

Middle Ordovician phosphatic
inarticulate brachiopods from
Västergötland and Dalarna,
Sweden

Lars E. Holmer



FOSSILS AND STRATA

Number 26 · Oslo, 30th November, 1989

Universitetsforlaget · Oslo

FOSSILS AND STRATA

Editor

Stefan Bengtson, Institute of Palaeontology, Box 558, S-751 22 Uppsala, Sweden.

Editorial and administrative board

Stefan Bengtson (Uppsala), Fredrik Bockelie (Oslo), Valdemar Poulsen (Copenhagen).

Publisher

Universitetsforlaget, Postboks 2959, Tøyen, N-0608 Oslo 6, Norway.

Fossils and Strata is an international series of monographs and memoirs in palaeontology and stratigraphy, published in cooperation between the Scandinavian countries. It is issued in *Numbers* with individual pagination, listed cumulatively on the back of each cover.

Fossils and Strata forms part of the same structured publishing programme as the journals *Lethaia* and *Boreas*. These two journals are fully international and accept papers within their respective sectors of science without national limitations or preferences. *Fossils and Strata*, however, is an outlet for more comprehensive systematic and regional monographs emanating primarily from the five countries of Norden. Contributions from other countries may also be included if this series is deemed appropriate with regard to distribution and availability. Articles can normally only be accepted if they are heavily subsidized by the national Research Council in their country of origin or by other funds. All income is re-invested in forthcoming numbers of the series.

Manuscripts should conform with the instructions on p. 3 of this cover. Normally the text should be submitted as word-processor

files (the editor will provide the necessary information on request). Manuscript processing is designed to ensure rapid and inexpensive production without compromising quality. Proofs are produced from the edited text files using desk-top-publishing techniques. Galley proofs are sent to the authors to provide opportunity to check the editor's changes and to revise the text if needed. Page proofs let the authors check the page layout, cross-references, word-breaks, etc., and to correct any remaining errors in the text. The final type will be produced on a high-resolution phototypesetter, and both text and illustrations are printed on high-quality coated paper.

Although articles in German and French may be accepted, the use of English is strongly preferred. An English abstract should always be provided, and non-English articles should have English versions of the figure captions. Abstracts or summaries in one or more additional languages may be added.

Many regional or systematic descriptions and revisions contain a nucleus of results which are of immediate and general interest in international palaeontology and stratigraphy. It is expected that authors of such papers will to some extent duplicate their publication in the form of an article for a journal, in the first place *Lethaia* or *Boreas*.

Individual numbers and standing subscriptions may be ordered from Universitetsforlaget (address as above). Prices (subject to revision) are listed on the back side of each issue. IPA members generally have a 50% discount on older issues (ask for information from Universitetsforlaget), and until the end of 1989 standing subscribers may purchase a set of back numbers 1–18 (except for Nos. 2, 4, 11, and 13, which are out of stock) for a total price of USD 33.00. All prices exclude postage and handling.

LETHAIA



An International Journal of
Palaeontology and Stratigraphy

Editor

Lars Ramsköld, Department of Palaeozoology, Swedish Museum of Natural History, Box 50007, S-104 05 Stockholm 50, Sweden.

Lethaia publishes articles of international interest in the fields of palaeontology and stratigraphy. Articles on the morphology and anatomy of fossil plants and animals should be of general interest to palaeontologists, and articles on systematic palaeontology should deal with the higher units in systematics or key forms on which our concepts of classification are based. New features, new forms and significant changes in the known distribution of fossils organisms also constitute important criteria for the acceptance of articles. Palaeobiology – particularly palaeoecology – and ecostratigraphy are the core topics of the journal. Articles on stratigraphy should meet the same requirements for general interest as the palaeontological articles and deal with stratigraphic principles, correlation of at least continent-wide importance, stratotype areas of key character, new occurrences or revisions which establish major features in palaeogeography, etc.

Lethaia, like its sister journal *Boreas*, forms part of a publishing system with special ambitions to apply and develop modern techniques, methodology and standards in scientific publication. These journals are semi-specialized, intending to cover and provide information within the respective interest ranges of large groups of earth and life scientists. They do not duplicate the functions of extant, strictly specialized journals in their field, national series, or monograph and memoir series.

Subscription to LETHAIA 1989

Ordinary price (non-members of IPA, institutions, libraries, etc.): Nordic countries NOK 630,00; all other countries USD 115.00 (1989).

Discount subscription to LETHAIA and membership for 1989 in the International Palaeontological Association

Subscribing membership for individual palaeontologists in the International Palaeontological Association (IPA, affiliated to the International Union of Geological Sciences, IUGS) may be obtained by payment of NOK 330,00 (Nordic countries) or USD 60.00 (all other countries) to Universitetsforlaget, Box 2959, Tøyen, N-0608 Oslo 6, Norway. The applicant must sign a statement that he undertakes to retain his discount copy of *Lethaia* as a personal copy and not deposit it in a public or institutional library.

Back volumes (1–21, 1968–1988) may be ordered on the same conditions.

Middle Ordovician phosphatic inarticulate brachiopods from Västergötland and Dalarna, Sweden

LARS E. HOLMER

Holmer, L. E. 1989 11 30: Middle Ordovician phosphatic inarticulate brachiopods from Västergötland and Dalarna, Sweden. *Fossils and Strata*, No. 26, pp. 1–172. Oslo. ISSN 0300-9491. ISBN 82-00-37425-4. [Revised and published version of doctoral thesis presented at the Faculty of Science, Uppsala University, 1988.]

Phosphatic inarticulate brachiopods are described from Middle Ordovician (Viru Series) strata in Västergötland and Dalarna, Sweden. The material originates from a series of closely spaced samples through the sequences of the Fjäckå and Kårgårde sections, Dalarna, and at Gullhögen quarry, Västergötland. Fifty-six species (34 named, of which 22 are new) are described, assigned to 29 named genera (of which three are new). The new acrotretacean subfamily Biernatinae is proposed, together with the new acrotretacean genera *Cyrtonotreta* and *Biernatia*; the problematical genus *Tegulella* is erected. For the discinaceans and most of the lingulaceans open nomenclature is applied; the taxonomically complicated Family Paterulidae has been excluded from systematic treatment altogether. The lingulaceans and discinaceans share a common type of shell structure which is clearly distinguishable from that of the acrotretaceans. The early ontogeny of many species is described. In the examined members of the Lingulacea and Discinacea the larval shell is large and smooth, whereas the acrotretaceans have a comparatively small and pitted larval shell. Although the protogular stage as a rule is not observable in fossil material, the cementing ventral valves of some eoconulids preserve the mould of an organic embryonic (or early larval) shell. The evolution of the phosphatic-shelled inarticulates is discussed. Within the order Acrotretida (*sensu lato*) the acquisition of a ventral valve with holoperipheral growth and a pedicle foramen could have taken place convergently several times from a lingulid stock, leading to the acrotretaceans, discinaceans, and siphonotretaceans, respectively; the latter two superfamilies are considered to belong to separate orders, the Discinida and the Siphonotretida. The usefulness of the inarticulates for biostratigraphical correlation is demonstrated. □ *Brachiopoda, phosphatic inarticulates, Lingulacea, Discinacea, Siphonotretacea, Acrotretacea, new subfamily Biernatinae, new genera Biernatia, Cyrtonotreta, Tegulella, shell structure, ontogeny, evolution, biostratigraphy, palaeoecology, Middle Ordovician, Västergötland, Dalarna, Sweden, N5815 N6050 E1520 E1337.*

Lars E. Holmer, Institute of Palaeontology, Box 558, S-751 22 Uppsala, Sweden; 1988 12 13, revised 1989 02 28.

Contents

Introduction	3	Uhakuan Stage	20
Historical review	3	Dalby Limestone	24
Material and methods	4	Discussion	26
Middle Ordovician stratigraphy in Västergötland and		Life habits	26
Dalarna	5	Epifauna	29
Localities	6	Endofauna	29
Gullhögen quarry	6	Morphological terms	30
Kårgårde section	9	Shell structure	30
Fjäckå section	12	Lingulacea, Discinacea and Acrothelidae	31
Biostratigraphy and palaeoecology	12	Lingulacea	31
Distribution, abundance and lithofacies	12	Discinacea	35
Kundan Stage	13	Acrothelidae	36
Aserian Stage	13	Discussion	36
Lasnamägian Stage	20	Acrotretacea	42

Acrotretinae and Torynelasmatinae	42	Genus <i>Torynelasma</i> Cooper, 1956	106
Ephippelasmatinae and Biernatinae	46	<i>Torynelasma suecicum</i> sp. nov.	107
Scaphelasmatinae	47	<i>Torynelasma</i> sp.	110
Eoconulidae	48	Genus <i>Acrotretella</i> Ireland, 1961	110
Discussion	48	<i>Acrotretella</i> sp.	110
Summary	52	Subfamily Linnarssoniinae Rowell, 1965	110
Ontogeny	52	Genus <i>Aktassia</i> Popov, 1976	110
Lingulacea and Discinacea	55	<i>Aktassia</i> cf. <i>triangularis</i> Popov, 1976	110
Lingulacea	55	Subfamily Ephippelasmatinae Rowell, 1965	112
Recent Discinacea	56	Genus <i>Myotreta</i> Goryanskij, 1969	113
Discinacea	59	<i>Myotreta</i> aff. <i>crassa</i> Goryanskij, 1969	113
Discussion	59	<i>Myotreta dalecarlica</i> sp. nov.	114
Acrotretacea	61	<i>Myotreta orensis</i> sp. nov.	117
Acrotretinae and Torynelasmatinae	61	Genus <i>Rhinotreta</i> Holmer, 1986	119
Ephippelasmatinae	62	<i>Rhinotreta davidi</i> sp. nov.	119
Biernatinae	63	Genus <i>Numericoma</i> Popov, 1980	121
Scaphelasmatinae	63	<i>Numericoma simplex</i> sp. nov.	122
Eoconulidae	63	<i>Numericoma perplexa</i> sp. nov.	124
Discussion	64	<i>Numericoma</i> ? <i>spinosa</i> (Biernat, 1973)	127
Siphonotretacea	65	Genus <i>Ephippelasma</i> Cooper, 1956	130
Summary	65	<i>Ephippelasma minutum</i> Cooper, 1956	131
Predation and malformation	65	Subfamily Biernatinae subfam. nov.	131
Phylogeny and evolution	67	Genus <i>Biernatia</i> gen. nov.	133
Phosphatic inarticulates and brachiopod phylogeny	67	<i>Biernatia holmi</i> sp. nov.	134
Evolution of the Class Lingulata Goryanskij & Popov	69	<i>Biernatia</i> sp.	138
Systematic palaeontology	70	Subfamily Scaphelasmatinae Rowell, 1965.	139
Class Lingulata Goryanskij & Popov, 1985		Genus <i>Scaphelasma</i> Cooper, 1956	139
Order Lingulida Waagen, 1885	70	<i>Scaphelasma mica</i> Popov, 1975	139
Superfamily Lingulacea Menke, 1828	70	<i>Scaphelasma</i> sp. nov. a	143
Family Obolidae King, 1846	70	<i>Scaphelasma</i> cf. <i>pusillum</i> Popov, 1980	144
Subfamily Obolinae King, 1846	72	<i>Scaphelasma</i> ? <i>rugosum</i> Goryanskij, 1969	144
Genus <i>Rosobolus</i> Havlíček, 1982	72	Family Eoconulidae Rowell, 1965.	147
<i>Rosobolus</i> ? sp. nov. a	72	Genus <i>Eoconulus</i> Cooper, 1956	147
Subfamily Lingulellinae Schuchert, 1893	72	<i>Eoconulus</i> cf. <i>clivus</i> Popov, 1975	148
Genus <i>Expellobolus</i> Havlíček, 1982	72	<i>Eoconulus</i> cf. <i>semiregularis</i> Biernat, 1973	150
<i>Expellobolus</i> ? sp. nov. a	72	<i>Eoconulus</i> sp. nov. a	153
Genus <i>Lingulella</i> Salter, 1866	72	<i>Eoconulus</i> cf. <i>cryptomyus</i> Goryanskij, 1969	153
<i>Lingulella</i> ? <i>alata</i> sp. nov.	72	<i>Eoconulus robustus</i> sp. nov.	155
Genus <i>Spinilingula</i> Cooper, 1956	73	Order Discinida Kuhn, 1949	157
<i>Spinilingula radiolamellosa</i> sp. nov.	74	Superfamily Discinacea Gray, 1840	157
Genus <i>Paldiskites</i> Havlíček, 1982	74	Family Trematidae Schuchert, 1893.	158
<i>Paldiskites</i> ? sp. nov. a	74	Genus <i>Trematis</i> Sharpe, 1848	158
Genus <i>Rowellella</i> Wright, 1963	76	<i>Trematis</i> ? sp.	158
<i>Rowellella</i> cf. <i>lamellosa</i> Popov, 1976	76	Family Discinidae Gray, 1840.	158
<i>Rowellella hollenensis</i> sp. nov.	77	Subfamily Orbiculoideinae Schuchert & LeVene, 1929	158
Lingulellinae gen. et spp.	79	Genus <i>Orbiculoidea</i> D'Orbigny, 1847	158
Subfamily Glossellinae Cooper, 1956	79	<i>Orbiculoidea</i> ? sp. a	158
Genus <i>Pseudolingula</i> Mickwitz, 1909	79	<i>Orbiculoidea</i> ? sp. b	158
<i>Pseudolingula</i> sp.	79	<i>Orbiculoidea</i> ? sp. c	158
Glossellinae gen. et sp.	79	Genus <i>Schizotreta</i> Kutorga, 1848	159
Order Acrotretida Kuhn, 1949	81	<i>Schizotreta</i> sp. a	160
Suborder Acrotretidina Kuhn, 1949	81	Order Siphonotretida Kuhn, 1949	161
Superfamily Acrotretacea Schuchert, 1893	81	Superfamily Siphonotretacea Kutorga, 1848	161
Family Acrotretidae Schuchert, 1893	81	Family Siphonotretidae Kutorga, 1848	161
Subfamily Acrotretinae Schuchert, 1893	81	Subfamily Schizamboniinae Havlíček, 1982	161
Genus <i>Conotreta</i> Walcott, 1889	81	Genus <i>Nushbiella</i> Popov, 1986	161
<i>Conotreta</i> ? <i>mica</i> Goryanskij, 1969	81	<i>Nushbiella lilliana</i> sp. nov.	161
<i>Conotreta</i> ? <i>siljanensis</i> sp. nov.	84	Subfamily Acanthamboniinae Cooper, 1956	162
Genus <i>Hisingerella</i> Henningsmoen, 1948	89	Genus <i>Acanthambonia</i> Cooper, 1956	163
<i>Hisingerella billingensis</i> sp. nov.	90	<i>Acanthambonia delicata</i> sp. nov.	163
<i>Hisingerella</i> ? <i>unguicula</i> sp. nov.	90	<i>Acanthambonia</i> sp. nov. a	165
Genus <i>Cyrtonotretagen</i> gen. nov.	93	Order Paterinida Rowell, 1965	165
<i>Cyrtonotreta vestrogothica</i> sp. nov.	94	Superfamily Paterinacea Schuchert, 1893	165
<i>Cyrtonotreta</i> sp. a	96	Family Paterinidae Schuchert, 1893.	165
<i>Cyrtonotreta</i> ? <i>striata</i> sp. nov.	96	Genus <i>Dictyonites</i> Cooper, 1956	165
<i>Cyrtonotreta</i> ? sp. b	99	<i>Dictyonites fredriki</i> sp. nov.	165
Genus <i>Physotreta</i> Rowell, 1966	99	<i>Dictyonites</i> sp.	166
<i>Physotreta deformis</i> sp. nov.	99	Problematica	167
Genus <i>Spondylotreta</i> Cooper, 1956	104	Genus <i>Tegulellagen</i> gen. nov.	167
<i>Spondylotreta orsaensis</i> sp. nov.	104	<i>Tegulella minuta</i> sp. nov.	167
<i>Spondylotreta</i> sp. nov. a	104	References	168
Subfamily Torynelasmatinae Rowell, 1965	106		

Introduction

Phosphatic inarticulate brachiopods are easily obtainable in great quantities from many sequences of Lower Palaeozoic limestones throughout the world (e.g., Rowell, 1966). The majority of them may be classified as microfossils, because the maximum dimension is generally less than 2 mm. However, detailed studies using micropalaeontological techniques, such as isolation with weak acids, began only fairly recently (Bell 1946, 1948), and in many parts of the world such investigations have still not been undertaken.

During the Ordovician Period the inarticulate faunas reached their highest known generic diversity (Williams 1965, Fig. 150). In Sweden the Ordovician platform sequence was dominated by deposition of carbonate muds with a low average rate of sedimentation (in the order of 1–5 mm per 1000 years; Lindström 1963; Jaanusson 1973). Consequently, the total thickness of the Ordovician beds in this region is comparatively small, and phosphatic and organic microfossils are concentrated in the limestones by comparison with many other regions where the average rates of sedimentation were higher.

There are only a few modern studies of Ordovician phosphatic inarticulates from Baltoscandia, notably by Goryanskij (1969), Biernat (1973), Bednarczyk & Biernat (1978), Bednarczyk (1986), and Popov & Nölvak (1987). In Sweden the first such study dealt with a fauna from beds around the Middle–Upper Ordovician boundary in Västergötland (Holmer 1986). The main object of the investigation presented here is to study the systematics and biostratigraphy of Middle Ordovician phosphatic inarticulate brachiopods from Västergötland and Dalarna. The terms Lower, Middle, and Upper Ordovician are used here as synonyms for the Baltoscandian ‘regional series’ Oeland, Viru, and Harju (Kaljo, Röömusoks & Männil 1958).

It is necessary to discuss briefly what is to be understood by ‘inarticulate brachiopods’. The Class Inarticulata Huxley, 1869 (*sensu* Rowell 1965, p. H260), is structurally and anatomically heterogeneous; it includes forms with both phosphatic and calcareous shells (apart from other morphological and anatomical differences). Recent proposals have suggested that this difference is of fundamental systematic importance, and should be recognized at a higher taxonomic level than that currently used. Indeed, the most

recent of these proposals, by Goryanskij & Popov (1985, 1986), suggests that the phosphatic-shelled inarticulates constitute a clade quite separate from the Phylum Brachiopoda. Although this notion is not supported here (see also p. 67), the Lingulata Goryanskij & Popov, 1985 (phosphatic inarticulate brachiopods), is accepted as a class within a monophyletic Phylum Brachiopoda.

The remainder of the scheme of Goryanskij & Popov (1985, 1986) concerns the systematic position of the calcareous-shelled inarticulates that is not commented upon here, but it is somewhat doubtful if the Class Inarticulata Huxley should be used in the very restricted sense of Goryanskij & Popov, to include only the calcareous craniaceans and craniopsids, and the aragonitic trimerellaceans; in order to avoid confusion it is probably better to introduce a new name for such a group. The term ‘inarticulate brachiopods’ can then, in a broad sense, still be used as a designation for non-articulate brachiopods, including both the phosphatic and the calcareous inarticulate stocks.

Historical review

Goryanskij (1969, pp. 9–12) compiled a general review of publications dealing mainly with inarticulate brachiopods from Estonia and the Leningrad district. Papers describing Swedish material were not included in that account, and therefore a short review is given here of publications illustrating and describing Swedish Ordovician phosphatic inarticulate brachiopods. A broad historical account of the class Inarticulata was given by Muir-Wood (1955).

The first description of a Swedish Ordovician phosphatic inarticulate brachiopod was published by Wahlenberg (1818), who named but did not illustrate the Hirnantian (uppermost Ordovician) discinacean *Patellites* [= *Orbiculoides*] *concentricus* from the Dalmanitina beds at Bestorp on Mösseberg in Västergötland (see also Bergström 1968b). Later, Hisinger (1837) described, but did not figure, the acrotretine *Atrypa*? [= *Hisingerella*] *nitens* (see also Henningsmoen 1948; Holmer 1986) from the Harju age Fjäckå Shale of Dalarna. Lindström (*in* Angelin & Lindström 1880) was the first to figure Swedish phosphatic inarticulates; he described *Discina* [= *Orbiculoides*?] *gibba* Lindström from the Upper Ordovician Boda Limestone of Dalarna

(see also Holmer 1987b), as well as *Obolella?* [= *Hisingerella nitens* (Hisinger)]. Lindström (1888) summarized (in stratigraphical faunal lists) the Lower Palaeozoic fossil faunas of Sweden; from the entire Ordovician sequence, only a total of six named species of phosphatic inarticulates were listed.

Around 1900 Gerhard Holm planned a comprehensive work on 'Acrotreta', based on Cambrian and Ordovician material from Baltoscandia. Unfortunately, the work was never completed, but the unpublished plates, figures, and sketches are kept at the Swedish Museum of Natural History in Stockholm, together with the material.

The Tremadoc age *Obolus*, *Dictyonema* and *Ceratopyge* beds of Baltoscandia are generally very rich in, and frequently dominated by, phosphatic inarticulate brachiopods. This fauna attracted the attention of many of the early workers (see also Walcott 1912). In two articles dealing with Cambrian and Ordovician faunas of the marine South Bothnian sequence (based on material collected from erratic boulders), Wiman (1905, 1908) recorded numerous phosphatic inarticulates from the Tremadoc beds.

The rich Swedish Tremadoc faunas were studied also by Moberg & Segerberg (1906), who described seven new species from the *Dictyonema* and *Ceratopyge* beds in Skåne and on Öland, comprising four lingulaceans and three acrotretaceans. The poorly known *Lamanskya splendens* Moberg & Segerberg (reputedly an articulate), from the *Ceratopyge* beds of Öland, is also a phosphatic inarticulate; it belongs to the elkaniids. A few species of phosphatic inarticulate brachiopods, from the same sequence in Skåne and on Öland, were described by Walcott (1908) and Westergård (1909). Later, Walcott (1912, pp. 144–145) listed a total of 17 species of phosphatic inarticulate brachiopods from the lowermost Ordovician of Sweden, and his work still remains the most recent synthesis of these faunas.

Hede (1951) recorded the inarticulates from the Lower and Middle Ordovician beds of the Fågelsång core in Skåne, and Waern (1952) illustrated some species from the *Dictyonema* beds of the Bödahamn core on Öland.

Lower Palaeozoic shales and mudstones commonly have conspicuous faunas of small brachiopods, and many of the early descriptions of phosphatic inarticulate taxa, prior to the development of standard techniques for isolating phosphatic shells from limestones (Bell 1946, 1948), are based on material from such lithologies. The Middle to Upper Ordovician *Dicellograptus* Shale of Skåne is rich in, and occasionally dominated by such forms. These faunas were first studied by Hadding (1913), who described a total of eleven new species, including eight lingulaceans, two acrotretacean brachiopods, *Acrotreta* [= *Hisingerella*] *nana* and *Acrotreta dubia* [= *Hisingerella nitens* (Hisinger)], as well as the discinacean *Discina* [= *Schizocrania*] *compressa*.

Troedsson (1918) studied the uppermost Ordovician Tommarp Mudstone of Skåne, and described two new species, *Conobreta* [= *Biernatia?*] *acuta* (see also p. 133) and *Discina* [= *Orbiculoidea*] *radiata* (see also Temple 1965). Funkquist (1919) illustrated some phosphatic inarticulates from the Middle Ordovician Killeröd Formation in Skåne, and the faunas of the Middle–Upper Ordovician sequence in the Koängen core were studied by Nilsson (1977; see also Jaanusson 1984).

The phosphatic inarticulates from the Upper Ordovician argillaceous sequences in Västergötland have received attention mainly through Henningsmoen (1948), who illustrated specimens from the Fjäckå Shale of the Kullatorp core. Bergström (1968b) studied the Hirnantian brachiopods of Västergötland, which included *Orbiculoidea concentrica* (Wahlenberg) and some unnamed lingulaceans.

Acknowledgements. – This work was initiated at the Department of Palaeobiology, Uppsala University, where the late Anders Martinsson kindly provided working space and facilities. The major part of the study has been carried out at the Palaeontological Institute, Uppsala University, where my assistant supervisor, Stefan Bengtson, kindly helped, encouraged and offered constructive criticism during all stages of the work, and lately also at the Department of Palaeozoology, Swedish Museum of Natural History, Stockholm, where my supervisor Valdar Jaanusson has offered never failing support since I became interested in palaeontology around 1973. I am also grateful to Michael Bassett (Cardiff), Leonid Popov (Leningrad), Ivar Puura (Tallinn), Aarvo Rõõmusoks (Tartu), Michal Mergl (Prague), Gertruda Biernat (Warsaw), and Wiesław Bednarczyk (Warsaw) for help in obtaining comparative material, and for stimulating discussions on brachiopods in general.

The assistance of Meit Lindell (Uppsala) in the extensive laboratory work and in the painstaking picking of thousands of inarticulate specimens, as well as of Tommy Westberg (Uppsala), Martin Feuer (Uppsala), Uno Samuelsson (Stockholm), and Göran Blom (Stockholm) in the dark-room work, is greatly appreciated, as is that of Lennart Andersson (Stockholm) and Björn Lindsten (Stockholm) in completing the drawings. Stig Bergström (Columbus, Ohio) kindly supplied samples from the Pratt Ferry beds of Alabama, and permitted the use of his processed samples from the Fjäckå section, Dalarna. Anita Löfgren (Lund) supplied her residues from pertinent parts of the sequence in Jämtland. I am grateful to Albert Rowell (Lawrence, Kansas) for refereeing and commenting on the manuscript, and also to Michael Bassett (Cardiff) for correcting and improving both the language and scientific content.

My work has been supported by grants from the Royal Swedish Academy of Sciences (*Gustav Lindströms Minnesfond* and *Hierta Retzius Stipendiefond*), Uppsala University (*Liljewalchs* and *Lenanders stipendiefonder*), Palaeontological Institute and Department of Palaeobiology (Uppsala University), Department of Palaeozoology (Swedish Museum of Natural History), and by the Swedish Natural Science Research Council. The authorities of Kopparberg County permitted access to the Kårgårde and Fjäckå Nature Reserves, and Cementa AB kindly permitted sampling at Gullhögen quarry. My work could not have been completed without the continuing help of my wife (and private chauffeur) Lillian, who offered company in the field, as well as moral support.

Material and methods

Samples (1–2 kg) were taken at close intervals (generally 25–50 cm) throughout the Middle Ordovician sequence at Gullhögen quarry (sample series GB81, 84), Västergötland (Fig. 2), and in the Kårgårde section (sample series DLK83, 84), Dalarna (Fig. 5). Of these, 160 samples were used, and from each roughly 1 kg (or, more rarely, 500 g) of uncrushed limestone was dissolved in 10% acetic acid, using the method developed by Jeppsson *et al.* (1985). The samples from the Viru beds above the Dalby Limestone are not included in this study, as in Västergötland the Skagen Limestone is siliceous and does not dissolve easily in weak acids; in Dalarna the Skagen and Moldå limestones are

Series Balto-scandian	British	Graptolite zones	zones	Conodont subzones	Balto-scandian stages	Västergötland	Dalarna
						Billingen	Siljan district
Middle Ordovician (Viru)	Caradoc	<i>Diplograptus multdens</i>	<i>Amorphognathus tvaerensis</i>	<i>Prioniodus alobatus</i>	Unnamed	Skagen Limestone	
						<i>Nemagraptus gracilis</i>	Dalby Limestone
		<i>Glyptograptus teretiusculus</i>		Lower			
				Llandello		<i>Eoplacognathus lindstroemi</i> <i>Eoplacognathus robustus</i> <i>Eoplacognathus reclinatus</i>	<i>Pygodus serra</i>
	Gullhögen Formation						
	<i>Didymograptus murchisoni</i>	Lasnamägian	Skövde beds		Folkeslunda Limestone		
			<i>Eoplacognathus suecicus</i> <i>Panderodus sulcatus</i>		Aserian	Våmb Ls.	
	Segerstad Ls.	Skärlov Limestone					
		Vikarby Limestone					
	Llanvirn	<i>Didymograptus artus</i>	<i>Eoplacognathus suecicus</i>	Kundan	Holen Limestone	Kårgärde Limestone	

Fig. 1. Stratigraphical subdivision of the Middle Ordovician in Västergötland and in the Siljan district, Dalarna. After Jaanusson 1982a, Fig. 4.

comparatively poor in acid-resistant microfossils; a detailed study of this fauna requires additional sampling.

The residues were sieved into two fractions (larger than 1 mm and 1–0.075 mm). Both fractions were picked, yielding a total of about 31,000 specimens (separate dorsal and ventral valves, and complete shells) from the two sections (Kårgärde section, 16,354 specimens; Gullhögen quarry, 14,535 specimens). Neither heavy liquid nor any other method of concentrating the microfossils was used, for the reasons stated by Holmer (1986, p. 98).

Through the courtesy of Stig M. Bergström (Columbus, Ohio) and the Department of Historical Geology and Palaeontology, Lund, the insoluble residues from samples (series D59, 60) through the uppermost Furudal Limestone and Dalby Limestone of the Fjäckå section, Dalarna, could be used. Picking of the 'heavy' (and some of the 'light') fractions of the residues (treated with bromoform) yielded a total of 4,246 specimens.

In the SEM work standard orientations were used with the 'light' coming from the left (that is, the detector being

positioned to the left), and all plane views were photographed at about 10–20° tilt (of the stub), as it reduces deep shadows.

Middle Ordovician stratigraphy in Västergötland and Dalarna

Exhaustive reviews of previous work dealing with the stratigraphy of the Viru age sequences of Västergötland and Dalarna were given by Jaanusson (1963, 1964), who also introduced a modern combined litho- and 'topostratigraphical' (*sensu* Jaanusson 1960, 1976) classification for the Middle Ordovician of these provinces. Recently, the existing information on the Ordovician in Dalarna and Västergötland was summarized by Jaanusson (1982b, c), and his stratigraphical classification is followed here (Fig. 1).

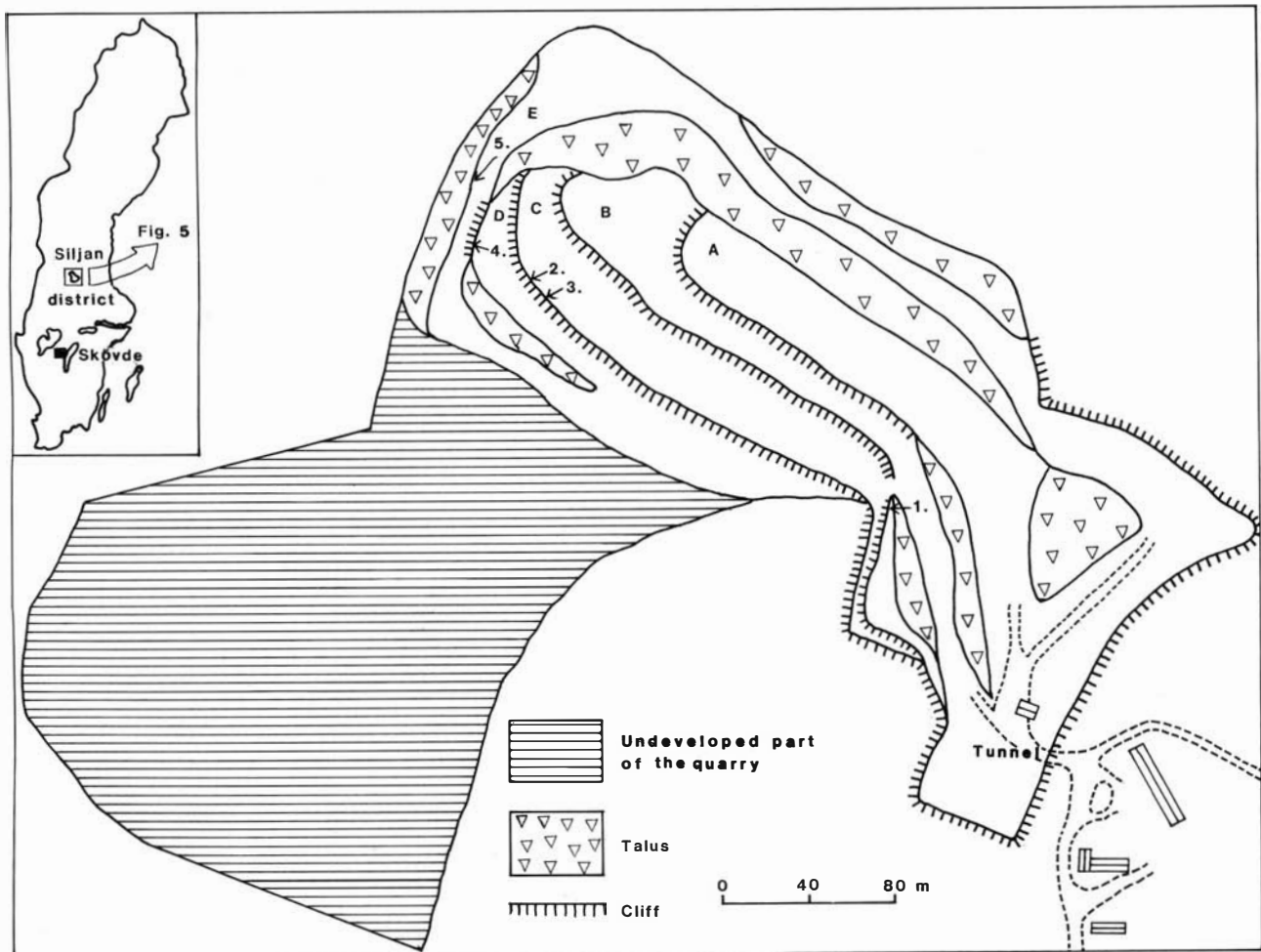


Fig. 2. Diagrammatic map of Gullhögen quarry, Skövde, Västergötland, showing the location of the sections (1–4) investigated (section 5 was described by Holmer 1986). A, Upper Cambrian to lower Hølen Limestone; B, upper Hølen Limestone to lower Gullhögen Formation; C, upper Gullhögen Formation to lowermost Dalby Limestone; D, lower to upper Dalby Limestone; E, uppermost Dalby Limestone (from the lower bentonitic bed) to lower Jonstorp Formation. Based on a map supplied by Cementa AB. Figure prepared by Björn Lindsten (Stockholm).

Localities

Gullhögen quarry

This locality exposes a section almost 70 m thick ranging from the Upper Cambrian to the lower part of the Upper Ordovician. The quarry is on the south-eastern slope of northern Billingen, in the outskirts of the town of Skövde (Fig. 2). Commercial quarrying is still proceeding and will probably continue until around the year 2000. Fig. 2 (based on a more detailed map kindly supplied by Cementa AB) shows the outline of the present quarry (as of summer 1984), and the planned maximum extent (shaded) of the future quarry.

The exposed sequence was first described in detail by Thorslund & Jaanusson (1960, p. 17); at that time the highest exposed beds were within the Middle Ordovician Ryd Formation (see also Jaanusson 1964). At present the top of the exposure is within the lower part of the Harju age lower Jonstorp Formation (Section 5, Fig. 2; see also Holmer 1986). A brief description of the Ordovician sequence in the quarry was compiled by Jaanusson (1982c, pp. 176–179). The stratigraphy of the uppermost Viru and lower

Harju sequence (comprising an unnamed upper Viru unit, the Slandrom and Bestorp limestones, and the Fjäckå Shale) in the quarry was revised recently (Holmer 1986).

This monograph deals with the phosphatic inarticulate brachiopod fauna of the sequence between the uppermost Oeland age Hølen Limestone (top of the *Didymograptus artus* Biozone; Fortey & Owens 1987) and the Viru age Skagen Limestone (basal part within the *Diplograptus multidentis* Biozone). This interval comprises, in ascending order, the Våmb Limestone, Skövde beds, Gullhögen Formation, and the Ryd and Dalby limestones (Fig. 1). A single sample from the uppermost Hølen Limestone was included for comparison with the Middle Ordovician faunas (Figs. 1, 8A). The Lower Ordovician sequence in the quarry (Latorp, Lanna, and Hølen limestones) has never been studied in detail, apart from by Lindström & Vortisch (1983) and Lindström (1984). The Viru lithostratigraphical succession in the quarry is almost identical to that of the Stora Åsbotorp core, situated about 1.5 km to the north (Jaanusson 1964; Grahn 1981).

A brief description of the Viru sequence under consideration, in ascending order, is given below. Measurements were taken from the discontinuity surface at the base of the

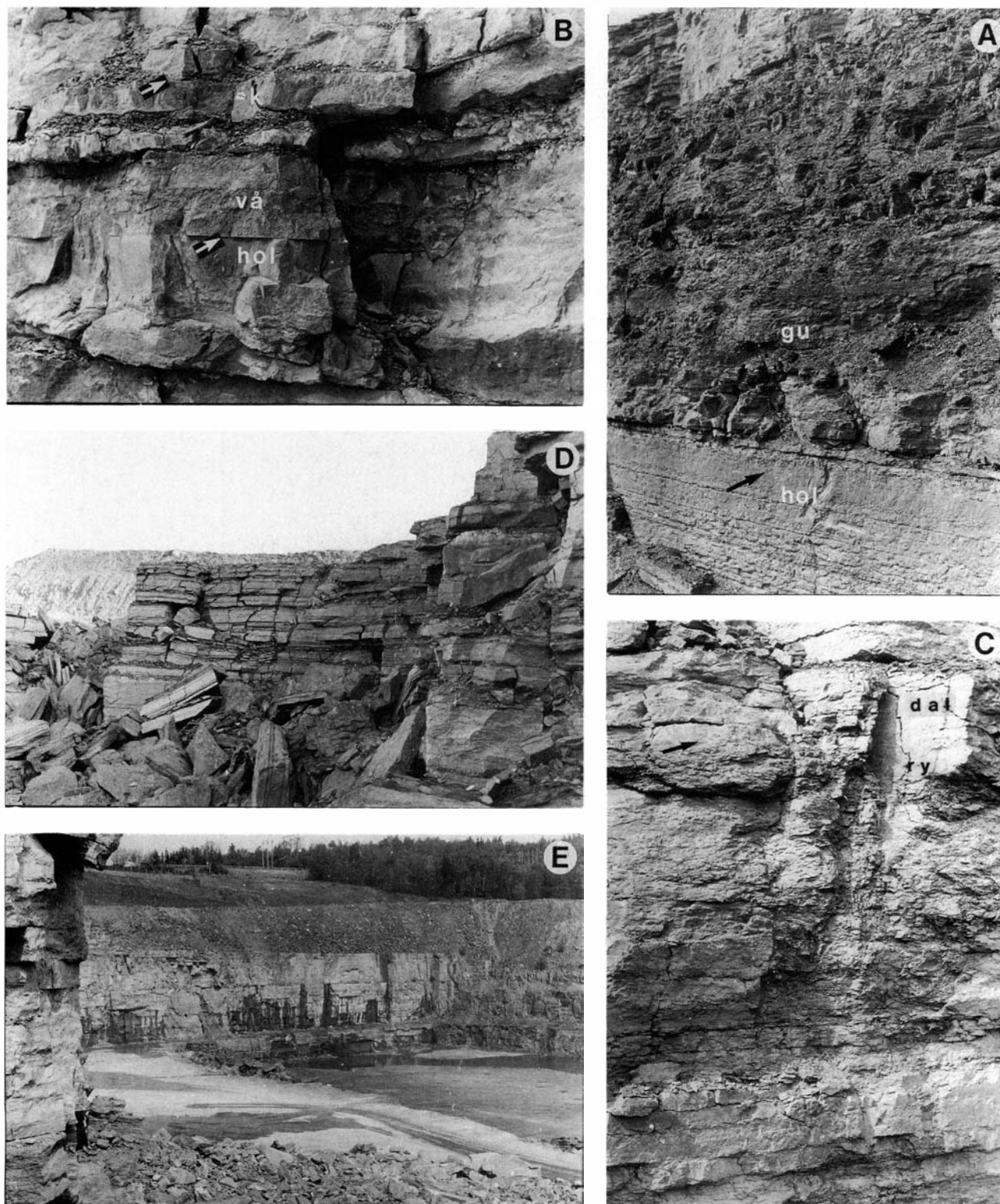


Fig. 3. Gullhøgen quarry. □A. Section 1 (see Fig. 2), showing the uppermost Holen Limestone (hol), the Våmb Limestone, the Skövde beds, and the Gullhøgen Formation (gu). The basal Viru discontinuity surface is indicated by an arrow. □B. Section A (situated some 5 m south of section 1 in Fig. 2), showing the Holen Limestone (hol), Våmb Limestone (vå), Skövde beds (sk), and the lowermost Gullhøgen Formation. The basal Viru discontinuity surface and the discontinuity surface at the top of the Skövde beds are indicated by arrows. □C. The upper part of Section 3, showing the uppermost part of the finely nodular Ryd Limestone (ry); the boundary to the Dalby Limestone (dal) is indicated by an arrow. □D. Section 4, showing the upper Dalby Limestone. □E. View of the north-western part of the quarry (taken from section 3 towards section 5), showing a section from the Holen Limestone at the base (cliff B in Fig. 2) to the Jonstorp Formation (cliff E in Fig. 2).

Våmb Limestone upwards. The thickness of the units given by Jaanusson (1964, 1982c) does not always agree exactly with those based on my measurements; in all probability

this is because the sequence could not be measured along a continuous section, but had to be pieced together from different parts of the quarry (Fig. 2).

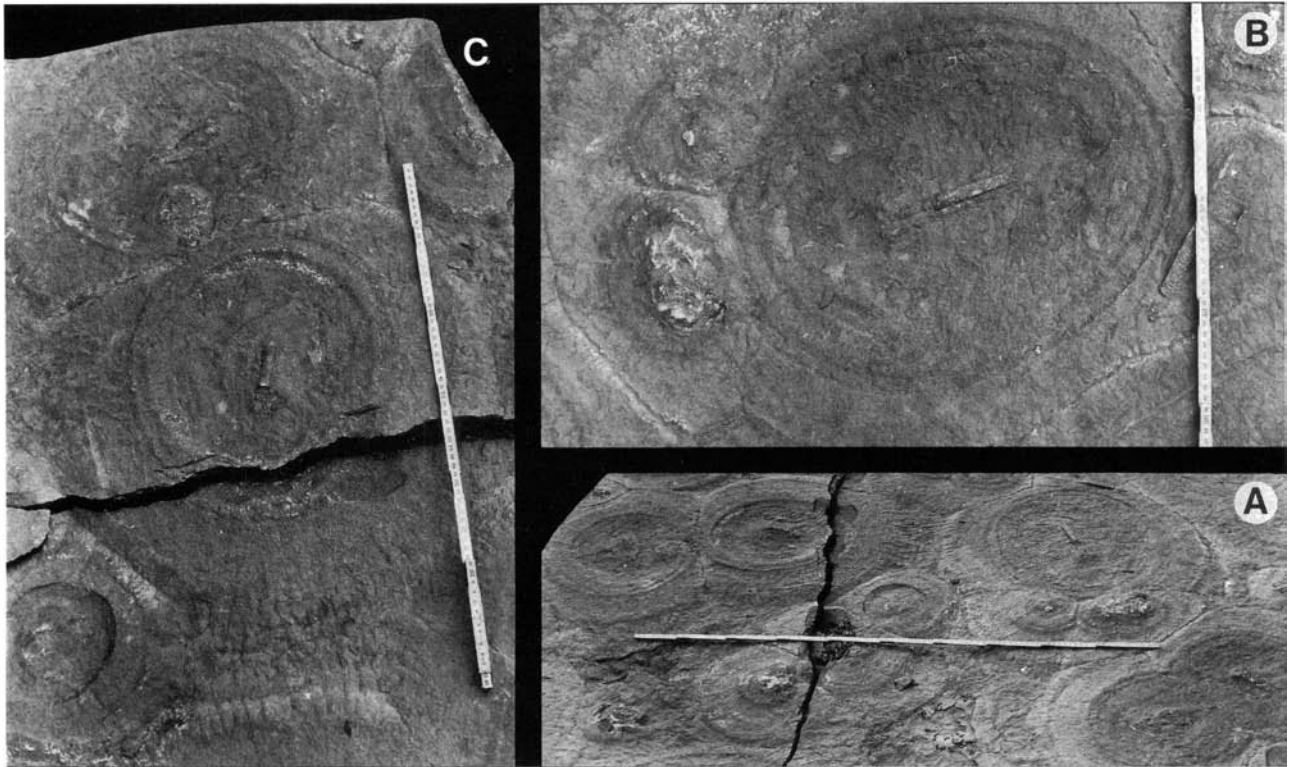


Fig. 4. Gullhøgen quarry. □A–C. Bedding plane from the upper Dalby Limestone showing orthoconic cephalopods enveloped by laminated encrustations, which may represent stromatolites. Total length of ruler 1 m.

Jaanusson (1964) referred the lowermost Viru beds in the quarry to the Vikarby Limestone. However, Jaanusson (1982c) introduced the Våmb Limestone (0–0.1 m; Fig. 8B) for this part of the sequence, because the conodont succession suggests that it is a lateral equivalent to the lower part of the Skårlöv Limestone. Moreover, these beds do not appear to be contiguous with the Vikarby Limestone in the Siljan district. The Våmb Limestone is bounded by discontinuity surfaces and varies from 0 to 12 cm thick within the quarry (Holmer 1983); the upper surface is furrowed in places, with the furrows having a V-shaped cross section, indicating that they may represent desiccation cracks. In addition, there are numerous, laterally impersistent intraformational discontinuity surfaces (Holmer 1983). The Våmb Limestone is rich in ferruginous ooids (see Sturesson 1989 for details), and in the lowermost bed it includes laminated stromatolite-like structures (Fig. 8A; Holmer 1983). The lower planar discontinuity surface (referred to as the basal Viru discontinuity surface by Jaanusson 1964 and Holmer 1983) indicates a considerable break in the sequence, comprising equivalents of most of the Aserian Stage as developed elsewhere.

The quarry is the type locality of the Gullhøgen Formation and the Skövde beds (0.1–12.4 m from the base of the Våmb Limestone; Fig. 8A–B). The lowermost limestone beds of the Gullhøgen Formation can be distinguished as an informal subdivision, the Skövde beds (Figs. 3A–B, 8A–B). The unit is bounded by discontinuity surfaces and varies in thickness from 10 to 45 cm within the quarry; in places, the upper discontinuity surface of the Skövde beds is missing (Holmer 1983). It is possible that the Skövde

beds constitute a wedge of the Folkeslunda Limestone (Jaanusson 1964). The Gullhøgen formation is 12.3 m thick (including the Skövde beds), and composed mainly of dark grey mudstone with calcilititic nodules, but it includes also beds of calcilititic limestone (Fig. 3A). There is a phosphatized discontinuity surface in about the middle of the unit (at 7.5 m from the base of the Våmb Limestone; Fig. 8B). A few reddish calcarenitic irregular limestone beds close to the lower boundary of the formation contain ferruginous ooid-like structures (Fig. 8A–B; see Sturesson 1989 for details).

The Ryd Limestone (12.4–21.4 m from the base of the Våmb Limestone in Fig. 8C) is 9.0 m thick, and dominated by grey, thick-bedded calcilitites, with some finely nodular intercalations (Figs. 3C, 8C); it can be regarded as a wedge of the upper Furudal Limestone (Jaanusson 1964). The lower boundary is defined clearly lithologically, whereas the upper is not, and drawn on faunal evidence (Jaanusson 1964).

The Dalby Limestone (21.4–33.2 m from the base of the Våmb Limestone in Fig. 8C–D) can be divided into (unnamed) upper and lower members on lithological grounds (Jaanusson 1982c).

The lower member is 6.3 m thick (5.6 m in Jaanusson 1982c). The compact limestone is grey, thick bedded and predominantly calcilititic in the lower part, and calcarenitic in the upper part. In places, there are intercalations of finely nodular limestone (Fig. 8C–D).

The upper member is 5.5 m thick (6.3 m in Jaanusson 1982c), and composed mainly of grey, bedded to nodular calcarenites with intercalations of calcareous mudstone

(Figs. 3D, 8D). The limestone is most commonly siliceous and does not dissolve readily in weak acid (see also Schallreuter 1984). In at least two beds of the upper member, large macrofossils (mostly orthoconic cephalopods) are enveloped by laminated encrustations, which may represent stromatolites. In the uppermost of these two beds (at 30.5 m above the base of the Våmb Limestone; Fig. 8D), the stromatolite-like structures are developed as large disc-shaped nodules that vary in size, reaching about 40 cm in diameter and 10 cm in thickness. In the lower bed (at 29.2 m above the base of the Våmb Limestone; Fig. 8D) the stromatolitic structures reach a still larger size, up to 60 cm in diameter (Fig. 4). According to Jan Johansson (*in Jaanusson 1982c*), there is also a level with stromatolitic structures close to the lower boundary of the upper member. The upper boundary of the member is marked by a bentonitic bed, 1.1 m thick.

Few previous studies have been made of the Viru–Harju faunas at Gullhögen quarry. Fåhraeus (1966) studied the conodonts of the Våmb Limestone and Skövde beds. Some ostracodes from the upper Dalby Limestone were described by Schallreuter (1984). Holmer (1986) studied the uppermost Viru and lower Harju faunas of phosphatic inarticulate brachiopods, and described some unusual microfossils (Holmer 1987a). Owen (1987) described the trilobite *Tretaspis percontator*, which previously (Jan Johansson *in Jaanusson 1982c*) was identified as *Tretaspis ceriodes* (Angelin). The graptolites from the Viru–Harju sequence in the nearby Stora Åsbotorp core were studied by Jaanusson & Skoglund (1963) and Skoglund (1963), and the palaeocope ostracodes by Jaanusson (1957). The Viru and Harju chitinozoans were studied by Grahn (1981).

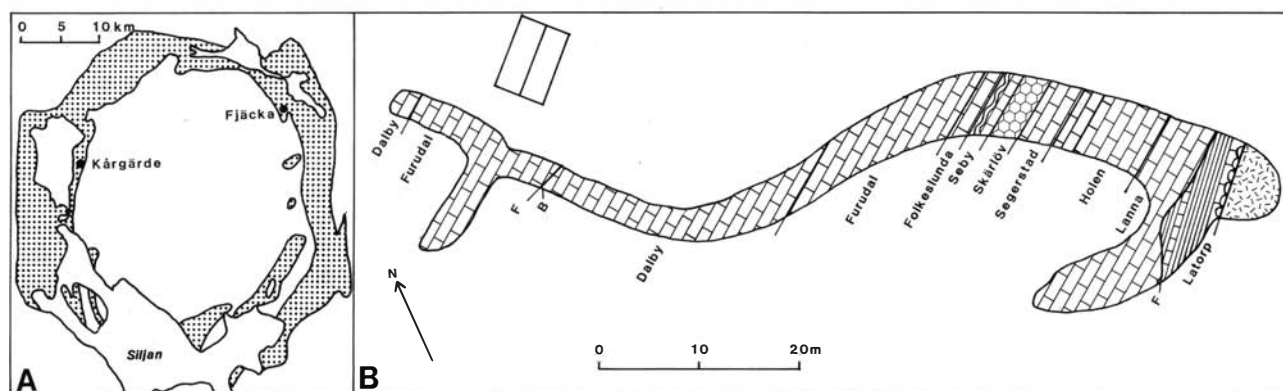


Fig. 5. □A. Map of the Siljan District, Dalarna, showing distribution of Palaeozoic rocks (shaded). □B. Map of the Kårgårde section. After a map produced by L. Karis (Uppsala). Figure prepared by Björn Lindsten (Stockholm).

Kårgårde section

The Kårgårde section is situated close to Holen village in the northwestern part (parish of Orsa) of the Siljan district, Dalarna (Fig. 5). Scattered exposures in the Kårgårde area have been studied scientifically since the late 19th Century (Törnquist 1883).

Cambrian rocks have been thought to be absent over the whole of the Siljan district. However, the occurrence of the acrotretacean *Ceratreta tanneri* (Metzger, 1922), in erratic boulders of the so-called 'Obolus Sandstone' from Gårdsjö, appears to indicate a late Cambrian age for the earliest transgression into the Siljan district; this brachiopod is restricted to the Upper Cambrian within Baltoscandia (Popov & Holmer, unpublished). In the Kårgårde section Arenig rocks rest directly on Precambrian basement. In 1947 V. Jaanusson and H. Mutvei excavated a continuous section from the Lanna Limestone up to the lower Furudal Limestone, and in 1976 a section was prepared from the basement to the top of the Dalby Limestone along the course of the previous excavation. This section is now preserved as a Nature Reserve (Fig. 5).

The dip of the exposed beds in the Kårgårde area is close to vertical (Fig. 5). The Viru sequence, from the Segerstad Limestone to the lowermost Dalby Limestone, was de-

scribed in detail by Jaanusson & Mutvei (1953) and Jaanusson (1963). A brief description of the entire section was made by Lars Karis (*in Jaanusson 1982b*), but the new exposure has never been studied in detail. Bergström (1971) established the North Atlantic conodont zone of *Pygodus serra*, and its subzones (mid Skärilöv Limestone to mid Furudal Limestone; Fig. 1), for which the Kårgårde section is the type locality. Sturesson (1988a) studied the occurrence of ferruginous ooids in the Lower Ordovician sequence at Kårgårde.

A short description of the Middle Ordovician beds is given below in ascending stratigraphical order. Exposures in the Furudal and lowermost Dalby limestones in the western part of the Kårgårde area are separated from the main section by a major fault (Fig. 5), and were not studied for this paper.

Deep red, thick-bedded limestones dominate the lowermost Viru Segerstad Limestone (0–3.0 m; Fig. 9A). In the Kårgårde section the formation is 3.0 m thick. It can be divided into two subdivisions; the Kårgårde and Vikarby limestones (Jaanusson 1963).

The Kårgårde Limestone is composed mainly of reddish, thick-bedded to finely nodular calcilutites (Figs. 6A–B, 9A);

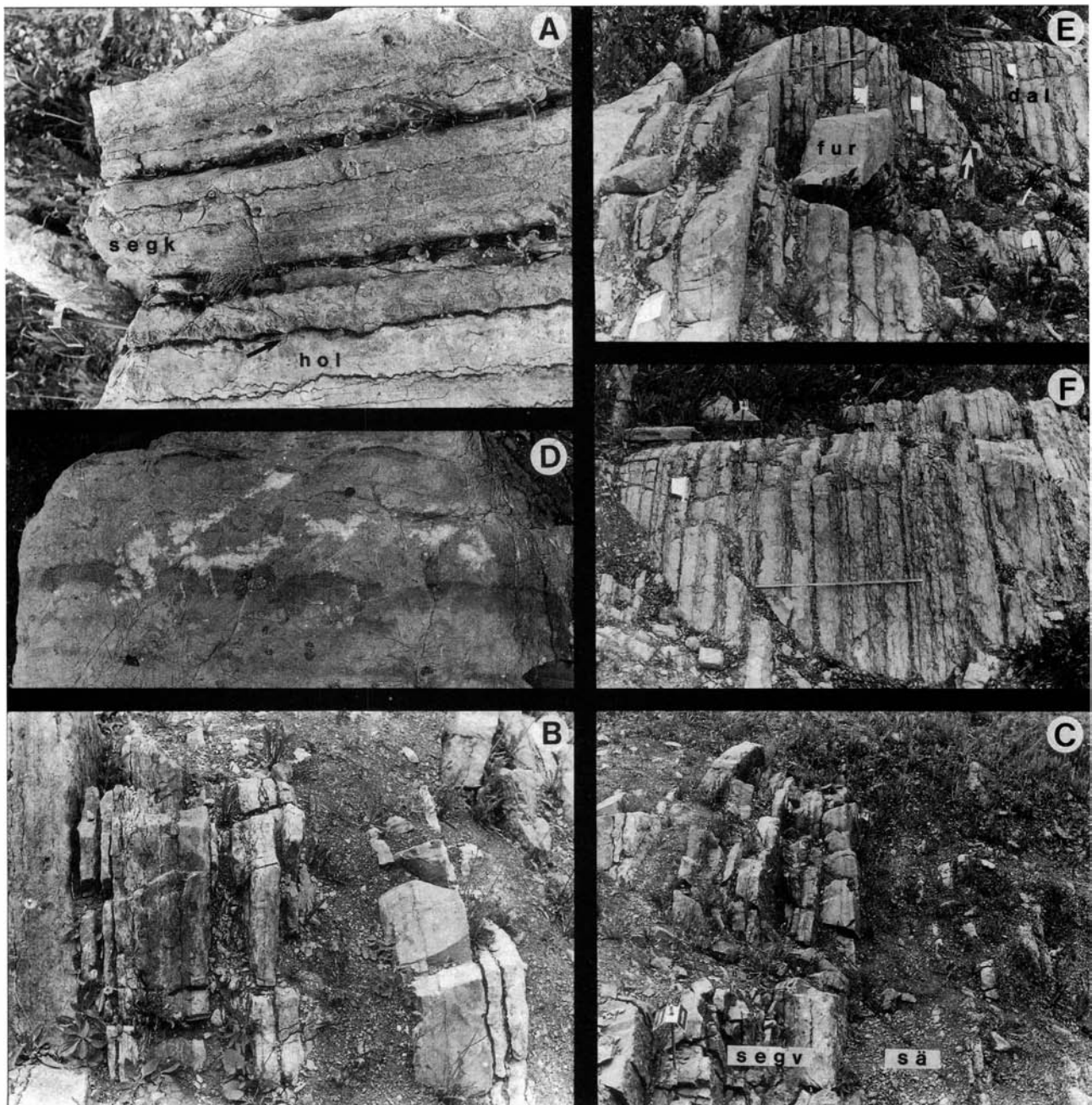


Fig. 6. Kårgärde section, Dalarna. □A. Bedded limestones in the uppermost Holen (hol) and lowermost Kårgärde limestones (segk); the Lower–Middle Ordovician boundary is indicated by an arrow. □B. The middle part of the Kårgärde Limestone, showing the alternation between bedded and finely nodular limestone. □C. The contact between the bedded Vikarby Limestone (segv) and the finely nodular Skärlov Limestone (sä). □D. Upper Seby Limestone (the interval 7.2–7.3 m in Fig. 9A), showing stromatolite-like domes. □E. The contact between the Furudal (fur) and Dalby (dal) limestones; the approximate level of the boundary is indicated by an arrow. □F. Typical bedding in the lower Dalby Limestone.

for further details see Jaanusson & Mutvei (1953). At Kårgärde, which is the type locality of the member, the lowermost beds have stromatolite-like structures which are almost identical to those higher up in the Vikarby and Seby limestones (Fig. 9A). In the Vikarby section (situated some 30 km south-east of Kårgärde) the stromatolitic bed at the base of the Kårgärde Limestone is 6 cm thick (Jaanusson 1982b; Fig. 7C).

The Vikarby Limestone is 50 cm thick and consists of mottled red and grey calcarenites (Fig. 6C). In the middle

part (at 2.8 m; Fig. 9A) there is a bed with stromatolite-like structures (Fig. 7B).

The Skärlov Limestone (3.0–6.3 m above the base of the Segerstad Limestone; Fig. 9A) is 3.3 m thick, and consists of a uniform sequence of red to grey, finely nodular calcilutites with partings of calcareous mudstone (Fig. 6C). The level of the boundary between the Aserian and Lasnamägian stages is situated within the lower part of the formation, but the exact position cannot be determined at present (Jaanusson 1963).

The Seby Limestone (6.3–7.9 m above the base of the Segerstad Limestone; Fig. 9A) is 1.6 m thick. In the lower half it is composed of thick-bedded limestones, whereas the upper part is dominated by mottled red and grey, finely nodular calcilutites (Fig. 9A). The uppermost bed of the formation includes a conspicuous level with finely laminated, haematite-rich, stromatolite-like domes (Fig. 7A) of the LLH-C type (closely-linked, lateral-linked hemispheroid type of Logan *et al.* 1964). There are two additional stromatolitic levels of the same type, lower down in the Seby Limestone (Figs. 6D, 9A). The stromatolite-like domes are up to about 6 cm in diameter and 3 cm high. The lamination is accentuated by alternating haematite-rich and haematite-poor laminae. Previously, similar structures were described from the Lunne Limestone of the autochthonous sequence in Jämtland (Larsson 1973). However, the algal origin of these structures was questioned by Lindström (1979, 1984) and Lindström *et al.* (1983). Closely similar stromatolite-like structures have also been reported from roughly coeval beds in northeastern Poland (Szymanski 1985).

The Folkeslunda Limestone (7.9–10.5 m above the base of the Segerstad Limestone; Fig. 9A) is 2.6 m thick. The lower boundary of the Folkeslunda Limestone is situated below a bed of grey calcarenite, 15 cm thick (Fig. 9A). The lower 1 m is dominated by grey, thin-bedded calcarenitic to calcilutitic limestone with intercalations of calcareous mudstone. Above there is a 1.6 m thick interval with grey, thick-bedded calcarenites (Fig. 9A).

The Furudal Limestone (10.5–19 m above the base of the Segerstad Limestone; Fig. 9A–B) is 8.5 m thick (9.2 m according to L. Karis *in* Jaanusson 1982b) and is composed mainly of uniform, grey, thin- to thick-bedded calcilutites, alternating with thin beds of calcareous mudstone (Figs. 6E, 9A–B).

The Dalby Limestone (19.0–38.8 m from the base of the Segerstad Limestone; Fig. 9B–C) is 19.8 m thick (18.1 m according to L. Karis, *in* Jaanusson 1982b). The detailed position of the lower boundary has not been determined in the locality (Fig. 6E); lithologically it is not marked clearly, and exact correlation with the type locality of the Furudal and Dalby limestones, at the main Fjäckå section, has not yet been made. The boundary is placed tentatively for this study, roughly a metre below the level suggested by L. Karis (*in* Jaanusson 1982b), based on the appearance of *Ephippelasma minutum*. The formation consists mainly of grey, bedded to nodular limestone with some intercalations of calcareous mudstone (Fig. 6E–F). According to L. Karis (*in* Jaanusson 1982b), a change from calcilutitic to calcarenitic

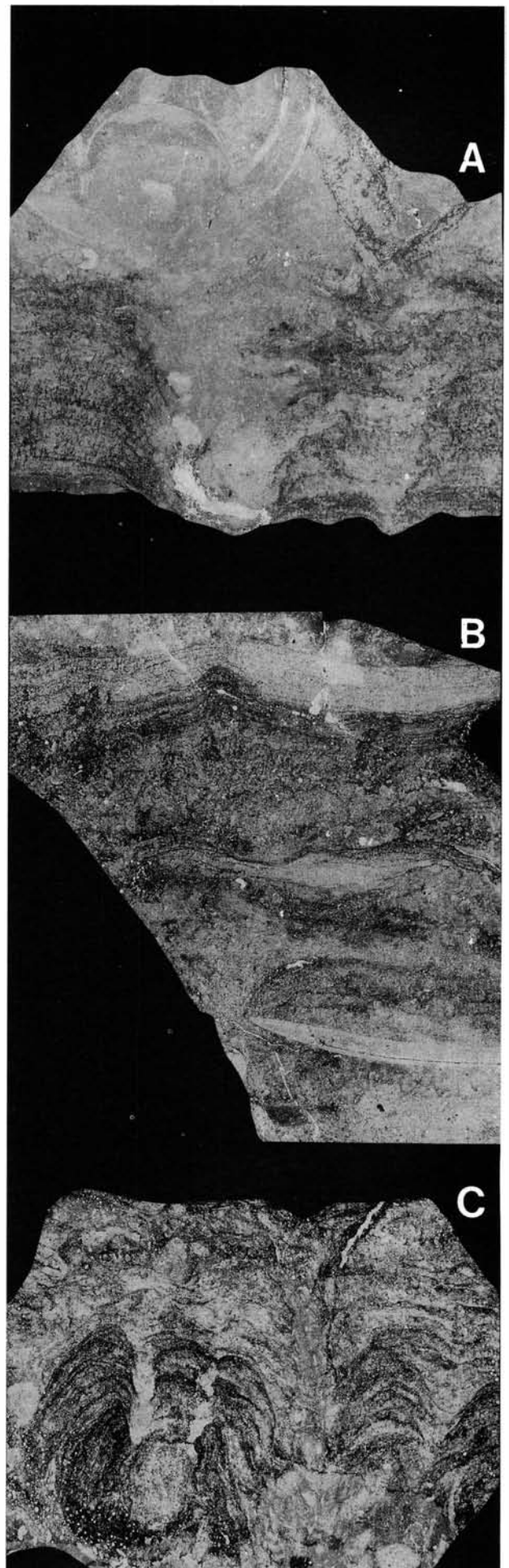


Fig. 7. □A. Stromatolite-like structures in the upper Seby Limestone (sample DLK83-se-5), Kårgårde section; Peel; SGU (Swedish Geological Survey, Uppsala) Rock Original 96; $\times 1.5$. □B. Stromatolite-like structures in the Vikarby Limestone (sample DLK83-segv-2), Kårgårde section; Peel; SGU Rock Original 97; $\times 1.0$. □C. Stromatolite-like structures in the lowermost bed of the Kårgårde Limestone (taken from sample D-179, level indicated *in* Jaanusson & Mutvei 1953, Fig. 5), Vikarby section; Peel; SGU Rock Original 98; $\times 1.0$.

limestone takes place 1.5 m above the lower boundary of the formation. The upper boundary of the unit is marked by a bed of bentonitic clay, 15 cm thick (Fig. 9C). Three additional, thinner bentonitic beds occur within the uppermost metre of the formation.

Fjäckå section

This is a classic locality, cut into the bedrock by the Fjäckå stream at Moldå in Dalby village, parish of Ore, in the northeastern part of the Siljan district, Dalarna (Fig. 5). It has been reported scientifically since its first mention by Törnquist (1867), mostly as scattered exposures but including a small, now abandoned quarry. Excavations in 1945–1946 exposed a complete section ('the main section') from the upper Furudal Limestone to the Jonstorp Formation (Jaanusson & Martna 1948). In 1976 the area was prepared (and further excavated) for preservation of the section as a Nature Reserve (see also Jaanusson 1982b).

Only the lower portion of the main section at Fjäckå is covered by this study, including the uppermost 2 m of the Furudal Limestone and the entire Dalby Limestone. The Fjäckå section is the type locality for both units. The samples used for this paper were collected by Stig M. Bergström in 1959 and 1960 (sample series D59 and D60 in Fig. 10). The conodont zonation based on the material from these samples was summarized by Bergström (1971), who designated Fjäckå as the type locality for three North Atlantic conodont zones (*Pygodus anserinus*, *Amorphognathus tvaerensis*, and *Amorphognathus superbis*; Fig. 1). The palaeoecology of ostracodes from the same series of samples was studied by Jaanusson (1963, 1976), and the chitinozoans by Laufeld (1967).

Two subdivisions of the Dalby Limestone were distinguished by Jaanusson (1982b). The lower member consists of 6.6 m of grey, thick-bedded limestones that are calcarenitic in the upper, and calcilutitic in the lower part (Fig. 10). The lower boundary of the formation is drawn at the level of a conspicuous faunal change (Jaanusson 1963, 1976, 1982b). The upper member is 13.3 m thick, consisting of grey, bedded to slightly nodular calcarenitic argillaceous calcilutites and calcarenites. Close to the lower boundary of the upper member, there is a thin bentonitic bed (Fig. 10).

As elsewhere in Sweden there is a complex of bentonitic beds in the uppermost portion of the Dalby Limestone. At Fjäckå seven such beds can be distinguished (Jaanusson & Martna 1948), the upper of which is 26 cm thick (Fig. 10). The lower thin bentonitic bed, 1.8 m from the top of the formation, is used as a reference level for measurements (Jaanusson 1963).

This monograph is a contribution to the (informal) Project Fjäckå, initiated by Valdar Jaanusson in 1945. Previous contributions include Jaanusson & Martna (1948), Martna (1955), Jaanusson (1963, 1976, 1982b), Laufeld (1967), and Bergström (1971).

Biostratigraphy and palaeoecology

Distribution, abundance and lithofacies

It is assumed commonly that changes in bio- and lithofacies are controlled mainly by changes in water depth. For example, the change from coarse-grained to fine-grained sediments, and a related change in the benthic faunas, is usually thought to be due mainly to an increase in the depth. The concept of depth related, so-called Benthic Assemblages (in the sense of Boucot 1975, pp. 21–24) is well known; Swedish upper Viru and Harju assemblages of brachiopods were classified with reference to such Benthic Assemblages by Sheehan (1979). However, this model appears to be too simplistic to explain the distribution of litho- and biofacies in the Ordovician of Baltoscandia (Jaanusson 1973, 1976).

An alternative to the concept of depth-related Benthic Assemblages was proposed by Jaanusson (1984); he suggested that changes in Ordovician benthic associations (including phosphatic inarticulate brachiopods) along environmental gradients (e.g., from graptolitic shale to coarse grained sediments) were more substrate-dependent than depth-related (although, of course, depth remains one of the parameters).

The distribution of bio- and lithofacies within Baltoscandia is related to the presence of so-called confacies belts – a term which was introduced by Jaanusson (1976; see also Männil 1966; Jaanusson 1973; Jaanusson & Bergström 1980) to describe the pattern of spatially stable ecological zones defined by a combination of litho- and biofacial features. The environmental factors, controlling the distribution of such ecological zones are not known, but Jaanusson & Bergström (1980, p. 107) suggested that temperature, rather than depth, could have been one of the more important parameters.

As noted by Jaanusson (1982a) the depositional conditions in the central Baltoscandian confacies belt has been interpreted mainly in two widely different ways. Lindström (1963, 1972, 1979, 1984), Lindström & Vortisch (1983), and Lindström *et al.* (1983), suggested that the deposition, for most of the Ordovician Period, took place in a fairly deep sea, whereas other workers, notably Jaanusson (1973, 1982a) and Larsson (1973), have presented evidence for more shallow water with possible intervals of emergence (for a summary and review, see, e.g., Jaanusson 1982a, and Lindström 1984).

The distribution and composition of associations of Palaeozoic phosphatic inarticulate brachiopods and their relationship to lithofacies and depth are poorly known; Rowell & Brady (1976), Rowell & Krause (1973), and Krause & Rowell (1975) have provided the only detailed studies on the subject. Rowell & Brady (1976) studied the distribution of inarticulate brachiopods in the Upper Cambrian of the Great Basin (Utah and Nevada), where inarticulates are comparatively abundant in rocks representing outer and inner shelf environments, whereas they are rare, or completely missing, in the shallow carbonate shoal and lagoonal facies. Krause (1972), Rowell & Krause (1973),

and Krause & Rowell (1975) investigated the composition of the fauna, and the distribution of species, relative to the lower Whiterock stromatactis-bearing carbonate mound at Meiklejohn Peak in Nevada (Ross *et al.* 1975).

Because of the limited number of sequences that have been investigated to date, it is difficult to analyze the distribution of assemblages and species of phosphatic inarticulate brachiopods in relation to lithofacies and confacies belts. The three sections under consideration here are all within the central Baltoscandian confacies belt (Jaanusson 1973, Text-fig. 7) and, as already mentioned, there are few previous studies from other parts of Baltoscandia.

A total of more than 35,000 specimens of phosphatic inarticulate brachiopods were identified, and the vertical distributions of various species in the three sections are recorded in faunal logs (Figs. 8, 9, 10). The quantitative composition of the inarticulates in each sample yielding 20 specimens or more is presented in diagrams of relative abundance (Figs. 11, 12). Only species that form 20% or more of the total number of inarticulates in at least one sample are shown; the rest are grouped as 'others'. In the counts each separate dorsal and ventral valve or complete shell was counted as one specimen. Fragmented valves were counted only in the cases where more than half of the larval shell was preserved; no lower size limit was applied.

Only the faunas isolated from Gullhøgen quarry and the Kårgårde section were investigated quantitatively; data from Fjäckå were considered as unreliable, because the insoluble residues had been separated with heavy liquids, and only the 'heavy' fractions were picked completely for inarticulates.

Kundan Stage

The red bedded limestones of the Lower Ordovician Holen Limestone of Dalarna and Västergötland represent part of a widespread litho- and biofacies, which in the central

Baltoscandian confacies belt of Sweden is referred to traditionally as the 'orthoceratite limestone' (ranging from the Hunnebergian to the Lasnamägian; see also Löfgren 1978, pp. 5-7). The dominant sediment in the Kundan Stage in this region seems to have been carbonate mud mixed with skeletal sand (Jaanusson 1973, Fig. 2; Männil 1966, Fig. 53). In the central confacies belt of Sweden, the depositional conditions in the Kundan Stage appear to have been comparatively stable, and no major breaks are known.

This lithofacies contains rich and well preserved assemblages of phosphatic inarticulate brachiopods that are uniform in composition but have not yet been studied in detail. For the present study, only two samples were included, one from the uppermost portion of the formation at Gullhøgen (sample GB81-0), and the other from the Kårgårde section (sample DLK84-hol-25). These beds yielded 52-92 mostly well preserved specimens per 100 g (Figs. 11A, 12A). In the Holen Limestone at both localities, *Numericoma? spinosa* is the dominant species, forming up to 92% of the assemblages (Figs. 11A, 12A). *Hisingerella? unguicula* and *Scaphelasma* sp. nov. a are also present at both localities (Figs. 8A, 9A), whereas *Conotreta? mica* was recorded only at Gullhøgen (Fig. 8A). *Myotreta* aff. *crassa* is known from Kårgårde (Fig. 9A), and questionably from the Holen Limestone in Jämtland.

Aserian Stage

In the central confacies belt, depositional conditions appear to have been changed at the transition to the Middle Ordovician. In Dalarna, Jämtland, and on Öland, the Segerstad Limestone contains structures interpreted by some as possible desiccation cracks and stromatolites (Jaanusson 1960, 1973, 1982b; Jaanusson & Mutvei 1982; Larsson 1973), but by others as possible diagenetic phenomena (Lindström 1979, 1984; Lindström *et al.* 1983). The Segerstad Limestone in Jämtland includes numerous discontinu-

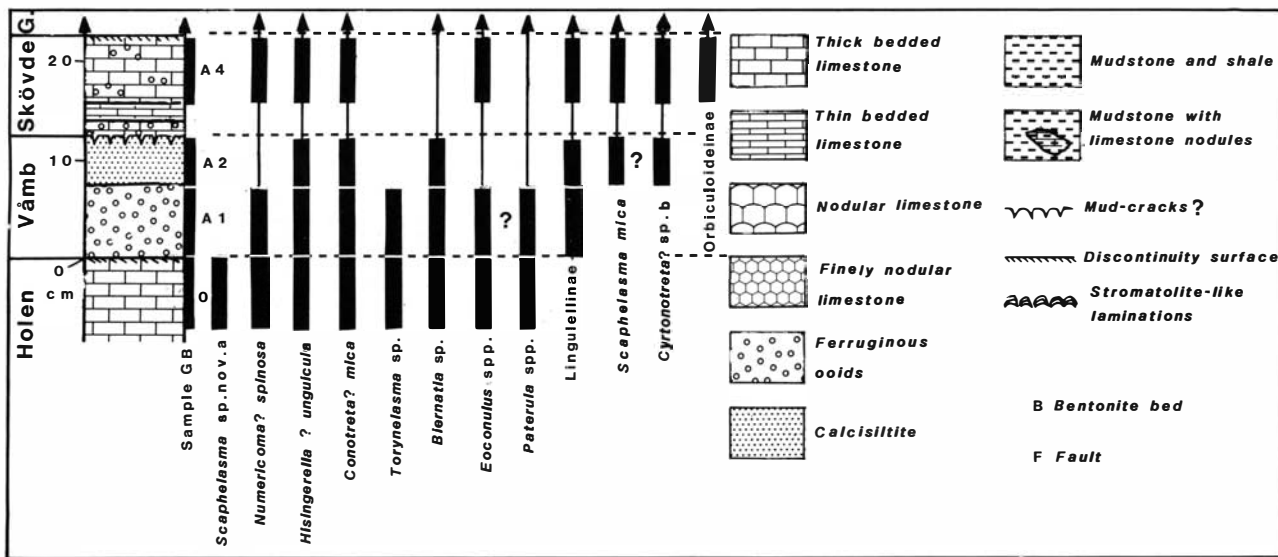


Fig. 8. Faunal logs from Gullhøgen quarry, showing distribution of phosphatic inarticulates. □A (this page). Section A, situated some five meters south of section 1 in Fig. 2. □B (p. 14). Sections 1-2 (see Fig. 2). □C (p. 15). Sections 2-4 (see Fig. 2). □D (p. 16). Sections 4-5 (see Fig. 2). V, Våmb Limestone; S, Skövde beds; G, Gullhøgen Formation; R, Ryd Limestone.

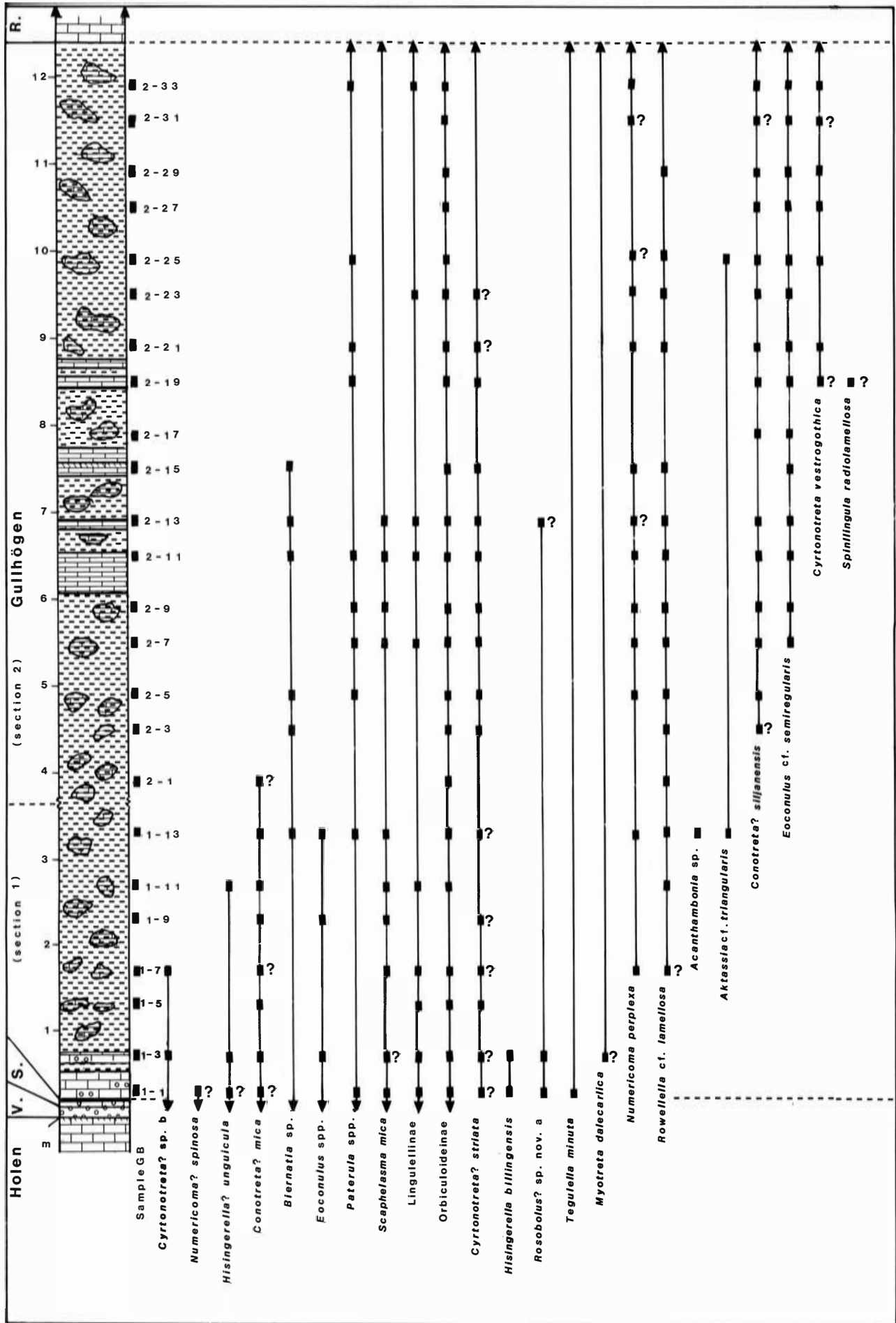


Fig. 8B (caption on p. 13).

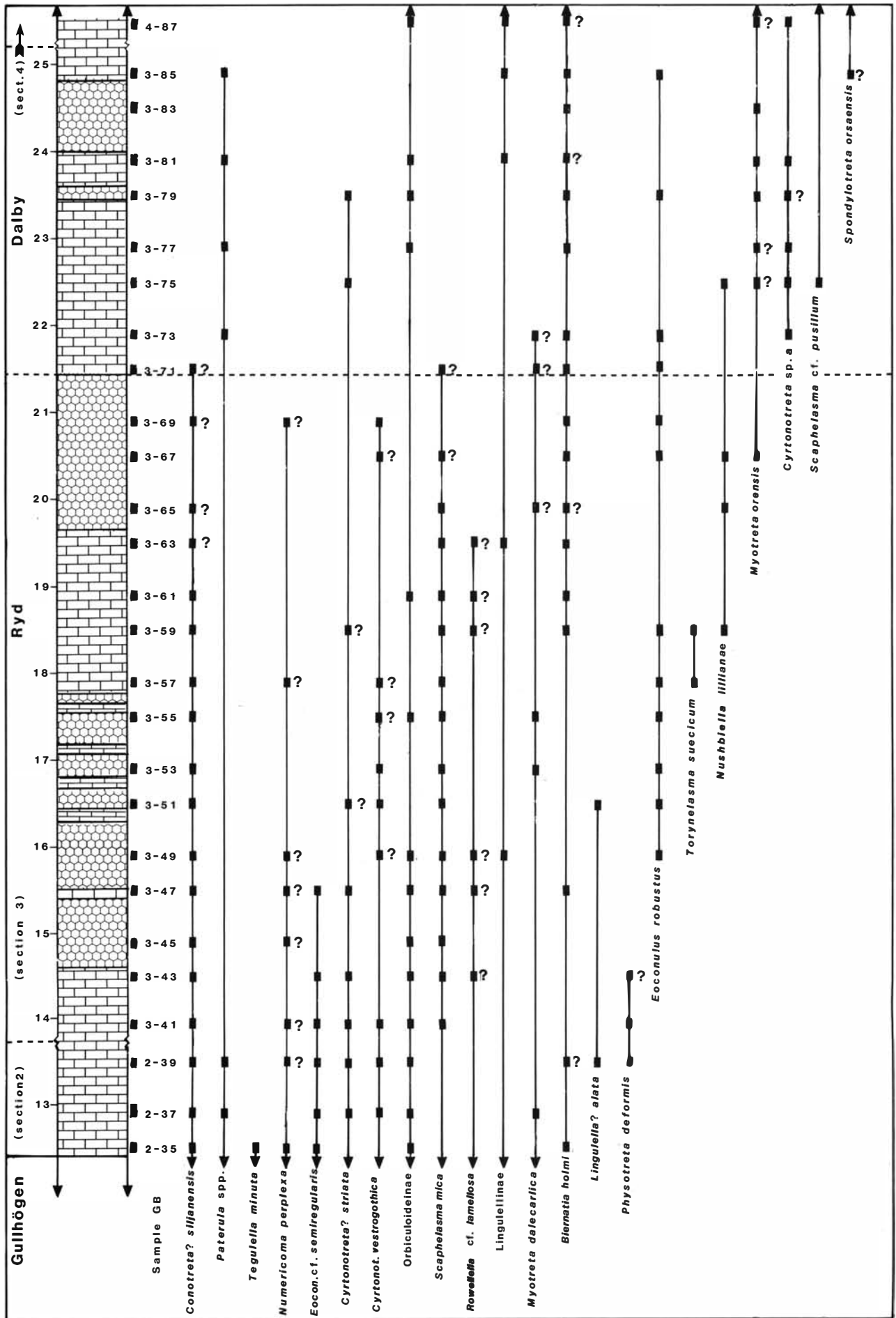


Fig. 8C (caption on p. 13).

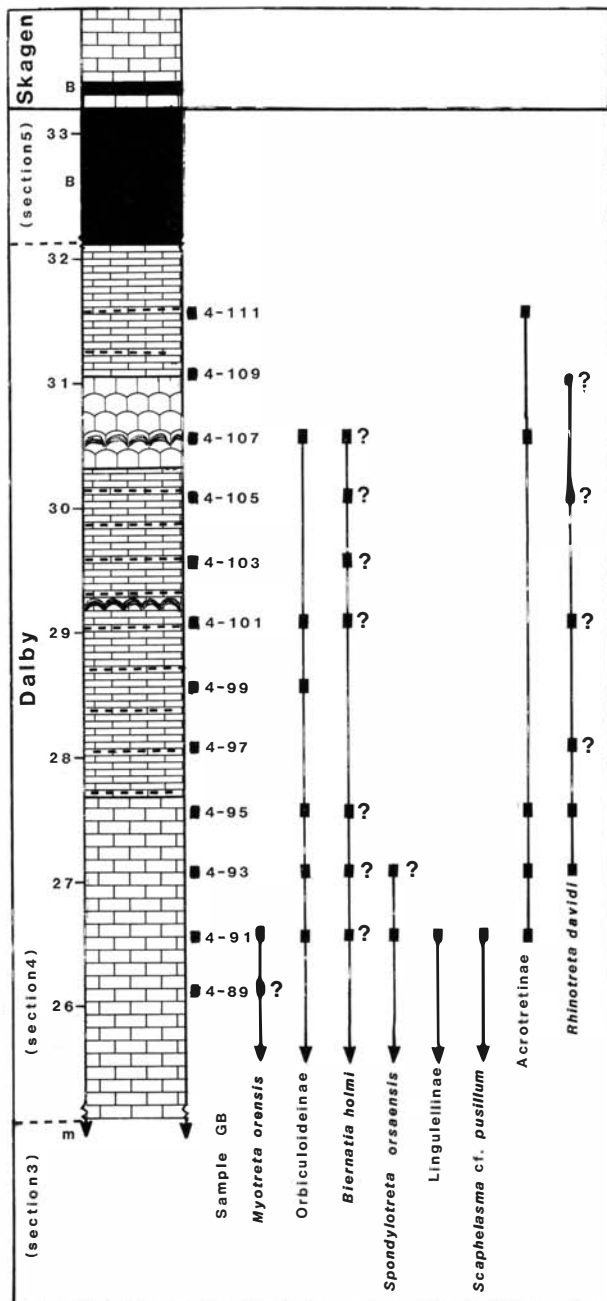


Fig. 8D (caption on p. 13).

ity surfaces as well as an intraformational conglomerate (Larsson 1973). Moreover, in Västergötland there are major breaks, marked by discontinuity surfaces, comprising most of the Aserian Stage. The thin, condensed sequence contains levels with possible desiccation cracks and stromatolite-like laminations (Jaanusson 1964, 1982c; Holmer 1983).

The boundary between the Oeland and Viru Series is associated with a marked turnover in the benthic faunas (Männil 1966; Jaanusson 1960, 1976, 1982b), and numerous new taxa of phosphatic inarticulate brachiopods appear. At Kårgårde *Scaphelasma mica*, *Myotreta dalecarlica*, *Numericoma simplex*, *Spondylotreta* sp. nov. a, *Lingulella? alata?*, *Scaphelasma? rugosum*, *Physotreta deformis?*, and *Acanthambonia delicata* all appear at the base of the of the Viru

(Fig. 9A). The Kårgårde Limestone is rich in phosphatic inarticulates, with a maximum abundance of 109 specimens per 100 g (on average 25 per 100 g; Fig. 12A). Each sample yielded, on average, eight species. The preservation in these beds is generally poor and the specimens are almost invariably abraded and fragmented.

In the Kårgårde Limestone the assemblages are dominated by the following five species (with maximum abundance given in brackets): *Conotreta? mica* (83% in sample DLK83-segk-5), *Scaphelasma? rugosum* (60% in sample DLK83-segk-7), *Numericoma simplex* (52% in sample DLK83-segk-6), *Myotreta dalecarlica* (38% in sample DLK83-segk-10), and *Hisingerella? unguicula* (42% in sample DLK83-segk-1; Fig. 12A).

Closely related assemblages are known from the Segerstad Limestone on Öland and in Jämtland. In Sweden *Scaphelasma? rugosum*, *Eoconulus* cf. *cryptomyus* and *Eoconulus* sp. nov. a, have so far been recorded only from the Segerstad Limestone. In Dalarna and on Öland *Numericoma? spinosa* is absent from the Segerstad Limestone, whilst there is a questionable occurrence from Jämtland.

A similar fauna that includes *Conotreta? mica* and *Scaphelasma? rugosum* is present in the Segerstad Limestone in southern Estonia ('Livonian Tongue', Jaanusson 1976, Text-fig. 7; see also Männil 1966, Fig. 54), and in the Pskov district, Russia (Goryanskij 1969).

At Kårgårde there is a marked decrease in the frequency of inarticulates in the upper member of the Segerstad Limestone. The Vikarby Limestone consists mainly of calcarenites and yielded up to 10 poorly preserved specimens per 100 g (Fig. 12A). However, it should be noted that from the Vikarby section (some 30 km south-east of Kårgårde) a frequency of 40 specimens per 100 g has been reported (Jaanusson 1984, Fig. 7). *Myotreta dalecarlica* has a frequency of up to 36% (sample DLK83-segv-1), and dominates the fauna together with *Conotreta? mica* (up to 27% in sample DLK83-segv-1; Fig. 12A). *Rowellevella* cf. *lamellosa* appears at the base of the Vikarby Limestone, whilst the top of the formation coincides with the disappearance of *Eoconulus* sp. nov. a (Fig. 9A).

The transition from the bedded limestones of the Segerstad Limestone to the more argillaceous and finely nodular calcilitites of the Skårlöv Limestone is associated with the appearance of *Eoconulus* cf. *clivus* and *Expellobolus? sp. nov. a* (Fig. 9A); the former constitutes 18–61% of the fauna in the lower to middle part of the formation (samples DLK83-så-1–6; Fig. 12A). *Expellobolus? sp. nov. a* is restricted to the Skårlöv Limestone (Fig. 9A). The frequency (in specimens per 100 g) of inarticulates varies from 6 in the lower part to 77 in the upper part of the formation (Fig. 12A).

Numericoma? spinosa reappears abruptly in the middle Skårlöv Limestone (66% in sample DLK83-så-4; Fig. 12A). The uppermost two samples of the Skårlöv Limestone are dominated by *Numericoma simplex* (67% in sample DLK83-så-7) and *Conotreta? mica* (70% in sample DLK83-så-8; Fig. 12A).

At Gullhöggen most of the Aserian Stage is missing at the level of the basal Viru discontinuity surface; the Våmb Limestone is approximately equivalent to the uppermost

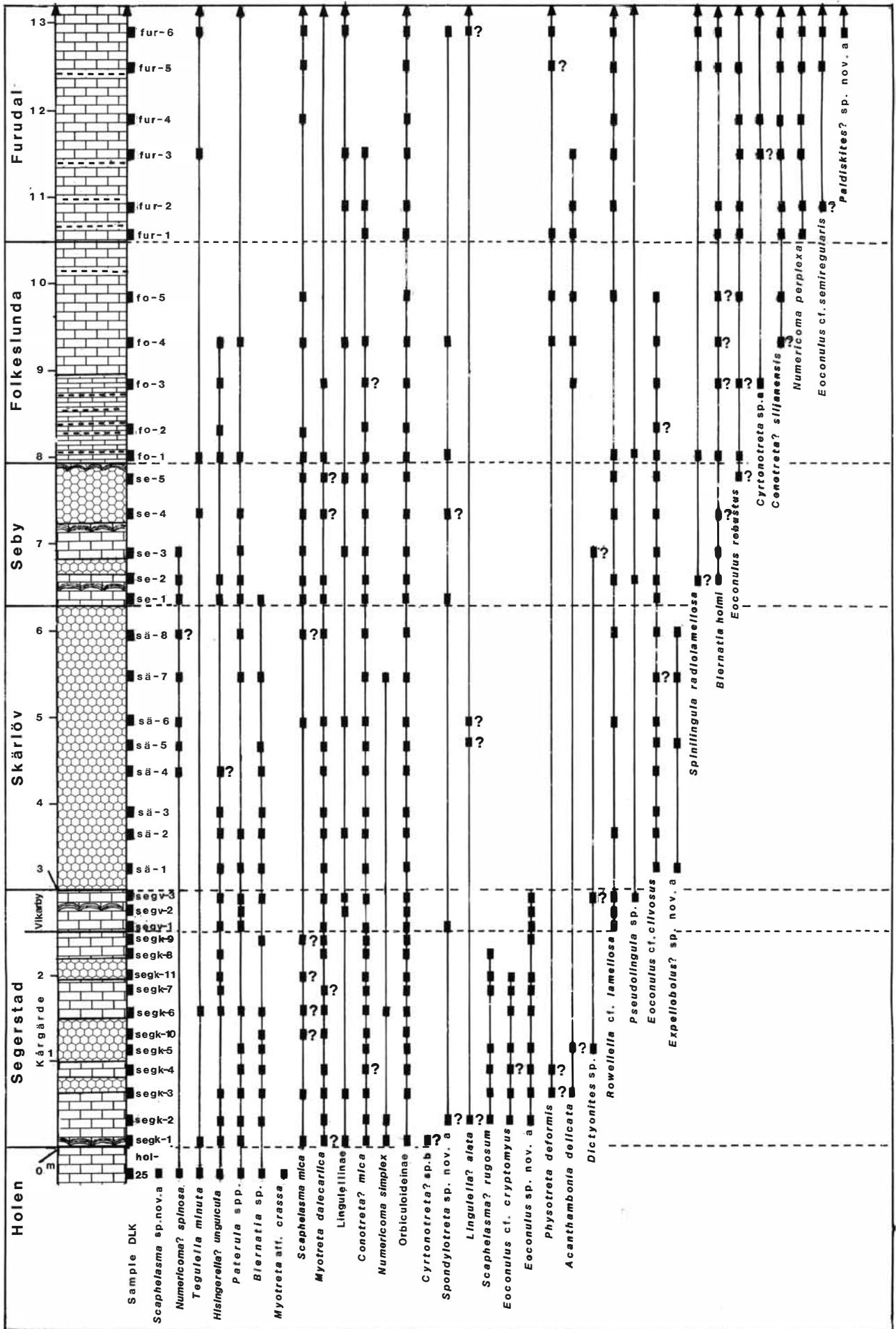


Fig. 9. □A-C (pp. 17-19). Faunal logs from Kårgårde, showing distribution of phosphatic inarticulates (for legend see Fig. 8A).

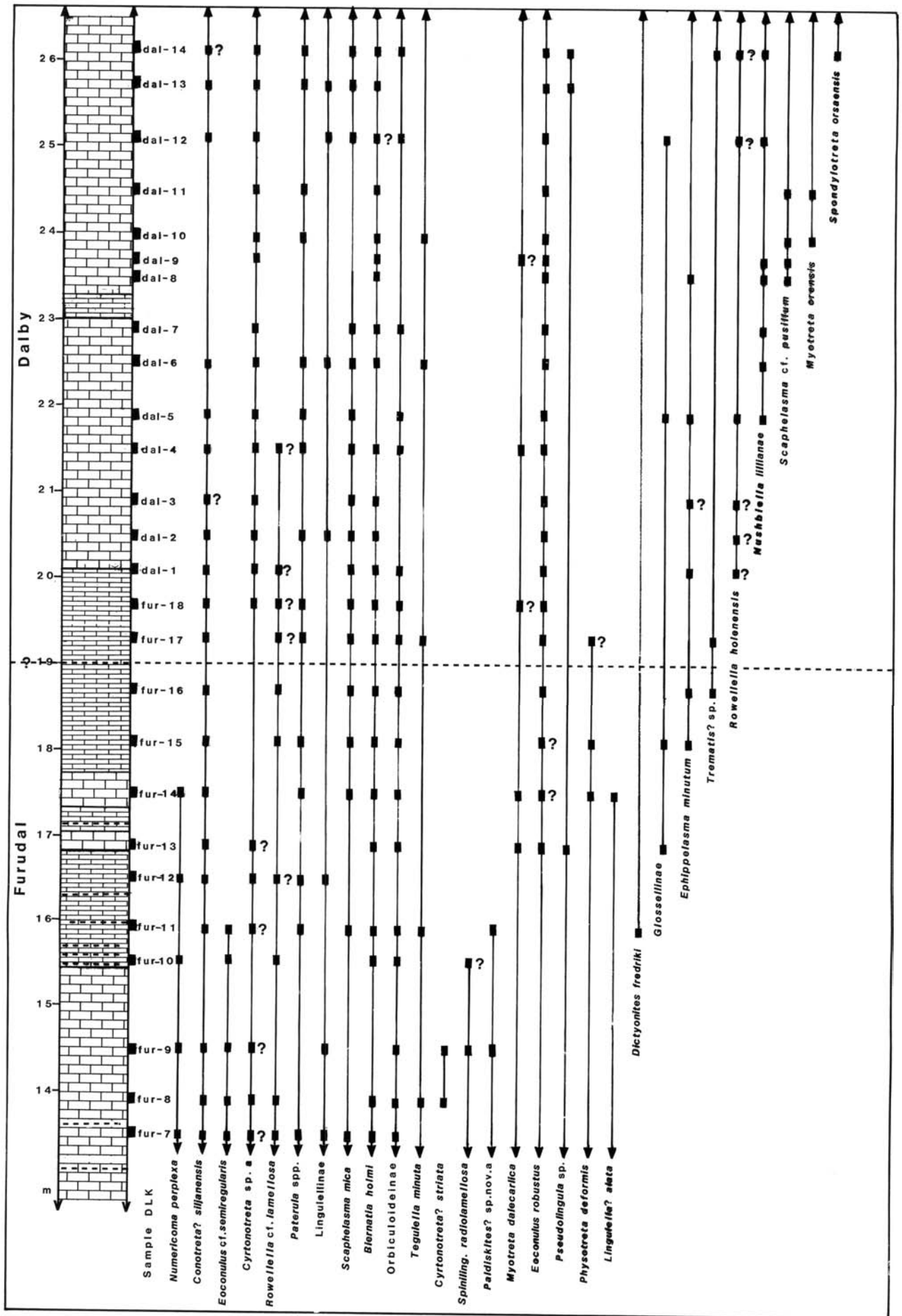


Fig. 9B (caption on p. 15).

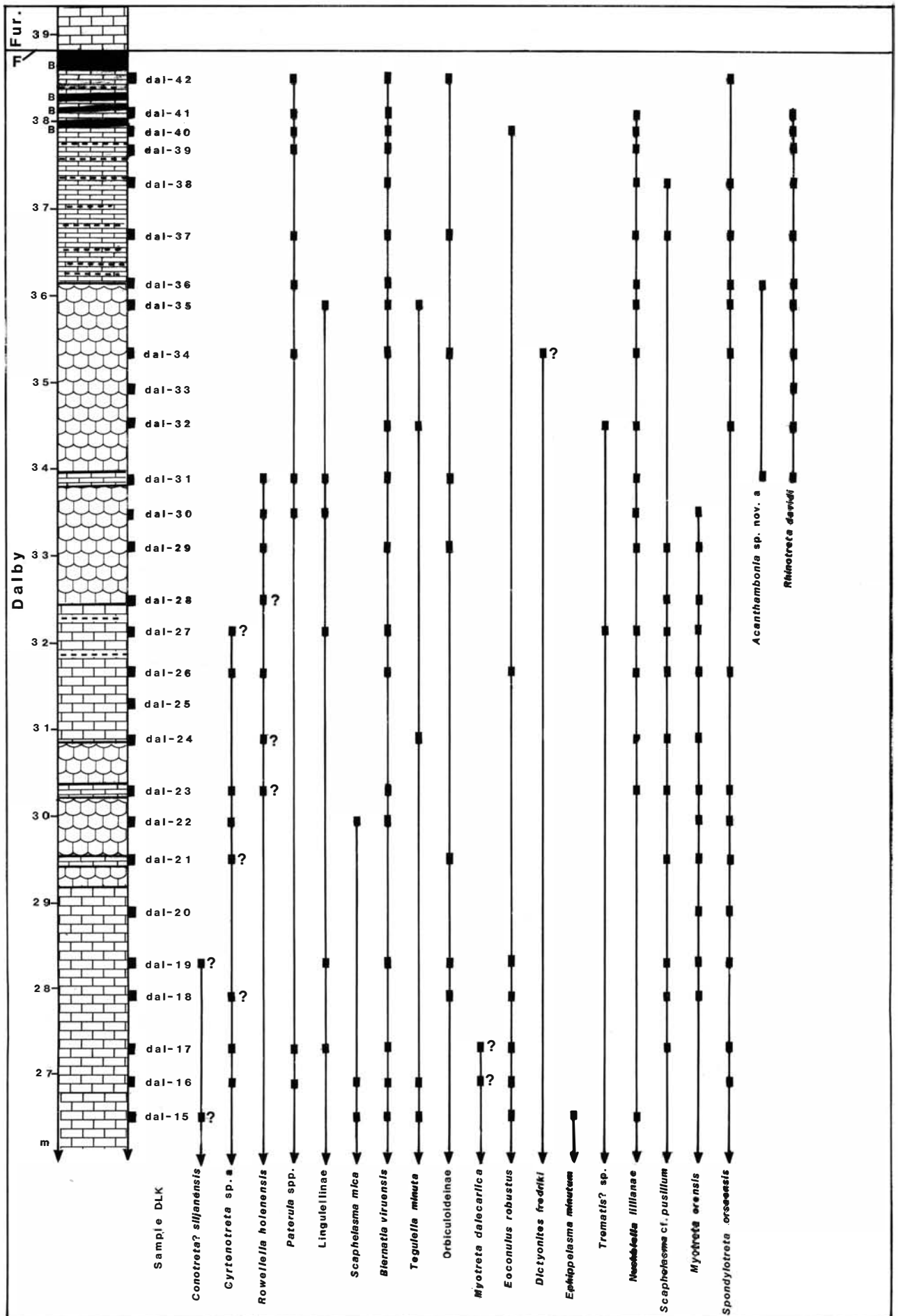


Fig. 9C (caption on p. 15).

part of the Skärlov Limestone (Fig. 1; see also Jaanusson 1982b). The oolitic beds (sample GB84-A1) in the lower half of the Våmb Limestone yielded 113 poorly preserved specimens per 100 g (Fig. 11A); *Numericoma? spinosa* is the dominant species, having a frequency of 71% (Fig. 11A). There is a tenfold decrease in the frequency of inarticulate specimens in the upper calcisiltite lithology of the formation (sample GB84-A2, which includes the desiccation cracks described by Holmer 1983); in this part, *Conotreta? mica* has a frequency of 89% (Fig. 11A).

Lasnamägian Stage

At Gullhögen most of the Lasnamägian Stage is missing at the level of the upper discontinuity surface in the Våmb Limestone (Fig. 1). In the Kårgårde section the Aserian-Lasnamägian boundary is situated somewhere in the middle of the Skärlov Limestone, but there is no conspicuous faunal change marking the level (Fig. 1; see also Jaanusson 1963).

The major part of the Lasnamägian Stage consists of red and grey calcarenites belonging to the Seby and Folkeslunda limestones, which represent the uppermost two units of the 'orthoceratite limestone'. At Kårgårde both units yielded up to 30 specimens per 100 g (Fig. 12A), whereas a much lower frequency was reported from the Seby and Folkeslunda limestones in the Vikarby section (Jaanusson 1984, Fig. 7). In the lower Seby Limestone *Numericoma? spinosa* disappears. *Hisingerella? unguicula* and *Eoconulus cf. clivosus* have their last occurrences within the Folkeslunda Limestone (Fig. 9A); a new assemblage, including *Spinilingula radiolamellosa*, *Biernatia holmi*, *Eoconulus robustus*, and *Conotreta? siljanensis*, appears within the Seby-Folkeslunda interval (Fig. 9A). However, *Conotreta? mica* is still the dominant faunal element, forming 19–47% of the assemblages both in the Seby (samples DLK83-se-1–5) and Folkeslunda limestones (samples DLK83-fo-1, 2, 4), whilst *Scaphelasma mica* (46% and 57% in samples DLK83-se-5 and fo-2), and *Myotreta dalecarlica* (31% in sample DLK83-se-1) are only occasionally dominant (Fig. 12A).

At Gullhögen the argillaceous Skövde beds are possibly equivalent to the uppermost Lasnamägian Folkeslunda Limestone (Fig. 1); the fauna of phosphatic inarticulate brachiopods is poorly preserved, yielding 62 specimens per 100 g, of which 67% belong to *Conotreta? mica* (sample GB84-A4; Fig. 11A). Both the Våmb Limestone and Skövde beds appear to represent condensed sequences, and possibly the phosphatic shells have been redeposited and mixed; the specimens are generally strongly worn and fragmentary.

Uhakuan Stage

Jaanusson (1982b, p. 21) noted that the transition to the Uhakuan sequence marks the beginning of a period of more stable depositional conditions within the central Baltoscandian confacies belt, possibly due to increased water depth. The assemblages of phosphatic inarticulate brachiopods from Uhakuan sequences in Västergötland and Dalarna are the richest and best preserved of all those considered in this monograph. In Dalarna the Uhakuan Stage is

represented by bedded calcilutites of the Furudal Limestone, yielding on average 33 specimens per 100 g (Fig. 12A–B); a maximum of 14 species per sample (DLK83-fur-6) has been recorded from these beds. In Västergötland the Gullhögen Formation, which yielded on average 30 specimens per 100 g (Fig. 11A), is also calcilutitic, but has a much higher content of terrigenous clay; it probably represents a sedimentary wedge contiguous with the facies in the Oslo region (Jaanusson 1973, 1982b).

In both the Kårgårde section and at Gullhögen, the lower boundary of the Uhakuan Stage is associated with a conspicuous change in the fauna. At Kårgårde *Conotreta? mica* disappears in the lower part of the Furudal Limestone, and it is replaced already as a dominant species by *Conotreta? siljanensis* in the uppermost sample of the Folkeslunda Limestone (where it has an abundance of 40%; Fig. 12A). In the lower five samples in the Furudal Limestone (samples DLK83-fur-1–5), *Numericoma perplexa* is the dominant species and forms 28–40% of the assemblages (Fig. 12A–B).

Eoconulus cf. semiregularis also appears at the base of the Furudal Limestone; it becomes the dominant species in the middle part of the unit (samples DLK83-fur-6–11), forming 20–59% of the fauna (Fig. 12A–B). In the upper part of this formation (samples DLK83-fur-12–16), *Eoconulus cf. semiregularis* disappears and *Numericoma perplexa* again becomes the most common species, occasionally with a frequency of up to 87% (sample DLK83-fur-12), together with *Conotreta? siljanensis* (56% in sample DLK83-fur-13; Fig. 12B). In the Kårgårde section *Eoconulus cf. semiregularis*, *Numericoma perplexa* and *Paldiskites? sp. nov.* are restricted to the Furudal Limestone (Fig. 9A–B).

At Gullhögen the fauna of the lower Uhakuan Gullhögen Formation is similar to that of the Furudal Limestone (Fig. 8B), with *Conotreta? mica* initially present (55% in sample GB84-1-5), and then replaced by *Conotreta? siljanensis* (in sample GB84-2-3; Fig. 11A). As in the Furudal Limestone, *Numericoma perplexa* and *Eoconulus cf. semiregularis* are important constituents in the lower Uhakuan sequence, with the former dominant in six samples (GB84-1-13, 2-3, 5, 21, 23, 33; Fig. 11A), where it forms 41–71% of the assemblages. *Eoconulus cf. semiregularis* constitutes 27–62% of the faunas in seven samples (GB84-2-7, 13, 19–27), primarily in the upper Gullhögen Formation (Fig. 11A). *Scaphelasma mica* is locally abundant in the lower part of the formation (71% in sample GB84-1-7). Specimens of *Rowellia cf. lamellosa* are also comparatively numerous (23–28% in samples GB84-1-11, 2-7, 11, 13, 25, 29; Fig. 11A).

Hisingerella billingensis, *Rosobolus? sp. nov.* a, and *Cyrtotreta? striata* appear at the base of the Gullhögen Formation (Fig. 8B), with the first two restricted to the lower part of the formation. The rare species *Aktassia cf. triangularis* is also restricted to the Gullhögen Formation (Fig. 8B).

The upper part of the Uhakuan Stage at Gullhögen is represented by bedded calcilutites of the Ryd Limestone (yielding on average 20 specimens per 100 g; Fig. 11A–B); the unit is a wedge of the upper Furudal Limestone (Fig. 1). The boundary between the Gullhögen Formation and the Ryd Limestone is associated with the appearance of a new fauna, including *Biernatia holmi*, *Lingulella? alata*, *Phys-*

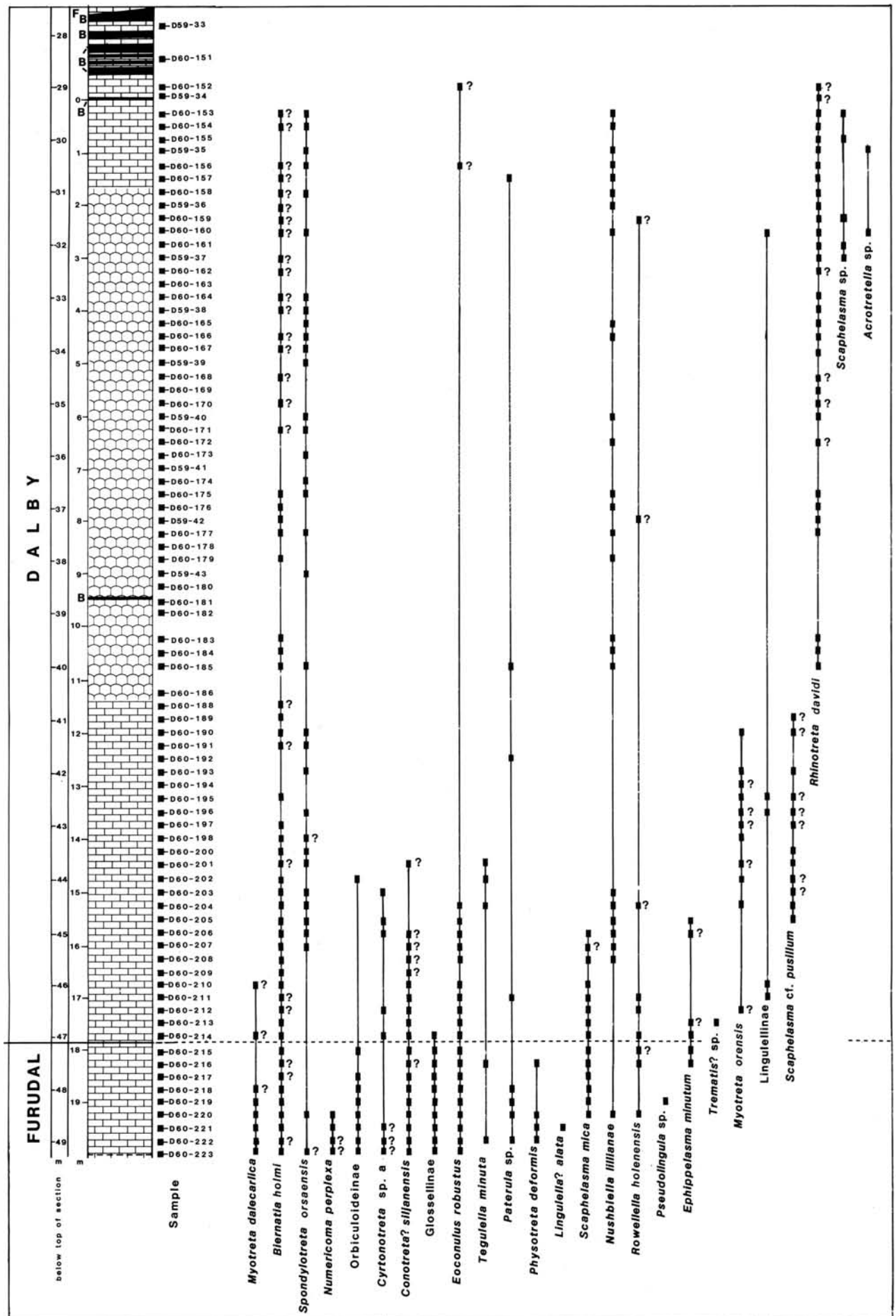


Fig. 10. Faunal log from the main section at Fjåcka, showing distribution of phosphatic inarticulates (for legend see Fig. 8A).



Fig. 11. □A-B (pp. 22–23). Relative frequencies of phosphatic inarticulates at Gullhøgen, Västergötland. To the left, frequency of specimens per 100 g limestone. The remaining columns show the relative frequencies of those species that form at least 10% of the total fauna in at least one sample. 'Others' include all taxa that constitute less than 10% in all samples. The total number of specimens is given in the column farthest to the right. H, Holen Limestone; Sk, Skövde beds. Figure prepared by Björn Lindsten (Stockholm).

otreta deformis, and Eoconulus robustus (Fig. 8C). In the Kår-gårde section these species are known already from the lower Furudal Limestone. The assemblages in the Ryd Limestone are dominated by Scaphelasma mica, forming up

to 81–85% of the assemblages (samples GB84-3-45, 65; Fig. 11A–B). In the lower part of the formation (samples GB84-2-37, 39), Cyrtotreta? striata occasionally forms 36–61% of the faunas, whereas Conotreta? siljanensis is abundant

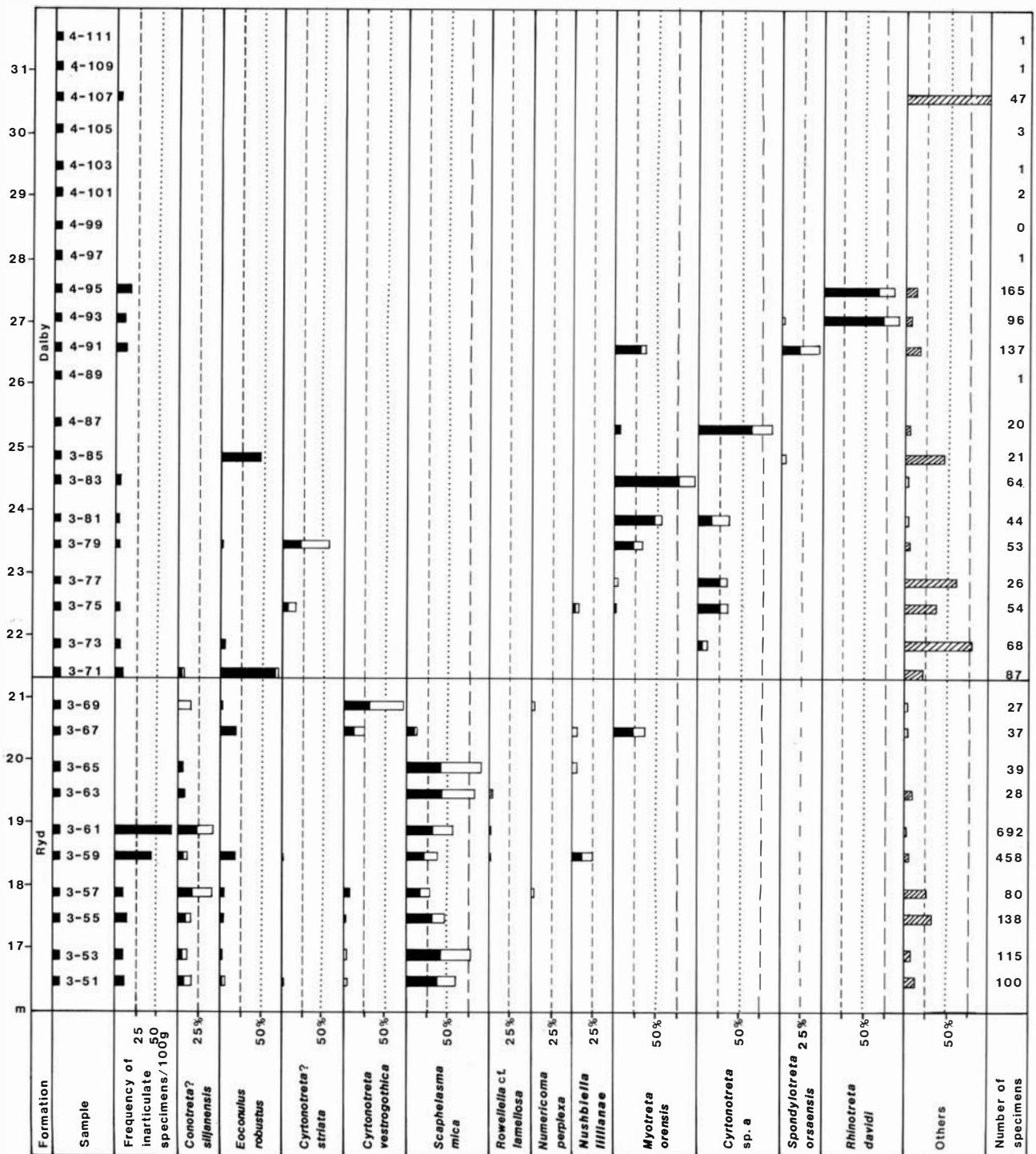


Fig. 11B.

throughout the Ryd Limestone (generally forming around 20% of the assemblages; Fig. 11A–B). *Torynelasma suecicum* is the only species at Gullhögen that is restricted to the unit (Fig. 8C).

A single sample (1 kg) from the type locality of the calcilitic lower Uhakuan Källa Limestone (Jaanusson 1960) on northern Öland (a wedge of the lower Furudal Limestone) yielded an assemblage ($N=123$) that includes (in order of descending frequency) *Eoconulus* cf. *semiregularis* (26%), *Conotreta? siljanensis* (24%), *Biernatia holmi*

(24%), *Scaphelasma mica* (8%), *Spinilingula radiolamellosa* (6%), *Tegulella minuta* (3%), *Numericoma perplexa* (2%), *Spondylotreta* sp. nov. a (2%), and *Physotreta deformis?* (1%).

The fauna ($N=463$) extracted from a sample (1 kg) of the calcilitic Furudal Limestone at Gräsgårds Hamn on southern Öland is dominated by *Eoconulus* cf. *semiregularis* (76%), but includes also *Numericoma perplexa* (17%), *Rowellia* cf. *lamellosa* (3%), *Cyrtotonotreta vestrogothica* (2%), *Spinilingula radiolamellosa* (1%), *Conotreta? siljanensis* (1%), and *Lingulella? alata* (>1%). A sample (1 kg) from the calc-

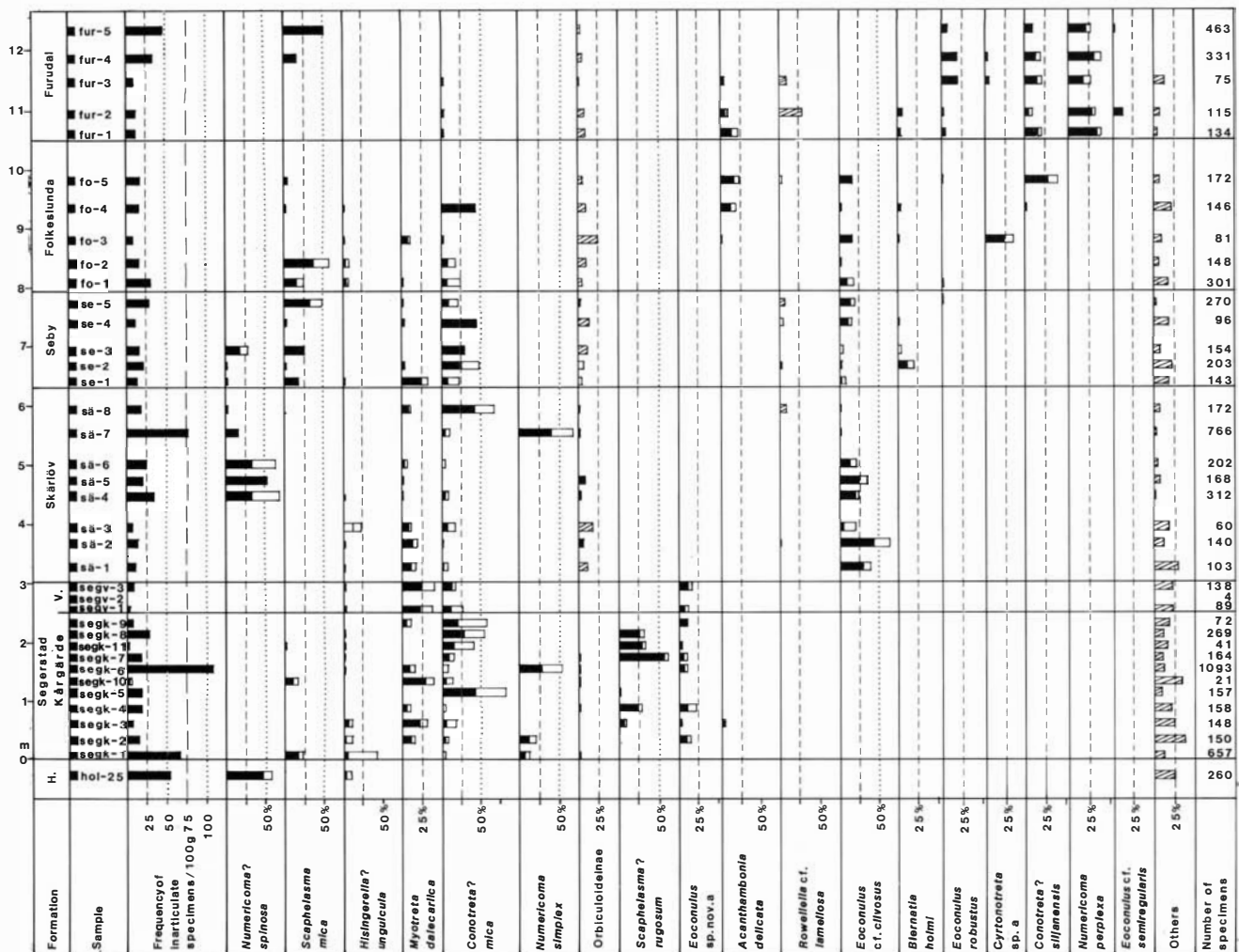


Fig. 12. □A–C (pp. 24–26). Relative frequencies of phosphatic inarticulates at Kårgårde, Dalarna. To the left, frequency of specimens per 100 g limestone. The remaining columns show the relative frequencies of those species that form at least 10% of the total fauna in at least one sample. 'Others' include all taxa that constitute less than 10% in all samples. The total number of specimens is given in the column farthest to the right. H, Holen Limestone; V, Vikarby Limestone. Figure prepared by Björn Lindsten (Stockholm).

arenitic upper Uhakuan Persnäs Limestone (a wedge of the upper Furudal Limestone) on northern Öland lacked identifiable phosphatic inarticulate brachiopods.

In the Scanian confacies belt the upper Uhakuan of the lower 'Dicellograptus Shale' (*Glyptograptus teretiusculus* Biozone) consists primarily of fine-grained graptolitic shales (e.g., Jaanusson 1973, Fig. 4D). These beds are dominated by phosphatic inarticulates; in the Koängen core, they make up about one half of the entire fauna (Nilsson 1977), and about 80% of the benthic fauna (Jaanusson 1984, Fig. 1).

The inarticulate brachiopods of the 'Dicellograptus Shale' have not been subjected to detailed systematic study since the investigations by Hadding (1913), and they are in need of revision. Nevertheless, it is clear that the faunas from these beds are markedly different compared with those of the contemporaneous sequence in the central confacies belt. The taxonomic diversity is lower, with only six species being recorded from the upper Uhakuan of the 'Dicellograptus Shale' (Nilsson 1977, Table 3). Of these, 34% belong to the thin-shelled acrotretacean *Hisingerella nana* (see Harper, in Harper *et al.* 1984 for a discussion of

this species), whereas the remainder of the assemblage is made up of lingulaceans (Nilsson 1977, p. 8; Jaanusson 1984, Fig. 1).

Dalby Limestone

In Dalarna and Västergötland the change from the calcilitic Furudal Limestone to the mainly calcarenitic Dalby Limestone probably marks an increase in water energy, and this is associated with a change in the benthic faunas (Jaanusson 1976; 1982b). There is a corresponding decrease in the abundance and state of preservation of the specimens.

At Gullhögen the lower part of the Dalby Limestone yielded on average six specimens per 100 g; and at Kårgårde 17 per 100 g (Figs. 11B, 12B). In all three sections investigated *Numericoma perplexa*, *Lingulella? alata*, and *Physotreta deformis* have their last occurrences within the upper part of the Uhakuan sequence (Figs. 8C, 9B, 10). At Kårgårde and Fjäcka a new assemblage appears near the base of the Dalby Limestone. It includes *Nushbiella lilliana*, *Ephippelasma minutum*, *Myotreta orensis*, *Rowellia holenensis*, *Spondylotreta orsaensis*, and *Scaphelasma cf. pusillum* (Figs. 9B,

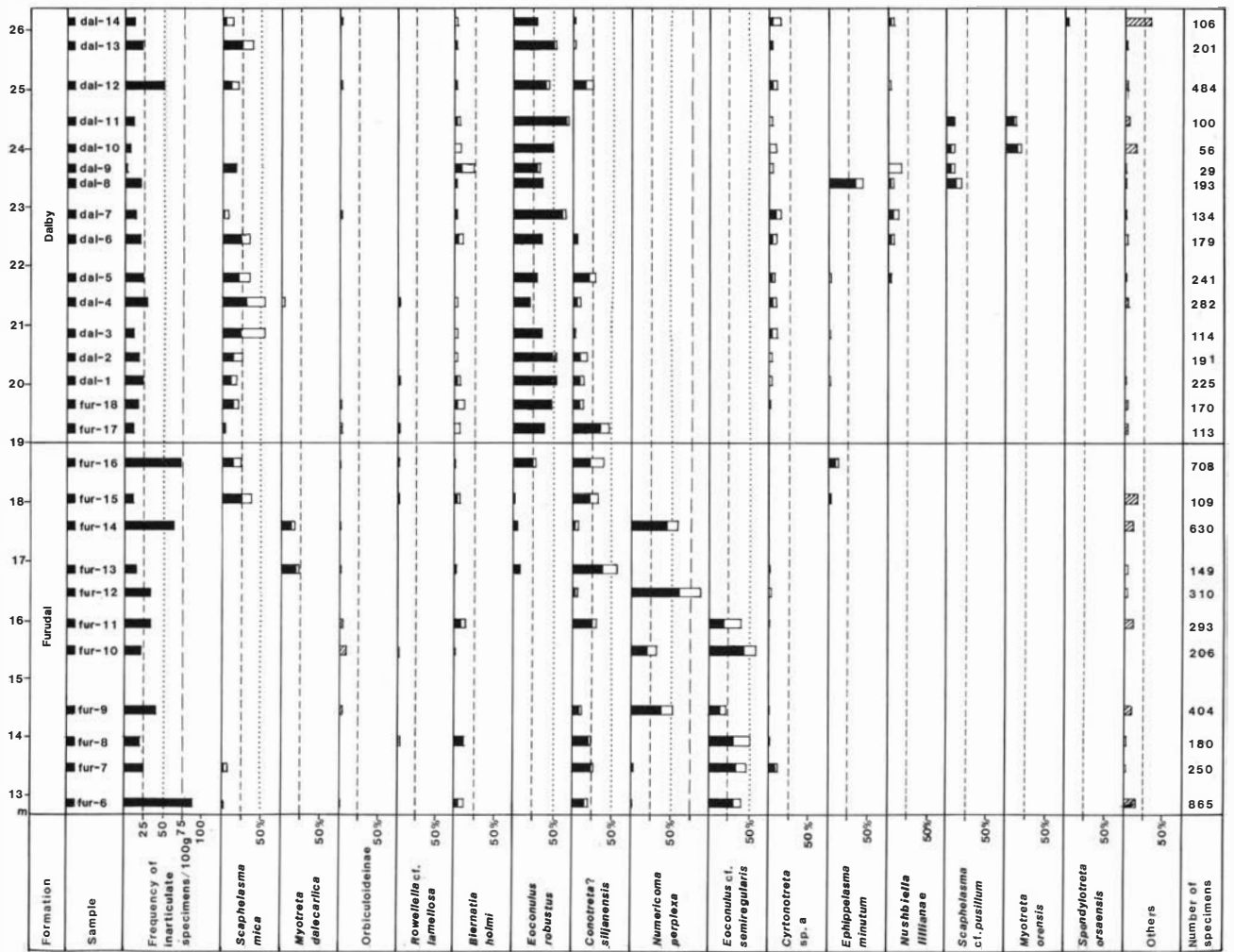


Fig. 12B.

10). The fauna of the same interval at Gullhögen is somewhat different, and *Ehippelasma minutum* and *Rowelleta hollenensis* are absent (Fig. 8C).

In the Kårgärde and Fjäcka sections *Conotreta? siljanensis* and *Ehippelasma minutum* have their last occurrence within the lower part of the Dalby Limestone (Figs. 9B–C, 10). At Kårgärde the lower Dalby Limestone is dominated by *Eoconulus robustus* and *Scaphelasma mica*. The former species constitutes 20–68% of the assemblages (samples DLK83-fur-16 – dal-15, 17; Fig. 12B–C). *Scaphelasma mica* is generally less abundant, with a frequency of 3–54% in the same part of the sequence. There are abundant fragments of an unnamed species of the Glossellinae at both Fjäcka and Kårgärde (Figs. 9B, 10); at Gullhögen the glosselline is missing in the lower Dalby Limestone, and *Eoconulus robustus* dominates only in two samples (GB84-3-71, 85; Fig. 11B–C). Moreover, *Scaphelasma mica* and *Conotreta? siljanensis* are absent (Fig. 8C).

At Kårgärde there is a further decrease in the frequency of phosphatic inarticulate brachiopods from the middle Dalby Limestone and upwards; the upper Dalby Limestone yielded on average only three specimens per 100 g (Fig. 12B–C). *Myotreta orensis* and *Scaphelasma cf. pusillum* dominate in the lower part of the upper Dalby Limestone (samples DLK83-dal-18 – 29); the latter forms 10–50% of the

assemblages, and the former has a frequency of 24–52% (Fig. 12B–C).

In all three sections under consideration *Myotreta orensis* disappears and is replaced by *Rhinotreta davidi* in the upper part of the Dalby Limestone. At Kårgärde *Acanthambonia* sp. nov. a is restricted to the same part of the sequence (Figs. 8D, 9C, 10). *Rhinotreta davidi* occurs at frequencies of up to 85–91% in the top part of the Dalby Limestone, both in the Kårgärde section (sample DLK83-dal-41) and at Gullhögen (samples GB84-4-93, 95). There are almost no inarticulates in the upper five metres of the Dalby Limestone; this part of the sequence yielded on average less than one specimen per 100 g (Figs. 11B, 12C).

In the Scanian confacies belt the boundary between *Glyptograptus teretiusculus* and *Nemagraptus gracilis* biozones, situated within the 'Dicellograptus Shale', is associated with an overall change in the faunas (Hadding 1913; Nilsson 1977). The thin-shelled acrotretacean '*Hisingerella nitens*' (see Holmer 1986 for a discussion of this species), '*Paterula bohémica*', in addition to four lingulaceans and one discinacean, enter at the base of the *N. gracilis* Biozone (Nilsson 1977, Table 3). However, as noted above, the changes in this fauna must be interpreted with caution, because the phosphatic inarticulates in these beds have not been revised recently.

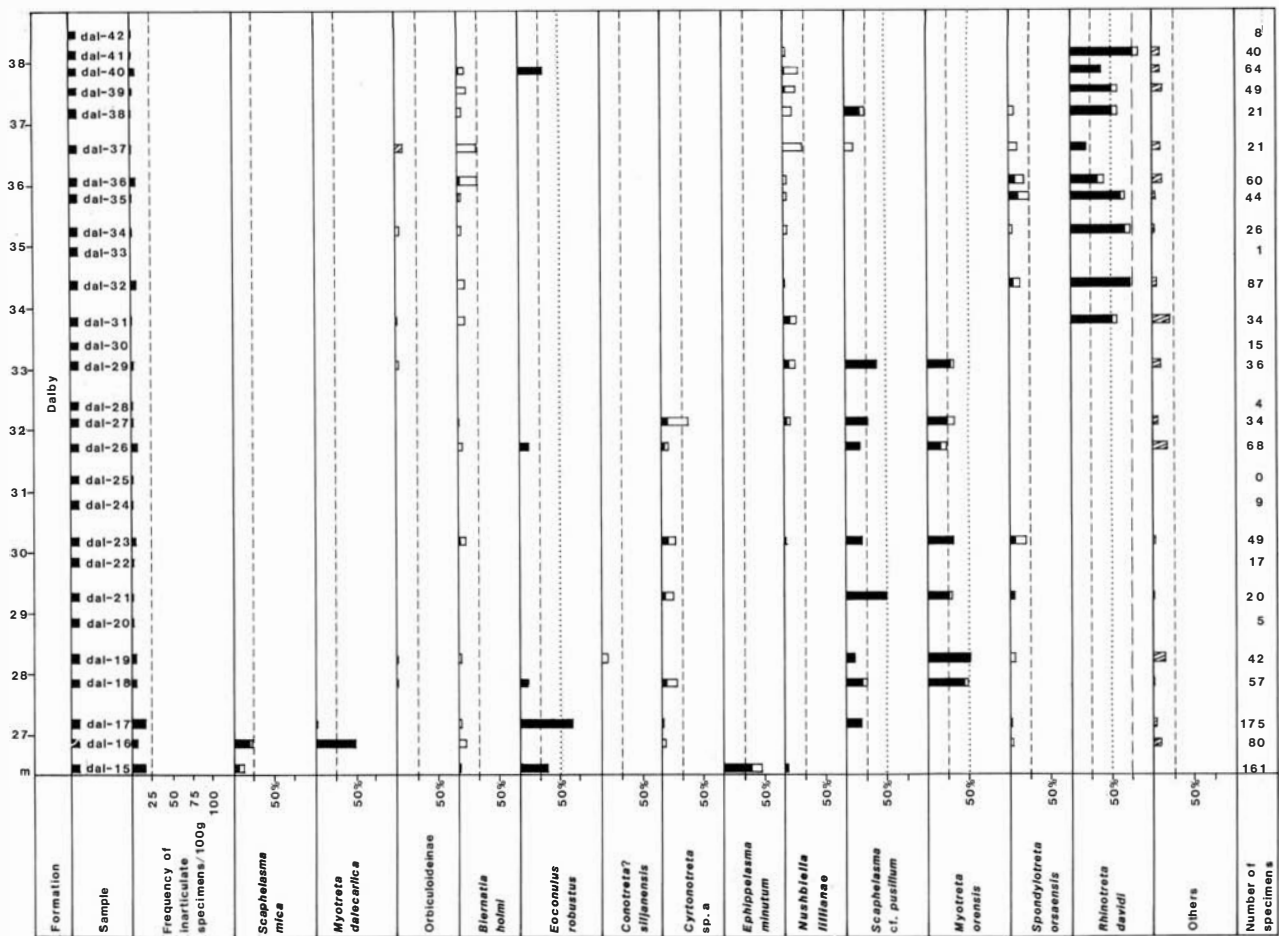


Fig. 12C (caption on p. 24).

Discussion

The results of this and previous investigations (Bednarczyk 1964, 1971, 1986; Bednarczyk & Biernat 1978; Goryanskiy 1969; Biernat 1973; Holmer 1986; Kaljo *et al.* 1986) indicate clearly that Ordovician phosphatic inarticulate brachiopods can be useful for biostratigraphic correlations. However, data sufficient for a regional biostratigraphical zonation are not yet available.

In the Viru sequence of Dalarna and Västergötland successive lithostratigraphic units are characterized by distinct assemblages of phosphatic inarticulates, permitting satisfactory correlations between the two provinces (Fig. 13, Table 1). In Dalarna and Västergötland there are major changes in the fauna primarily at the following five stratigraphical levels: (1) the Kundan–Aserian boundary, (2) the Seby–Folkeslunda interval, (3) the Lasnamägian–Uhakuan boundary, (4) the Uhakuan–Dalby boundary, and (5) at the boundary between the lower and middle Dalby Limestone (Fig. 13, Table 1). These levels are also associated with major changes in the fauna of trilobites, articulate brachiopods, and ostracodes (see Jaanusson 1976 for details). The environmental parameters that controlled the distribution of other benthic organisms in the Ordovician of Baltoscandia seem to have affected the phosphatic inarticulate brachiopod faunas as well.

In general, the Ordovician faunas appear to be richer and more diverse in calcarenitic calcilitutes than in calcarenites. It is also clear that the spatial distribution of phosphatic inarticulate brachiopod assemblages was influenced by the ecological factors controlling the confacies belts. For example, the faunas of the Scanian confacies belt are completely different from those of the central confacies belt.

The biostratigraphic succession from other districts within Sweden has not yet been studied in detail, but preliminary results presented here indicate that the Viru sequences in Jämtland and on Öland contain closely comparable assemblages.

A few of the species investigated appear to be distributed widely also outside Baltoscandia; for example, the specimens here assigned to *Scaphelasma mica* Popov and *Ehippelasma minutum* Cooper are indistinguishable morphologically from those described from the Middle Ordovician of Kazakhstan (*S. mica*) and Alabama (*E. minutum*). At the generic level many phosphatic inarticulates appear to have almost cosmopolitan distribution (see also Rowell 1986).

Life habits

As noted above, the distribution in time and space of most Ordovician phosphatic inarticulate brachiopods appears to

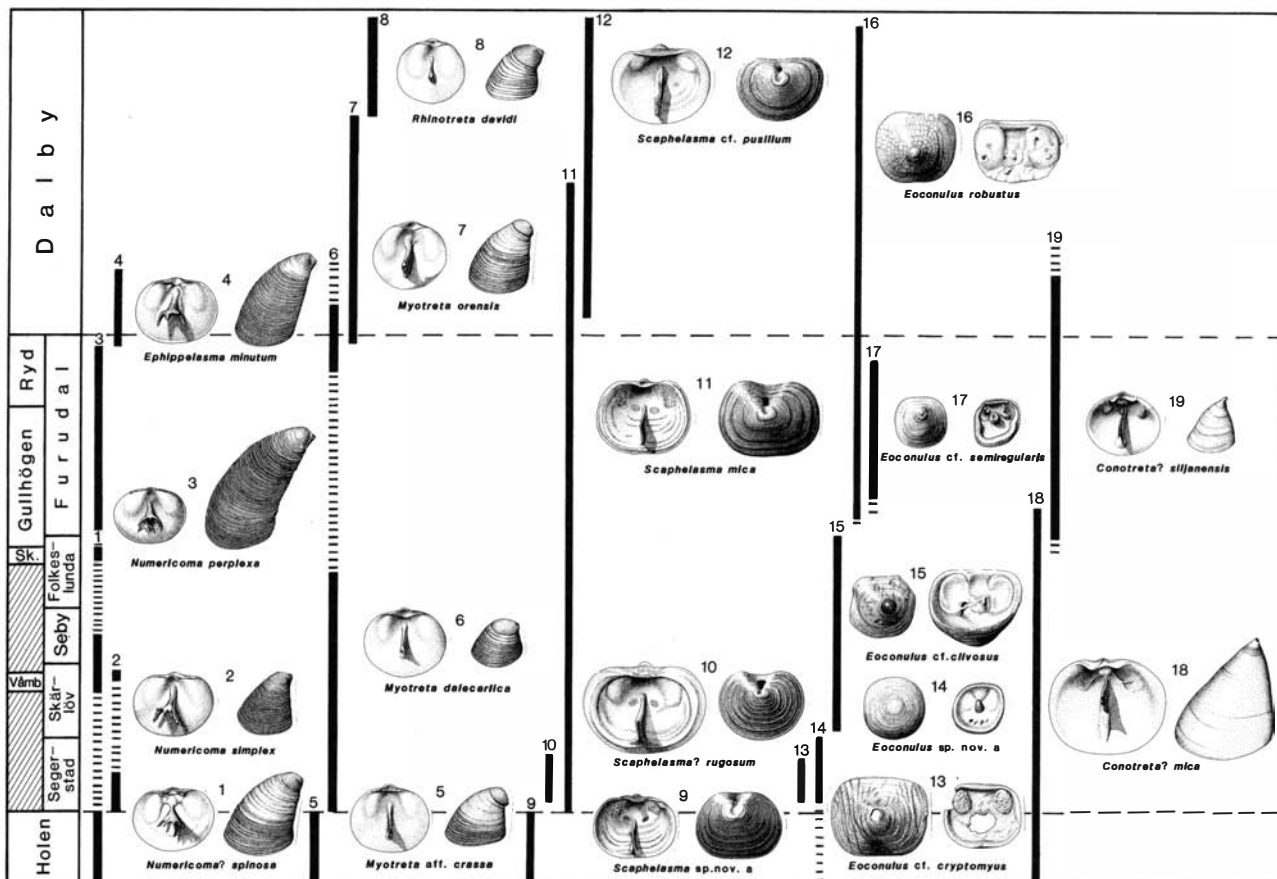


Fig. 13. Pooled stratigraphical ranges of selected species of phosphatic inarticulate brachiopods in the examined sequence. Figure prepared by Lennart Andersson (Stockholm).

be comparable with that of other benthic organisms. However, some species appears to have a wide, and sometimes almost cosmopolitan distribution, which is otherwise quite uncommon during the Ordovician; this can possibly be explained by an extensive larval dispersal through a prolonged pelagic larval phase (see Rowell 1986 for a detailed discussion).

There is no direct evidence for a planktic or epiplanktic mode of life among the phosphatic inarticulate brachiopods investigated for this study, possibly with one exception – species of *Paterula* appear to be distributed world-wide during the Ordovician, and in all types of lithofacies; *Paterula* is common in the Viru graptolitic shales of Scania, as well as in the contemporaneous limestone sequences. Moreover, Popov *et al.* (1982) suggested that the specialized pitted surface ornamentation of the extremely thin-shelled paterulids indicates a highly vesicular periostracum, which may be associated with a prolonged postlarval planktic stage, possibly spanning most of the adult stage.

Nevertheless, it has been suggested repeatedly that many of the small-shelled lower Palaeozoic inarticulates were epiplanktic, and attached to some kind of floating object, e.g., *Sargassum*-type algae. As noted by Jaanusson (1984) and Bassett (1984), little evidence (save for the occasional chance attachment of craniaceans and discinaceans to cephalopods; see, e.g., Havlíček 1972; Lockley & Antia 1980) has been presented, so far, in support of this very specialized mode of life. Although the numerous proposals

have been reviewed previously, notably by Rowell & Krause (1973), Percival (1978), Williams & Lockley (1983), Williams & Rickards (1984), and Harper *et al.* (1984), the subject merits some further comment. The following four points need to be considered:

(1) The presence of rich assemblages of minute, thin-shelled brachiopods in black graptolitic shales originally lead Schuchert (1911), Ruedeman (1934), and Bulman (1964) to argue for an epiplanktic mode of life, as these sediments supposedly represent an anoxic benthic environment. However, it is evident that black shales (in a broad sense) can be formed in various environments, from shallow water down to the deep sea, and probably also in moderately oxic conditions (e.g., Wetzel 1982, p. 431).

(2) Havlíček (1967) and Bergström (1968a) presented more direct evidence for an epiplanktic life habit, and illustrated assemblages of minute and thin-shelled aegiro-menines and obolids, arranged in rows or clusters, and occasionally in contact with possible traces of 'algal' remains. However, Sheehan (1977) and Hurst (1979) noted that these assemblages might equally well have been attached to benthic algae. Sheehan (1977), Jaanusson (1984), and Bassett (1984) have pointed out that the small, thin-shelled brachiopods could have tolerated oxygen deficiency and lived in or upon a fine-grained soft bottom (see also Thayer 1975; Fürsich & Hurst 1974). Moreover, Jaa-

Table 1. Summary of stratigraphical distribution of species in Dalarna and Västergötland. Open symbols denote questionable identifications.

	Dalarna								Västergötland					
	Ho	Kå	Vi	Sk	Se	Fo	Fu	Da	Ho	Vå	Sk	Gu	Ry	Da
Lingulacea														
<i>Rosobolus?</i> sp. nov. a												*		
<i>Expellobolus?</i> sp. nov. a				*									*	
<i>Lingulella?</i> <i>alata</i>		⊛		⊛			*						*	
<i>Spinilingula radiolamellosa</i>					⊛	*	*					⊛		
<i>Paldiskites?</i> sp. nov. a							*							
<i>Rowellella</i> cf. <i>lamellosa</i>			*	*	*	*	*	⊛				*	⊛	
<i>Rowellella hollenensis</i>							*	*						
<i>Pseudolingula</i> sp.			*		*	*	*	*						
Lingulellinae		*	*	*	*	*	*	*		*	*	*	*	*
Glossellinae							*	*						
Acrotretacea														
<i>Conotreta?</i> <i>mica</i>		*	*	*	*	*	*		*	*	*	*	*	
<i>Conotreta?</i> <i>siljanensis</i>						*	*	*				*	*	⊛
<i>Hisingerella billingensis</i>												*		
<i>Hisingerella?</i> <i>unguicula</i>	*	*	*	*	*	*			*	*	*	*		
<i>Cyrtotreta vestrogothica</i>												*	*	
<i>Cyrtotreta</i> sp. a						*	*	*						*
<i>Cyrtotreta?</i> <i>striata</i>							*					*	*	*
<i>Cyrtotreta?</i> sp. b		⊛									*	*		
<i>Physotreta deformis</i>		⊛				*	*	⊛					*	
<i>Spondylotreta orsaensis</i>							*	*						*
<i>Spondylotreta</i> sp. nov. a		⊛	*		*	*	*							
<i>Torynelasma suecicum</i>													*	
<i>Torynelasma</i> sp.									*	*				
<i>Acrotretella</i> sp.								*						
<i>Aktassia</i> cf. <i>triangularis</i>												*		
<i>Myotreta</i> aff. <i>crassa</i>	*													
<i>Myotreta dalecarlica</i>		*	*	*	*	*	*	*				⊛	*	⊛
<i>Myotreta oreensis</i>								*					*	*
<i>Rhinotreta davidi</i>								*						*
<i>Numericoma simplex</i>		*		*										
<i>Numericoma perplexa</i>							*					*	*	
<i>Numericoma?</i> <i>spinosa</i>	*		*	*					*	*	*	⊛		
<i>Ephippelasma minutum</i>							*	*						
<i>Biernatia holmi</i>					*	*	*	*					*	*
<i>Biernatia</i> sp.	*	*	*	*	*	*	*	*	*	*	*	*	*	*
<i>Scaphelasma mica</i>		*		*	*	*	*	*		⊛	*	*	*	⊛
<i>Scaphelasma</i> sp. nov. a	*								*					
<i>Scaphelasma</i> cf. <i>pusillum</i>								*						*
<i>Scaphelasma?</i> <i>rugosum</i>		*												
<i>Eoconulus</i> cf. <i>clivus</i>				*	*	*								
<i>Eoconulus</i> cf. <i>semiregularis</i>							*					*	*	
<i>Eoconulus</i> sp. nov. a		*												
<i>Eoconulus</i> cf. <i>cryptomylus</i>		*												
<i>Eoconulus robustus</i>						⊛	*	*					*	*
Discinacea														
<i>Trematis?</i> sp.							*	*						
Orbiculoideinae		*	*	*	*	*	*	*			*	*	*	*
Siphonotretacea														
<i>Nushbiella lillianae</i>							*	*					*	*
<i>Acanthambonia delicata</i>		*				*	*							
<i>Acanthambonia</i> sp. nov. a								*						
Paterinacea														
<i>Dictyonites fredriki</i>							*	⊛						
<i>Dictyonites</i> sp.		*	⊛		⊛									
Problematica														
<i>Tegulella minuta</i>	*	*			*	*	*	*				*	*	

nusson (1984) noted that the aegiromenines lacked a pedicle by which to attach themselves to the floating algae.

(3) In many instances the inarticulates occurring in the graptolitic shales were obviously components of the benthic fauna. Silurian lingulaceans from graptolitic laminated argillaceous sequences in the Welsh Borderland have been found in apparent life position, perpendicular to the bedding (Cherns 1979; Bassett 1984). Moreover, Cisne (1973, p. 15) noted the occurrence of still articulated lingulacean brachiopods in laminated argillaceous graptolitic rocks ('Beecher's trilobite bed') in the Upper Ordovician of New York State. Cisne's analysis of this assemblage (which is known mainly through the excellent preservation of trilobites with soft parts) indicates that it was formed by an almost instantaneous burial by a turbidity flow; it is evident that the lingulaceans in this case belonged to the benthic fauna. Lingulids in life position from Ordovician deep water carbonates have also been reported by Pickerill *et al.* (1984, and references therein).

(4) The entire fauna of the black Harju Fjåcka Shale (a widespread unit in Sweden) was interpreted as representing an epiplanktic *Sargassum*-type assemblage by Spjeldnaes (1978). However, among other things, the phosphatic inarticulate brachiopods from these beds include well preserved, articulated specimens of an undescribed obolid species (probably a glosselline; see also Savazzi 1986, p. 59). The shells of this species have well developed terrace lines that in all probability represent burrowing sculptures, thus pointing towards an infaunal life habit of the obolid (Savazzi 1986 and references therein). As noted by many previous authors (e.g., Cherns 1979; Jaanusson 1984), it is most unlikely that the pedicle, in demonstrably closely related lingulacean species, could have functioned both for an infaunal and epiplanktic mode of life.

(5) The fauna associated with the minute and thin-shelled brachiopods in many Lower Palaeozoic graptolitic shales includes trilobites, phyllocarids, bivalves, gastropods, hyoliths, machaeridians, annelids, and sponges (see, e.g., Jaanusson 1984, Fig. 2; Nilsson 1977, Table 3). It is most unlikely that all of these forms were planktic or epiplanktic.

Epifauna

Most of the acrotretaceans seem to have been part of the benthic epifauna, and the following three possible types of strategies may be envisaged for the taxa under consideration:

(1) A persistent peduncular attachment throughout life appears to have been the most common strategy in the faunas investigated. The brachiopods were probably able to attach themselves to relatively small scattered skeletal grains in the soft bottoms (see Bassett 1984, for a review of this life habit). It is somewhat surprising that the phosphatic inarticulates appear to be more common in fine grained and calcilititic limestones than in calcarenites. It would appear that the availability of suitable grains for attachment should have been higher in coarser grained sediments, but these were probably formed in high water-

energy environments, which may have been less suitable for these small and relatively delicate organisms.

Perishable organic substance (algae, etc.) may have been used for attachment (see also Bassett 1984), and living or dead sponges could also have provided substrate. The Middle Cambrian paterinid *Dictyonina* was found attached to the sponge *Pirania* from the Burgess Shale of British Columbia (Whittington *in* Conway Morris *et al.* 1982, p. 25, Pl. R); among fossil and Recent articulate brachiopods attachments to sponges are well known (see Ager 1967, and references therein). Attachment of small-shelled inarticulates to sponges has been suggested more recently by Percival (1978) and Holmer (1986).

(2) Among the phosphatic inarticulate brachiopods, an encrusting mode of life appears to have developed independently at least twice. Rowell & Krause (1973) discussed this life habit, known from species of *Undiferina* and *Eoconulus*. They suggested that algae formed a possible substratum for species of *Eoconulus*, the ventral valve of which frequently has a cylindrical attachment scar (Fig. 37A). However, most species of *Eoconulus* do not seem to have been restricted to a specific substrate. Ventral valves of a species in an assemblage show a number of different types of attachment scars, indicating the following types of substratum: (1) flat (Fig. 106E), (2) cylindrical (Fig. 37A), (3) ridges with (Fig. 106A) or without (Fig. 107A) nodes, and (4) completely irregular (Fig. 107C). Fragments of conulariid tests, ornamented with noded ridges that agree with the configuration of the attachment scar of *Eoconulus* are common in the insoluble residues, but no attached euconulid ventral valve has been observed. The ventral periostracum of the euconulids was probably not attached to the substrate as firmly as that in Recent craniaceans (see, e.g., Williams & Wright 1970), or else the substrate was calcareous (and has disappeared in the etching process).

Ventral valves of species of *Eoconulus* are less common than dorsal valves (Figs. 11, 12); this fact led Popov (1975) to suggest that *Eoconulus* had an epiplanktic mode of life. However, it is evident that the ventral valve of all euconulid species was mineralized late in ontogeny; the adult ventral valve of *E. cf. cryptomyus* and *E. robustus* (Fig. 109) was commonly mineralized only partially.

(3) The pedicle of some siphonotretaceans, like *Acanthambonia delicata* (Fig. 114A-K) seems to have atrophied during ontogeny, and adults of such species were free-living, probably using the spines for stabilization. Popov & Nölvak (1986, Pl. 1:1) illustrated some hook-like spines of *Acanthambonia portranensis*, indicating attachment to minute cylindrical objects, possibly sponge spicules (L. E. Popov, personal communication 1986).

Endofauna

It is generally assumed that most Palaeozoic lingulaceans had a burrowing, infaunal life habit, similar to that of their Recent representatives. Although direct evidence for this is lacking for most species, there is a considerable number of reports of Palaeozoic lingulaceans still found in vertical life

position (for a summary, see Paine 1970 and Pickerill *et al.* 1984).

Seilacher (1972) and Savazzi (1986) noted that the specialized ornamentation (with so-called terrace lines) of several lingulacean genera appears to be analogous to the burrowing sculptures found among several infaunal arthropods and molluscans. Moreover, the general shell shape of most lingulacean brachiopods, as well as the distribution of repaired injuries on the shell margin support the interpretation that these forms were infaunal organisms (Savazzi 1986 and references therein).

Of the lingulacean species incorporated in this study, only *Spinilingula radiolamellosa* (Fig. 50A–E) and an unnamed species of the Glossellinae (Fig. 53G–H) possess well developed divaricate terraces that are more or less identical to those described by Savazzi (1986, Fig. 8) in *Spinilingula intralamellata* and *Glossella papillosa*. The poorly preserved fragments of *Pseudolingula* (Fig. 53A–D) from the Viru sequence do not show evidence of the burrowing terraces described by Savazzi (1986, Fig. 4E) from the Upper Ordovician *Pseudolingula quadrata* (see also Goryanskij 1969, Pl. 6:6).

None of the lingulaceans discussed in this paper were found in life position, but an undescribed species of *Glossella* is known to occur in such a position in the Middle Ordovician Skålberget Limestone at Skålberget quarry, Dalarna (Valdar Jaanusson, personal communication 1985), and I have also found several species of *Pseudolingula* (including *P. quadrata*) in vertical positions (with the anterior margin pointing upwards) in the Ordovician sequence in Sweden and Estonia.

Bassett (1984) suggested that some of the minute lower Palaeozoic acrotretaceans (like the elongate Silurian *Opisiconidion*) could have been adapted to an interstitial way of life, comparable with that of the Recent articulate brachiopod *Gwynia capsula*. The fact that the faunas described here are more abundant and diverse in calcilititic sequences (where the size of individual pores in the sediment must have been extremely small), seems to suggest that such a life habit was uncommon.

Morphological terms

The terminology used currently in describing the morphology of phosphatic inarticulate brachiopods is comparatively stable; only a few additions to the list of Williams & Rowell (1965a) have been made. Krause & Rowell (1975, p. 14) introduced the term *surmounting plate* for the platform that is developed on top of the dorsal median septum in members of the acrotretid subfamilies Torynelasmatinae and Biernatinae (see, e.g., Figs. 74, 96). The same term has been used in describing the dorsal median septum of *Numericoma* and *Ephippelasma* (e.g., Figs. 86–89), but it should be noted that the formation of the surmounting plate in most ephippelasmatinae is different from that in the biernatinae and the torynelasmatinae (see also below, p. 122).

The term *median buttress* was introduced by Krause & Rowell (1975) to denote the thickened knob-like projec-

tion situated at the posterior end of the dorsal median septum in many acrotretines (see, e.g., Fig. 54B). They also introduced the term *interridge*, signifying a convex exterior ridge running from the apex to the posterior margin on the ventral pseudointerarea of some acrotretids (cf. *intertrough*, Williams & Rowell 1965a, p. H146; see, e.g., Fig. 61H).

Havlíček (1982, p. 13) proposed that *internal area* should be used for the low pseudointerareas of most members of the subfamily Lingulellinae (cf. *pseudointerarea*, Williams & Rowell 1965a, p. H151; see, e.g., Fig. 48K, N). Many previous workers have used *median plate* or *median depression* (see, e.g., Rowell 1965, p. H263; Havlíček 1982, p. 13), when referring to the concave central part of the dorsal pseudointerarea (see, e.g., Figs. 50B, 61E). However, *median groove* is preferred here.

The new term *posterior platform* is introduced for the raised area at the posterior end of the dorsal median septum of the biernatinae (see, e.g., Fig. 95G).

The descriptive terms *fila*, *ruga*, *lamella*, *capilla*, applied to various types of brachiopod ornamentation, are used in the sense of Williams & Rowell (1965a); the spacing is given in numbers per millimetre, or, if minute, as distance in micrometres between elements. *Growth line* is used widely for any unspecified kind of concentric ornamentation related to periodic growth.

The terminology describing the shell structure, ontogeny, and micro-ornamentation of the inarticulate brachiopods is discussed separately below.

Shell structure

The detailed shell structure of Recent phosphatic inarticulate brachiopods has been poorly known until recently, but studies by Iwata (1981a, 1981b, 1982; see also Watabe & Pan 1984) on the ultrastructure and mineralization of *Lingula anatina*, *Glottidia pyramidata*, and *Discinisca laevis* have greatly expanded our knowledge in this field; the work by Williams & MacKay (1979) on the morphology of the periostracum of *Discinisca strigata*, *Discina striata*, *Pelagodiscus atlanticus*, *Glottidia pyramidata*, and *Lingula anatina*, and by Williams (1977) on the ultrastructure of the mantle edge in *Glottidia pyramidata*, have also contributed significantly to the understanding of the formation and structure of phosphatic brachiopod shells.

Much less is known about the shell structure of fossil phosphatic brachiopods, with only a few detailed studies based on SEM investigations of etched sections. Poulsen (1971) published some SEM-photographs of cross-sections of fractured shell surfaces in an unnamed acrotretacean species (probably a member of the subfamily Acrotretinae) from the Middle Ordovician 'Ampyx Limestone' of Norway. Biernat & Williams (1971) studied the shell structure of Ordovician siphonotretacean brachiopods. The shell structure of some lingulaceans and acrotretaceans was illustrated by Hewitt (1980), and more recently, Popov & Ushatinskaya (1986) illustrated cross-sections of broken shell surfaces in some Cambrian and Ordovician phosphatic

inarticulates. Passing reference to the shell structure of these brachiopods has been made by, e.g., Popov *et al.* (1982), Rowell & Henderson (1978), Holmer (1986), and Rowell (1986).

The following section of this monograph describes the shell structure of phosphatic inarticulate brachiopods (mostly from the Middle Ordovician) by means of SEM investigations and examination of thin sections in transmitted light. Two main types of shell structure can be distinguished, the first typified by members of the superfamilies Lingulacea and Discinacea (Fig. 21), whilst the second was found exclusively in the examined acrotretaceans (Fig. 40). The shell structure of the siphonotretaceans was not examined (for this group, see Biernat & Williams 1971 and Popov & Nölvak 1987).

Most of the material used comes from the Viru sequence under consideration, but some well preserved Cambrian and Silurian forms from other areas have been included for the purpose of comparison.

For the study of internal structure under the SEM, specimens embedded in plastic resin (Polyester Giesshartz-GTS, manufactured by Vosschemie) were sectioned, polished and subsequently etched with 4% HCl for about four seconds before coating. In most cases the counterpart of the embedded and sectioned valves was used to make thin sections for examination in transmitted light.

The outermost shell layer is called the *primary layer*. Interior to this there is a *secondary layer*, and occasionally, a *tertiary layer* can be distinguished. The term *laminae* is used to denote shell layers thicker than 4 µm, whereas *lamellae* are comparatively thinner layers, 1–4 µm thick. In this way, a lamina can consist of several lamellae (e.g., Fig. 40).

The detailed composition of the shell mineral was not determined, but previous investigations have indicated that it consists of francolite (e.g., McConnell 1963). SEM examination (including some EDAX analysis) indicates that the shells consist of the following three morphological types of calcium phosphate: (1) granular apatite, (2) acicular apatite, and (3) an unidentified type of cryptocrystalline ('collophane-like') calcium phosphate, which in the following is abbreviated to CCP. The first two types are generally birefringent in polarized light, and show a preferred orientation of the apatite *c*-axes. In the CCP, the birefringence is comparatively weaker or missing altogether, which probably indicates that the size of the crystallites is very small or that the apatite *c*-axes do not have a preferred orientation. The CCP is generally more resistant to etching (in 4% HCl) than the granular and acicular apatite. In etched sections examined under the SEM and in transmitted light, the CCP has a more porous appearance than the two first types, but it is probable that the etching process has exaggerated the porosity somewhat; in some sections the plastic resin (used in the embedding process) has partly filled the empty spaces.

The term *crystallite* (in discussing the shape and size under the SEM), is used in a morphological sense, as neither X-ray diffraction nor any other method of determining single crystals were used.

The terms *baculae* (Latin *baculum*, small rod) and *baculate structure* are introduced here to denote the minute apatitic

rods that form a criss-crossing ('lattice-like' of Iwata 1982; 'X' figures of Watabe & Pan 1984) pattern in the organic laminae of the secondary shell layers of Recent lingulaceans (*Glottidia*; Fig. 21) and discinaceans (*Discinisca*; Fig. 21). The baculate structure was first described by Iwata (1982, e.g., Fig. 1:2), who showed that the baculae represent mineralized organic fibrils. Baculate structures are here identified also from the secondary layers of Ordovician and Silurian discinaceans and lingulaceans (e.g., Figs. 15, 18).

In acrotretaceans, the term *columnar layer* (Fig. 40) is introduced to denote a secondary or tertiary layer in which discrete lamellae are connected to each other by minute columns (referred to as pillars by Poulsen 1971 and Rowell 1986) that are perpendicular to the lamellae (e.g., Fig. 22F; see also Poulsen 1971, Pl. 5). The term *camerate layer* (Latin *camera*, chamber; Fig. 40) is used in describing a secondary layer, in which discrete lamellae are connected to each other by thin perpendicular walls (referred to as supporting ridges by Rowell 1986). The walls form irregularly shaped polygonal chambers in a honeycomb-like pattern, which is best observed on the surface of exfoliated specimens, where the primary layer is peeled off (e.g., Fig. 28A; see also Holmer 1986, Fig. 5O and Rowell 1986, Fig. 1:3–4). The chambers of the camerate layer are sometimes elongated in the direction of growth, to form parallel 'tubes' of rectangular cross section (see also Poulsen 1971, Fig. 4).

Lingulacea, Discinacea and Acrothelidae

Lingulacea

Of the five lingulaceans described and discussed below, two are from outside the study area, but have a shell structure that is considered significant for the interpretation of the three Middle Ordovician species.

(1) The stratigraphically oldest shells examined belong to the early Tremadoc *Ungula ingraca* (= *Obolus apollinis* Eichwald of most previous authors, including Mickwitz 1896, p. 133, and Rowell 1965, p. H264; *sensu* Popov in Kaljo *et al.* 1986, p. 101) from the Maardu Member, Kallavere Formation at Jägala Juga, northern Estonia. The shell structure of this species (referred to as *Obolus Apollinis* var. *maximus*) was described by Mickwitz (1896, pp. 102–106, Pl. 3:30–32; see also Walcott 1908, p. 152, Fig. 5, Pl. 12:11–12, 1912, p. 300, Fig. 15). In the available material, both valves are fragmentary and heavily worn. The specimens were prepared mechanically from the friable sandstone, and some midsagittal sections were studied in transmitted light and under the SEM.

The outermost primary layer (referred to as the '*äussere Schalenlamellen*' by Mickwitz 1896, p. 103, Pl. 3:30) is not preserved in the material investigated here, but the secondary and tertiary layers (referred to collectively as the '*Verdickungslamellen*' by Mickwitz 1896) are well shown (Fig. 14A).

The secondary layer is of variable thickness, reaching up to about 0.6 mm anteriorly. As noted by Mickwitz (1896),

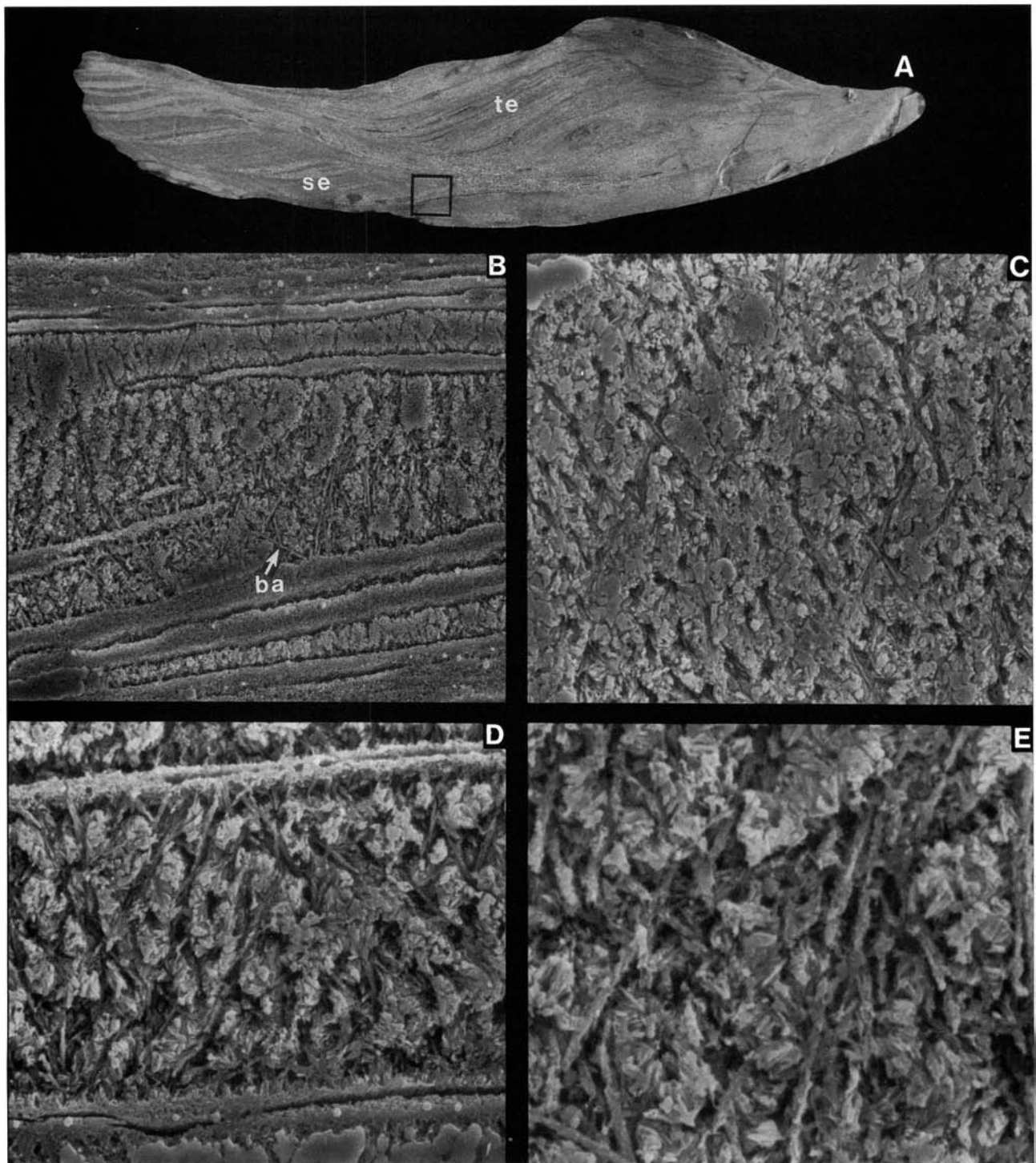


Fig. 14. □A. Midsagittal section through a dorsal valve of the lower Tremadoc *Ungula ingrica* (Eichwald, 1829) *sensu* Popov (1986, p. 101, in Kaljo et al. 1986), showing the secondary (se) and tertiary (te) layers; the location of B–E is indicated by an open square; Maardu Member, Kallavere Formation, Jägala Jüga, Estonia; Br133665, $\times 26$. □B. Detail of A, showing the secondary layer with an alternation between baculate and lamellose laminae; *ba*, baculum; $\times 1200$. □C. Detail of A, showing criss-crossing baculae in the secondary layer; $\times 3071$. □D. Detail of A, showing baculate laminae; $\times 3700$. □E. Detail of D, showing baculae consisting of acicular apatite crystallites; $\times 5700$.

this layer consists of two alternating types of laminae, both of which are wedge-shaped in sagittal section and inclined at about $20\text{--}30^\circ$ relative to the exterior of the valve. The first type consists of numerous thin apatitic lamellae, which have a homogeneously granulose appearance (described as ‘*homogene hornige Masse*’ by Mickwitz 1896, p. 105; Fig. 14B);

the orientation of the apatite *c*-axes is parallel to the lamellae.

The second type of lamina lacks lamellae, and it is proportionally thicker than the first type (Fig. 14A); these laminae have a porous appearance. They have a baculate structure, with a criss-crossing pattern of apatitic baculae

(about 15 μm long and 350 nm wide), which are inclined at varying angles to the laminae. This structure was described by Mickwitz (1896, p. 105) as 'kalkige, mit feinen verzweigten Röhrensystem durchsetzte Masse'. The baculae consist of needle-shaped apatite crystallites (Fig. 14B–E); the individual crystallites are about 200 nm wide and 2000 nm long, arranged with their long axis parallel to the baculae. The alignment of the crystallites appears to agree with the preferred c -axis orientation. The interbacular spaces are filled with CCP (Fig. 14E).

Interior to the secondary layer, a tertiary layer is developed (about 1 mm thick), consisting of numerous thin granulose lamellae, whereas the baculate laminae are even thinner or lacking (Fig. 14A). The layer has a very weak birefringence; the preferred orientation of the c -axes appears to be parallel to the lamellae.

On the interior of the dorsal and ventral valves of *U. ingriva*, there are numerous shallow 'pores' (referred to as 'Bohrgänge (?) von Parasiten' by Mickwitz 1896, Pl. 3:31).

(2) The stratigraphically youngest lingulacean examined is an as yet undescribed species of *Pseudolingula*?, from the Silurian Hemse beds of Gotland. This species is represented by some articulated shells, still within matrix. The primary layer is 4 μm thick and has a granular structure (Figs. 15A–B, 21). The birefringence is weak; the preferred c -axis orientation appears to be parallel to the outer surface.

The secondary layer is about 35 μm thick. Posteriorly, it consists of a single lamina parallel to the outer surface. Anteriorly, wedge-shaped laminae are developed, inclined at about 10–30° relative to the outer surface. All laminae have criss-crossing baculae, about 700 nm wide and 15 μm long (Figs. 15, 21), consisting of flattened, stacked platelets of apatite (Fig. 15B–C). The spaces between the baculae are filled with CCP (Fig. 15A) or less commonly empty (secondarily filled with drusy calcite; Figs. 15B–C, 21). The secondary layer has a strong birefringence, with c -axes almost perpendicular to the outer surface of the valve. Inside this layer there is a single lamella consisting of granular apatite; it is strongly birefringent, with the c -axis parallel to the lamella.

The shell structure of *Pseudolingula quadrata* (Eichwald), from the Upper Ordovician Vormsian Stage of Estonia, appears to be similar to that of the Silurian species described above (see also Mickwitz 1896, p. 107, Pl. 3:36–37).

(3) Some unoriented sections through the ventral valves of an unnamed lingulacean, *Obolina*? gen. et sp. a, from the Seby Limestone show a primary layer, 3 μm thick, which has a granular appearance (Figs. 16A, 21). The secondary layer is of uniform thickness (about 20 μm) and consists of a single lamina parallel to the outer surface; it appears to consist entirely of CCP, and has a porous appearance. There are criss-crossing hollow tubes of circular cross section, about 450 nm wide and 10 μm long (Fig. 16A). The empty tubes may have contained unmineralized organic fibres, but it is also possible that they were formed through the etching process (see also discussion below).

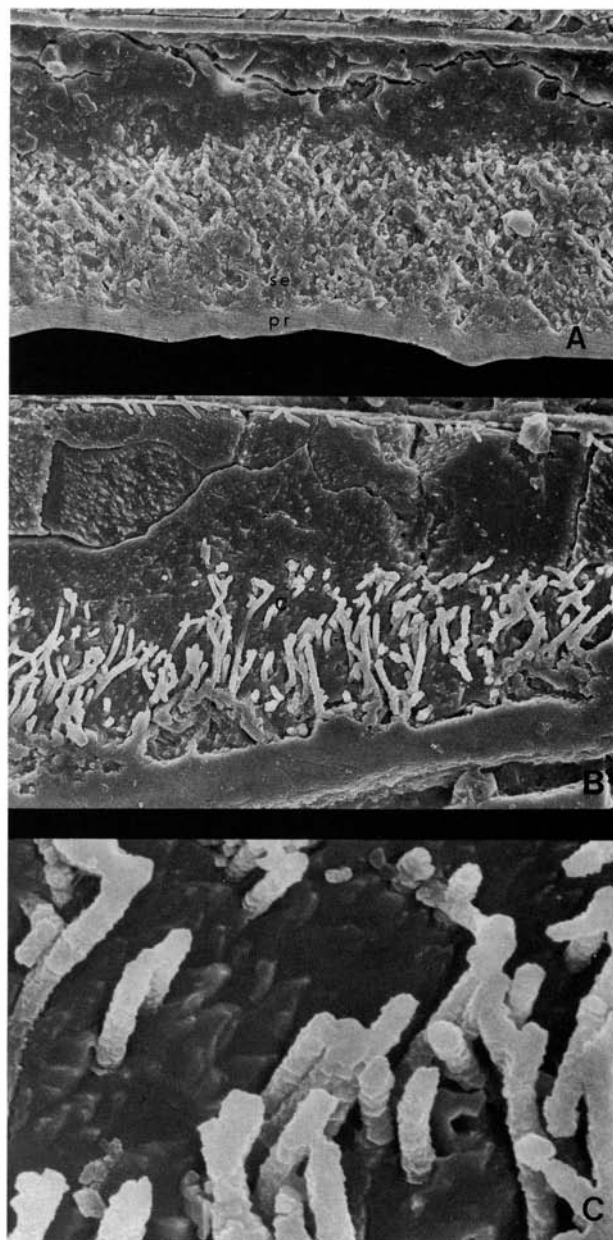


Fig. 15. □A. Midsagittal section through a dorsal valve of a complete articulated shell of the Silurian (Ludlow) *Pseudolingula* sp. nov., showing the criss-crossing pattern of baculae and interbacular spaces filled with cryptocrystalline apatite (CCP); *pr*, primary layer; *se*, secondary layer; Hemse beds, Petesvik, Gotland; Br124967, $\times 1000$. □B. Detail from another section of A, showing the apatitic baculae surrounded by secondary calcite, the location of C is indicated; $\times 1400$. □C. Detail of B, showing baculae which appear to consist of stacked platelets of apatite; $\times 7000$.

(4) In a midsagittal section through the ventral valve of *Rosobolus*? sp. nov. a (Fig. 16B–D), the primary and secondary layers are poorly developed. There is a very thin outermost primary layer, which is absent in sections through the umbonal region, where the larval shell forms a well defined plate, 8 μm thick (indicated by an arrow in Fig. 16B).

In the secondary layer there is an alternation between thick laminae consisting of numerous thin lamellae, and proportionally thinner non-lamellose laminae. The thick lamellae have a granular microstructure; they are strongly birefringent with the c -axes oriented parallel to the

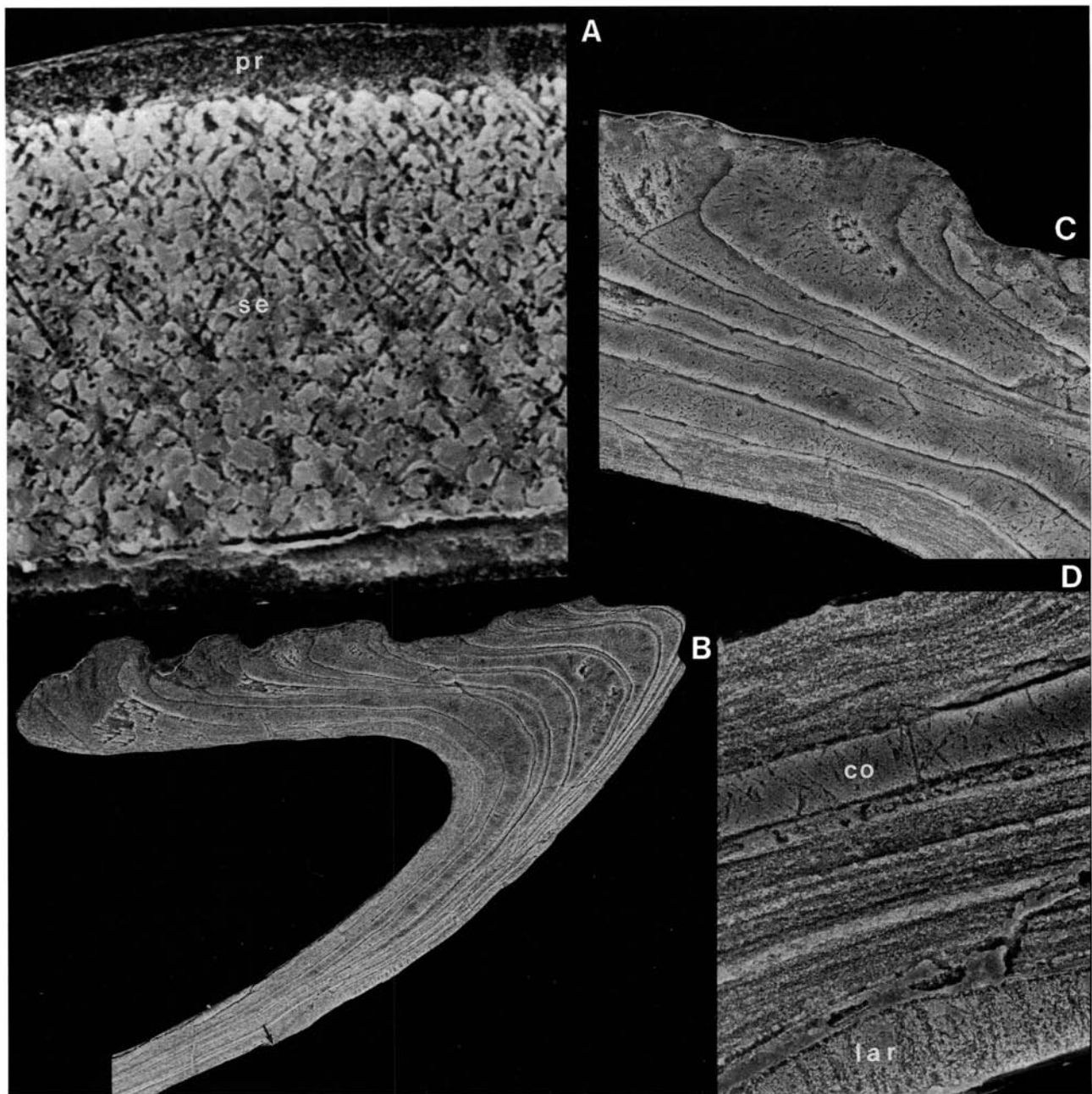


Fig. 16. □A. Section through a fragmentary ventral valve of *Obolinae?* gen. et sp. a, showing the criss-crossing pattern of hollow tubules in the CCP; note that this pattern might be partly due to the etching process; *pr*, primary layer; *se*, secondary layer; Seby Limestone (sample DLK83-se-2); Br133614b, $\times 3328$. □B–D. Midsagittal section through a ventral valve of *Rosobolus?* sp. nov. a; Gullhöggen Formation (sample GB84-1-1); Br132594c. □B. Posterior portion of the valve, showing the shelf-like pseudointerarea; the edge of the larval shell is indicated by an arrow; $\times 207$. □C. Detail of B, showing numerous laminae, which consist of porous 'collophane-like' CCP; $\times 665$. □D. Detail of B, *lar* = larval shell, *co* = cryptocrystalline apatite (CCP); $\times 1908$.

lamellae (Fig. 16D). The thinner laminae are of uniform thickness (about $5 \mu\text{m}$) and appear to consist of porous CCP (Fig. 16D). As in the unnamed oboline species described above, there is a criss-crossing system of empty tubes in the CCP. The larval shell consists of a CCP-like substance, and in both cases the birefringence is weak. In sections through the shelf-like raised pseudointerarea, the laminae of CCP are more numerous and thicker than in the remainder of the shell (Fig. 16B–C).

(5) In the ventral valves of *Rowellella* cf. *lamellosa*, the primary layer is $4 \mu\text{m}$ thick and lamellose, with a granular

microstructure (Fig. 17C). The primary layer is weakly birefringent, with a preferred orientation of the *c*-axes parallel to the outer surface; this layer is absent in sections through the umbo, where the larval shell is developed (Fig. 17A).

As in *Rosobolus?* sp. nov. a, the secondary layer consists of lamellose laminae that are separated by non-laminose laminae (Fig. 17B). The lamellose laminae are of uniform thickness (about $12 \mu\text{m}$); they are strongly birefringent, and have the apatite *c*-axis arranged parallel to the lamellae. The non-lamellose laminae are wedge-shaped, up to

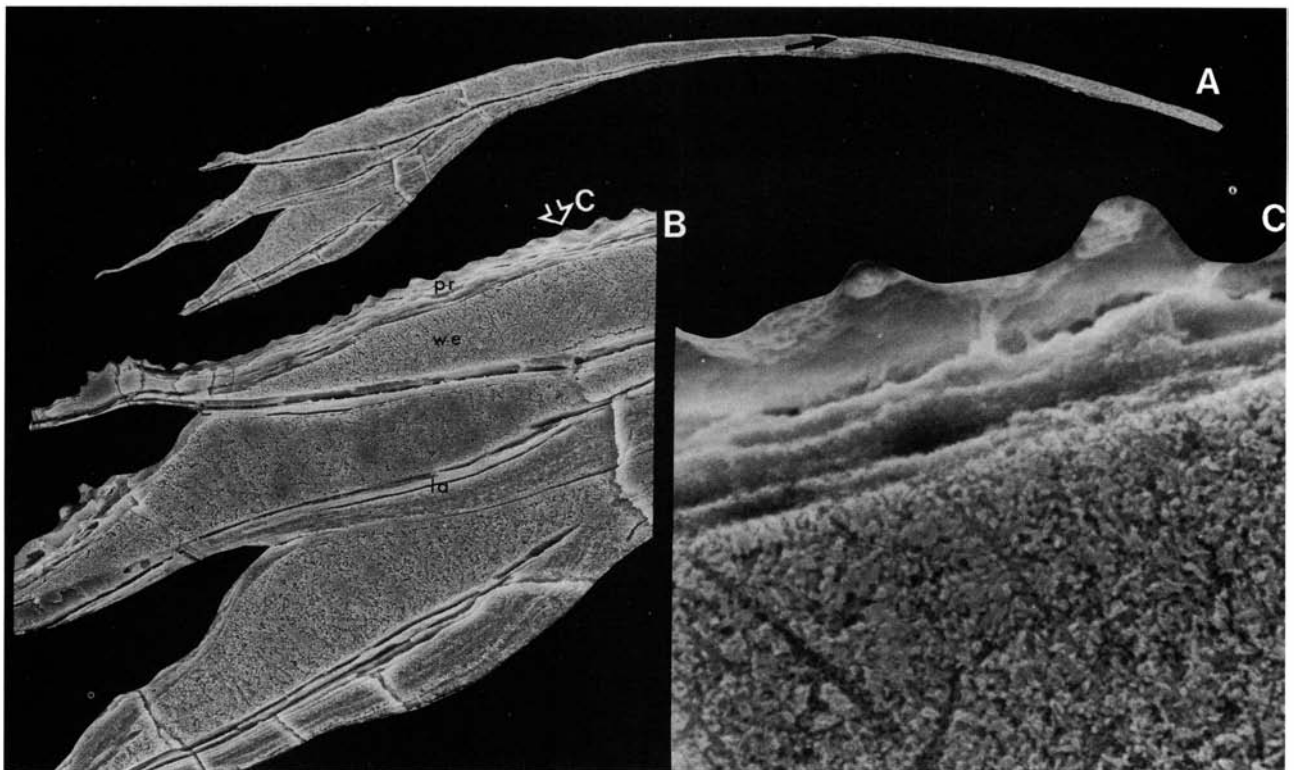


Fig. 17. □A. Midsagittal section through a ventral valve of *Rowellella* cf. *lamellosa* Popov; the edge of the larval shell is indicated by an arrow; Ryd Limestone (sample GB84-3-43); Br132856b, $\times 200$. □B. Detail of the anterior section of A, showing the primary layer (pr) and the alternation between wedge-shaped laminae (we) and lamellose laminae (la) in the secondary layer; the location of C is indicated; $\times 600$. □C. Detail of B, showing the granular and lamellose primary layer, and the CCP in the wedge-shaped laminae; $\times 4500$.

180 μm long and 30 μm thick, with a somewhat granular appearance (Fig. 17B–C), but there is no birefringence observed in polarized light. The larval shell is a well defined separate plate (arrow in Fig. 17A), consisting of a substance that is similar to that of the non-lamellose laminae.

Discinacea

The shell structure of three species of the discinacean subfamily Orbiculoideinae was examined. The first is from outside the study area, whereas the latter two are from the Viru sequence under consideration.

(1) In a midsagittal section through a ventral valve of *Orbiculoidea pilidium* (Lindström) from the Silurian Eke beds on Gotland, the primary layer is about 30 μm thick; it has a granular microstructure with minute apatite granulae, 90–300 nm across (Figs. 18A, C, 21), and the birefringence is weak.

The secondary layer consists of wedge-shaped laminae inclined at about 30–40° relative to the shell surface (Fig. 18A); these laminae have a well developed baculate structure almost identical to that of the lingulaceans described above (cf. *Ungula ingraca* and *Pseudolingula?* sp.; Fig. 21). The criss-crossing apatitic baculae are about 600 nm wide and 15 μm long, inclined obliquely to the laminae (Fig. 18B), and with a granular microstructure; the interbacular spaces are empty (that is, filled with a secondary drusy calcite; Fig. 21).

(2) Sagittal sections through the dorsal (Fig. 19D–H) and ventral valves (Fig. 19I–J) of *Orbiculoidea?* sp. b, and the dorsal valve of *Schizotreta* sp. a (Fig. 19A–C) were examined. In both species the primary and secondary layers are well developed (Fig. 19C, G, J). In the dorsal valves the primary layer is about 3 μm thick, but it is generally somewhat thinner in *Orbiculoidea?* sp. b (Fig. 19C, E). The layer has a granular microstructure (Fig. 19C, G); examination in polarized light indicates that the c -axis orientation is parallel to the shell surface. In the single ventral valve of *Orbiculoidea?* sp. b, the primary layer is 15 μm and lamellose (Fig. 19I–J). In all examined discinaceans the granular primary layer is missing in sections through the smooth larval shell.

The secondary layer consists of wedge-shaped laminae, inclined at a much varying angle to the outer surface, alternating with thin granulose lamellae (Fig. 19B, D, G, J). The preferred c -axis orientation in the latter is parallel to the laminae. The wedge-shaped laminae increase in thickness in the direction of growth, but gradually merge in the opposite direction. They are most common posteriorly, reaching a length of 0.15 mm and a thickness of 24 μm (Fig. 19B, G); anteriorly, they are fewer and more uniform in thickness (Fig. 19A, D).

In etched sections (embedded in plastic resin) the wedge-shaped laminae of both species consist of a substance with a porous CCP-like microstructure; however, it is apparent that the empty spaces have been partly filled with plastic resin (Fig. 19C, J). As in some of the examined lingulaceans (*Obolinae?* gen. et sp. a and *Rosobolus?* sp. nov.

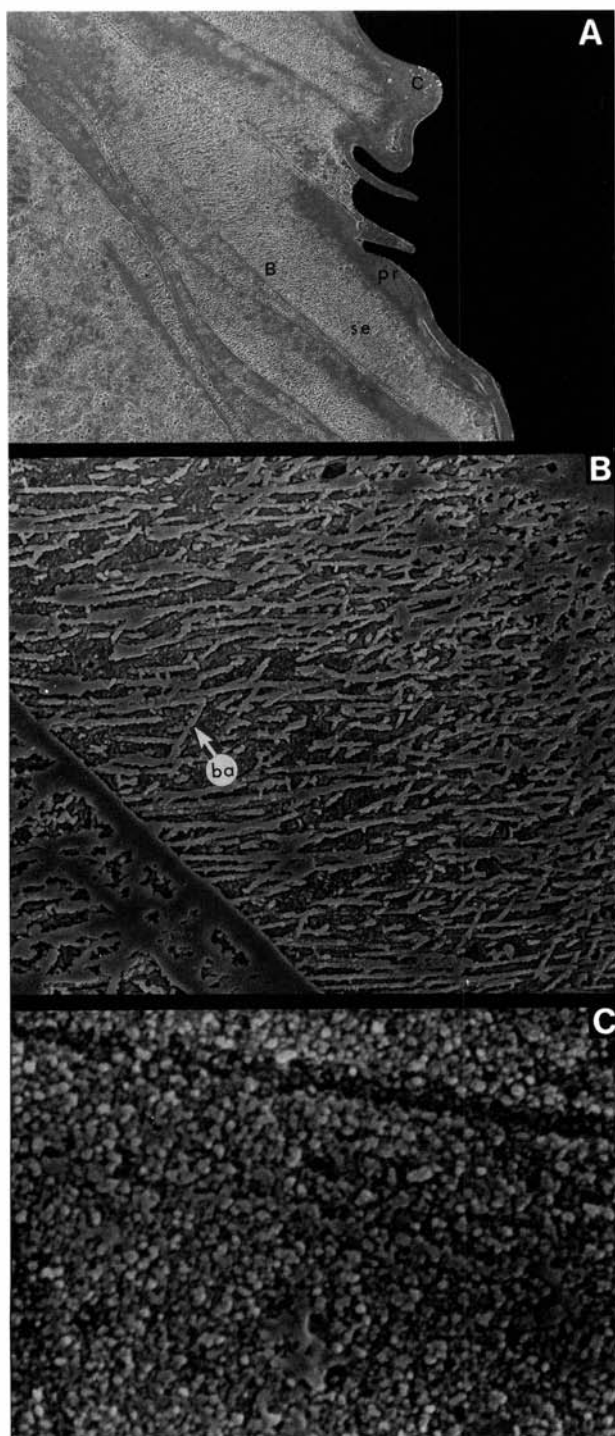


Fig. 18. □A. Detail of the anterior portion of a midsagittal section through a ventral valve of the Silurian (Ludlow) *Orbiculoidea pilidium* (Lindström, 1861), showing the primary (pr) and secondary (se) layers; the location of B and C is indicated; Eke beds, Lau backar, Gotland; Br24478, $\times 170$. □B. Detail of A, showing the criss-crossing baculae (ba) and the surrounding secondary calcite; $\times 1100$. □C. Detail of A, showing the granular structure of the primary layer; $\times 11000$.

a), there is a criss-crossing pattern of hollow tubes, with a diameter of about $0.5 \mu\text{m}$ (Fig. 19C, E, J). However, in unetched fractured shells (not embedded in plastic resin) a baculate structure can be observed, with baculae up to $13 \mu\text{m}$ long and 450 nm wide (Fig. 19G–H). In yet another

fractured and unetched fragment from the same specimen, the baculate structure of the secondary layer can not be observed (Fig. 19F); here the interbacular spaces appear to be almost completely filled with CCP. The wedge-shaped laminae are birefringent, and has the preferred ϵ -axis orientation at an angle to the laminae (almost perpendicular to the exterior shell surface). As suggested above, the empty tubes could have contained unmineralized organic fibrils, but at least in *Orbiculoidea?* sp. b they appear to have been formed through the etching process; that is, a mould of the baculum has formed in the surrounding CCP and plastic resin.

Acrothelidae

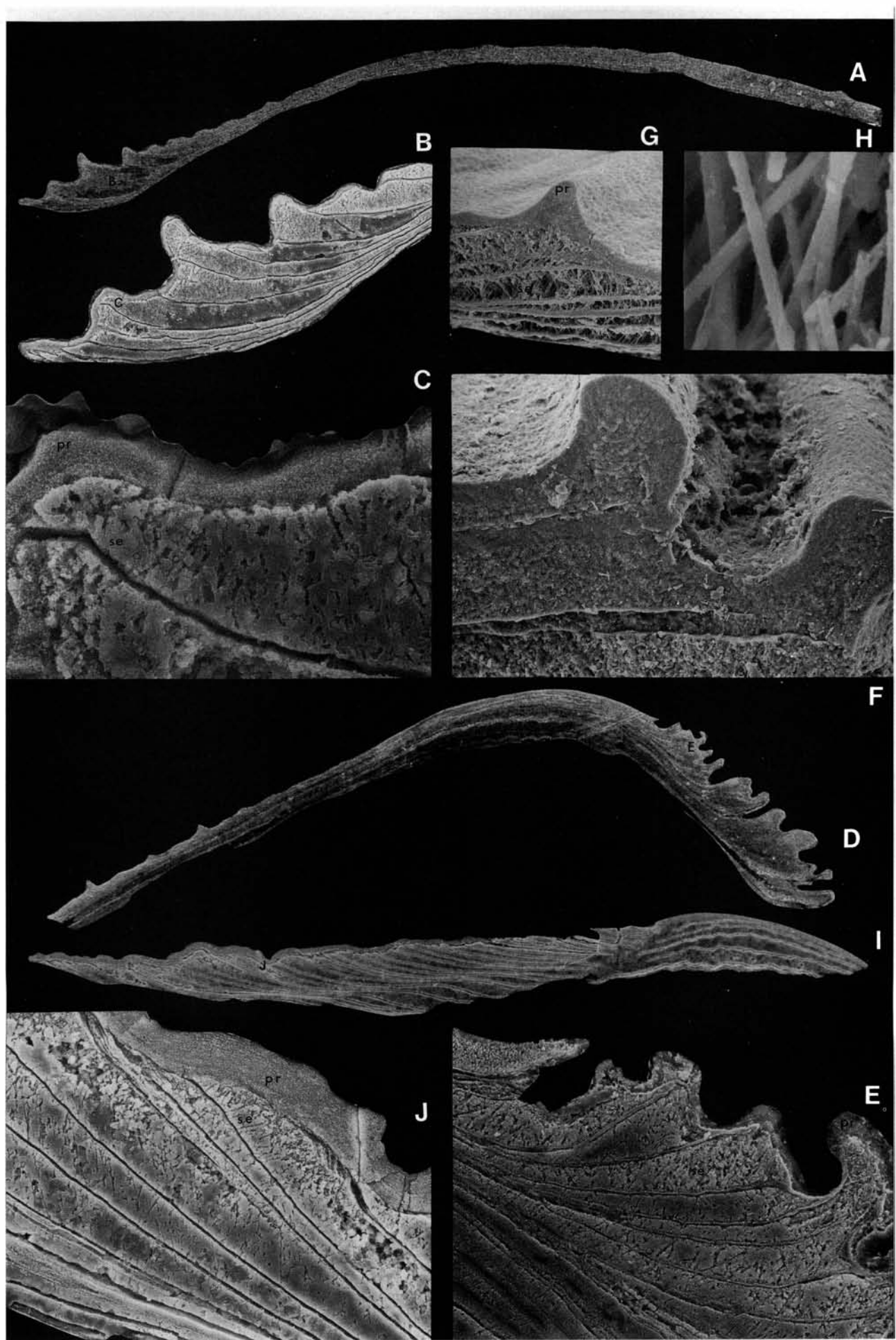
This acrothelacean family became extinct during the early Ordovician. Their shell structure was examined for comparison with the discinaceans; they have been proposed as an ancestral stock for the latter group (Rowell 1965). For this study some material of the Middle Cambrian *Acrothele coriacea* (type species of *Acrothele* Linnarsson) from Västergötland (Djupadal) was examined (Fig. 20).

In the single examined ventral valve there is no obvious division into primary and secondary layers. The anterior portion of the valve consists of flat-lying laminae, $5\text{--}25 \mu\text{m}$ thick (Fig. 20A); these have criss-crossing baculae, about 175 nm wide and $7 \mu\text{m}$ long (Fig. 20B–C). The interbacular spaces are filled with porous CCP. The laminae have a weak birefringence, but indicating a preferred orientation of apatite ϵ -axes inclined at about $40\text{--}60^\circ$ relative to the outer surface.

Discussion

It is well known that the shell of Recent lingulaceans has alternating subparallel organic and phosphatic layers (e.g., Williams & Rowell 1965a). However, recent studies by Iwata

Fig. 19. Etched sections (embedded in plastic resin) and unetched fractured surfaces (not embedded in plastic resin) through dorsal and ventral valves of Viru discinaceans; pr, primary layer; se, secondary layer. □A–C. *Schizotreta* sp. a, a dorsal valve; Skärlov Limestone (sample DLK83-sä-5); Br133608d. □A. The location of B is indicated; $\times 150$. □B. Detail of the posterior section of A, showing the distribution of wedge-shaped laminae in the secondary layer; the location of C is indicated; $\times 350$. □C. Detail of B, showing the granular primary layer and the secondary layer; note that plastic resin has partly filled the pores in the CCP of the secondary layer; $\times 2400$. □D–J. *Orbiculoidea?* sp. b; Gullhögen Formation (sample GB84-2-9). □D. Dorsal valve; the location of E is indicated; Br132676f, $\times 130$. □E. Detail of D, showing the distribution of wedge-shaped laminae in the secondary layer; note that the hollow tubules in the secondary layer (CCP and plastic resin) partly is due to the etching process; $\times 960$. □F. Detail of a fractured shell surface through D (not embedded in plastic resin), showing the homogeneous appearance of both the primary and secondary layers on an unetched surface; $\times 622$. □G. Detail of the same fragment as in F, showing a secondary layer with baculae; note that the interbacular spaces are only partly filled with CCP; $\times 421$. □H. Detail of G, showing criss-crossing baculae in the secondary layer; $\times 7600$. □I. Ventral valve; the location of J is indicated; Br132676g, $\times 130$. □J. Detail of I, showing the primary and secondary layer; note that the plastic resin has partly filled the pores of the secondary layer; $\times 740$.



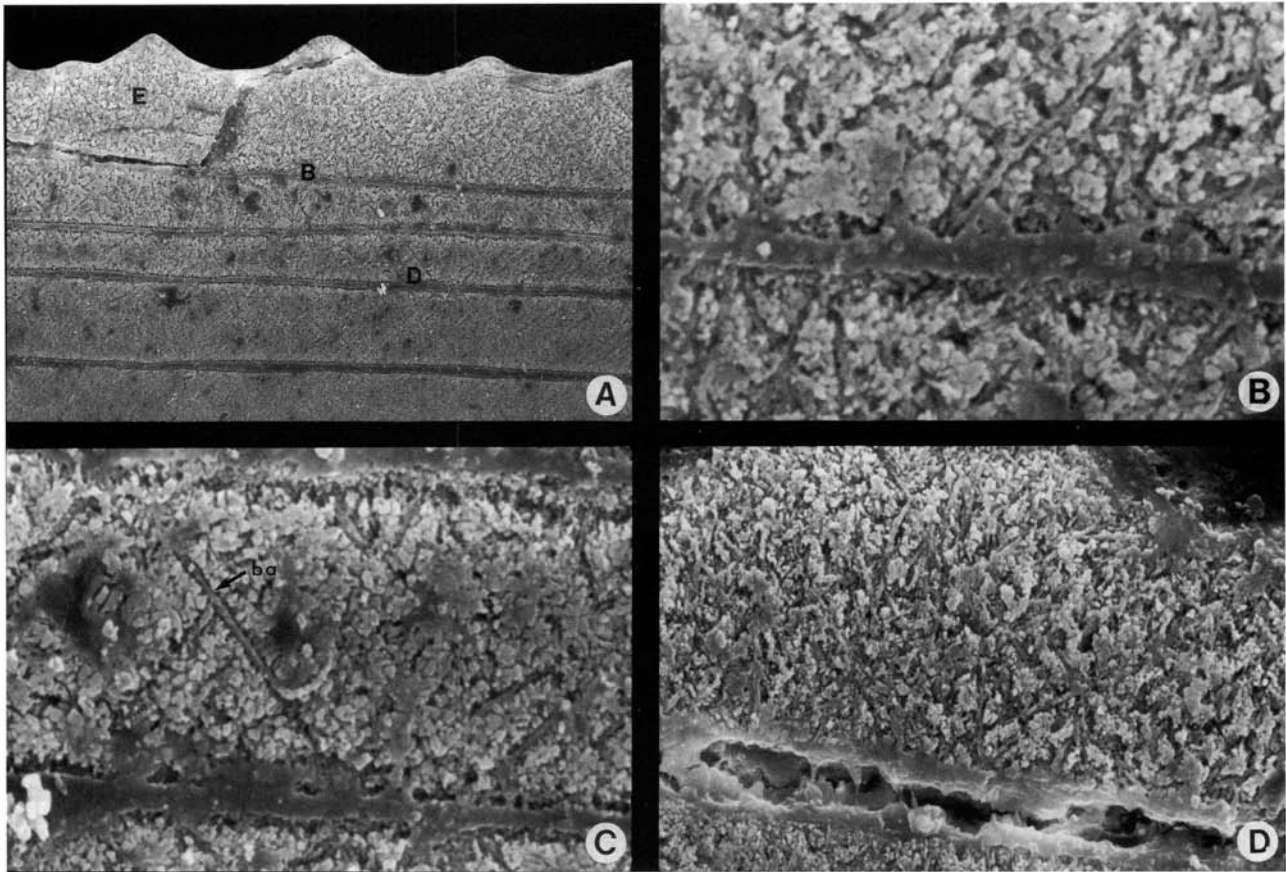


Fig. 20. □A. Detail of the anterior portion of a midsagittal section through a ventral valve of the Middle Cambrian (*Paradoxides paradoxissimus* Biozone) *Acrothele coriacea* Linnarsson, 1876; the location of B–D is indicated; Djupadal, Västergötland; Br1718d, $\times 930$. □B. Detail of A, showing a contact between two laminae; $\times 7150$. □C. Detail of A, showing criss-crossing baculae (ba) in the laminae; note that the interbacular spaces are filled with CCP; $\times 5700$. □D. Detail of A, showing the baculate structure in the outermost laminae; $\times 3500$.

(1981a, 1981b, 1982), indicate that there are fundamental differences in shell structure between the two extant genera, *Lingula* and *Glottidia*. The phosphatic layers of *Glottidia pyramidata* consist primarily of acicular apatite crystallites, arranged almost parallel to the layer (Fig. 21). In contrast, the phosphatic layers of *Lingula anatina* are divided into three 'zones', where each discrete zone consists of either subparallel acicular crystallites (A-zone), coalescent acicular crystallites (B-zone), or 'amorphous crystalline materials' and granular crystallites (C-zone; Iwata 1981b).

Moreover, the organic layers of *Glottidia pyramidata* are fibrous; the organic fibres (300 nm wide) cross one another at 50–90°, forming a reticulated (here termed criss-crossing) pattern (Iwata 1982). Most of the organic fibres are mineralized (that is, impregnated with apatite crystallites), and form apatite rods, here termed baculae (Fig. 21). However, some of the organic fibres in the baculate layer of *Glottidia* are unmineralized (Iwata 1982, Fig. 3:1; Fig. 21).

There is no baculate structure in the organic layer of *Lingula* (see Iwata 1981a, b, for details). The shell of *Lingula* is less mineralized than that of *Glottidia*, and has phosphatic layers only in the median portion of the valves, whereas the remainder of the shell consists exclusively of organic layers.

The shell structure of *Glottidia* is similar to that of Recent *Disciniscia laevis*, also described by Iwata (1982). The disciniscan shell consists of obliquely arranged, wedge-shaped laminae, and extremely finely punctate structures (the punctae are omitted in Fig. 21). This structure was described originally by Blochmann (1900). The shell of *D. laevis* can be divided into three layers, primary, secondary, tertiary (Fig. 21), where the primary and tertiary layers consist of phosphatic laminae only. In the secondary layer there is an alternation between wedge-shaped organic laminae and phosphatic laminae (Iwata 1982; Fig. 21). The phosphatic laminae consist of extremely fine, granular crystallites (Fig. 21). As in *Glottidia*, the organic laminae have criss-crossing baculae 0.1 μm in diameter (Iwata, 1982, Fig. 3, Pl. 5:1–2; Fig. 21).

The ultrastructure of *Glottidia pyramidata* was also studied by Watabe & Pan (1984), whose description does not agree with that of Iwata (1982). According to them, the primary layer and the phosphatic laminae of the secondary layer are made up of spherulites that consist of acicular crystallites (Watabe & Pan, 1984, p. 978, Fig. 2). In the organic laminae of the secondary layer (referred to as the chitin layers by Watabe & Pan), aggregates of spherulites form rods; 'These rods often branch out and form 'X' figures that are oriented obliquely to the shell surface' (Watabe & Pan,

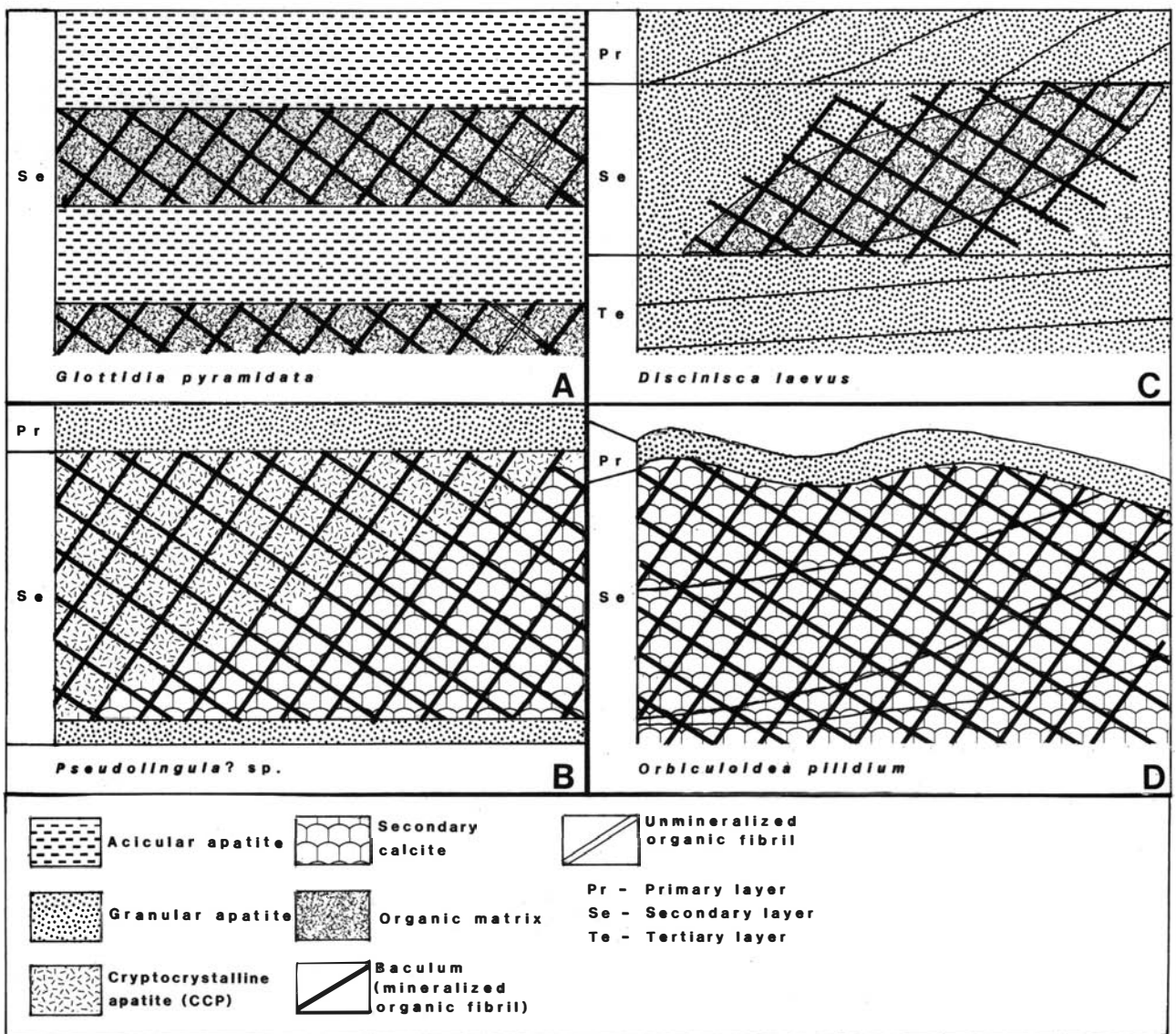


Fig. 21. Diagrammatic comparison of shell structures of some Recent and lower Palaeozoic lingulaceans and discinaceans; not to scale. □A. Recent *Glottidia pyramidata*, showing the structure of the secondary layer, with alternation between phosphatic laminae consisting of acicular apatite crystallites with parallel c -axis orientation, and organic laminae with criss-crossing baculae and unmineralized organic fibrils; punctae omitted; after Iwata 1982, Fig. 1. □B. Silurian *Pseudolingula?* sp. from the Hemse beds, Petesvik, Gotland, showing a primary layer consisting of granular apatite, and a secondary layer with baculate structure; after Br124967. □C. Recent *Discinisca laevis*, showing the primary and tertiary layers with granular apatite, and the alternation between wedge-shaped organic laminae with baculae, and laminae of granular apatite in the secondary layer; punctae omitted; after Iwata 1982, Fig. 2. □D. Silurian *Orbiculoidea pilidium* from the Eke beds, Lau backar, Gotland, showing the primary layer of granular apatite, and the wedge-shaped baculate laminae in the secondary layer; after Br24478.

1984, p. 979, Fig. 3). According to the same authors the baculae illustrated by Iwata (1982) from *G. pyramidata* are lacking. However, it appears that the pattern of 'X' rods (although thicker and consisting of 'spherulites' rather than 'apatite needles') is comparable with the criss-crossing baculate structure described by Iwata.

The shell structure of the Lower Palaeozoic lingulaceans examined for this study is similar to that of *Glottidia pyramidata* (cf. Fig. 21) in that there is a well defined phosphatic primary layer (in *Pseudolingula?* sp., *Obolina?* gen. et sp. a, and *Rowellella* cf. *lamellosa*), as well as baculate structure in the laminae of the secondary layer (in *Ungula ingraca* and *Pseudolingula?* sp.; Fig. 21).

Similarly, the Lower Palaeozoic discinaceans have a shell structure that agrees closely with that of *Discinisca laevis*.

The wedge-shaped baculate laminae in the secondary layer in *Orbiculoidea pilidium* and *Orbiculoidea?* sp. b are considered to be homologous with the organic laminae with baculate structure in the secondary layer of *D. laevis* (Fig. 21).

The detailed structure of the baculate laminae differs between the fossil and Recent forms. According to Iwata (1982) the baculae in Recent *Glottidia pyramidata* are about 0.3 μ m in diameter and consist of granular apatite. The same author notes also that the baculae in *Discinisca laevis* are similar in structure to those of *Glottidia* but are smaller, about 0.1 μ m in diameter. In contrast, the baculae described above are more variable in diameter; from about 0.2 μ m in *Acrothele coriacea* to 0.7 μ m in *Pseudolingula?* sp. They consist of the following three types of apatite crystal-

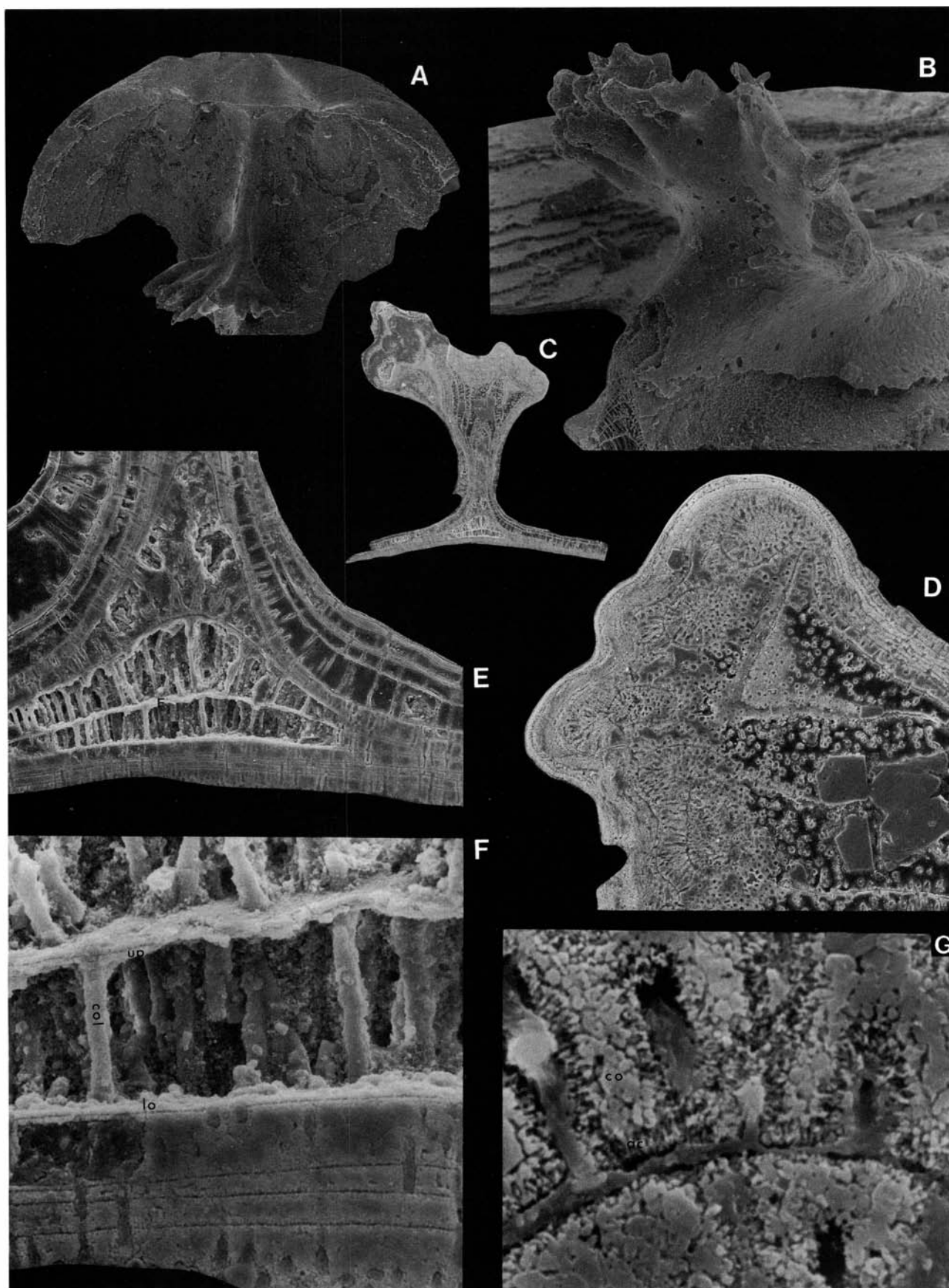


Fig. 22. □A. Dorsal valve of *Prototreta attenuata* (Meek, 1873); Middle Cambrian Swasey Limestone, Topaz Mountains, Utah (coll. R.A. Robison); Br133660, $\times 30$. □B. Oblique anterior view of the median septum of A; $\times 100$. □C. Transverse section through A; $\times 78$. □D. Detail of C, showing the columnar structure of the median septum; $\times 320$. □E. Detail of C, showing the columnar structure of the secondary layer, $\times 360$. □F. Detail of C, showing that the laminae consist of upper (up) and lower (lo) lamellae, connected by columns (col); $\times 1600$. □G. Detail of C, showing the normal orientation of acicular apatite crystallites (ac) in the lamellae and columns, and the CCP (co) in the intracolumnar spaces; $\times 6000$.

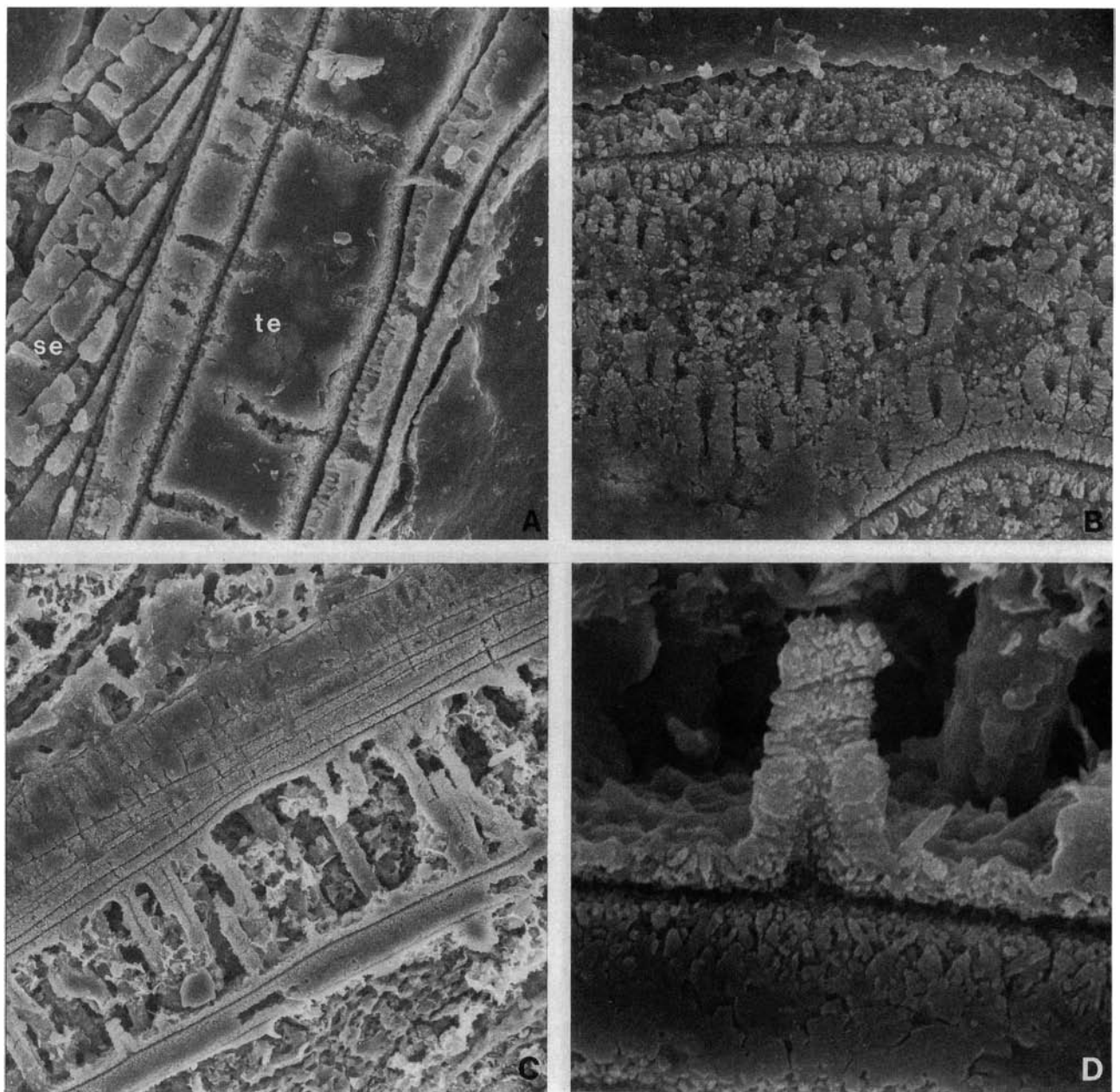


Fig. 23. □A. Detail of an oblique section through a ventral valve of *Conotreta? mica* Goryanskij, showing the wedge-shaped laminae in the camerate secondary layer (se), and the columnar tertiary layer (te); Skärlov Limestone (sample DLK83-sä-7); Br129003b, $\times 2000$. □B. Detail of the apical process of A, showing the columnar tertiary layer; $\times 2000$. □C. Detail of an oblique section through a ventral valve of *Conotreta? mica* Goryanskij, showing the columnar laminae of the tertiary layer; Skärlov Limestone (sample DLK83-sä-8); Br133611b, $\times 1000$. □D. Detail of C; note that the columns and lamellae consist of acicular apatite crystallites; $\times 6600$.

lites: (a) needle-shaped (*Ungula ingrlica*), (b) minute granulae (*Orbiculoidea pilidium*, *Orbiculoidea?* sp. b), or (c) flattened platelets (*Pseudolingula?* sp.). The variation in shape and structure of the apatite is possibly due to some recrystallisation.

There is also some difference between Recent and fossil species in the structure and composition of the apatite that fills the interbacular spaces. In Recent *Glottidia* and *Discinisca* these spaces are filled entirely with organic matrix (Fig. 21; see also Watabe & Pan 1984). In contrast, the interbacular spaces of the Lower Palaeozoic species are most frequently filled with an undifferentiated type of cryptocrystalline ('collophane-like') calcium phosphate

(CCP), which generally lacks or has only a weak birefringence. The apatite has a porous microstructure and contains a considerable amount of empty spaces; in life the empty spaces may have contained organic matrix.

The amount of remaining organic material in the fossil species was not determined, but previous examinations of Lower Palaeozoic lingulaceans and discinaceans have shown that they contain about 4–19% organic substances (e.g., Rhodes & Bloxam 1971, Table 3).

In many of the examined lingulaceans and discinaceans (*Orbiculoidea?* sp. b, *Schizotreta* sp. a, *Rosobolus?* sp. nov. a, *Rowwella* cf. *lamellosa*, and obolinae gen. et sp. a) the laminae of the secondary layer sections appear to lack baculae.

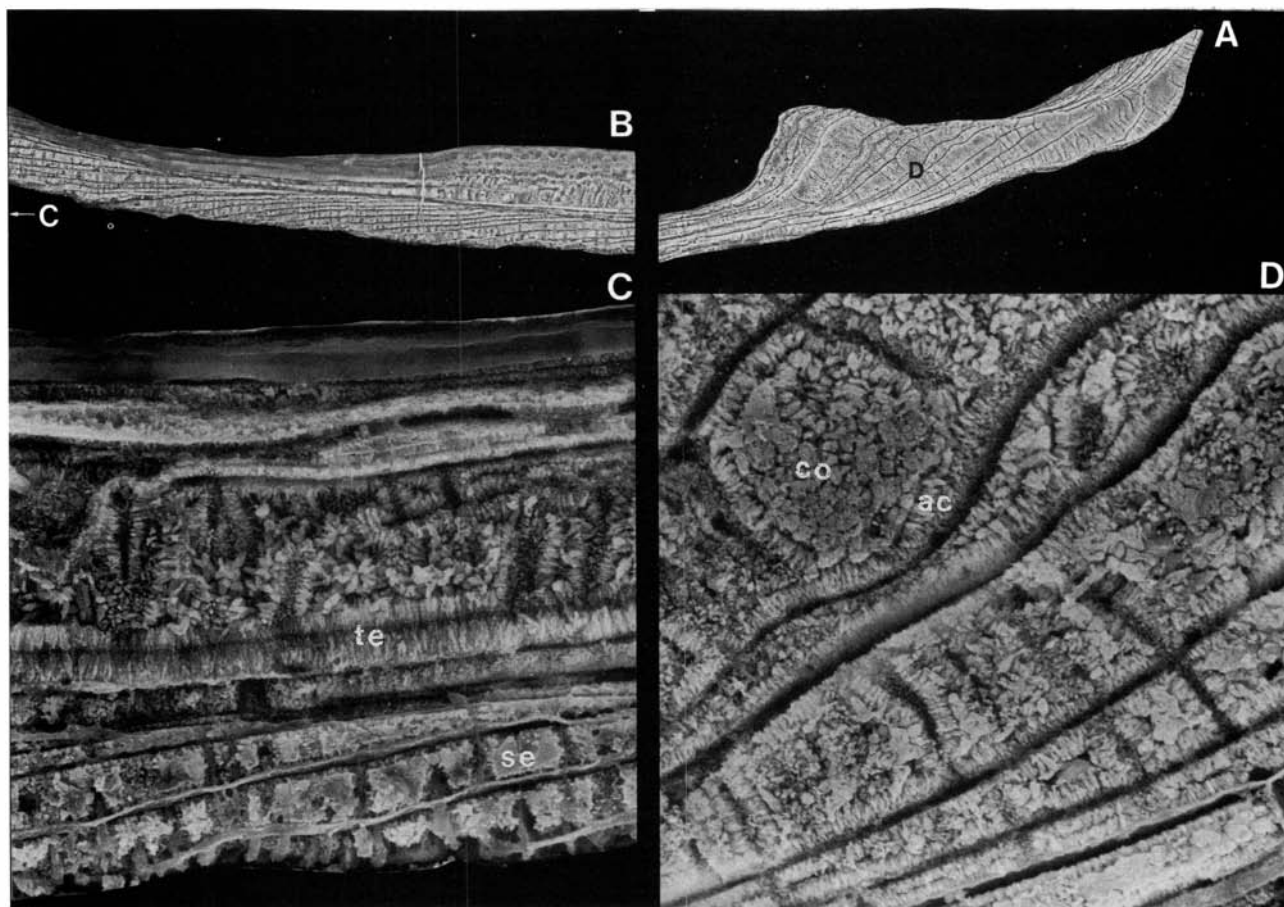


Fig. 24. □A. Detail of the posterior portion of a midsagittal section through a dorsal valve of *Spondylotreta* sp. nov. a; the location of D is indicated; Folkelslunda Limestone (sample DLK83-fo-1); Br133628b, $\times 200$. □B. Detail of the median section of A; the location of C is indicated; $\times 360$. □C. Detail of A, showing the wedge-shaped camerate laminae in the secondary layer (se), and the columnar tertiary layer (te); $\times 2000$. □D. Detail of A, showing the structure of the columnar tertiary layer; ac, acicular apatite crystallites; co, CCP; $\times 2000$.

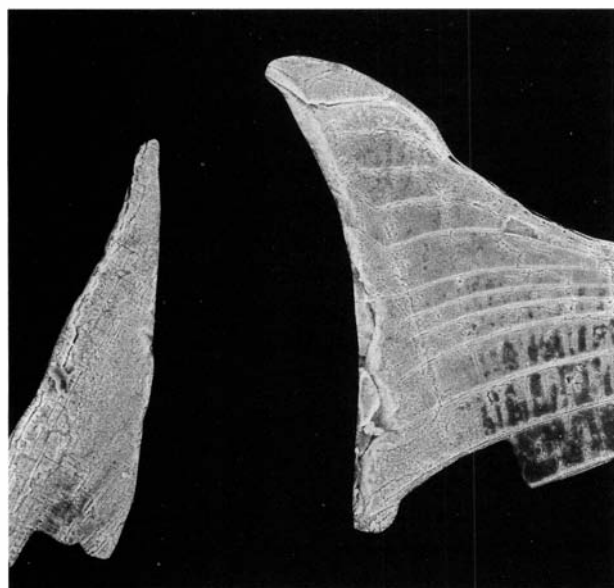


Fig. 25. Midsagittal section through a ventral valve of *Physotreta deformis* sp. nov., showing the columnar laminae in the apical process; Folkelslunda Limestone (sample DLK83-fo-5); Br133636c, $\times 160$.

Instead they consist almost entirely of CCP, in which there is a criss-crossing pattern of hollow tubes. As noted above, there are both mineralized (baculae) and unmineralized organic fibres in the organic laminae of *Glottidia* (Iwata 1982, Fig. 3:1); the hollow tubes could have contained unmineralized organic fibres that have disappeared post-mortem, but it is also possible that the thin baculae were dissolved in the etching process; at least this seems to have been the case in *Orbiculoidea?* sp. b., where the hollow tubes are encountered in the embedded and etched sections (Fig. 19E, J), whilst many fractured and unetched surfaces show well developed baculae (Fig. 19G–H). In specimens of *Pseudolingula?* sp. and *Orbiculoidea pilidium*, sectioned while still within matrix, some interbacular spaces (which otherwise would have been empty) are filled with secondary calcite (Fig. 21).

Acrotretacea

Acrotretinae and Torynelasmatinae

The shell structure of one Middle Cambrian and several Middle Ordovician acrotretines, as well as one torynelasma-

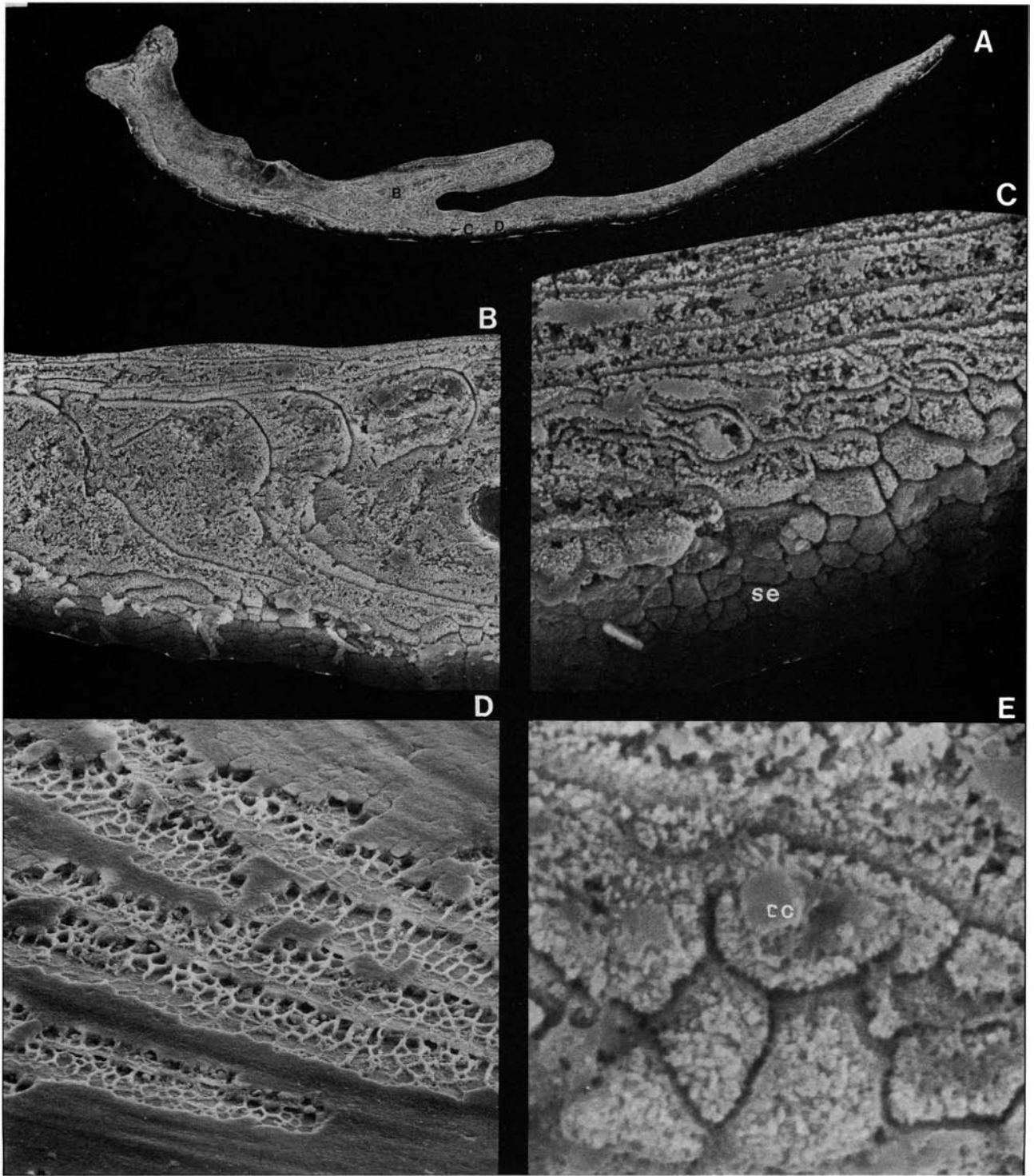


Fig. 26. □A. Midsagittal section through a dorsal valve of *Hisingerella unguicula* sp. nov.; the location of C and D is indicated; Seby Limestone (sample DLK83-se-1); Br133612c, $\times 230$. □B. Detail of A, showing the columnar laminae in the median septum; $\times 1100$. □C. Detail of A, showing the camerate secondary layer (se); $\times 2600$. □D. Detail of Fig. 62A, showing a dorsal exterior where the primary layer is partly exfoliated; note the 'honeycomb-like' arrangement of empty chambers in the camerate secondary layer; Gullhög Formation (sample GB84-1-1); Br128625, $\times 1000$. □E. Detail of A, showing the chambers of the camerate secondary layer; note that the chambers are filled with CCP (co); $\times 7800$.

tine, was examined both under the SEM and in polarized light; the structure of the two subfamilies is very similar, and they are therefore discussed together.

(1) In the Middle Cambrian *Prototreta attenuata*, a primary layer could not be identified in sections examined under the SEM, probably because of the thinness of the layer.

Moreover, the contact between the surface of the specimen and the embedding resin is frequently not perfect, and the resulting gap can obscure details of a thin outermost layer. Judging from the surface of slightly exfoliated shells, the primary layer is a very thin granular 'sheet', less than $1 \mu\text{m}$ thick.

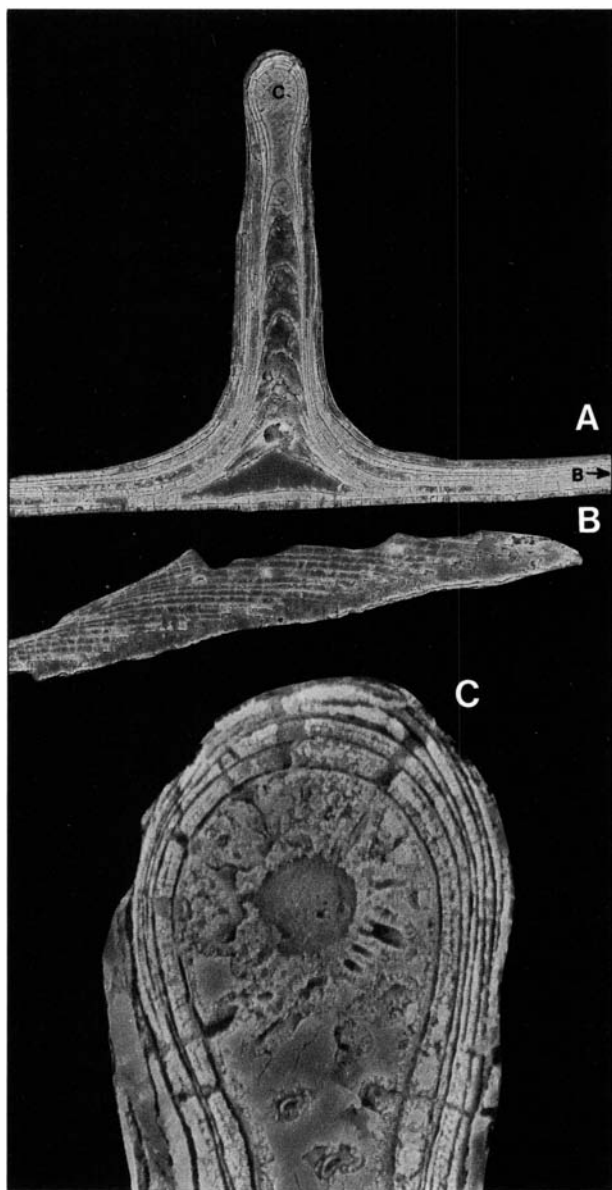


Fig. 27.

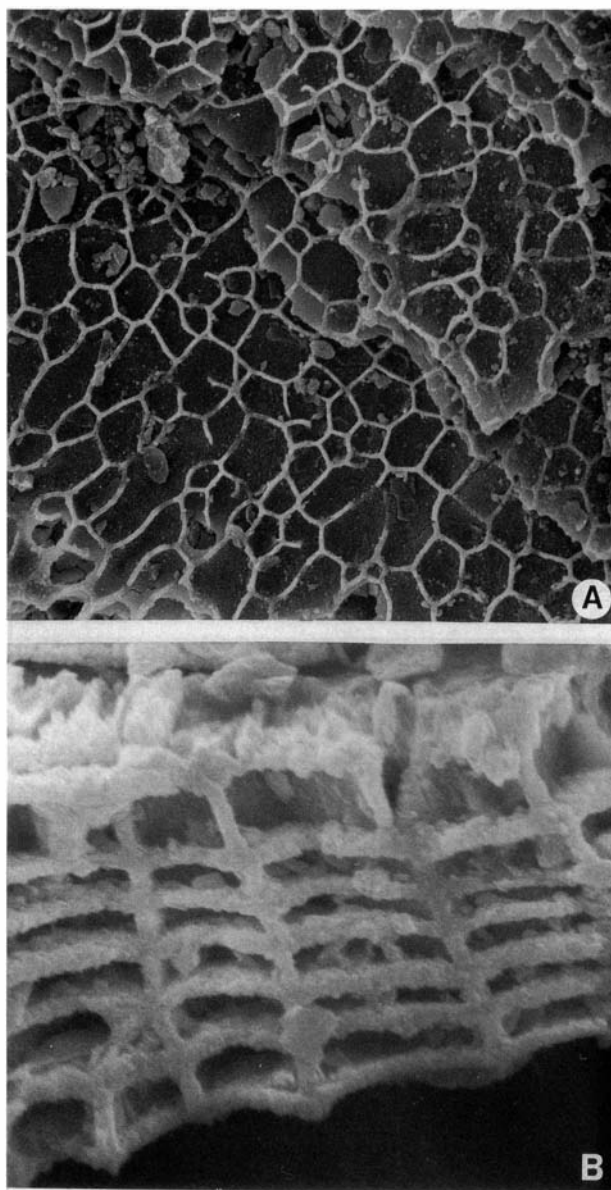


Fig. 28.

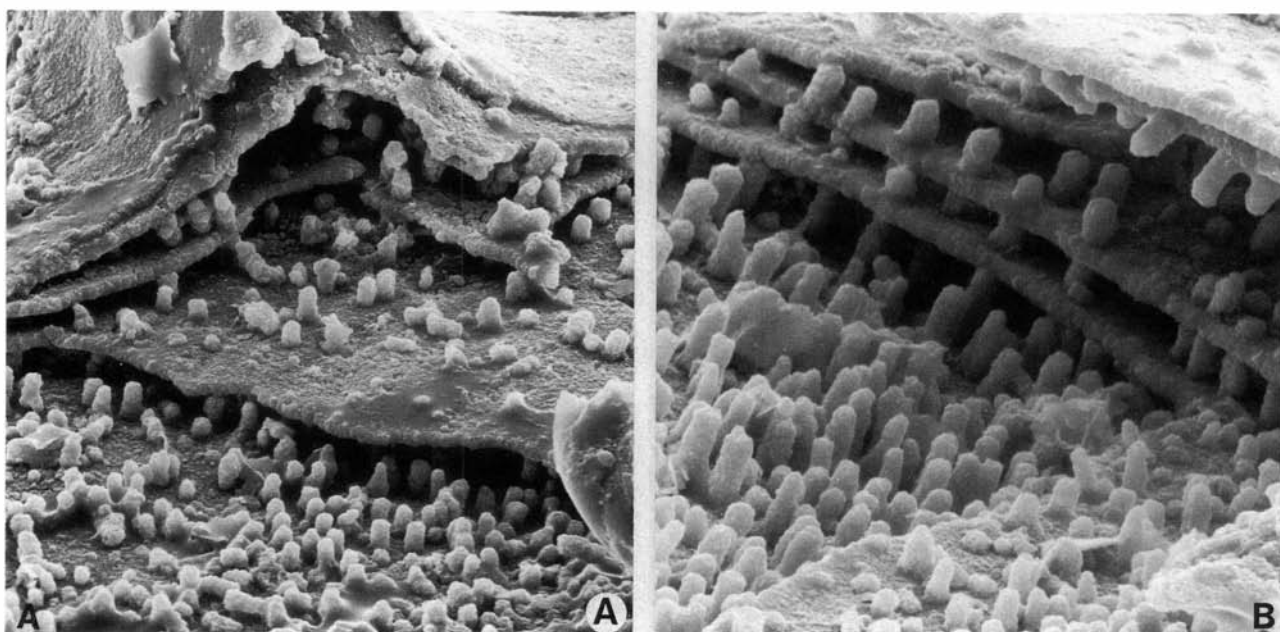


Fig. 29 .

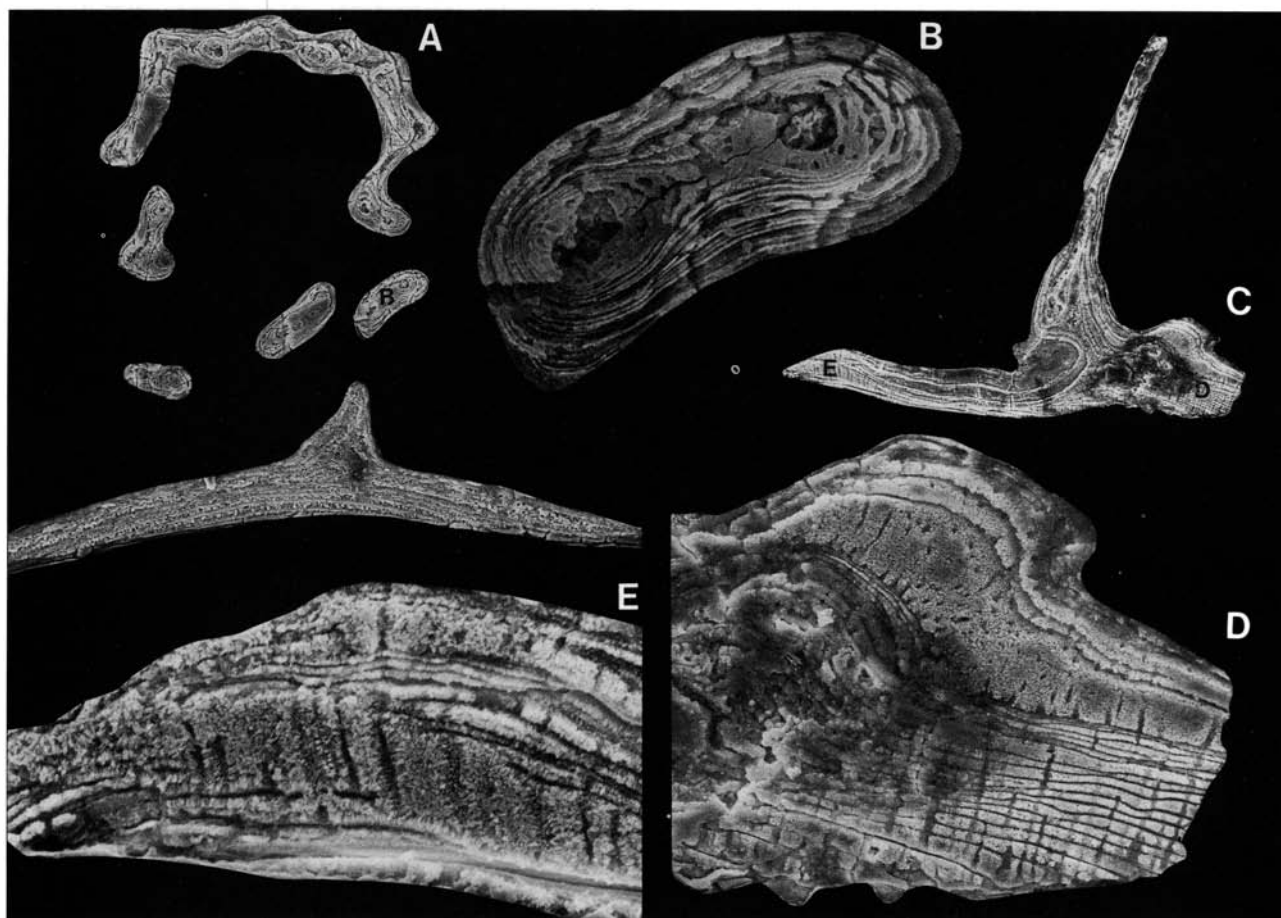


Fig. 30. □A–B. Transverse section through a dorsal valve of *Numericomma perplexa* sp. nov.; Furudal Limestone (sample DLK83-fur-12); Br132394d. □A. Section through the median septum; the location of B is indicated; $\times 10$. □B. Detail of A; $\times 1300$. □C–E. Midsagittal section through a dorsal valve of *Numericomma simplex* sp. nov.; Kårgårde Limestone (sample DLK83-segk-6); Br133595m. □C. The location of D and E is indicated; $\times 160$. □D. Detail of the posterior portion of C, showing the columnar secondary layer; $\times 720$. □E. Detail of the anterior section of C; $\times 1200$.

The secondary layer of the Middle Cambrian species is well developed and thick, forming all of the interior morphological features (Fig. 22). In section it consists of numerous columnar laminae, varying in thickness from about 3 to 42 μm (Fig. 22E). Each discrete lamina is defined by a

Fig. 27 (opposite page, top left). □A. Detail of a transverse section through a dorsal valve of *Conotreta? siljanensis* sp. nov., showing the structure of the median septum; the location of B and C is indicated; Gullhøgen Formation (sample GB84-2-19); Br132719b, $\times 260$. □B. Lateral section of A, showing the wedge-shaped camerate laminae in the secondary layer; $\times 200$. □C. Detail of A, showing the columnar laminae in the median septum; $\times 1600$.

Fig. 28 (opposite page, top right). □A. Detail of the shell structure of the exterior of a slightly exfoliated dorsal valve (see also Fig. 74D) of *Torynelasma suecicum* sp. nov., showing the camerate secondary layer; Ryd Limestone (sample GB84-3-59); Holotype; Br128826, $\times 1000$. □B. Detail of the shell structure of A, showing the columnar tertiary layer; $\times 3900$.

Fig. 29 (opposite page, bottom). □A. Detail of shell structure of a slightly exfoliated dorsal interior of *Numericomma perplexa* sp. nov., showing the columnar secondary layer; Furudal Limestone (sample D60-220); Br128783, $\times 1500$. □B. Detail from the same general area as in A; $\times 2200$.

thin upper and a lower lamella, about 1 μm thick. The lamellae are connected by numerous columns (about 3 μm in diameter), and aligned perpendicular to the lamellae (Fig. 22E–G). The columns are hollow, with a central canal about 1 μm in diameter (Fig. 22G).

The lamellae and columns consist of needle-shaped apatite crystallites, about 170 nm wide and 1 μm long, with the *c*-axis orientation perpendicular to the lamellae and columns (Fig. 22G). The intercolumnar spaces are occasionally empty, thus exposing the columns in relief (Fig. 22E–F), but more commonly the spaces are filled with CCP (Fig. 22F–G).

The relatively complex spinose median septum of *Prototreta attenuata* is formed entirely through successive discrete columnar laminae wrapped into various shapes (Fig. 22C–D); septal spines are formed by finger-shaped projections from the laminae (Fig. 22D).

(2) The acrotretines *Conotreta? mica* (Fig. 23), *Conotreta? siljanensis* (Fig. 27), *Spondylotreta* sp. nov. a (Fig. 24), *Physotreta deformis* (Fig. 25) and *Hisingerella? unguicula* (Fig. 26) share a common type of shell structure (Fig. 40A).

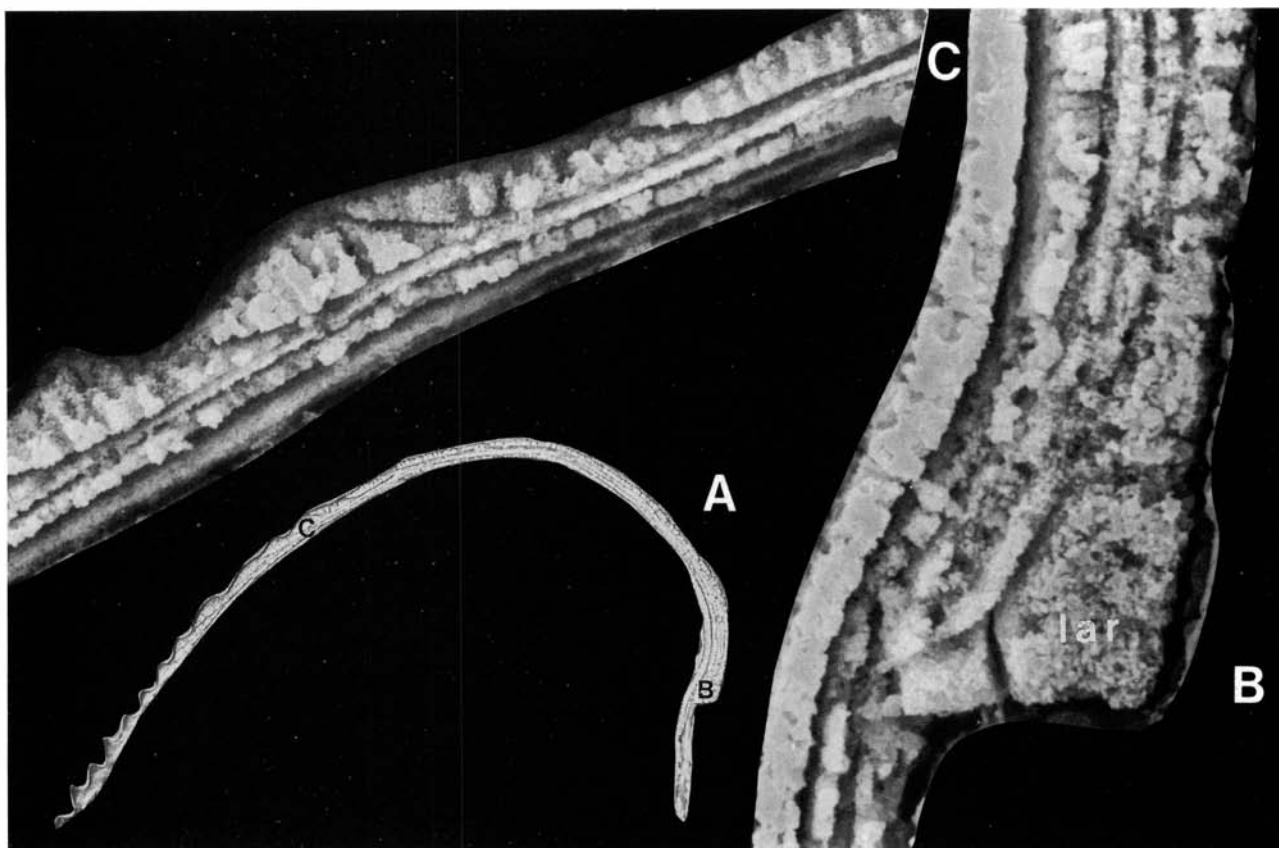


Fig. 31 (opposite page). □A. Midsagittal section through a ventral valve of *Myotreta dalearlica* sp. nov.; the location of B and C is indicated; Skärlov Limestone (sample DLK83-sä-6); Br133609h, $\times 276$. □B. Detail of the posterior section of A, showing the edge of the larval shell; $\times 3315$. □C. Detail of A, showing the wedge-shaped columnar laminae in the secondary layer; $\times 2070$.

From slightly exfoliated surfaces (e.g., Fig. 26D), it appears that there is a thin (less than $1\ \mu\text{m}$), outermost primary layer of granular apatite that covers the camerate secondary layer (Fig. 40A). However, the primary layer could not be identified in sections, neither under the SEM nor in transmitted light.

In the acrotretines the secondary layer consists of camerate laminae. In sagittal sections they are wedge-shaped, about $4\ \mu\text{m}$ thick, and inclined at $10\text{--}30^\circ$ to the outer surface of the valve (Figs. 23A, 24B–C, 26D, 27B, 40A). Each of the camerate laminae is defined by an upper and a lower lamellae, $1\ \mu\text{m}$ thick (Fig. 24C), which are connected by perpendicular walls, $3\ \mu\text{m}$ thick (Figs. 26C, E, 40A).

The camerate structure is best observed in slightly exfoliated specimens, where the primary layer has been peeled off to expose the honeycomb-like pattern of small polygonal chambers beneath (e.g., Figs. 26D, 64C). The lamellae and walls are made up of needle-shaped crystallites in which the long axes are normal to the surfaces. Examination in polarized light indicates that this agrees with the c -axis orientation. In broken and exfoliated valves the space inside the chambers is occasionally empty (Fig. 26D), but they are more commonly filled with CCP (Figs. 26E, 40A).

The acrotretine species examined have a columnar tertiary layer (Fig. 40A) that forms all interior structures of both valves, such as the median septum (Fig. 26A–B, 27A, C), the apical process (Figs. 23B, 25), and the muscle scars (Fig. 24A, D). As in *Prototreta*, this layer consists of laminae of

varying thickness, with an upper and a lower lamellae connected by perpendicular columns (Figs. 23C–D, 24C–D, 25). The needle-shaped crystallites are arranged with their c -axis normal to the lamellae and walls (Figs. 23D, 24D). In sections through the apical process the columnar laminae are arranged more or less perpendicular to the outer surface (Fig. 25). The median septum is formed as in *Prototreta* (Figs. 26B, 27A, C). In more thin-shelled species like *Hisingerella? unguicula* the tertiary layer is comparatively thin and the valves consist almost exclusively of the secondary layer (Fig. 26A).

Broken and exfoliated surfaces of the acrotretines *Cyrtotreta vestrogothica* (Fig. 64C), *Cyrtotreta? striata* (Fig. 66B), *Hisingerella billingensis* (Fig. 61I), *Spondylotreta orsaensis*, and the torynelasmatine *Acrotretella* sp. (Fig. 76E) indicate that camerate secondary and columnar tertiary layers are present in these species also.

(3) The single examined torynelasmatine, *Torynelasma suecicum*, has a shell structure close to that of the acrotretines (Fig. 40A). Some exfoliated and broken valves show a camerate secondary layer (Fig. 28A), in addition to a columnar tertiary layer (28B).

Ephippelasmatinae and *Biernatinae*

Middle Ordovician species of these two subfamilies have the same type of shell structure, with a thin primary layer and a thicker columnar secondary layer (Fig. 29). Camer-

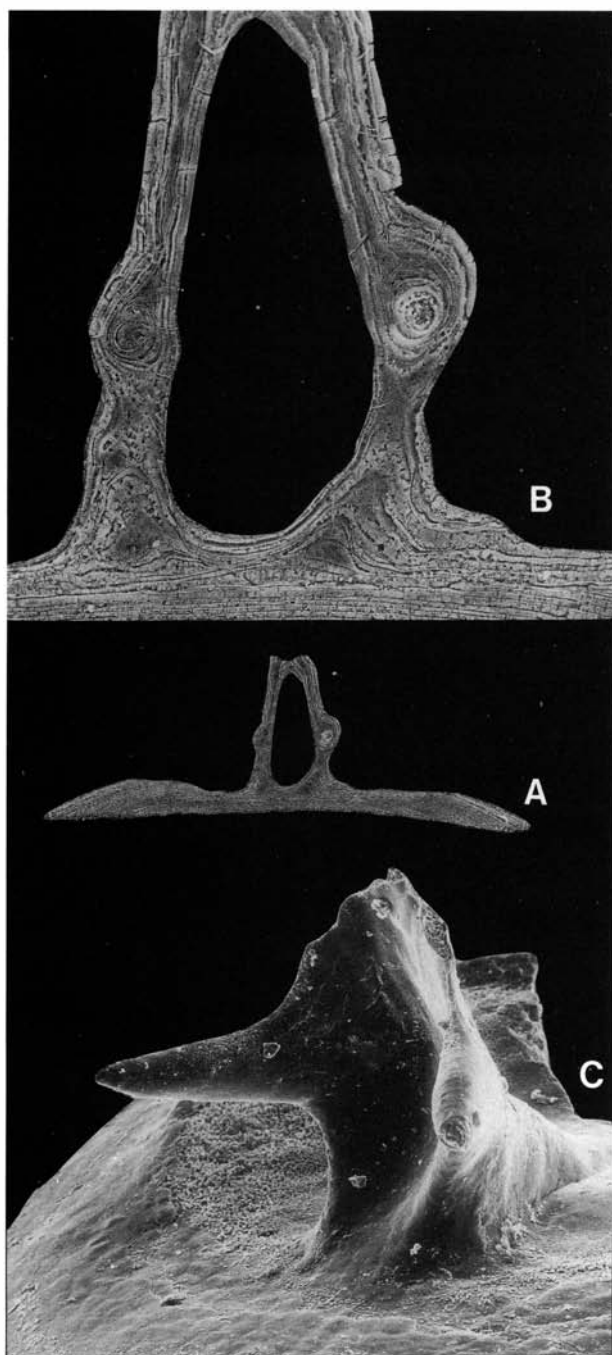


Fig. 32. Dorsal valves of *Ehippelasma minutum* Cooper, 1956 □A. Transverse section through the median septum; Furudal Limestone (sample DLK83-fur-16); Br132430c, $\times 100$. □B. Detail of A; $\times 440$. □C. Oblique anterior view of a median septum; Furudal Limestone (sample D60-215); Br128652, $\times 240$.

ate structures have not been identified from members of either subfamily (Fig. 40B).

The shell structure of the following Ehippelasmatinae was studied in transmitted light and/or under the SEM: *Numericoma perplexa* (Figs. 29, 30A–B), *Numericoma simplex* (Fig. 30C–E), *Numericoma? spinosa* (Fig. 33), *Myotreta dalecarlica* (Fig. 31) and *Ehippelasma minutum* (Fig. 32).

The primary layer of the ehippelasmatinae is difficult to recognize in the sections. The secondary layer consists of columnar laminae, varying in thickness from about 1 to

20 μm . The outer laminae of both valves are wedge-shaped in cross section (Figs. 30E, 31C, 32A, 33D). In some species there are subparallel columnar laminae of uniform thickness interior to the wedge-shaped laminae, (Figs. 31C, 33D), but no well defined tertiary layer can be distinguished. The columnar laminae are identical to those described from other acrotretaceans (Figs. 29, 30D–E, 40B).

There are minute needle-shaped crystallites, about 1 μm long, in the lamellae and columns of *Numericoma simplex* (Fig. 29D–E). The needles are oriented with their *c*-axis normal to the lamellae and the columns (Fig. 30D–E). Identical crystallites are also present in specimens of *Ehippelasma minutum*.

The fine structure of all examined valves of *Numericoma perplexa*, *Numericoma? spinosa*, and *Myotreta dalecarlica* is different from that described above. The lamellae have a granular microstructure (Figs. 30A–B, 31, 33), and the preferred *c*-axis orientation appears to be almost parallel to the lamellae. The significance of this difference is not yet understood, but it could be due to recrystallisation.

In slightly exfoliated and broken valves of most ehippelasmatinae species the intercolumnar spaces are empty, and the columns stand out in relief (Fig. 29A–B). In undamaged valves, however, the space is filled with CCP (Figs. 30D–E, 40B). The dorsal median septum of the ehippelasmatinae is formed as in all other acrotretaceans (Figs. 29A–C, 32).

Sections through the umbonal part of, e.g., *Myotreta dalecarlica* indicate that the larval shell constitutes a well separated plate (Fig. 31A–B), which consists of CCP.

Biematia holmi (Figs. 34, 35) has a shell structure that is identical to that of the ehippelasmatinae (Fig. 40B).

Scaphelasmatinae

In *Scaphelasma mica* the primary layer is identical to that of all other acrotretaceans (Fig. 40C). Interior to the primary layer there is a well developed secondary layer with camerate laminae. In sagittal sections the laminae are elongately wedge-shaped and meet the outer surface of the valve at a much varying, oblique angle (Figs. 36B–C, E, 40C). As in the acrotretines, the camerate laminae are built up by an upper and a lower lamella, connected by perpendicular walls (Figs. 36B–C, E, 40C). The optical properties of the sectioned valves are not readily determinable; the birefringence of the shell is very weak.

The camerate laminae are observed best on the interior surface of both valves, in places where the inner lamella is slightly exfoliated (e.g., Figs. 99H, 100F, 102D); the chambers of the camerate laminae are elongated in the direction of growth, and form parallel 'tubes' of rectangular cross section (cf. Poulsen 1971, Fig. 4). As in the acrotretines, the spaces within the chambers are empty in most exfoliated specimens, but in sections through undamaged shells, the chambers are filled with CCP (Fig. 36B–C, E). Examination of internal exfoliated surfaces indicates that the connecting walls of the camerate laminae are formed by closely spaced rows of columns that gradually merge in the direction of growth (Fig. 100F).

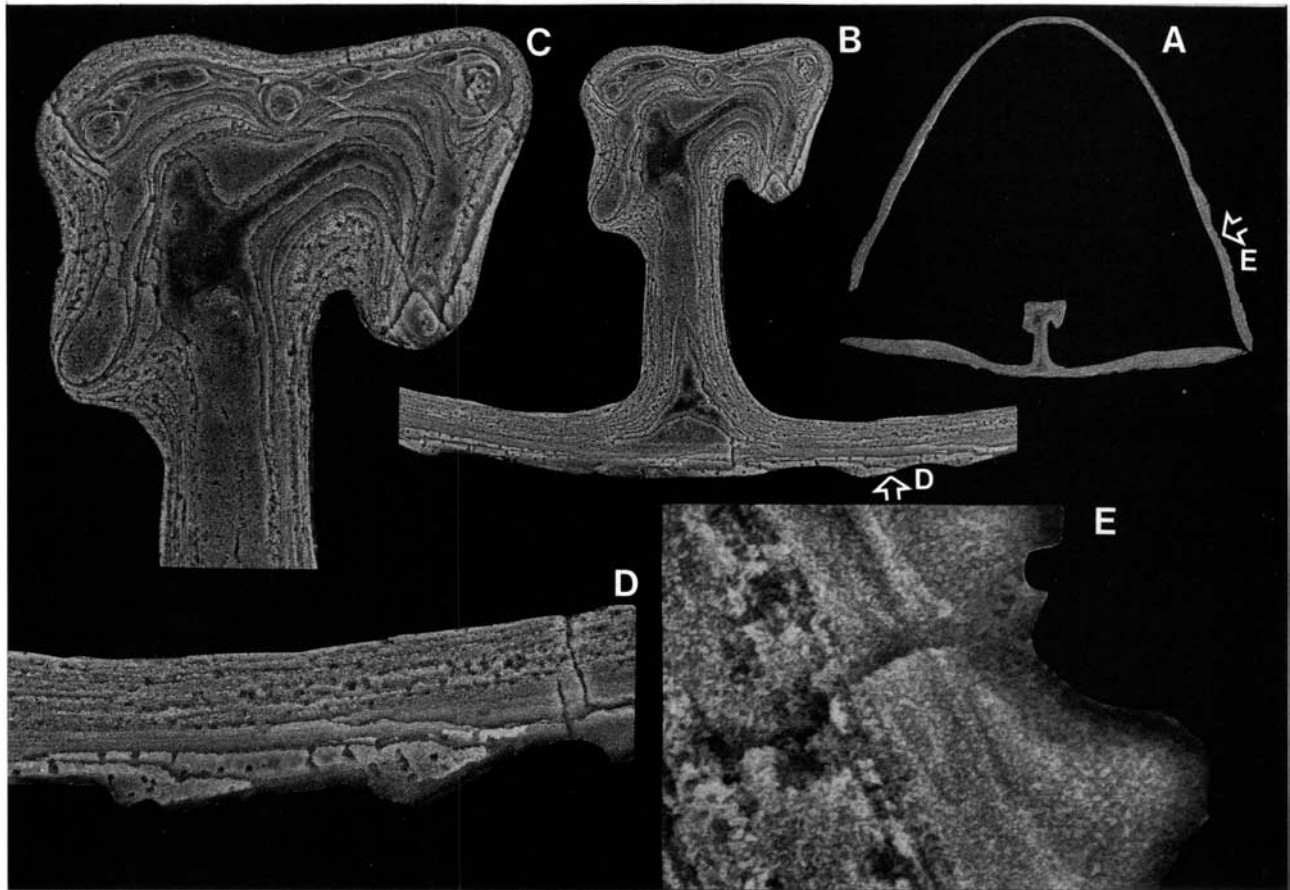


Fig. 33. □A. Transverse section through a complete shell of *Numericomma? spinosa* (Biernat, 1973); the location of E is indicated; Skärlov Limestone (sample DLK83-sä-8); Br133609f, $\times 72$. □B. Detail of A; the location of D is indicated; $\times 400$. □C. Detail of B, showing structure of median septum; $\times 780$. □D. Detail of B, showing the wedge-shaped laminae in the secondary layer; $\times 1000$. □E. Detail of A; $\times 4800$.

Eoconulidae

The shell structure was examined in *Eoconulus* cf. *clivosus* Popov (Figs. 38A–B, 39A–H), *E. cf. cryptomyus* Goryanskij (Fig. 38C), and *E. sp. nov. a* (Figs. 38D, 37); the pattern of development remains somewhat unclear.

(1) The single dorsal valve of *Eoconulus* cf. *clivosus* examined shows little structure under the SEM; there are some poorly developed laminae that are slightly wedge-shaped and meet the outer surface at a much varying angle (Fig. 38A–B).

In contrast, there are no wedge-shaped laminae in the sectioned ventral valves of *E. cf. clivosus*. Instead, numerous very fine, parallel, successive lamellae are stacked one on top of the other (Fig. 39E–H). The outermost lamella must have been secreted first (at about the adult stage), and the successive lamellae were then deposited inwards. Examination of the ventral and dorsal valves in polarized light gave no clear indications of the ϵ -axis orientation.

The external and internal surfaces of the ventral valve of *E. cf. clivosus* have numerous 'pores' which never penetrate the entire shell thickness (Fig. 39A–D). The lamellae are observed to follow the outline of the 'pores'.

(2) A dorsal valve of *Eoconulus* sp. nov. a has wedge-shaped columnar laminae. Interior to this a layer with fine subparallel lamellae is developed (Fig. 38D).

The ventral valve of the same species is relatively thin (Fig. 37). There is a poorly defined outer layer (Fig. 37B), and in the central portion it consists of a single $3\ \mu\text{m}$ thick lamella. Away from the centre, the outer layer becomes up to $7\ \mu\text{m}$ thick, and there are well developed wedge-shaped laminae (Fig. 37C–D). Interior to this there are thin parallel lamellae (Fig. 37C). The wedge-shaped laminae appear to consist of CCP, whereas the lamellae are minutely granulose (Fig. 37D). The exterior of the ventral valve has some 'pores' (Fig. 37A), but none were observed in the sections examined.

(3) The dorsal valve of *Eoconulus* cf. *cryptomyus* has an almost homogeneous shell, with only some subparallel lamellae that consist of minute granular crystallites, $400\ \text{nm}$ across (Fig. 38C)

Discussion

The shell structure of acrotretaceans was described briefly by Williams & Rowell (1965a, p. H78, Fig. 77:4A–B). In the ceratretine *Keyserlingia* (= *Clistotrema* Rowell) they noted wedge-shaped, thick laminae, inclined obliquely relative to the outer surface. The laminae in *Keyserlingia* were reported to 'have a strongly fibrous structure, the fibres being arranged normal to the lamellae' (Williams & Rowell 1965a, p. H78), alternating with thinner bands that lack the fibrous structure. According to Williams & Rowell (1965a),

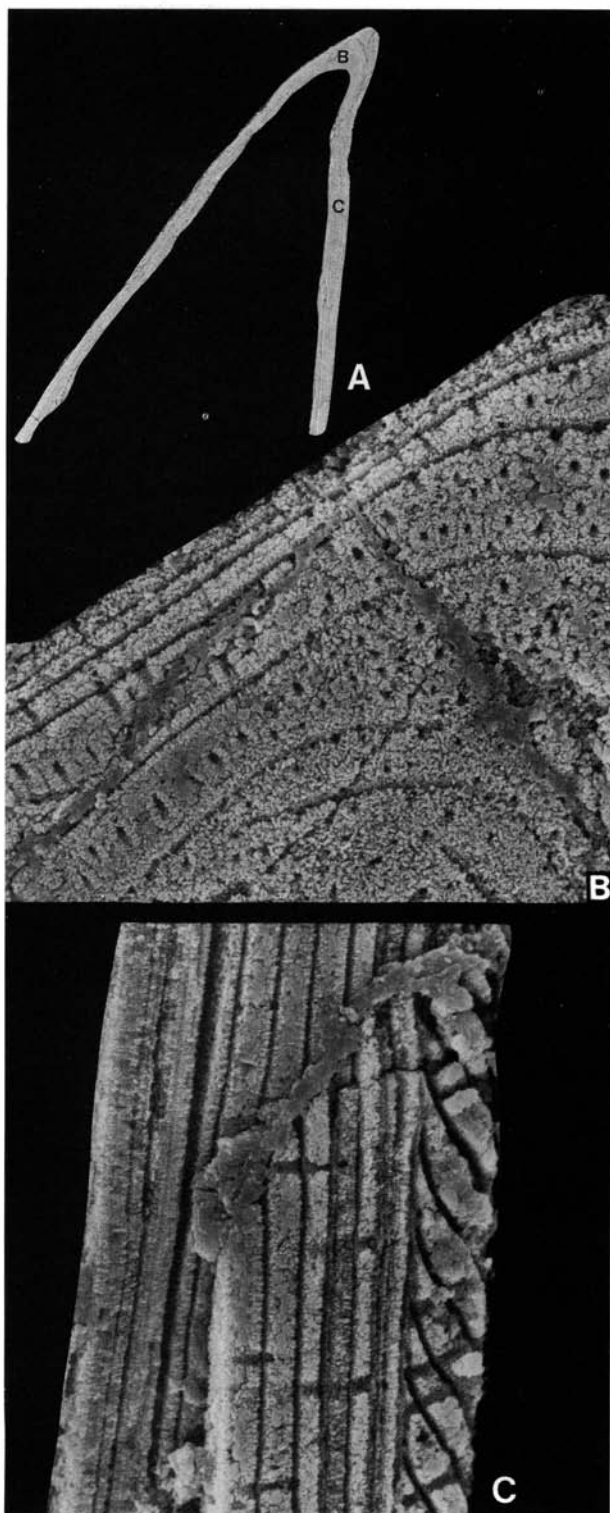


Fig. 34. □A. Midsagittal section through a ventral valve of *Biernatia holmi* gen. et sp. nov.; the location of B and C is indicated; Seby Limestone (sample DLK83-se-2); Br133613e, $\times 78$. □B. Detail of A, showing the columnar secondary layer in the apex; $\times 2000$. □C. Detail of A, showing the columnar secondary layer in the posterior wall; $\times 2000$.

the thicker fibrous laminae represent the mineralized layers, whereas the thinner bands are organic layers which were phosphatized during diagenesis.

The ceratretine type of shell structure described by Williams & Rowell (1965a) is comparable with that of an unnamed Middle Ordovician acrotretacean species (prob-

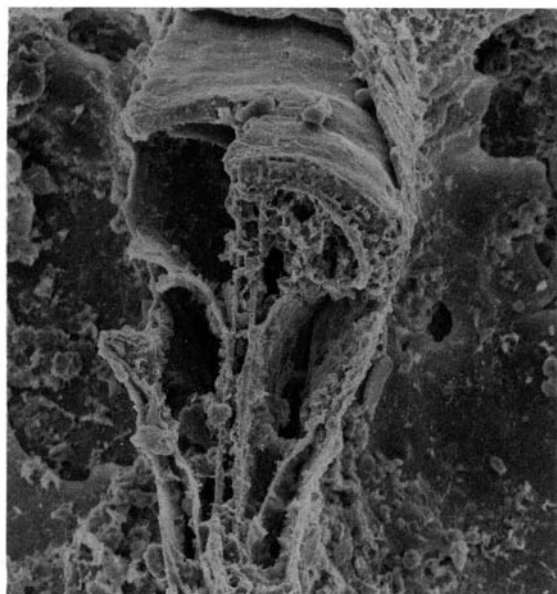


Fig. 35. Anterior view of a broken dorsal median septum of *Biernatia holmi* gen. et sp. nov. (see also Fig. 95G); Seby Limestone (sample DLK83-se-2); Br129043, $\times 500$.

ably an acrotretine) illustrated by Poulsen (1971). Poulsen's species has a thin primary layer which is partly exfoliated in the illustrated specimens, in addition to a camerate secondary layer (referred to as the outer layer by Poulsen) and a columnar tertiary layer (referred to as the inner layer by Poulsen).

The camerate laminae in Poulsen's species are wedge-shaped in sagittal sections (Poulsen 1971, Pl. 2:3-4, 4:1); these are defined by an upper and a lower lamella, connected by perpendicular walls that define elongated parallel 'tubes' of rectangular cross section (Poulsen 1971, Pl. 4). This type of secondary layer has been described also from members of the Scaphelasmatinae (Holmer 1986). A columnar tertiary layer forms the interior thickenings (such as the apical process and the muscle scars in Poulsen's species). The columnar laminae have an upper and a lower lamellae which are connected by perpendicular columns (Poulsen 1971, Pl. 5-6); this type of layer is present in all acrotretaceans examined so far, apart from the scaphelasmatinae.

In Poulsen's species the spaces between the columns and within the chambers are empty. According to him (1971, p. 269) 'the empty spaces between the phosphatic bands may be interpreted as the sites of former organic bands', whereas the comparatively thin phosphatic lamellae in the shell represent the mineralized portion. Poulsen's (1971) interpretation of the acrotretacean shell structure is preferred here to that of Williams & Rowell (1965a). The latter model requires a considerable amount of secondary phosphatization, which is difficult to account for; at least, there is no evidence for phosphatization in the associated fauna examined for this study. The empty spaces within the columnar and camerate laminae probably contained most of the organic matrix of the shell, whereas the thin lamellae and the primary layer correspond to the phosphatic layers. In all probability, the columns and walls also represent

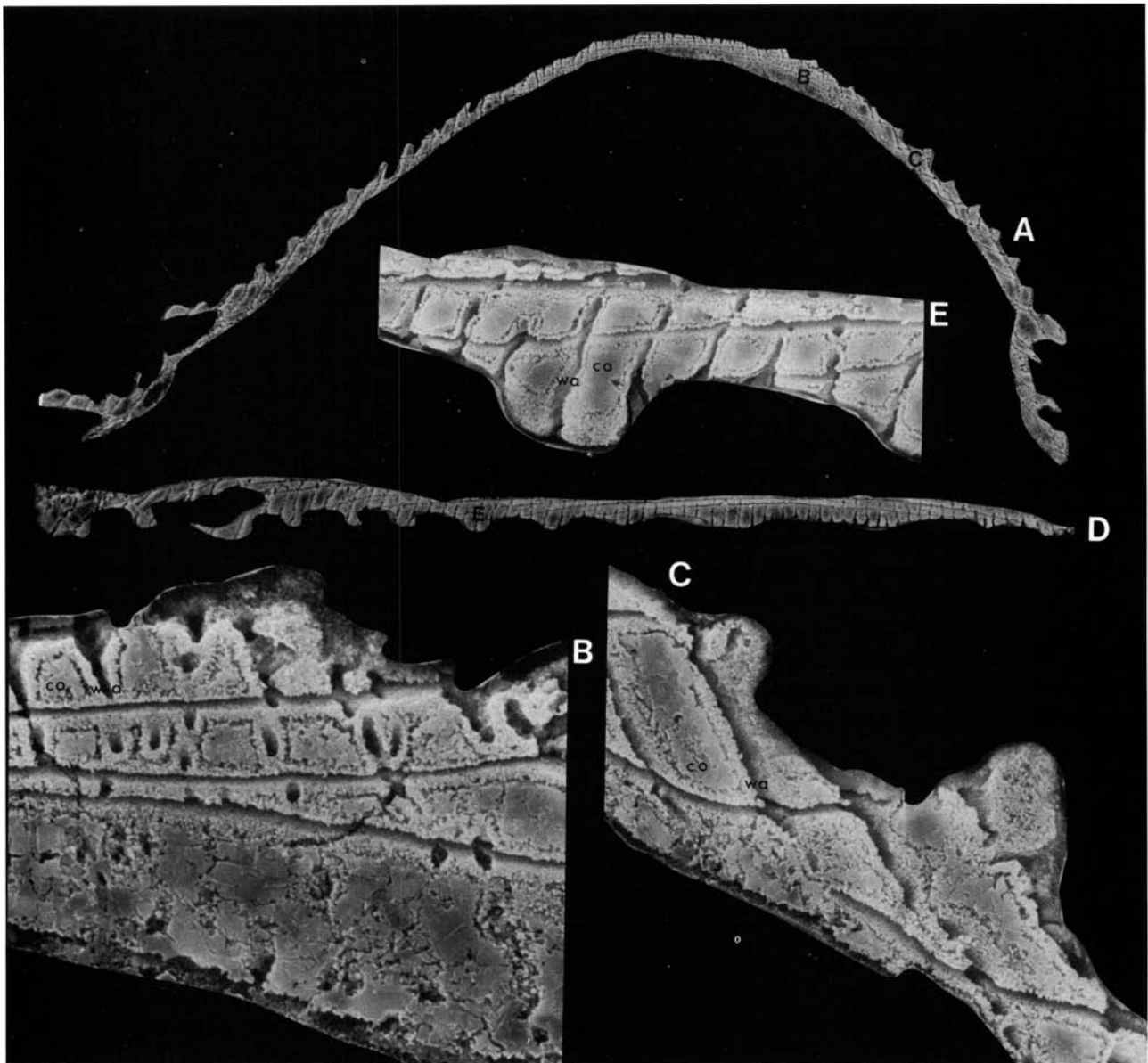


Fig. 36. Midsagittal sections through *Scaphelasma mica* Popov, 1975; Gullhög Formation (sample GB84-2-9); *wa*, chamber wall; *co*, CCP. □A. Ventral valve; the location of B and C is indicated; Br132676b, $\times 230$. □B-C. Details of A, showing the wedge-shaped camerate laminae in the secondary layer; $\times 2400$ (B) and $\times 2000$ (C). □D. Dorsal valve; the location of E is indicated; Br132676c, $\times 310$. □E. Detail of D, showing the wedge-shaped camerate laminae in the secondary layer; $\times 1500$.

original mineralized portions of the shell, rather than being diagenetically phosphatized 'punctae' as was proposed by Poulsen (1971, p. 270).

Rowell & Henderson (1978, Pl. 1:7) illustrated columnar laminae in some Cambrian members of the subfamily Acrotretinae, and noted that the 'voids' within them might have been filled with organic material; their suggestion that the voids could have been empty seems highly unlikely. A camerate secondary layer was also described by Holmer (1986, Figs. 5O, 6I) from the Ordovician acrotretines *Hisingerella tenuis* and *Conotreta? orbicularis*.

The shell structure of the Cambrian *Rhondellina dorei* Rowell (subfamily Linnarssoniinae?) was discussed recently by Rowell (1986, p. 1062, Figs. 1:3-4, 2:7). The secondary layer (referred to as the inner shell layers by Rowell) of this species has numerous camerate laminae that are closely

comparable with the camerate secondary layer of most Acrotretinae described above. In shell structure *R. dorei* is most similar to the scaphelasmataines; it is comparatively thin-shelled and lacks a columnar layer (Fig. 40C).

The shell structure of the examined members of the subfamilies Ephippelasmatainae and Biernatinae differs slightly from that of the acrotretines; there is no camerate layer developed, and the secondary layer is entirely of the columnar type.

The shell structure of *Eoconulus* is not well known, and requires further study. As outlined above, it is apparently comparable with that of the acrotretaceans; there are some indications of columnar laminae in both valves of *E. sp. nov. a*.

The aberrant shell structure of most eoconulid ventral valves is most probably due to the fact that they become

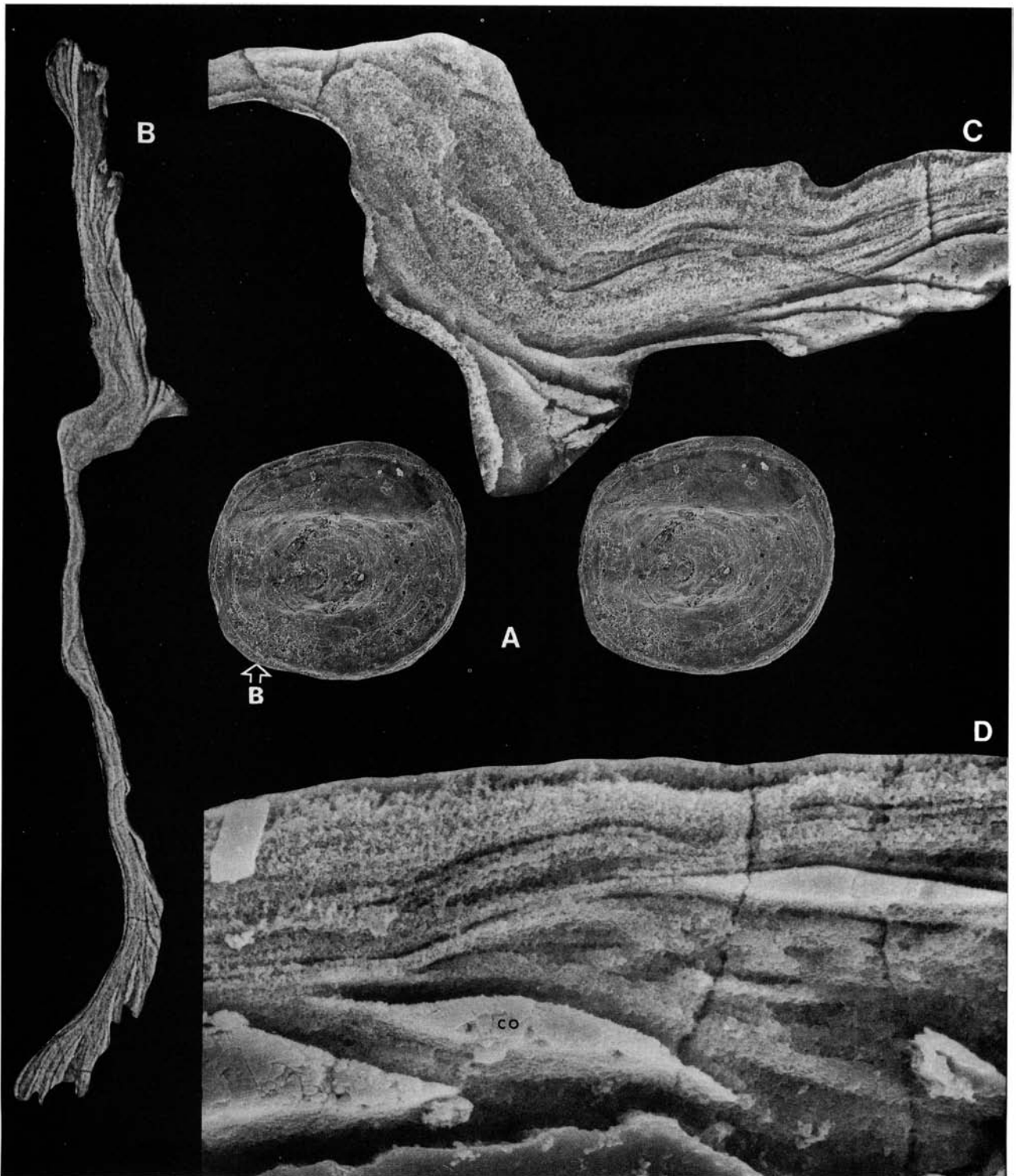


Fig. 37. □A. Stereo-pair; ventral exterior of *Eoconulus* sp. nov. a, showing a cylindrical attachment scar; the location of the section in B is indicated; Kårgårde Limestone (sample DLK83-segk-4); Br128923, $\times 93$. □B. Section through A; the location of C and D is indicated; $\times 391$. □C. Detail of B, showing the outer wedge-shaped laminae, and the inner granulose lamellae; $\times 1302$. □D. Detail of B showing the CCP (co) in the laminae; $\times 3324$.

mineralized late in ontogeny (see also below, p. 64); the simple lamellose shell of the ventral valve of *Eoconulus* cf. *clivus* lacks evidence of normal peripheral accretionary growth. The lamellae represent interior thickenings, deposited during, or subsequent to, the adult stage.

The 'pores' in the ventral valves of most eoconulids seem to have been formed contemporaneously with the secre-

tion of the shell, and in all probability do not represent predatory borings. The function of the 'pores' is not obvious, but they might have been related to the early attachment of the valve; they can also possibly be comparable with the 'koskinoid perforations' in the Orthotetacea (Grant 1980).

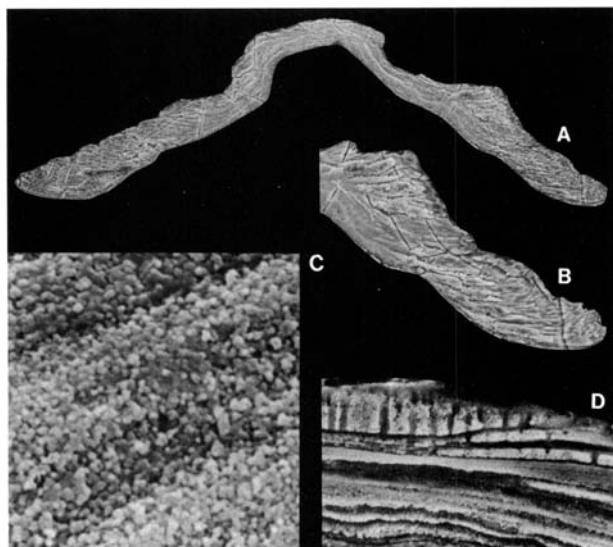


Fig. 38. □A–B. *Eoconulus cf. clivosus* Popov, 1975. □A. Midsagittal section through a dorsal valve; Skärlov Limestone (sample DLK83-sä-2); Br133605d, $\times 122$. □B. Detail of A; $\times 212$. □C. Detail of a section through a dorsal valve of *Eoconulus cf. cryptomyus* Goryanskij, 1969, showing the minute granular apatite crystallites in the lamellae; Kårgårde Limestone (sample DLK83-segk-6); Br133595n, $\times 4900$. □D. Detail of a section through a dorsal valve of *Eoconulus* sp. nov. a, showing the wedge-shaped columnar laminae; Kårgårde Limestone (sample DLK83-segk-6); Br133595o, $\times 965$.

Summary

(1) The Ordovician and Silurian lingulaceans and discinaceans that have been examined possess a thin primary layer in which the apatite c -axes are oriented parallel to the shell surface; the layer has a granular appearance under the SEM.

The secondary layer generally comprises thick baculate laminae that have criss-crossing slender baculae consisting of granulae, needles or platelets of apatite. The baculae probably represent mineralized organic fibres, similar to those present in the organic layers of Recent *Glottidia* and *Discinisca*. The interbacular spaces are empty or filled with 'collophane-like' calcium phosphate (CCP). The CCP has a porous microstructure and the empty spaces may have contained organic matrix. The baculate laminae alternate with lamellose laminae, consisting of thin apatite lamellae of similar structure as in the primary layer.

The shell structure of the acrothelids appears to be comparable with that of the lingulaceans and discinaceans.

(2) The Cambrian and Ordovician acrotretaceans investigated for this study possess a very thin, granular primary layer that is not readily observable in thin sections.

The following two types of secondary and tertiary layers are identified in the examined acrotretaceans: (a) The columnar layer appears to be developed in all acrotretacean subfamilies apart from the Scaphelasmatinae. In sagittal section this layer has wedge-shaped columnar laminae. The laminae are defined by an upper and a lower lamella that are connected by columns perpendicular to the lamellae. (b) The camerate secondary layer has been found only

in the subfamilies Acrotretinae, Torynelasmatinae, and Scaphelasmatinae (and possibly also in the Linnarssoniinae). The camerate laminae have upper and lower lamellae connected by walls that form polygonal chambers in a honeycomb-like pattern. In the scaphelasmatinines (and the species figured by Poulsen 1971) the chambers of the camerate laminae are elongated, and form parallel 'tubes' of rectangular cross section.

In both types of layers there are needle-shaped apatite crystallites with their c -axis oriented normal to the lamellae, walls and columns. The spaces between the columns and walls are empty (in broken specimens), or filled with CCP.

The primary layer and the apatitic lamellae, walls, and columns of the secondary and tertiary layers are considered to form the original mineralized shell. The empty or CCP-filled spaces within the secondary and tertiary layers probably contained most of the organic matrix.

Ontogeny

Many of the described species of phosphatic inarticulate brachiopods are represented (in the samples used for this study) by almost all ontogenetic stages. The following growth stages of the shell are distinguished: protegular, larval, juvenile (brepic and neanic), adult, and gerontic. The definitions of the two earliest stages require some special explanation.

The term *protegulum* was introduced by Beecher (1891, p. 344) to denote the 'common form of embryonic shell' of the brachiopods. Williams & Rowell (1965a, p. H151) defined protegulum as the 'first-formed shell of organic material (chitin or protein), secreted simultaneously by both mantles'.

Among Recent inarticulate brachiopods, a protegulum, about 0.2–0.3 mm wide and 0.1–0.2 mm long, consisting of two joined semicircular valves, has been observed in the ontogeny of *Lingula* (Yatsu 1902; Chuang 1962, 1977; Hammond 1982) and *Glottidia* (Paine 1963). The lingulacean protegulum is secreted by the non-feeding embryo, at about the time of appearance of the first pair of lophophoral filaments and while the embryo is still within the vitelline membrane. The disturbance in growth at the end of the protegular stage is probably a result of the change to a free-swimming planktotrophic larva. Discinaceans lack a protegulum (Chuang 1977; Hammond 1980), whilst the earliest ontogenetic stages of Recent craniaceans are unknown (Rowell 1960). The so-called protegulum of Recent articulate brachiopods was discussed and described in detail by Stricker & Reed (1985a, 1985b, 1985c), but in a strict sense this represents a postlarval shell (see also Chuang 1977), as it is secreted after settlement and metamorphosis.

Protegula have been reported from many fossil inarticulate brachiopods. However, as has been pointed out repeatedly (Chuang 1971a, 1971b, 1977; Popov *et al.* 1982; Rowell 1986), it is questionable whether the traces of early shell-bearing ontogenetic stages actually correspond to embryonic shells in a strict sense (that is, a shell secreted by the embryo while still within the vitelline membrane). Obviously, there are no absolute criteria by which to determine

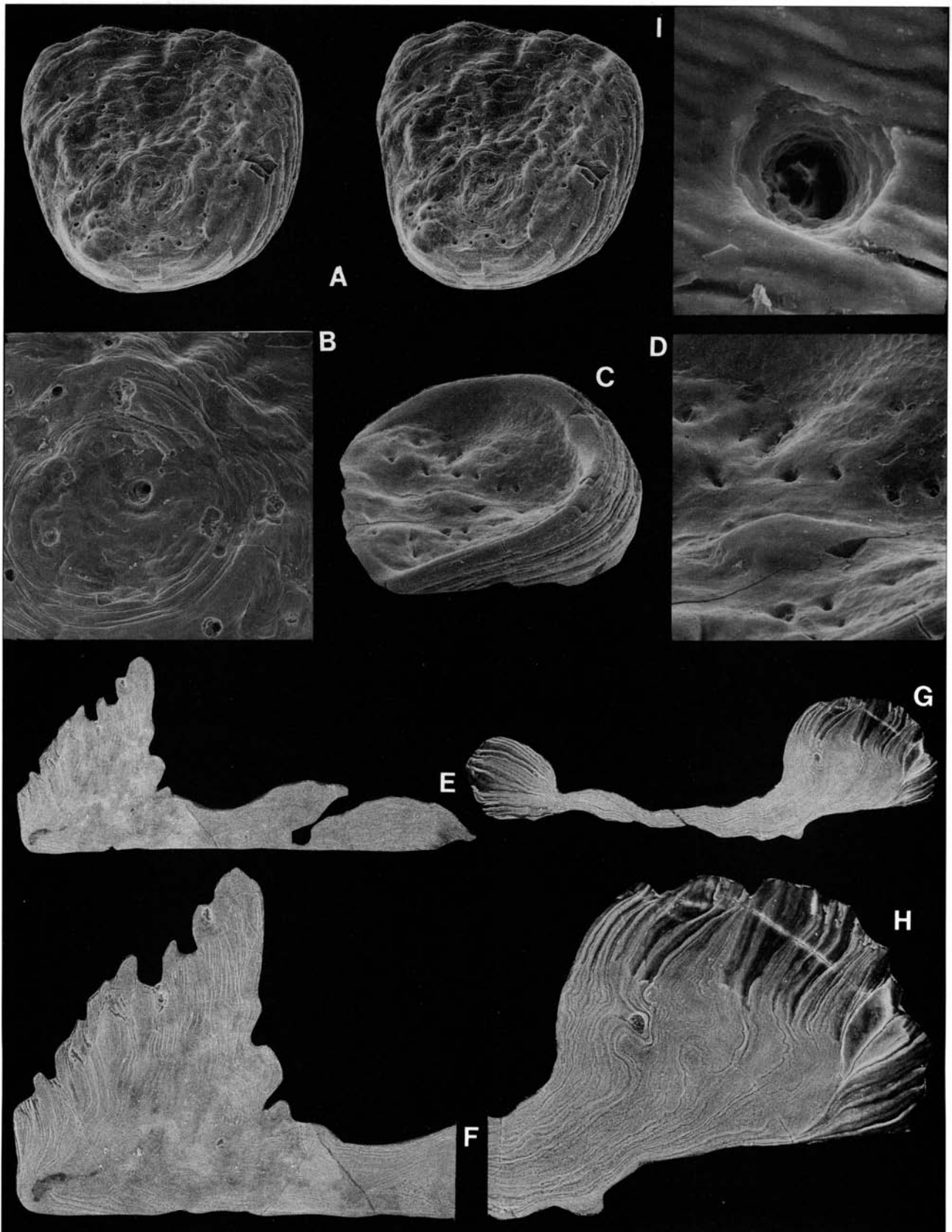


Fig. 39. □A–H. *Eoconulus* cf. *clivus* Popov, 1975. □A. Stereo-pair; exterior of a ventral valve, showing an irregular attachment scar; Skövde beds (sample GB84-D5); Br128907, $\times 59$. □B. Detail of A, showing the shallow 'pores' and the poorly defined larval shell; note that the central 'pore' may represent a closed pedicle foramen; $\times 186$. □C. Side view of the interior of A, showing the muscle scars and the apical process; $\times 65$. □D. Detail of the apical process of A, showing the 'pores' and the polygonal pattern of epithelial moulds; $\times 152$. □E. Midsagittal section through a ventral valve; note the flat attachment scar and the apical process; Skärlov Limestone (sample DLK83-så-5); Br133608c, $\times 76$. □F. Detail of the anterior wall of F, showing the anteroventral direction of the 'inside growth'; note the thin granular lamellae; $\times 138$. □G. Midsagittal section through a ventral valve; note the irregular attachment scar; Skövde beds (sample GB84-D5); Br132576, $\times 127$. □H. Detail of the anterior wall of G; $\times 303$. □I. Detail of the ventral exterior of *Eoconulus* cf. *semiregularis* Biernat, 1973, showing a 'pore'; Gullhøgen Formation (sample GB84-2-19); Br132719d, $\times 2756$ (see also Fig. 106E).

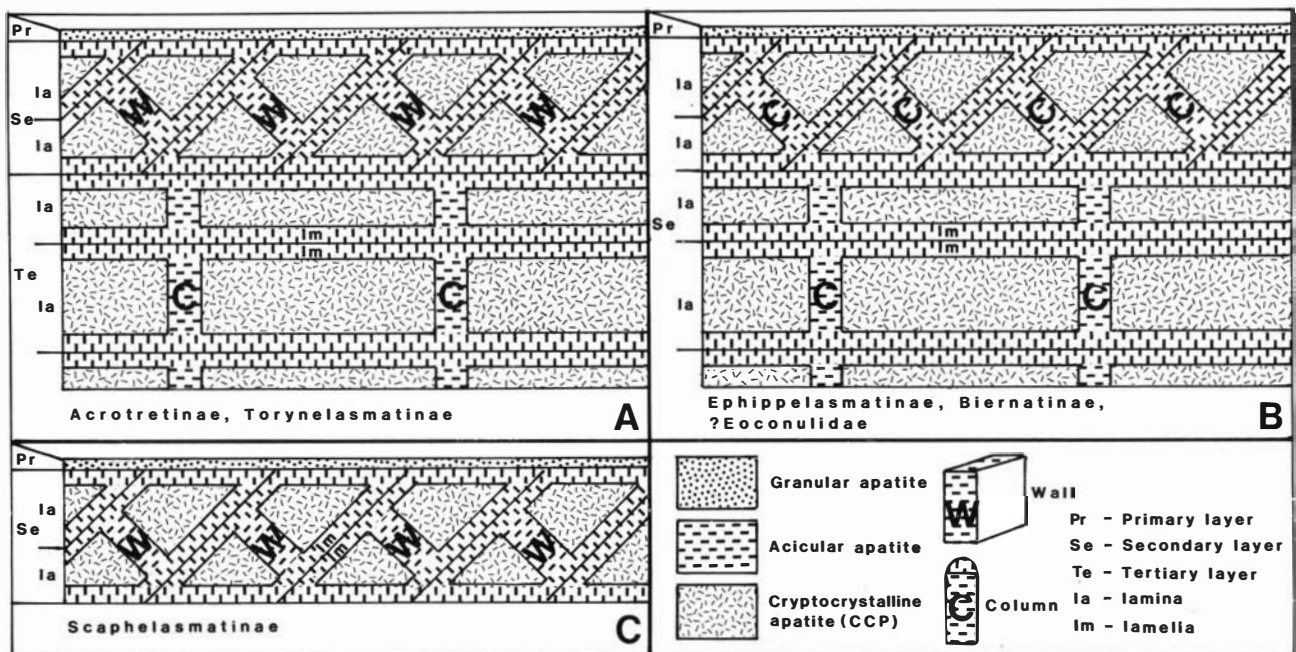


Fig. 40. Diagrammatic comparison between the three main types of shell structure in the examined acrotretacean subfamilies. □A. The acrotretines and torynelasmatinae have a camerate secondary layer with wedge-shaped laminae, where the upper and lower lamellae are connected by walls, in addition to a columnar tertiary layer with perpendicular columns. □B. The secondary layer of the ehippelasmatinae and biernatinae is entirely columnar; the shell structure of the eoconulids is not well known, but some species appear to have a columnar secondary layer. □C. The scaphelasmatinae have a thin camerate secondary layer with wedge-shaped laminae. Note that the empty spaces, which are commonly present within the columns and walls, and between successive laminae have been omitted; they may have contained some of the organic matrix. Not to scale.

the specific ontogenetic stages represented by fossil material, but among other things, the so-called protegula of most Palaeozoic acrotretaceans possess a dorsal pseudo-interarea as well as a pedicle foramen that are indicative of later growth stages (Popov *et al.* 1981; Rowell 1986). In all probability these early structures (which are preserved on the umbo of most fossil acrotretaceans and lingulaceans) represent a mould of the organic larval shell. As noted by Rowell (1986) this fact is of some importance when discussing the dispersal of brachiopods, and also in attempts to compare different kinds of ontogenetic developments.

Although it appears that a protegulum (in a strict sense) is generally unobservable in fossil material, the peculiar pitted plate preserved on the ventral valve of *Eoconulus* (described on p. 63; e.g., Fig. 107E) could be related to the embryonic (or possibly early postembryonic) stage.

The term *larval* stage is used here in the sense of Chuang (1971a, 1971b, 1977), Popov *et al.* (1982), and Rowell (1986). In Recent discinaceans and lingulaceans this stage of development begins approximately when the lophophore has two pairs of filaments, whereas the time of settlement (in terms of days and number of lophophoral filaments) of the planktotrophic larvae varies between the two superfamilies. In *Glottidia* settlement occurs after a maximum of about 20 days when the lophophore has up to about 20 filaments (Paine 1963). At the time of settlement, the discinacean larvae are up to about six days old and have four filaments (Chuang 1977). In postlarval shells of Recent phosphatic inarticulates, the outline of the larval shell is seen clearly as a circle of disturbance in the growth,

probably caused by settlement of the larva and the change from a planktotrophic to sedentary life (Paine 1963; Chuang 1977). In *Lingula anatina* the larval shell is about 0.45–0.75 mm wide and 0.55–0.94 mm long, and on average 80% as wide as long (Chuang 1961, 1962). The larval shell of Recent *Glottidia* is around 0.70 mm long, but in exceptional cases can exceed 1 mm in length, apparently due to a prolongation of the larval stage (Paine 1963). The larval shell of Recent discinaceans is generally somewhat smaller, around 0.40 mm across (Chuang 1977; Figs. 40–43).

The size of the larval shell in phosphatic inarticulates appears to remain roughly constant within the superfamilies, rather than being proportional to the size of the adult animal. For example, the maximum width of the dorsal larval shell of *Lingula anatina* is around 0.75 mm (Chuang 1962, Table 1), constituting about 3% of the maximum adult width (22.3 mm according to Chuang 1962, Table 3). The same ratio for the Ordovician lingulacean *Spinilingula radiolamellosa* is about 28%; the width of the dorsal larval shell is 0.64 mm, whereas the maximum width is only 2.25 mm.

Between the last three postlarval ontogenetic stages (juvenile, adult, and gerontic) the boundaries are transitional, and it is difficult to define unambiguous criteria for recognizing meaningful and comparable ontogenetic stages. *Juvenile* is used for stages that lack fully developed adult morphological features (see below). The juvenile stage of many acrotretaceans can be divided into a *brephic* (=nepionic, Beecher 1892, p. 150; or early juvenile) and *neanic*

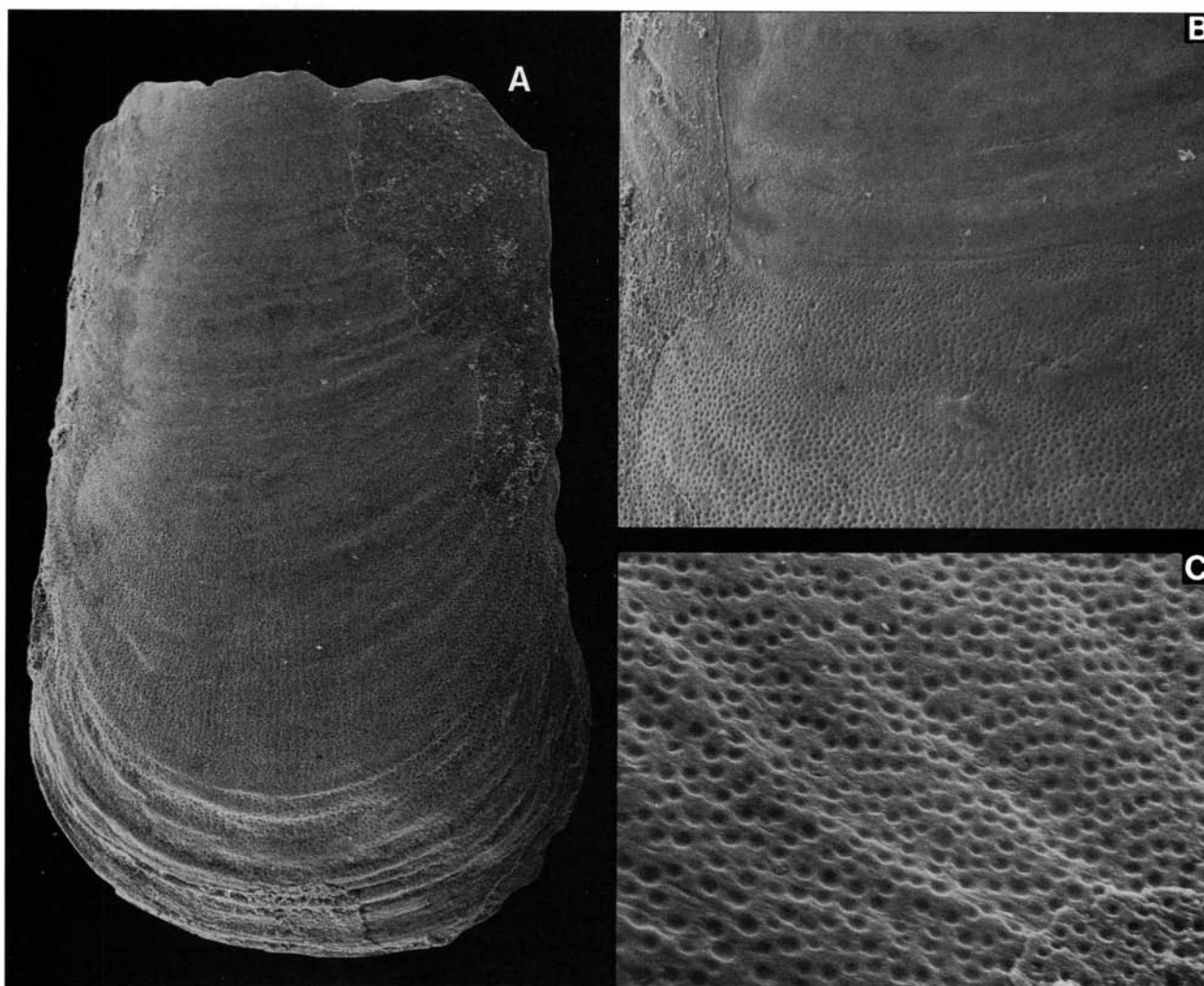


Fig. 41. □A. Ornamentation of a ventral valve of *Rowellella holenensis* sp. nov.; Dalby Limestone (sample DLK83-dal-36); Br132978, $\times 160$. □B. Detail of A, showing the contact between the larval and the adult shells; $\times 360$. □C. Detail of A, showing the pitted ornamentation of the adult shell; $\times 1000$.

(=neologic, Beecher 1892, p. 151; or late juvenile) stage, by reference to the developmental stages of the dorsal pseudointerarea (see also Holmer 1986). Breplic is used, essentially in the sense of Williams & Rowell (1965a, p. H141), for the earliest juvenile stages that have well developed growth lines and a crescent-shaped incipient dorsal pseudointerarea, consisting of a thin, undivided plate that lacks propleas. The transition to the neanic stage is marked by the appearance of a divided widened dorsal pseudointerarea with propleas (see also Williams & Rowell 1965a, p. H148). *Adult* acrotretaceans have one or several of the following, fully developed characters: (1) thickened cardinal muscle scars, (2) an apical process, (3) a median buttress, and (4) an elaborate median septum. In *gerontic* individuals the adult characters are more strongly pronounced and the internal structures of the valves increase in thickness.

The following section outlines and discusses different types of early ontogenetic development, and their associated types of micro-ornamentation.

Lingulacea and Discinacea

Lingulacea

In the material studied the lingulaceans are represented mostly by juveniles and/or fragments of adults.

No obvious traces of a protegulum, comparable in size to that of Recent lingulaceans (e.g., Chuang 1962), have been identified, but a growth disturbance on the umbo of many lingulaceans defines an oval plate that is similar in size and shape to the larval shell of Recent forms (see also Popov *et al.* 1982). The disturbance is commonly, but not always, associated with a change in ornamentation; the larval shell is mostly smooth, whilst the postlarval surface commonly has well developed growth lines, fila, rugae, lamellae, papillae or pits.

The following four types of early ontogeny can be distinguished:

(1) The lingulelline *Rowellella* cf. *lamellosa* (Fig. 51) and *R. holenensis* (Figs. 41, 52) have a well defined larval shell, but

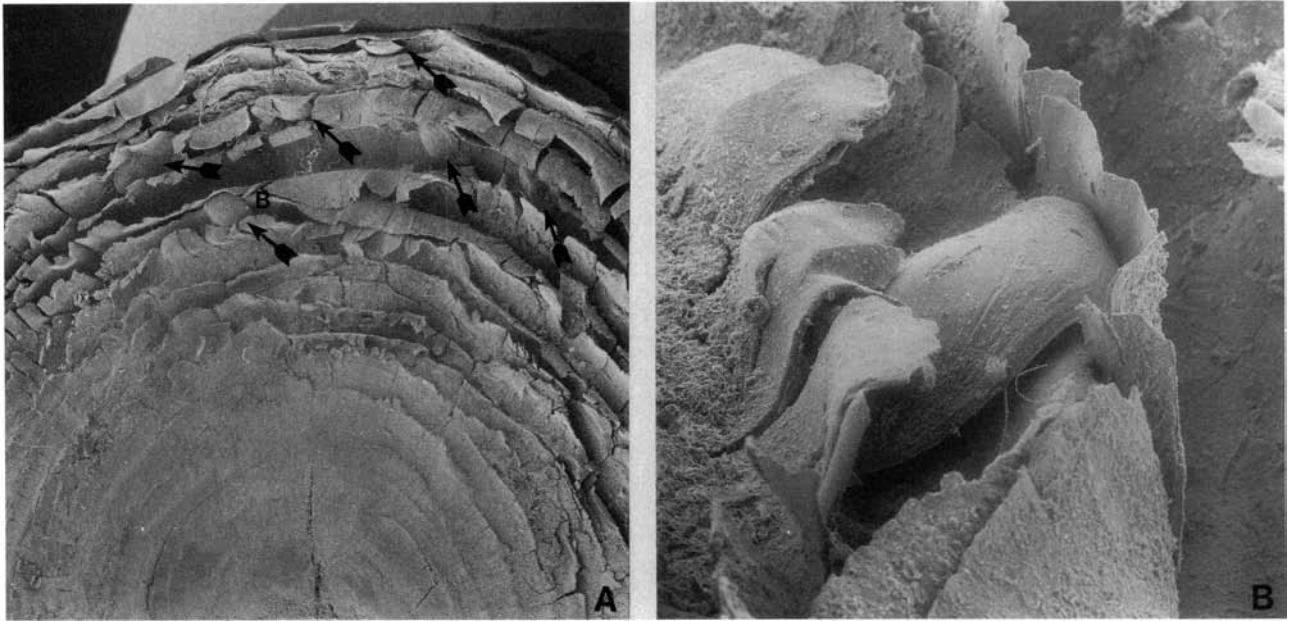


Fig. 42. □A. Detail of the anterior portion of a ventral valve of Recent *Discinisca lamellosa*; the location of B and five other attached juvenile shells is indicated by arrows; Chile; Br133667a, $\times 10$. □B. Detail of A, showing a lateral view of an attached juvenile; $\times 75$.

in older individuals it is generally broken off (Figs. 51, 52H). In sections through *R. cf. lamellosa* the larval shell is a thin and well defined plate, which lacks the primary shell layer (Fig. 17A).

In juveniles of *R. hollenensis* the larval shell is better preserved; it is as long as wide, about 0.50 mm in diameter. The surface is smooth, apart from some faint concentric lines laterally (Figs. 41, 52C–D). The boundary with the postlarval shell is fairly sharp and is accentuated further by the ornamentation of shallow pits, which starts at the edge of the larval shell (Figs. 41B, 52D). The pits on the postlarval shell are closely spaced and distributed evenly over the surface of the valve. They are circular and of almost uniform size, with a diameter of 2–3 μm (Fig. 41C).

(2) In the other members of the Lingulellinae and Glossellinae, the larval shell is best defined when the postlarval shell is strongly ornamentated, as in *Spinilingula radiolamellosa* (Figs. 46, 50A, D), and in some undeterminable fragments of a glosselline (Fig. 53G–H). In *S. radiolamellosa* a growth disturbance forming a circular line, about 0.46–0.64 mm wide, indicates the boundary of the larval shell; the lamellose ornamentation starts a short distance in front of the the larval shell (Figs. 46, 50A, D). The lamellae of the postlarval surface are provided with short spines, arranged along radiating lines (Fig. 50A; see also Savazzi 1986).

In some fragments of a ventral valve of a glosselline (Fig. 53H), a circular line of disturbance in growth defines a smooth circular shell which is over 2 mm long and may correspond to a prolonged larval stage. The surface of the remainder of the valve is strongly papillose, with papillae (up to 50 μm long) arranged in more or less straight rows (Fig. 53G–H).

(3) In many of the lingulaceans, such as *Rosobolus?* sp. nov. a (Fig. 48A), *Expellobolus?* sp. nov. a (Fig. 48E, I), *Lingulella?*

alata (Fig. 49A, G), and *Paldiskites?* sp. nov. a (Fig. 50G, K, J), the umbo bears a number of subdued circular lines of growth disturbances. It is not clear which of these lines defines the larval shell; the associated change in ornamentation is poorly accentuated. In these species the approximate width of the larval shell varies from about 0.5 mm (in *Rosobolus?* sp. nov. a) to 0.8 mm (in a ventral valve of *Lingulella?* *alata?*; Fig. 49I). In a longitudinal section through the umbo of the ventral valve of *Rosobolus?* sp. nov. a, the larval shell is sharply delineated and constitutes a separate plate (Fig. 16B, D).

(4) The exact growth stage represented by the two illustrated young ventral valves of an unnamed species of *Lingulella?* (W 0.50–0.64; Fig. 48L–M) is uncertain. It is probable that they represent the early postlarval stage, and already at this stage there is a well developed internal area (Fig. 48M), with a shallow pedicle groove and minute propareas. On the exteriors of both valves there is a line of growth disturbance, defining a shell about 0.3–0.4 mm wide. In front of this line concentric ornamental lines are more crowded; in all probability this marks the edge of the larval shell (Fig. 48L). The exterior of both these valves has a micro-ornamentation with minute polygonal ‘scales’ (up to 2 μm across) and arranged in terraces (see also Holmer 1986, Fig. 4G–I).

Recent Discinacea

For the purpose of comparison, the micro-ornamentation of some dry dorsal and ventral valves of the Recent *Discinisca lamellosa* were examined (Figs. 42–44). This species occurs commonly in clusters that include individuals of varying size (e.g., Rowell 1965, Fig. 178:3A; Fig. 42). In young growth stages the material shows some previously unknown details of the micro-ornamentation of the perios-tracum.

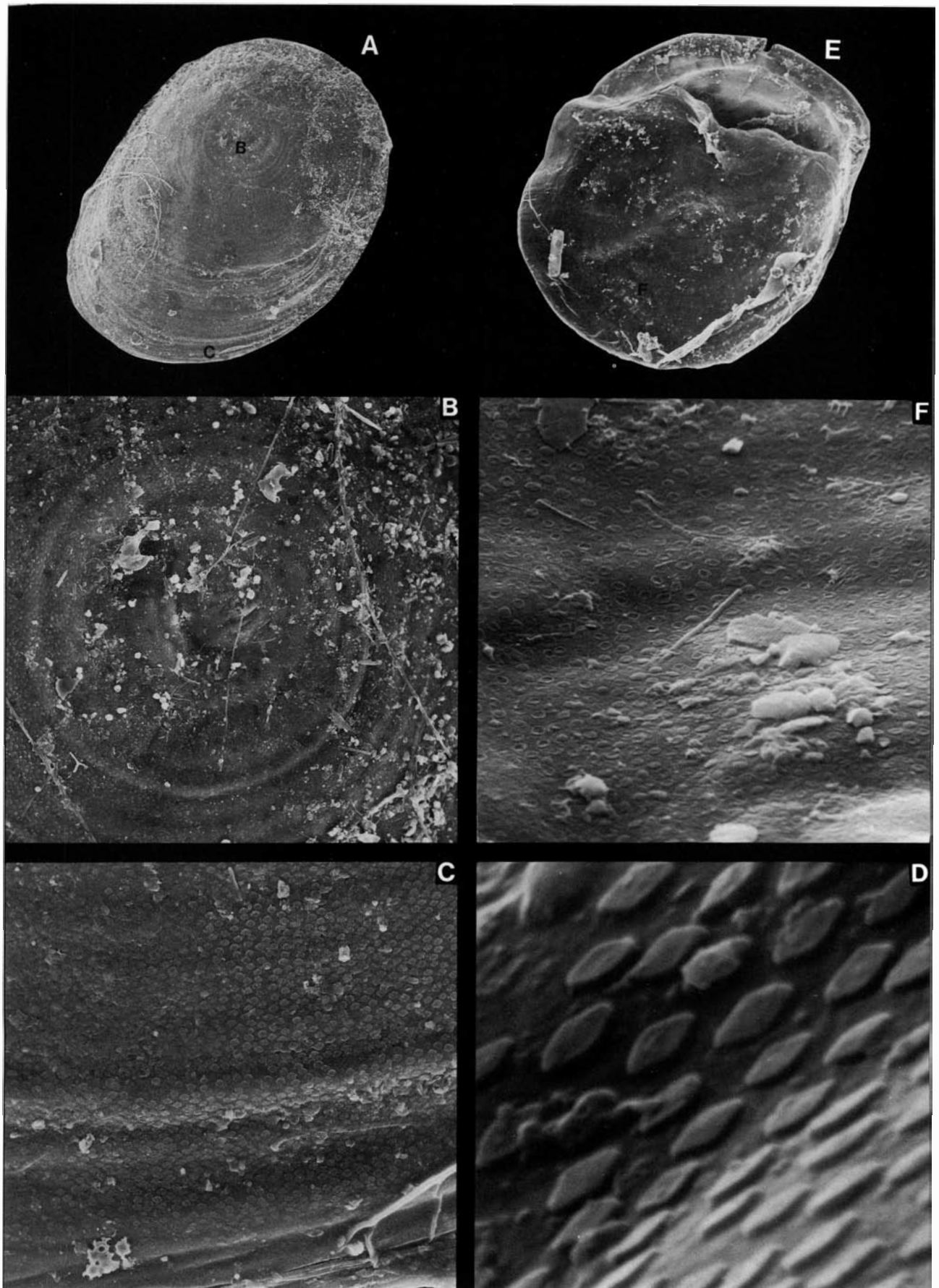


Fig. 43. □A–D. Early juvenile dorsal valve of *Discinisca lamellosa* (removed from the adult shown in Fig. 42); Br133643. □A. The location of B and C is indicated; $\times 100$. □B. Detail of A, showing the possible larval shell; $\times 440$. □C. Detail of A, showing the arrangement of minute vesicle-like structures in the periostracum; $\times 1000$. □D. Detail of A, showing a side view of the vesicle-like structures; $\times 10000$. □E–F. Early juvenile shell of *Discinisca lamellosa*, removed from an adult dorsal valve; Br133667b. □E. Ventral view; the location of F is indicated; $\times 120$. □F. Detail of E, showing the vesicle-like structures; $\times 2600$.

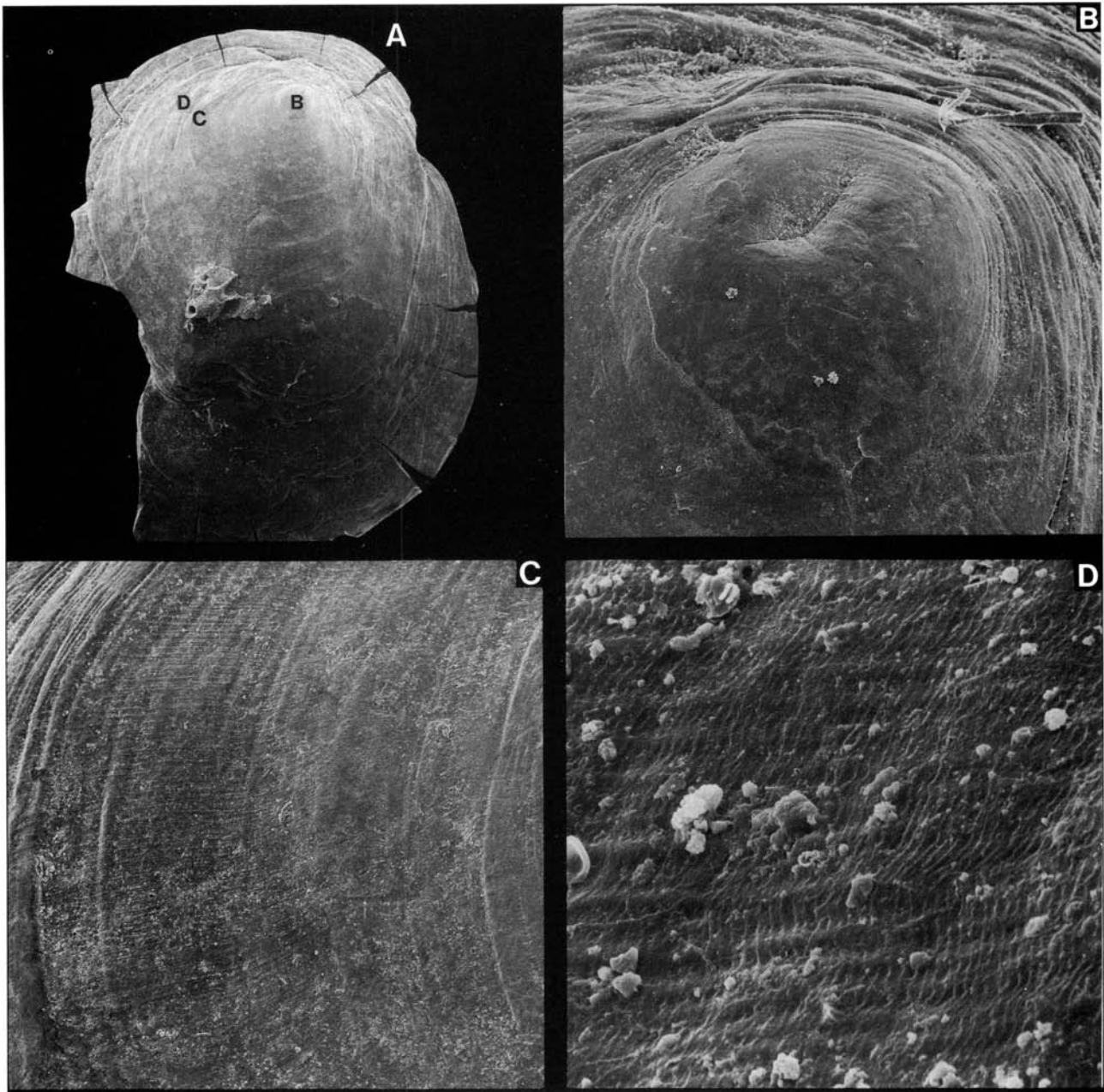


Fig. 44. □A. Dorsal valve of Recent *Discinisca lamellosa*; the location of B–D is indicated; Chile; Br133666, $\times 10$. □B. Detail of the apical portion of A, showing the outline of the larval shell; $\times 100$. □C. Detail of A, showing the ornamentation of concentric ridges and radial capillae; $\times 100$. □D. Detail of of A; $\times 1000$.

Seven complete, attached shells of *D. lamellosa* have a subcircular outline, 0.5–0.7 mm in diameter. No pedicle notch is developed in the ventral valves, but the posterior margin is slightly concave (Fig. 43E). The shells resemble the late planktotrophic discinacean larvae with four pairs of lophophoral filaments, first described by Müller (1860; see also Chuang 1977 for a review).

The dorsal valves show three major concentric lines, each marking a disturbance in the shell growth (Fig. 43A). The circles have a diameter of about 53, 100, and 450 μm , respectively (Fig. 43A–C). The area outside the third line of growth disturbance possibly marks the change from planktotrophic to filter feeding (see also Chuang 1977). At this stage, formation of regular growth lines begins (Fig. 43C). The significance of the earlier growth disturbances is

not obvious; the ventral valve of a complete shell, 0.5 mm in diameter, shows only a single outer line of growth disturbance (Fig. 43E).

In all examined larval shells the surface of the periostracum is ornamented with densely spaced, minute, vesicle-like structures distributed evenly over the entire exterior surface outside the innermost line of disturbance. The density of these structures averages about 250 000 per mm^2 , which corresponds to about 49 000 vesicles per valve (Fig. 43B–D, F). On a somewhat larger dorsal valve (0.7 mm in diameter) the vesicles disappear gradually towards the outermost line of disturbance (Fig. 43C). The vesicles of the dorsal valve are oval, about 1.5 μm long, with the maximum dimension perpendicular to the direction of growth. The vesicles on the examined ventral valve are

more rounded in outline and generally somewhat smaller, about 1.0 μm long (Fig. 43F).

An etched section (in 2% EDTA for 10 min) through one of the young dorsal valves (0.5 mm in diameter) showed that it is about 11 μm thick. The vesicles are developed in a thin uppermost layer (about 300 nm thick) of the periostracum (up to 3 μm thick). Beneath the periostracum there is a layer, up to 6 μm thick, which appears to be at least partly mineralized.

The umbo of the examined adult dorsal and ventral valves has a conspicuous, smooth, subcircular area (Fig. 44A–B), corresponding to the larval shell (cf. Chuang 1977, Fig. 11).

In both valves of *D. lamellosa* an ornamentation of closely spaced fila starts abruptly at the edge of the larval shell (Fig. 44B). The fila are transversed by fine, low, radial capillae, up to 7 μm apart, intersected by concentric ridges, up to 2 μm apart (Fig. 44C–D). This micro-ornamentation is apparently developed in the periostracum. The minute concentric ridges resemble those described by Williams & MacKay (1979, p. 730) from the periostracum of Recent *Discinisca strigata*.

Discinacea

The ontogeny and micro-ornamentation of the discinaceans is illustrated best in *Orbiculoidea?* sp. b and *Schizotreta* sp. a.

No isolated early stages were found, but the larval shell on older individuals is well defined; it is invariably almost completely smooth, with the exception of some very faint concentric lines (Fig. 45A–B, D). The larval shell is almost circular, on average 0.50 mm wide and 0.42 mm long (range WL 0.44–0.56, LL 0.32–0.51; $N=4$) in *Orbiculoidea?* sp. b, and up to 0.64 mm wide and 0.54 mm long in *Schizotreta* sp. a (Fig. 46, 112J). There is no pedicle notch in the ventral larval shell of any of the examined species (Fig. 112D–E, G, J). Sections through the larval shell of both species show that it constitutes a separate plate, not covered by primary shell. In both species ornamentation comprising shallow pits starts abruptly at the edge of the larval shell (Figs. 45B, 46, 112H); it is developed continuously over the remainder of the juvenile and adult growth stages but is missing on the ventral listrium of *Orbiculoidea?* sp. b.

In *Orbiculoidea?* sp. b the distribution, density, and size range of the pits are uniform over the entire postlarval shell surface of both valves. The shape of the pits varies from roughly circular on the early postlarval shell to somewhat oval in later growth stages; these oval pits are arranged with their maximum dimension almost perpendicular to the direction of growth (Fig. 45B–C). The size of the pits varies from less than 1 μm in diameter close to the larval shell, to about 5 μm long and 3 μm wide in later stages. The pits are closely spaced, separated by ridges about 2–7 μm wide (Fig. 45B–C).

The micro-ornamentation of *Schizotreta* sp. a differs from that of *Orbiculoidea?* sp. b mainly in having pits developed in two size-groups: (a) rounded small pits up to about 0.6 μm in diameter, and (b) larger pits of varying outline, up to 7 μm long and 4 μm wide (Figs. 45D–F, 112H). The

smaller pits are closely spaced and distributed evenly over the surface of the postlarval shell (Fig. 45F). The larger pits are arranged along discontinuous radial rows (Fig. 45D–E, 112H).

During the larval and brephic stages of the dorsal valve of both species, growth is hemiperipheral (Fig. 112J), and shell material is not secreted posterior to the larval shell until the valve is about 0.6–1 mm wide (Fig. 112C–E, G).

Neanic ventral valves of both species have a pedicle notch (Fig. 113D–E, J). *Orbiculoidea?* sp. b, has a listrium, but the central posterior portion of the ventral mantle edge did not start to secrete shell material until the valve was about 2–3 mm wide (Fig. 113D).

Discussion

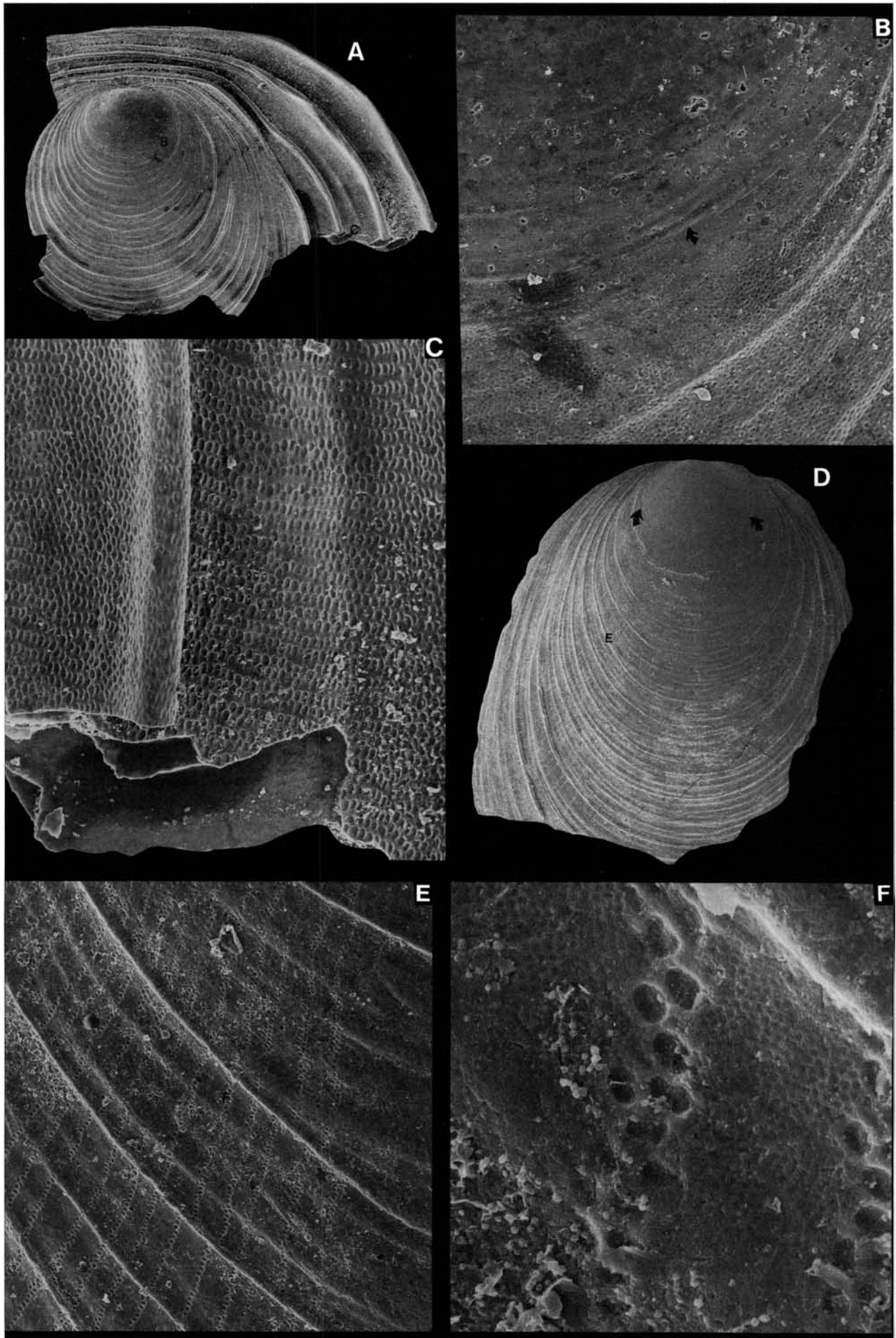
The larval shell of the Ordovician lingulaceans and discinaceans examined here is invariably smooth and around 0.4–0.5 mm wide (with the exception of the single valve of an unnamed species of Glossellinae, where it is about 2 mm long). This corresponds closely to the larval shells in many previously described Lower Palaeozoic lingulaceans and discinaceans. For example, from the illustrations of Krause & Rowell (1975, Pl. 1:1, 4, 10), the larval shell (WL 0.61, LL 0.52) of the Lower Ordovician *Lingulella bullata* is identifiable.

Holmer (1986, Fig. 4A–I) described isolated young valves of an unnamed Ordovician lingulacean (*Lingulella?* sp. a) that are considered to represent larval or early postlarval stages. The smooth larval shell of this species is around 0.4–0.5 mm wide and 0.6 mm long. It has a poorly defined ventral internal area (Holmer 1986, Fig. 4F), and lacks a dorsal internal area. On the umbo of larger valves, the larval shells are well defined and marked by lines of growth disturbances (Holmer 1986, Fig. 4C). A micro-ornamentation of minute polygonal 'scales' was found in *Lingulella?* sp. a (Holmer 1986, Fig. 4G–I).

Discinacean larval shells, similar in size and morphology to those discussed above, have also been figured previously in an unnamed Ordovician *Schizotreta* (Holmer 1986, Fig. 11A, D) and from the upper Viru *Orbiculoidea?* *kullsborgensis* (Holmer 1987b, Fig. 4B).

Apart from the micro-ornamentation with 'scales', all examined larval shells of Ordovician lingulaceans and discinaceans appear to be almost smooth. The only exception to this is the extremely thin-shelled aberrant lingulacean *Paterula*, in which the circular larval shell is distinctly pitted, with circular pits comparable with those of acrotretacean brachiopods (Popov *et al.* 1982, Fig. 1:2; Holmer 1986, Fig. 4N–O). The postlarval shell surface of this species is also very distinct, with a regular divaricate pattern of rhombical pits, unlike those of any other lingulacean.

In sections through the umbonal region of lingulaceans (*Rowellella* cf. *lamellosa* and *Rosobolus?* sp. nov. a) and discinaceans, the larval shell comprises a separated plate that is not covered by the primary layer. The postlarval ornamentation is developed on a distinct, granular primary layer. It is possible that this change in secretional behaviour of the mantle is connected with the first appearance of the 'con-



veyor belt system' (cf. Biernat & Williams 1970), and the change to sedentary postlarval life.

The vesicle-like structures in the larval shells of Recent *Discinisca lamellosa* clearly require further study. However, they can be interpreted as indicating a vesicular structure of the larval periostracum. The possible advantages of a vesicular periostracum in dispersion of acrotretacean larvae have been discussed by, among others, Biernat & Williams (1970) and Rowell (1986), but such a structure has never been observed in the larval periostracum of Recent brachiopods. The minute periostracal vesicles of *D. lamellosa* appear to be developed in the uppermost periostracal layer and do not leave an imprint upon the mineralized shell.

In lingulaceans the postlarval ornamentation is relatively well known. The development and significance of the ornamentation, forming divaricate patterns, have been discussed in detail by Seilacher (1972), Wright (1981), and Savazzi (1986).

The pitted nature of the postlarval shell surface of some trematid discinaceans was discussed by Wright (1981), and the minutely pitted postlarval micro-ornamentation of Ordovician orbiculoidines was described by Holmer (1986, 1987b).

Acrotretacea

A detailed description of the ontogeny of various acrotretacean species is given in the systematic section of this monograph. However, some common patterns are outlined and discussed immediately below.

Acrotretinae and Torynelasmatinae

The material of these two subfamilies did not include any isolated larval shells; on the apex of postlarval valves, the larval shell is preserved as a well defined plate.

The outline of the larval shell is invariably slightly elongated transversely. Within a species, the size of the larval shell is fairly constant, with a width that varies from about 0.15 mm in the torynelasmatines (Figs. 46, 74C, 76B) to about 0.41 mm in *Physotreta deformis* (Fig. 71C). In most other species the larval shell is around 0.20 mm wide, corresponding to about 10–20% of the maximum adult

width (Fig. 46). In lateral profile the dorsal larval shell is flattened with one or three nodes at about the centre of the valve (e.g. Figs. 55C, 67H). The ventral larval shell is around 0.10–0.30 mm high and invariably provided with a pedicle foramen that does not appear to have become widened by resorption during subsequent growth stages.

The larval shell of the acrotretines and torynelasmatines is always pitted, although the pits may have become obliterated subsequently, resulting in a smooth surface (e.g., *Acrotretella* sp., Fig. 76B). The size and density of the pits vary slightly between various species. Three types of larval ornamentation can be distinguished. (1) Pits of uniform size (1.6–5.0 µm) that overlap one another. For example, *Conotreta? mica*, *C.? siljanensis*, and *Hisingerella billingensis* have this kind of ornamentation (Figs. 54F, 57C, 61J). (2) Pits of somewhat varying size, up to about 3 µm in diameter, that do not generally overlap. Examples include *Cyrtonotreta*, *Physotreta*, and *Spondylotreta*; e.g., Figs. 71B, 73F). (3) Large pits, up to about 6 µm in diameter, surrounded by clusters of smaller pits, up to 2 µm across, that do not overlap. In the examined material only *Hisingerella? unguicula* has this type of larval pitting (Fig. 62D). The pits of all three types decrease gradually in size towards the edges of the larval shell (see, e.g., 67I).

The boundary with the postlarval shell is marked by the disappearance of the pits and the appearance of growth lines. In most acrotretines and torynelasmatines this change in ornamentation is enhanced further by a line of growth disturbance (e.g., 67H), but occasionally the boundary appears to be transitional (e.g., 67B).

The youngest isolated acrotretine and torynelasmatine shells belong to the brephic stage (Figs. 59, 67J–K, 75A–K). The brephic dorsal pseudointerarea is minute, undivided and lacks propareas (Figs. 46, 59A, C, E, 67J, 75D). A simple median septum with an upper septal rod is developed early, during the juvenile stage (Figs. 59B, D, 67K, 75C), whereas the interior of the brephic ventral valve (Fig. 59F–H) completely lacks recognizable structures.

In acrotretines and torynelasmatines the transition to the neanic stage is marked by the development of a widened dorsal pseudointerarea with propareas. In *Torynelasma suecicum* the beginning of the neanic stage is associated with the appearance of a surmounting plate (Figs. 67C, 75G). The approximate width at which the dorsal propareas are developed varies from around 0.46 mm in *Torynelasma suecicum*, to 0.62 mm in *Cyrtonotreta rydensis*, corresponding to about 20–30% of the maximum adult width (Fig. 46). Occasionally, neanic valves have a pair of weakly impressed cardinal muscle scars. In ventral valves of *Conotreta? siljanensis* there is a minute apical process.

In addition to a fully developed dorsal median septum, adult shells of acrotretines and torynelasmatines normally possess an apical process, a median buttress, and a pair of distinct cardinal muscle scars. The approximate width at which this stage is reached varies from 0.93 mm in *T. suecicum* to 1.13 mm in *Cyrtonotreta? striata*. In some species, such as *Conotreta? siljanensis* and *Torynelasma suecicum*, excessively thickened valves indicate a possible gerontic stage in the ontogenetic development (Fig. 46).

Fig. 45. □A–C. Ornamentation of a dorsal valve of *Orbiculoidea? sp. b*; Gullhögen Formation (sample GB84-1-3); Br132613. □A. The location of B and C is indicated; ×24. □B. Detail of A; the edge of the larval shell is indicated by an arrow; ×330. □C. Detail of A, showing the pitted exterior of the adult shell; note that the pits are arranged in discontinuous rows; ×240. □D–F. Ornamentation of a dorsal valve of *Schizotreta sp. a*; Furudal Limestone (sample DLK83-fur-6); Br129053. □D. The edge of the larval shell is indicated by arrows; the location of E is indicated; ×20. □E. Detail of D, showing the pitted exterior of the adult shell; note that the large pits are arranged in discontinuous radial bands; ×180. □F. Detail of E; ×1300.

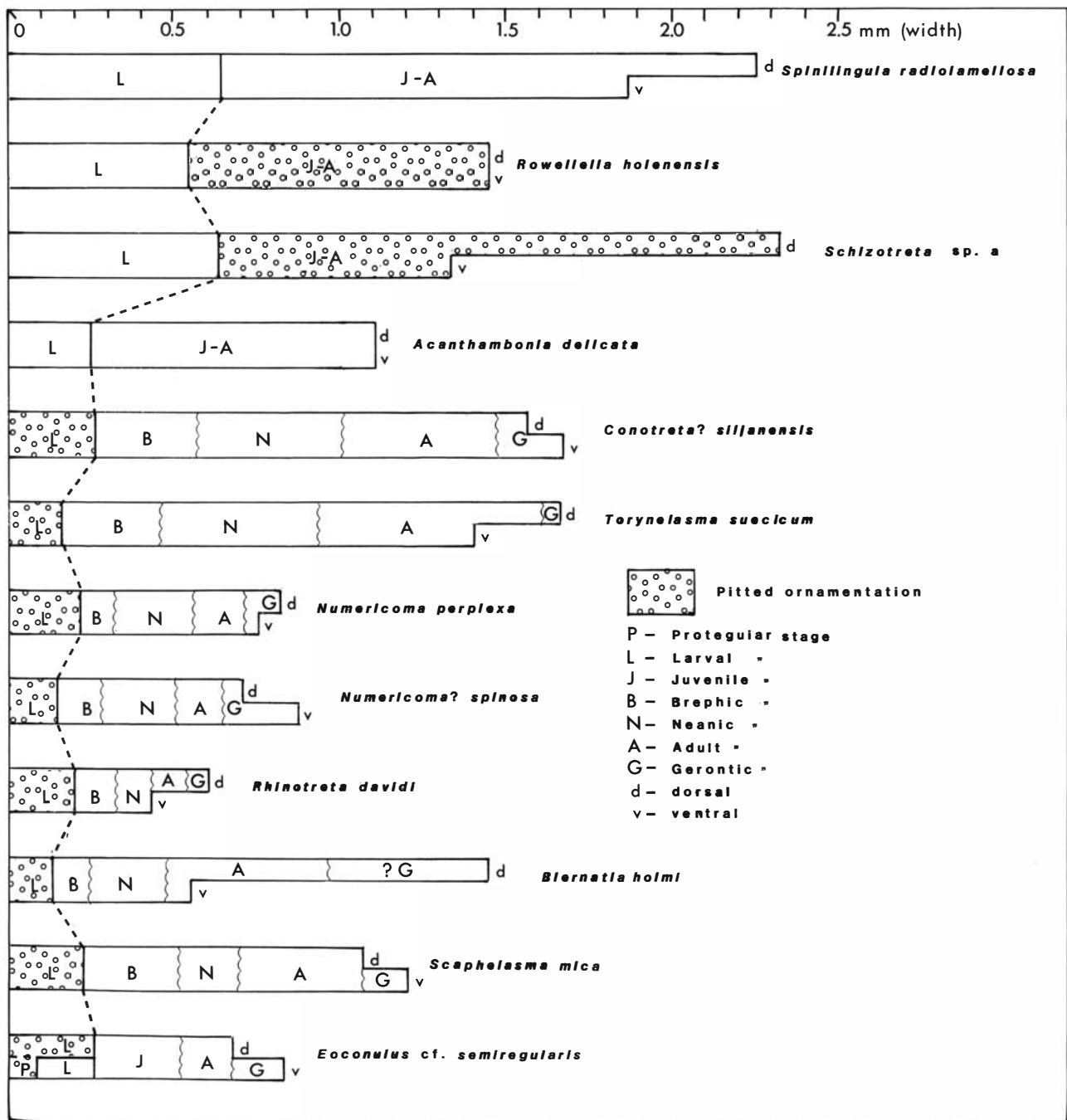


Fig. 46. Diagrammatic comparison between the ontogenies of selected species of phosphatic inarticulate brachiopods. The average widths of the protegular, larval, brephic, neanic, adult and gerontic shells are compared between 12 lingulacean, discinacean, siphonotretacean, and acrotretacean species. The distribution of pitted ornamentation is shown.

Ephippelasmatinae

Isolated larval shells of ephippelasmatine are rarely found (e.g., *Rhinotreta davidi*; Fig. 84F). Compared with the acrotretines, the ephippelasmatine larval shell occupies a relatively large area, around 20–40%, of the adult shell (Fig. 46). In spite of this, the average size of the larval shell is somewhat smaller than in the acrotretines; the width of the transversely suboval larval shell varies from about 0.16 mm in *Numericoma? spinosa* (Fig. 89B) to 0.22 mm in *Numericoma perplexa* (Fig. 87E).

In lateral profile the dorsal larval shell is flattened and has a centrally situated node (e.g., Fig. 87D). The ventral

valve is up to 0.15 mm high, and there is commonly an exterior pedicle tube (e.g., Fig. 87H). The surface of both valves is ornamented with deep circular pits of varying size, up to about 3 μ m in diameter; they are densely spaced, but do not overlap (e.g., Fig. 87F).

As in all other acrotretaceans, the transition to the juvenile shell is marked by the disappearance of the pits and the appearance of growth lines; in most specimens there is also a line of disturbance in the growth (e.g., Figs. 80B, 89B). The postlarval ontogeny varies slightly between different species of the subfamily. A brephic stage can be distinguished by its minute and undivided pseudointerarea. All

examined ephippelasmatine species, except for *Numericoma? spinosa* (Fig. 90A), lack a median septum during the earliest part of the brephic stage (Figs. 81B, 84A, 88A).

The width at which the ephippelasmatine neanic stage is attained varies from 0.27 mm in *Numericoma? spinosa* to 0.36 mm in *Rhinotreta davidi* (Fig. 46). This corresponds to about 30–60% of the maximum width of the shell. During the neanic stage, the ephippelasmatine dorsal median septum is formed. In all species of *Myotreta* and *Rhinotreta* the neanic septum is a flat, triangular plate (Figs. 81D, 84C), whereas in *Numericoma* and *Ephippelasma* it becomes twisted rapidly either to the left or to the right (Figs. 88E, 90D).

A fully grown ephippelasmatine shell is about 0.43–0.57 mm wide. Some particularly thick shells can belong to the gerontic stage (Fig. 46).

Biernatinae

The ontogeny of only a single biernatine species, *Biernatia holmi*, could be examined in detail (Figs. 46, 97). Compared with the ephippelasmatines and acrotretines, the larval shell of this species is small. It is 0.12 mm wide and 0.11 mm long, corresponding to about 8% of the maximum adult shell width (Fig. 46). The pitting of the larval shell is distinct, with large, circular, flat-bottomed pits, up to 6 µm in diameter, that are surrounded by clusters of minute pits, up to about 600 nm across (e.g., Fig. 96C). The dorsal larval shell has a median sulcus (e.g., Fig. 98D). The strongly apsacline (e.g., Fig. 98F) ventral larval shell is about as high as wide.

During the comparatively short brephic stage, the dorsal valve has a crescent-shaped pseudointerarea, in addition to a simple median septum with an upper septal rod (Fig. 97A). The development of dorsal propareas and a surmounting plate, associated with the transition to the neanic stage, takes place when the shell is about 0.23 mm wide (Fig. 97C); this corresponds to about 16% of the maximum width of the fully grown shell (Fig. 46). The surmounting plate of the dorsal median septum becomes convex during the later part of the neanic stage. The late neanic ventral valve is highly conical, with the H/W ratio above 100%. The end of the neanic stage is reached when the dorsal median septum is fully developed and develops a posterior platform.

Most adult shells of *B. holmi* are less than 1.0 mm wide. A few rare dorsal valves reaching widths of up to 1.43 mm may possibly belong to a gerontic stage (Figs. 46, 95G).

Scaphelasmatinae

The four scaphelasmatines described in this paper have a closely comparable ontogeny, best illustrated by *Scaphelasma mica*. Some early ontogenetic stages of this species were described by Popov (1975 and in Nazarov & Popov 1980) and Holmer (1986).

The larval shell of *S. mica* and *S. cf. pusillum* is about 0.22 mm wide and 0.19 mm long, whilst in *S.? rugosum* it is almost circular and 0.17 mm across (Figs. 99G, 101B, 102C, 103A). In isolated dorsal larval shells of *S. mica* an incipient pseudointerarea is already developed. The ventral larval

shell has a posteriorly unrestricted pedicle notch. The scaphelasmatine larval shell corresponds to about 20% of the maximum width of the adult shell. There is a distinct larval ornamentation with large circular pits, up to 4 µm across, surrounded by clusters of smaller pits, up to 1 µm across. The boundary with the brephic stage is mostly transitional.

The brephic stage of *S. mica* is comparatively long and can be divided into the following three phases: (1) at first, a dorsal median septum is lacking, and the pedicle notch is unrestricted posteriorly (Fig. 103B, E), (2) later a low septum develops, and (3) during the late part of the brephic stage, a pedicle foramen is formed; that is, the posterior median sector of the ventral mantle starts to secrete shell material (Fig. 103D). In contrast, the entire brephic stage of *S.? rugosum* lacks both a dorsal median septum and a pedicle foramen (Fig. 103G–H). In both species the maximum width of the brephic shell corresponds to about 40% of the maximum shell width (Fig. 46).

During the short neanic stage of *S. mica* and *S.? rugosum* the dorsal pseudointerarea is slightly widened and develops a pair of propareas (Fig. 46). The neanic valves of the latter species develop a foramen, a dorsal median septum (Fig. 103F), and up to five lamellae, whereas the former species has only one or two lamellae. The adult stage of both species is reached when the cardinal muscle scars become thickened (Fig. 46).

Eoconulidae

There are few isolated early ontogenetic stages of the five eoconulid species examined; most ventral valves appear to belong to the adult stage. In the larval and juvenile stages the ventral valve was probably either poorly mineralized or not mineralized at all.

The cementing ventral valve of *Eoconulus cf. semiregularis* and *E. sp. nov.* preserves the earliest ontogenetic stages known in fossil brachiopods (Fig. 46). At about the centre of the ventral valve these two species have a depression defining an oval to circular plate, up to 70 µm wide, that has a most peculiar morphology (e.g., Fig. 107D). At about the centre of the plate there is a spherical to oval 'bubble', up to 40 µm across, which is here termed *bulla* (Fig. 106G). The bulla has two lateral circular apertures, up to 7 µm across, and in some specimens, a minute perforated cone is telescoped into the aperture (Fig. 106H). The bulla is frequently deformed and shows 'scars', as if it had been attached to some object (Fig. 107E).

The bulla is connected to the circular plate by a rounded constricted 'neck' (Fig. 106G), and whereas the plate itself is pitted, the surface of the bulla is completely smooth (e.g., Fig. 107E). The pits on the central plate are of two types, comprising large flat-bottomed pits up to 4 µm across, separated by smaller overlapping round-bottomed pits, up to 1 µm in diameter (Fig. 106C). Anterior to the bulla, there is a distinct notch in the plate, up to about 20 µm wide and 30 µm long, where the pits are missing (Fig. 107D–E).

The pitted plate and the bulla occur within the limits of the ventral larval shell and represent an earlier ontogenetic stage (see discussion below).

The boundary with the larval stage on the ventral valve of *E. cf. semiregularis* and *E. sp. nov. a* is marked by the disappearance of the pits, and the ventral larval shell of the euconulids lacks both pits and true growth lines. The shape of the euconulid ventral larval shell appears to follow the configuration of the substrate; the larval attachment scar is flat (Fig. 106F), wrinkled and irregular (Fig. 39B), cylindrical (Fig. 105E), or ridge-like (Fig. 107B), and there are numerous scattered 'pores' (Fig. 39B). The ventral larval shell of *E. cf. cryptomyus* and *E. robustus* is poorly defined.

The dorsal larval shell of all euconulids is almost circular, and up to 0.25 mm across; it is invariably pitted, with overlapping pits that are flat-bottomed, up to 9 µm across, separated by clusters of smaller pits up to 800 nm across (Figs. 105D, 110C). The boundary with the juvenile stage is either transitional (Fig. 110C) or abrupt (Fig. 110F). Some specimens of *E. robustus* already show a growth disturbance within the dorsal larval shell, whose outline appears to follow the configuration of the substrate (Fig. 110J). In *E. cf. clivosus* some dorsal larval shells have bulbous nodes, each about 50 µm across, which are also probably related to the configuration of the substrate (Fig. 110B, F).

The ventral valve of all examined euconulid species apparently became mineralized late in ontogeny. By comparison with *E. cf. semiregularis* and *E. sp. nov. a*, the ventral valves of *E. cf. cryptomyus*, *E. robustus*, and *E. cf. clivosus* were mineralized still later in ontogeny, which could be the reason why the earliest developmental stages are preserved in the former two species, but missing in the latter. In some specimens of *E. cf. clivosus* and *E. cf. cryptomyus*, the apex of the dorsal valve appears to have been broken, and possibly sealed off during a later part of ontogeny (Fig. 110H).

Discussion

As noted above, it is unlikely that any of the previously described so-called protegula of acrotretacean brachiopods in fact represent an embryonic shell secreted within the vitelline membrane (see also Popov *et al.* 1982 and Rowell 1986). However, the earliest preserved stages in the ontogeny of the euconulids, *Eoconulus cf. semiregularis* and *E. sp. nov. a*, were probably formed early during, or even prior to, the larval stage. The circular pitted plate and the bulla of the ventral valve appear to have been flexible and were probably not mineralized; in this preservation they probably represent a mould, secreted as a mineralized sheet beneath the periostracum (see also Biernat & Williams 1970). This preservation is probably a reflexion of the encrusting life habit of the Eoconulidae; the structure had a protected location on the exterior of the cementing ventral valve.

The interpretation of the peculiar smooth spherical bulla of the ventral valve is not obvious. It is probable that both the bulla and the pitted plate were formed at the same time as a chitinous shell, secreted either by the embryo, as a protegulum, or by the early larva. The protegular or larval periostracum of the circular plate was vesicular (cf. Biernat

& Williams 1970), whereas the flexible, chitinous layer of the bulla did not have the vesicular structure.

The width of the pitted plate is about 1/3 that of the protegulum of *Lingula*. The circular shape and the possession of a posterior notch agrees with that of the ventral larval shell of the scaphelasmatine, although the latter is about three times larger. In size the pitted plate is closest to the earliest larval shell of *Discinisca*, which is about 20–70 µm across and is secreted during the stage with three pairs of lophophoral filaments (Chuang 1977, Fig. 6).

The euconulids were probably derived from the scaphelasmatine (L. E. Popov, personal communication 1986), and the minute notch in the pitted ventral plate of the former may correspond to the pedicle notch in the ventral larval shell of the latter. The bulla is situated within this 'pedicle' notch, which invariably faces towards the posterior margin of the ventral valve. For this reason, the bulla might represent an incipient 'pedicle', of which a mould of the chitinous cuticle is preserved. It is difficult to envisage the function of the two lateral apertures of the 'pedicle' bulla, but they might have been used somehow in early attachment to the substrate.

No Recent inarticulate brachiopod larvae develop a pedicle before or during the early larval stage; in lingulaceans and discinaceans the pedicle is first seen late during the larval stage, just prior to settlement.

Popov *et al.* (1982, p. 99, Fig. 2:6) noted that the edge of the dorsal larval shell of some specimens of *Eoconulus semiregularis* reproduces the irregularities of the substrate. This fact is also apparent from some dorsal larval shells of *E. cf. semiregularis* and *E. robustus*, which means that the secretion of the 'larval shell' must have continued also some time after settlement. As settlement marks the end of the larval stage (in a strict sense), this indicates that the end of the so-called 'larval stage' in acrotretaceans is not always correlated with settlement.

The pitted nature of the larval shells of acrotretacean brachiopods has attracted attention ever since it was first reported by Biernat & Williams (1970). Popov *et al.* (1982) adequately summarized previous studies on the fine structure of the larval shells of inarticulate brachiopods. It is generally agreed that the pitting represents the negative replica of an organic and vesicular shell (Biernat & Williams 1970; see also Ludvigsen 1974; and Bitter & Ludvigsen 1979). In this context it is interesting to note the vesicular nature of the periostracum of some larval shells in Recent *Discinisca lamellosa*, described briefly above.

In the euconulids and other acrotretaceans the end of the larval stage is correlated with a change in the secretional pattern. As suggested by Biernat & Williams (1970), it is possible that this is due partly to the appearance of the 'conveyor belt system' of the epithelium. In thin section, the acrotretacean larval shell constitutes a thin separate plate that probably represents a mould of the larval periostracum. The plate lacks a primary shell layer; secretion of the primary layer starts first in the juvenile stage.

Siphonotretacea

Two siphonotretacean species, *Acanthambonia delicata* and *Nushbiella lillianae*, yielded some information on early ontogeny this group, but few isolated early stages were found.

In *Acanthambonia delicata* the larval shell is smooth, circular, and about 0.25 mm across. The ventral larval shell is pierced by a minute pedicle foramen that became atrophied during later growth (Fig. 115I). The boundary with the juvenile stage is marked by the development of growth lines and spines. The ontogeny of the closely related *Acanthambonia portranensis* was described in greater detail by Popov & Nölvak (1986).

In *Nushbiella lillianae* the smooth larval shell is about 0.28 mm wide and 0.23 mm long, but it is not always well defined on older individuals. The ventral larval shell is partitioned roughly into three lobes, with a central posterior lobe that is bulbous and elevated in lateral profile, and two lateral lobes. The valve is penetrated practically along its whole length by an anteriorly unrestricted, keyhole-shaped pedicle notch. However, in some specimens the anterior margin of the ventral larval shell appears to be entire. The outline of the dorsal larval shell is not known in detail. The larval shells of both valves are smooth and the boundary with the brephic stage is marked by the appearance of spinose lamellae.

The larval shells of other siphonotretaceans (*Siphonotreta*, *Multispinula*, and *Helmersenina*) are also smooth, but somewhat larger, around 0.40 long (Biernat & Williams 1971).

The brephic and juvenile stages of both valves of *Nushbiella lillianae* are extremely thin. The posterior part of the keyhole-shaped pedicle foramen is plugged in all specimens examined; only the anterior part appears to have remained open throughout the ontogeny. As far as could be determined, no resorption took place during the development of the pedicle foramen; it is of an almost constant size in all observed ontogenetic stages and is not observed cutting through growth lines.

In contrast, the ontogenetic development of the pedicle foramen of many other siphonotretaceans includes some degree of resorption (e.g., Rowell 1962).

Summary

There is no obvious trace of a protegular shell in the ontogeny of the examined Middle Ordovician phosphatic inarticulate brachiopods. However, the cementing ventral valve of *Eoconulus* cf. *semiregularis* and *E.* sp. nov. has a very small central pitted circular plate that possibly corresponds to a mould of a chitinous vesicular embryonic or early postembryonic valve.

All fossil and Recent phosphatic inarticulates have some sort of larval shell that is secreted by a planktotrophic larva. In the morphology of the larval shell and with respect to details of the postlarval development the following three types can be distinguished:

(1) In fossil and Recent lingulaceans and discinaceans the larval shell is large (as compared with that of the acrotreta-

ceans) and lacks a pedicle notch. Its surface is smooth and well delineated from the remainder of the shell by a line of growth disturbance. The larval shell constitutes a well defined plate, which lacks a primary shell layer. Some isolated larval shells of Recent *Disciniscia lamellosa* have an highly vesicular outer periostracal layer. The vesicles do not appear to have left any marks upon the mineralized shell.

The beginning of the juvenile stage is marked by a change in the secretional pattern of the mantle. A thin outer primary shell layer is deposited, in which the ornamentation (pits, spines etc.) is developed.

The discinacean pedicle opening (along with the listrium, pedicle tube etc.) is formed during the juvenile stage, when the posterior median sector of the ventral mantle starts to secrete shell material.

(2) The larval shell of the two examined siphonotretacean species is smooth, circular, and has a pedicle foramen. The boundary with the juvenile stage is marked by a line of growth disturbance, associated with formation of spinose lamellae. In adults of two species of *Acanthambonia*, the pedicle foramen is atrophied, whereas in *Nushbiella lillianae* it is only partly plugged.

(3) All examined members of the superfamily Acrotretacea have a comparatively small, circular, pitted larval shell. The ventral larval shell has a pedicle foramen, except in the scaphelasmates, which have a pedicle notch that is open at the posterior margin. The central posterior section of the ventral mantle of the scaphelasmates starts to secrete shell material during the early juvenile stage.

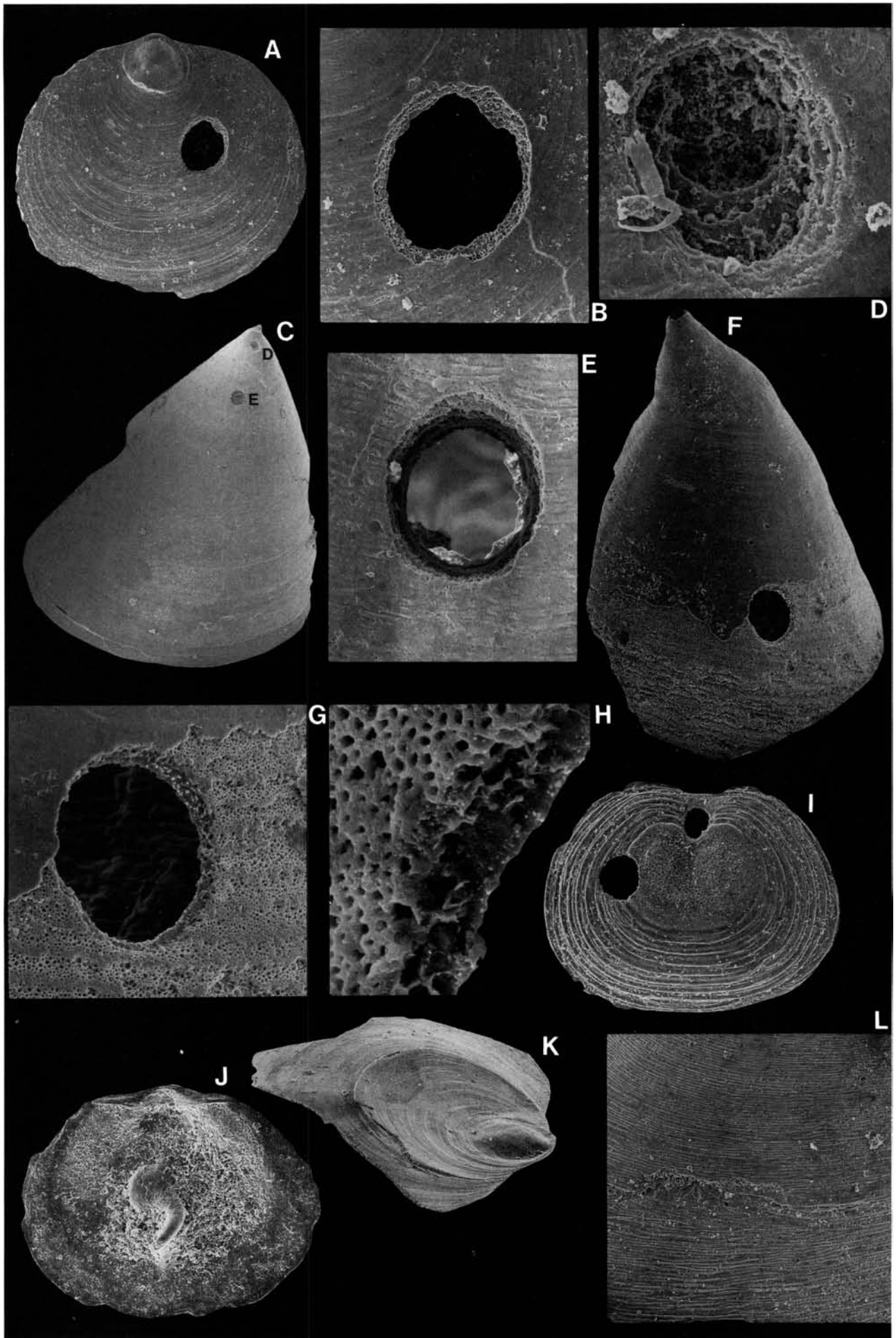
The acrotretacean larval shell constitutes a separate plate, which lacks a primary shell layer. The boundary with the juvenile stage is marked by disappearance of larval pits and a line of disturbance in shell growth; at about that time the mantle starts to secrete the outer primary shell layer.

All brephic dorsal valves have a minute pseudointerarea that is undivided. In a few acrotretacean species an incipient dorsal pseudointerarea is developed already in the larval shells. The neanic stage of the acrotretaceans starts when the propleareas of the dorsal pseudointerarea are formed.

Predation and malformation

There is little evidence of any extensive predation in the faunas of the Middle Ordovician phosphatic inarticulate brachiopods; among more than 35 000 specimens examined, less than 30 specimens have unquestionable predatory borings.

In the upper Ryd Limestone a single sample (GB84-3-61) yielded 16 specimens with predatory borings – two dorsal and five ventral valves of *Scaphelasma mica* (Fig. 47I), and four dorsal and five ventral valves of *Conotreta?* *siljanensis* (Fig. 47A–B, F–H). The relative frequency of valves with borings in the sample is about 2% of the specimens of *S. mica* and 5% in *C.?* *siljanensis*. A few ventral valves of *Cyrtotreta?* *striata* (Fig. 66F–G, J) and *Cyrtotreta* sp. (Fig.



47C–E) from the Dalby Limestone also have predatory borings.

Normally there is a single borehole per valve. Only in one case, a ventral valve of *Cyrtotreta* sp. a, was a valve bored twice, but one of the borings does not penetrate the shell (Fig. 47D–E). Due to the limited number of bored specimens available, neither the possible preferential location of the boreholes, nor the relative frequency of bored dorsal *versus* ventral valves were determined.

The boreholes have a circular to slightly elliptical outline and appear to penetrate the surface of the shell at about 90°. The external diameter varies from about 70 µm (Fig. 47I) to 220 µm (Fig. 47A–B). In most specimens the holes are countersunk, and the external diameter exceeds the inner diameter by up to 30 µm (Fig. 47B, D–E, F–H). A few holes lack a well defined countersunk rim (Fig. 47I).

Predatory borings with an identical morphology have been described and discussed in detail from Silurian acrotretacean brachiopods (*Artiotreta parva*, *Opsiconidion* sp.) by Chatterton & Whitehead (1987; see this work for a full discussion of acrotretacean boreholes). The material described by them differs by a somewhat higher frequency of bored specimens (8% of the total number of specimens of *Artiotreta parva*) and the slightly smaller size range of the holes (diameter 60–130 µm). In *Artiotreta parva* the boreholes were distributed about equally between dorsal and ventral valves. They were located preferentially around the pedicle opening on the ventral valve, and between the umbo and the median septum on the dorsal valve, where the valves are relatively thin. As noted by the authors, the failed boreholes, together with countersunk edges, indicate that penetration was from the outside, and that they are predatory borings rather than made for domicile. The identity of the boring organism cannot be determined with any degree of certainty, but the borings are similar to those produced by Recent muricid gastropods (Chatterton & Whitehead 1987, p. 73).

Fig. 47. □A–I. Possible predatory boreholes in acrotretids. □A. Dorsal valve of *Conotreta? siljanensis* sp. nov., showing a countersunk borehole; Ryd Limestone (sample GB84-3-61); Br132914, ×55. □B. Detail of A; ×165. □C. Side view of a ventral valve of *Cyrtotreta* sp. a, showing both an unfinished and a completed borehole; the location of D and E is indicated; Dalby Limestone (sample DLK83-dal-12); Br132526, ×20. □D. Detail of C, showing the unfinished borehole through the apical process; ×413. □E. Detail of A, showing the completed countersunk borehole; ×207. □F. Side view of a ventral valve of *Conotreta? siljanensis* sp. nov.; Ryd Limestone (sample GB84-3-61); Br132912, ×106. □G. Detail of F; ×379. □H. Detail of the edge of the countersunk borehole in G; ×1860. □I. Ventral valve of *Scaphelasma mica* Popov, 1975, showing a borehole at the edge of the larval shell; note that the edges are not countersunk; Ryd Limestone (sample GB84-3-61); Br132915, ×121. □J–L. Examples of deformations in acrotretids. □J. Dorsal valve of *Myotreta dalecarlica* sp. nov., showing a deformed median septum; Kårgårde Limestone (sample DLK83-segk-6); Br128908, ×90. □K. Side view of a deformed dorsal valve of *Conotreta? mica?* Goryanskij, 1969; Gullhögen Formation (sample GB84-1-1); Br132598, ×80. □L. Detail of the disturbed growth in a ventral valve of *Conotreta? mica?* Goryanskij, 1969; Skärlov Limestone (sample DLK83-sä-7); Br129003a, ×90.

Malformations and disturbances in the growth of the *Viru* inarticulates are not common, but have been noted in some ephippelasmates and acrotretines. In some specimens of *Myotreta dalecarlica* the growth of the otherwise regular dorsal median septum has been disturbed (Fig. 47J), and in some specimens of *Conotreta? mica?* the direction of growth of the dorsal valve is deflected temporarily during the neanic stage, resulting in a concave surface of the valve (Fig. 47K).

Large specimens of lingulaceans and acrotretaceans occasionally show traces of repaired external damages (Figs. 47L, 50A).

Phylogeny and evolution

Phosphatic inarticulates and brachiopod phylogeny

Although the basic unity of the phylum has long been accepted generally, there have been some suggestions recently to the effect that brachiopods arose polyphyletically from several independently developing phoronid-like (or 'brachiophorate', Wright 1979) lineages (Cowen & Valentine *in* Valentine 1973; Valentine 1975, 1977). The Brachiopoda would then constitute a grade of organization rather than a monophyletic clade. An analysis and review of these proposals was presented by Rowell (1981a, 1981b, 1982).

A recent provocative scheme for a polyphyletic derivation of the brachiopods was developed by Goryanskij & Popov (1985, 1986). They propose to restrict the phylum to the inarticulates having a calcium carbonate shell (*Craniida*, *Craniopsida*, *Trimerellida*, *Kutorginida*, and *Obolellida*) and the articulates. In their opinion phosphatic inarticulates, together with the phoronids and the ectoprocts, diverged from the lineage leading to true brachiopods at a very early stage of lophophorate evolution, before the acquisition of a bivalved and mineralized shell (Goryanskij & Popov 1985, Fig. 5; 1986, Fig. 2).

Goryanskij & Popov (1985) erected the new taxon *Lingulata* of the rank of class to accommodate the ousted phosphatic inarticulates, but did not state to what higher taxon this new class should belong. The main basis for their proposal is the inferred differences in the partition of coelomic spaces in living brachiopods; according to them, the mantle, body cavity and shell of the articulates and *Crania* are not homologous with the mantle, body cavity and shell of the phosphatic brachiopods (Goryanskij & Popov 1986, p. 234). Traditionally brachiopods are considered to be trimerous organisms with proto-, meso- and metacoel; the coelom of the mantle and body cavity represents the metacoel, whereas the mesocoel (and 'proto-coel') is within the lophophore (e.g., Hyman 1959). In the view of Goryanskij & Popov this is only true for the phosphatic inarticulates.

According to Percival (1944), the larva of the articulate brachiopod *Terebratalia inconspiqua* has two pairs of coelomic sacs; the anterior is within the mantle lobe and the posterior occupies the pedicle lobe of the larva. In the view of Goryanskij & Popov (1986, p. 233) these represent the

mesocoel and metacoel, respectively. In a similar way the coelomic partition of *Crania* is reinterpreted; according to Starobogatov (1979) and Goryanskij & Popov, the main part of the body represents the mesocoel and the 'anal chamber' (e.g. Hyman 1959, Fig. 198A) a reduced metacoel.

As noted by Goryanskij & Popov (1986, p. 233), 'it is known that coelomic partitioning in brachiopods is not obvious and may be a debatable feature', and Hyman (1959, p. 576) pointed out that Percival (1944) does not give details as to the fate of the coelomic sacs through later ontogeny. In fact, Percival (1944) also suggested that articulates and inarticulates do not belong to the same phylum. However, this proposal was based on the erroneous identification of a pair of 'ventral' muscles in the dorsal larval shell of *T. inconspicua*. Later, Percival (1953) withdrew his earlier suggestion.

Percival's (1944) type of well developed division of coelom could not be observed by Conklin (1902) in the ontogeny of *Terebratulina septentrionalis*, and Franzén (1969) found that no coelom is developed in the pedicle lobe of free-swimming larva of *Terebratulina retusa*. The mode of coelom formation in the latter species is unlike any other described from the articulate brachiopods, and appears to be more related to the schizocoelic type, as found in *Lingula* (Franzén 1969, p. 171). Moreover, recent studies on the ontogeny of *Terebratalia transversa* (Stricker & Reed 1985a, 1985c, 1985d) did not prove the presence of a separate coelom in the pedicle lobe, and the mode of coelom formation in this species apparently cannot be equated with the ordinary enterocoely and schizocoely shown by other brachiopods (Stricker & Reed 1985a, p. 244). It is evident that further detailed ontogenetic studies are needed in order to clarify the nature of coelom formation in Recent brachiopods.

The best case for a monophyletic origin of the phylum was argued by Rowell (1981a, 1981b, 1982). As he noted (Rowell 1982, p. 305) the detailed structure of the brachiopod lophophore presents the most formidable arguments against polyphyly. It is difficult to argue that the structural and functional integrity of this distinctive organ arose convergently several times. Moreover, as suggested by Valentine (1981; Valentine & Erwin 1987) the solution to suspension feeding life habit (or body plan) exhibited by brachiopods appears to require the presence of a 'rigid' filtering chamber. The brachiopod lophophore is stiff and cartilaginous with a long ciliated food groove and a feeding stream that passes between the tentacles, unlike the lophophore of ectoprocts and phoronids which has a hydraulic skeleton and a feeding stream directed toward the mouth (see earlier references in Valentine 1981; Valentine & Erwin 1987; also Gilmour 1978, 1981). The brachiopod type of feeding mechanism cannot function without a bivalved shell, where there are separate inhalant and exhalant chambers (Valentine 1981, p. 199). The development of this type of suspension feeding represents another potential synapomorphy for a monophyletic phylum. A hypothetical 'prototypic brachiopod' (or proto-brachiopod) like that of Williams & Hurst (1977, p. 88) could then be the oldest common ancestor with the following characters:

(1) a 'brachiopod type' of suspension feeding (in the sense of Valentine 1981), (2) a 'rigid' but unmineralized shell, and (3) hydraulic opening mechanism (for other inferred characters of the proto-brachiopod, see Williams & Hurst 1977, Fig. 8).

However, it is important to note that the anatomy and morphology of the 'proto-brachiopod' must not necessarily be modelled after the Recent lingulids, as has been the usual practise (e.g. Williams & Hurst 1977, Fig. 8); the recurved gut and other peculiarities of the living lingulids might as well have evolved secondarily, and there is no need to assume that the U-shaped gut originated before the true 'proto-brachiopod' as suggested by Goryanskij & Popov (1985, 1986). The anatomy of the Recent craniids (with a posterior anus) might actually represent a retained primitive character for the phylum (e.g., Helmcke 1939, Fig. 155; Hyman 1959).

Although closely similar, the lophophores of Recent inarticulates and articulates are not identical; Gilmour's (1978, 1981) work on the articulate *Laqueus californianus* and the inarticulate *Glottidia pyramidata* indicated some previously unknown differences between these two species in the ultrastructure of the tentacles and the solution to waste-rejection.

Basically the two opposing viewpoints, the monophyletic or polyphyletic derivation of the brachiopods, try to explain and emphasize the relative importance of similarities interpreted as representing synapomorphies and symplesiomorphies (or convergences). As is suggested from the above discussion, evidence presented so far is inconclusive, and much further work would be required to negate the traditional concept of a monophyletic brachiopod phylum.

The classification and inferred evolution of groups within the Brachiopoda are open to widely different opinions. In the classification of Williams & Rowell (1965c) the phylum is divided into two main classes, the Inarticulata and the Articulata. Although there is relatively little confusion about what constitutes an articulate brachiopod, it can very well be argued that the Inarticulata is a very heterogeneous grouping (see, e.g., Wright 1979). The proposal by Goryanskij & Popov (1985, 1986) to group the phosphatic inarticulates in a separate higher taxon (i.e. a Class) is acceptable also within a monophyletic phylum. It can very well be argued that changes in skeletal chemistry are unlikely to have taken place convergently several times within the phylum (six times, according to Williams 1984, p. 744). It is possible that the acquisition of a skeleton (whether phosphatic or calcareous) from an unmineralized 'proto-brachiopod' ancestor, once it had occurred, did not involve any subsequent changes in skeletal chemistry. However, in the case of the aragonitic trimerellids (Jaanusson 1966), a change in skeletal mineralogy may have been involved.

New information on the detailed morphology of the poorly known trimerellids and obolellids, such as a possible articulate type of opening mechanism as presented by Goryanskij & Popov (1985, 1986), clearly indicates that the systematic position of the non-phosphatic inarticulates must be reevaluated.

Evolution of the Class Lingulata Goryanskij & Popov

Traditionally, the phosphatic inarticulates have been placed within three separate orders, the Lingulida, Acrotretida, and Paterinida. As suggested by Goryanskij & Popov (1985, 1986; see also above), these orders are now restricted to forms which have a phosphatic shell. Together these three groups are considered to constitute a separate Class, the Lingulata.

Apart from such poorly known and aberrant lingulacean families as the Paterulidae and Andobolidae, the Order Lingulida (in the sense of Goryanskij & Popov 1985, 1986) appears to represent a natural grouping of closely related forms. The text-book examples of evolutionary stability within this group, which ranges from the Cambrian to the Recent, are well known, although many of the common records of Palaeozoic *Lingula* must be strongly questioned and should be re-examined.

Although the morphology of the lingulaceans may have remained comparatively unchanged through time, there appear to be some differences in shell structure between early Palaeozoic and Recent forms. The shell of the type species, *Lingula anatina*, is poorly mineralized; it lacks a well defined primary layer, and has alternating apatitic and organic layers only in the median portion of the valves. The remainder of the shell consists exclusively of organic substance (e.g., Iwata 1981a, b). In contrast, most Palaeozoic lingulaceans appear to have an outer apatitic primary layer, and alternating mineralized and organic layers throughout the valves. Moreover, the shell structure in the Ordovician and Silurian lingulaceans examined for the present study is unlike that of Recent *Lingula* (Iwata 1981a, b), but agrees more closely with that of Recent *Glottidia* (Iwata 1982).

The Order Acrotretida as defined by Rowell (1965, p. H274) is heterogenous and probably does not represent a monophyletic clade; the superfamilies Acrotretacea, Discinacea, and Siphonotretacea have a ventral valve with a pedicle foramen and holoperipheral growth in common, but show fundamental differences in ontogeny and shell structure.

The only surviving phosphatic Acrotretida (in the sense of Rowell 1965) are members of the Discinacea. Contrasting views as to the systematic position of the discinaceans were summarized very briefly by Holmer (1987b). As noted by Helmcke (1939) and Williams & Rowell (1965b, p. H167), the anatomy and ontogeny of the Recent discinaceans agree closely with the Recent lingulaceans (see, e.g., Helmcke 1939 and Hyman 1959, for details). There is also a great deal of resemblance in shell structure between Recent discinaceans and lingulaceans (Iwata 1982).

By contrast, the musculature of Palaeozoic acrotretaceans such as *Linnarssonella* is quite unlike the musculature of Palaeozoic lingulaceans such as *Lingulella* (Williams & Rowell 1965b, p. H167). Moreover, the difference in shell structure and ontogeny between the Palaeozoic represen-

tatives of these two groups examined so far is fundamental. According to Williams & Rowell (1965b), the similarities in anatomy between Recent lingulaceans and discinaceans are due to convergence.

It is proposed herein that the Discinacea, the Siphonotretacea, and the Acrotretacea were derived convergently from the Lingulacea; it is most unlikely that the two former superfamilies originated from an acrotretacean stock as suggested by Williams & Rowell (1965b), for the following reasons:

(1) A pedicle foramen is also present in members of the recently described lingulacean family *Lingulellotretidae* Koneva & Popov, 1983, where it develops late in ontogeny; I suggest that the evolution of an 'acrotretid' type of ventral valve – with a pedicle foramen and holoperipheral growth – from a lingulacean stock could have been accomplished comparatively easily, and could have taken place convergently three times within the Acrotretida (*sensu lato*).

(2) The acrotretacean larval shell is small and distinctly pitted. As suggested by Rowell (1986), this type of ontogeny can be considered to represent a derived character for the acrotretaceans (including the families *Eoconulidae*, *Acrothelidae* and *Botsfordiidae*). The smooth and comparatively large larval shell of the discinaceans can be regarded as a primitive character, shared with the lingulaceans. The smooth larval shell of the siphonotretaceans is probably closer to the lingulacean–discinacean type than to the acrotretacean type.

(3) The acrotretacean type of shell structure can be regarded as representing a further derived character for this Superfamily, whereas the discinacean shell structure agrees with that of the lingulaceans, representing a symplesiomorphy for these groups. The acrothelids also appear to have retained the primitive lingulacean type of shell structure. The shell structure of the siphonotretaceans is not well known, but appears to be more closely related to the lingulacean–discinacean than to the acrotretacean type (Popov & Nölvak 1986).

Consequently, the Order Acrotretida is here restricted to the families *Acrotretidae*, *Eoconulidae*, *Acrothelidae*, and *Botsfordiidae*. The superfamilies *Siphonotretacea* and *Discinacea* are considered to belong to two separate orders, the *Siphonotretida* and *Discinida*. Each one of these three orders probably originated separately from a lingulid stock.

Thus, the following classification of the inarticulate brachiopods with a phosphatic shell seems to reflect best our present knowledge of relationships.

Class Lingulata Goryanskij & Popov, 1985

Order Lingulida Waagen, 1885

Order Acrotretida Kuhn, 1949

Order Discinida Kuhn, 1949

Order Siphonotretida Kuhn, 1949

?Order Paterinida Rowell, 1965

Systematic palaeontology

Most of the figured material below comes from the Fjåcka and Kårgårde sections (Fig. 5) and from Gullhøgen quarry (Fig. 2).

Additional comparative unfigured material was examined from the Viru sequence of several Cambrian–Silurian districts of Sweden. From the island of Öland, material was isolated from the following formations (for the detailed location of the localities, see Jaanusson 1960): (1) Lowermost Segerstad Limestone (quarry 300 m NW of the railway station at Skärlov, coll. V. Jaanusson 1958); (2) Furudal Limestone (shore at Gräsgårds Hamn, coll. V. Jaanusson 1952); (3) Källa Limestone (quarry at Källa, coll. V. Jaanusson 1949).

A single erratic boulder of the Dalby Limestone (coll. S. Hagenfelt), derived from the submarine South-Bothnian Cambrian–Ordovician district, was available for examination, found on the small island of Alskäret about 36 km NE of the town of Norrtälje, Norrpadra Archipelago, County of Stockholm. Through the courtesy of Anita Löfgren (Lund), the inarticulate brachiopods from insoluble residues of the lower Viru sequence of Jämtland were also studied, including the upper Holen (sample J70-161), Segerstad (samples J70-165, 166), and Skärlov (sample J70-167) limestones of the Gammalbodberget section and the upper Holen (sample J69-28) and Segerstad (samples J69-35, 37, 38, 40–43) limestones of the Gusta section (for the location of the localities, see Löfgren 1978).

For comparative purposes, some specimens are figured also from the following additional regions: (1) U.S.S.R., Estonia, Kohtla (coll. G. Troedsson), Viivikonna Formation, Kiviõli Member, Kukrusean Stage (*Pygodus anserinus* Biozone); (2) U.S.A., Alabama, Pratt Ferry (sample 68B9-1, coll. S. M. Bergström) Pratt Ferry beds (top part of *P. anserinus* Biozone, Bergström 1971); (3) U.S.S.R., Kazakhstan, Karakan (Locality 2033, coll. L. E. Popov), Llanvirn, Karakan Formation (Nazarov & Popov 1980); (4) U.S.S.R., Russia, Pskov district, Pechory core (483.35 m), Kundan Stage.

All measurements are in millimetres unless stated otherwise, and with specimens oriented in the conventional manner, defined as follows: W = maximum width, L = maximum length, H = maximum height of ventral valve, T = maximum thickness of complete biconvex shell, WI = maximum width of pseudointerarea (or internal areas), LI = maximum length of pseudointerarea (or internal areas), WP = maximum width of pedicle groove (or foramen), LP = maximum length of pedicle groove (or foramen), WM = maximum combined width of dorsal cardinal muscle scars, LM = maximum length of dorsal cardinal muscle scar (measured from the midsagittal posterior margin, unless stated otherwise), BS = point of origin of median septum (measured from the midsagittal posterior margin), LS = length of median septum (measured from the sagittal posterior margin), HS = maximum height of dorsal median septum, WL = maximum width of larval shell, LL = maximum length of larval shell. The mean (\bar{W} , \bar{L} , \bar{H} etc.), observed range (OR), standard deviation (S_{n-1}) and number (N) of measurements are given.

Figured specimens are deposited in the Department of Palaeozoology, Swedish Museum of Natural History (abbreviated RM), Stockholm, unless stated otherwise. Only figured specimens are given individual numbers. The original material is mounted on slides with numbers (RM)Br128492–129100, 132371–133500, 133587–133642.

Class Lingulata Goryanskij & Popov, 1985 Order Lingulida Waagen, 1885

Superfamily Lingulacea Menke, 1828

Diagnosis. – See Rowell (1965, p. H262).

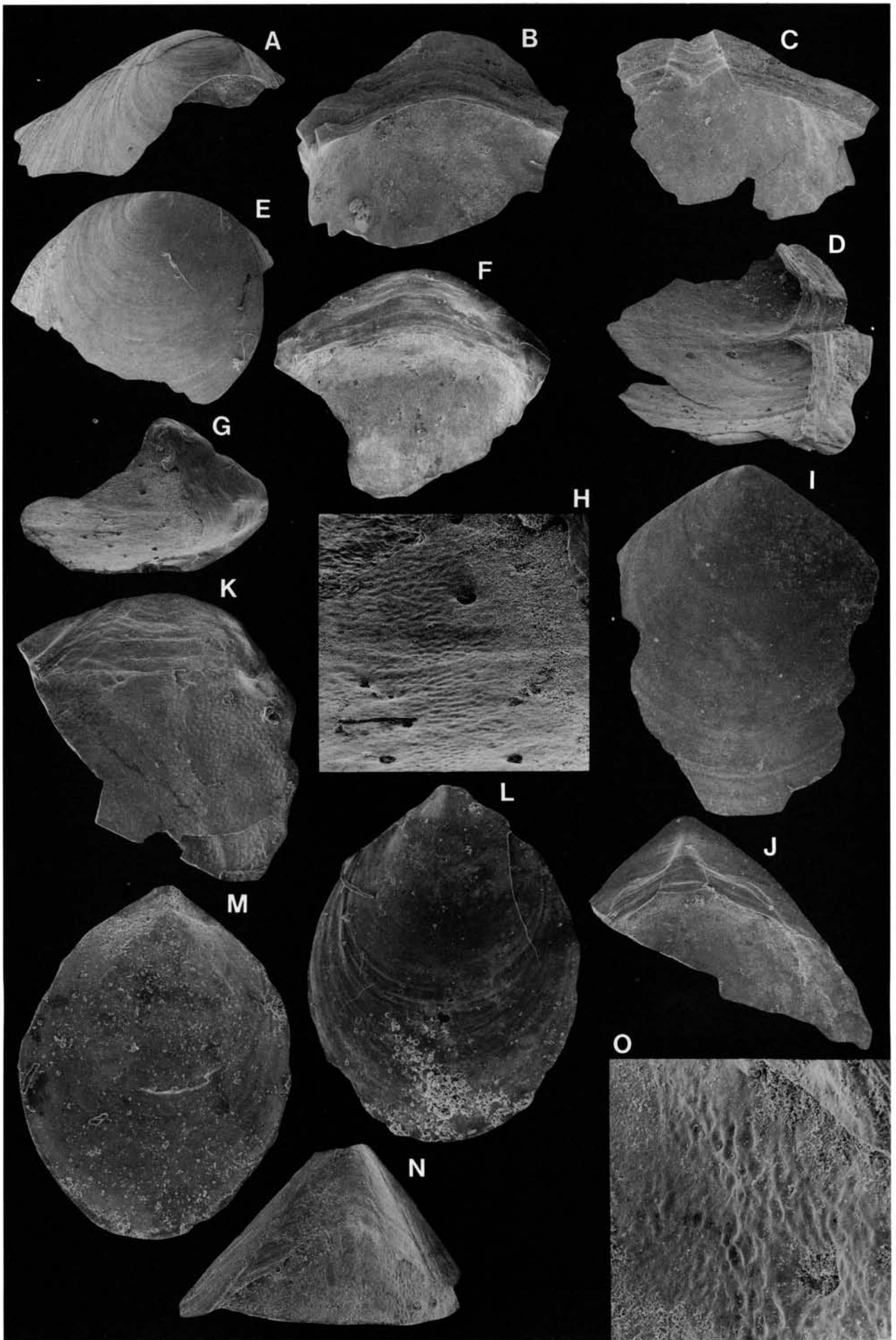
Discussion. – Many lingulaceans are relatively large as compared with most other phosphatic inarticulates; well preserved specimens are rare, but even when the shell is complete the valves are commonly fractured and disintegrate during the etching process. Selective collecting in the field of macroscopic material has not produced any recognizable specimens; examination of museum collections did not yield additional material. For this reason, the use of open nomenclature is commonly unavoidable. The Family Paterulidae, although represented by fairly abundant and well preserved material (some 700 specimens), have been excluded from detailed study, because this taxonomically complicated group requires special investigation. However, the stratigraphical distribution of the paterulids is recorded.

Family Obolidae King, 1846

Diagnosis. – See Rowell (1965, p. H263).

Discussion. – As noted by Havlíček (1982, p. 13), assigning species of the general obolid and lingulid morphotype into the subfamilies Obolinae, Lingulellinae or Glossellinae presents difficulties. According to him, the obolines have clearly raised pseudointerareas, whereas in the lingulellines pseudointerareas, or so called internal areas, are less raised. However, the distinction between these two subfamilies is still not always clear.

Fig. 48. □A–D. *Rosobolus?* sp. nov. a; Gullhøgen Formation (sample GB84-1-1). □A. Exterior of a dorsal valve; Br132601, ×29. □B. Interior of a dorsal valve; Br132600, ×37. □C. Ventral interior; Br132603, ×44. □D. Side view of the interior of C; ×67. □E–J. *Expellobolus?* sp. nov. a; Skärlov Limestone (sample DLK83-så-1). □E. Dorsal exterior; Br128992, ×22. □F. Interior of a dorsal valve; Br128993, ×22. □G. Side view of the interior of F; ×24. □H. Detail of G, showing the pitted interior and the shallow ‘pores’; ×245. □I. Exterior of a ventral valve; Br128990, ×32. □J. Interior of a ventral valve; Br128991, ×27. □K–O. Lingulellinae gen. et sp. □K. Dorsal interior, showing a polygonal mosaics of pits; Gullhøgen Formation (sample GB84-1-3); Br132611, ×31. □L. Exterior of a juvenile ventral valve; Gullhøgen Formation (sample GB84-2-13); Br132714, ×105. □M. Interior of a juvenile ventral valve; Gullhøgen Formation (sample GB84-2-2); Br132663, ×84. □N. Ventral interior; Gullhøgen Formation (sample GB84-1-1); Br132604, ×23. □O. Detail of N, showing the pitted interior; ×103.



Subfamily Obolinae King, 1846 (*sensu* Havlíček 1982, p. 15)

Genus *Rosobolus* Havlíček, 1982

Type species. – Original designation; *Rosobolus robertinus* Havlíček, 1982, p. 19, from the Tremadoc Trenice Formation, Holoubkov quarry, Prague basin, Bohemia.

Diagnosis. – See Havlíček (1982, p. 18).

Species assigned. – *Rosobolus robertinus* Havlíček, 1982.

Rosobolus? sp. nov. a

Figs. 16B–D, 48A–D

Material. – Figured; Br132600, Br132601, Br132603, Br132594c (section). Total of 9 fragmentary dorsal valves and 10 fragmentary ventral valves.

Description. – No complete valves are known to give an indication of the outline. Both valves have shelf-like anacline pseudointerareas (Fig. 16B). The ventral valve has a deep, subtriangular pedicle groove. There is a ventral umbonal muscle scar (Fig. 48C–D). The dorsal pseudointerarea lacks a median groove (Fig. 48B). The valves are ornamented with weakly developed fila (Fig. 48A). The shell structure is described above (p. 33, Fig. 16B–D).

Discussion. – This species is assigned tentatively to *Rosobolus*, mainly because of similarities in the development of the pseudointerareas. In the type species *R. robertinus* Havlíček (1982, Pl. 3:1–9) these features are anacline and shelf-like, and the pedicle groove is well developed. *Hyperobolus feistmanteli* (Barrande) (Havlíček 1982, Pl. 1:1–8) also has shelf-like pseudointerareas, but these are orthocline. Moreover, *H. feistmanteli* is several times larger than *Rosobolus?* sp. nov. a, and has lamellose ornamentation. Because of the fragmentary state of the available material, no close comparison is possible.

Occurrence. – *Rosobolus?* sp. nov. a is known only from Västergötland, where it is restricted to the Gullhøgen Formation (Fig. 8B).

Subfamily Lingulellinae Schuchert, 1893 (*sensu* Havlíček 1982, p. 25).

Genus *Expellobolus* Havlíček, 1982

Type species. – Original designation; *Lingula expulsa* Barrande, 1879, Pl. 110, Fig. 9:1–4, from the Tremadoc Trenice Formation, Krušná Hora, Prague basin, Bohemia.

Diagnosis. – See Havlíček (1982, p. 25).

Species assigned. – *Expellobolus expulsus* (Barrande, 1879).

Expellobolus? sp. nov. a

Fig. 48E–J

Material. – Figured; Br128990, Br128991, Br128992, Br128993. Total of 5 fragmentary dorsal valves and 8 fragmentary ventral valves.

Description. – No complete outline is preserved of either valve, but it appears to have been broadly subquadrate. Both valves have internal areas, which are not raised above the inner surface of the valve. The ventral internal area has a shallow triangular pedicle groove, up to 0.4 mm wide (Fig. 48J). The dorsal internal area lacks a median groove (Fig. 48F–G). The inner surface of both valves is distinctly pitted with a polygonal mosaics of pits, defined by elevated ridges (Fig. 48H); in addition there are numerous ‘pores’, about 60 µm across, that do not penetrate the entire thickness of the valve (Fig. 48H). The valves are ornamented with faint radial capillae (Fig. 48E, I).

Discussion. – *Expellobolus?* sp. nov. a is similar to the type species, *E. expulsus* (Barrande) (Havlíček 1982, Pl. 4:2–8). The internal areas of both lack a dorsal median groove, whereas they have a shallow ventral pedicle groove. The interior ‘pores’ in the Swedish specimens appear to be similar to those present in the unnamed glosselline (cf. Fig. 53I). This is only the second record of *Expellobolus*.

Occurrence. – *Expellobolus?* sp. nov. a is restricted to the Skärlov Limestone of Dalarna (Fig. 9A).

Genus *Lingulella* Salter, 1866

Type species. – Subsequent designation by Dall, 1870, p. 159; *Lingula davisii* M’Coy, 1851, from the Upper Cambrian Ffestiniog Flags Formation, Gwynedd, Wales, U.K.

Diagnosis. – The broad diagnosis of *Lingulella* by Krause & Rowell (1975, p. 14) is followed here.

Lingulella? *alata* sp. nov.

Fig. 49A–H, ?I

Name. – Latin *alatus*, winged; alluding to the strongly recurved dorsal propareas.

Holotype. – Br132863, fragmentary dorsal valve, Fig. 49D–E, from the Ryd Limestone, Gullhøgen quarry (sample GB84-3-51), Västergötland.

Paratypes. – Figured; Br132865, Br132862, Br132864, Br132839, ?Br128999. Total of 16 fragmentary dorsal valves and 7 fragmentary ventral valves.

Diagnosis. – Valves with wide posterior margin. Dorsal internal area relatively narrow and short, not raised above inner surface. Dorsal propareas ‘wing-like’, of extremely variable inclination, from slightly hypercline to apsacline. Ornamentation with rugae, up to 14 per mm.

Description. – The complete outline is not known from either valve, but it appears to have been broadly oval. The ventral internal area has a well developed triangular pedicle groove, up to 0.40 mm wide (Fig. 49H). The dorsal internal area has a subtriangular median groove (Fig. 49D–F); the propareas are ‘wing-like’, and recurved almost 180° (Fig. 49B, E). The larval shell is comparatively sharply delineated and smooth, about 0.80 mm wide and 0.50 mm long. The valves are ornamented with regularly spaced, discontinuous rugae, up to about 14 per mm (Fig. 49G, I).

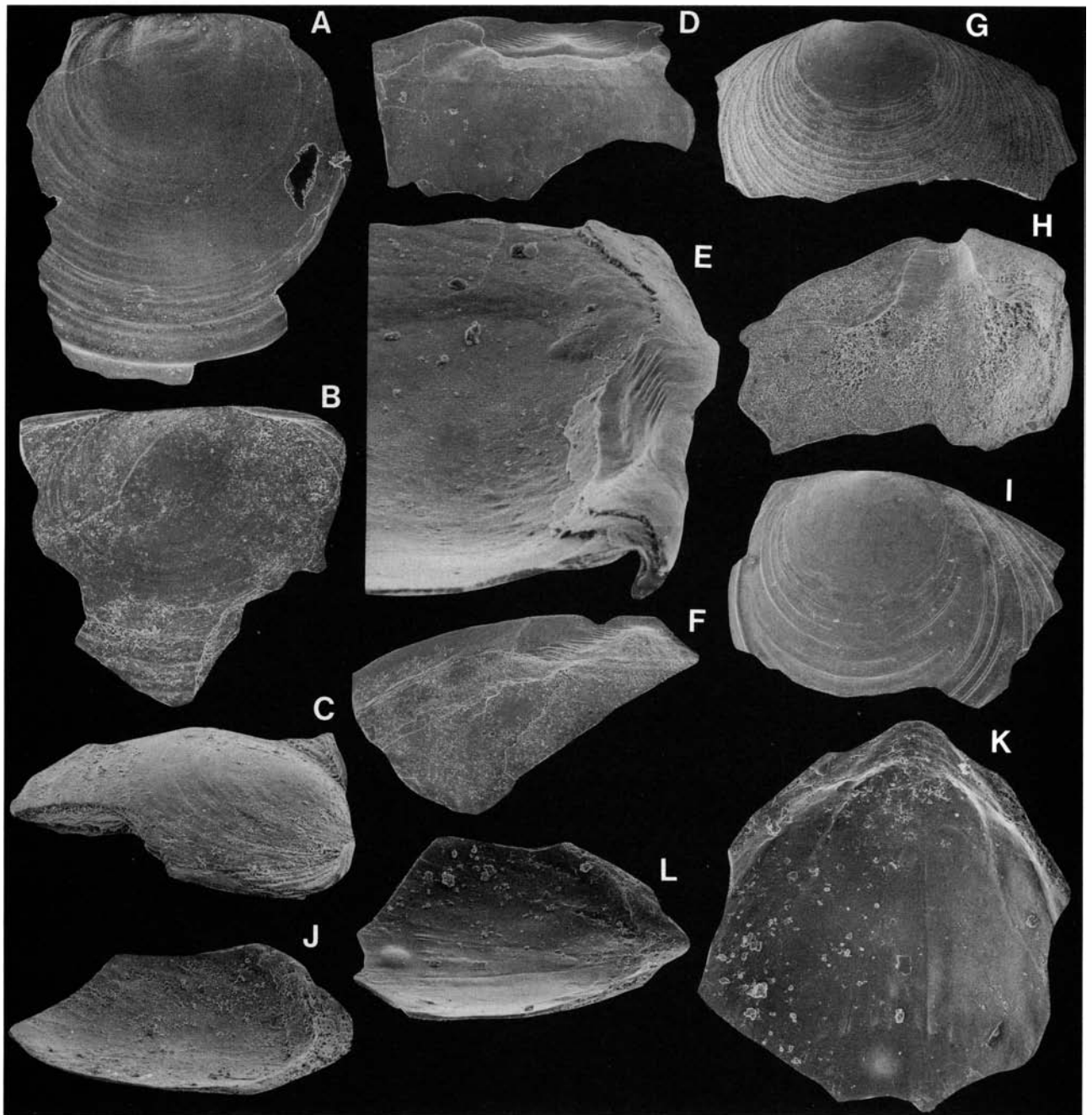


Fig. 49. □A–I. *Lingulella? alata* sp. nov. □A. Exterior of a dorsal valve; Ryd Limestone (sample GB84-3-51); Br132865, ×72. □B. Dorsal exterior; Ryd Limestone (sample GB84-3-51); Br132862, ×55. □C. Side view of B; ×64. □D. Holotype; interior of a dorsal valve; Ryd Limestone (sample GB84-3-51); Br132863, ×55. □E. Side view of the internal area of D; ×146. □F. Dorsal interior; Ryd Limestone (sample GB84-3-51); Br132864, ×44. □G. Exterior of a ventral valve; Ryd Limestone (sample GB84-2-39); Br132839, ×29. □H. Interior of G; ×34. □I. *Lingulella? alata?* sp. nov.; ventral exterior; Skärlov Limestone (sample DLK83-sä-6); Br128999, ×34. □J–L. *Lingulellinae* gen. et. sp.; Dalby Limestone (sample DLK83-dal-19). □J. Side view of the interior of a dorsal valve; Br132961, ×76. □K. Ventral interior; Br132959, ×90. □L. Side view of K; ×76.

Discussion. – *Lingulella? alata* is referred tentatively to *Lingulella* in preference to the erection of a new genus. It differs from most other species referred to *Lingulella* (*sensu lato*) in having a broad and rounded posterior margin, and rugose ornamentation.

Occurrence. – In Västergötland this species occurs in the Ryd Limestone (Fig. 8C). In Dalarna it is known from the Furudal Limestone, and there are questionable records from the Kårgårde and Skärlov limestones (Fig. 9A–B). On

southern Öland it is questionably present in the Furudal Limestone.

Genus *Spinilingula* Cooper, 1956

Type species. – Original designation; *Spinilingula intralamelata* Cooper, 1956, p. 210, from the Middle Ordovician (*Pygodus anserinus* Biozone) Pratt Ferry beds, Pratt Ferry, Alabama, U.S.A.

Diagnosis. – See Cooper (1956, p. 210).

Species assigned. – *Spinilingula intralamellata* Cooper, 1956; *S. bracteata* Krause & Rowell, 1975; *S. radiolamellosa* sp. nov.

Discussion. – The three known species assigned to this genus range from the Lower to Middle Ordovician. The oldest of these, *S. bracteata*, was described by Krause & Rowell (1975) from the lower Whiterock of Nevada; this American species was also recorded later from the Lower and Middle Ordovician Kogashi and Karakan stages of Kazakhstan (Nazarov & Popov 1980). Savazzi (1986) suggested that the distinctive ornamentation of *Spinilingula*, with spinous lamellae arranged in roughly radial terraces, could be analogous with the divaricate surface ornamentation of burrowing bivalve molluscs. This possibly indicates a similar mode of life for these brachiopods.

Spinilingula radiolamellosa sp. nov.

Fig. 50A–F

Name. – Latin *radius*, ray and *lamella*, lamina; alluding to the ornamentation.

Holotype. – Br129050, slightly damaged dorsal valve, Fig. 50A–C, (W 2.25, L 2.70), from the Furudal Limestone, Kårgårde section (sample DLK83-fur-6), Dalarna.

Paratypes. – Figured; Br129051 (damaged), Br129052 (W 0.93, L 1.07). Total of 7 dorsal valves and 9 ventral valves.

Diagnosis. – Elongated, oval *Spinilingula* with ventral umbonal muscle scar divided by anteriorly directed extension of internal area. Dorsal internal area with well developed median groove.

Description. – The valves have an elongated, oval outline (Fig. 50A, D). The ventral internal area is on average 47% as long as wide (\overline{WI} 1.05, \overline{LI} 0.49; $N=3$), with a well developed pedicle groove that is about as long as wide, up to 0.48 mm wide and 0.46 mm long (\overline{WP} 0.38, \overline{LP} 0.37; $N=3$; Fig. 50E). The ventral umbonal muscle scar is divided by an anteriorly directed triangular extension of the internal area (Fig. 50E). The dorsal valve is 81% as wide as long (\overline{W} 1.27, \overline{L} 1.57; $N=3$) with an internal area that is comparatively short and narrow, 30% as long as wide (\overline{WI} 0.40, \overline{LI} 0.12; $N=2$). The propareas are minute and anacline; the median groove is well developed and deep (Fig. 50B). The dorsal interior has distinct and bilaterally arranged markings that may correspond to the umbonal, central, and anterior lateral muscle scars (Fig. 50C, F). The larval shell is distinct and nearly circular (\overline{WL} 0.37, \overline{LL} 0.37). The postlarval ornamentation consists of concentric lamellose growth lines, each bearing short, flattened marginal spines, which are arranged in divaricate terrace lines (on average 10 per mm) beginning approximately 0.90 mm from the posterior margin (Fig. 50A, D). The early ontogeny of *S. radiolamellosa* is discussed briefly above (p. 56, Fig. 46).

Discussion. – The type species, *Spinilingula intralamellata* Cooper (1956, Pls. 2A:1–5, 11J:25–32), differs from *S. radiolamellosa* in having (1) a proportionally narrower ventral internal area (WP/LP ratio 65–68%; Pl. 11J:29–30), (2) a long, deep and narrow ventral pedicle groove, and (3) an undivided dorsal internal area. Moreover, the type species

lacks a triangular extension of the ventral internal area. *S. bracteata* Krause & Rowell (1975, Pl. 2:5–12, 12:4) is similar to the Swedish species in having (1) a ventral internal area, about half as long as wide, (2) the dorsal valve on average 82% as wide as long (Krause & Rowell 1975, Table 9), and (3) a distinct median groove in the dorsal internal area (LI/WI ratio on average 31%, Table 9). *S. bracteata* differs from *S. radiolamellosa* mainly in the lack of a triangular extension of the ventral internal area, but also in having relatively sharper and more pointed spines, forming a less regular pattern of divaricate terraces. Krause & Rowell (1975, p. 21) noted the presence of some bilaterally symmetrical markings in the ventral valve of *S. bracteata*. However, these are not discernable on their published figures. The markings described from *S. radiolamellosa* are present in several valves representing different growth stages (Fig. 50C, F); it is most probable that they represent sites of muscle attachment.

Occurrence. – In Dalarna *S. radiolamellosa* appears questionably in the Seby Limestone, and ranges through the Folkeslunda and Furudal limestones (Fig. 9A–B). On Öland the species is found also in the Furudal and Källa limestones; in Västergötland there is a questionable record from the Gullhögen Formation (Fig. 8B).

Genus *Paldiskites* Havlíček, 1982

Type species. – Original designation; *Lingula sulcata* Barrois, 1879, Pl. 106:3, Fig. 1–3, from the Lower Ordovician (Arenig) Klabava Formation, Rokycany, Prague basin, Bohemia.

Diagnosis. – See Havlíček (1982, p. 34).

Species assigned. – See Havlíček (1982, p. 34).

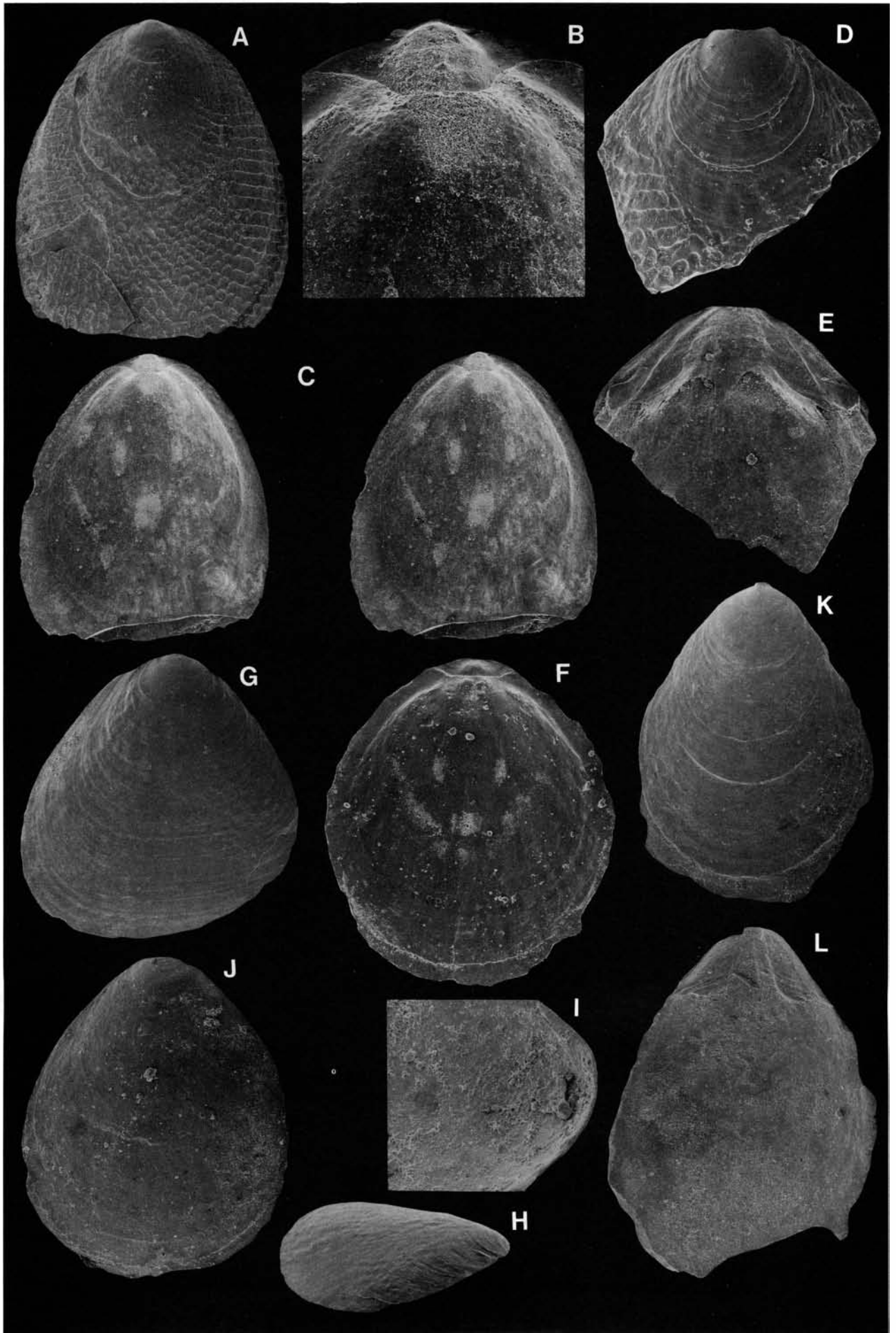
Paldiskites? sp. nov. a

Fig. 50G–L

Material. – Figured; Br132388 (W 1.80, L 1.90), Br132377 (W 0.87, L 1.18), Br132378 (W 1.05, L 1.30), Br132380 (W 0.59, L 0.71), Br132379 (W 0.95). Total of 7 dorsal and 3 ventral valves.

Description. – The valves have an elongated, oval outline. The ventral internal area is low, on average 45% as long as

Fig. 50. □A–F. *Spinilingula radiolamellosa* sp. nov.; Furudal Limestone (sample DLK83-fur-6). □A. Holotype; exterior of a dorsal valve; Br129050, ×24. □B. The pseudointerarea of A; ×80. □C. Stereo-pair; the interior of A; ×22. □D. Ventral exterior; Br129051, ×45. □E. Interior of D; ×45. □F. Interior of a juvenile dorsal valve; Br129052, ×60. □G–L. *Paldiskites?* sp. nov. a. □G. Dorsal exterior; Furudal Limestone (sample DLK83-fur-11); Br132388, ×29. □H. Side view of G; ×23. □I. Side view of a dorsal pseudointerarea; Furudal Limestone (sample DLK83-fur-9); Br132380, ×110. □J. Dorsal exterior; Furudal Limestone (sample DLK83-fur-9); Br132378, ×47. □K. Exterior of a ventral valve; Furudal Limestone (sample DLK83-fur-9); Br132377, ×53. □L. Ventral interior; Furudal Limestone (sample DLK83-fur-9); Br132379, ×53.



wide (\overline{WI} 0.51, \overline{LI} 0.23; $N=2$); the pedicle groove is up to 0.16 mm wide and 0.20 mm long (Fig. 50L). The dorsal valve is 81% as wide as long (\overline{W} 0.82, \overline{L} 1.01; $N=2$; Fig. 50J). The low internal area is crescent-shaped, up to 0.59 mm wide and 0.20 mm long, with a poorly defined median groove and a pair of propareas (Fig. 50I). The maximum midsagittal length of the internal area is about 0.10 mm. The valves are weakly ornamented with growth lines; the dorsal valve has faint discontinuous capilla (Fig. 50G–H, J).

Discussion. – Similarities in the morphology of the ventral internal area of the type species, *P. sulcatus* (Barrande; Havlíček 1982, Pl. 7:1–12), allow this species to be referred tentatively to *Paldiskites*. *P.?* sp. nov. a is also similar to the type species in that it has discontinuous capilla on the dorsal valve. However, in *P. sulcatus* the ornamentation is stronger. *P. sulcatus* has a shelf-like orthocline dorsal pseudointerarea, whereas the Swedish species has a low dorsal internal area. *P.?* sp. nov. a also differs from *P.?* *subditivus* (Williams, 1974) from the lower Llanvirn of the Shelve district, Shropshire, as the British species has a subcircular outline and an orthocline dorsal pseudointerarea. *P.?* sp. nov. a is the third species assigned to the genus and the first from the Middle Ordovician.

Occurrence. – *Paldiskites?* sp. nov. a is restricted to the Furu-dal Limestone of Dalarna (Fig. 9A–B).

Genus *Rowellella* Wright, 1963

Type species. – Original designation; *Rowellella minuta* Wright, 1963, p. 233, from the Upper Ordovician (Ashgill, Cautleyan) Portrane Limestone, Portrane Co., Ireland.

Diagnosis. – See Wright (1963, p. 233).

Species assigned. – *Rowellella minuta* Wright, 1963; *R. rugosa* Goryanskij, 1969; *R. margarita* Krause & Rowell, 1975; *R. lamellosa* Popov, 1976; *R. distincta* Bednarczyk & Biernat, 1978; *R. parallela* Bednarczyk, 1986; *R. multilamellata* Bednarczyk, 1986; *R. hollenensis* sp. nov.

Discussion. – Krause & Rowell (1975) summarized the then available information on *Rowellella*. Since that time four additional occurrences have been described and the genus now has a known range from the Lower Ordovician (Tremadoc; Biernat 1973) to the Upper Ordovician (Cautleyan; Wright 1963). Popov (*in* Nazarov & Popov 1976) described the Middle Ordovician (Llandeilo–Caradoc) *R. lamellosa* from the Bestamak Formation of Kazakhstan. Bednarczyk & Biernat (1978) erected *R. distincta* from the Lower Ordovician (Arenig) of the Holy Cross Mountains, Poland. An unnamed species of *Rowellella* occurs in some upper Viru calcilitites from Västergötland (Holmer 1986). More recently Bednarczyk (1986) described *R. parallela* and *R. multilamellata* from the lower Arenig of northern Poland.

Rowellella is a taxonomically complicated genus. Meaningful definitions of new species, as well as comparison with previously described species are difficult; biometric analysis cannot be performed on the mostly fragmentary specimens. It is even difficult to tell the ventral and dorsal valves apart. Moreover, the relative convexity and ornamentation

are extremely variable within species such as *R. cf. lamellosa*, described below.

The pitted postlarval micro-ornamentation seems to be a general feature of *Rowellella* (see also Holmer 1986). This ornamentation is similar to the postlarval pits of most orbiculoidines.

Rowellella cf. *lamellosa* Popov, 1976

Figs. 17, 51

Synonymy. – □v cf. 1976 *Rowellella lamellosa* Popov, sp. nov. – Nazarov & Popov, p. 36, Pl. 3:1–3.

Material. – Figured; Br128995 (W 0.67), Br128996 (damaged), Br132653 (W 0.93), Br132654 (W 0.74), Br132693 (W 1.21), Br132652 (W 1.02), Br132856b (section). Total of 916 mostly fragmentary valves; the exact proportions of dorsal and ventral valves could not be determined.

Diagnosis. – See Nazarov & Popov (1976, p. 36).

Description. – The valves are quite variable in outline and ornamentation. The larval shell of both valves is always damaged. The ventral valve generally broadens anteriorly (Fig. 51B, D, F), and has a convex lateral profile (Fig. 51E, G). Compared with the ventral valve, the dorsal is slightly more elongated, less convex, and more flattened in lateral view (Fig. 51A, C), but the relative convexity of both valves appears to be very variable. The larval shell is sharply delineated and is smooth apart from some very faint concentric fila (Fig. 51D). On average the larval shell is 0.59 mm wide ($N=5$), but the exact length is not known because the anterior portion is always broken off (Fig. 51C–D, F–G). The postlarval shell is ornamented with rugae, about 25 per mm, superposed on lamellae, about 7 per mm (Figs. 51C, E–G, 17C); this ornamentation starts abruptly at the edge of the larval shell. The lamellae and rugae are laterally discontinuous initially, but they become concentric during later growth (Fig. 51F). The shell structure is discussed above (p. 34, Fig. 17).

Discussion. – The Kazakhstani specimens of *R. lamellosa* are roughly contemporaneous with the Swedish material and are similar in outline and ornamentation, but their variability is not known. *R. cf. lamellosa* differs from *R. lamellosa* in (1) the lack of a thickening inside the ventral valve, (2) the lack of muscle scars in the dorsal valve, and (3) the lack of pitted postlarval ornamentation (reported from topotype material of *R. lamellosa* supplied by L. E. Popov; Holmer 1986, p. 105). However, the absence of thickenings and muscle scars is a doubtful specific character as indicated by the variability of these features in the Swedish material. The lack of a pitted postlarval ornamentation in the Swedish material could be preservational.

Occurrence. – In the lower Viru Series of Sweden *Rowellella* cf. *lamellosa* is a common and widely distributed species. In Dalarna it ranges from the Vikarby Limestone to the Furu-dal Limestone, and there are questionable occurrences in the lower part of the Dalby Limestone (Fig. 9A–B). In Västergötland it is known from the Gullhøgen Formation and questionably also from the Ryd Limestone (Fig. 8B–C).

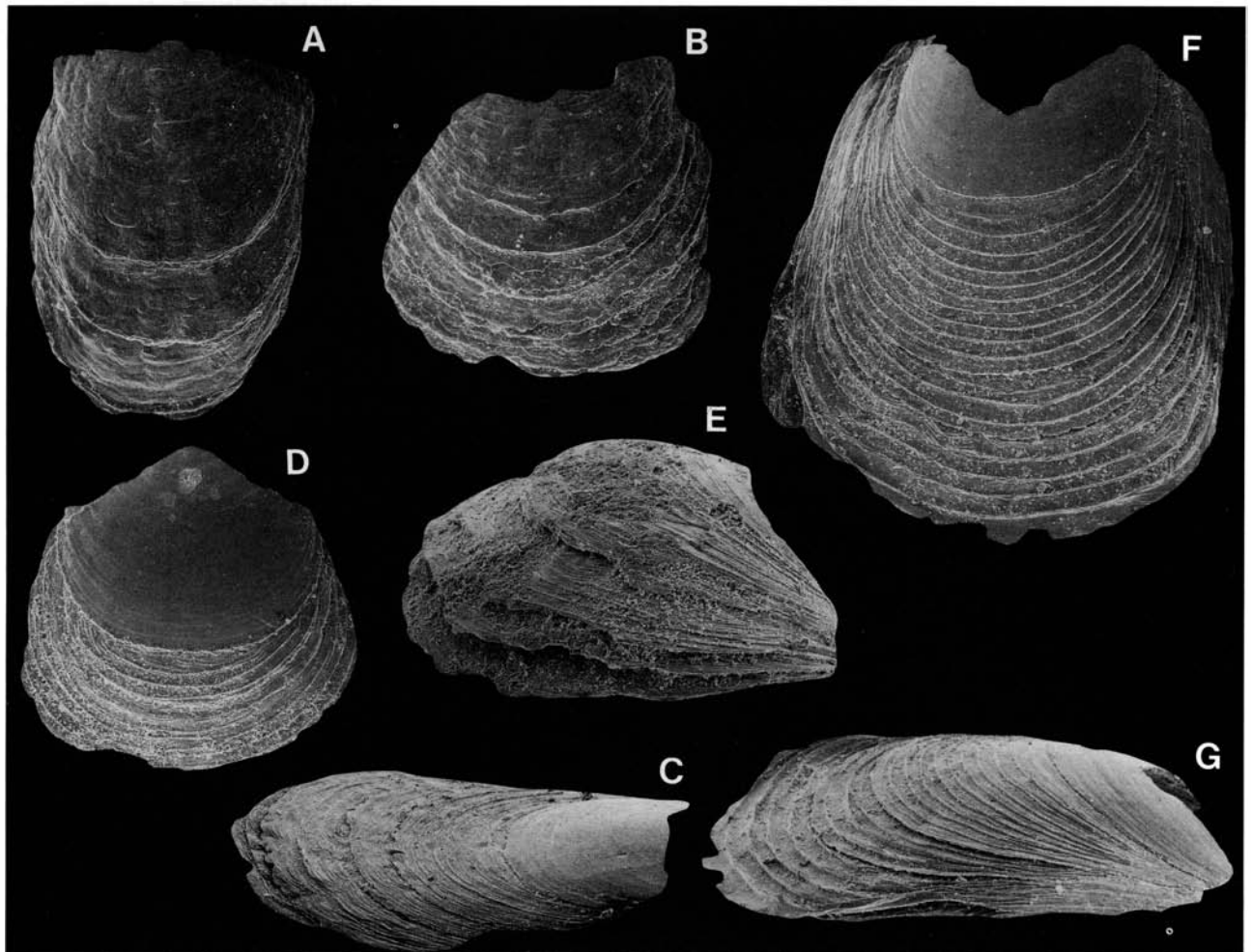


Fig. 51. *Rowellella* cf. *lamellosa* Popov, 1976. □A. Exterior of a dorsal valve; Skärlov Limestone (sample DLK83-sä-2); Br128995, $\times 57$. □B. Exterior of a ventral valve; Skärlov Limestone (sample DLK83-sä-2); Br128996, $\times 57$. □C. Side view of a dorsal valve; Gullhög Formation (sample GB84-2-7); Br132653, $\times 57$. □D. Ventral exterior; note the distinct boundary between the larval and juvenile shells; Gullhög Formation (sample GB84-2-7); Br132654, $\times 57$. □E. Side view of a ventral valve; Gullhög Formation (sample GB84-2-9); Br132693, $\times 57$. □F. Ventral exterior; Gullhög Formation (sample GB84-2-7); Br132652, $\times 57$. □G. Side view of F; $\times 57$.

In Jämtland it occurs in the Skärlov Limestone (sample J70-167); on southern Öland it is recorded from the Furudal Limestone.

Rowellella holenensis sp. nov.

Figs. 41, 52

Name. – From Holen village, close to the type locality.

Holotype. – Br132977, complete ventral valve, Fig. 52F–G (W 0.74, L 1.09), from the Dalby Limestone, Kårgärde section (sample DLK83-dal-26), Dalarna.

Paratypes. – Figured; Br132471 (W 1.44, L 1.88), Br132457 (W 0.52, L 0.72), Br128724 (damaged), Br132978 (W 0.64). In addition there are 69 fragmentary valves, 1 dorsal valve, 1 ventral valve, and 1 complete shell; the proportion of dorsal and ventral valves could not be determined.

Diagnosis. – Valves of elongate suboval outline, flattened in lateral profile; ventral valve only slightly larger and more convex than dorsal valve. Ventral valve with short, wide, crescent-shaped internal area, without a pedicle groove.

Dorsal internal area short, with median groove. Postlarval ornamentation with concentric rugae and minute pits.

Description. – The valves have an elongated, suboval outline, 72% as wide as long in two specimens; in lateral profile they are flattened. The ventral valve is slightly larger and more convex than the dorsal valve (Fig. 52B, G–H), but the identification of the ventral and dorsal valve is not always clear. The larval shell of both valves is very thin and most frequently broken off, whilst the anterior portion of both valves is thickened. The ventral internal area is minute; the midsagittal length is barely 0.03 mm in one specimen, occupying about 4% of the total valve length. The dorsal internal area is also minute, about 21% as long as wide, and has a shallow median groove (Fig. 52E). The interior of both valves is without recognizable structures. The larval shell is about as wide as long (diameter 0.47–0.55; $N=2$). The exterior is smooth with only some faint concentric growth lines (Figs. 41B, 52C–D). The postlarval shell is ornamented with irregularly spaced, concentric rugae (Fig. 52A, C, F–H); the surface is pitted with minute, closely spaced, circular pits, 2–3 μm across (see also above, p. 56, Figs. 41, 46, 52D).

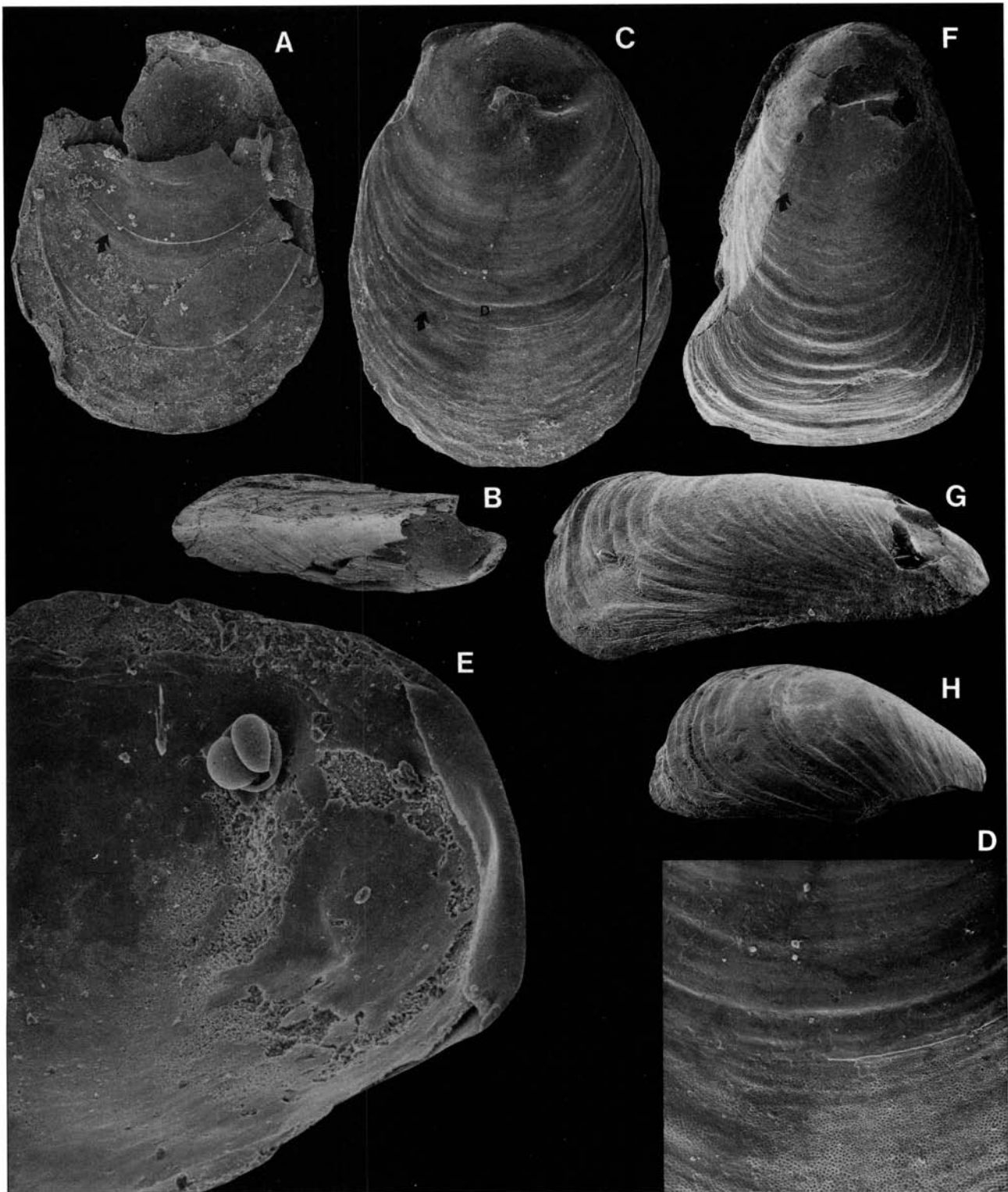


Fig. 52. *Rowellella holenensis* sp. nov. □A. Dorsal view of a complete shell; Dalby Limestone (sample DLK83-dal-5); Br132471, $\times 35$. □B. Side view of A; $\times 37$. □C. Dorsal exterior; the edge of the larval shell is indicated by an arrow; the location of D is indicated; Dalby Limestone (sample DLK83-dal-4); Br132457, $\times 107$. □D. Detail of the ornamentation of C, showing the boundary between the smooth larval shell and the pitted juvenile shell; $\times 228$. □E. Side view of the interior of C, showing the dorsal pseudointerarea; $\times 300$. □F. Holotype; ventral exterior; the edge of the larval shell is indicated; Dalby Limestone (sample DLK83-dal-26); Br132977, $\times 64$. □G. Side view of F; $\times 64$. □H. Side view of a ventral valve; Dalby Limestone (sample D60-211); Br128724, $\times 71$.

Discussion. — *R. holenensis* is similar to *R. lamellosa* Popov, 1976, from which it is distinguished mainly by the lack of lamellose ornamentation and in having a less sharply delineated larval shell. *R. distincta* Bednarczyk & Biernat, 1978 (p. 302, Pl. 17:1–2), *R. rugosum* Goryanskij, 1969 (p. 48, Pl.

8:4–7), and the type species *R. minuta* Wright differ from *R. holenensis* in having densely spaced lamellae. *R. margarita* Krause & Rowell, 1975 (p. 24, Pl. 3:8–15) from the lower Whiterock of Nevada differs in having (1) a ventral internal area with a better developed pedicle groove, (2) a more

elongated outline, and (3) a 'lip' along the ventral anterior margin.

Occurrence. – *R. holenensis* is restricted to the uppermost Furudal Limestone and the Dalby Limestone of Dalarna (Figs. 9B–C, 10).

Lingulellinae gen. et spp.

Figs. 48K–O, 49J–L

Material. – Figured; Br132611, Br132714 (W 0.50, L 0.67), Br132663 (W 0.64, L 0.82), Br132604, Br132961, Br132959. Total number of specimens not determined.

Remarks. – The fragmentary nature of fairly abundant lingulelline material prevents a close taxonomic evaluation; more than one genus and several species are probably represented. No attempt has been made to describe these in any detail. However, some relatively well preserved specimens representing two species are figured (Figs. 48K–O, 49J–L). The internal surface of both valves of the first taxon has a polygonal mosaic of pits (Fig. 48K, O), comparable with that described by Curry & Williams (1983). The juveniles of this species are ornamented with closely spaced, somewhat irregular 'scales', about 2 µm across. This type of ornamentation has also been observed in *Lingulella?* sp. a (Holmer 1986, Fig. 4G–I). A second species has a short ventral internal area with a distinct pedicle groove (Fig. 49K). The ventral interior has two distinct and diverging striae, defining a triangular area (Fig. 49K–L). The dorsal valve has an undivided and slightly raised internal area (Fig. 49J).

Occurrence. – Fragments of lingulellines are distributed throughout most of the sequence studied (Figs. 8, 9, 10).

Subfamily Glossellinae Cooper, 1956

Diagnosis. – See Havlíček (1982, p. 43).

Genera included. – *Pseudolingula* Mickwitz, 1909; in addition to genera listed by Rowell (1965) and Havlíček (1982).

Genus *Pseudolingula* Mickwitz, 1909

Type species. – Original designation; *Crania quadrata* Eichwald, 1829, p. 273, from the Upper Ordovician Vormsian Stage, Estonia, U.S.S.R.

Diagnosis. – See Williams (1974, p. 35).

Discussion. – The genus has generally been included in the Lingulellinae (Rowell 1965, p. H267). Williams (1974) referred *Pseudolingula* to the Glossellinae because of its reduced dorsal pseudointerarea, and this placement is tentatively supported here (but see also Havlíček 1982, p. 46). Fragments of species of *Pseudolingula* are comparatively common throughout the Ordovician succession in Sweden. A relatively well preserved but as yet undescribed species occurs in the upper Viru Kullberg Limestone of Dalarna (Holmer, unpublished).

Pseudolingula sp.

Fig. 53A–D

Material. – Figured; Br128763, Br132539, Br128762, Br132399. Total of 7 fragmentary dorsal valves and 4 fragmentary ventral valves.

Description. – Complete outlines are unknown for either valve. The ventral valve has a well developed pseudointerarea, with a deep, triangular pedicle groove and wide propleareas (Fig. 53D), whereas the dorsal pseudointerarea is reduced and almost catacline (Fig. 53A–B); there is trace of a low, ridge-like median septum (Fig. 53B). The larval shell of both valves is sharply delineated. The postlarval shell is ornamented with concentric growth lines (Fig. 53C).

Discussion. – Fragments of the dorsal valve (Fig. 53A–B) show the reduced pseudointerarea of *Pseudolingula*, supporting the suggestion by Williams (1974) that it should be included in the Glossellinae. The reduced dorsal pseudointerarea of the type species *P. quadrata* was figured by Goryanskij (1969, Pl. 6:6A).

Occurrence. – Fragments of one or several species of *Pseudolingula* have been isolated from the Vikarby, Seby, Folkelslunda, Furudal and Dalby limestones of Dalarna (Figs. 9A–B, 10).

Glossellinae gen. et sp.

Fig. 53E–I

Material. – Figured; Br132515, Br132514, Br128750a, Br128785, Br128753a. Total of 2 fragmentary ventral valve and 1 fragmentary dorsal valve in addition to an undetermined number of numerous smaller fragments.

Description. – The outline is unknown for either valve. The ventral pseudointerarea is well developed, orthocline, and divided into propleareas by a deep pedicle groove (Fig. 53F). The dorsal pseudointerarea is completely reduced (Fig. 53E). The postlarval shell is ornamented with minute papillae, arranged in roughly radial terraces. The larval shell is sharply delineated (Fig. 53G, H). The interior of both valves has deep, circular 'pores' that are up to 0.05 mm across, but they do not penetrate the entire thickness of the valves (Fig. 53I).

Discussion. – Although none of the numerous fragments is determinable, their placement within the Glossellinae is likely because of the reduced dorsal pseudointerarea and the distinct ornamentation; the papillose ornamentation is well known from species of *Glossella* Cooper (Rowell 1965, p. H269, Fig. 162:7A). *Lingulasma* Ulrich also has this type of ornamentation (Rowell 1965, p. H271, Fig. 165:1C), but both valves of this genus are provided with muscular platforms.

Occurrence. – In Dalarna numerous fragments of this glosselline appear in the uppermost Furudal Limestone and range into the lower Dalby Limestone (Figs. 9B, 10).

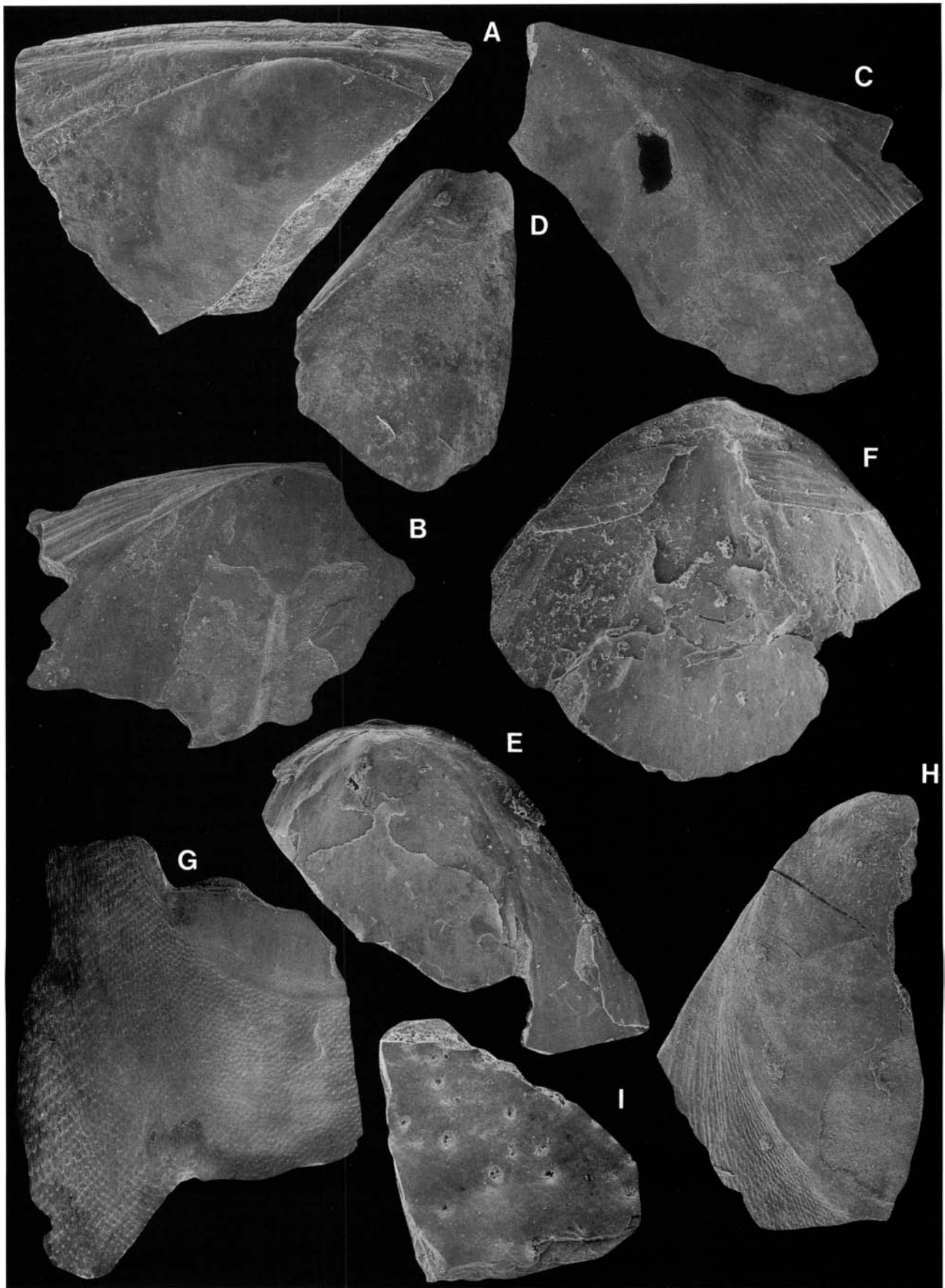


Fig. 53. □A–D. *Pseudolingula* sp. □A. Dorsal exterior; Furudal Limestone (sample D60-219); Br128763, ×85. □B. Exterior of a fragment of the posterior portion of a dorsal valve, showing the larval shell and the reduced pseudointerarea; Dalby Limestone (sample DLK83-dal-14); Br132539, ×29. □C. Ventral exterior, showing the smooth larval shell and the boundary to the juvenile shell with growth lines; Furudal Limestone (sample D60-219); Br128762, ×32. □D. Interior of a ventral valve; Furudal Limestone (sample DLK83-fur-13); Br132399, ×17. □E–I. Glossellinae gen. et sp. □E. Dorsal interior; Dalby Limestone (sample DLK83-dal-12); Br132515, ×64. □F. Interior of a ventral valve;

Order Acrotretida Kuhn, 1949 (*sensu*
Kuhn, 1949, p. 101)

Suborder Acrotretidina Kuhn, 1949

Superfamily Acrotretacea Schuchert, 1893

Family Acrotretidae Schuchert, 1893

Subfamily Acrotretinae Schuchert, 1893

Genus *Conotreta* Walcott, 1889

Type species. – Original designation; *Conotreta rusti* Walcott 1889, p. 365, from the Middle Ordovician Trenton Group ('Trenton Limestone') of New York State, U.S.A.

Diagnosis. – See Cooper (1956, p. 247).

Discussion. – Although Cooper's definition of the genus is generally accepted, it is important to emphasize that the type species *C. rusti* Walcott is poorly known. Walcott (1889, Figs. 1–3) figured only two ventral valves, mainly preserved as internal moulds. The third valve figured by him (Fig. 4) has a strikingly different outline and convexity; it does not appear to belong to the same species.

Without isolating additional material from the type locality, no detailed comparison with *C. rusti* is possible. In the following discussion, assignments to *Conotreta* (*sensu lato*) are tentative. The well known and well illustrated species, *C. multisinuata* Cooper, 1956, may serve as a provisional standard of reference until more information on the type species becomes available. More than thirty species have been assigned to the genus, embracing a very wide range of morphological variation. Cooper's (1956) monograph on North American Middle Ordovician Brachiopoda alone lists eleven species of *Conotreta*, five of which come from a single unit, the Pratt Ferry beds of Alabama.

Conotreta? *mica* Goryanskij, 1969

Figs. 23, 47K–L, 54, 55, 60

Synonymy. – □v*1969 *Conotreta mica* Gorjansky sp. nov. – Goryanskij, p. 64, Pl. 11:1–9. □aff. 1975 *Conotreta mica?* Goryanskij, 1969 – Krause & Rowell, p. 38, Pl. 4:17–24.

Holotype. – CNIGR Museum no. 130/9960 (VSEGEI, Leningrad), complete dorsal valve, Goryanskij 1969, Pl. 11:6 (W 1.8, L 1.6) from the Aseri Stage, Pechory core (459.4 m), Pskov district (near village of Panikovich), Russia, U.S.S.R.

Material. – Figured; Br129003b (section), Br133611b (section), ?Br132598 (damaged), Br128939 (W 1.78, L 1.52), Br128941 (W 2.14, L 1.83), Br128610 (W 1.40, L 1.16), Br128897 (W 1.47, L 1.26), Br128898 (W ~1.04, L ~0.86, H ~0.68), Br128944 (W ~1.22, L ~1.07, H ~1.08), Br128899 (damaged), Br129017 (W 1.71, L 1.57), Br129018 (W 1.47, L 1.36), Br129011 (W 2.32, L 1.95, H 2.32), Br129019 (W

1.77, L 1.41, H 1.63), Br129002 (damaged), Br129003a (damaged), Br129005 (W 0.90, L 0.78, H 0.74). Total of 850 dorsal and 847 ventral valves.

Diagnosis. – Ventral valve procline, with robust apical process and strongly impressed, pinnate mantle canal pattern. Dorsal valve with clearly raised pair of cardinal muscle scars and robust median buttress; pseudointerarea wide and short. Median septum high with up to three anterior denticles.

Description of the Swedish material. – The valves average 88% as long as wide (OR 77–100%; N=25; Table 2). The ventral valve (\bar{W} 1.58, \bar{L} 1.38; OR W 1.08–2.32, L 0.96–1.95; N=6) is highly conical, and 78% (OR 66–100%) as high as wide (\bar{H} 1.29; OR H 0.78–2.32; N=6). The ventral pseudointerarea is mostly procline (Fig. 54I), but slightly apsacline in some gerontic specimens (Fig. 55E). The interridge is poorly delineated (Figs. 54H, 55F). The pedicle foramen is about 0.03–0.06 mm wide (Figs. 54I, 55E) and continues internally as a very short tube (Fig. 55I); an exterior pedicle tube is developed in some specimens (Fig. 55G). The ventral interior is dominated by a robust apical process (Figs. 54L, 55H–I), which sometimes occupies about 40% of the height of the valve. The mantle canal pattern is well developed and pinnate (Figs. 54L, 55H). A pair of raised ventral cardinal muscle scars are present on the posterior wall (Fig. 55H). The dorsal valve (\bar{W} 1.39, \bar{L} 1.22; N=19; Table 2) has a shallow sulcus starting on the larval shell (Fig. 55A). The dorsal pseudointerarea is wide and short, 18% (OR 13–24%) as long as wide (\bar{W} 0.67, \bar{L} 0.12; N=32; Table 2); it has a distinct median groove and anacline propareas (Figs. 54B, 55B). The dorsal cardinal muscle scars are raised and oval, about half as long as wide (Table 2) and occupy about 35–40% of the total length (Figs. 54B, D, 55B). The median buttress is up to 0.15 mm long. The median septum is high and has up to three denticles (septal rods) on the anterior declivity (Fig. 54G); the septum occupies 79% (OR 70–88%) of the total length and is about 31% as high as wide in one specimen (Fig. 54G). The valves are ornamented with weakly developed fila, about 8–26 μ m apart. The dorsal larval shell is well delineated, slightly protruding (Fig. 54E, 55C), and generally about 0.22–0.28 mm wide and 0.19–0.26 mm long. On both valves, it is distinctly pitted with overlapping pits of uniform size, up to 2.5 μ m across (Fig. 54F). The shell structure is discussed above (p. 45, Fig. 23).

Discussion. – The Swedish material is assigned to *C.?* *mica* mainly because of similarities in the dorsal valve. Both species have a dorsal valve with (1) a length/width ratio of 80–90% (see Goryanskij 1969, p. 64), (2) a wide, well developed pseudointerarea, about 15–20% as long as wide, (3) a robust median buttress, (4) well developed, raised cardinal muscle scars, about 50% as long as wide, and (5) a high

Dalby Limestone (sample DLK83-dal-12); Br132514, $\times 85$. □G. Exterior of a fragmentary valve, showing the 'terrace-lines' and the edge of the larval shell; Furudal Limestone (sample D60-223); Br128750a, $\times 38$. □H. Ventral exterior, showing the boundary between the smooth larval shell and the papillose juvenile shell; Dalby Limestone (sample D60-214); Br128785, $\times 35$. □I. Interior of a fragmentary valve, showing the scattered 'pores'; Furudal Limestone (sample D60-215); Br128753a, $\times 58$.

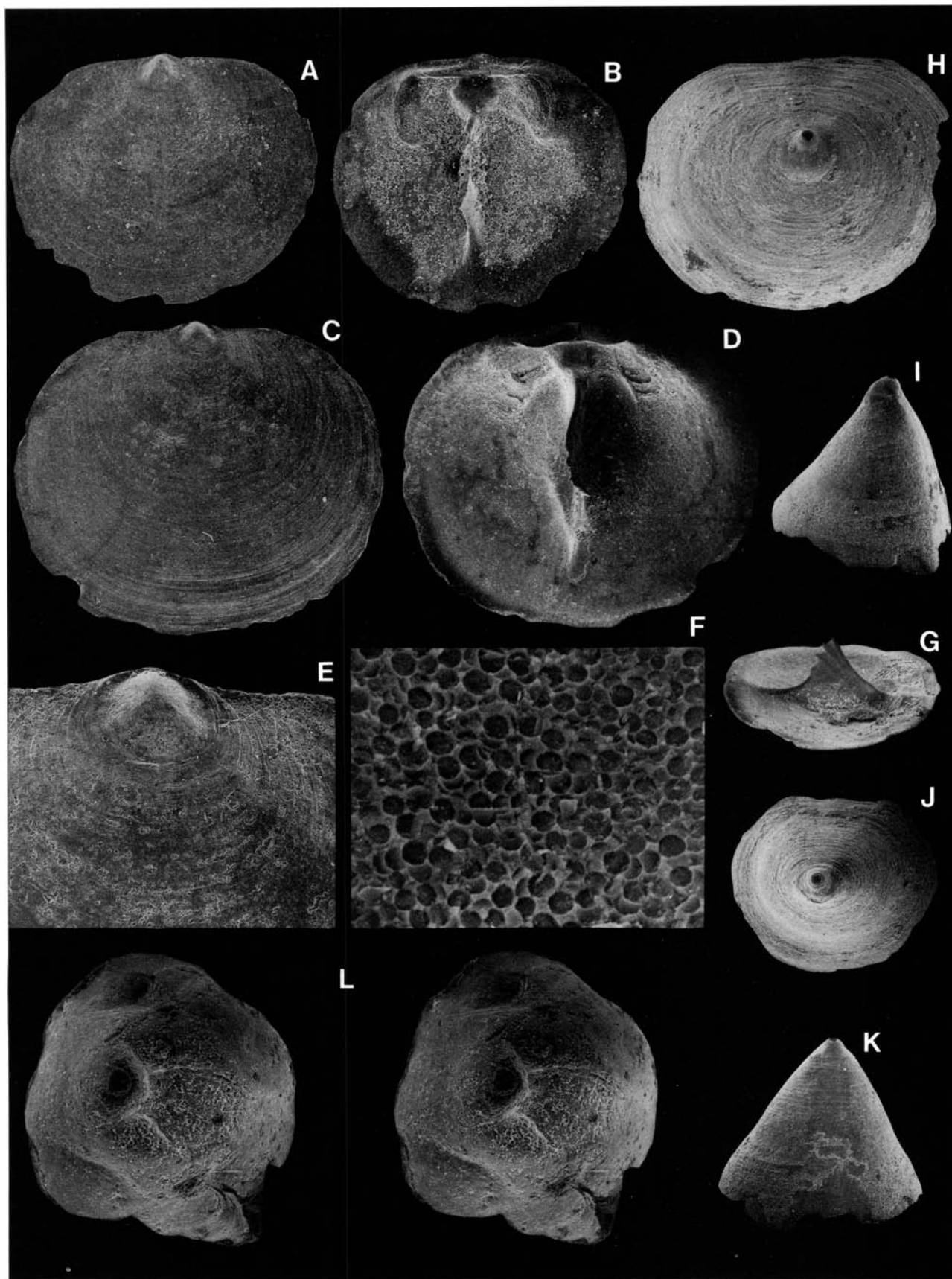


Fig. 54. *Conotreta mica* Goryanskij, 1969. □A. Exterior of a dorsal valve; Kårgårde Limestone (sample DLK83-segk-5); Br128939, $\times 29$. □B. Interior of A; $\times 29$. □C. Dorsal exterior; Kårgårde Limestone (sample DLK83-segk-6); Br128941, $\times 29$. □D. Interior of C; $\times 29$. □E. Larval valve of C; $\times 82$. □F. Ornamentation of a dorsal larval shell; Gullhøgen Formation (sample GB84-1-3); Br128610, $\times 2000$. □G. Side view of a dorsal valve; Våmb Limestone (sample GB84-A2); Br128897, $\times 29$. □H. Ventral exterior; Skövde beds (sample GB84-A4); Br128898, $\times 50$. □I. Side view of a ventral valve; Kårgårde Limestone (sample DLK83-segk-8); Br128944, $\times 29$. □J. Exterior of I; $\times 29$. □K. Posterior view of I; $\times 29$. □L. Stereo-pair; ventral interior; Skövde beds (sample GB84-A4); Br128899, $\times 50$.

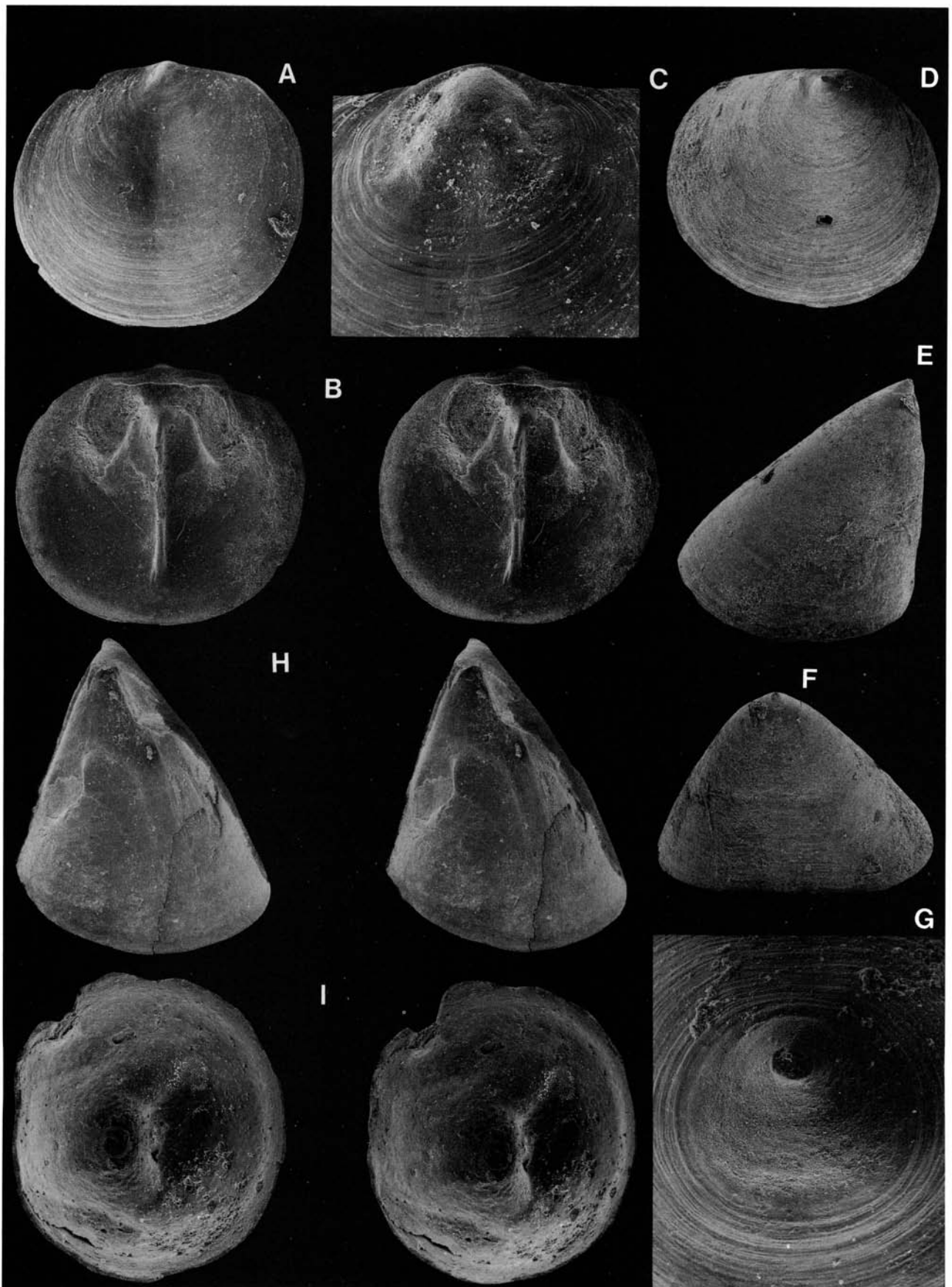


Fig. 55. *Conotreta? mica* Goryanskij, 1969. □A. Exterior of a dorsal valve; Furudal Limestone (sample DLK83-fur-3); Br129017, ×29. □B. Stereo-pair; interior of A; ×29. □C. Dorsal larval shell; Folkeslunda Limestone (sample DLK83-fo-4); Br129018, ×140. □D. Ventral exterior; Seby Limestone (sample DLK83-se-5); Br129011, ×20. □E. Side view of D; ×20. □F. Posterior view of D; ×20. □G. Ventral larval shell; Folkeslunda Limestone (sample DLK83-fo-4); Br129019, ×140. □H. Stereo-pair; side view of a ventral interior; Skärlov Limestone (sample DLK83-sä-5); Br129002, ×20. □I. Stereo-pair; interior of a juvenile ventral valve; Skärlov Limestone (sample DLK83-sä-8); Br129005, ×60.

Table 2. *Conotreta? mica* Goryanskij, average dimensions and ratios of dorsal valves.

	W	L	L/W	WI	LI	LI/WI	WM	LM	LM/WM	LS	BS
GB81-50											
<i>n</i>	8	8	8	11	11	11	5	5	5	11	11
mean	1.26	1.11	89%	0.55	0.10	19%	0.79	0.44	56%	0.92	0.24
<i>s</i>	0.365	0.314	2.977	0.140	0.017	3.142	0.990	0.062	1.483	0.260	0.048
min	0.78	0.70	85%	0.34	0.08	15%	0.70	0.39	54%	0.56	0.16
max	1.86	1.61	93%	0.74	0.12	24%	0.93	0.54	58%	1.24	0.31
DLK83-sä-8											
<i>n</i>	5	5	5	5	5	5				3	3
mean	1.48	1.34	91%	0.68	0.12	18%				1.20	0.25
<i>s</i>	0.467	0.426	3.564	0.208	0.028	2.950					
min	0.78	0.70	88%	0.39	0.08	13%				1.15	0.25
max	1.95	1.74	97%	0.93	0.16	20%				1.24	0.25
DLK83-se-5											
<i>n</i>	6	6	6	6	6	6				6	6
mean	1.48	1.24	83%	0.65	0.10	15%				0.95	0.22
<i>s</i>	0.506	0.434	3.674	0.274	0.038	2.563				0.371	0.055
min	0.93	0.82	77%	0.39	0.05	12%				0.65	0.16
max	2.29	1.95	88%	1.12	0.16	18%				1.64	0.23

median septum occupying about 80% of valve length (see Goryanskij, Fig. 11:5–6, 9).

In the Russian material the ventral valve of *C. mica* is poorly known but it appears to be somewhat less conical than in the Swedish specimens (42% as high as wide according to Goryanskij 1969, p. 64). However, the ventral valves in both collections have a well developed mantle canal pattern, a robust apical process, internal and external pedicle tubes, a poorly developed pseudointerarea, and a likewise poorly developed interr ridge (cf. Goryanskij 1969, p. 64).

Some lower Whiterock material of *Conotreta* from Nevada was referred tentatively to *C. mica* by Krause & Rowell (1975, p. 38). The dorsal valves of the American species are similar to those described here in having (1) a length/width ratio of about 80–95%, (2) a pseudointerarea about 15% as long as wide, (3) a robust median buttress, (4) cardinal muscle scars about 50% as long as wide, and (5) a high median septum occupying about 80% of the valve length (Krause & Rowell 1975, pp. 38–40, Fig. 31, Plate 4:17–24, Table 14). The ventral valve of the American species differs from the Swedish material mainly in being less conical (about 54% as high as wide according to Krause & Rowell, Table 13). The median septum of the Nevadan species has only an upper septal rod (Krause & Rowell, Plate 4:23–24).

The Swedish specimens of *Conotreta? mica* are quite variable, especially the ventral valves (Figs. 54H–K, 55D–I).

Occurrence. – *Conotreta? mica* is common and widely distributed in Baltoscandia. In Sweden and Russia it appears in the upper Kundan Stage and ranges into the lowermost Uhakuan Stage. In Västergötland it is known from the upper Holen Limestone to the lower Gullhøgen Formation (Fig. 8A–B). In Dalarna *C. mica* is not known from the uppermost part of the Holen Limestone, but ranges from the Segerstad Limestone to the lower Furudal Limestone

(Fig. 9A). In Jämtland it has been found in the Segerstad (samples J69-35, 38, 40–43; J70-165, 166) and Skärlov (sample J70-167) limestones. On Öland the lower Segerstad Limestone has yielded some specimens.

Conotreta? siljanensis sp. nov.

Figs. 27, 47A–B, F–H, 56–60

Name. – After lake Siljan, Dalarna.

Holotype. – Br132374, complete dorsal valve, Fig. 56C–D (W 1.07, L 0.95), from the Furudal Limestone, Kårgårde section (sample DLK83-fur-8), Dalarna.

Paratypes. – Figured; Br132393 (W 1.38, L 1.22), Br128677 (damaged), Br128799 (W 0.82, L 0.65, H 0.68), Br129022 (W 1.52, L 1.19, H 1.79), Br132667 (W 1.07, L 0.96), Br129010 (W 1.35, L 1.19), Br129008 (W 1.26, L 1.12, H 1.01), Br129009 (W 1.22, L 1.05, H 0.87), Br132467 (W 1.22, L 1.05), Br128694 (damaged), Br132466 (W 1.43, L 1.19), Br132445 (W 1.72, L 1.38, H 1.74), Br132446 (W 1.43, L 1.19, H 1.49), Br132912 (damaged), Br132914 (W 0.98, L 0.87), Br132719b (section), Br132468 (W 0.37, L 0.37), Br132797 (W 0.39, L 0.38), Br132419 (W 0.46, L 0.43), Br132835 (W 0.42, L 0.38, H 0.25), Br132447 (W 0.50, L 0.43, H 0.30). Total of 2057 dorsal valves, 1047 ventral valves and one complete shell.

Diagnosis. – Ventral valve procline, with long snout-shaped exterior pedicle tube. Apical process small; pinnate mantle canal pattern weakly impressed. Dorsal valve with raised pair of cardinal muscle scars and median buttress; pseudointerarea wide and short. Median septum high with up to five anterior denticles.

Description. – The valves average 89% as long as wide (OR 77–100%; $N=110$; Tables 3, 4); the ventral valve (\bar{W} 0.85, \bar{L}

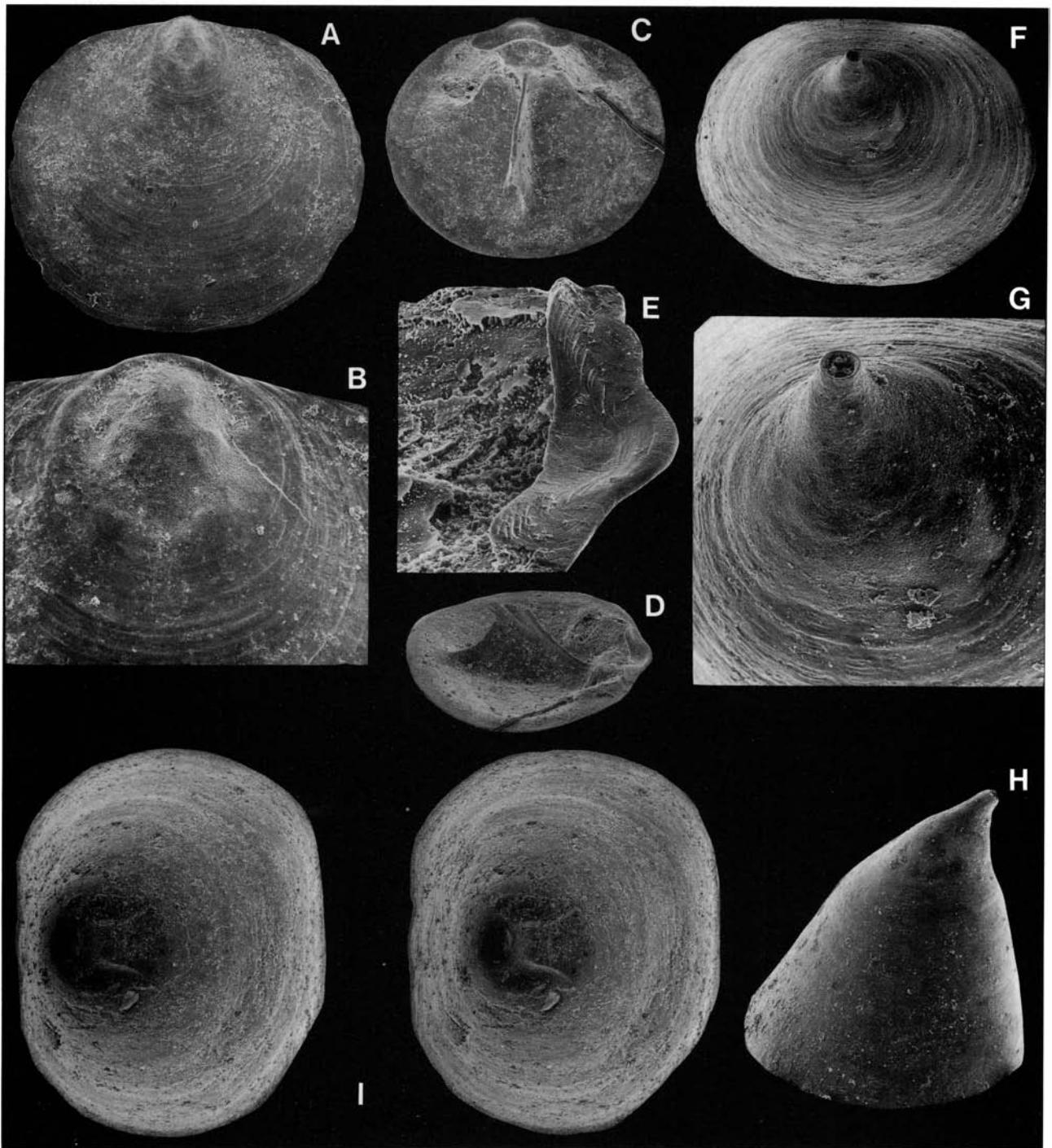


Fig. 56. *Conotreta? siljanensis* sp. nov. □A. Exterior of a dorsal valve; Furudal Limestone (sample DLK83-fur-11); Br132393, $\times 40$. □B. The larval shell of A; $\times 140$. □C. Holotype; dorsal interior; Furudal Limestone (sample DLK83-fur-8); Br132374, $\times 40$. □D. Side view of C; $\times 40$. □E. Side view of a dorsal pseudointerarea; Furudal Limestone (sample D60-218); Br128677, $\times 200$. □F. Ventral exterior; Furudal Limestone (sample D60-215); Br128799, $\times 64$. □G. The larval shell of F; $\times 174$. □H. Side view of F; $\times 64$. □I. Stereo-pair; ventral interior; Furudal Limestone (sample DLK83-fur-6); Br129022, $\times 40$.

0.74, \bar{H} 0.70; $N=36$; Table 3) 79% ($N=36$; Table 3) as high as wide. In lateral profile the outline of the posterior surface of the ventral valve is flattened to flat, whereas the anterior surface is slightly convex (Figs. 56H, 57H, 58G). The ventral pseudointerarea is poorly delineated, catacline to slightly procline (Figs. 56H, 57G). The interridge is poorly developed (Figs. 56F, 57H, 45F). The exterior pedicle tube is long and snout-shaped (Figs. 56G–H, 57G, I, 58G); it continues as a short interior tube (Fig. 58H). The

ventral interior has a small apical process and a poorly developed pinnate mantle canal pattern (Figs. 56I, 57J, 58H); the posterior wall has a pair of cardinal muscle scars (Fig. 53I). In lateral profile the dorsal valve (\bar{W} 0.94, \bar{L} 0.85; $N=74$; Table 4) is flattened (Fig. 57E) or slightly convex (Fig. 56D). The dorsal pseudointerarea averages 23% as long as wide (\bar{W} 0.39, \bar{L} 0.09; $N=74$; Table 4), occupying 41% of the width of the valve. The median groove is well developed and the propleareas are anacline or nearly catacl-

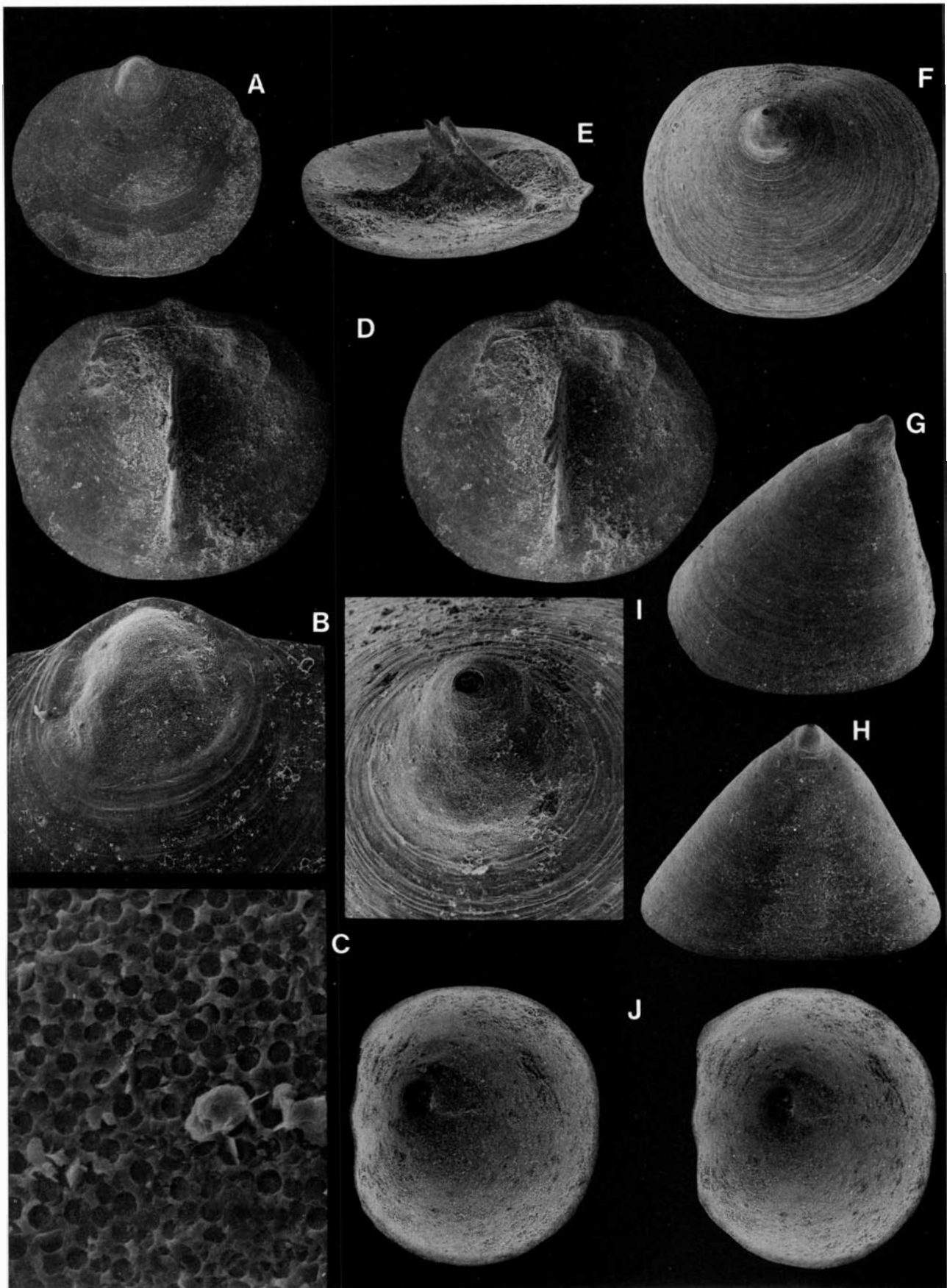


Fig. 57. *Conotreta? siljanensis* sp. nov. □A. Dorsal exterior; Gullhøgen Formation (sample GB84-2-7); Br132667, $\times 40$. □B. The larval shell of A; $\times 150$. □C. Ornamentation of the larval shell of A; $\times 2000$. □D. Stereo-pair; interior of a dorsal valve; Folkeslunda Limestone (sample DLK83-fo-5); Br129010, $\times 40$. □E. Side view of D; $\times 40$. □F. Ventral exterior; Folkeslunda Limestone (sample DLK83-fo-5); Br129008, $\times 40$. □G. Side view of F; $\times 40$. □H. Posterior view of F; $\times 40$. □I. The larval shell of F; $\times 150$. □J. Stereo-pair; ventral interior; Folkeslunda Limestone (sample DLK83-fo-5); Br129009, $\times 40$.

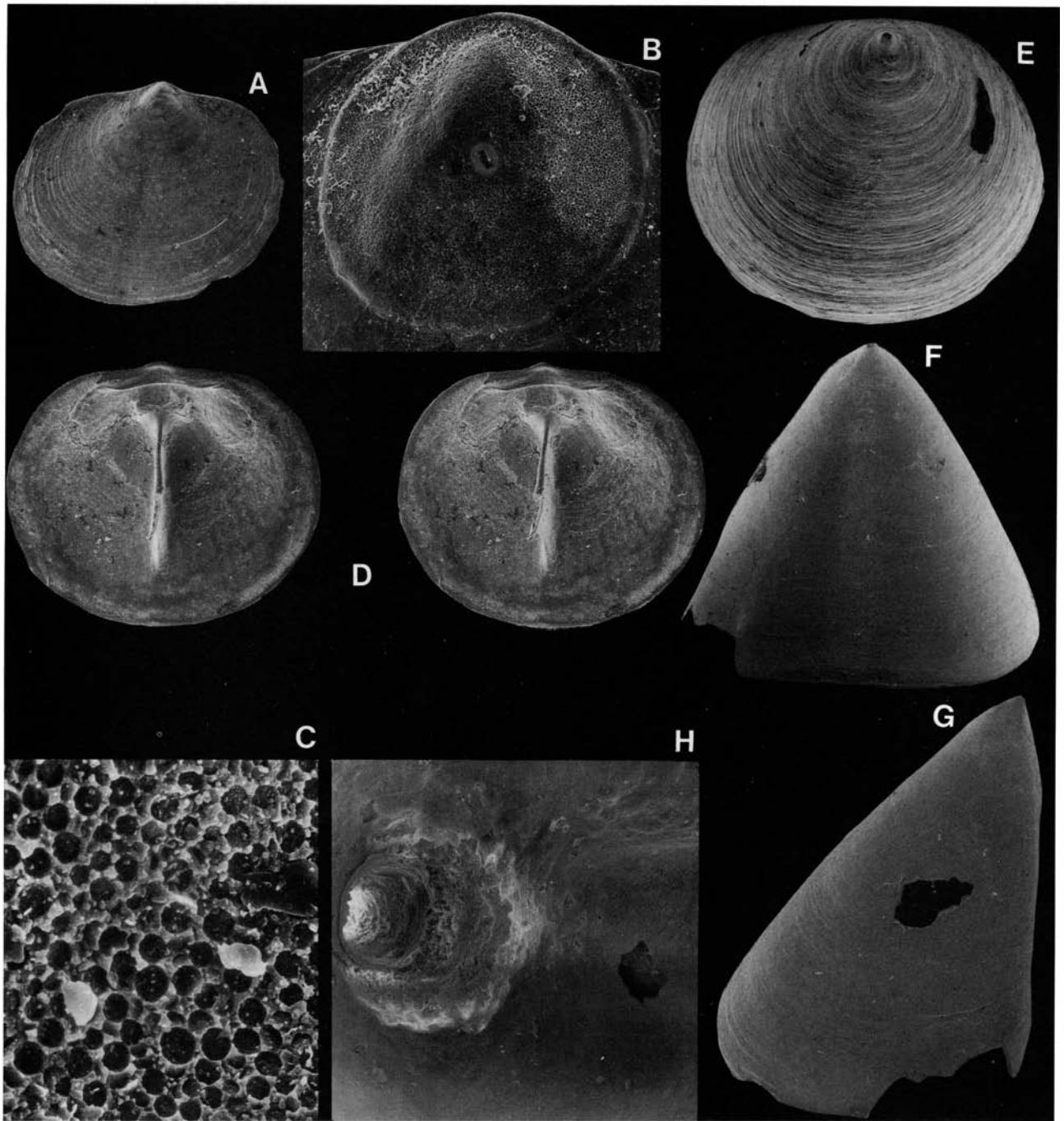


Fig. 58. *Conotreta siljanensis* sp. nov. □A. Exterior of a dorsal valve; Dalby Limestone (sample DLK83-dal-5); Br132467, $\times 33$. □B. Dorsal larval shell; Dalby Limestone (sample D60-214); Br128694, $\times 210$. □C. Ornamentation of the larval shell of B; $\times 1900$. □D. Stereo-pair; dorsal interior; Dalby Limestone (sample DLK83-dal-5); Br132466, $\times 33$. □E. Exterior of a ventral valve; Dalby Limestone (sample DLK83-dal-2); Br132445, $\times 33$. □F. Posterior view of E; $\times 33$. □G. Side view of E; $\times 33$. □H. Ventral interior, showing the pedicle tube and the apical process; Dalby Limestone (sample DLK83-dal-2); Br132446, $\times 170$.

ine (Figs. 56E, 57D, 58D). The median buttress is well developed. The cardinal muscle scars average 62% (OR 44–79%) as long as wide (WM 0.57, LM 0.35; $N=41$; Table 4; Figs. 56C, 57D, 58D). In one specimen, the median septum is about 30% as high as long; it occupies 77% (OR 62–88%; $N=62$) of the total length of the valve (Figs. 56D, 57E), and has up to five anterior denticles (septal rods). The ornamentation of the valves is like that of *C. mica*; the larval shell is sharply delineated, ornamented with overlap-

ping pits of uniform size, up to 5 μm wide (Figs. 57C, 58C). The shell structure is described above (p. 45, Fig. 23).

Ontogeny. – The larval shell is about 0.26 mm wide and 0.25 mm long (Figs. 56B, 57B, 58B); that of the ventral valve is about 0.25 mm high (Fig. 56H). In the brephic stage (W 0.26–0.56, L 0.25–0.54) the dorsal valve (Fig. 59) has a narrow, undivided pseudointerarea (WI ?–0.23, LI ?–0.05). The median septum originates as a minute trian-

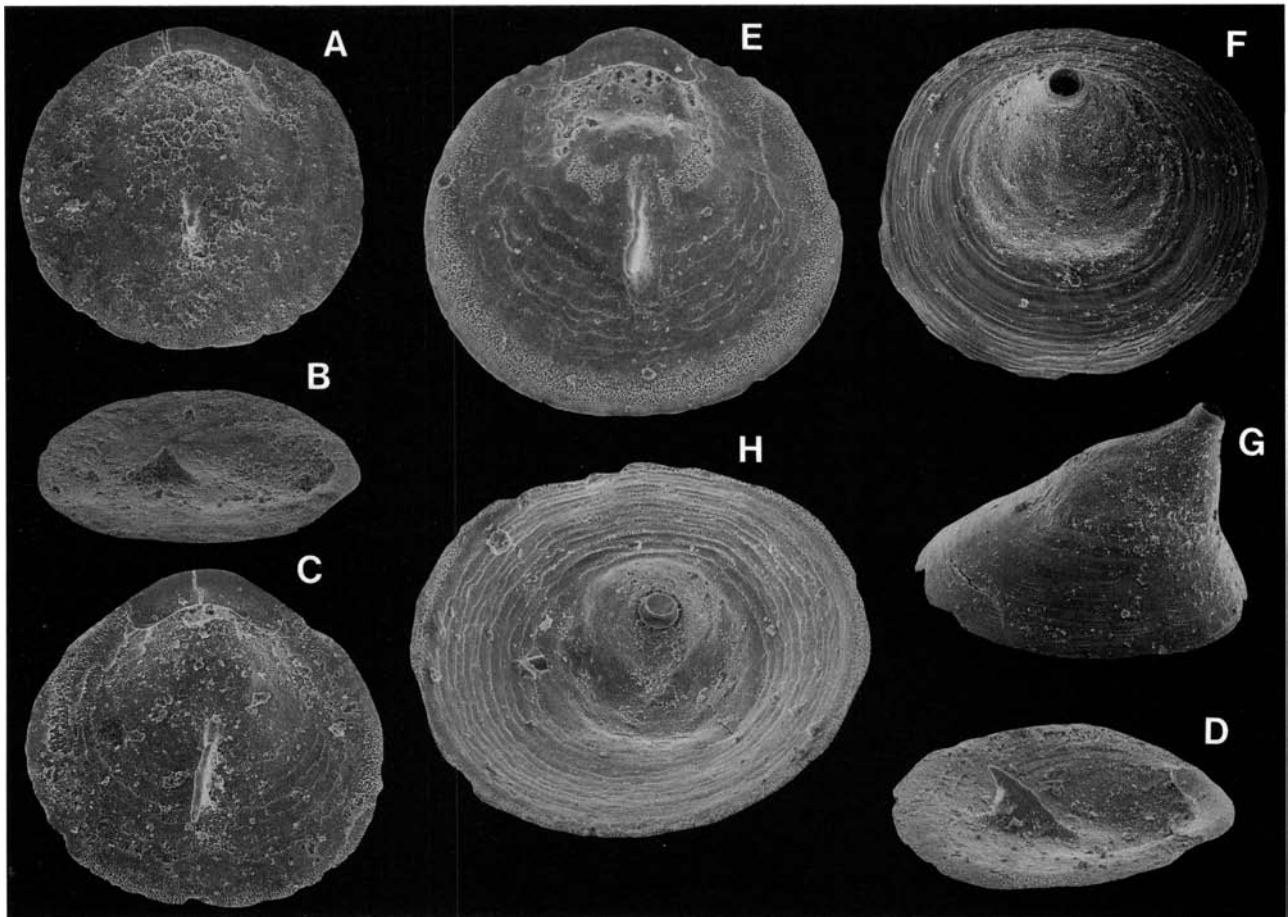


Fig. 59. Ontogeny of *Conotreta? siljanensis* sp. nov. □A. Interior of a brephic dorsal valve; Dalby Limestone (sample DLK83-dal-5); Br132468, ×120. □B. Side view of A; ×120. □C. Interior of a brephic dorsal valve; Gullhøgen Formation (sample GB84-2-33); Br132797, ×120. □D. Side view of C; ×120. □E. Interior of a juvenile dorsal valve; Furudal Limestone (sample DLK83-fur-16); Br132419, ×120. □F. Exterior of a brephic ventral valve; Ryd Limestone (sample GB84-2-39); Br132835, ×120. □G. Side view of F; ×120. □H. Interior of a brephic ventral valve; Dalby Limestone (sample DLK83-dal-2); Br132447, ×120.

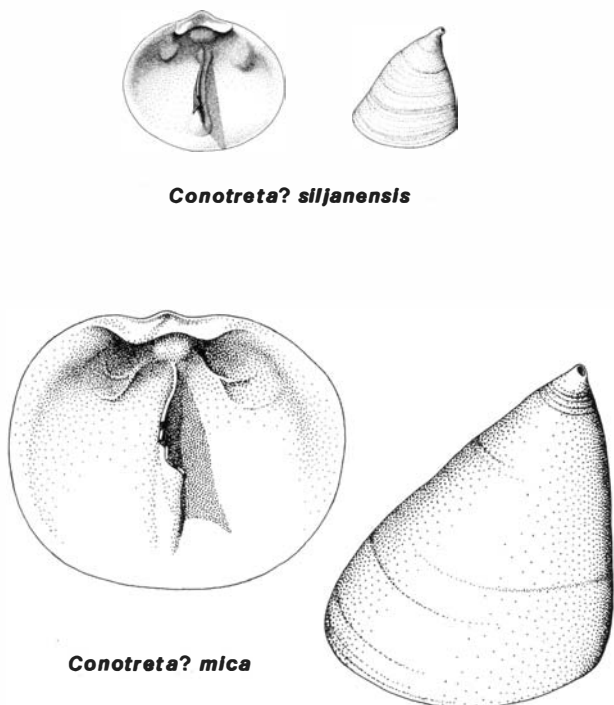


Fig. 60. Comparison between *Conotreta? mica* and *C.? siljanensis*. Figure prepared by Lennart Andersson (Stockholm).

gular plate at about the centre of the valve (Fig. 59A–B). At the end of the brephic stage the median septum develops an upper septal rod (Fig. 59C–D, E). The brephic ventral valve (H 0.25–0.42) lacks all recognizable interior structures (Fig. 59F–H). In neanic shells (W 0.56–1.01, L 0.54–0.90) the dorsal pseudointerarea (WI 0.23–0.42, LI 0.05–0.10) is divided by a median groove; the propareas are well developed. The median buttress and the raised cardinal muscle scars (WM 0.31–0.56, LM 0.23–0.33) are also developed during the neanic stage. In the ventral valve (H 0.42–0.81) an apical process is formed as well as a pseudointerarea. In adults (W 1.01–1.46, L 0.90–1.32) the dorsal valve is thickened and the median septum (up to about 0.40 mm high) develops a maximum of three to five septal rods. A few valves exceeding 1.46 mm in width are considered to represent the gerontic stage. Some gerontic ventral valves are slightly apsacline (see also Fig. 46).

Discussion. – *Conotreta? siljanensis* differs from *C.? mica* in several distinct features (Fig. 6D). *C.? siljanensis* has (1) a smaller apical process, (2) a poorly developed mantle canal pattern, (3) a snout-like exterior pedicle tube, and (4) smaller average and maximum size (\bar{W} 0.94, maximum W 1.57 in *C.? siljanensis* compared with \bar{W} 1.39, maximum W 2.29 in *C.? mica*). As in *C.? mica* there is some temporal change in the morphology of the species. The material of

Table 3. *Conotreta? siljanensis* sp. nov., average dimensions ratios of ventral valves.

	W	L	L/W	H	H/W
GB84-2-7, 2-39					
<i>n</i>	11	11	11	11	11
mean	0.84	0.74	88%	0.62	73%
<i>s</i>	0.185	0.155	1.567	0.176	6.373
min	0.62	0.56	86%	0.39	61%
max	1.13	0.98	90%	0.93	82%
DLK83-fur-16					
<i>n</i>	18	18	18	18	18
mean	0.77	0.66	86%	0.62	80%
<i>s</i>	0.126	0.107	3.924	0.137	6.122
min	0.56	0.48	77%	0.42	73%
max	0.95	0.79	92%	0.84	89%
DLK83-dal-2, 5					
<i>n</i>	7	7	7	7	7
mean	1.09	0.95	88%	1.02	88%
<i>s</i>	0.421	0.344	4.776	0.532	17.727
min	0.45	0.43	83%	0.28	62%
max	1.67	1.40	97%	1.67	113%

C.? siljanensis is abundant and well preserved, which would allow the pattern of this change to be studied in detail, but such a study is outside the scope of the present paper. The morphology of the ventral valve appears to vary more than that of the dorsal valve (cf. Figs. 56H, 57G, 58G; Tables 3–4); in particular, the H/W ratio as well as the size and shape of the apical process show considerable variation. The new species appears to be similar to *C.? apicalis* Cooper, 1956 (p. 249, Pl. 17B:15–28) and *C.? multisinuata* Cooper, 1956 (p. 253, Pl. 16G:28–40) from the Pratt Ferry beds of Alabama. The mantle canal pattern of the two American species is much better developed than that of *C.? siljanensis* and the dorsal pseudointerarea is proportionally longer and narrower. Moreover, the median septum of *C.? siljanensis* has 3–5 septal rods, whereas both American species have a more simple septum with only an upper septal rod.

Occurrence. – *Conotreta? siljanensis* is the third most abundant species in the Viru sequence investigated and it has a long stratigraphical range. In Dalarna it appears first in the uppermost Folkeslunda Limestone and is found in virtually all samples up into the lower Dalby Limestone (Figs. 9, 10). In Västergötland *C.? siljanensis* appears within the lower part of the Gullhögen Formation and ranges up into the Ryd Limestone. In addition there is a questionable record from the lowermost sample in the Dalby Limestone (Fig. 8B–C). On Öland it is known from the Furudal and Källa limestones.

Type species. – Original designation; *Atrypa? nitens* Hisinger, 1837, p. 77, from the lower Harju Fjäcka Shale, Draggån, Dalarna.

Genus Hisingerella Henningsmoen, 1948

Diagnosis. – See Holmer (1986, p. 107).

Species assigned. – *Conotreta? devota* Krause & Rowell, 1975; *Hisingerella billingensis* sp. nov.; *H.? unguicula* sp. nov.; in addition to the species listed by Holmer (1986).

Discussion. – As noted by Holmer (1986), the Upper Ordovician type species, *H. nitens* is inadequately known be-

Table 4. *Conotreta? siljanensis* sp. nov., average dimensions and ratios of dorsal valves.

	W	L	L/W	WI	LI	LI/WI	WM	LM	LM/WM	LS	BS
DLK83-fo-5											
<i>n</i>	14	14	14	14	14	14	6	6	6	9	9
mean	1.20	1.08	91%	0.51	0.11	21%	0.77	0.43	56%	0.97	0.25
<i>s</i>	0.288	0.254	2.921	0.132	0.024	3.851	0.175	0.088	5.924	0.112	0.030
min	0.45	0.43	87%	0.19	0.06	18%	0.54	0.36	48%	0.82	0.19
max	1.57	1.41	97%	0.70	0.12	33%	0.98	0.56	66%	1.12	0.29
GB84-2-7, 2-39											
<i>n</i>	24	24	24	24	24	24	14	14	14	24	24
mean	0.96	0.86	90%	0.39	0.09	23%	0.60	0.36	61%	0.68	0.20
<i>s</i>	0.264	0.221	3.836	0.109	0.019	3.867	0.115	0.076	8.206	0.191	0.034
min	0.37	0.37	85%	0.16	0.04	17%	0.36	0.23	44%	0.26	0.16
max	1.36	1.22	100%	0.57	0.11	32%	0.73	0.46	79%	0.96	0.26
DLK83-fur-16											
<i>n</i>	18	18	18	18	18	18	15	15	15	17	17
mean	0.82	0.74	91%	0.33	0.08	25%	0.48	0.30	64%	0.58	0.18
<i>s</i>	0.268	0.223	3.490	0.121	0.022	3.948	0.146	0.080	6.224	0.187	0.038
min	0.42	0.39	86%	0.17	0.04	19%	0.28	0.14	53%	0.33	0.14
max	1.29	1.12	97%	0.54	0.11	33%	0.78	0.46	74%	0.85	0.25
DLK83-dal-2, 5											
<i>n</i>	18	18	18	18	18	18	6	6	6	13	13
mean	0.84	0.75	90%	0.35	0.08	22%	0.54	0.34	65%	0.61	0.19
<i>s</i>	0.265	0.214	3.183	0.123	0.024	3.218	0.166	0.071	7.202	0.226	0.030
min	0.56	0.50	84%	0.20	0.05	16%	0.31	0.23	54%	0.33	0.14
max	1.43	1.19	97%	0.59	0.11	29%	0.78	0.42	75%	1.05	0.23

cause of the poor preservation of the type material; it is possibly a senior synonym of *H. tenuis* Holmer, 1986 from the lower Harju Bestorp Limestone. *H. tenuis* may serve as a provisional reference species, until good comparative topotype material of *H. nitens* has been located.

Hisingerella billingensis sp. nov.

Fig. 61

Name. – After the Billingens district, Västergötland.

Holotype. – Br128616, complete dorsal valve, Fig. 61A–E (W 0.98, L 0.91), from the Gullhøgen Formation, Gullhøgen quarry (sample GB84-1-1), Västergötland.

Paratypes. – Figured; Br128615 (W 0.97, L 0.91, H 0.57), Br128614 (damaged). Total of 45 dorsal valves and 27 ventral valves.

Diagnosis. – Ventral valve procline with maximum height at umbo; apical process small. Pseudointerarea of dorsal valve with wide median groove and small propareas.

Description. – The valves are approximately circular in outline, on average 93% as long as wide (OR 90–95%; $N=5$; Table 5). In one specimen the ventral valve is 59% as high as wide with the maximum height at the umbo. In lateral profile the outline of the posterior surface of the ventral valve is procline and flattened, whilst the anterior surface is convex (Fig. 61G). The ventral pseudointerarea is poorly delineated and has a wide interr ridge (Fig. 61F–H). The ventral interior has a distinct apical process, as well as a pair of cardinal muscle scars on the posterior wall (Fig. 61L). The exterior pedicle tube is short; it is not continued into the interior (Fig. 61J). The dorsal valve is flattened in lateral profile (Fig. 61D), with a pseudointerarea on average 29% as long as wide (Table 5) and occupying about 43% of the total width. The median groove is well developed and the propareas are orthocone (Fig. 61E). The cardinal muscle scars are slightly raised in adults, on average 53% as long as wide (Table 5). The median septum has a single upper septal rod. The septum originates about 0.20 mm from the posterior margin (Table 5), and occupies about 80% of the length (Fig. 61D). The valves are ornamented with faint, closely spaced fila (Fig. 61A, F). The larval shell is nearly circular, about 0.22 mm in diameter; it is ornamented with overlapping circular pits of uniform size (up to 1.6 μm in diameter; Fig. 61K).

Discussion. – *Hisingerella billingensis* is related closely to *H. tenuis* Holmer, 1986 (p. 107, Figs. 5A–P, 10A–C), from the Upper Ordovician Bestorp Limestone. The two species are similar in having (1) an almost circular outline (L/W ratio about 93% in both species), (2) a wide interr ridge on the ventral valve, (4) a dorsal pseudointerarea with a wide, well developed median groove, (5) a simple median septum, and (6) a circular larval shell with overlapping pits of uniform size. Both species are also thin-shelled. The Middle Ordovician species differs from *H. tenuis* mainly in having (1) a distinct apical process, (2) a procline ventral valve, (3) a short exterior pedicle tube, and (4) poorly developed dorsal propareas. In addition, the ventral valve

of *H. tenuis* is recurved, with the maximum height slightly anterior to the depressed umbo. The type material of the Middle Ordovician species *H. nana* (Hadding, 1913) from the 'Dicellograptus Shale' of Scania is too poorly preserved for a detailed comparison (see also Harper *et al.* 1984).

Occurrence. – *Hisingerella billingensis* is restricted to the lowermost part of the Gullhøgen Formation of Västergötland (Fig. 8B).

Hisingerella? unguicula sp. nov.

Figs. 26, 62

Name. – Latin *unguiculus*, small fingernail; alluding to the lateral profile of the dorsal valve.

Holotype. – Br129006, complete dorsal valve, Fig. 62E–F (W 0.87, L 0.76), from the Folkeslunda Limestone, Kårgårde section (sample DLK83-fo-1), Dalarna.

Paratypes. – Figured; Br128625 (W 0.78, L 0.71), Br128598 (W 0.88, L 0.78), Br128871 (damaged), Br128631 (damaged), Br128879 (damaged), Br128900 (damaged), Br133612c (section). Total of 193 dorsal valves and 379 ventral valve.

Diagnosis. – Ventral valve with long, narrow, posteriorly inclined exterior pedicle tube. Ventral interior with poorly developed apical process. Dorsal valve deep; fingernail-shaped in lateral profile.

Description. – The valves are approximately circular. The ventral valve is highly conical with maximum height at the umbo. In lateral profile the outline of the posterior surface of the ventral valve is slightly concave, whilst the anterior surface is flattened to convex (Fig. 62J). There is a posteriorly inclined, pointed exterior pedicle tube (Fig. 62J). The ventral pseudointerarea is poorly delineated, procline and has a faint interr ridge (Fig. 62K). The apical process is just a slight thickening, and there is no interior pedicle tube (Fig. 62L). The dorsal valve averages 94% as long as wide (Table 6); 0.16 mm deep in the holotype. In lateral profile it is fingernail-shaped (Fig. 62B). The dorsal pseudointerarea averages 28% as long as wide (Table 6), occupying some 44% (OR 38–52%; $N=10$) of the width of the valve. The median groove is well developed, and the propareas are small and anacone (Fig. 62G–H). The median buttress is robust. In the holotype, the dorsal cardinal muscle scars are about 72% as long as wide (Fig. 62E). The median septum originates about 0.18 mm from the posterior margin and occupies about 80–90% of the total length. In lateral profile the septum is low and has a single upper septal rod (Fig. 62F). The valves are ornamented with closely spaced concentric fila (Fig. 62A, I). The larval shell is about 90–95% as long as wide, up to 0.24 mm wide and 0.22 mm long. It is ornamented with pits of two size groups; large pits, up to 6 μm wide, separated from small pits, 830 nm to 2 μm wide (Fig. 62D). For shell structure, see above (p. 45, Fig. 26).

Discussion. – This species is similar to other described species of *Hisingerella* in having (1) a reduced apical process, (2) a dorsal pseudointerarea with a deep median groove,

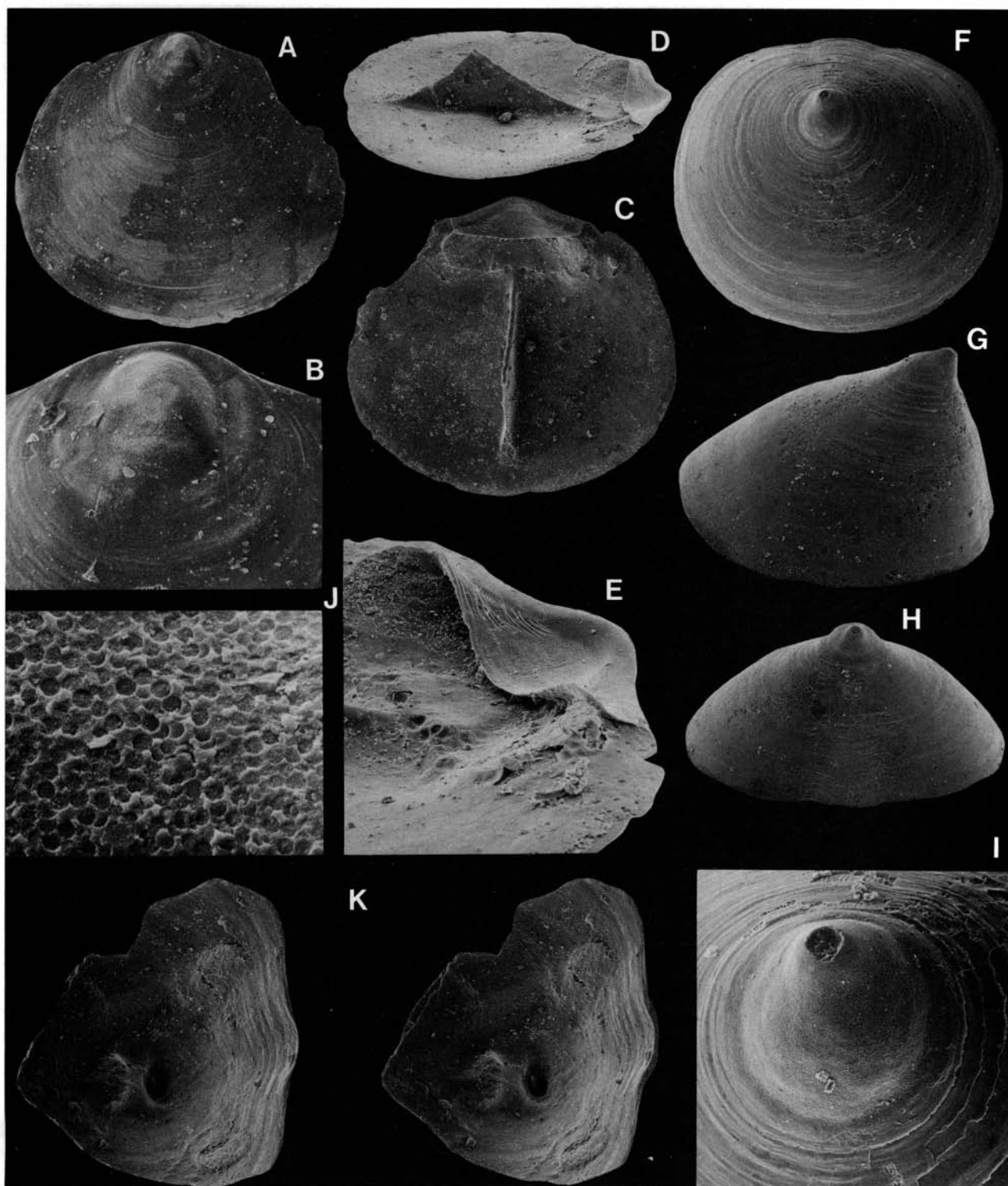


Fig. 61. *Hisingerella billingensis* sp. nov., Gullhöggen Formation (sample GB84-1-1). □A. Holotype; dorsal exterior; Br128616, ×55. □B. The larval shell of A; ×165. □C. Interior of A; ×55. □D. Side view of C; ×59. □E. Detail of the pseudointerarea of C; ×178. □F. Ventral exterior; Br128615, ×55. □G. Side view of F; ×60. □H. Posterior view of F; ×55. □I. The larval shell of F; ×186. □J. The larval ornamentation of F; ×1860. □K. Stereo-pair; interior of a ventral valve; Br128614, ×60.

Table 5. *Hisingerella billingensis* sp. nov., average dimensions and ratios of dorsal valves.

	W	L	L/W	WI	LI	LI/WI	WM	LM	LM/WM	LS	BS
GB84-1-1											
n	3	4	3	4	4	4	3	3	3	4	4
mean	0.91	0.88	93%	0.41	0.12	29%	0.49	0.26	53%	0.71	0.20
min	0.68	0.64	90%	0.31	0.09	26%	0.43	0.25	50%	0.43	0.16
max	1.07	0.99	95%	0.48	0.14	32%	0.53	0.26	57%	0.85	0.23

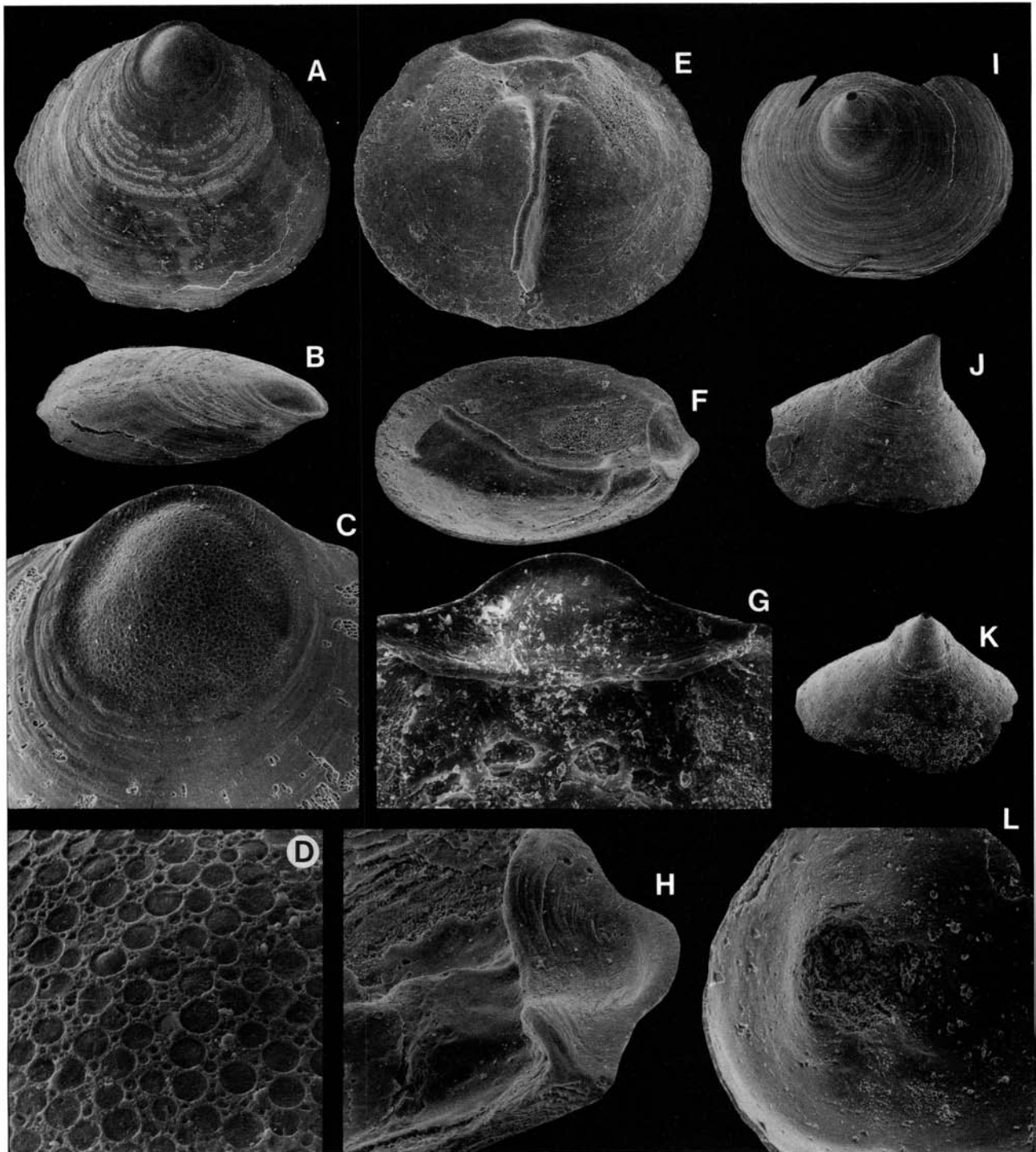


Fig. 62. *Hisingerella? unguicula* sp. nov. □A. Dorsal exterior; Gullhögen Formation (sample GB84-1-3); Br128625, $\times 64$. □B. Side view of A; $\times 64$. □C. The larval shell of A; $\times 185$. □D. The larval ornamentation of A; $\times 1200$. □E. Holotype; dorsal interior; Folkeslunda Limestone (sample DLK83-fo-1); Br129006, $\times 64$. □F. Side view of E; $\times 64$. □G. Detail of a dorsal pseudointerarea; Våmb Limestone (unnumbered sample); Br128598, $\times 185$. □H. Side view of a dorsal pseudointerarea; Kårgårde Limestone (sample DLK83-segk-1); Br128871, $\times 185$. □I. Ventral exterior; Holen Limestone (sample GB81-0); Br128631, $\times 64$. □J. Side view of a ventral valve; Kårgårde Limestone (sample DLK83-segk-1); Br128879, $\times 64$. □K. Posterior view of J; $\times 64$. □L. Interior of a ventral valve; Skövde beds (sample GB84-A4); Br128900, $\times 150$.

Table 6. *Hisingerella? unguicula* sp. nov., average dimensions and ratios of dorsal valves.

	W	L	L/W	WI	LI	LI/WI	WM	LM	LM/WM	LS	BS
GB84-A1, DLK83-fo-2											
<i>n</i>	10	10	10	11	11	11	1	1	1	10	10
mean	0.65	0.61	94%	0.29	0.08	28%	0.39	0.28	72%	0.49	0.18
<i>s</i>	0.066	0.055	3.479	0.049	0.016	2.914				0.068	0.011
min	0.54	0.53	88%	0.22	0.06	24%				0.42	0.16
max	0.78	0.71	98%	0.40	0.11	32%				0.62	0.18

and (3) a simple median septum; it also lacks an interior pedicle tube, and the thin shell and ornamentation are also suggestive of *Hisingerella*. *H. unguicula* differs from other described species of the genus in having a strongly convex dorsal valve and a different type of larval pitting. Moreover, the ventral valve lacks an interr ridge. *H. unguicula* appears to be similar to *H. devota* (Krause & Rowell, 1975, p. 35, Pls. 4:1–16, 12:5) from the lower Whiterock of Nevada. The dorsal valves of both taxa have (1) a strongly convex outline in lateral and anterior views, (2) cardinal muscle scars shaped like a ‘Spanish wineskin’ (*sensu* Krause & Rowell 1975, p. 35; see also Fig. 62E), (3) the pseudointerarea around 30% as long as wide, occupying about 46% of total width, with deep median groove and anacline propareas, and (4) a simple triangular median septum occupying about 86% of the valve length. The median septum of the American species has up to two septal spines, whereas *H. unguicula* invariably has a single upper septal rod. The ventral valve of *H. devota* differs from the Swedish species in (1) a more recurved convexity of the valve, (2) the development of a distinct interr ridge, and (3) a more robust apical process.

Occurrence. – In Jämtland (sample J69-28), Dalarna, and Västergötland this species is known from the the upper part of the Lower Ordovician Holen Limestone. In Dalarna and Jämtland (sample J69-35) it also occurs in the Segerstad Limestone; in the former district it ranges up into the

Folkeslunda Limestone (Fig. 9A). In Västergötland the Skövde Limestone and Gullhøgen Formation have also yielded specimens (Fig. 8A–B).

Genus *Cyrtonotreta* gen. nov.

Name. – Greek *Cyrton*, humpback and *tretos*, perforated; alluding to the lateral profile of the ventral valve.

Type species. – *Conotreta depressa* Cooper, 1956, p. 251, Pl. 17C:29–57, from the Middle Ordovician Pratt Ferry beds, Pratt Ferry, Alabama, U.S.A.

Cooper stated that all the Pratt Ferry material originates from the lower three feet, corresponding to the *P. serra* Biozone (Bergström 1971). However, the conodonts from Cooper’s samples were examined by Sweet & Bergström (1962), indicating the *Pygodus anserinus* Biozone (Bergström 1971). Some topotypic specimens are figured in Fig. 63.

Diagnosis. – Ventral valve widely conical with rounded apex sometimes recurved (‘humpbacked’) in lateral view. Ventral pseudointerarea procline to apsacline, frequently with interr ridge. Ventral interior with large apical process and deeply impressed pinnate mantle canal pattern; internal pedicle tube long. Dorsal valve flattened in lateral profile, with wide, almost straight pseudointerarea, frequently occupying more than half the total width; long propareas and shallow, wide median groove. Simple low median septum,

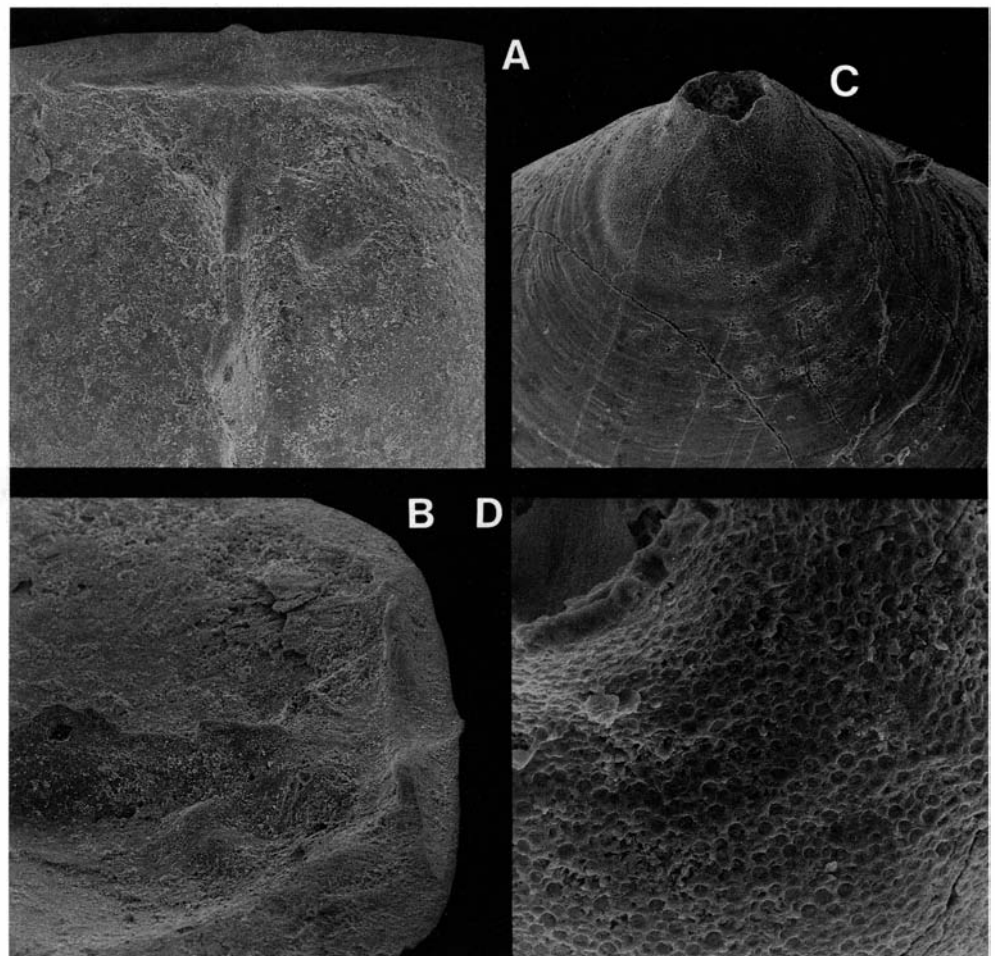


Fig. 63. *Cyrtonotreta depressa* (Cooper, 1956); Pratt Ferry Limestone (*Pygodus anserinus* Biozone), Pratt Ferry, Alabama (sample 68B9-1, coll. S.M. Bergström). □A. Detail of the pseudointerarea of a dorsal valve; Br133668, ×52. □B. Side view of A; ×60. □C. Detail of the larval shell of a ventral valve; Br133669, ×175. □D. Detail of the ornamentation of C; ×795.

extending about 60–70% of total length; single upper septal rod.

Species assigned. – *Conotreta depressa* Cooper, 1956; *Cyrtonotreta vestrogothica* sp. nov.; *C.? striata* sp. nov.

Discussion. – The three species assigned to the genus are all restricted to the Middle Ordovician. *Cyrtonotreta* is related to *Conotreta* Walcott, 1889, the type species of which (as discussed above) is poorly known. Using the definition of Cooper (1956), *Cyrtonotreta* differs from *Conotreta* in having (1) a relatively wider and less conical ventral valve, (2) a dorsal valve with a wide and almost straight pseudointerarea, most frequently occupying more than 50% of the total width (WI/W ratio most commonly less than 40% in *Conotreta*), (3) more widely spaced dorsal cardinal muscle scars, and (4) a low median septum, extending about 60–70% of total length (LS/L ratio most commonly 80–90% in *Conotreta*), and invariably with a single upper septal rod. Topotypes of *C. depressa* (Cooper) from the uppermost part (sample 68B9-1; within the *Pygodus anserinus* Biozone; supplied by S. M. Bergström) of the Pratt Ferry beds of Alabama are illustrated here (Fig. 63). The dorsal pseudointerarea of *Cyrtonotreta* is somewhat similar to that of *Physotreta* Rowell, 1966. However, compared with *Cyrtonotreta*, this genus has a much greater maximum size and a more widened and elongated dorsal pseudointerarea.

Cyrtonotreta vestrogothica sp. nov.

Figs. 64, 67I–N

Name. – Latinized form of Västergötland.

Holotype. – Br132844, slightly damaged dorsal valve, Fig. 64E–F (W ~2.51, L 2.26), from the Ryd Limestone, Gullhøgen quarry (sample GB84-3-41), Västergötland.

Paratypes. – Figured; Br132783 (W 2.64, L 2.39), Br132941 (W 3.07, L 2.73), Br132784 (damaged), Br132785 (lost during SEM), Br132786 (lost during SEM), Br133937 (W 0.65), Br132796 (damaged), Br132771 (W 0.62, L 0.55), Br132768 (W 0.74, L 0.64, H 0.33). Total of 77 dorsal valves and 88 ventral valves.

Diagnosis. – Ventral valve widely conical; pseudointerarea procline with interridge. Interior of ventral valve with well developed and robust apical process, occupying large portion of apex. Dorsal valve flattened in lateral profile, with wide pseudointerarea and almost straight posterior margin.

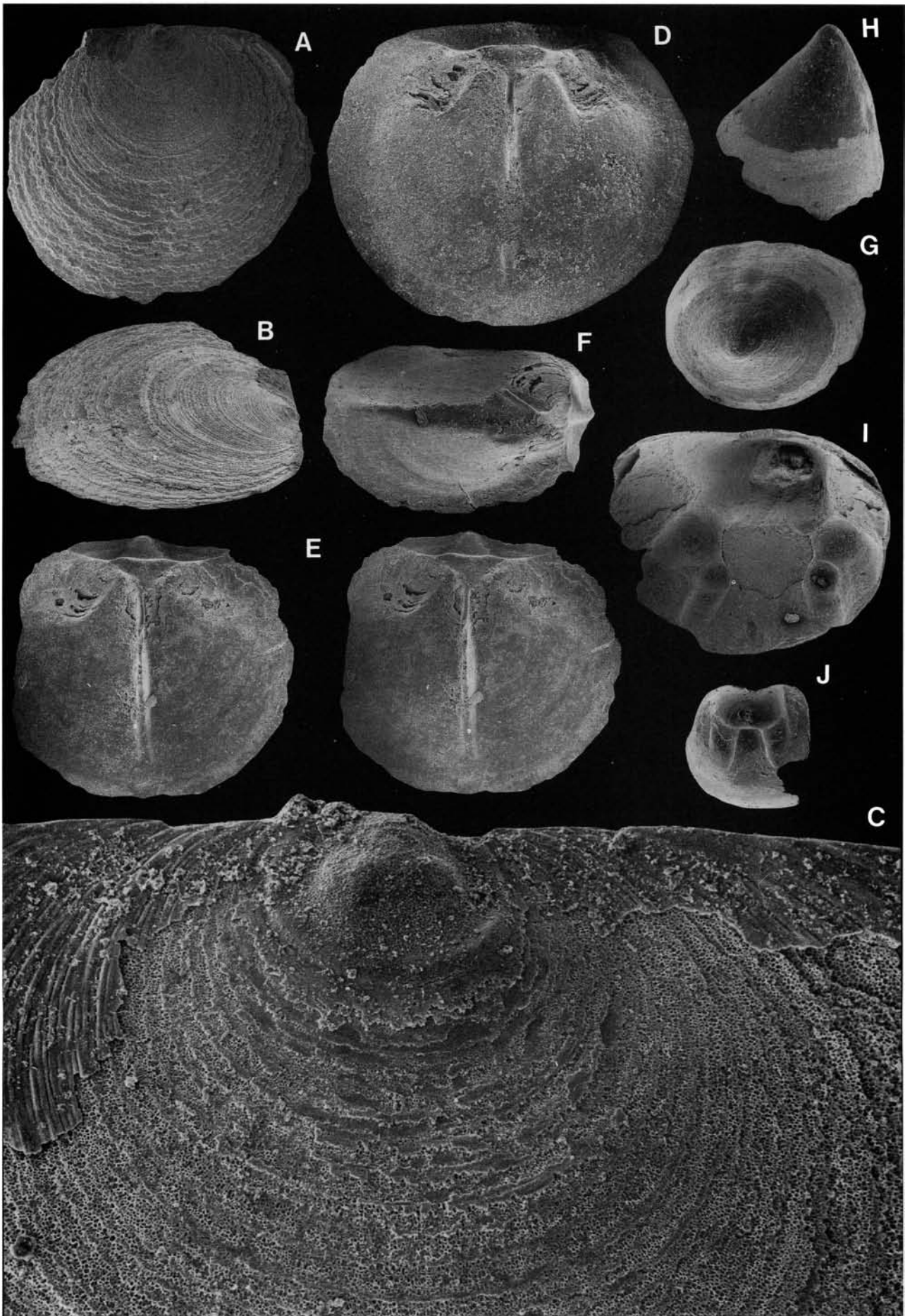
Description. – The outline of the valves is broadly oval. Preserved ventral valves are invariably fragmentary, but it appears to be widely conical and has a rounded apex, lacking an exterior pedicle tube (Fig. 64H). In lateral profile the ventral pseudointerarea is procline and slightly convex; the interridge is wide (Fig. 64G–H). The ventral interior is dominated by a well developed apical process, penetrated by a long interior pedicle tube. The mantle canal pattern is deeply impressed (Fig. 64I–J). The dorsal valve is on average 91% as long as wide (Table 7). In lateral profile it is flattened, and in dorsal view the posterior margin is almost straight (Fig. 64A–B). The dorsal pseudointerarea is on average 14% as long as wide (Table 7), and occupies well over 50% of the width of the valve. The propareas are wide and anacline, with a shallow and wide median groove (Fig. 64D–F). The median buttress is robust. The cardinal muscle scars are on average 57% as long as wide (Table 7); they are widely separated and diverge anteriorly, occupying about 40% of the total length (Fig. 64D–E). The median septum originates about 0.44 mm from the posterior margin (Table 7) and occupies about 80% of the valve length. In lateral view it is low and has a single upper septal rod. The exterior of both valves is commonly exfoliated, exposing the camerate secondary layer (Fig. 64C). The valves are ornamented with weakly developed, evenly spaced concentric growth lines, about 7–8 µm apart.

Remarks on ontogeny. – Some juvenile valves appear to belong to *Cyrtonotreta vestrogothica*, but in many cases it is difficult to distinguish these from juveniles of *Conotreta? siljanensis* and *Cyrtonotreta? striata* (see, e.g., Figs. 59, 67). The larval shell of dorsal valves is relatively small for the subfamily, up to 0.20 mm wide and 0.18 mm long, with

Fig. 64 (opposite page). *Cyrtonotreta vestrogothica* gen. et sp. nov. □A. Exterior of a dorsal valve; Gullhøgen Limestone (sample GB84-2-25); Br132783, ×21. □B. Side view of A; ×21. □C. Detail of A, showing the larval shell; note that the primary layer of the adult shell is exfoliated, exposing the camerate shell structure of the secondary layer; ×200. □D. Dorsal interior; Ryd Limestone (sample GB84-3-69); Br132941, ×21. □E. Holotype; stereo-pair; dorsal interior; Ryd Limestone (sample GB84-3-41); Br132844, ×21. □F. Side view of E; ×21. □G. Exterior of a ventral valve; Gullhøgen Limestone (sample GB84-2-25); Br132784, ×21. □H. Side view of G; ×21. □I. Ventral interior; Gullhøgen Limestone (sample GB84-2-25); Br132785, ×30. □J. Interior of a ventral valve; Gullhøgen Limestone (sample GB84-2-25); Br132786, ×30.

Table 7. *Cyrtonotreta vestrogothica* sp. nov., average dimensions of dorsal valves.

	W	L	L/W	WI	LI	LI/WI	WM	LM	LM/WM	LS	BS
GB84-3-41, 3-69											
n	4	3	3	4	4	4	2	2	2	3	3
mean	2.81	2.47	91%	1.52	0.21	14%	1.56	0.90	57%	1.98	0.44
min	2.48	2.26	90%	1.30	0.14	13%	1.46	0.84	57%	1.55	0.40
max	3.07	2.73	92%	1.70	0.25	16%	1.67	0.96	57%	2.39	0.46



three nodes (Fig. 64E). The pits of the dorsal larval shell are of varying size, about 1–3 μm in diameter (Fig. 67I). One juvenile dorsal valve (W 0.62, L 0.55) has a narrow and undivided pseudointerarea (WI 0.22, LI 0.04), and a short median septum with a single upper rod. The median septum originates about 0.17 mm from the posterior margin, extending to about the centre of the valve (Fig. 67J–K). On adult ventral valves the larval shell cannot be observed in detail, but some juvenile ventral valves have an almost circular larval shell, about 0.24 mm across with a minute apical foramen, about 0.05 mm across (Fig. 67L–M). One juvenile ventral valve is a low cone with a strongly procline lateral profile (Fig. 67N); the interior is without recognizable structures.

Discussion. – *Cyrtonotreta vestrogothica* is most similar to the type species *C. depressa* (Cooper, 1956, p. 251, Pl. 17C:29–57 and Fig. 63 herein), which differs in having (1) a more depressed, strongly apsacline ventral valve, (2) a well developed ventral pseudointerarea that almost lacks an interridge, (3) a less well developed apical process, (4) a wider and straight dorsal pseudointerarea (Fig. 63A–B), and (5) a lower and shorter median septum, extending about 70% of total length (LS/L ratio about 80% in *C. vestrogothica*). The larval shell of *C. depressa* is circular, about 0.18 mm in diameter (Fig. 63C).

Occurrence. – *Cyrtonotreta vestrogothica* occurs in the Gullhög Formation and Ryd Limestone of Västergötland (Fig. 8B–C).

Cyrtonotreta sp. a

Figs. 47C–E, 65, 67G–H

Material. – Figured; Br128695 (damaged), Br 132526 (damaged), Br132528 (damaged), Br132527 (W 2.57, H 1.95), Br132503 (deformed), Br132967 (damaged), Br133038 (W 0.71, L 0.64). Total of 188 mostly fragmentary dorsal valves and 187 mostly fragmentary ventral valves. (Description based on some of the better preserved material from the Dalby Limestone).

Description. – The complete outline is unknown from either valve. In one specimen the ventral valve is broadly conical, and about 76% as high as wide (Fig. 65E). The ventral pseudointerarea is flattened, wide and nearly catacline; it lacks an interridge (Figs. 47C, 65E–F, H). There is no exterior pedicle tube (Fig. 65G); the pedicle foramen is continued as an interior pedicle tube. The apical process is narrow and long. The mantle canal pattern is well developed, pinnate (Fig. 65I). The dorsal pseudointerarea is wide, short and anacline. The median groove is poorly defined (Fig. 65C–D). The dorsal median septum and muscle scars are not known. The valves are ornamented with regular concentric growth lines. The dorsal larval shell of the preserved adult valves is generally damaged, about 0.20 mm wide (Fig. 65B). In one ventral valve, the larval shell is about 0.25 mm wide and 0.22 mm long, with an apical foramen, 0.08 mm in diameter (Fig. 65G). Some juvenile dorsal valves possibly belonging to this species (Fig. 67G) preserve a larval shell about 0.24 mm wide and

0.21 mm long. The larval pitting is identical to that of *Cyrtonotreta vestrogothica*.

Discussion. – The specimens from the Dalby Limestone are better preserved than those occurring lower in the sequence. *Cyrtonotreta* sp. a differs from *C. vestrogothica* in having (1) an almost catacline ventral valve that lacks an interridge, (2) a ventral interior with less well developed apical process, and (3) a dorsal pseudointerarea with a very faint median groove.

Occurrence. – In Dalarna *Cyrtonotreta* sp. a ranges from the Folkeslunda to the Dalby limestones (Figs. 9, 10). In Västergötland it is restricted to the lower Dalby Limestone (Fig. 8C).

Cyrtonotreta? *striata* sp. nov.

Figs. 66, 67A–F

Name. – Latin *striatus*, striated; alluding to the ornamentation of the species.

Holotype. – Br132615, complete dorsal valve, Fig. 66C–D (W 2.42, L 2.11), from the Gullhög Formation, Gullhög quarry (sample GB84-1-5), Västergötland.

Paratypes. – Figured; Br132382 (W 1.70, L 1.52), Br132720 (W 2.32, L 2.02), Br133034 (damaged), Br132721 (damaged), Br133036 (damaged), Br132827 (W 1.95, L ~1.74, H 1.33), Br132824 (L 1.44), Br132825 (W 1.13, 1.01), Br132938 (W 0.93, L 0.74, H 0.66). Total of 409 dorsal valves and 207 ventral valves.

Diagnosis. – Ventral valve strongly procline with broad apical process. Dorsal valve with pseudointerarea occupying about 43% of total width. Median septum low, occupying about 73% of total length. Ornamentation of faint radial striae.

Description. – The valves average 89% as long as wide (Table 8; $N=17$). The ventral valve is broadly conical, about 50–60% as high as wide (maximum W 0.85, maximum H 0.50; $N=3$). In lateral profile the anterior and posterior surfaces are gently convex (Fig. 66L). The exterior pedicle tube is short (Fig. 66G, L) and continues interiorly (Fig. 66I). The ventral pseudointerarea is strongly procline and has an interridge (Fig. 66F–G). The ventral interior has a broad apical process, and a poorly defined pinnate mantle canal pattern (Fig. 66H, J). In lateral profile the dorsal valve is flattened to slightly convex (Fig. 66D–E). The dorsal pseudointerarea is on average 18% as long as wide (Table 8), occupying about 43% of the width of the valve; the median groove is well developed and the propareas are anacline (Fig. 66C–E). The median buttress is robust. The cardinal muscle scars are raised, widely spaced and diverge anteriorly; on average 53% as long as wide (Table 8; Fig. 66C–E). In some specimens there is a pair of anterocentral muscle scars (Fig. 66E). The median septum originates about 0.38 mm from the posterior margin (Table 8), and occupies about 60–70% of the length. In lateral view the septum is very low, on average 19% as high as wide (Table 8), with the highest point at about the centre of the valve.

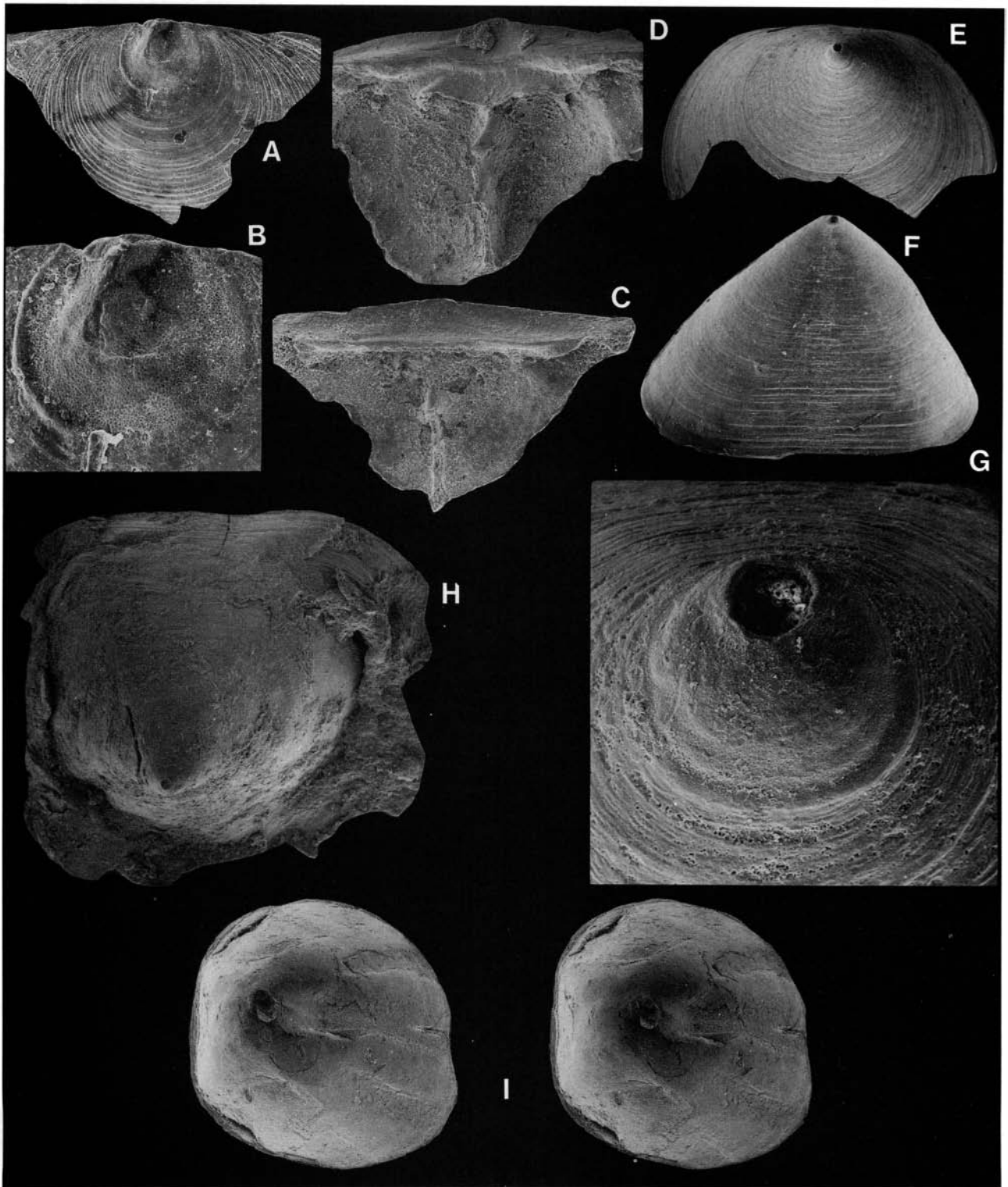


Fig. 65. *Cyrtontreta* sp. a. □A. Exterior of a dorsal valve; Dalby Limestone (sample D60-206); Br128695, $\times 68$. □B. The larval shell of A; $\times 200$. □C. Interior of A; $\times 68$. □D. Dorsal interior; Dalby Limestone (sample DLK83-dal-12); Br132528, $\times 34$. □E. Exterior of a ventral valve; Dalby Limestone (sample DLK83-dal-12); Br132527, $\times 21$. □F. Posterior view of E; $\times 21$. □G. The larval shell of E; $\times 200$. □H. Exterior of a slightly deformed ventral valve; Dalby Limestone (sample DLK83-dal-10); Br132503, $\times 21$. □I. Stereo-pair; ventral interior; Dalby Limestone (sample DLK83-dal-22); Br132967, $\times 17$.

The single upper septal rod is commonly obscured in adult valves (Fig. 66C–E). The valves are ornamented with weakly developed, closely spaced concentric fila, as well as radial discontinuous striae (Fig. 66A–B, F, M). The larval shell is

92% as long as wide (\overline{WL} 0.26, \overline{LL} 0.24; $N=12$). The pitted ornamentation is identical to that of *C. vestrogothica*.

Remarks on the ontogeny. – As noted above, it is difficult to distinguish between early stages of species belonging to

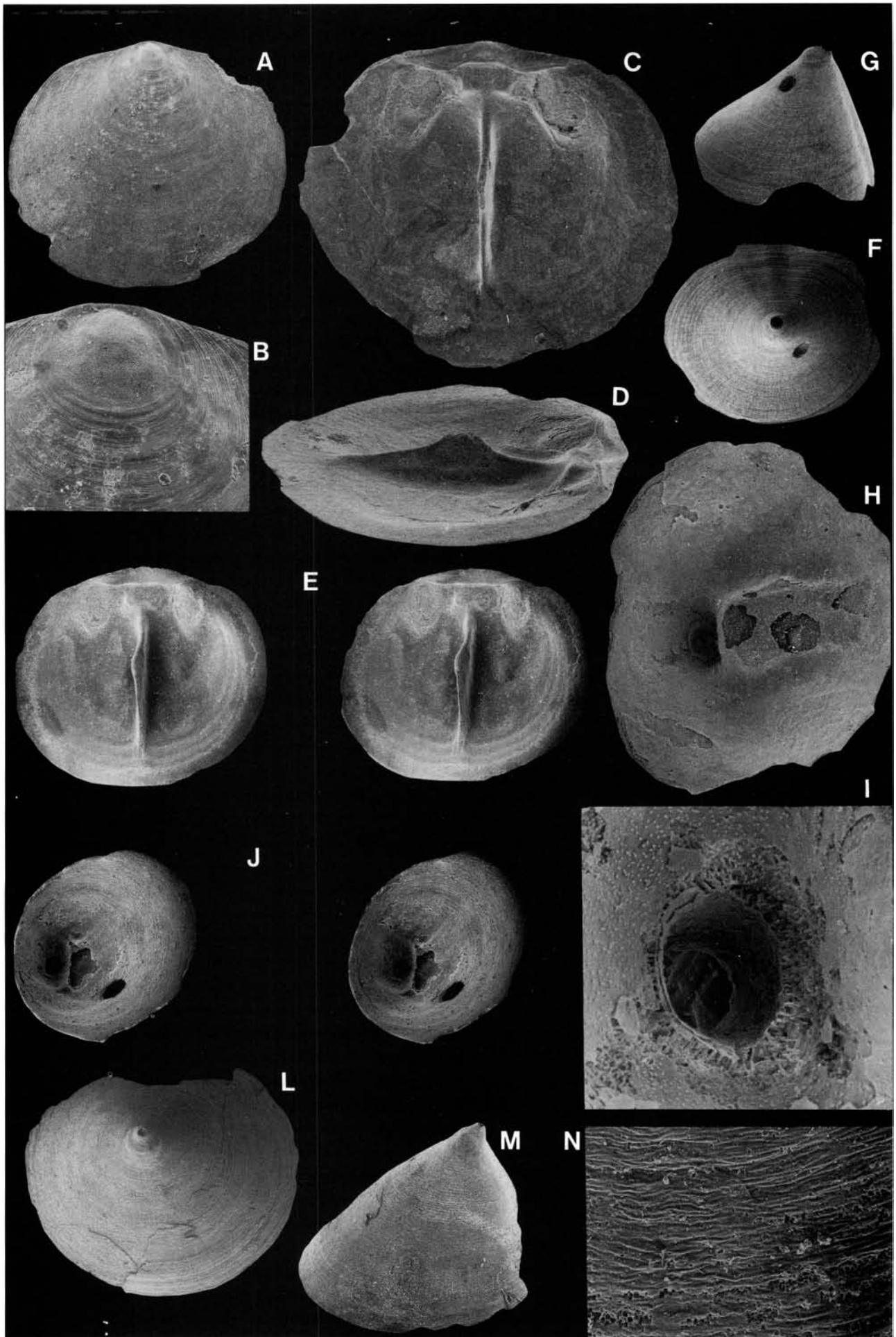


Table 8. *Cyrtontreta?* *striata* sp. nov., average dimensions of dorsal valves.

	W	L	L/W	WI	LI	LI/WI	WM	LM	LM/WM	LS	BS	HS	HS/W
GB84-1-1, 5, 2-9, 19, 37, 39, 41													
n	16	16	16	16	16	16	9	9	9	15	15	15	15
mean	2.11	1.88	89%	0.91	0.16	18%	1.24	0.65	53%	1.38	0.38	0.42	19%
s	0.459	0.426	4.070	0.190	0.030	2.620	0.179	0.095	5.210	0.367	0.082	0.049	3.521
min	0.71	0.67	85%	0.42	0.09	14%	0.95	0.50	46%	0.59	0.22	0.34	13%
max	2.64	2.57	98%	1.15	0.22	24%	1.43	0.78	63%	2.02	0.50	0.50	25%

Cyrtontreta and *Conotreta*. However, some juvenile valves of *Cyrtontreta?* *striata* have been identified (Fig. 67A–F). One dorsal valve is 89% as long as wide (W 1.13, L 1.01) with the pseudointerarea 26% as long as wide (WI 0.42, LI 0.11). The median septum has a single upper septal rod (HS 0.16), originating 0.24 mm from the posterior margin (Fig. 67C–D). One juvenile ventral valve is about 80% as long as wide (W 0.93, L 0.74, H 0.66; Fig. 67E–F). The ventral interior is without recognizable structures.

Discussion. – *Cyrtontreta?* *striata* is similar to other species of the genus in having (1) a broadly conical ventral valve, (2) a distinct apical process, (3) a pinnate mantle canal pattern, and (4) a low, comparatively short median septum. It differs mainly in having a narrower dorsal pseudointerarea, occupying up to about 43% of total width. This ratio is generally above 50% in species of *Cyrtontreta*. The larval shell of *C.?* *striata* is generally larger than that of *Cyrtontreta* (cf. Fig. 67B, H).

Occurrence. – *Cyrtontreta?* *striata* has a range from the Gullhøgen Formation to the lowermost Dalby Limestone of Västergötland (Fig. 8B–C). In Dalarna it is known from only two levels within the upper Furudal Limestone (Fig. 9B).

Cyrtontreta? sp. b

Fig. 68A–H, ?I–J

Material. – Figured; Br128613 (W 1.86, L 1.70), Br128600 (1.77, L 1.58), Br132566 (damaged), Br128896 (damaged), ?Br128876 (damaged). Total of four dorsal and four ventral valves.

Fig. 66. *Cyrtontreta?* *striata* gen. et sp. nov. □A. Dorsal exterior; Furudal Limestone (sample DLK83-fur-9); Br132382, ×30. □B. The larval shell of A; ×110. □C. Holotype; interior of a dorsal valve; Gullhøgen Formation (sample GB84-1-5); Br132615, ×30. □D. Side view of C; ×30. □E. Stereo-pair; dorsal interior; Gullhøgen Formation (sample GB84-2-19); Br132720, ×20. □F. Exterior of a ventral valve; Dalby Limestone (sample GB84-3-75); Br133034, ×30. □G. Side view of F; ×30. □H. Ventral interior; Gullhøgen Formation (sample GB84-2-21); Br132721, ×60. □I. The pedicle tube of H; ×270. □J. Stereo-pair; interior of a ventral valve; note the possible predatory borehole; Dalby Limestone (sample GB84-3-75); Br133036, ×30. L. Ventral exterior; Ryd Limestone (sample GB84-2-37); Br132827, ×30. M. Side view of L; ×30. □N. Detail of ornamentation of L; ×230.

Remarks. – The poorly preserved specimens of this species resemble *Cyrtontreta?* *striata*, but differ in the lack of well developed striae (Fig. 68A) and a ventral interridge (Fig. 68F, I). Because of the fragmentary nature of the material, no closer taxonomic evaluation is attempted.

Occurrence. – This species occurs in the Våmb and Skövde limestones and in the lowermost Gullhøgen Formation of Västergötland (Fig. 8A–B). In Dalarna there is a questionable record from the lowermost Kårgårde Limestone (Fig. 9A).

Genus *Physotreta* Rowell, 1966

Type species. – Original designation; *Acrotreta spinosa* Walcott, 1905, p. 302, from the Upper Cambrian *Dunderbergia* Zone, Eureka Co., Nevada, U.S.A.

Diagnosis. – See Rowell (1966, p. 19).

Species assigned. – *Acrotreta spinosa* Walcott, 1905; ?*Conotreta gigantea* Cooper, 1956; *Physotreta rugosa* Popov, 1980; *P. deformis* sp. nov.

Physotreta deformis sp. nov.

Figs. 25, 69–71

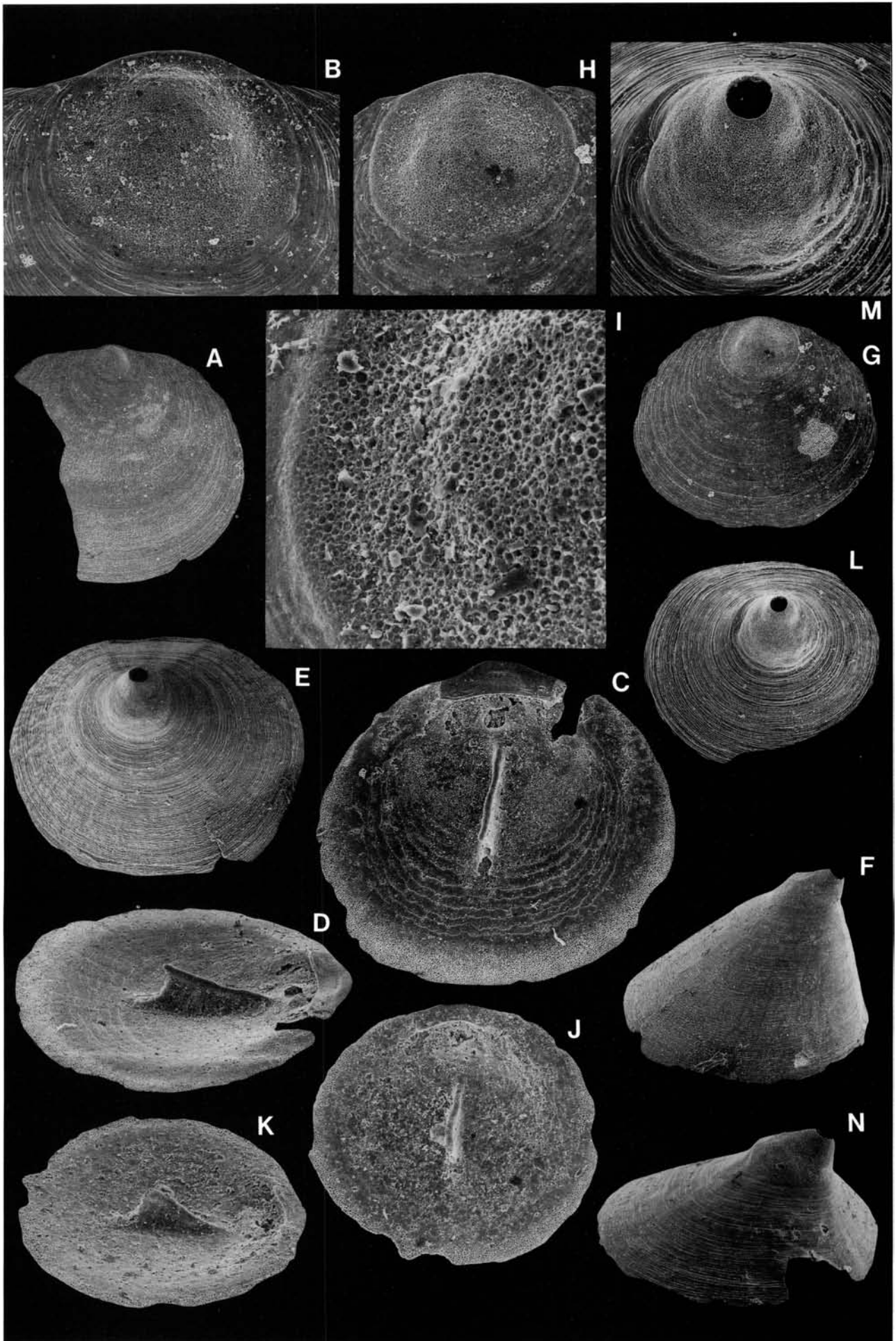
Name. – Latin *deformis*, misshapen; alluding to the misshapen lateral profile of the ventral valve.

Holotype. – Br129024, slightly damaged ventral valve, Fig. 71F–I, from the Folkeslunda Limestone, Kårgårde section (sample DLK83-fo-5), Dalarna.

Paratypes. – Figured; Br132405 (damaged), Br132406 (damaged), Br132407 (damaged), Br132831 (damaged), Br5611 (W 5.94, L ~5.31), Br133636c (section), SGU (Swedish Geological Survey, Uppsala) Type 6098 (W ~6.5, L ~5.4, H ~4.3). Total of 67 fragmentary dorsal valves and 66 fragmentary ventral valves.

Diagnosis. – Ventral valve broadly convex. Ventral interior with apical process filling entire apex, perforated by pedicle tube. Dorsal valve with pseudointerarea extremely wide and long; well developed triangular median groove. Median septum very low.

Description. – The complete outline is not preserved in either valve. However, the ventral valve appears to be very broadly convex, about half as high as wide, with the maximum height at the umbo (or somewhat behind the umbo in gerontic valves; Fig. 71G, J). In one specimen it is about



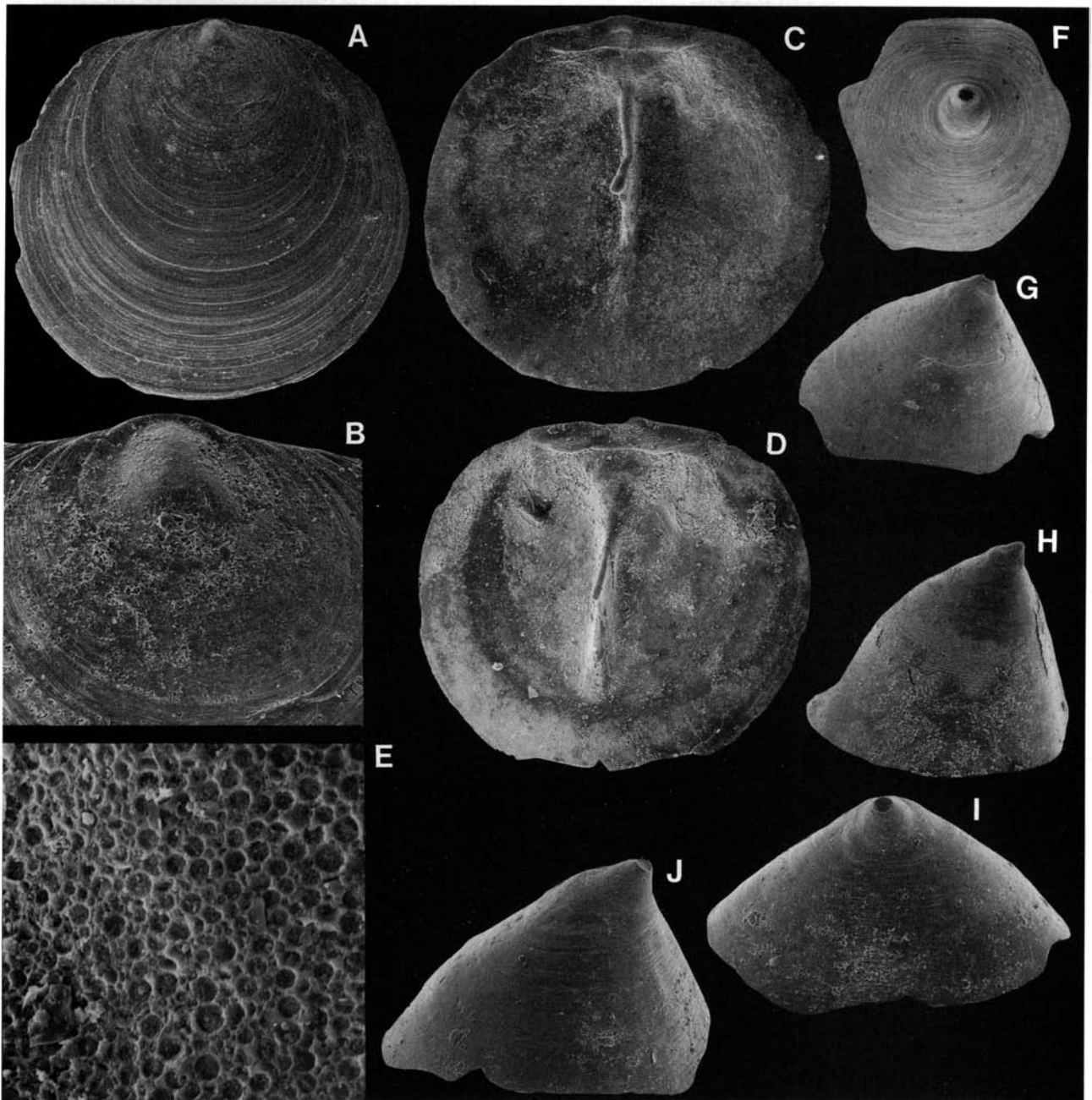


Fig. 68. □A–H. *Cyrtonotreta?* sp. b. □A. Dorsal exterior; Gullhøgen Formation (sample GB84-1-7); Br128613, ×33. □B. The larval shell of A; ×110. □C. Interior of A; ×33. □D. Interior of a dorsal valve; Gullhøgen Formation (sample GB80-50 cm above the base); Br128600, ×33. □E. The larval ornamentation of D; ×1650. □F. Exterior of a ventral valve; Skövde beds (sample GB84-A4); Br132566, ×33. □G. Side view of F; ×33. □H. Side view of a ventral valve; Våmb Limestone (sample GB84-A2); Br128896, ×33. □I. *Cyrtonotreta?* sp. b?; posterior view of a ventral valve; Kårgårde Limestone (sample DLK83-segk-1); Br128876, ×80. □J. Side view of I; ×80.

Fig. 67 (opposite page). □A–F. *Cyrtonotreta? striata* gen. et sp. nov. □A. Dorsal exterior; Ryd Limestone (sample GB84-2-37); Br132824, ×32. □B. The larval shell of A; ×165. □C. Interior of a juvenile dorsal valve; Ryd Limestone (sample GB84-2-37); Br132825, ×62. □D. Side view of C; ×62. □E. Exterior of a juvenile ventral valve; Ryd Limestone (sample GB84-3-69); Br132938, ×62. □F. Side view of E; ×62. □G–H. *Cyrtonotreta* sp. a. Dalby Limestone (sample GB84-3-75). □G. Exterior of a juvenile dorsal valve; Br133038, ×62. □H. The larval shell of G; ×165. □I–N. *Cyrtonotreta vestrogothica* gen. et sp. nov. □I. Ornamentation of a dorsal larval shell; Ryd Limestone (sample GB84-3-69); Br132937, ×700. □J. Dorsal interior; Gullhøgen Formation (sample GB84-2-21); Br132771, ×86. □K. Side view of J; ×86. □L. Exterior of a ventral valve; Gullhøgen Formation (sample GB84-2-33); Br132796, ×62. □M. The larval shell of L; ×165. □N. Side view of a ventral valve; Gullhøgen Formation (sample GB84-2-21); Br132768, ×86.

66% as high as wide (Fig. 70). In lateral profile the posterior surface of the ventral valve is flattened; the anterior surface is strongly convex (Figs. 70, 71G). The ventral pseudointerarea is nearly catacline (but procline in early growth stages) with a poorly developed interr ridge (Figs. 70, 71H). The pedicle foramen is wide (maximum width about 0.10 mm), and continues as an interior pedicle tube (Fig. 71I). The apical process is very large and fills the entire apex (Figs. 70, 71I). The mantle canal pattern is not known. The dorsal valve is about 89% as long as wide in one specimen, and flattened in lateral profile (Fig. 69B). The dorsal pseudointerarea is wide, about 13% as long as wide, occupying nearly 60% of the total width. The median groove is wide, triangular and shallow; the propleas are

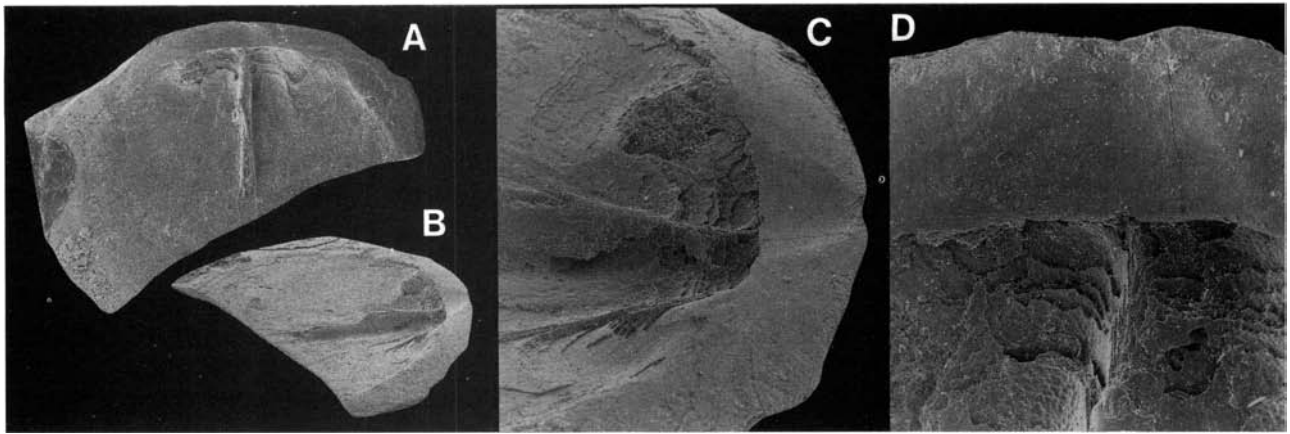
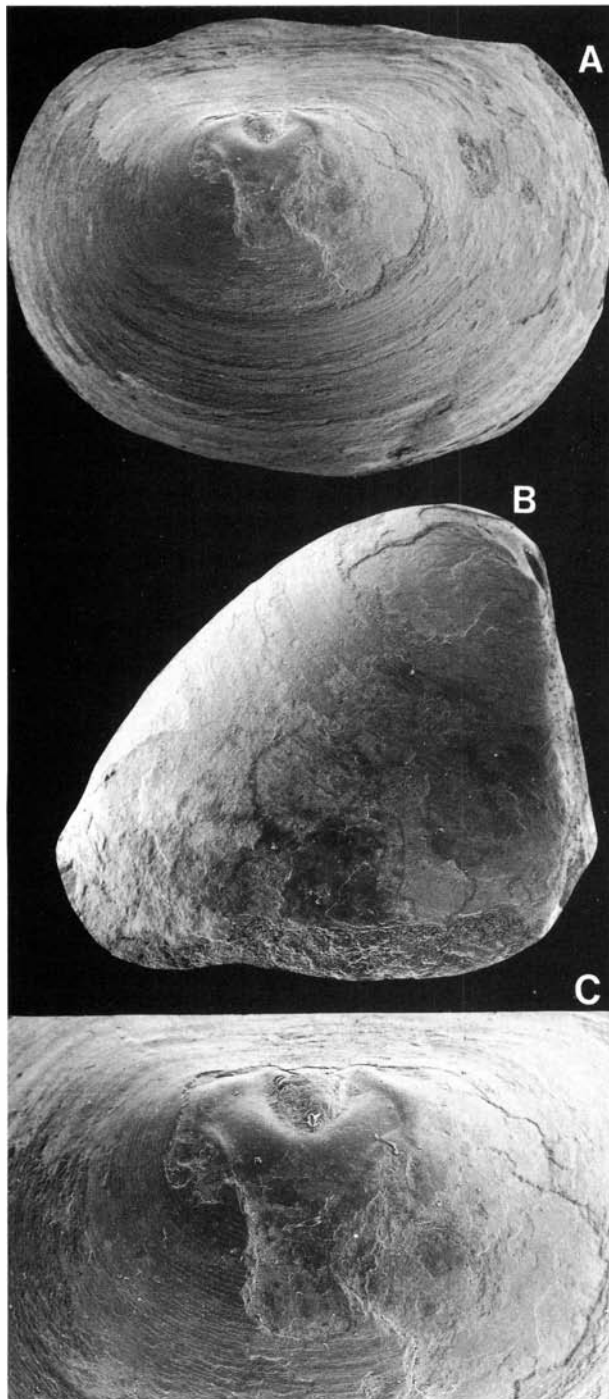


Fig. 69. *Physotreta deformis* sp. nov. □A. Dorsal interior; Folkeslunda Limestone, Grangärdet (coll. G. Holm); Br5611, $\times 8$. □B. Side view of A; $\times 8$. □C. Detail of the pseudointerarea of A; $\times 34$. □D. Detail of the median groove of A; $\times 60$.



slightly anacline (Figs. 69, 71D–E). There is no median buttress, and the cardinal muscle scars are indistinct (Fig. 69C). The median septum is low and short, occupying about 60% of the length of the valve (Fig. 69). The valves are ornamented with closely spaced, concentric fila (Fig. 71A, F). The larval shell is about 70–80% as long as wide. It is large for the subfamily, up to 0.41 mm across, with pitted ornamentation as described for *Cyrtonotreta vestrogothica* (Fig. 71B–C, K).

Discussion. – *Physotreta deformis* is the largest of the examined acrotretaceans. It is similar to the type species, *Physotreta spinosa*, in having (1) a broadly conical ventral valve, (2) a poorly defined pseudointerarea with a poorly developed interridge, (3) a ventral interior with a conspicuous apical process plugging the apex, perforated by a long pedicle tube, (4) a dorsal valve with a wide pseudointerarea and a triangular median groove, and (5) a low simple median septum. It differs mainly in having a strongly lamellose ornamentation, and a dorsal pseudointerarea that is proportionally longer. *P. rugosa* Popov, 1980 (Fig. 25:1–6) from the Lower Ordovician (Tremadoc) of Kazakhstan is different from *P. deformis* in having (1) a procline ventral valve with poorly developed apical process, (2) a dorsal valve with the pseudointerarea wide and short, and (3) a much stronger rugose ornamentation. The Middle Ordovician *P. gigantea* (Cooper, 1956, Pl. 16E:18–23, 17D:58, 17E:59–60) has a higher ventral valve.

Occurrence. – In Dalarna *Physotreta deformis* ranges from the Folkeslunda Limestone to the Furudal Limestone; there are questionable records from the Kårgårde and the Dalby limestones (Figs. 9A–B). In Västergötland it is known only from the lower Ryd Limestone (Fig. 8C) and on northern Öland it occurs in the Källa Limestone.

Fig. 70. *Physotreta deformis* sp. nov. □A. Ventral exterior; Folkeslunda Limestone, Altsarbyn, Mora (coll. G. von Schmalensee 1895); SGU (Swedish Geological Survey, Uppsala) Type 6098, $\times 12$. □B. Side view of A; $\times 12$. □C. Detail of the exfoliated apex of A; $\times 24$.

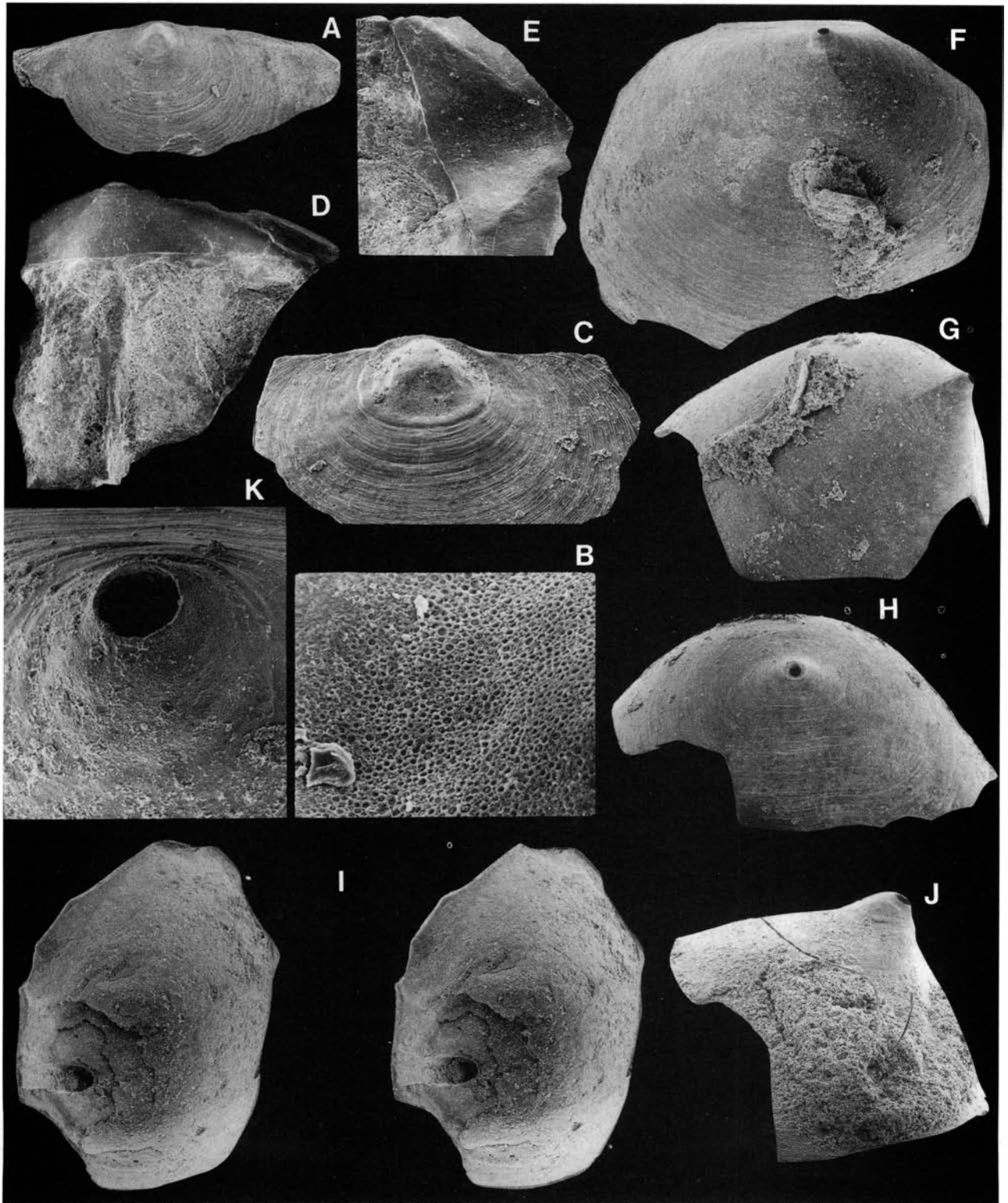


Fig. 71. *Physotreta deformis* sp. nov. □A. Dorsal exterior; Furudal Limestone (sample DLK83-fur-14); Br132405, ×26. □B. Detail of the larval ornamentation of A; ×583. □C. Exterior of a dorsal valve; Br132406, ×53. □D. Dorsal interior; Furudal Limestone (sample DLK83-fur-14); Br132407, ×37. □E. Side view of the pseudointerarea of D; ×60. □F. Holotype; exterior of a ventral valve; Folkeslunda Limestone (sample DLK83-fo-5); Br129024, ×18. □G. Side view of F; ×18. □H. Posterior view of F; ×18. □I. Stereo-pair; interior of F; ×14. □J. Side view of a ventral valve; Ryd Limestone (sample GB84-2-39); Br132831, ×35. □K. Detail of the larval shell of J; ×140.

Genus *Spondylotreta* Cooper, 1956

Type species. – Original designation; *Spondylotreta concentrica* Cooper, 1956, p. 255, from the Middle Ordovician (*Pygodus anserinus* Biozone) Pratt Ferry beds, Pratt Ferry, Alabama, U.S.A.

Diagnosis. – See Cooper (1956, p. 255).

Species assigned. – *Spondylotreta maior* Bednarczyk & Biernat, 1978; *S. parva orientalis* Popov, 1980; *S. orsaensis* sp. nov.; in addition to the species listed by Krause & Rowell (1975, p. 41).

Discussion. – Eight species have been assigned to *Spondylotreta*; the genus has a range from the Lower (Tremadoc; Biernat 1973) to the Upper Ordovician (Cautleyan; Wright 1963). Krause & Rowell (1975) summarized the existing information on the genus; they also discussed an unnamed species of *Spondylotreta* from the lower Whiterock of Nevada. Bednarczyk & Biernat (1978, p. 305) described *S. maior* from the Arenig of the Holy Cross Mountains, Poland. Popov (*in* Nazarov & Popov 1980, p. 96) described *S. orientalis* from the Upper Ordovician of Kazakhstan.

Spondylotreta orsaensis sp. nov.

Fig. 72

Name. – From Orsa parish, in which the Kårgårde section is situated.

Holotype. – Br132946, complete dorsal valve, Fig. 72D–E (W 1.32, L 1.13), from the Dalby Limestone, Kårgårde section (sample DLK83-dal-17), Dalarna.

Paratypes. – Figured; Br133056 (W 1.36, L 1.30), Br133057 (W 1.16, L 1.01), Br133060 (damaged), Br128647 (damaged), Br128706 (damaged). Total of 91 dorsal valves and 161 ventral valves.

Diagnosis. – Ventral valve broadly conical with depressed apex, poorly delineated pseudointerarea, procline; interior with long pedicle tube and wide median septum. Dorsal valve with median buttress poorly developed to absent; median septum with up to three septal rods.

Description. – The valves are almost subcircular in outline. The ventral valve is relatively low for the genus, procline, and has the highest point at, or slightly anterior to, the umbo. In lateral profile the outline of both the posterior and anterior surfaces of the ventral valve is convex. The ventral pseudointerarea has a narrow interridge (Fig. 72I). The exterior pedicle tube is short, up to 0.06 mm wide (Fig. 72H, J), and continues as a long interior tube with a rectangular cross-section. The pedicle tube is connected with a ventral median septum which is slightly swollen in the centre (Fig. 72K). The dorsal valve is about 86–96% as long as wide ($N=3$). In lateral view it is gently convex and has a shallow median sulcus (Fig. 72A–B). The pseudointerarea is about 13–18% as long as wide ($N=3$), and has a well developed median groove and a pair of wide, anacline propareas. The median buttress and the muscle scars are

poorly developed. The septum is low and has three septal rods; it originates about 0.23 mm from the posterior margin and extends about 70–80% of the total length (Fig. 72D–E). The valves are ornamented with regularly spaced fila (Fig. 72A, F). The larval shell is poorly delineated, nearly circular in outline and about 0.23 mm in diameter. The larval ornamentation is similar to that of *Spondylotreta* sp. nov. a (Figs. 72C, J, 73F).

Discussion. – Almost all previously described species of *Spondylotreta* have (1) a highly conical ventral valve (in the Tremadoc *S. faceta* up to almost twice as high as long), (2) a narrow, sometimes forked ventral median septum, (3) a median buttress, and (4) a median septum that originates directly anterior to the pseudointerarea. *S. orsaensis* is distinguished from these species in having (1) a ventral valve that is low and depressed, (2) a wide ventral median septum, (3) a dorsal median septum originating some distance (about 0.23 mm) from the pseudointerarea, and (4) no median buttress. *S. orsaensis* is most similar to the Upper Ordovician *S. parva* Wright (1963, Pl. 2:17, 20–25, Pl. 3:1, 5, 9, 15) from the Portrane Limestone of Ireland; both species have a wide ventral median septum, and a three-pronged dorsal median septum originating some distance from the pseudointerarea. However, the ventral valve of the Irish species is a much higher, almost as high as long.

Occurrence. – *Spondylotreta orsaensis* is restricted to the Furdal and Dalby limestones of Dalarna (Figs. 9B–C, 10). In Västergötland it occurs only in the lower Dalby Limestone (Fig. 8C–D).

Spondylotreta sp. nov. a

Figs. 24, 73

Material. – Figured; Br133628b (section), Br129030, Br129031, Br129034, Br129033. Total of 8 dorsal and 25 ventral valves.

Description. – No complete outline is preserved in either valve (Fig. 73A). The ventral valve is procline. In lateral profile the outline of the posterior surface is gently convex, with the anterior surface gently concave. The highest point is slightly anterior to the umbo (Fig. 73E). The ventral pseudointerarea is well developed and has a wide interridge (Fig. 73D). The interior pedicle tube is long and has a rectangular cross-section. The ventral median septum is forked (Fig. 73G). In lateral profile the dorsal valve is gently convex. The dorsal pseudointerarea is poorly defined, but has a wide median groove and a pair of anacline propareas (Fig. 73B–C). Directly anterior to the pseudointerarea there is a thickened and raised area, possibly corresponding to a poorly developed median buttress (Fig. 73B). The dorsal median septum originates some distance from the pseudointerarea; it has a single, thick upper septal rod (Fig. 73C). The larval shell is poorly delineated, with circular pits (up to 2.5 μ m in diameter; Fig. 73F). The valves are ornamented with weak, concentric fila (Fig. 73A, D). The shell structure is discussed above (p. 45, Fig. 24).

Discussion. – This species is most similar to *S. orsaensis*, but differs in having (1) a lower ventral valve, (2) a concave

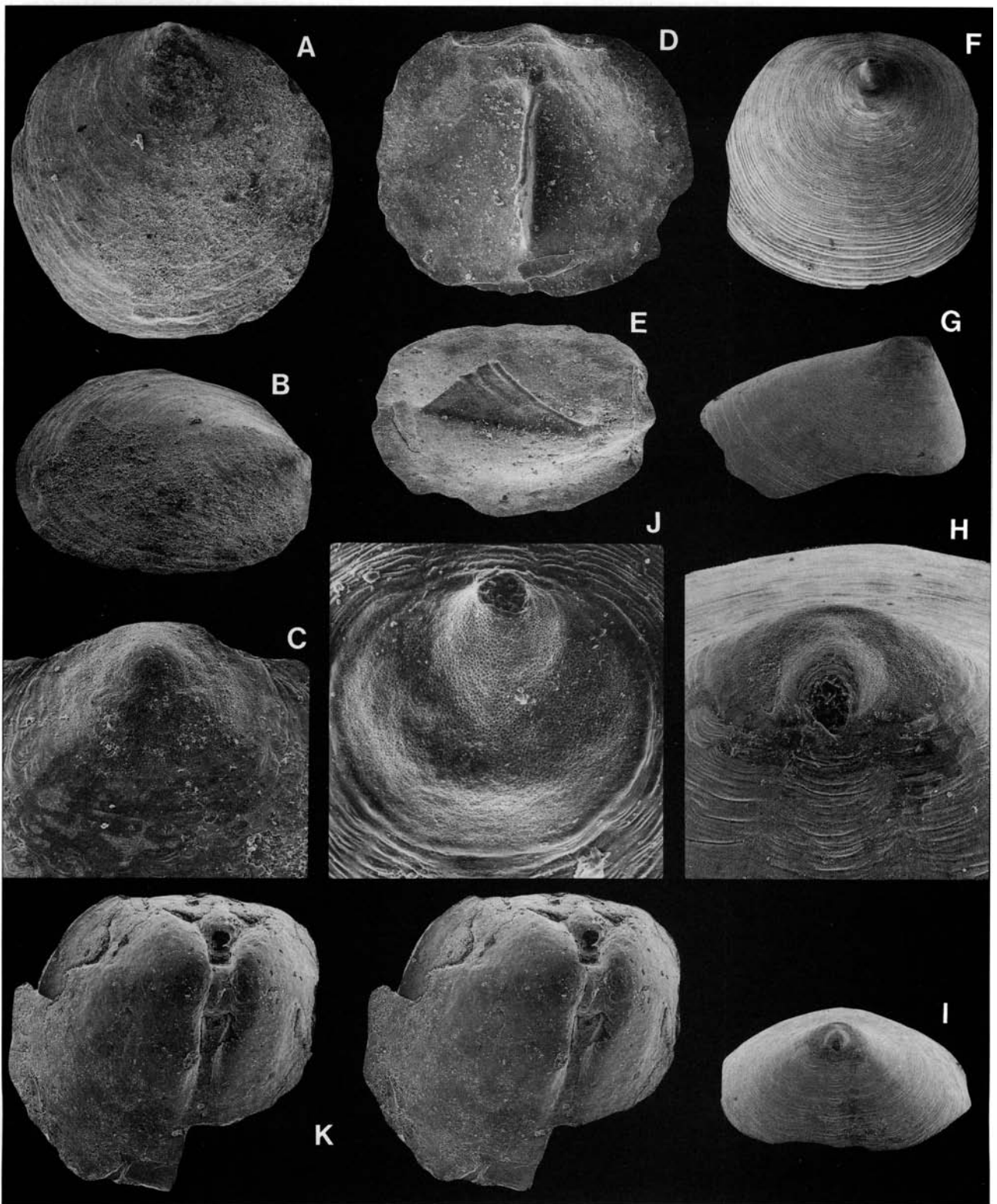


Fig. 72. *Spondylotreta orsaensis* sp. nov. □A. Dorsal exterior; Dalby Limestone (sample GB84-3-91); Br133056, $\times 40$. □B. Side view of A; $\times 40$. □C. Dorsal larval shell; Dalby Limestone (sample GB84-3-91); Br133057, $\times 170$. □D. Holotype; interior of a dorsal valve; Dalby Limestone (sample DLK83-dal-17); Br132946, $\times 40$. □E. Side view of D; $\times 40$. □F. Ventral exterior; Dalby Limestone (sample GB84-3-91); Br133060, $\times 40$. □G. Side view of F; $\times 40$. □H. Posterior view of the larval shell of F; $\times 170$. □I. Posterior view of F; $\times 40$. □J. Ventral larval shell; Furudal Limestone (sample D60-220); Br128647, $\times 250$. □K. Stereo-pair; ventral interior; Dalby Limestone (sample D60-201); Br128706, $\times 54$.

ventral anterior surface, (3) a forked ventral median septum, and (4) a dorsal median septum with a single upper septal rod.

Occurrence. — *Spondylotreta* sp. nov. a is known only from Dalarna where it ranges from the Segerstad to the lower Furudal limestones (Fig. 9A).

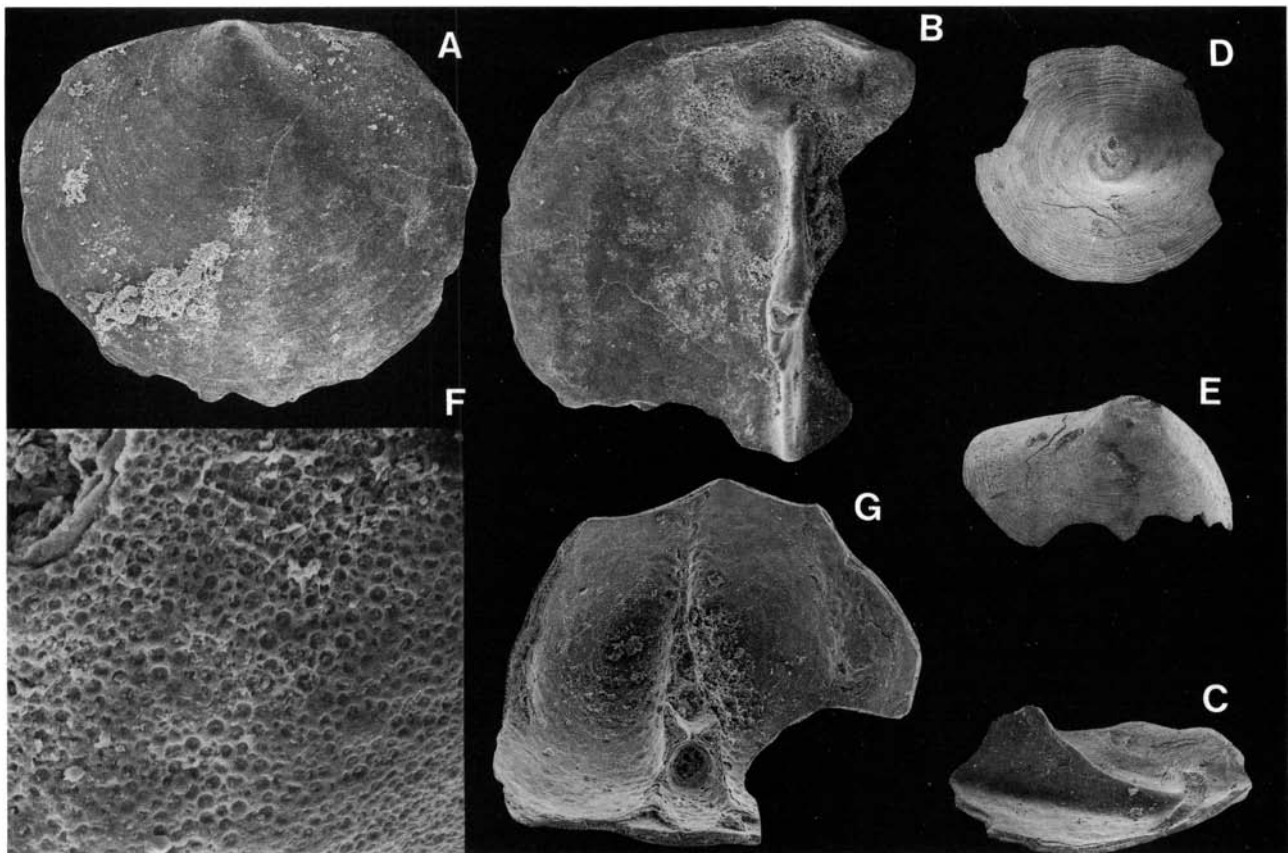


Fig. 73. *Spondylotreta* sp. nov. a. □A. Dorsal exterior; Folkeslunda Limestone (sample DLK83-fo-1); Br129030, ×40. □B. Interior of a dorsal valve; Folkeslunda Limestone (sample DLK83-fo-1); Br129031, ×40. □C. Side view of B; ×40. □D. Ventral exterior; Folkeslunda Limestone (sample DLK83-fo-4); Br129034, ×40. □E. Side view of D; ×40. □F. Ornamentation of the larval shell of D; ×800. □G. Interior of a ventral valve; Folkeslunda Limestone (sample DLK83-fo-4); Br129033, ×70.

Subfamily Torynelasmatinae Rowell, 1965

Diagnosis. – Valves with rounded triangular outline and straight, widened posterior margin. Ventral valve with well developed and wide pseudointerarea, procline, catacline to slightly apsacline; triangular in posterior view, with inter-ridge poorly developed or obsolete. Ventral interior with apical process. Dorsal valve with widened, poorly divided pseudointerarea; well developed and raised dorsal cardinal muscle scars. Median septum high, frequently with surmounting platform, commonly with spines.

Genera included. – *Torynelasma* Cooper, 1956; *Acrotretella* Ireland, 1961; *Issedonia* Popov, 1980; *Polylasma* Popov, 1980; *Myloconotreta* Williams & Curry, 1985.

Discussion. – As erected originally by Rowell (1965, p. H279), the Torynelasmatinae included *Torynelasma* Cooper (see discussion below) and tentatively also the Silurian genus *Acrotretella* Ireland. The definition of Rowell (1965) has been followed in all subsequent papers. *Opsiconidion* Ludvigsen, 1974 was assigned to the subfamily by von Bitter & Ludvigsen (1979, p. 706), but this genus is here referred to the new subfamily Biernatinae (see below). Popov (in Nazarov & Popov 1980, p. 103–105) erected *Issedonia* and *Polylasma*; both genera have a straight posterior margin and a complex *Torynelasma*-like dorsal median septum with spines. Williams & Curry (1985, p. 203) described *Mylo-*

conotreta that clearly also is a torynelasmatine. At present, the five genera have a combined range from the Lower and questionably into the Upper Ordovician. The subfamilies Torynelasmatinae and Biernatinae are compared below.

Genus *Torynelasma* Cooper, 1956

Type species. – Original designation; *Torynelasma toryniferum* Cooper, 1956, p. 258, Pls. 9C:9, 18E:28–30, 35–36, 28E:13–16, non Pls. 9C:10, 18E:31–34, from the Middle Ordovician (*Pygodus anserinus* Biozone) Pratt Ferry beds, Pratt Ferry, Alabama, U.S.A.

Diagnosis. – As for subfamily; invariably with well developed surmounting platform, flat to concave, but lacking spines. Ventral valve catacline to slightly apsacline.

Species assigned. – *Torynelasma toryniferum* Cooper, 1956; *T. papillosum* Krause & Rowell, 1975; *T. suecicum* sp. nov.

Discussion. – As defined originally (Cooper 1956, p. 257) the genus included two species; the type species and the minute *Torynelasma minor*. Both species come from the same level at Pratt Ferry. The dorsal valves of the two are similar in that they have a median septum with a surmounting platform. In the view of Cooper (1956, p. 257) and subsequent authors, this is a unique and characteristic feature that unites the species, of otherwise varying mor-

phology, that have been placed within the genus. However, this view is not adopted here.

The dorsal posterior margin and pseudointerarea of *T. toryniferum* is widened and nearly straight in dorsal view. By contrast, the dorsal valve of *T. minor* is 'nearly circular in outline' according to Cooper (1965, p. 257). The dorsal valves of all subsequently described species of *Torynelasma* (*sensu lato*) fall into either of these two, clearly separated groups. The first includes *T. minor* Cooper, *T. rossicum* Goryanskij, 1969, *T. rara* Biernat, 1973, *T. forte* Popov, 1975, *T. curvatum* Holmer, 1986, and *T. planum* Holmer, 1986, which are all nearly circular in outline and have a reduced dorsal pseudointerarea. The second group includes *T. toryniferum* Cooper, *T. papillosum* Krause & Rowell, 1975, and *T. suecicum*, which have a dorsal valve with a roughly triangular outline and a wide pseudointerarea. The division of the torynelasmatines (*sensu lato*) into these two groups is first found in the Lower Ordovician (lower Arenig) of Baltoscandia (Holmer unpublished).

It is suggested that the two groups are not closely related, and that the similarities in the median septum points to a similarity in function, rather than to a common ancestry. The six species in the 'first group' of the torynelasmatines (*sensu lato*) are here referred to the new genus *Biernatia* within the new subfamily Biernatinae (see below); the remaining three species are retained within the restricted genus *Torynelasma*.

Understanding of the type species *T. toryniferum* is complicated because Cooper illustrated two widely different types of ventral valves as belonging to the dorsal valve of this species. In his collections there are (1) numerous acutely conical valves that lack a pseudointerarea, and have a rounded posterior margin (Pl. 9C:10, 18E:31–34), and (2) one ventral valve (only figured in posterior view by Cooper) with a clearly defined triangular pseudointerarea (28E:16). This obvious mistake was commented on by both Goryanskij (1969, p. 71) and Krause & Rowell (1975, p. 58). In the view of these workers, only the first type of ventral valve belongs to the type species. However, the reverse interpretation is suggested here.

According to the description of Cooper (1965, p. 258), the dorsal valve of *T. toryniferum* has a 'shelflike area, short but wide' that is clearly seen at the posterior margin in the illustrations of the holotype (Pl. 9C:9). It is not clear how a dorsal valve with a wide and almost straight posterior margin can be fitted to a ventral valve whose posterior margin is 'convex in cross section and thus without a conspicuous pseudointerarea' (Cooper 1956, p. 258). Examination of the type specimens (M. G. Bassett, personal communication 1987) confirms the suspicion that the valves of the first type, do not fit to the dorsal valves illustrated by Cooper. Probably, the second type of ventral valve (116825e; Pl. 28E:16) is the correct corresponding valve. However, this question clearly needs further study based on topotype material.

Torynelasma suecicum sp. nov.

Figs. 28, 74A–L, 75A–K

Name. – Latinized form of Sweden.

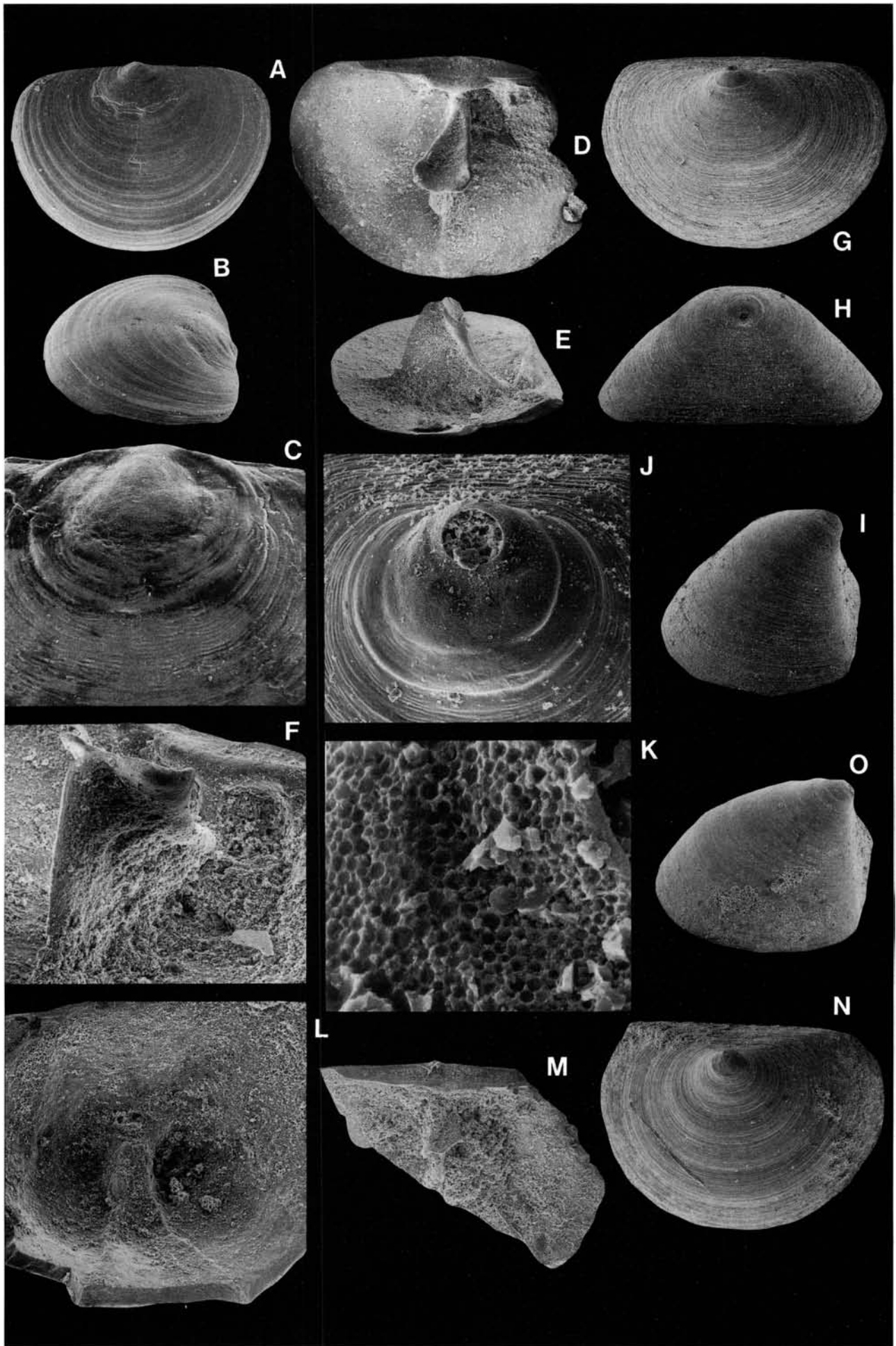
Holotype. – Br128826, slightly broken dorsal valve, Fig. 28B, 74D–F (W ~1.61, L 1.15), from the Ryd Limestone, Gullhögen quarry (sample GB84-3-59), Västergötland.

Paratypes. – Figured; Br128829 (W 1.29, L 0.96), Br128832 (W 0.46, L 0.37), Br128828 (W 1.40, L 0.95, H 0.71), Br128833 (W 0.56, L 0.42, H 0.20; lost during SEM), Br128830 (damaged, sectioned), Br128831 (W 0.39, L 0.29). Total of 14 dorsal valves and 8 ventral valves.

Diagnosis. – Ventral valve with depressed apex, and wide, triangular pseudointerarea lacking interridge. Ventral interior with pedicle tube and forked median septum.

Description. – The valves average 75% as long as wide (Tables 9, 10; Fig. 74A, G). The ventral valve is about half as high as wide (Table 9) with a depressed apex; the highest point is somewhat anterior to the umbo (Fig. 74I). The ventral pseudointerarea is wide and straight (Fig. 74G), triangular in posterior view and lacks an interridge (Fig. 74H); in lateral profile it is procline to almost catacline, with a slightly concave outline, whilst the anterior surface is strongly convex (Fig. 74I). The pedicle foramen is about 0.05 mm wide (Fig. 74J), and continues internally as a pedicle tube. The ventral median septum is forked (Fig. 74L). The ventral interior has traces of a pair of cardinal muscle scars on the posterior wall. In lateral profile the dorsal valve is strongly convex (Fig. 74B), up to 10–15% as deep as wide with a straight posterior margin. The pseudointerarea is well developed and wide, on average 11% as long as wide (Table 10), occupying up to more than 70% of the valve width; the median groove is triangular and the propareas are wide and anacline (Fig. 74D–E). The median septum is high (HS/W ratio up to 40%; Table 10) and long, occupying up to 80% of the valve length (Fig. 74D–E). The surmounting plate is strongly concave, up to 0.30 mm wide; it is supported dorsally by a vertical median plate (Fig. 74F). The dorsal cardinal muscle scars are generally raised, about half as long as wide (Table 10). The valves are ornamented with closely spaced, concentric fila (Fig. 74A, G). The larval shells on adult valves are poorly delineated, and generally smooth, whilst the larval shell on juvenile valves is pitted (Fig. 74C, J), with circular pits up to 1 µm in diameter (Fig. 74K, 60F).

Ontogeny. – The larval shell is relatively small (WL ~0.15, LL ~0.10) about 60–80% as long as wide; on both valves it is slightly bulbous; the ventral, less than 0.1 mm high (Fig. 74C, J). At the brephic stage (W 0.15–0.46, L 0.10–0.37; Fig. 75A) an undivided dorsal pseudointerarea (WI ?–0.20, LI ?–0.03) is present, occupying about 40% of the total width (Fig. 75B, D). The dorsal median septum is a low triangular plate, which originates about 0.12 mm from the posterior margin and extends about 70–80% of the total length (Fig. 75B). The septum is less than 0.10 mm and about 0.12 mm high, and has an upper septal rod (Fig. 75C). The brephic ventral valve is strongly procline, about 0.20 mm high, and



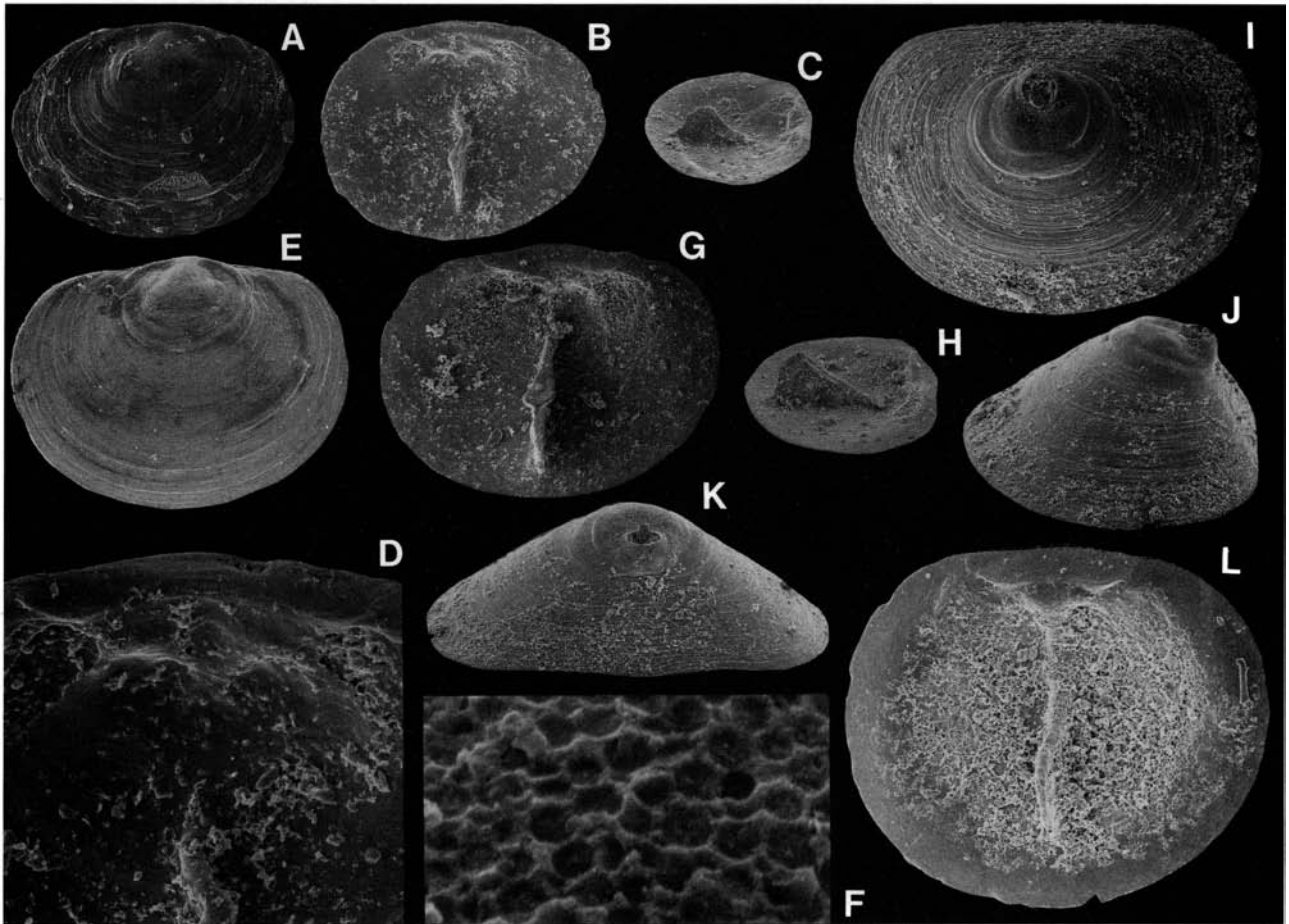


Fig. 75. □A–K. Ontogeny of *Torynelasma suecicum* sp. nov.; Ryd Limestone (sample GB84-3-59). □A. Exterior of a brephic dorsal valve; Br128831, $\times 90$. □B. Interior of A; $\times 90$. □C. Side view of B; $\times 70$. □D. Detail of the pseudointerarea of A; $\times 300$. □E. Exterior of a juvenile dorsal valve; Br128832, $\times 90$ (see also Fig. 74C). □F. Detail of the ornamentation of the larval shell of E; $\times 4200$. □G. Interior of E; $\times 90$. □H. Side view of G; $\times 70$. □I. Exterior of a juvenile ventral valve; Br128833, $\times 90$ (see also Fig. 74J–K). □J. Side view of I; $\times 90$. □K. Posterior view of I; $\times 90$. □L. Interior of a juvenile dorsal valve of *Torynelasma* sp.; Holen Limestone (sample GB81-0); Br132593, $\times 90$.

is without recognizable interior structures. At the subsequent neanic stage (W 0.46–0.93, L 0.37–0.67; Fig. 75E) the dorsal pseudointerarea (WI 0.20–0.59, LI 0.03–0.05) is widened, extending about 40–60% of the valve width, and the propareas are formed (Fig. 75G). The neanic dorsal median septum (HS 0.12–0.36) forms a narrow (about 0.10 mm wide), flattened surmounting platform through the lateral thickening of the septal rod (Fig. 75G–H). In some specimens there are traces of dorsal cardinal muscle scars (WM 0.34–0.56, LM 0.23–0.26). The neanic ventral valve (H 0.20–0.40) remains procline and lacks recogniz-

able interior structures (Fig. 75I–K). The adult growth stage (W 0.93–1.61, L 0.67–1.15) is reached when (1) the dorsal pseudointerarea occupies above 60% of the length of the valve, (2) the surmounting platform is above 0.10 mm wide and strongly concave, and (3) the internal pedicle tube and median septum of the ventral valve (H 0.40–0.71) are formed (see also Fig. 46).

Discussion. – *T. suecicum* is distinguished from previously described species mainly by the ventral valve which has (1) a recurved and depressed umbo, (2) an internal pedicle tube, and (3) a forked ventral median septum. However, as mentioned above, the original description and illustrations of the ventral valve of the type species are ambiguous. Only one of the two illustrated types of ventral valves (Cooper 1956, Pl. 28E:16) has a flattened, sharply delineated and triangular pseudointerarea, comparable with that of *T. suecicum*. It is assumed that this is the correct ventral valve, but unfortunately the detailed morphology of this valve is not known. The ventral valve of the second described species, the lower Whiterock *T. papillosum* Krause & Rowell (1975) from Nevada, also has a ventral valve with a well developed pseudointerarea. It differs from the Swedish species in having papillose ornamentation and

Fig. 74. □A–L. *Torynelasma suecicum* sp. nov.; Ryd Limestone (sample GB84-3-59). □A. Dorsal exterior; Br128829, $\times 36$. □B. Side view of A; $\times 36$. □C. Dorsal larval shell; Br128832, $\times 230$. □D. Holotype; interior of a dorsal valve; Br128826, $\times 36$. □E. Side view of D; $\times 36$. □F. Median septum of D; $\times 89$. □G. Ventral exterior; Br128828, $\times 36$. □H. Posterior view of G; $\times 36$. □I. Side view of G; $\times 36$. □J. Ventral larval shell; Br128833, $\times 230$. □K. Detail of the ornamentation of the larval shell of J; $\times 2300$. □L. Ventral interior; Br128830, $\times 75$. □M–O. *Torynelasma* sp. □M. Interior of a dorsal valve; Holen Limestone (sample GB81-0); Br132585, $\times 36$. □N. Ventral exterior; Våmb Limestone (sample GB84-A1); Br132556a, $\times 36$. □O. Side view of N; $\times 36$.

a flattened dorsal valve. The dorsal valve of *T. suecicum* is most similar to the Middle Ordovician *T. cf. toryniferum* Cooper (Popov *in* Nazarov & Popov, 1980) from Kazakhstan, but the ventral valve of this species is not known. The median septum of the Kazakhstan species extends to about 90–100% of the total length (compared with about 80% in *T. suecicum*).

Occurrence. *Torynelasma suecicum* is only known from the Ryd Limestone of Västergötland (Fig. 8C).

Table 9. *Torynelasma suecicum* sp. nov., average dimensions and ratios of ventral valves.

	W	L	L/W	H	H/W
GB84-3-59					
<i>n</i>	6	6	6	5	5
mean	0.76	0.56	74%	0.37	45%
<i>s</i>	0.350	0.220	4.355	0.206	3.633
min	0.39	0.31	68%	0.17	41%
max	1.40	0.95	79%	0.71	51%

Table 10. *Torynelasma suecicum* sp. nov., average dimensions and ratios of dorsal valves.

	W	L	L/W	WI	LI	LI/WI	WM	LM	LM/WM	LS	BS	HS
GB84-3-59												
<i>n</i>	13	11	11	13	13	13	7	7	7	13	13	9
mean	0.95	0.78	75%	0.57	0.06	11%	0.75	0.37	49%	0.62	0.14	0.31
<i>s</i>	0.422	0.289	2.966	0.324	0.034	2.931	0.296	0.120	5.057	0.272	0.055	0.198
min	0.39	0.37	72%	0.11	0.02	8%	0.34	0.23	44%	0.26	0.11	0.10
max	1.66	1.30	80%	1.21	0.12	18%	1.21	0.54	59%	1.16	0.23	0.65

Torynelasma sp.

Figs. 74M–O, 75L

Material. – Figured; Br132585 (damaged), Br132556a (W 1.41, L 1.04, H 0.67), Br132593 (W 0.68, L 0.57). Total of 2 dorsal valves and 1 ventral valve.

Remarks. – The single well preserved ventral valve appears to be more depressed than that of *T. suecicum* (Fig. 74N–O). A single adult dorsal valve has a wide pseudointerarea and traces of a median septum with surmounting platform (Fig. 74M). A juvenile dorsal valve was also found (Fig. 75L).

Occurrence. – This rare species occurs in the uppermost Hølen Limestone and the Våmb Limestone of Västergötland (Fig. 8A).

Genus *Acrotretella* Ireland, 1961

Type species. – Original designation; *Acrotretella siluriana* Ireland, 1961, p. 1139, from the upper Silurian of Oklahoma, U.S.A.

Diagnosis. – See Holmer (1986, p. 119).

Discussion. – Holmer (1986) briefly discussed the systematic position of *Acrotretella* and recorded an unnamed species from the upper Viru and lower Harju Series of Västergötland and Östergötland. The morphology of the ventral valve, the larval ornamentation (Holmer 1986, Fig. 9N), and the camerate shell structure (Fig. 76E) appear to indicate that the genus is best placed among the torynelasmates.

Acrotretella sp.

Fig. 76

Material. – Figured; Br128711, Br128795. Total of 2 fragmentary dorsal valves.

Remarks. – The ventral valve is unknown. The dorsal pseudointerarea is wide and long, with a well developed median groove and anacline propareas (Fig. 76C–F). The median septum is low and poorly developed in one of the specimens (Fig. 76C–D); in the other the septum is high and has a well developed, concave surmounting platform (Fig. 76F). The larval shell is poorly delineated, but apparently nearly circular and about 0.15 mm in diameter, with a bulbous central node (Fig. 76B); the larval pitting is not preserved. The valves are ornamented with concentric fila (Fig. 76A). This is the third record of the genus as a whole and the second from the Ordovician.

Occurrence. – This rare species was only found in the Dalby Limestone in Dalarna (Fig. 10).

Subfamily Linnarsoniinae Rowell, 1965

Genus *Aktassia* Popov, 1976

Type species. – Original designation; *Aktassia triangularis* Popov, 1976, from the Middle Ordovician (Llandeilo–Caradoc) Bestamak Formation, Chingiz Range, Kazakhstan, U.S.S.R.

Diagnosis. – See Popov (*in* Nazarov & Popov 1976, p. 37).

Aktassia cf. *triangularis* Popov, 1976

Fig. 77

Synonymy. – □v cf. 1976 *Aktassia triangularis* Popov, sp. nov. – Nazarov & Popov, p. 37, Pl. 3:4–7.

Material. – Figured; Br132645 (W 0.31, L 0.34), Br132646 (W 0.32, L 0.37), Br132788 (W 0.28, L 0.31, H 0.12). Total of 2 dorsal and 1 ventral valve.

Diagnosis. – See Popov (*in* Nazarov & Popov 1976, p. 37).

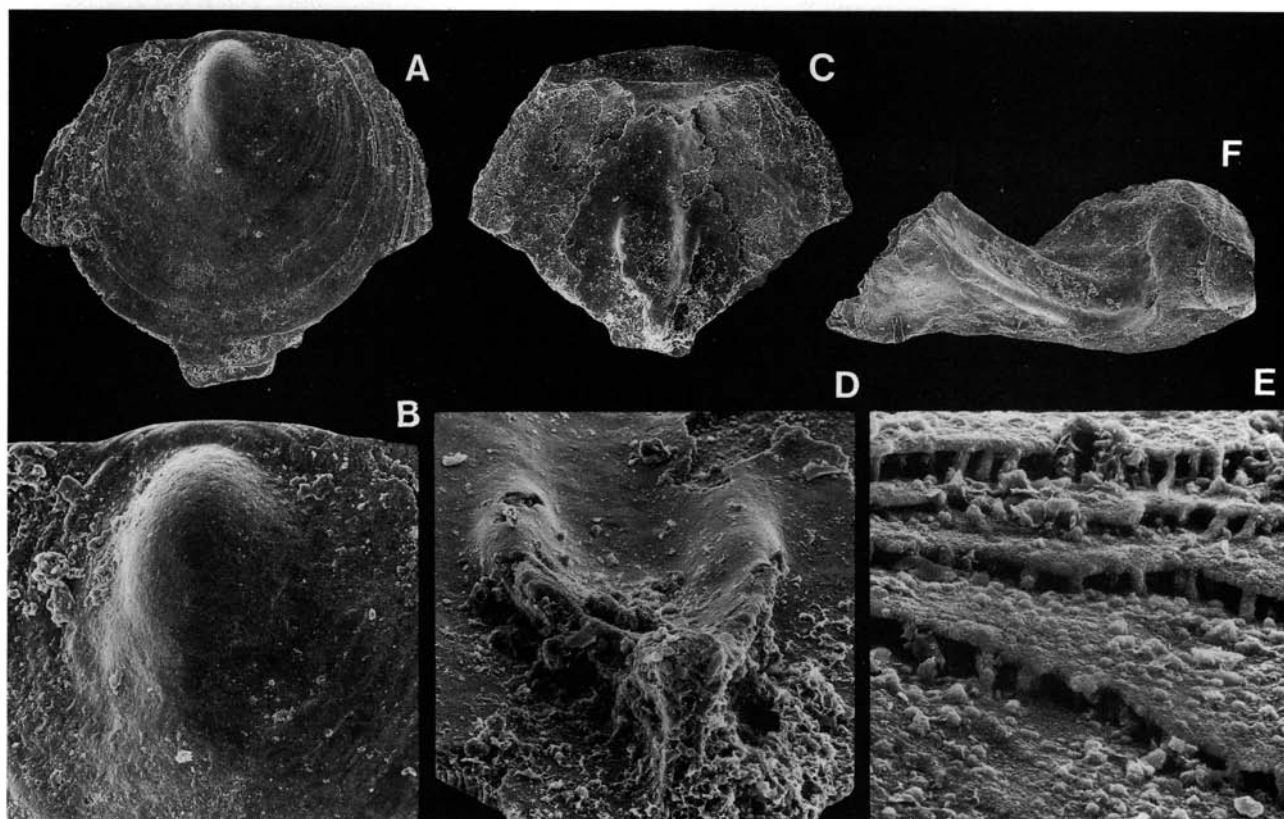


Fig. 76. *Acrotretella* sp. □A. Dorsal exterior; Dalby Limestone (sample D60-160); Br128711, ×107. □B. The larval shell of A; ×257. □C. Interior of A; ×92. □D. Oblique anterior view of the spoon-like median septum of B; ×357. □E. Detail of the interior of A, showing the camerate shell structure of the secondary layer; ×1286. □F. Side view of the interior of a dorsal valve; note the high spoon-like median septum; Dalby Limestone (sample D59-35); Br128795, ×71.

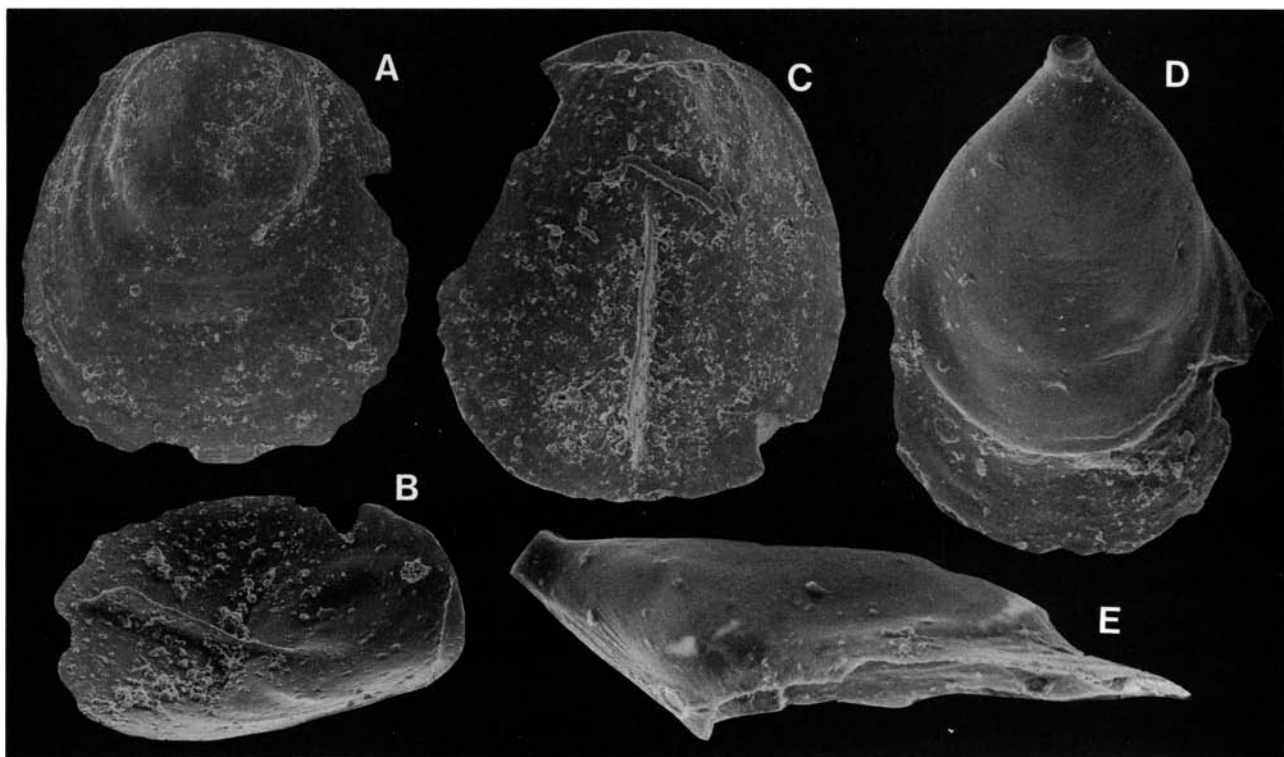


Fig. 77. *Aktassia* cf. *triangularis* Popov, 1976 □A. Dorsal exterior; Gullhøgen Limestone (sample GB84-1-13); Br132645, ×167. □B. Interior of a dorsal valve; Gullhøgen Limestone (sample GB84-1-13); Br132646, ×167. □C. Side view of B; ×155. □D. Ventral exterior; Gullhøgen Limestone (sample GB84-2-25); Br132788, ×189. □E. Side view of D; ×232.

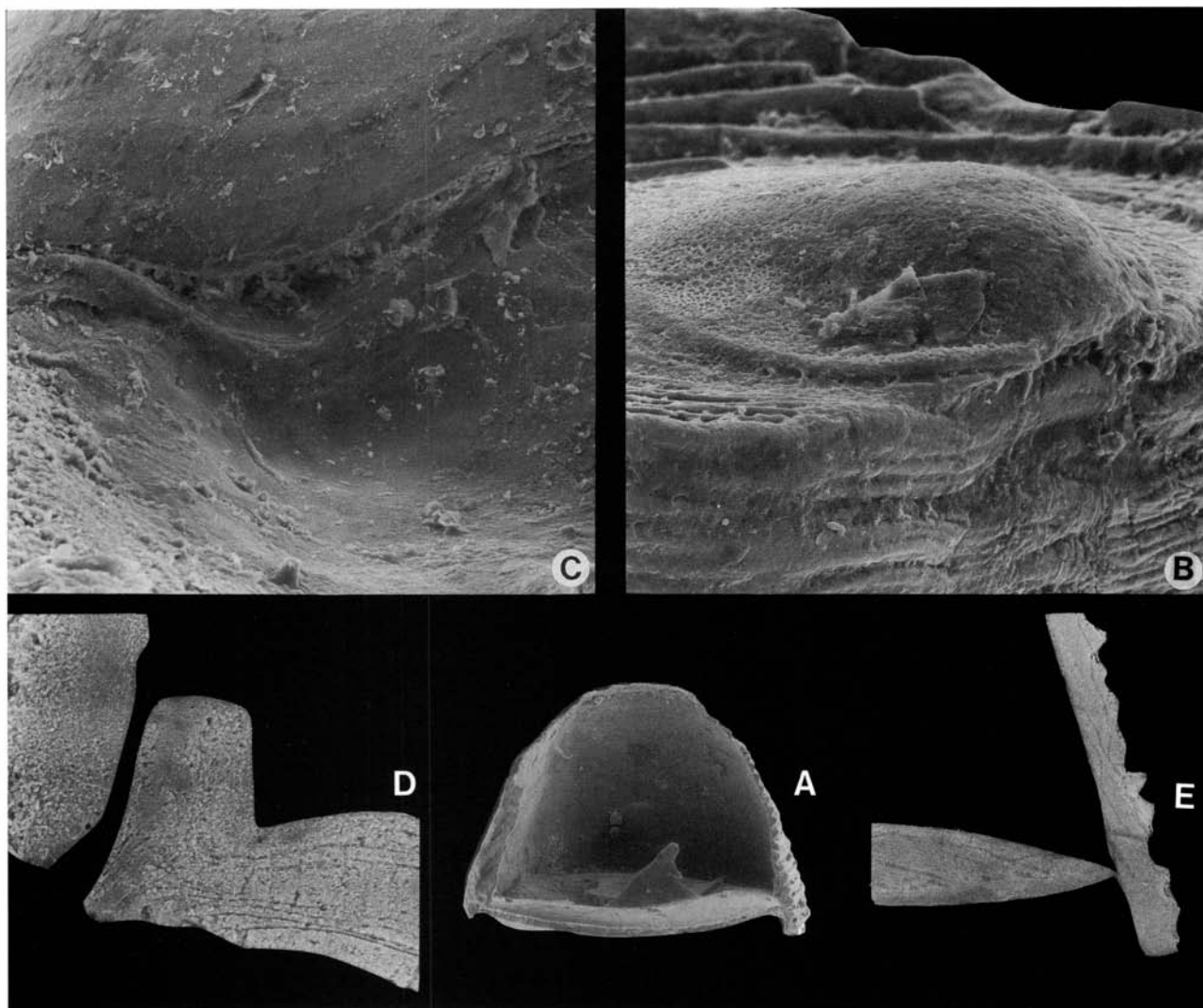


Fig. 78. □A–C. *Myotreta dalecarlica* sp. nov.; Furudal Limestone (sample D60-220); Br128800. □A. Side view of the shell; $\times 90$. □B. Detail of A, showing an external view of the commissure; $\times 430$. □C. Detail of A, showing an interior view of the commissure; $\times 500$. □D–E. Detail of a sagittal section through a complete shell of *Ehippelasma minutum* Cooper, 1956; Furudal Limestone (sample DLK83-fur-16); Br132430b. □D. Posterior portion of the shell, showing the commissure; $\times 410$. □E. Anterior portion of the shell, showing the commissure; $\times 1370$.

Description. – The valves are elongated and oval in outline (Fig. 77C–D), on average 89% as wide as long. The single ventral valve is about 43% as high as wide, and strongly apsacline. The ventral interior lacks recognizable structures (Fig. 77D–E). The dorsal pseudointerarea is minute and lacks a median groove. The dorsal median septum is low and originates about 0.13 mm from the posterior margin; it occupies about 90% of the total length of the valve (Fig. 77B–C). The valves are ornamented with faint fila (Fig. 77A, D).

Remarks. – The morphology of the Swedish specimens agrees closely with the Middle Ordovician material of *A. triangularis* from Kazakhstan (Nazarov & Popov 1976, Pl. 3:4–7). The present material includes three juveniles, and the identification at the specific level is uncertain. The main difference between the Swedish and Kazakhstani specimens is the lack of a median groove in the dorsal pseudointerarea of *A. cf. triangularis*. This is only the second record of *Aktassia*.

Occurrence. – In Västergötland *Aktassia cf. triangularis* occurs in the Gullhögen Formation (Fig. 8B).

Subfamily Ehippelasmatinae Rowell, 1965

Diagnosis. – See Holmer (1986, p. 112).

Genera assigned. – *Pomeraniotreta* Bednarczyk, 1986; in addition to the genera listed by Holmer (1986, p. 112).

Discussion. – A short review of previous works dealing with ehippelasmatines was given by Holmer (1986, p. 112). Bednarczyk (1986) described the Lower Ordovician *Pomeraniotreta* (= the unnamed acrotretacean in Poulsen 1971, Pl. 1:1–2, 2:1), which he referred to the torynelasmatines. However, this assignment is not supported here. Following Biernat (1973, p. 81) and Holmer (1986, p. 112) this genus is included in the Ehippelasmatinae (which includes the subfamily Myotretinae Biernat, 1973).

In comparison with other acrotretaceans the ehippelasmatines have a comparatively high frequency of articu-

lated shells; about 1% of the total number of specimens of *Numericoma perplexa* and *Ephippelasma minutum* is represented by articulated shells. This is probably due to the well developed 'articulation' in the ephippelasmatine shells, where the flat dorsal valve functions as an 'operculum'. In a closed shell, the anterior commissure is sunk into the ventral valve (Fig. 78A, E). The dorsal pseudointerarea fits snugly to the ventral valve (Fig. 78B–D).

Genus *Myotreta* Goryanskij, 1969

Type species. – Original designation; *Myotreta crassa* Goryanskij, 1969, p. 67, from the upper Kundan Stage in the Pechory core (479.1 m), Pskov district, Russia, U.S.S.R.

Diagnosis. – See Biernat (1973, p. 80).

Species assigned. – *Myotreta crassa* Goryanskij, 1969; *M. estoniana* Biernat, 1973; ?*M. goryansky* Bednarczyk, 1986; *M. dalecarlica* sp. nov.; *M. oreensis* sp. nov.

Discussion. – Species of *Myotreta* are common in the Lower and Middle Ordovician of Baltoscandia. Their main distinction from *Numericoma* Popov, 1980, and *Ephippelasma* Cooper, 1956, is in the more complex morphology of the median septum in the latter two genera. However, in ontogeny the saddle-shaped spinose median septum of *Ephippelasma* and *Numericoma* originates as a simple, flat plate with a triangular lateral profile. The step from a simple septum, like that of *Myotreta*, to a laterally folded septum, as in *Ephippelasma* and *Numericoma*, is not great; in *M. estoniana* Biernat (1973, Fig. 30), there is a tendency to form lateral folds. *Myotreta* is similar to *Rhinotreta* Holmer, 1986, and *Veliseptum* Popov, 1976 (see Popov in Nazarov & Popov 1976 and Holmer 1986 for a comparative discussion). The described species of *Myotreta* and *Rhinotreta* are compared in Fig. 85.

Myotreta aff. *crassa* Goryanskij, 1969

Figs. 79, 81A–B, 85

Synonymy. – □v aff. 1969 *Myotreta crassa* Gorjansky sp. nov. – Goryanskij, Pl. 11:10–27.

Material. – Figured; Br128842 (W 0.65, L 0.54), Br128841 (W 0.63, L 0.54), Br128844 (damaged), Br128845 (damaged), Br128843 (W 0.39, L 0.34). Total of 23 dorsal and 22 ventral valves.

Description. – The valves average 82% as long as wide (Table 11; N=7). The ventral valve is approximately 70% as high as

wide; in lateral profile it is recurved and has a slightly depressed apex (Fig. 79H). The ventral pseudointerarea is poorly defined, catacline to slightly apsacline with an intertrough (Fig. 79H–I). The pedicle foramen is up to 0.02 mm wide (Fig. 79J); it continues interiorly as a short pedicle tube, the anterior edge of which is sharply pointed; the tube is buttressed by a short median septum (Fig. 79K). The dorsal pseudointerarea averages 16% as long as wide (Table 11; Fig. 79D), occupying 43% (OR 33–55%; N=6) of the total width. The median groove is well developed, and the propareas are short and anacline (Fig. 79D–F). The dorsal median septum is moderately high; the HS/W ratio is about 30% in one valve (Fig. 79E). It originates around 0.13 mm from the posterior margin (Table 11), and extends 80% of the total length of the valve (OR 69–85%; N=7; Fig. 79D). The dorsal cardinal muscle scars are about 67% as long as wide, and originate during the late adult stage (W 0.60–0.70, L 0.50–0.60). The larval shell is sharply delineated and nearly circular (\overline{WL} 0.16, \overline{LL} 0.16; N=6; Fig. 79B, J). The dorsal larval shell has a distinct subcentral node in lateral profile; it is ornamented with circular pits, up to 3 μ m in diameter (Fig. 79C). The valves are ornamented with regularly spaced, concentric fila, up to 0.05 mm apart (Fig. 79A, G). The ontogeny is not known in detail, but it appears to be closely related to that of *M. dalecarlica*; the dorsal valve of the brephic and neanic stages (W 0.16–0.39, L 0.16–0.34; Fig. 81A) has a pseudointerarea (WI ?–0.15, LI ?–0.02), but a median septum is missing (Fig. 81B).

Discussion. – *M. crassa* Goryanskij (1969, Pl. 11:10–27; some topotypic specimens were kindly supplied by G. Biernat) from the Pskov district differs from the Swedish specimens mainly in that have (1) a strongly apsacline ventral valve, (2) a pair of well developed cardinal muscle scars, which are present already in the juvenile growth stage, and (3) a dorsal median septum with two septal rods. Moreover, the maximum size of the Russian specimens appears to be smaller than that of *M. aff. crassa*. Some specimens of *M. crassa* from the Volkhovian Stage at Paldiski, Estonia, illustrated by Goryanskij (1969, Pl. 11:26–27) appear to differ from the type specimens. However, the Estonian material is similar to the Swedish specimens in having less well developed dorsal cardinal muscle scars, and an almost catacline ventral valve.

Occurrence. – *Myotreta* aff. *crassa* is restricted to the Holen Limestone of Dalarna (Fig. 9A). In Jämtland there is a questionable occurrence from the same unit (sample J69-28).

Table 11. *Myotreta* aff. *crassa* Goryanskij, average dimensions and ratios of dorsal valves.

	W	L	L/W	WI	LI	LI/WI	LS	BS
DLK84-hol-25								
<i>n</i>	6	6	6	9	9	8	8	8
mean	0.49	0.40	82%	0.24	0.04	16%	0.37	0.13
<i>s</i>	0.110	0.087	3.077	0.069	0.010	4.970	0.088	0.027
min	0.34	0.29	79%	0.12	0.02	11%	0.25	0.09
max	0.60	0.51	86%	0.33	0.05	25%	0.48	0.17

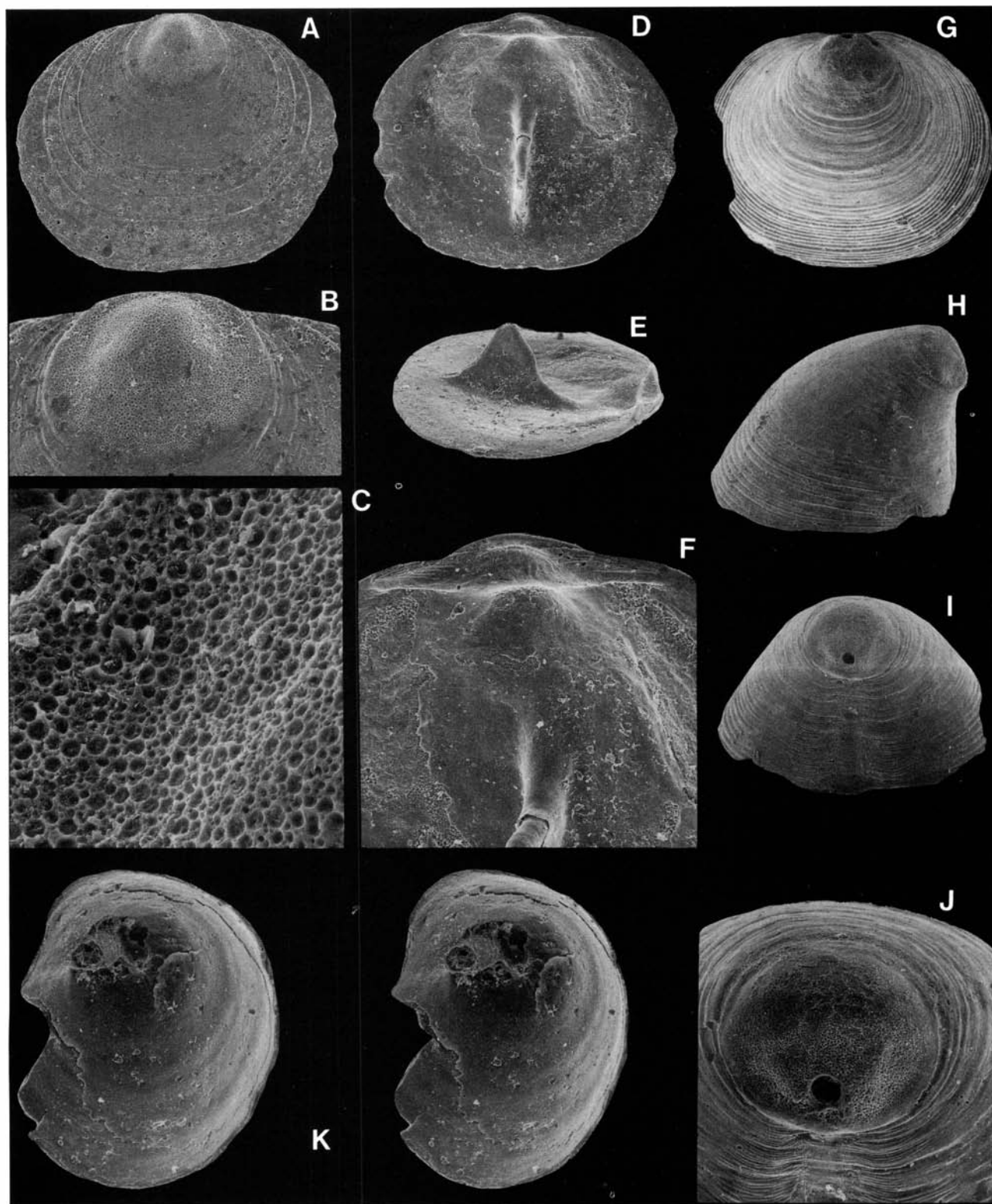


Fig. 79. *Myotreta* aff. *crassa* Goryanskij, 1969; Holen Limestone (sample DLK84-hol-25). □A. Dorsal exterior; Br128842, $\times 80$. □B. The larval shell of A; $\times 185$. □C. The larval ornamentation of A; $\times 1200$. □D. Interior of a dorsal valve; Br128841, $\times 80$. □E. Side view of D; $\times 80$. □F. The pseudointerarea of D; $\times 185$. □G. Ventral exterior; Br128844, $\times 80$. □H. Side view of G; $\times 80$. □I. Posterior view of G; $\times 80$. □J. The larval shell of G; $\times 185$. □K. Stereo-pair; interior of a ventral valve, showing the pedicle tube and traces of a median septum; Br128845, $\times 150$.

Myotreta dalecarlica sp. nov.

Figs. 31, 47J, 78A–C, 80, 81C–F, 85

Name. – Latinized form of Dalarna.

Holotype. – Br128924, complete dorsal valve, Fig. 80C (W 0.60, L 0.50), from the Kårgårde Limestone, Kårgårde section (sample DLK83-segk-3), Dalarna.

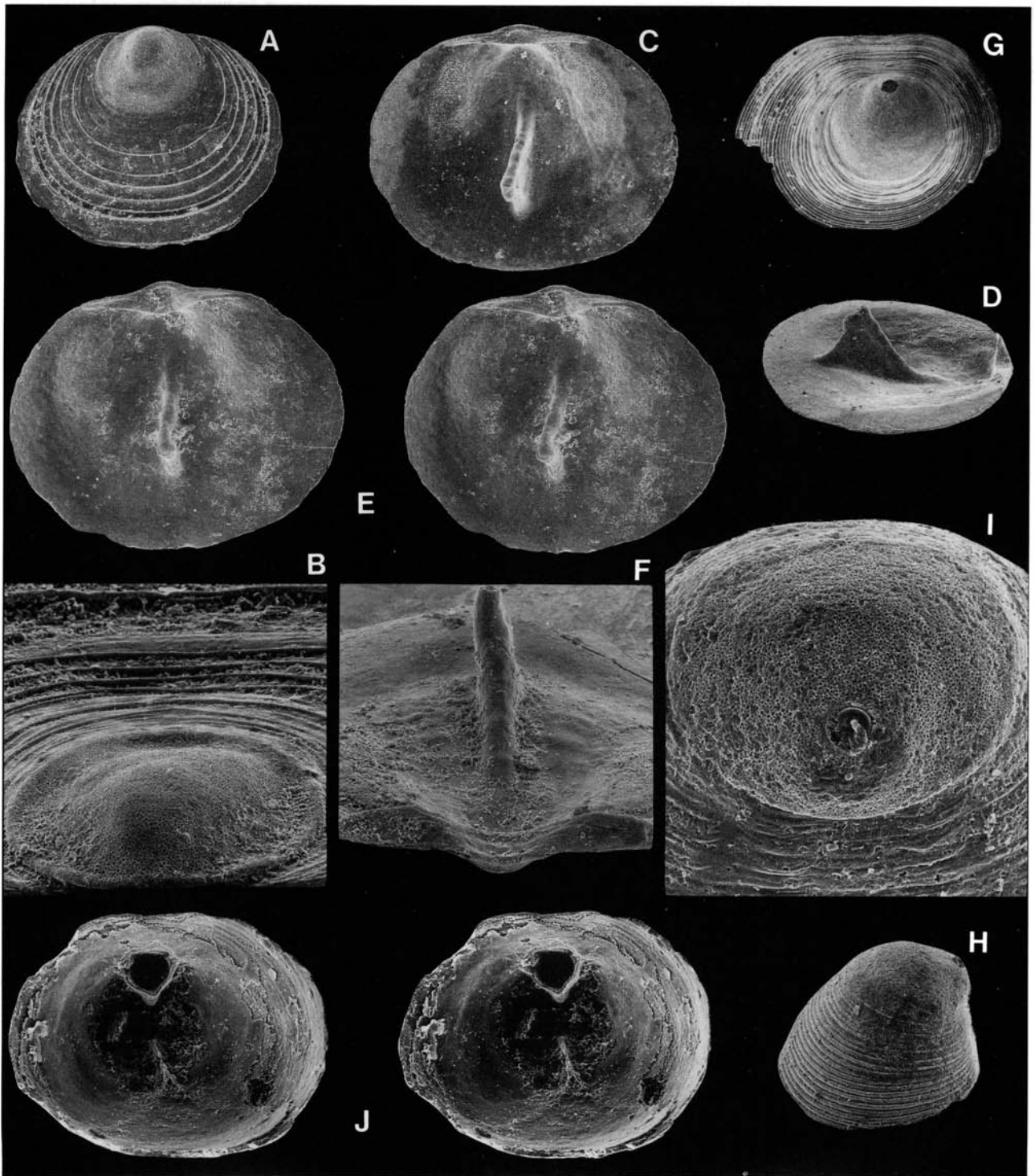


Fig. 80. *Myotreta dalecarlica* sp. nov. □A. Dorsal exterior; Kårgårde Limestone (sample DLK83-segk-6); Br128909, ×80. □B. Posterior view of a dorsal larval shell; Furudal Limestone (sample D60-222); Br128643, ×250. □C. Holotype; interior of a dorsal valve; Kårgårde Limestone (sample DLK83-segk-3); Br128924, ×80. □D. Side view of C; ×80. □E. Stereo-pair; dorsal interior; Furudal Limestone (sample D60-221); Br128778, ×80. □F. Posterior view of a dorsal pseudointerarea; Furudal Limestone (sample D60-220); Br128801, ×206. □G. Exterior of a ventral valve; Vikarby Limestone (sample DLK83-segv-3); Br128973, ×80. □H. Side view of a juvenile ventral valve; Kårgårde Limestone (sample DLK83-segk-6); Br128910, ×80. □I. Posterior view of the larval shell of H; ×250. □J. Stereo-pair; ventral interior; Furudal Limestone (sample D60-222); Br128648, ×135.

Paratypes. – Figured; Br128800 (W 0.59, L 0.45), Br133609h (section), Br128908 (W 0.64, L 0.50), Br128909 (W 0.53, L 0.43), Br128643 (W ~0.59, L 0.48), Br128778 (W 0.65, L 0.53), Br128801 (W 0.82, L 0.68), Br128973 (W 0.51, L

~0.40, H 0.36), Br128910 (W 0.51, L 0.39, H 0.28), Br128648 (damaged), Br128913 (W 0.43, L 0.37), Br128912 (W 0.31, L 0.28), Br128967 (W 0.34, L 0.28, H 0.16). Total of 761 dorsal valves and 252 ventral valves.

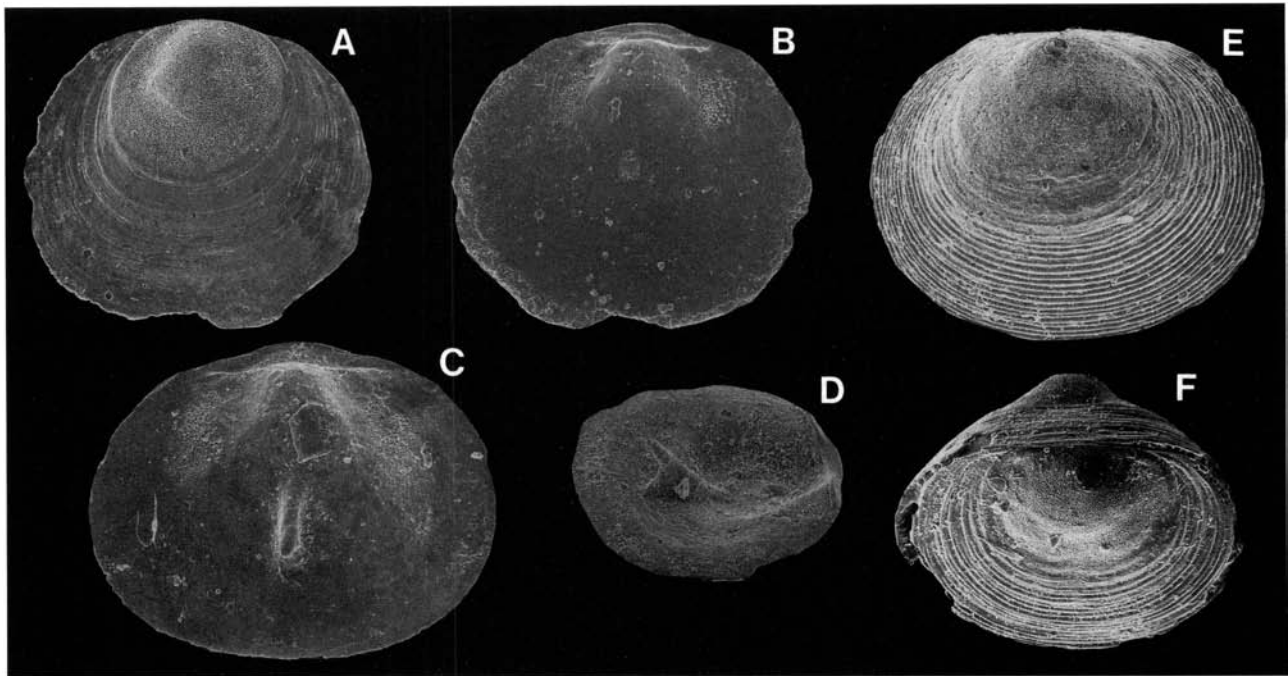


Fig. 81. □A–B. Juvenile dorsal valve of *Myotreta* aff. *crassa* Goryanskij, 1969; Hølen Limestone (sample DLK83-hol-25). □A. Dorsal exterior; Br128843, ×117. □B. Interior view of A; ×117. □C–F. *Myotreta dalecarlica* sp. nov. □C. Interior of a juvenile dorsal valve; Kårgårde Limestone (sample DLK83-segk-6); Br128913, ×117. □D. Side view of the interior of a dorsal valve; Kårgårde Limestone (sample DLK83-segk-6); Br128912, ×117. □E. Exterior of a juvenile ventral valve; Kårgårde Limestone (sample DLK83-segk-6); Br128910, ×102 (see also Fig. 80H–I). □F. Oblique posterior view of a complete juvenile valve; Skårlöv Limestone (sample DLK83-sä-4); Br128967, ×117.

Diagnosis. – Ventral valve with flattened pseudointerarea, procline to catacline and lacking intertrough. Ventral interior with pedicle tube; low and bifurcating median septum along anterior surface. Dorsal valve with wide pseudointerarea.

Description. – The valves average 85% as long as wide (OR 75–96%; *N*=46; Table 12); the ventral valve 54% as high as wide (OR 47–65%; *N*=4; Fig. 80H). In lateral profile the ventral pseudointerarea is flattened, procline to slightly catacline; there is no intertrough (Fig. 80G, I). The pedicle foramen is about 0.02 mm in diameter (Fig. 80I), continued internally as a pedicle tube with a triangular cross-section (Fig. 80J). There is a low, bifurcating median septum along the anterior wall (Fig. 80J). The dorsal pseudointerarea is wide, occupying 47% of the total width of the valve

(OR 30–61%; *N*=44; Table 12; Fig. 80C, E) and averaging 17% as long as wide (OR 8–26%; *N*=44; Table 12); it has a deep median groove and a pair of wide, anacline propareas (Fig. 80F). The dorsal median septum originates on average 0.16 mm from the posterior margin (Table 12), and extends about 71% of the total length (OR 56–92%; *N*=37); it is moderately high, with a maximum HS/W ratio of 27% (*N*=20; Table 12), and has a single upper septal rod (Fig. 80D). A few large, possibly gerontic, dorsal valves have a pair of cardinal muscle scars (LM/WM ratio on average 76%; *N*=2). The larval shell is ornamented with pits, identical to those of *M. aff. crassa*. The dorsal larval shell has a distinct subcentral node and an elevated outer rim (Fig. 80B). The posterior edge of the larval shell is not covered by the dorsal pseudointerarea (Fig. 80B, F). The shell structure is described above (p. 47, Fig. 31).

Table 12. *Myotreta dalecarlica* sp. nov., average dimensions and ratios of dorsal valves.

	W	L	L/W	WI	LI	LI/WI	WM	LM	LM/WM	LS	BS	HS
DLK83-segk-2, 3, 6												
<i>n</i>	26	26	26	26	26	26	1	1	1	22	22	14
mean	0.47	0.40	85%	0.22	0.04	17%	0.43	0.31	72%	0.29	0.16	0.05
<i>s</i>	0.080	0.078	4.877	0.059	0.015	4.310				0.072	0.027	0.042
min	0.29	0.26	75%	0.09	0.02	8%				0.17	0.14	0.02
max	0.62	0.54	96%	0.33	0.06	26%				0.43	0.22	0.17
D60-221												
<i>n</i>	18	18	18	18	18	18	1	1	1	15	15	6
mean	0.49	0.41	85%	0.24	0.04	17%	0.43	0.34	79%	0.30	0.15	0.15
<i>s</i>	0.116	0.091	3.466	0.077	0.014	3.548				0.075	0.015	0.037
min	0.29	0.26	80%	0.11	0.02	11%				0.19	0.14	0.11
max	0.67	0.54	93%	0.36	0.06	25%				0.42	0.19	0.20

Remarks on ontogeny. – The larval shell is almost circular (WL 0.20, LL 0.19; $N=12$; Fig. 80B, I) and like that of *M. aff. crassa*. The brephic and neanic stages (W 0.20–0.42, L 0.19–0.34; Fig. 81F) have a dorsal pseudointerarea (WI ?–0.14, LI ?–0.02) but lack a dorsal median septum (as in *M. aff. crassa*; Fig. 81B). The brephic and neanic ventral valve (H 0.08–0.20) is slightly procline. In the adult stage (W 0.42–0.67, L 0.34–0.54) the dorsal pseudointerarea is widened (WI 0.14–0.36, LI 0.02–0.06) and the median septum is formed. The dorsal cardinal muscle scars were first formed during the late adult (or gerontic) growth stage.

Discussion. – *Myotreta dalecarlica* is similar to *M. aff. crassa* Goryanskij, but differs from this species in having (1) a bifurcating ventral median septum, (2) a well developed ventral pseudointerarea, and (3) in lacking a ventral intertrough. Moreover, the dorsal pseudointerarea is proportionally somewhat wider in *M. dalecarlica* (Fig. 85).

Occurrence. – *M. dalecarlica* is a common and long ranging species in Sweden. In Dalarna, it appears in the Segerstad Limestone and ranges up into the lower Dalby Limestone (Figs. 9, 10). On Öland it occurs in the lowermost Segerstad Limestone; in Jämtland it is recorded from the Skärlov Limestone (samples J70-165–167, J69-37–38, 40–43). It is rare in Västergötland, but is known from a few horizons within the Ryd Limestone, and there are a few questionable occurrences from the lower Gullhögen Formation and the lower Dalby Limestone (Fig. 8B–C).

Myotreta oreensis sp. nov.

Figs. 82, 84, 85

Name. – From Ore parish, in which the Fjäckå section is situated.

Holotype. – Br128708, complete dorsal valve, Fig. 82A–C (W 0.56, L 0.51), from the Dalby Limestone, Fjäckå section (sample D60–204), Dalarna.

Paratypes. – Figured; Br132501 (W 0.59, L 0.48), Br132549 (W 0.73, L 0.64), Br133044 (damaged), Br133043 (W 0.62, L 0.50), Br132953 (W 0.45, L 0.39), Br133031 (W 0.57, L 0.43, H 0.45), Br132973 (W 0.43, L 0.37, H 0.33), Br133049

(W 0.29, L 0.26). Total of 423 dorsal valves and 67 ventral valves.

Diagnosis. – Outline of valves oval to circular. Dorsal pseudointerarea narrow and long. Dorsal cardinal muscle scars well developed and long. Median septum of variable height, low to high. Ventral valve catacline to slightly apsacline, lacking well defined pseudointerarea and intertrough. Ventral interior with long pedicle tube.

Description. – The valves are very variable in outline, on average 90% as long as wide (OR 75–103%; $N=60$; Table 13). The ventral valve is slightly less than 80% as high as wide in two specimens, with the highest point slightly anterior to the umbo. The pseudointerarea is poorly defined and lacks an intertrough. In lateral profile the ventral pseudointerarea is flattened, catacline to slightly apsacline (Fig. 82M). The interior pedicle tube is long (Fig. 82O). The morphology of the dorsal valve is very variable. The dorsal pseudointerarea is narrow and long, 21% as long as wide (OR 12–35%; $N=58$; Table 13), extending to 43% of the total width (OR 29–50%; $N=58$). The median groove is wide and deep; the propareas are narrow and anacline (Fig. 82B–C, G–K). The dorsal median septum is very low to very high (average HS/W ratio 29%; OR 8–57%; $N=10$), and has an upper septal rod (Fig. 82C, H, K); the septum originates about 0.14 mm from the posterior margin, and extends to 74% of the total length (OR 61–86%; $N=53$; Table 13; Fig. 82B, G, I–J). The dorsal cardinal muscle scars are well developed, 86% as long as wide (OR 55–100%; $N=18$; Table 13); they occupy over half of the total length (average LM/L ratio 64%; OR 51–72%; $N=18$; Fig. 82G, J). The valves are ornamented with concentric fila (Fig. 82D, L). The larval shell is sharply delineated, and nearly circular, about 0.17–0.20 mm in diameter, with pits identical to those of *M. aff. crassa* (Fig. 82E–F). The ontogenetic development is not known in detail, but appears to be more or less like that of *M. dalecarlica*; the brephic stage (W 0.20–0.36, L 0.20–0.33) lacks a median septum but has a minute pseudointerarea (WI ?–0.14, LI ?–0.03; Fig. 84A).

Discussion. – *Myotreta oreensis* is similar to *M. dalecarlica* and the distinction between these two species is not always clear when dealing with juveniles and small assemblages. *M. oreensis* differs from *M. dalecarlica* in having (1) a subcircular

Table 13. *Myotreta oreensis* sp. nov., average dimensions and ratios of dorsal valves.

	W	L	L/W	WI	LI	LI/WI	WM	LM	LM/WM	LS	BS
GB84-3-83											
<i>n</i>	18	18	18	18	18	18				14	14
mean	0.40	0.35	88%	0.16	0.03	20%				0.26	0.14
<i>s</i>	0.065	0.045	4.722	0.033	0.009	4.105				0.030	0.013
min	0.23	0.22	78%	0.09	0.02	12%				0.20	0.12
max	0.54	0.42	96%	0.19	0.05	26%				0.29	0.16
DLK83-dal-19, 22, 23, 27											
<i>n</i>	18	18	18	18	18	18	9	9	9	18	18
mean	0.49	0.44	90%	0.22	0.05	21%	0.37	0.30	82%	0.34	0.14
<i>s</i>	0.060	0.060	6.638	0.031	0.015	5.860	0.034	0.038	12.474	0.050	0.013
min	0.36	0.29	80%	0.16	0.02	12%	0.31	0.22	55%	0.22	0.11
max	0.59	0.51	103%	0.26	0.06	35%	0.42	0.33	94%	0.40	0.16

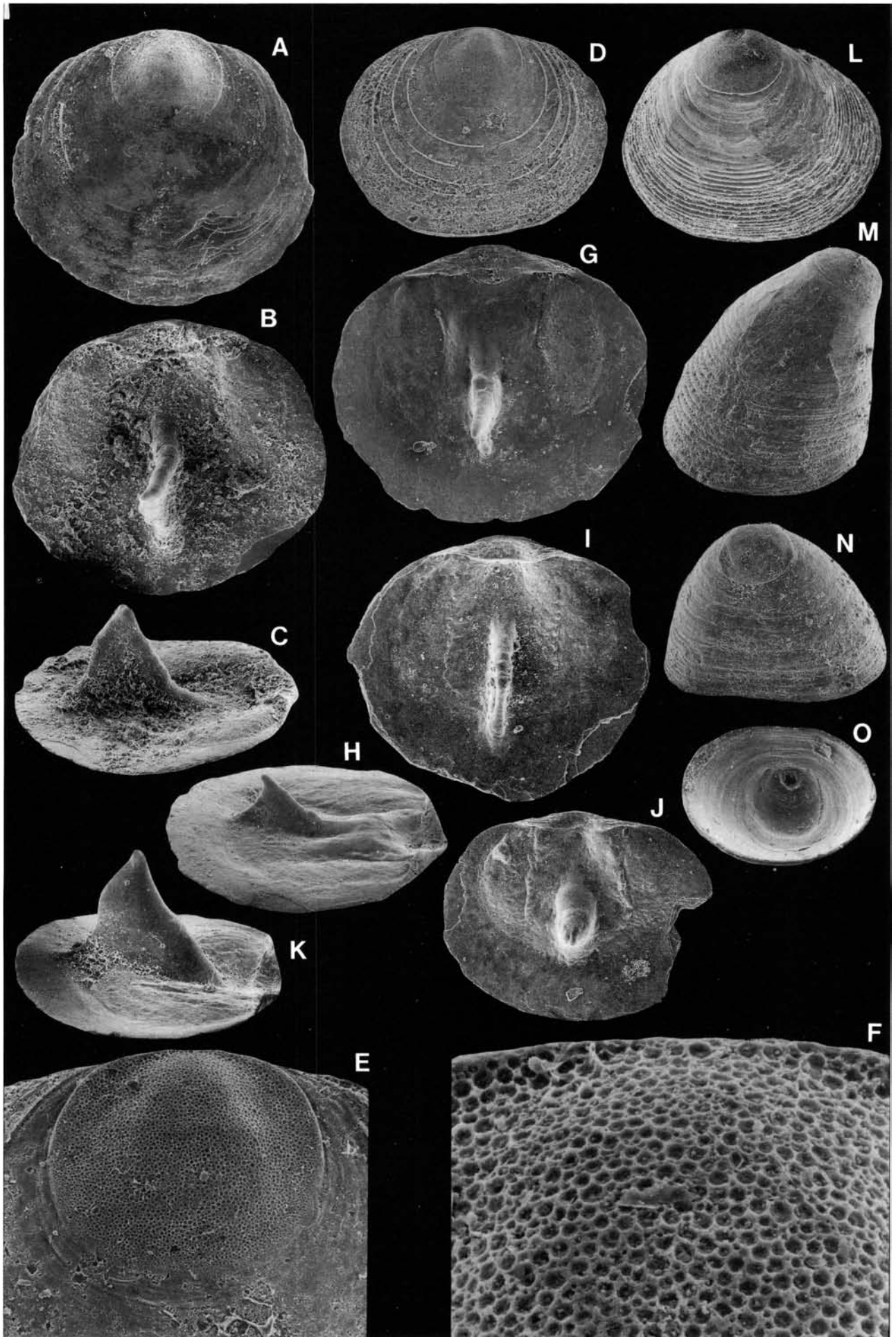


Table 14. *Rhinotreta davidi* sp. nov., average dimensions and ratios of dorsal valves.

	W	L	L/W	WI	LI	LI/WI	WM	LM	LM/WM	LS	BS
D60-185, 165, 157											
<i>n</i>	18	18	18	18	18	18	4	4	4	11	11
mean	0.40	0.39	97%	0.17	0.05	28%	0.28	0.26	94%	0.27	0.14
<i>s</i>	0.071	0.060	5.079	0.034	0.012	7.733	0.042	0.024	11.705	0.047	0.016
min	0.25	0.26	86%	0.11	0.02	14%	0.25	0.23	82%	0.20	0.12
max	0.54	0.51	110%	0.23	0.06	50%	0.34	0.28	108%	0.36	0.17
DLK83-dal-32											
<i>n</i>	18	18	18	18	18	18	10	10	10	17	17
mean	0.42	0.40	95%	0.20	0.05	24%	0.32	0.27	85%	0.31	0.15
<i>s</i>	0.066	0.056	4.221	0.034	0.011	4.914	0.040	0.035	7.011	0.040	0.013
min	0.29	0.28	89%	0.14	0.02	14%	0.26	0.22	72%	0.26	0.12
max	0.54	0.48	102%	0.26	0.06	31%	0.37	0.31	97%	0.43	0.16

outline, (2) a long and narrow dorsal pseudointerarea, and (3) a pair of well defined and long dorsal cardinal muscle scars. Moreover, *M. oreensis* lacks a well defined ventral pseudointerarea, as well as a ventral median septum; the morphology of the dorsal valve is more variable in outline, as are the relative height and length of the median septum.

Occurrence. – *Myotreta oreensis* is known from the uppermost Ryd Limestone and lower Dalby Limestone of Västergötland, (Fig. 8C–D). In Dalarna it is restricted to the lower Dalby Limestone (Figs. 9B–C, 10).

Genus *Rhinotreta* Holmer, 1986

Type species. – Original designation; *Rhinotreta muscularis* Holmer, 1986, p. 113, from the upper Viru (Middle Ordovician) unnamed 'unit A', Gullhøgen quarry (section 5 in Fig. 2), Västergötland.

Diagnosis. – See Holmer (1986, p. 113).

Species assigned. – *Rhinotreta muscularis* Holmer, 1986; *R. davidi* sp. nov.

Rhinotreta davidi sp. nov.

Figs. 83, 84B–F, 85

Name. – After my son David.

Holotype. – Br128707, slightly damaged ventral valve, Fig. 83J–M (W ~0.36, L ~0.36, H ~0.36), from the Dalby Limestone, Fjäckå section (sample D60-153), Dalarna.

Paratypes. – Figured; Br132999 (W 0.53, L 0.49), Br132988 (W 0.37, L 0.36), Br133013 (W 0.43, L 0.40, H 0.39), Br133019 (W 0.39, L 0.39, H 0.40), Br132991 (W 0.28, L 0.29), Br133012 (W 0.31, L 0.28), Br133000 (W 0.43, L 0.40), Br133016 (W 0.60, L 0.51), Br133014 (W 0.20, L 0.20). Total of 732 dorsal valves, 98 ventral valves and 1 complete shell.

Diagnosis. – Valves of subquadrate outline, almost as long as wide. Ventral valve almost as high as wide, with short exterior and long interior pedicle tube. Ventral pseudointerarea poorly defined, with intertrough.

Description. – The valves have a generally subquadrate outline, on average 96% as long as wide (OR 86–110%; *N*=38; Table 14), but it is variable (Figs. 83A, 84B, E). The ventral valve is about as high as wide (Fig. 83N), apsacline to catacline, and has a poorly defined pseudointerarea (Fig. 83I, K, M) with a well developed intertrough (Fig. 83E). The exterior pedicle tube is short (Fig. 83H, J, L), posteriorly inclined (Fig. 83I, M), and continues as a long internal pedicle tube. The dorsal pseudointerarea is narrow and long, 26% as long as wide (OR 14–50%; *N*=36; Table 14) and occupying 44% of the total width of the valve (OR 31–56%; *N*=36). The median groove is well developed and the propareas are short and anacline (Fig. 83D). In lateral profile the median septum is low and ridge-like; it originates about 0.15 mm from the posterior margin (Table 14) and extends to 71% of the total length (OR 58–84%; *N*=28; Fig. 83B–C). The dorsal cardinal muscle scars are well developed, of oval shape, and 88% as long as wide (OR 72–108%; *N*=14; Table 14); they form 70% of the total length (OR 58–96%; *N*=14; Fig. 83B). The valves are ornamented with evenly spaced growth lines (Fig. 83A, H). The larval shell is sharply delineated (Fig. 83F, L). The larval pits are similar to those of *Myotreta* aff. *crassa* (Fig. 83G). The dorsal larval shell has a subcentral node and an elevated outer ridge (Fig. 83E). The posterior part of the ridge is not covered by the dorsal pseudointerarea (Fig. 83D).

Fig. 82. *Myotreta oreensis* sp. nov. □A. Holotype; dorsal exterior; Dalby Limestone (D60-204); Br128708, ×100. □B. Interior of A; ×100. □C. Side view of A; ×100. □D. Exterior of a dorsal valve; Dalby Limestone (sample DLK83-dal-10); Br132501, ×80. □E. The larval shell of D; ×250. □F. Ornamentation of the larval shell of D; ×1200. □G. Interior of a dorsal valve; Dalby Limestone (sample DLK83-dal-16); Br132549, ×80. □H. Side view of G; ×80. □I. Dorsal interior; Dalby Limestone (sample GB84-3-81). Br133044, ×80. □J. Interior of a dorsal valve; Dalby Limestone (sample GB84-3-81); Br133043, ×80. □K. Side view of the interior of a dorsal valve; Dalby Limestone (sample DLK83-dal-18); Br132953, ×100. □L. Ventral exterior; Dalby Limestone (sample GB84-3-73); Br133031, ×80. □M. Side view of L; ×80. □N. Posterior view of L; ×80. □O. Interior of a ventral valve, showing the pedicle tube; Dalby Limestone (sample DLK83-dal-26); Br132973, ×80.

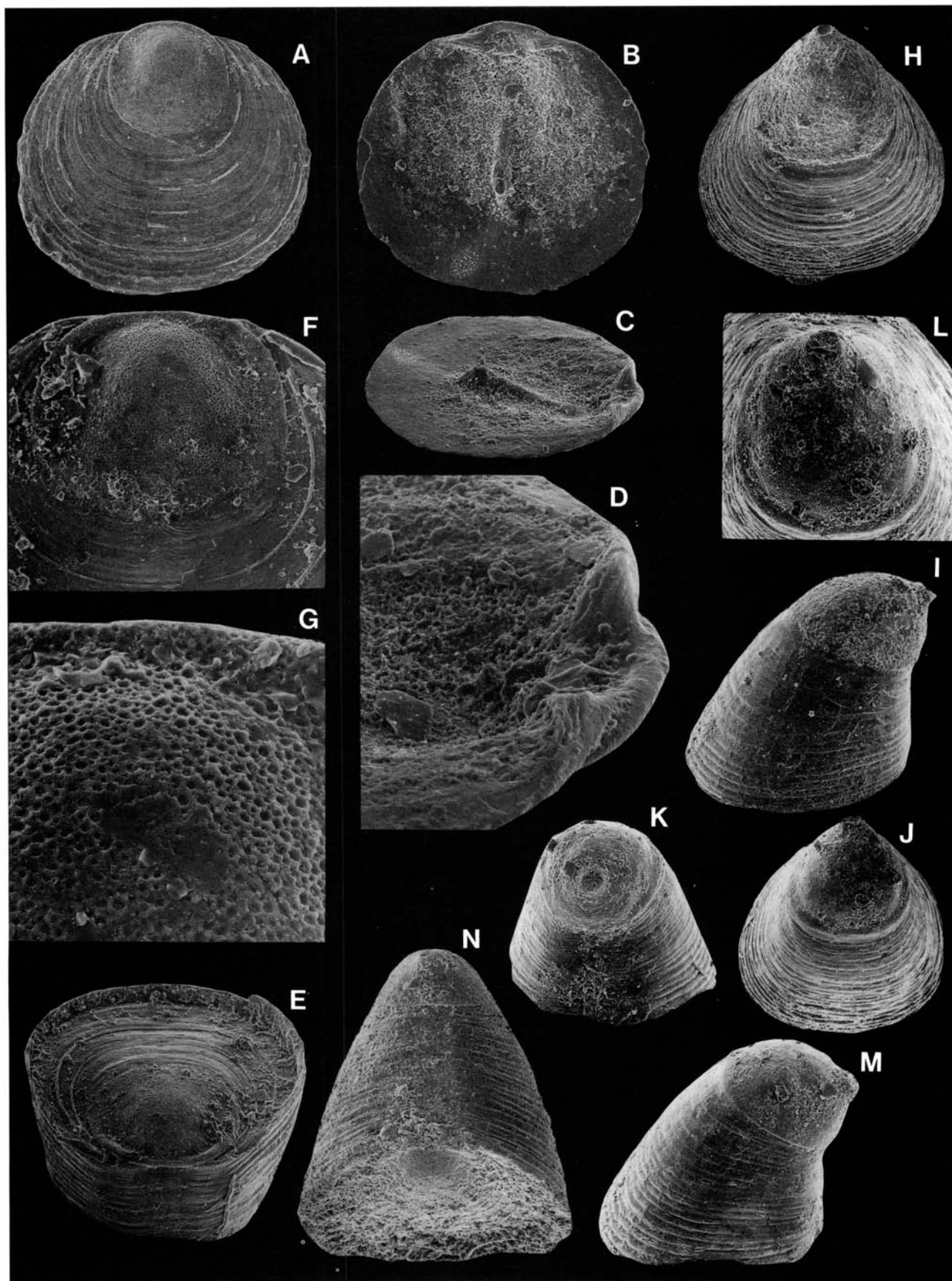


Fig. 83. *Rhinotrete davidi* sp. nov. □A. Exterior of a dorsal valve; Dalby Limestone (sample DLK83-dal-36); Br132999, $\times 100$. □B. Interior of A; $\times 100$. □C. Side view of B; $\times 100$. □D. Detail of the pseudointerarea of C; $\times 350$. □E. Oblique posterior view of a damaged complete shell; Dalby Limestone (sample DLK83-dal-33); Br132988, $\times 100$. □F. The larval shell of E; $\times 200$. □G. Ornamentation of the larval shell of E; $\times 800$. □H. Exterior of a ventral valve; Dalby Limestone (sample DLK83-dal-39); Br133013, $\times 100$. □I. Side view of H; $\times 100$. □J. Holotype; exterior of a ventral valve; Dalby Limestone (sample D60-153); Br128707, $\times 100$. □K. Posterior view of J; $\times 100$. □L. The larval shell of J; $\times 200$. □M. Side view of J; $\times 100$. □N. Posterior view of a complete shell; Dalby Limestone (sample DLK83-dal-41); Br133019, $\times 100$.

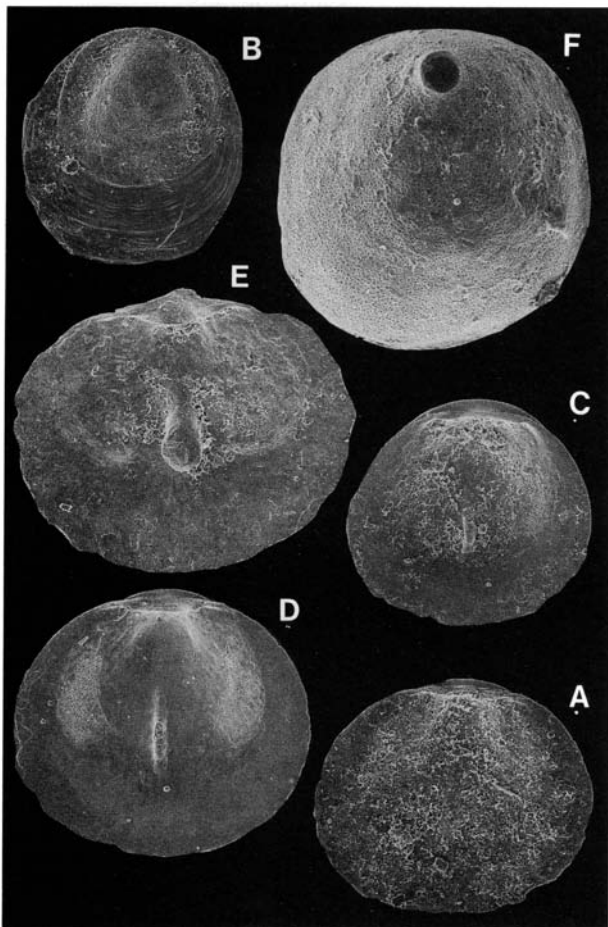
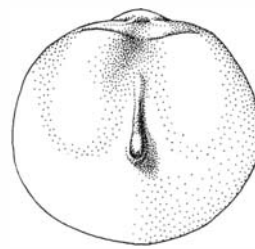


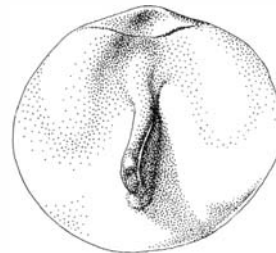
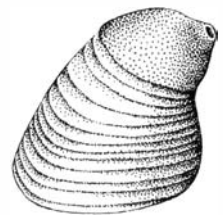
Fig. 84. □A. Interior of a brephic dorsal valve of *Myotreta orensis* sp. nov.; Dalby Limestone (sample GB84-3-83); Br133049, $\times 117$. □B–F. Ontogeny of *Rhinotrete davidi* sp. nov. □B. Exterior of a brephic dorsal valve; Dalby Limestone (sample DLK83-dal-34); Br132991, $\times 117$. □C. Interior of a brephic dorsal valve; Dalby Limestone (sample DLK83-dal-39); Br133012, $\times 117$. □D. Interior of a juvenile dorsal valve; Dalby Limestone (sample DLK83-dal-36); Br133000, $\times 102$. □E. Dorsal interior; Dalby Limestone (sample DLK83-dal-39); Br133016, $\times 83$. □F. Exterior of a ventral larval shell; Dalby Limestone (sample DLK83-dal-39); Br133014, $\times 240$.

Remarks on ontogeny. – The larval shell is almost circular (WL 0.20, LL 0.20). The ventral one (H 0.09) lacks an interior pedicle tube (Fig. 84F). The brephic dorsal valve (W 0.20–0.36, L 0.20–0.34) has a minute pseudointerarea (WI ?–0.19, LI ?–0.04). The low median septum (LS ?–0.26, BS ?–0.14; Fig. 84B–C) is formed during the neanic stage (W 0.36–0.43, L 0.34–0.40). The dorsal cardinal muscle scars (WM ?–0.28, LM ?–0.22; Fig. 84D) are formed during the adult stage. A few dorsal valves attaining widths of more than 0.54 mm appear to belong to the gerontic stage (see also Fig. 46).

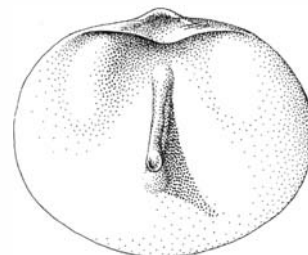
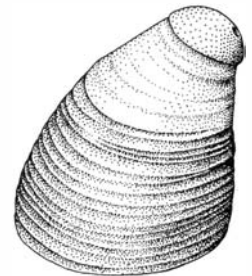
Discussion. – *Rhinotrete davidi* is very similar to the upper Viru type species *R. muscularis* Holmer (1986, Figs. 7H–Q, 10D–F), especially in the morphology of the dorsal valve. The ventral valve differs from that of *R. muscularis* in having (1) a shorter exterior pedicle tube, (2) an interior pedicle tube, and (3) a narrow, well developed intertrough. The dorsal valves of *R. davidi* are sometimes difficult to distinguish from those of *Myotreta orensis* (Figs. 82G–I, 83B–C),



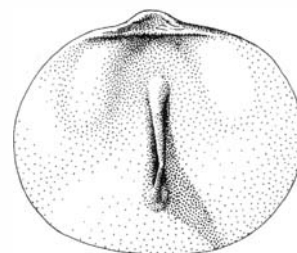
Rhinotrete davidi



Myotreta orensis



Myotreta dalecarlica



Myotreta aff. crassa

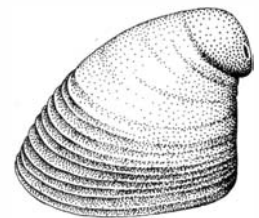


Fig. 85. Comparison between species of *Myotreta* and *Rhinotrete*. Figure prepared by Lennart Andersson (Stockholm).

but the median septum and cardinal muscle scars are developed at an earlier ontogenetic stage in the former (Fig. 84A, C–E).

Occurrence. – *Rhinotrete davidi* is restricted to the upper Dalby Limestone of Dalarna and Västergötland (Figs. 8D, 9C, 10).

Genus *Numericoma* Popov, 1980

Type species. – Original designation; *Numericoma ornata* Popov (in Nazarov & Popov 1980), p. 102, from the Llanvirn Kopalín Stage, Karakan (Locality 2033), Kazakhstan, U.S.S.R.

Diagnosis. – Ventral valve highly conical, catacline to apsacline with intertrough; commonly with interior pedicle tube.

Dorsal valve with wide, narrow pseudointerarea and well developed propareas. Dorsal median septum with numerous septal spines. Septum always asymmetrical in anterior view, forming simple or more complex 90° folds (left- or right-handed).

Species assigned. – *Numericoma ornata* Popov, 1980; *N. electa* Popov, 1980; *Ephippelasma spinosum* Biernat, 1973; *?E. latior* Biernat, 1973; *Numericoma simplex* sp. nov.; *N. perplexa* sp. nov.

Discussion. – The most distinguishing character of *Numericoma* is the complex dorsal median septum. In all species it is invariably asymmetrical in anterior view (apart from in a single specimen of *N. perplexa* [Fig. 88F–G], and in all specimens of *N.? spinosa* Biernat). It is important to emphasise that the development of the median septum of all species within *Numericoma* (and *Ephippelasma*) involves the folding of a single plate (see description of ‘Ontogeny’ below). The accepted division of the ephippelasmatine septum into a ‘buttressing septal plate’ and a ‘surmounting plate’ is somewhat unfortunate, as it gives the impression of a torynelasmatine (or a biernatine) type of septum, the formation of which is different (cf. Fig. 75). Thus the difference between *Numericoma* and *Ephippelasma* is not the lack of a ‘buttressing septal plate’ in the latter, but rather that the septum is asymmetrical and twisted only 90° in *Numericoma*, whereas it is symmetrical and twisted 180° in *Ephippelasma*.

At present *Numericoma* has a range from the lower Arenig Series to the upper Uhakuan Stage. In addition to the type species, Popov (*in* Nazarov & Popov, 1980) described *N. electa* from the Lower Ordovician (Arenig) Kogashi Stage of

Kazakhstan. Popov (p. 100) also assigned *Ephippelasma spinosum* Biernat, 1973 and *E. latior* Biernat, 1973 to the genus; both species from the lower Middle Ordovician of Poland. These two species are here only questionably retained within the genus. Krause & Rowell (1975) identified *N.? spinosa* from the lower Whiterock of Nevada, but in all probability this is a new species of *Numericoma*. Bednarczyk & Biernat (1978) illustrated specimens of a form from the lower Arenig of Poland, which they referred to *N.? spinosa*. The Swedish species of *Numericoma* (and *Ephippelasma*) are compared in Fig. 93.

Numericoma simplex sp. nov.

Figs. 30C–E, 86, 93

Name. – Latin *simplex*, single; alluding to the relatively simple type of median septum.

Holotype. – Br128947, complete dorsal valve, Fig. 86C (W 0.60, L 0.48), from the Kårgårde Limestone, Kårgårde section (sample DLK83-segk-6), Dalarna.

Paratypes. – Figured; Br133595m (section), Br128976 (W 0.45, L 0.39), Br128867a (W 0.82, L 0.64), Br128867b (damaged), Br128948 (W 0.51, L 0.40, H 0.43), Br128986 (W 0.74, L 0.57, H 0.79). Total of 659 dorsal valves, 520 ventral valves and 4 complete shells.

Diagnosis. – Ventral valve catacline to slightly apsacline, with short external pedicle tube. Dorsal valve with simple median septum, showing left- or right-handed dimorphism with single 90° loop.

Description. – The valves average 78% as long as wide (OR 72–90%; *N*=41; Tables 15, 16); the ventral valve 85% as high as wide (OR 78–107%; *N*=8; Table 15) with the highest point at the umbo (Fig. 86G). The exterior and interior pedicle tubes are short (Fig. 86F–H). The ventral pseudointerarea is catacline to slightly apsacline, with a well defined intertrough (Fig. 86G–H). In lateral profile the dorsal valve is slightly convex (Fig. 69E). The dorsal pseudointerarea averages 12% as long as wide (OR 8–15%; *N*=34; Table 16), forming 54% of the total width of the valve (OR 46–63%; *N*=34); the propareas are wide and anacline to catacline (Fig. 86C, E). The cardinal muscle scars are well developed, 59% as long as wide (OR 51–77%;

Table 15. *Numericoma simplex* sp. nov., average dimensions and ratios of ventral valves.

	W	L	L/W	H	H/W
DLK83-segk-6, sã-7					
<i>n</i>	7	7	7	7	7
mean	0.55	0.43	78%	0.46	82%
<i>s</i>	0.076	0.049	4.467	0.059	2.858
min	0.46	0.37	72%	0.40	78%
max	0.65	0.50	85%	0.54	86%

Table 16. *Numericoma simplex* sp. nov., average dimensions and ratios of dorsal valves.

	W	L	L/W	WI	LI	LI/WI	WM	LM	LM/WM	LS	BS
DLK83-segk-6											
<i>n</i>	17	17	17	17	17	17	5	5	5	15	15
mean	0.47	0.38	83%	0.25	0.02	11%	0.42	0.23	55%	0.29	0.11
<i>s</i>	0.126	0.092	4.802	0.083	0.005	2.849	0.025	0.016	3.209	0.093	0.010
min	0.31	0.28	75%	0.14	0.02	8%	0.39	0.22	51%	0.17	0.09
max	0.68	0.51	90%	0.39	0.03	15%	0.46	0.26	59%	0.51	0.12
DLK83-sã-7											
<i>n</i>	17	17	17	17	17	17	6	6	6	16	16
mean	0.60	0.49	82%	0.32	0.04	12%	0.47	0.29	63%	0.34	0.11
<i>s</i>	0.102	0.081	3.419	0.061	0.013	2.562	0.044	0.055	8.116	0.078	0.006
min	0.43	0.36	77%	0.22	0.03	8%	0.42	0.23	53%	0.20	0.09
max	0.73	0.62	88%	0.39	0.06	15%	0.51	0.39	77%	0.51	0.12

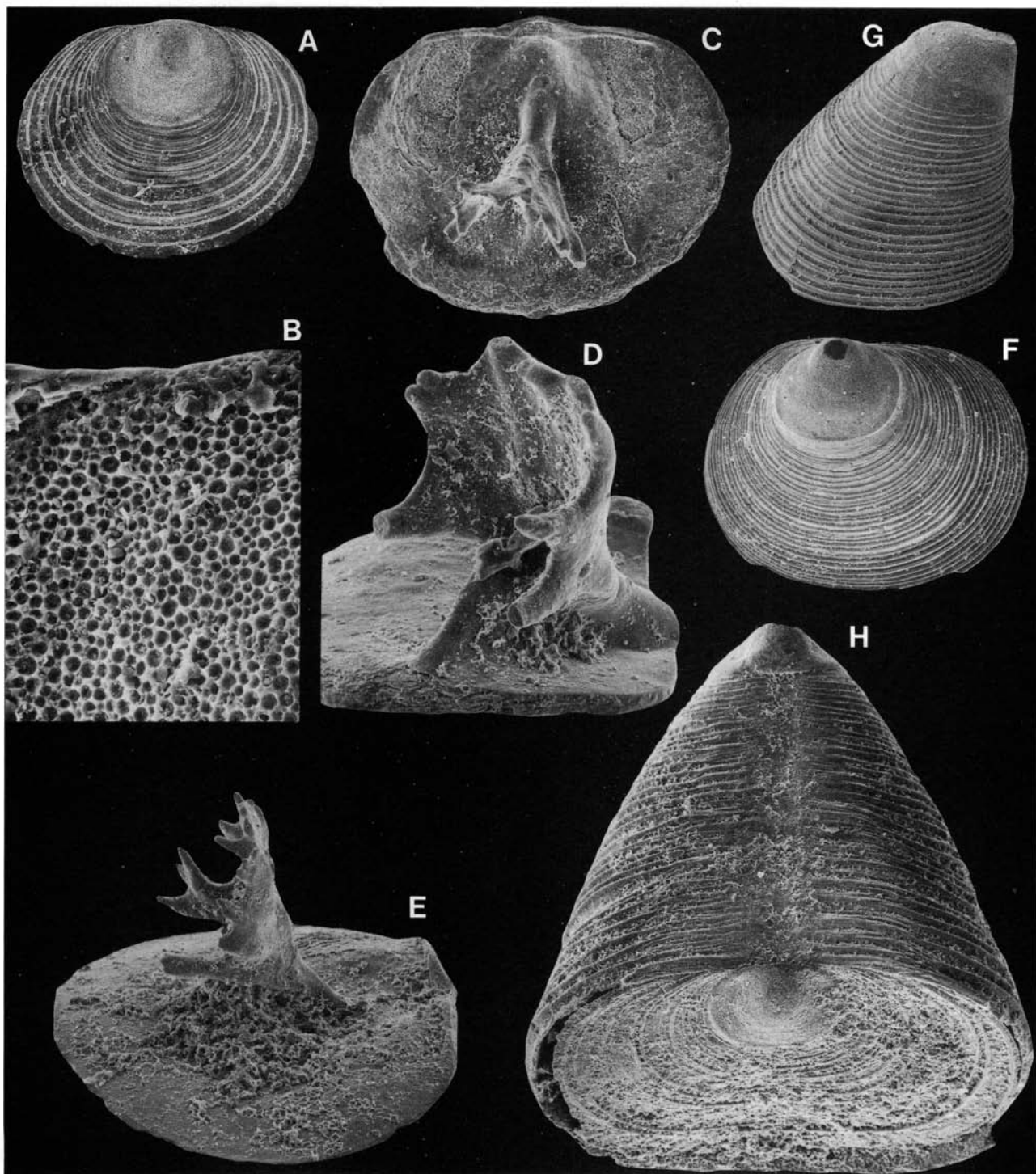


Fig. 86. *Numericoma simplex* sp. nov. □A. Dorsal exterior; Skärlov Limestone (sample DLK83-sä-7); Br128976, $\times 100$. □B. The larval ornamentation of A; $\times 1100$. □C. Holotype; interior of a dorsal valve; Kårgårde Limestone (sample DLK83-segk-6); Br128947, $\times 100$. □D. Oblique anterior view of the (left-handed) median septum of a dorsal valve; Kårgårde Limestone (sample DLK83-segk-1); Br128867b, $\times 190$. □E. Side view of the interior of a dorsal valve; Kårgårde Limestone (sample DLK83-segk-1); Br128867a, $\times 100$. □F. Exterior of a ventral valve; Kårgårde Limestone (sample DLK83-segk-6); Br128948, $\times 100$. □G. Side view of F; $\times 100$. □H. Posterior view of a complete shell; Skärlov Limestone (sample DLK83-sä-7); Br128986, $\times 100$.

$N=11$; Table 16; Fig. 86C). The median septum has numerous marginal spines (Fig. 86C–E); it originates about 0.11 mm from the posterior margin (Table 16), and extends 70% of the total length (OR 54–100%; $N=31$). In anterior view the septum is asymmetrical, showing dimorphism with right- or left-handed, 90° twisting in the single loop (Fig. 86C–E). The maximum height of the septum is

situated at about the centre of the valve (HS/W ratio around 50%; Figs. 30C, 86E). The valves are ornamentated with closely spaced fila (Fig. 86A, G). The larval shell is sharply delineated (WL 0.19, LL 0.17; $N=7$); the dorsal one has a central node. The larval pits are of varying sizes, up to 3 μm across (Fig. 86B). The shell structure is described above (p. 47, Fig. 30C–E).

Discussion. – *Numericoma simplex* is distinguished from all previously described species in having a comparatively simple median septum with a single 90° fold. It could possibly be related closely with the roughly contemporaneous *N.?* *latior* (Biernat, 1973) from Poland, which also appears to have a simple septum with a single fold (Biernat 1973, Pl. 24:1–3). However, the detailed morphology of the septum in this species is not known. Moreover, the Polish species differs from *N. simplex* mainly in having a narrower dorsal pseudointerarea with longer propareas.

Occurrence. *Numericoma simplex* appears in the Kårgårde Limestone and occurs also in the Skärlov Limestone of Dalarna (Fig. 9A). In Jämtland the Segerstad Limestone has yielded some specimens (samples J69-35, 40).

Numericoma perplexa sp. nov.

Figs. 29, 30A–B, 87, 88, 93

Name. – Latin *perplexus*, intricate; alluding to the complex median septum.

Holotype. – Br128780, complete dorsal valve, Fig. 87A–B (W 0.57, L 0.43), from the Furudal Limestone, Fjäckå section (sample D60-220), Dalarna.

Paratypes. – Figured; Br128783 (damaged), Br132394d (section), Br132734 (W 0.62, L 0.43, H 0.34), Br128748 (W 0.45, L 0.39), Br128634 (W 0.68, L 0.53, H 0.84), Br128638 (W 0.56, L 0.43, H 0.43), Br129045 (W 0.56, L 0.42, H 0.48), Br129046 (W 0.74, L 0.54, H 0.98), Br132736 (W 0.56, L 0.42, H 0.50), Br132631 (W 0.23, L 0.20), Br132702 (W 0.31, L 0.25), Br132656 (W 0.36, L 0.29), Br128781 (W 0.43, L 0.34), Br132735 (W ~0.60, L 0.45), Br128658 (W ~0.53, L 0.43), Br128768 (damaged), Br128730 (lost). Total of 3147 dorsal valves, 1879 ventral valves and 46 complete shells.

Table 17. *Numericoma perplexa* sp. nov., average dimensions and ratios of ventral valves.

	W	L	L/W	H	H/W
GB84-2-23					
<i>n</i>	18	18	18	18	18
mean	0.48	0.37	79%	0.45	89%
<i>s</i>	0.136	0.094	3.974	0.228	24.871
min	0.25	0.22	72%	0.12	48%
max	0.71	0.51	88%	0.88	124%

Table 18. *Numericoma perplexa* sp. nov., average dimensions and ratios of dorsal valves.

	W	L	L/W	WI	LI	LI/WI	WM	LM	LM/WM	LS	BS
DLK83-fur-14											
<i>n</i>	18	18	18	18	18	18	12	12	12	12	12
mean	0.58	0.46	80%	0.32	0.03	10%	0.48	0.25	51%	0.41	0.12
<i>s</i>	0.175	0.131	4.717	0.123	0.007	3.167	0.083	0.047	4.033	0.054	0.005
min	0.28	0.23	73%	0.12	0.02	5%	0.34	0.19	44%	0.34	0.11
max	0.82	0.62	92%	0.51	0.04	17%	0.64	0.31	58%	0.50	0.12

Diagnosis. – Ventral valve catacline to strongly apsacline, with snout-like, long exterior pedicle tube. Dorsal median septum of varying shape, but always with complex 90° loop showing both secondary twisting, as well as right- and left-handed dimorphism.

Description. – The valves average 80% as long as wide (OR 72–92%; *N*=36; Tables 17, 18); the ventral valve is 89% as high as wide (Table 17) with the highest point at the umbo, but in gerontic valves it is somewhat anterior to the umbo (Fig. 87K). The ventral pseudointerarea has a well developed intertrough (Fig. 87G); it is catacline to strongly apsacline in gerontic valves (Fig. 87K). A long, snout-like exterior pedicle tube (Fig. 87H) continues as an interior pedicle tube (Fig. 87L). In lateral profile the dorsal valve is slightly convex (Fig. 87A). The pseudointerarea is on average 10% as long as wide (Table 18) and occupies 53% of the total width (OR 43–64%; *N*=18); the propareas are wide and anacline (Fig. 87A). The dorsal cardinal muscle scars are well developed, on average 51% as long as wide (Table 18; Fig. 87A). A dorsal median septum originates about 0.12 mm from the posterior margin (Table 18), and extends to 77% of the total length (OR 74–80%; *N*=12); it shows right- and left-handed dimorphism, and both morphs occur in about equal numbers (*N*=70, in sample DLK83-fur-14). The septum is strongly spinose; in anterior view it is asymmetrical and slightly funnel-shaped, about 0.20 mm wide. Details of the twisting pattern vary from a relatively simple asymmetrical 180° loop (Fig. 88H) to more complex shapes; in most specimens it has a secondary fold that forms a horizontal platform anterior to the funnel (Figs. 87B–C, 88I). A single specimen (Br132735; GB84-2-21) has a nearly bilaterally symmetrical septum, formed by two opposite loops and a horizontal platform in between (Fig. 88F–G). The maximum height of the septum is situated somewhat anterior to the centre of the valve; the HS/W ratio is around 50%. The valves are ornamented with closely spaced fila (Fig. 87E, K). The larval shell is sharply delineated; the dorsal larval shell has a distinct node (Fig. 87D, H–I). The larval pits are up to 2 µm across (Fig. 87F). For shell structure, see above (p. 47, Figs. 29, 30A–B).

Ontogeny. – The larval shell is about 0.22 mm wide and 0.16 mm long. The ventral larval shell is about 0.10 mm high. At the brephic stage the dorsal valve (W 0.22–0.31, L 0.16–0.25) lacks a median septum, but an incipient dorsal pseudointerarea (WI ?–0.16, LI ?–0.02) is present (Fig. 88A). At the early neanic stage (W 0.31–0.43, L 0.25–0.34) a simple median septum (LS 0.17–0.28) is developed, first as a small knob (Fig. 88B) which then forms a *Myotreta*-like

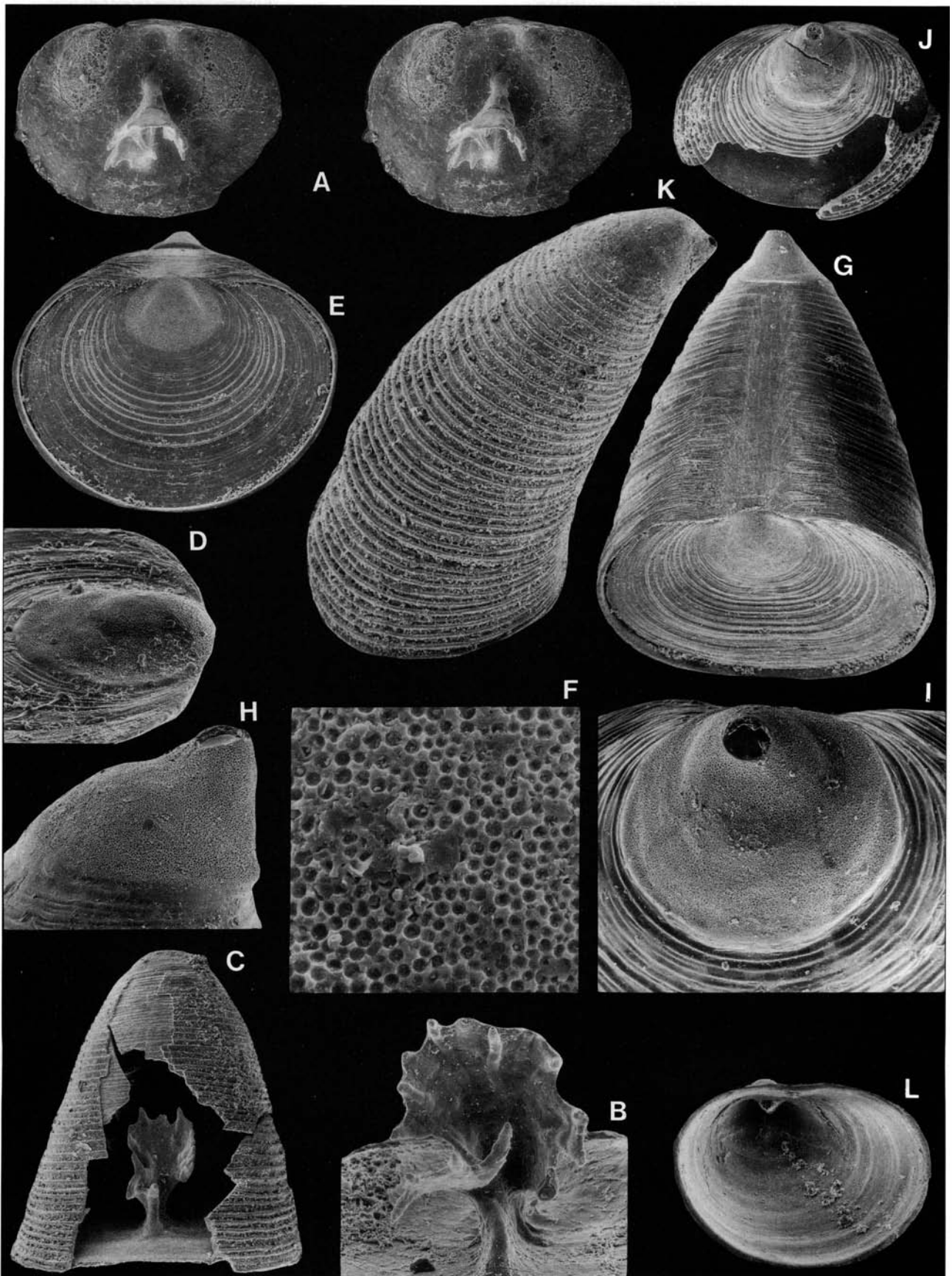
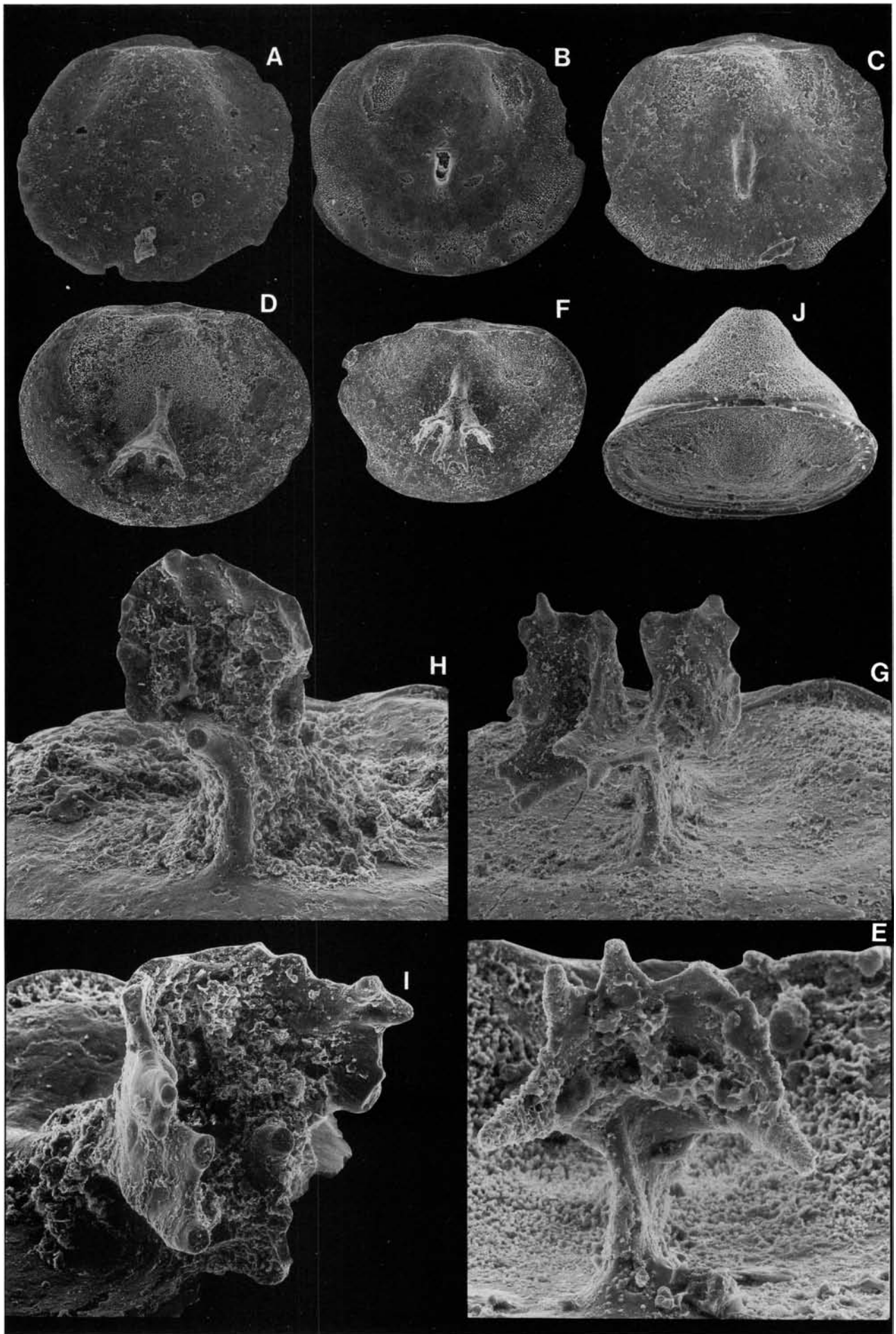


Fig. 87. *Numericomica perplexa* sp. nov. □A. Holotype; stereo-pair; dorsal interior; Furudal Limestone (sample D60-220); Br128780, $\times 80$. □B. Anterior view of the (left-handed) median septum of A; note the platform, and the funnel-shaped outline of the septum; $\times 200$. □C. Anterior view of a left-handed median septum; Gullhög Formation (sample GB84-2-21); Br132734, $\times 180$. □D. Side view of a dorsal larval shell; Furudal Limestone (sample D60-220); Br128748, $\times 200$. □E. Dorsal view of a complete shell; Gullhög Formation (sample GB84-1-7); Br128634, $\times 80$. □F. The larval ornamentation of E; $\times 1500$. □G. Posterior view of E; $\times 80$. □H. Side view of the ventral larval shell of E; $\times 200$. □I. Ventral larval shell; Gullhög Formation (sample GB84-1-7); Br128638, $\times 200$. □J. Ventral view of a complete shell; Furudal Limestone (sample DLK83-fur-3); Br129045, $\times 80$. □K. Side view of a ventral valve; Furudal Limestone (sample DLK83-fur-5); Br129046, $\times 80$. □L. Ventral interior; Gullhög Formation (sample GB84-2-21); Br132736, $\times 80$.



septum (Fig. 88C). During the neanic stage, the dorsal propareas (WI 0.16–0.21, LI 0.02–0.03) are formed (Fig. 88B–C); some specimens have traces of dorsal cardinal muscle scars (Fig. 88B). The early neanic ventral valve (H 0.10–0.36) is catacline, up to 80% as high as wide. During a later part of the neanic stage (W 0.43–0.57, L 0.34–0.45) the median septum (LS 0.28–0.36) forms the first 90° fold (Fig. 88D–E), and the dorsal pseudointerarea (WI 0.21–0.28, LI 0.03) is widened further (Fig. 88D). The late neanic ventral valve (H 0.36–0.68) is catacline to apsacline, 80–120% as high as wide. At the adult stage (W 0.57–0.71, L 0.45–0.54) the dorsal median septum attains its full complexity and distinct cardinal muscle scars are formed; the ventral valve (H 0.68–0.88) is strongly apsacline and up to 124% as high as wide. Some larger specimens (W 0.71–0.82) possibly represent the gerontic stage.

Discussion. – *Numericoma perplexa* is related closely to the approximately contemporaneous type species, *N. ornata* Popov, from Kazakhstan, which differs mainly in having a ventral valve that is less apsacline and less conical; the H/W ratio is 70% in one ventral valve of *N. ornata* Popov (1980, p. 102), compared with 122% in one valve of similar size of *N. perplexa*. *N. perplexa* differs from *N. simplex* in having a strongly apsacline ventral valve, and a more complex median septum.

Occurrence. – *Numericoma perplexa* is the most common species in the Viru sequence studied here. However, the range is short; it is restricted to the Furudal Limestone of Dalarna (Figs. 9A–B), and in Västergötland it ranges from the Gullhøgen Formation to the Ryd Limestone (Fig. 8B–C). On Öland the Källa and Furudal limestones have also yielded specimens.

Numericoma? *spinosa* (Biernat, 1973)

Figs. 33, 89, 90, 93

Synonymy. – □v*1973 *Ephippelasma spinosum* n.sp. – Biernat, p. 96, Pl. 23, 24:9, 26. □non 1975 *Ephippelasma spinosum* Biernat, 1973 – Krause & Rowell, p. 61, Pl. 8:7–22, 10:1–4, 7, 8, 11:2. □v?1978 *Ephippelasma spinosum* Biernat, 1973 – Bednarczyk & Biernat, p. 309, Pl. 21:1–13.

Fig. 88. Ontogeny of *Numericoma perplexa* sp. nov. □A. Interior of an early brephic dorsal valve; Gullhøgen Limestone (sample GB84-1-13); Br132631, ×225. □B. Interior of a brephic dorsal valve; Gullhøgen Limestone (sample GB84-2-11); Br132702, ×172. □C. Interior of a late brephic dorsal valve; Gullhøgen Limestone (sample GB84-2-7); Br132656, ×156. □D. Interior of a juvenile dorsal valve; Furudal Limestone (sample D60-220); Br128781, ×126. □E. Anterior view of the (left-handed) median septum of D; ×563. □F. Interior of an adult dorsal valve; Gullhøgen Limestone (sample GB84-2-11); Br132735, ×76. □G. Anterior view of the (symmetric) median septum of F; ×246. □H. Anterior view of a (left-handed) dorsal median septum; Furudal Limestone (sample D60-220); Br128658, ×276. □I. Oblique anterior view of a (right-handed) dorsal median septum; Furudal Limestone (sample D60-221); Br128768, ×307. □J. Posterior view of an early brephic complete shell; Gullhøgen Limestone (sample GB84-2-11); Br132730, ×229.

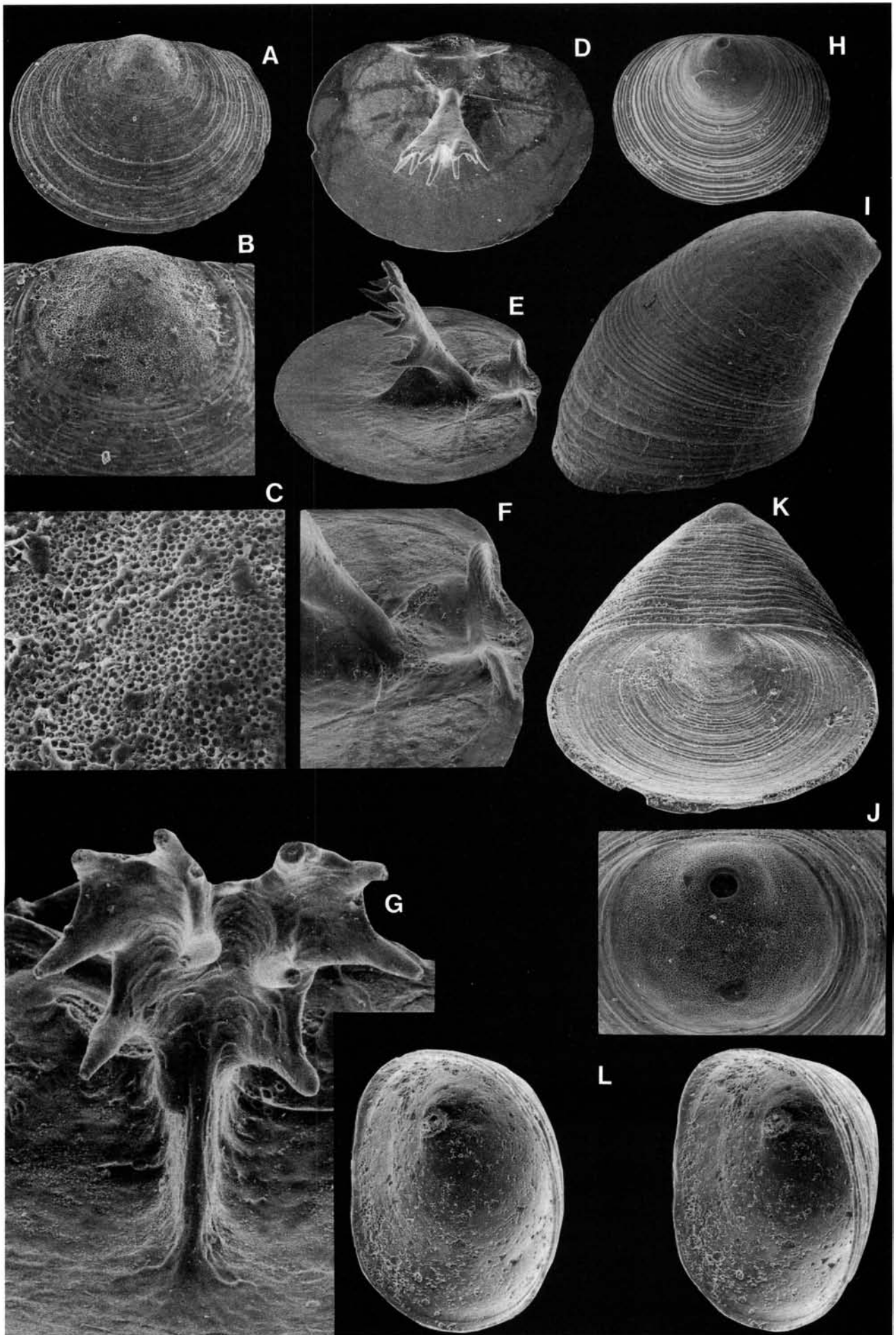
Holotype. – Brachiopod Type no. XV/12z (PAN, Warsaw), ventral valve, Biernat 1973, Pl. 23:11, from the Llanvirn of the Ketrzyn IG-1 core (1595.5 m), northern Poland.

Material. – Figured; Br133609f (section), Br128851 (W 0.59, L 0.46), Br128850 (W 0.64, L 0.51), Br128894 (W 0.48, L 0.39, H 0.23), Br128844 (W 0.71, L 0.54, H 0.62), Br128847 (W 0.73, L 0.54, H 0.50), Br128854 (W 0.56, L 0.42, H 0.45), Br128890 (W 0.27, L 0.25), Br128852 (W 0.42, L 0.36), Br128853 (W 0.50, L 0.39), Br128858 (W 0.67, L 0.54). Total of 1306 dorsal valves, 730 ventral valves and 14 complete shells.

Diagnosis. – Ventral valve catacline to apsacline, lacking exterior pedicle tube. Dorsal valve with pseudointerarea narrow and long. Dorsal median septum comparatively short, complex and very spinose, approaching bilateral symmetry.

Description of the Swedish material. – The valves average 80% as long as wide (OR 68–92%; $N=48$; Tables 19, 20); the ventral valve 54% as high as wide (Table 19); it is catacline to slightly apsacline, with the maximum height at the umbo (Fig. 89H, K). Some gerontic ventral valves are strongly apsacline, with the maximum height slightly anterior to the umbo. In lateral profile the outline of the anterior surface of the ventral valve is strongly convex, whilst the posterior surface is concave (Fig. 89I). The ventral pseudointerarea has a poorly defined intertrough (Fig. 89K). There is no exterior pedicle tube (Fig. 89J), but the circular foramen continues as a short interior tube, buttressed by a poorly developed median septum (Fig. 89L). The dorsal valve is flattened in lateral profile (Fig. 89E); it has a narrow pseudointerarea, which is on average 17% as long as wide (Table 20), occupying 48% of the total width (OR 42–62%; $N=27$; Fig. 89D). The propareas are narrow and anacline, and the median groove is wide and deep (Fig. 89E–F). Directly anterior to the pseudointerarea there is a raised area (Fig. 89F). The median septum is strongly spinose (Fig. 89D), originating about 0.10 mm from the posterior margin (Table 20); it is relatively high, with a maximum HS/W ratio of 50%, forming 64% of the total length (OR 54–72%; $N=26$). The maximum height of the septum is at about the centre of the valve (Fig. 89E); the upper surface (the surmounting plate) is flattened and up to 0.25 mm wide. The septum is almost bilaterally symmetrical in anterior view, and it has a short vertical plate (buttressing plate; Fig. 89G). The dorsal cardinal muscle scars are well developed, on average 60% as long as wide (Table 20; Fig. 89D). The larval shell is comparatively poorly delineated (Fig. 89B, J). The size of the larval pits varies, with the largest up to 2 μ m across (Fig. 89C). The valves are ornamented with weak fila (Fig. 89A, I).

Ontogeny. – The larval shell is relatively small, about 0.16 mm wide and 0.14 mm long. The ventral larval shell is about 0.10 mm high. During the brephic stage (W 0.16–0.27, L 0.14–0.25) the incipient dorsal median septum (LS ?–0.16) constitutes a small triangular plate with a single upper septal rod; it originates at about the centre of the valve, and is already twisted slightly to the right or to the left



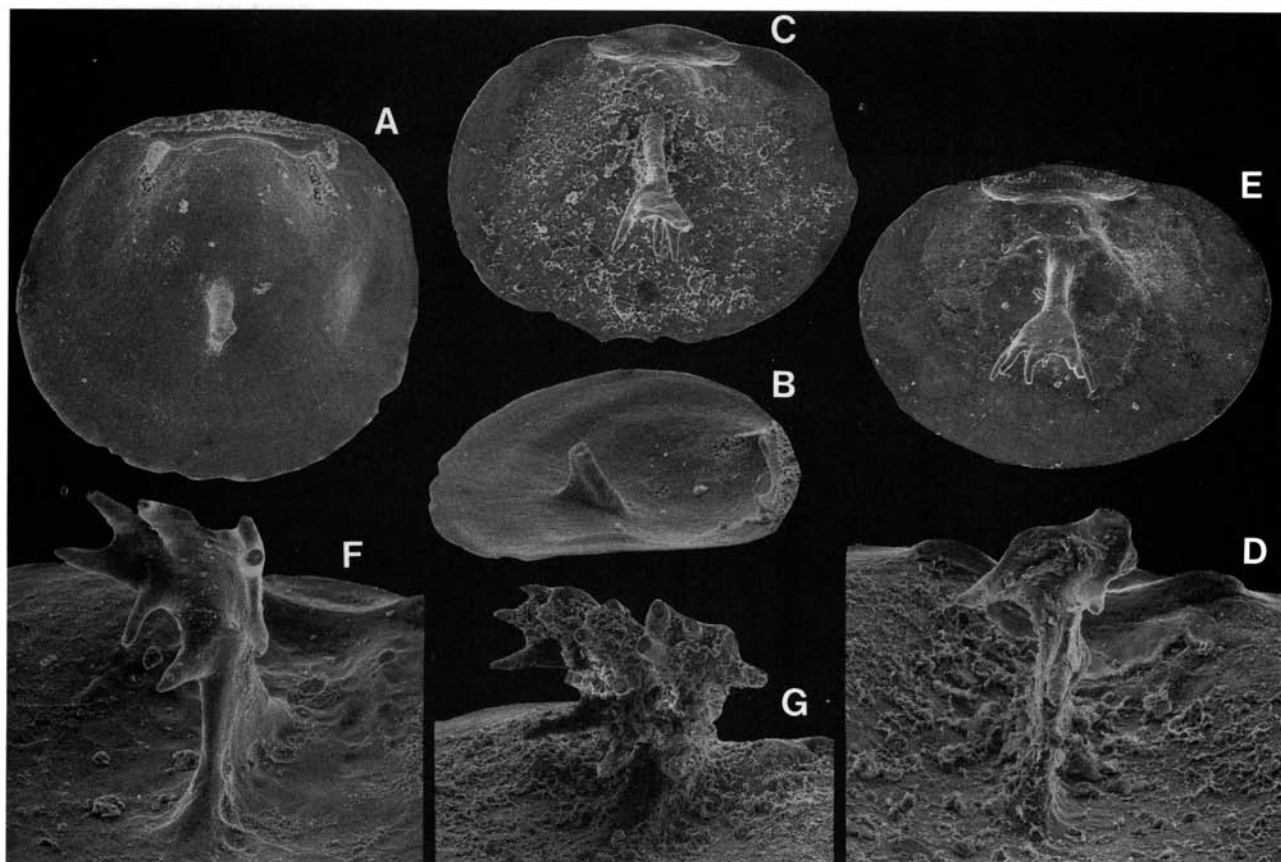


Fig. 90. Ontogeny of *Numericomma? spinosa* (Biernat, 1973). □A. Interior of brephic a dorsal valve; Våmb Limestone (sample GB84-A1); Br128890, $\times 198$. □B. Side view of A; $\times 198$. □C. Interior of a juvenile dorsal valve; Holen Limestone (sample GB81-0); Br128852, $\times 119$. □D. Anterior view of the median septum of C; $\times 269$. □E. Interior of an adult dorsal valve; Holen Limestone (sample GB81-0); Br128853, $\times 103$. □F. Anterior view of the median septum of E; $\times 248$. □G. Anterior view of the median septum of a gerontic dorsal valve; Holen Limestone (sample GB81-0); Br128858, $\times 124$.

at this stage. The incipient dorsal pseudointerarea (WI ≈ 0.13 , LI ≈ 0.3) is formed early during the brephic stage (Fig. 90A–B). The brephic ventral valve is catacline. The neanic stage (W 0.27–0.50, L 0.25–0.39) is reached when the dorsal pseudointerarea (WI 0.13–0.23, LI 0.03–0.05) is widened and develops propareas (Fig. 90C). The median septum (LS 0.16–0.26) acquires a single 90° loop (Fig. 90D). The ventral valve (H ≈ 0.26) remains catacline during the neanic stage. The adult stage (W 0.50–0.65, L 0.39–0.53) is attained about when the median septum develops a second 90° loop, opposite to the first (Fig. 90F). The dorsal cardinal muscle scars are also formed early during the adult stage (Fig. 90E). In some probably geron-

tic forms (W 0.65–0.70, L 0.53–0.56) the median septum is widened further (Fig. 90G). The gerontic ventral valves (W 0.65–0.87, L 0.46–0.62, H 0.39–0.56) are strongly apsacline (Fig. 89I) and up to 67% as high as wide (see also Fig. 46).

Discussion. – *Numericomma? spinosa* is not a typical member of the genus in that the shape of the septum approaches bilateral symmetry, but it is kept provisionally within the genus. The material of *N.? spinosa* described above is very close to the contemporaneous Polish material, figured by Biernat (1973), the main differences between them being in the ventral valve. The ventral valve figured by Biernat (Pl. 23:11) appears to be somewhat higher compared with those in the Swedish material. A second figured ventral valve (Biernat 1973, Pl. 23:12; stated as coming from the

Fig. 89. *Numericomma? spinosa* (Biernat, 1973), □A. Dorsal exterior; Holen Limestone (sample GB81-0); Br128851, $\times 80$. □B. The larval shell of A; $\times 200$. □C. The larval ornamentation of A; $\times 700$. □D. Interior of a dorsal valve; Holen Limestone (sample GB81-0); Br128850, $\times 80$. □E. Side view of D; $\times 80$. □F. Side view of the pseudointerarea of D; $\times 200$. □G. Anterior view of the median septum of D; $\times 300$. □H. Exterior of a ventral valve; Våmb Limestone (sample GB84-A1); Br128894, $\times 80$. □I. Side view of a ventral valve; Holen Limestone (sample DLK84-hol-25); Br128844, $\times 80$. □J. The larval shell of I; $\times 200$. □K. Posterior view of a complete shell; Holen Limestone (sample GB81-0); Br128847, $\times 80$. □L. Stereo-pair; ventral interior; Holen Limestone (sample GB81-0); Br128854, $\times 100$.

Table 19. *Numericomma? spinosa* (Biernat), average dimensions and ratios of ventral valves.

	W	L	L/W	H	H/W
DLK83-sä-4, 7					
<i>n</i>	15	15	15	15	15
mean	0.55	0.42	76%	0.31	54%
<i>s</i>	0.164	0.105	4.881	0.130	7.353
min	0.36	0.28	68%	0.16	44%
max	0.87	0.62	86%	0.56	64%

Table 20. *Numericoma?* *spinosa* (Biernat), average dimensions and ratios of dorsal valves.

	W	L	L/W	WI	LI	LI/WI	WM	LM	LM/WM	LS	BS
DLK83-hol-25											
<i>n</i>	33	33	33	27	27	27	4	4	4	26	26
mean	0.57	0.47	82%	0.28	0.05	17%	0.48	0.28	60%	0.30	0.10
<i>s</i>	0.075	0.052	3.614	0.051	0.010	3.460	0.026	0.041	6.557	0.044	0.013
min	0.40	0.36	76%	0.19	0.03	9%	0.45	0.23	51%	0.20	0.09
max	0.70	0.56	92%	0.34	0.06	26%	0.50	0.29	66%	0.37	0.14

Volkhovian Stage at Sukhrumägi quarry (Tallinn, Estonia, U.S.S.R.) is different from the Polish species in having a very distinct intertrough and a posteriorly directed pedicle foramen. The lower Whiterock material from Nevada, assigned to *N.?* *spinosa* by Krause & Rowell (1975), is in all probability a new species of *Numericoma*; it differs from the Polish and Swedish material in having (1) a wider and shorter dorsal pseudointerarea (average LI/WI ratio 11% in Table 25; as compared with 17% in *N.?* *spinosa*), (2) a longer median septum (average LS/L ratio 74% in Table 25; as compared with 64% in *N.?* *spinosa*), and (3) a septum that is of the asymmetrical *Numericoma*-type. Some yet undescribed species resembling *N.?* *spinosa* are present in the Lower Ordovician sequence of Sweden (Holmer, unpublished).

Occurrence. – In Sweden *Numericoma?* *spinosa* is abundant in the Lower Ordovician Holen Limestone of Dalarna and Västergötland, and in both districts it ranges into the Viru sequence. It is absent from the Segerstad Limestone of Dalarna and Öland, but reappears in the Skärlov Limestone and ranges up into the Seby Limestone (Fig. 9A). In Västergötland it ranges from the Våmb to the Skövde limestones, and occurs questionably also in the lowermost Gull-

högen Formation (Fig. 8A–B). In Jämtland there is a questionable record from the Segerstad Limestone (sample J70-167).

Genus *Ephippelasma* Cooper, 1956

Type species. – Original designation; *Ephippelasma minutum* Cooper, 1956, p. 261, from the Middle Ordovician (*Pygodus anserinus* Biozone) Pratt Ferry beds, Pratt Ferry, Alabama, U.S.A. Some topotypes (stored in the U.S. National Museum, Washington) are figured herein (Fig. 91).

Diagnosis. – Ventral valve highly conical, catacline to apsacline with intertrough; commonly with interior pedicle tube. Dorsal valve with bilaterally symmetrical median septum, having single right- or left-handed 180° loop.

Species assigned. – *Ephippelasma minutum* Cooper, 1956; *E. intutum* Popov, 1975.

Discussion. – Following Popov (*in* Nazarov & Popov 1980), the concept of the genus has been restricted to forms with a bilaterally symmetrical median septum. It appears to have been derived from a *Numericoma*-like stock. *Ephippelasma* (*sensu stricto*) appears at approximately the same level, at

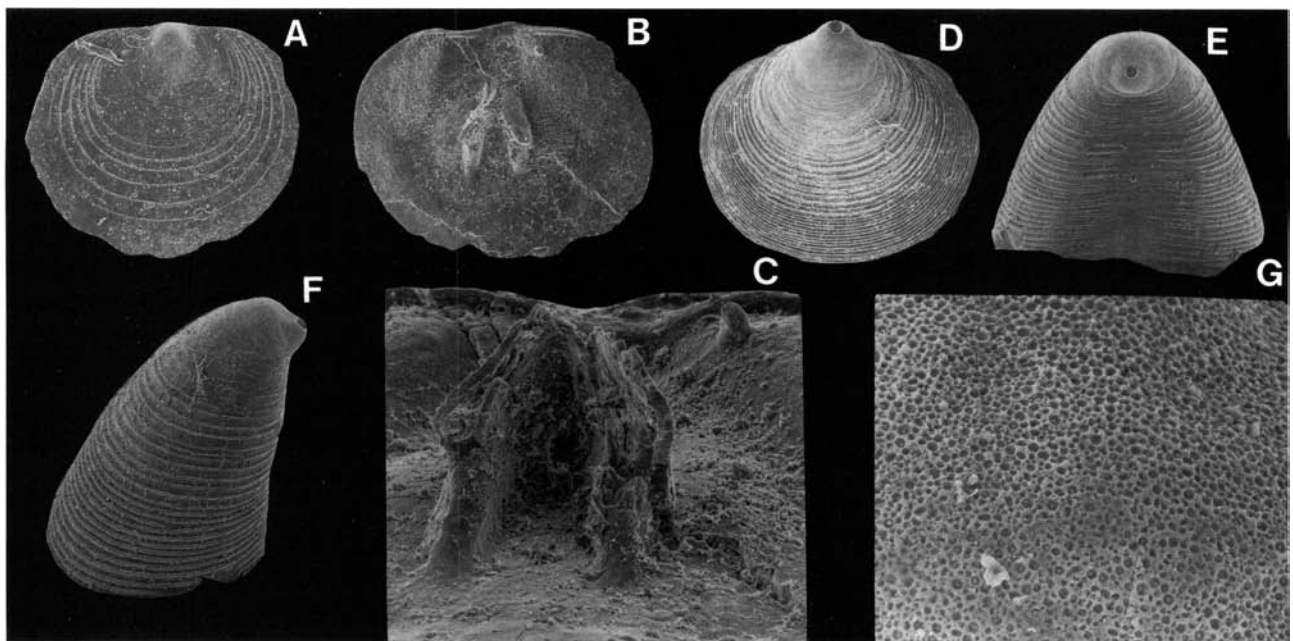


Fig. 91. *Ephippelasma minutum* Cooper, 1956, Pratt Ferry Limestone (*Pygodus anserinus* Biozone), Pratt Ferry, Alabama (all illustrated specimens from the U.S. National Museum, Washington). □A. Dorsal exterior; ×53. □B. Interior of a dorsal valve; ×53. □C. Anterior view of the broken median septum of B; ×127. □D. Ventral exterior; ×53. □E. Posterior view of D; ×53. □F. Side view of D; ×53. □G. The larval ornamentation of D; ×530.

about the upper Llandeilo–lower Caradoc (that is, the *Pygodus anserinus* Biozone), in (1) southern Appalachians (type species from the Pratt Ferry beds), (2) Kazakhstan (*E. intutum* Popov, 1975 from the upper Tselinograd Stage), and (3) Baltoscandia (*E. minutum* from the upper Furudal to lowermost Dalby limestones). An unnamed Upper Ordovician species of *Ephippelasma* has been described from the Ashgill Dulankara Stage of Kazakhstan (Popov 1980, p. 99), and by Wright (1963, p. 240) from the Cautleyan of Ireland.

Ephippelasma minutum Cooper, 1956

Figs. 32, 78D–E, 91, 92, 93

Synonymy. – □1956 *Ephippelasma minutum* Cooper, new species – Cooper, p. 261, Pl. 17A:1–14.

Holotype. – USNM no. 116821a (U.S. National Museum, Washington), complete shell, Pl. 17A:1–3, from the Pratt Ferry beds, Pratt Ferry, Alabama, U.S.A.

Material. – Figured; Br132430b (section), Br132430c (section), Br128652 (damaged), Br128700 (W 0.57, L 0.46, H 0.70), Br128649 (W 0.65, L 0.54), Br132489c (W 0.67, L 0.53), Br132489b (W 0.60, L 0.50), Br132489a (W 0.71, L 0.45, H 0.65). Total of 581 dorsal valves, 154 ventral valves and 8 complete shells.

Diagnosis. – See Cooper (1956, p. 261).

Description of Swedish material. – The valves average 81% as long as wide (OR 74–86%; $N=22$; Tables 21, 22). The ventral valve is catacline to apsacline, on average 92% as high as wide (Table 21), with the highest point slightly anterior to the umbo (Fig. 92F, J). In lateral profile the posterior surface of the ventral valve is flattened, whereas the anterior surface is convex. The intertrough is poorly defined (Fig. 92G). The short exterior pedicle tube (Fig. 92F–H) continues internally. In lateral profile the dorsal valve is strongly convex (Fig. 92E). The dorsal pseudointer-

area is on average 12% as long as wide (Table 22), extending 55% of total width (OR 46–63%; $N=18$). The median groove is relatively wide (Fig. 92B–C); the propareas are anacline to catacline (Fig. 32D, 92E). The median septum originates about 0.14 mm from the posterior margin (Table 22), and extends 63% of the total length (OR 49–70%; $N=18$). The septum is relatively high (HS/W ratio about 50–60%); in anterior view it is bilaterally symmetrical and forms a single 180° loop (Figs. 32, 92B–E), which is invariably three-pronged (Fig. 92B, I). The dorsal cardinal muscle scars are distinct, on average 54% as long as wide (Table 22; Fig. 92C). The valves are ornamented with closely spaced, minute fila (Fig. 92A, F). The larval shell is poorly delineated (Fig. 92K, H), but with a distinct pitting, where the pits are of varying size, up to 2 µm across (Fig. 91G). The ontogeny mainly follows that described for *Numericomma perplexa*. The shell structure is described above (p. 47, Fig. 32).

Discussion. – The ventral valves of *Ephippelasma minutum* illustrated by Cooper (1956, Pl. 17A:1–6; see also Fig. 91D–F) agree completely with those from Sweden. The dorsal valves illustrated by Cooper (Pl. 17A: 7–14) differ slightly in having (1) a sulcate valve, (2) a shorter pseudointerarea, and (3) a shorter median septum originating close to the posterior margin. However, a large collection of topotypes (isolated from samples of Pratt Ferry beds, supplied by S.M. Bergström) of *E. minutum* show that there are virtually no consistent differences between the specimens from Alabama and Sweden (see also Fig. 91A–C); the range of morphological variation in the dorsal valves from Pratt Ferry includes forms that are indistinguishable from the material illustrated here. Consequently, the Swedish specimens, which are contemporaneous with those from Alabama, are considered to be conspecific.

Occurrence. – In Dalarna *Ephippelasma minutum* is restricted to the uppermost Furudal and lowermost Dalby limestones (Figs. 9B–C, 10).

Subfamily Biernatinae subfam. nov.

Diagnosis. – Ventral valve highly conical, apsacline; without ventral apical process, pseudointerarea, and intertrough. Dorsal pseudointerarea reduced, with poorly defined median groove. Dorsal median septum high; with septal rods, or with convex, flat or slightly concave surmounting plate.

Genera assigned. – *Biernatia* gen. nov.; *Opsiconidion* Ludvigsen, 1974 (= *Caenotreta* Cocks, 1979).

Table 21. *Ephippelasma minutum* Cooper, average dimensions and ratios of ventral valves.

	W	L	L/W	H	H/W
DLK83-fur-16					
<i>n</i>	4	4	4	4	4
mean	0.58	0.44	77%	0.53	92%
<i>s</i>	0.123	0.094	2.630	0.153	11.790
min	0.42	0.33	74%	0.33	84%
max	0.68	0.53	79%	0.70	103%

Table 22. *Ephippelasma minutum* Cooper, average dimensions and ratios of ventral valves.

	W	L	L/W	WI	LI	LI/WI	WM	LM	LM/WM	LS	BS
DLK83-fur-16											
<i>n</i>	18	18	18	18	18	18	3	3	3	18	18
mean	0.60	0.49	82%	0.33	0.04	12%	0.47	0.25	54%	0.31	0.14
<i>s</i>	0.118	0.092	3.034	0.077	0.011	2.570	0.064	0.025	8.544	0.066	0.020
min	0.42	0.36	78%	0.22	0.02	8%	0.40	0.23	45%	0.19	0.09
max	0.81	0.70	86%	0.45	0.06	19%	0.51	0.28	62%	0.42	0.16

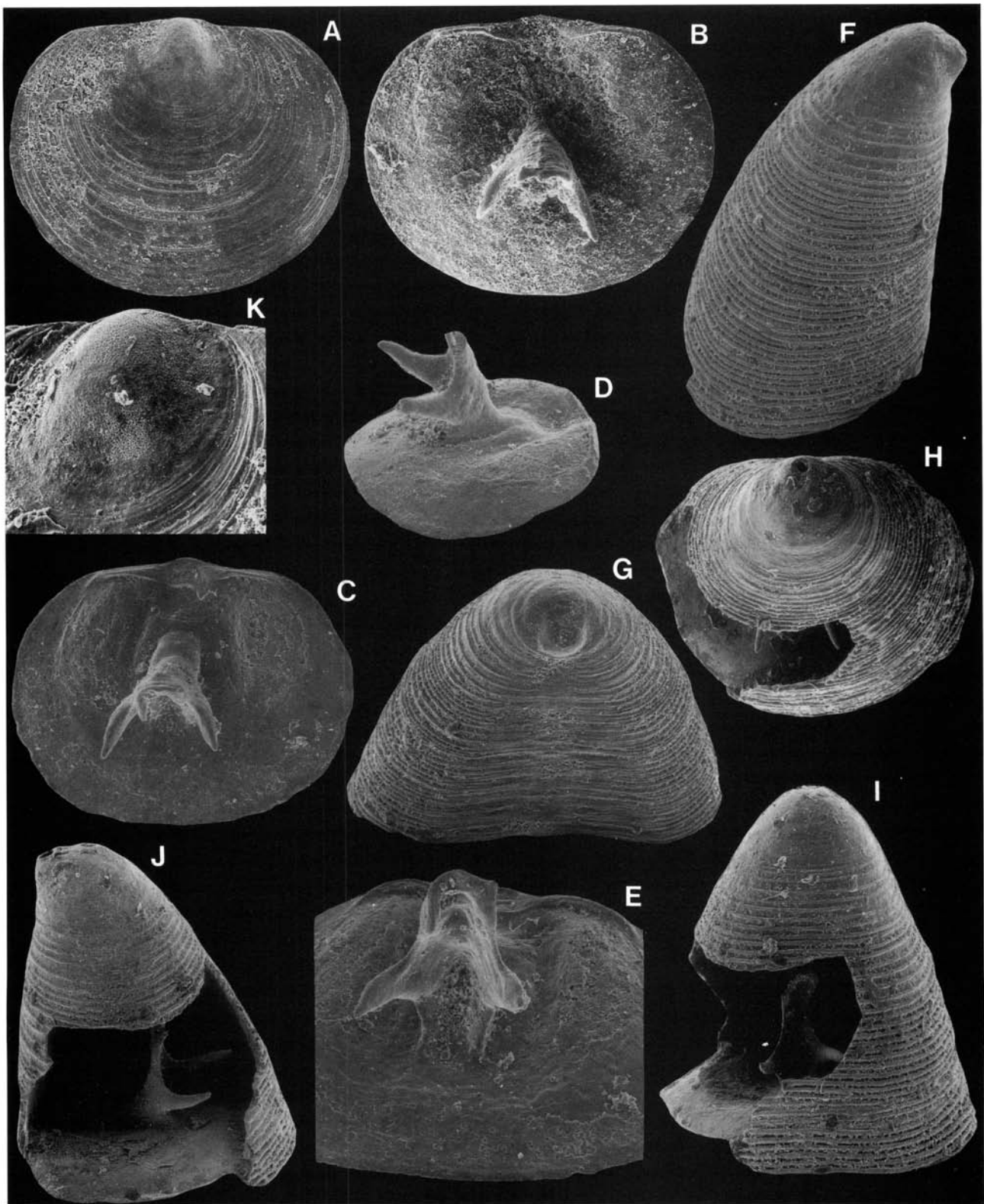


Fig. 92. *Ehippelasma minutum* Cooper, 1956. □A. Exterior of a dorsal valve; Furudal Limestone (sample D60-215); Br128649, ×85. □B. Interior of A; ×85. □C. Dorsal interior; Dalby Limestone (sample DLK83-dal-8); Br132489c, ×85. □D. Anterior view of the median septum of C; ×120. □E. Side view of a dorsal valve; Dalby Limestone (sample DLK83-dal-8); Br132489b, ×85. □F. Side view of a ventral valve; Dalby Limestone (sample DLK83-dal-8); Br132489a, ×85. □G. Posterior view of F; ×85. □H. Ventral view of a fragmentary shell; Dalby Limestone (sample D60-214); Br128700, ×85. □I. Anterior view of H; ×85. □J. Side view of H; ×85. □K. The dorsal larval shell of H; ×200.

Discussion. – Genera conforming with the above diagnosis were previously included in the Torynelasmatinae Rowell, 1965 (see also above, p. 106). However, the torynelasmatinines (*sensu stricto*) differ from members of the Biernatinae

in having (1) a widened, almost straight posterior margin, (2) a well defined, flattened, triangular ventral pseudo-interarea, (3) a proportionally less conical ventral valve (H/W ratio most frequently less than 100%), (4) a well

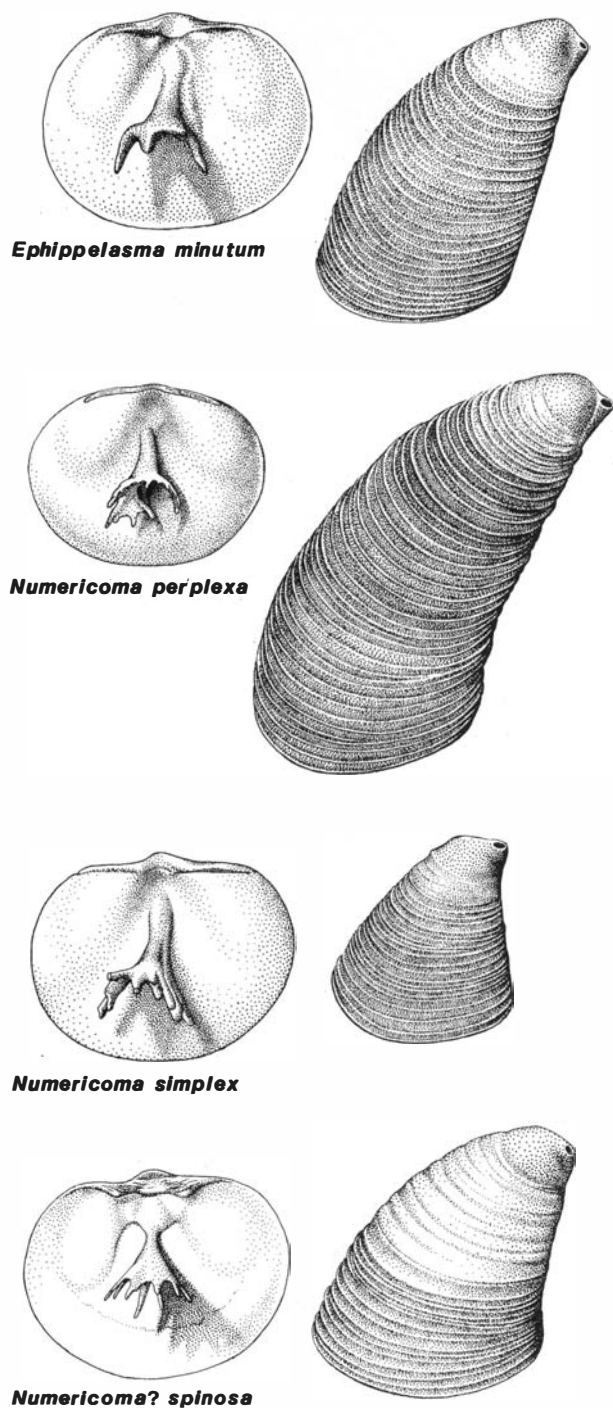


Fig. 93. Comparison between species of *Numericoma* and *Ehippelasma*. Figure prepared by Lennart Andersson (Stockholm).

developed apical process, (5) a well developed, wide dorsal pseudointerarea (WI/W ratio up to 70%), and (6) well developed and widely spaced dorsal cardinal muscle scars. Moreover, there are differences in ontogeny (Figs. 75, 97), shell structure (Figs. 28, 34), and in the ornamentation and shape of the larval shell (Figs. 74C, J–K, 95B–C, L). It appears that the biernatines are most closely related to, and possibly derived from the Ehippelasmatinae, whereas the torynelasmatines appear to have been derived from the Acrotretinae.

Genus *Biernatia* gen. nov.

Name. – In honour of the distinguished brachiopod specialist Gertruda Biernat.

Type species. – *Torynelasma minor rossicum* Goryanskij, 1969, p. 71, from the Kundan Stage, Pechory core (479.1 m), Pskov district, Russia, U.S.S.R. Some topotypes are figured in Fig. 94A–H.

Diagnosis. – Dorsal pseudointerarea very short. Surmounting plate flat, slightly concave or convex. Larval ornamentation with large pits surrounded by smaller pits.

Species assigned. – ?*Conotreta acuta* Troedsson, 1918; *Torynelasma minor* Cooper, 1956; *T. minor rossicum* Goryanskij, 1969; *T. magnum* Goryanskij, 1969; *T. rarum* Biernat, 1973; *T. forte* Popov, 1975; *T. curvatum* Holmer, 1986; *T. planum* Holmer, 1986; *Biernatia holmi* sp. nov.

Discussion. – As noted above, most of the species now referred to *Biernatia* were assigned previously to *Torynelasma*. *Opsiconidion* Ludvigsen, 1974 is closely related to *Biernatia*, but differs in having (1) a longer dorsal pseudointerarea, (2) a median septum with one or several septal rods, and (3) a larval shell with large cross-cutting pits, most commonly lacking the surrounding clusters of smaller pits. The nine species assigned currently to *Biernatia* has a range from the Tremadoc to the upper Ashgill series.

Troedsson's (1918) description of *Conotreta acuta* from the upper Ashgill of Skåne is the first record of a species assigned here to *Biernatia*. *C. acuta* has an acutely conical, *Biernatia*-like ventral valve, but the dorsal interior is not known in detail, and the species can only be referred tentatively to *Biernatia*. Cooper (1956) described *Torynelasma minor* from the Middle Ordovician Pratt Ferry beds of Alabama, and this species can be assigned unquestionably to *Biernatia*. The relationship between *T. minor* and *T. toryniferum* Cooper was discussed above (p. 107). *Torynelasma rossicum* Goryanskij, 1969, from the Lower Ordovician Kundan Stage of the Pskov district is designated type species of *Biernatia* because it is comparatively well known and well defined. Some topotype material (kindly supplied by G. Biernat) is figured herein (Fig. 94A–H). Goryanskij (1969, p. 72) recorded, but did not figure *Biernatia rossica* from the Middle Ordovician Kukrusean Stage of the Leningrad District and Estonia. This record is questioned here (see description of *B. holmi*). In addition, he described the poorly known Lower Ordovician (lower Arenig) *Torynelasma? magnum*, which has a highly conical ventral valve. However, the dorsal valve is unknown, and the species belongs only questionably to *Biernatia*. Biernat (1973) illustrated some Lower and Middle Ordovician material from Poland that was assigned to the type species. In addition, she described the Caradoc *Torynelasma rarum*, which appears to be unusually widely conical for *Biernatia*. Popov (1975) described a further member of the genus, the Middle Ordovician *Torynelasma forte* from the Tselinograd Stage of Kazakhstan. *Torynelasma curvatum* and *T. planum* were described from beds around the Viru–Harju boundary in Västergötland (Holmer, 1986), and are both typical species of *Biernatia*. In addition, *Torynelasma? sp.*, from the

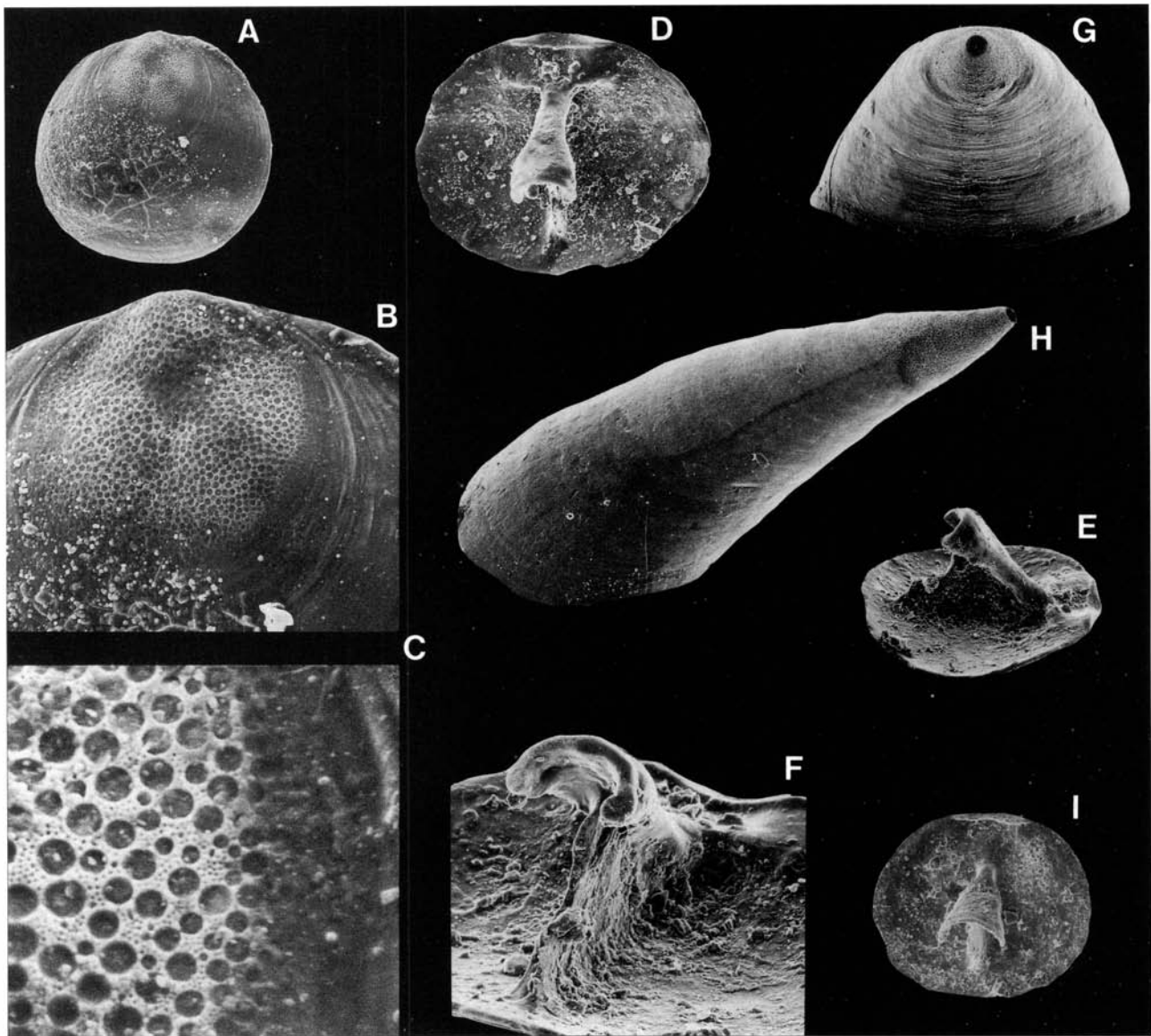


Fig. 94. □A–H. *Biernatia rossica* (Goryanskij, 1969), Kunda Stage, Pechorycore (483.35 m), Pskov, Leningrad district (material supplied by G. Biernat, Warszawa). □A. Exterior of a dorsal valve (stored in the collection of G. Biernat); $\times 90$. □B. The larval shell of A; $\times 270$. □C. The larval ornamentation of A; $\times 1400$. □D. Dorsal interior; Br133684, $\times 90$. □E. Side view of D; $\times 90$. □F. Oblique anterior view of the median septum of D; $\times 200$. □G. Anterior view of a ventral valve; Br133685, $\times 90$. □H. Side view of G; $\times 90$. □I. Interior of a juvenile dorsal valve of *Biernatia holmi* gen. et sp. nov.; Furudal Limestone (sample DLK83-fur-11); Br132391, $\times 90$.

Tremadoc of Wales (Rushton & Bassett *in* Owens et al. 1982) probably belongs to the genus, as well as two unnamed forms, *Torynelasma* sp. and ?*Conotreta* sp., described by Lockley & Williams (1981) from the Lower Ordovician of Wales.

Biernatia holmi sp. nov.

Figs. 34, 35, 94I, 95, 96, 97, ?98G–J

Name. – In honour of Gerhard Holm, who started an extensive study of Swedish ‘*Acrotreta*’.

Holotype. – Br129037, complete dorsal valve, Fig. 95D–F (W 0.88, L 0.70), from the Furudal Limestone, Kårgårde section (sample DLK83-fur-6), Dalarna.

Paratypes. – Figured; Br133613e (section), Br129043 (W 1.43, L 1.16), Br129041 (W 0.57, L 0.51), Br132905 (W 0.59, L 0.51, H 0.59), Br132505 (W 0.79, L 0.68), Br128663 (damaged), Br129038 (W 0.56, L 0.48, H 0.68), Br133675 (W 0.84, L 0.74), Br133676 (W 0.33, L 0.31), Br133677 (W 0.85, L 0.76), Br133678 (W 0.54, L 0.46, H 0.96), Br133679 (W 0.22, L 0.22), Br133680 (W 0.23, L 0.23), Br133681 (W 0.37, L 0.33), Br133682 (W 0.22, L 0.20, H 0.19), Br133683 (W 0.31, L 0.28, H 0.28), Br132391 (W 0.34, L 0.31), ?Br128667 (damaged), ?Br132532 (damaged), ?Br128699 (damaged). Total of 586 dorsal valves, 1033 ventral valves and 1 complete shell.

Diagnosis. – Ventral valve highly conical, apsacline, with H/W ratio above 100%. Dorsal valve with pseudointerarea, occupying about 33% of total width; well developed poste-

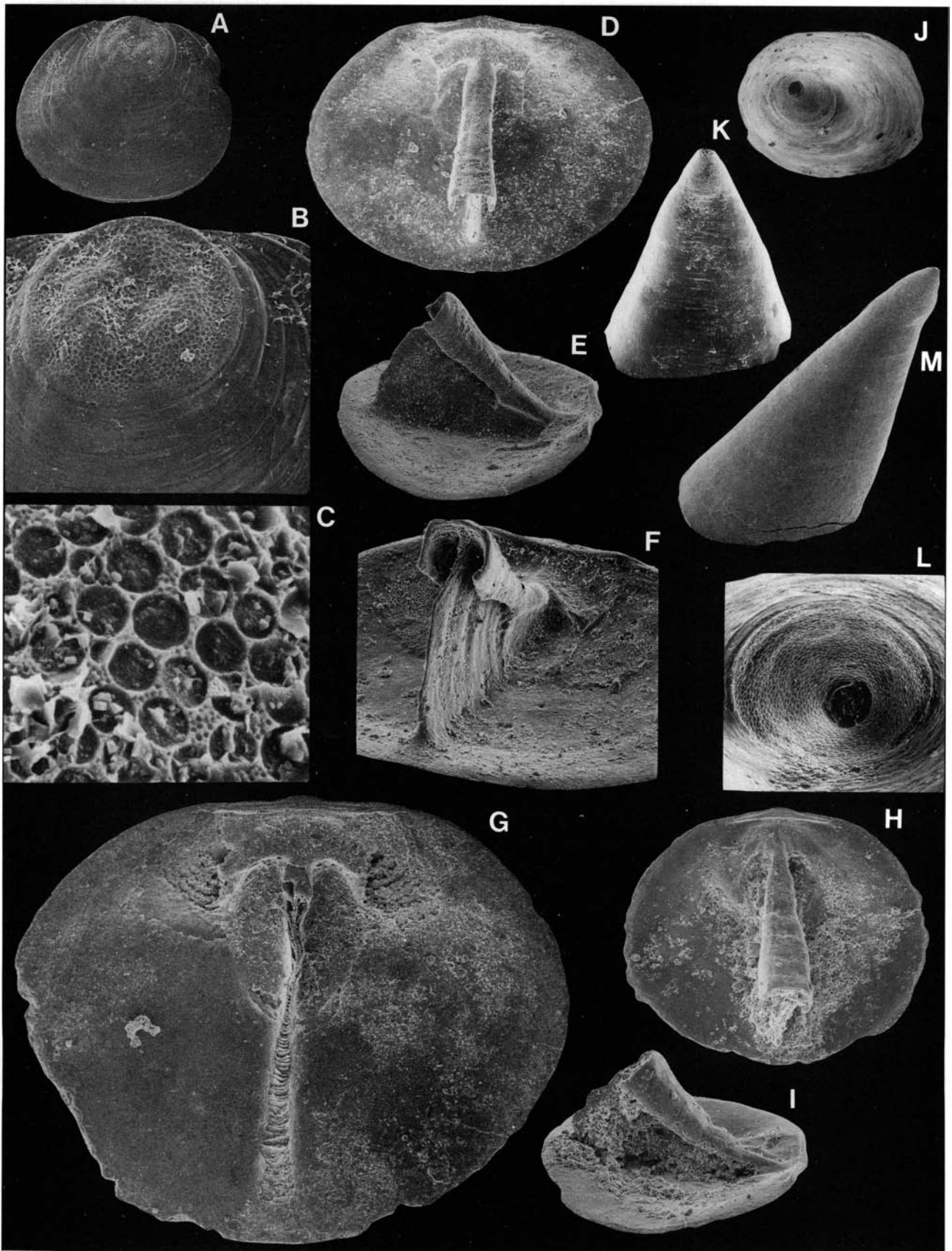


Fig. 95. *Biernatia holmi* gen. et sp. nov., □A. Dorsal exterior; Furudal Limestone (sample DLK83-fur-1); Br129041, ×65. □B. The larval shell of A; ×200. □C. Ornamentation of a ventral larval shell; Ryd Limestone (sample GB84-3-61); Br132905, ×2000. □D. Holotype; dorsal interior; Furudal Limestone (sample DLK83-fur-6); Br129037, ×65. □E. Side view of D; ×65. □F. Oblique anterior view of the median septum of D; ×100. □G. Interior of a dorsal valve; Seby Limestone (sample DLK83-se-2); Br129043, ×65. □H. Dorsal interior; Dalby Limestone (sample DLK83-dal-11); Br132505, ×65. □I. Side view of H; ×65. □J. Exterior of a ventral valve; Dalby Limestone (sample D60-218); Br128663, ×65. □K. Posterior view of J; ×65. □L. The larval shell of L; ×200. □M. Side view of a ventral valve; Furudal Limestone (sample DLK83-fur-6); Br129038, ×65.

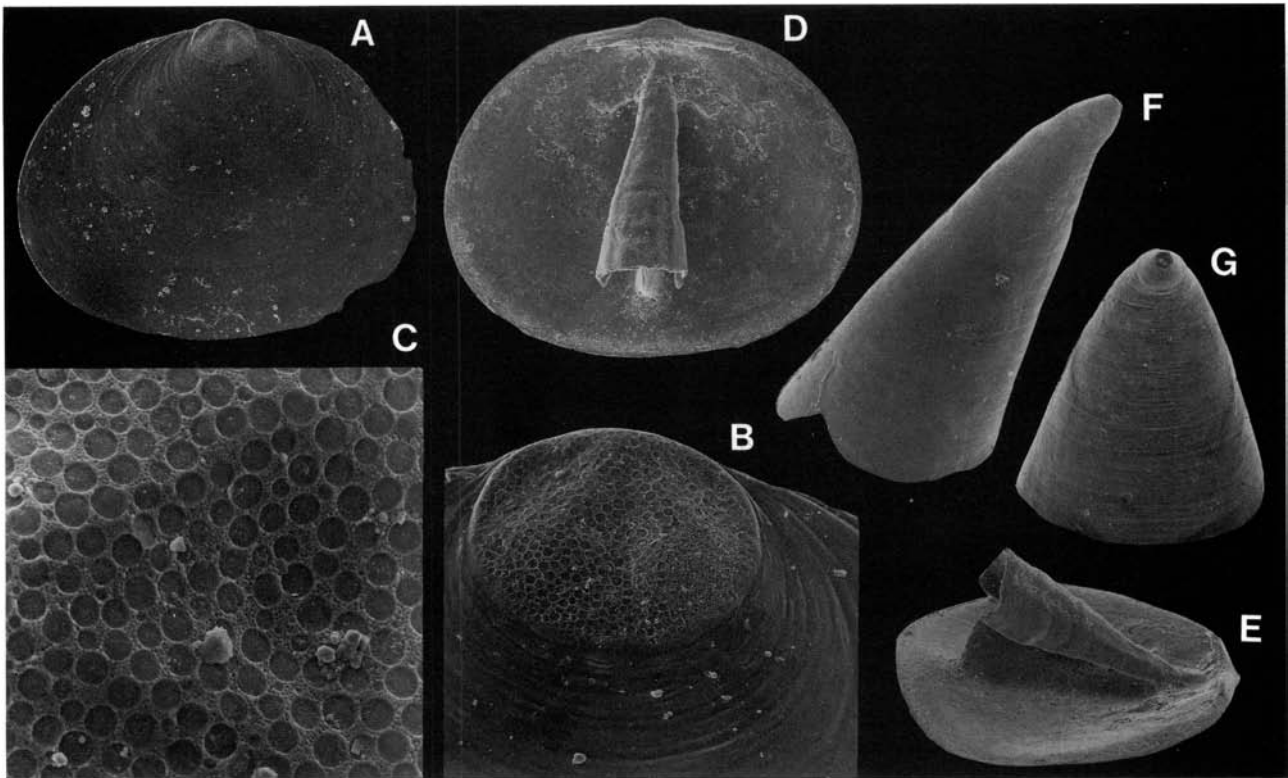


Fig. 96. *Biernatia holmi* gen. et sp. nov.; Viivikonna Formation (Kiviõli Member), Kohtla (coll. G. Troedsson), Estonia. □A. Dorsal exterior; Br133675, $\times 60$. □B. The larval shell of A; $\times 269$. □C. Ornamentation of a dorsal larval shell; Br133676, $\times 900$. □D. Dorsal interior; Br133677, $\times 60$. □E. Side view D; $\times 60$. □F. Side view of a ventral valve; Br133678, $\times 60$. □G. Posterior view of F; $\times 60$.

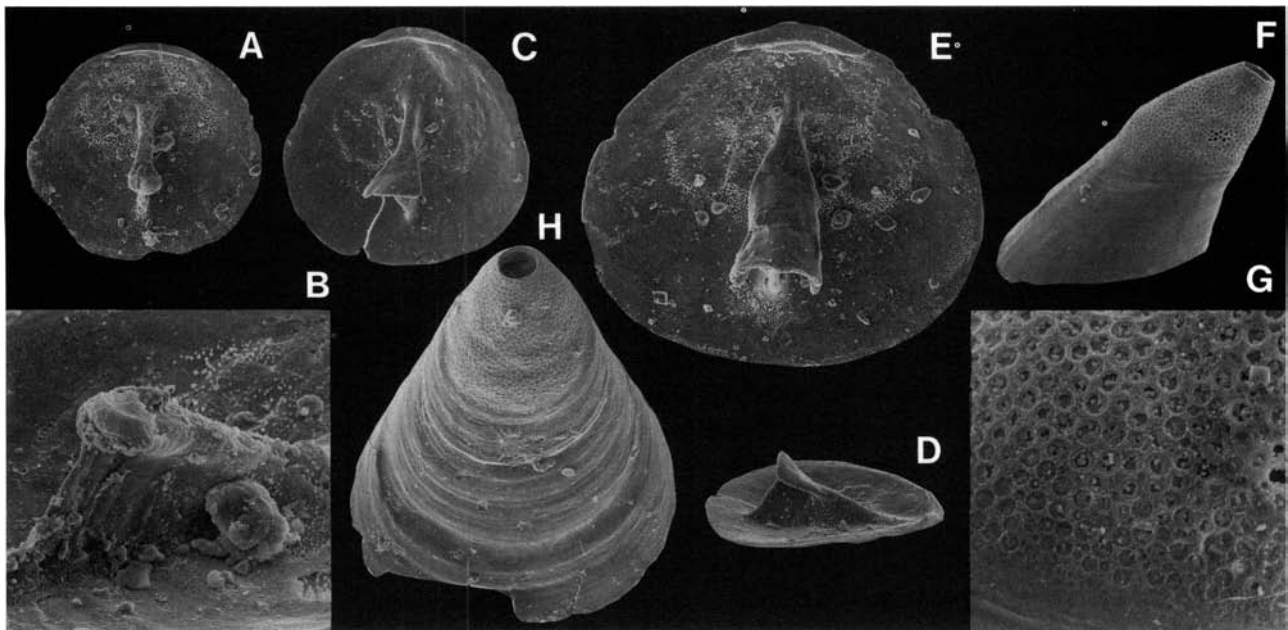


Fig. 97. Ontogeny of *Biernatia holmi* gen. et sp. nov.; Viivikonna Formation (Kiviõli Member), Kohtla (coll. G. Troedsson), Estonia. □A. Interior of an early brephic dorsal valve; Br133679, $\times 135$. □B. Oblique anterior view of the median septum of A; $\times 424$. □C. Interior of a late brephic dorsal valve; Br133680, $\times 135$. □D. Side view of C; $\times 135$. □E. Interior of a juvenile dorsal valve; Br133681, $\times 135$. □F. Side view of a brephic ventral valve; Br133682, $\times 135$. □G. Ornamentation of the larval shell of F; $\times 636$. □H. Exterior of a juvenile ventral valve; Br133683, $\times 135$.

rior platform. Dorsal median septum with strongly convex surmounting plate.

Description. – The valves average 90% as long as wide (OR 84–100%; $N=36$; Tables 23, 24); the ventral valve 105% as high as wide (OR 70–178%; $N=13$; Table 23). In lateral profile the outline of both the anterior and posterior surfaces of the ventral valve are flattened. The ventral interior is without recognizable structures (Figs. 95J–M, 96F–G). The ventral pseudointerarea is poorly defined, moderately apsacline, and lacks an intertrough (Figs. 95K, 96G). The dorsal valve is weakly sulcate (Fig. 96A) and is flattened in lateral profile (Figs. 95E, 96E). The pseudointerarea is 18% as long as wide (OR 11–25%; $N=23$; Table 24), and occupies 37% of the total width of the valve (OR 29–44%; $N=23$). The median groove is poorly defined and the propleas are anacline (Figs. 95D–E, G–I, 96D–E). The raised area directly anterior of the pseudointerarea (that is, the posterior platform) is up to 0.39 mm wide (Figs. 95D–I, 96D–E). The median septum originates about 0.07 mm from the posterior margin (Table 24), and extends 85% of the total length (OR 77–100%; $N=23$); it is high, with an HS/W ratio of about 50%, and there is a strongly convex surmounting plate which is up to 0.20 mm wide. In dorsal view it is mostly parallel-sided (Fig. 95D) or more rarely triangular in outline, widening anteriorly (Fig. 95H, 96D); the anterior end of the surmounting plate is not buttressed by the septal plate (Fig. 95F, 96E). The dorsal cardinal

muscle scars are poorly defined (Figs. 95D, G–H, 96D). The valves are ornamented with very faint fila (Figs. 95A, M, 96A, F). The dorsal larval shell is sharply delineated, with a slightly elevated outer ridge and a dorsal sulcus (Figs. 95B, L, 96B); it has large pits, up to 5.5 μm across, separated by clusters of small pits up to 500 nm across (Figs. 95C, 96C, 97G). For shell structure, see above (p. 47, Figs. 34, 35).

Ontogeny. – The larval shell is relatively small and almost circular, about 0.12 mm wide and 0.11 mm long. The ventral larval shell is about 0.11 mm high; it is apsacline and remains so throughout the ontogeny (Fig. 97F). In the subsequent brephic stage (W 0.12–0.23, L 0.11–0.23) the dorsal valve has an incipient crescent-shaped pseudointerarea (WI ?–0.09, LI ?–0.02; Fig. 97A); the median septum (LS ?–0.19) has a single upper septal rod (Fig. 97B). The brephic ventral valve (H 0.11–0.19) is invariably wider than high (H/W ratio about 86–96%; Fig. 97F). In an early part of the neanic stage (W 0.23–0.37, L 0.23–0.33) the septal rod of the median septum (LS 0.19–0.26) is thickened laterally, and forms a flat (or slightly convex) and triangular surmounting plate up to 0.08 mm wide (Figs. 94I, 97C–D). The pseudointerarea (WI 0.09–0.12, LI 0.02–0.03) is widened and develops minute propleas (Fig. 97C). In a later part of the neanic stage (W 0.37–0.48, L 0.33–0.45) the surmounting plate of the median septum (LS 0.26–0.36) becomes strongly convex; the pseudointerarea (WI 0.12–0.17) is further widened, but not elongated (Fig. 97E). The juvenile ventral valve (H 0.19–0.50) is generally less wide than high (H/W ratio about 86–112%; Fig. 97H). The adult stage (W 0.48–0.85, L 0.45–0.78) is reached when the dorsal posterior platform is developed. A few rare dorsal valves attain widths above 0.85 mm; possibly they represent the gerontic stage (Fig. 95G; see also Fig. 46).

Remarks. – Some poorly preserved dorsal valves from the Dalby Limestone are assigned only tentatively to *Biernatia holmi*. These have the dorsal pseudointerarea strongly elongated, with a wide posterior platform (Fig. 98H, J). The median septum is comparatively higher and the surmounting plate has a long, unsupported anterior end (Fig. 98I).

Discussion. – *Biernatia rossica* (Goryanskij, 1969, Pl. 12:15–21), differs from *B. holmi* in having (1) a strongly apsacline ventral valve (cf. Figs. 94H, 95M, 96F), (2) a less convex surmounting plate, and (3) a smaller maximum adult size,

Table 23. *Biernatia holmi* sp. nov., average dimensions and ratios of ventral valves.

	W	L	L/W	H	H/W
DLK83-fur-6					
<i>n</i>	5	5	5	5	5
mean	0.38	0.33	86%	0.42	109%
<i>s</i>	0.040	0.032	0.894	0.070	9.072
min	0.33	0.29	86%	0.34	94%
max	0.42	0.36	88%	0.50	119%
Kohtla, Estonia					
<i>n</i>	8	8	8	8	8
mean	0.32	0.29	89%	0.37	103%
<i>s</i>	0.115	0.091	4.241	0.260	33.298
min	0.22	0.20	84%	0.19	70%
max	0.54	0.46	97%	0.96	178%

Table 24. *Biernatia holmi* sp. nov., average dimensions and ratios of dorsal valves.

	W	L	L/W	WI	LI	LI/WI	LS	BS
DLK83-fur-6								
<i>n</i>	11	11	11	11	11	11	11	11
mean	0.47	0.42	89%	0.16	0.02	15%	0.36	0.08
<i>s</i>	0.123	0.102	2.401	0.051	0.005	4.125	0.100	0.011
min	0.28	0.26	86%	0.08	0.02	11%	0.20	0.06
max	0.68	0.59	92%	0.25	0.03	25%	0.53	0.09
Kohtla, Estonia								
<i>n</i>	12	12	12	12	12	12	12	12
mean	0.52	0.48	92%	0.20	0.04	21%	0.42	0.07
<i>s</i>	0.236	0.205	4.232	0.097	0.019	3.162	0.197	0.011
min	0.22	0.22	88%	0.09	0.02	16%	0.17	0.06
max	0.85	0.78	100%	0.37	0.08	25%	0.74	0.09

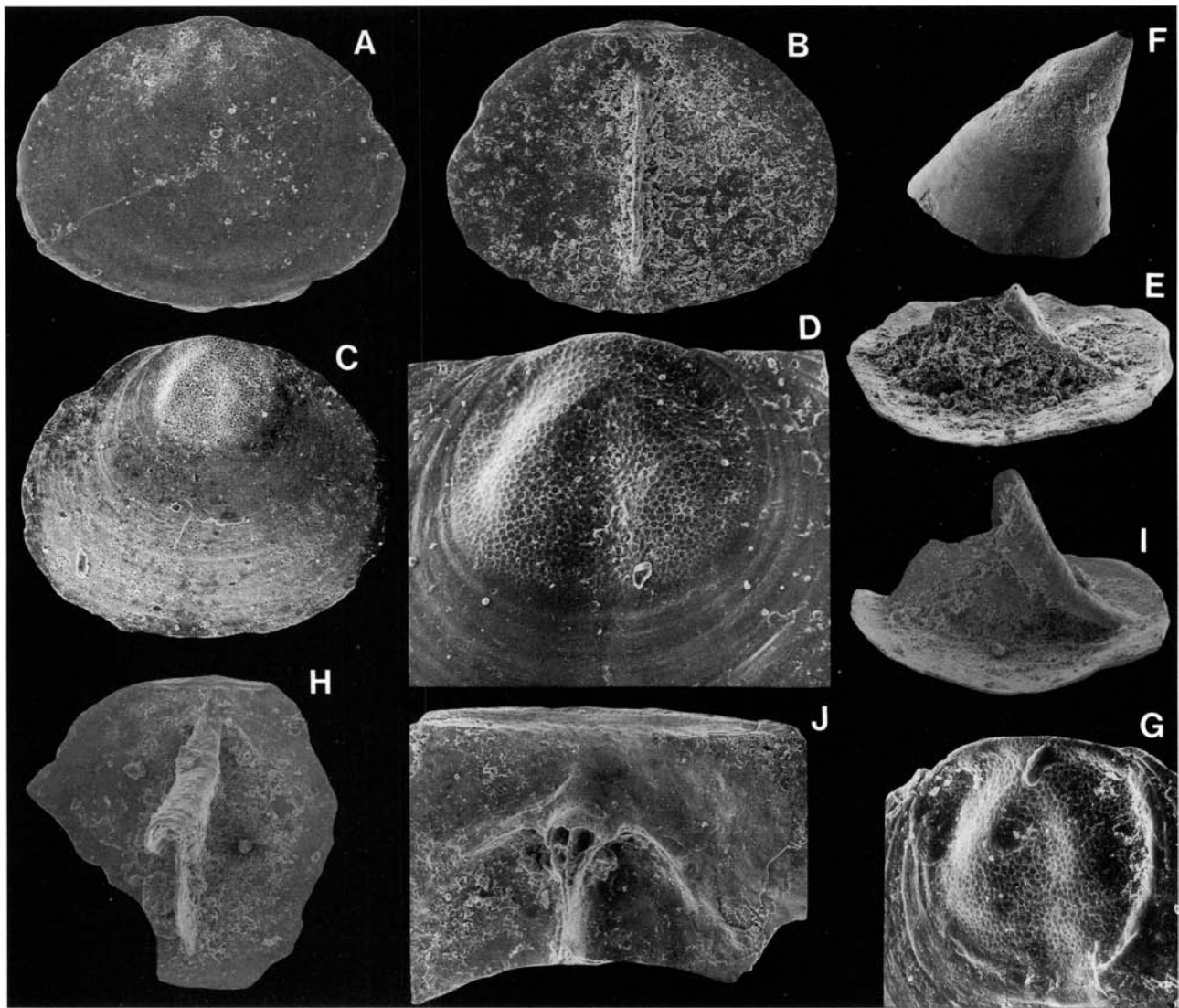


Fig. 98. □A–F. *Biernatia* sp. □A. Dorsal exterior; Holen Limestone (sample GB81-0); Br128860, ×90. □B. Interior of A; ×90. □C. Exterior of a dorsal valve; Kårgårde Limestone (sample DLK83-segk-2); Br128931, ×90. □D. Dorsal larval shell; Skärlov Limestone (sample DLK83-sä-7); Br128984, ×200. □E. Side view of the interior of a dorsal valve; Skärlov Limestone (sample DLK83-sä-4); Br128958, ×90. □F. Side view of a ventral valve; Våmb Limestone (sample GB84-A1); Br128892, ×90. □G–J. *Biernatia holmi?* gen. et sp. nov. □G. Dorsal larval shell; Furudal Limestone (sample D60-217); Br128667, ×200. □H. Interior of a dorsal valve; Dalby Limestone (sample DLK83-dal-13); Br132532, ×65. □I. Side view of H; ×65. □J. The pseudointerarea, anterior platform and broken median septum of a dorsal valve; Dalby Limestone (sample D60-201); Br128699, ×138.

around 0.40 mm in width. The Middle Ordovician, *B. minor* (Cooper, 1956, Pl. 181:57–64) differs from the Swedish species in having a slightly concave surmounting plate that is strongly arched in lateral view. Compared with *B. holmi*, the Middle Ordovician *B. forte* (Popov, 1975, Pl. 5:16–20) has a more complicated median septum. *B. holmi* is apparently related also to the Caradoc *B. rara* (Biernat, 1973, Pl. 20:12–13), but the ventral valve of this poorly known species appears to be more widely conical, with an H/W ratio around 50% (Biernat, Fig. 20:12a).

Occurrence. – *Biernatia holmi* is a common, widespread, and long-ranging species which appears in the Seby Limestone and ranges into the upper Dalby Limestone of Dalarna, (Figs. 9, 10). In Västergötland *B. holmi* was recorded from the Ryd to the Dalby limestones (Fig. 8C–D). A sample from the Kukrusean Stage of Kohtla, Estonia, also yielded numerous specimens.

Biernatia sp.

Fig. 98A–F

Material. – Figured; Br128860 (W 0.57, L 0.46), Br128931 (W 0.56, L 0.46), Br128984 (W 0.93, L 0.81), Br128958 (damaged), Br128892 (damaged). Total of 63 dorsal and 103 ventral valves.

Remarks. – Some poorly preserved specimens of *Biernatia* have the dorsal valve around 80% as long as wide (Fig. 98A–C). The dorsal pseudointerarea is narrow, and occupies less than 30% of the total width. The median septum is invariably broken, but it appears to have a convex surmounting plate (Fig. 98E). The ventral valve is apsacline (Fig. 98F). Additional, better preserved specimens are needed for a detailed taxonomic evaluation.

Occurrence. – In Dalarna and Västergötland fragments of this unnamed species are distributed through the Lower

Ordovician Hølen Limestone. It ranges from the Segerstad to the Seby limestones of Dalarna (Fig. 9A). In Västergötland it occurs in the Våmb Limestone and the Gullhögen Formation (Fig. 8A–B).

Subfamily Scaphelasmatinae Rowell, 1965.

Genus *Scaphelasma* Cooper, 1956

Type species. – Original designation; *Scaphelasma septatum* Cooper, 1956, p. 259, from the Middle Ordovician (*Pygodus anserinus* Biozone) Pratt Ferry beds, Pratt Ferry, Alabama, U.S.A.

Diagnosis. – See Krause & Rowell (1975, p. 49).

Species assigned. – *Scaphelasma septatum* Cooper, 1956; *S. septatum rugosum* Goryanskij, 1969; *S. subquadratum* Biernat, 1973; *S. lamellosum* Krause & Rowell, 1975; *S. tumidatum* Krause & Rowell, 1975; *S. anomalatum* Krause & Rowell, 1975; *S. mica* Popov, 1975; *S. bukowkense* Bednarczyk & Biernat, 1978; *S. pusillum* Popov, 1980.

Discussion. – At present nine species can be assigned to the genus, which has a range from the Arenig to the Upper Ordovician. The first illustration of a species now assigned to *Scaphelasma* appears to have been by Wang (1949, Pl. 1B:1–2), who described an unnamed form from the Upper Ordovician Maquoketa Shale of Iowa.

Information on *Scaphelasma* prior to 1975 was summarized by Krause & Rowell (1975), who also described three new species, *S. lamellosum*, *S. tumidatum*, and *S. anomalatum*, from the lower Whiterock of Nevada. The type species has been recorded from the Kundan Stage in the Pskov region by Goryanskij (1969, Pl. 12:5–11), but in all probability this material represents a new species. The Middle Ordovician *S. mica* was described by Popov (1975) from the Tselinograd Stage (Bestamak Formation) of Kazakhstan and was later recorded also from the Karakan Stage of the same area (Popov, 1980); specimens from this region are figured herein (Fig. 100). Holmer (1986) recorded some juvenile specimens assigned to *S. mica* from the upper Middle Ordovician of Västergötland. The oldest record of the genus is *S. bukowkense* Bednarczyk & Biernat, 1978, from the Arenig of Poland. The Upper Ordovician *S. pusillum* was described by Popov (1980), from the Dulankara Stage of Kazakhstan. Some Lower Ordovician specimens from the Tourmakeady Limestone of Ireland were assigned tentatively to the type species by Williams & Curry (1985).

As noted by Krause & Rowell (1975, p. 49), the distinction between *Scaphelasma* Cooper and *Rhysotreta* Cooper is sometimes unclear, due to morphological overlap. It seems that the latter is distinguished from the former mainly by (1) a more lamellose ornamentation, (2) a proportionally longer dorsal pseudointerarea (the maximum LI/L ratio is generally above 10% in *Rhysotreta*), (3) a proportionally higher ventral valve (the maximum H/W ratio is generally above 100%), which sometimes is apsacline, and (4) a more strongly developed pair of dorsal cardinal muscle scars.

Scaphelasma mica Popov, 1975

Figs. 36, 47I, 99D–N, 100, 101H–K, 103A–E, 104

Synonymy. – □v*1975 *Scaphelasma mica* Popov, sp. nov. – Popov, p. 39, Pl. 5:21–30. □v1980 *Scaphelasma mica* Popov, 1975 – Nazarov & Popov, p. 108, Pl. 25:12–14. □v?1986 *Scaphelasma mica* Popov, 1975 – Holmer 1986, p. 121, Fig. 10J–O.

Holotype. – CNIGR Museum no. 28/10696 (VSEGEL, Leningrad), complete shell, Popov, 1975, Pl. 5:21–30 (W 0.94, L 0.80, T 0.46), from the Middle Ordovician Bestamak Formation, Chingiz range, Kazakhstan, U.S.S.R.

Material. – Figured; Br132676b (section), Br132676c (section), Br132915 (W 0.45, L 0.37), Br128882 (damaged), Br132619 (W 1.08, L 0.82), Br132688 (W 1.21, L 0.90, H 0.50), Br132689 (W 1.07, L 0.84), Br132853 (damaged), Br132854 (W 0.96, L 0.79), Br132690 (W 0.99, L 0.79), Br128880 (W 1.07, L 0.81, H 0.34), Br132618 (W 0.96, L 0.60, T 0.29), Br128883 (damaged), Br128717 (W 0.67, L 0.57), Br132464 (W 0.73, L 0.54, H 0.34), Br128791 (damaged), Br132879 (W 0.22, L 0.19), Br132908 (W 0.36, L 0.28), Br132909 (W 0.39, L 0.29), Br132910 (W 0.45, L 0.37), Br128718 (W 0.36, L 0.28, T 0.16). Total of 3177 dorsal valves, 1658 ventral valves and 86 complete shells.

Diagnosis. – Ventral valve less than half as high as wide; pedicle foramen small, oval. Short groove extending from anterior margin of foramen to apex of valve. Ventral interior with or without apical process. Dorsal valve with narrow pseudointerarea and low median septum.

Description of the Swedish material. – The valves average 80% as long as wide (OR 71–88%; N=82; Tables 25, 26). The ventral valve is widely conical, less than 50% as high as wide (OR 20–50%). In lateral profile it is depressed, with the maximum height near the centre of the valve (Fig. 99J). In ventral view the ventral posterior margin is slightly concave. The pseudointerarea is strongly procline and has a distinct intertrough (Fig. 99J). The pedicle foramen is minute, oval, about 67% as wide as long (Table 25). Anterior to the apex, a short groove extends to the anterior margin of the foramen (Fig. 99J, L). The apical process is either wide and ridge-like (Fig. 99M–N), or narrow and high (Fig. 101J–K); it is bounded by a pair of anterocentral muscle scars (Figs. 99N, 101K). More rarely the process is absent. Other internal features include a pair of poorly developed cardinal muscle scars and possible traces of a pair of simple *vascula lateralia* (Fig. 99M). The dorsal valve is slightly sulcate (Fig. 99D–E). In lateral profile the umbo is strongly convex and recurved; the outline of the anterior surface of the dorsal valve is flat to slightly concave (Fig. 99F, I). The dorsal pseudointerarea is reduced, 23% as long as wide (OR 11–33%; N=47; Table 26); it forms 26% of the total width of the valve (OR 15–44%; N=47). The median groove is deeply concave, and the propleas are poorly defined (Fig. 99H, I). The median septum originates about 0.28 mm from the posterior margin (Table 26), and extends 93% of the total length (Fig. 99H); it is comparatively low with an average HS/W ratio of 32% (OR 17–39%; N=10); the anterior declivity of the septum is convex, with the postero-ven-

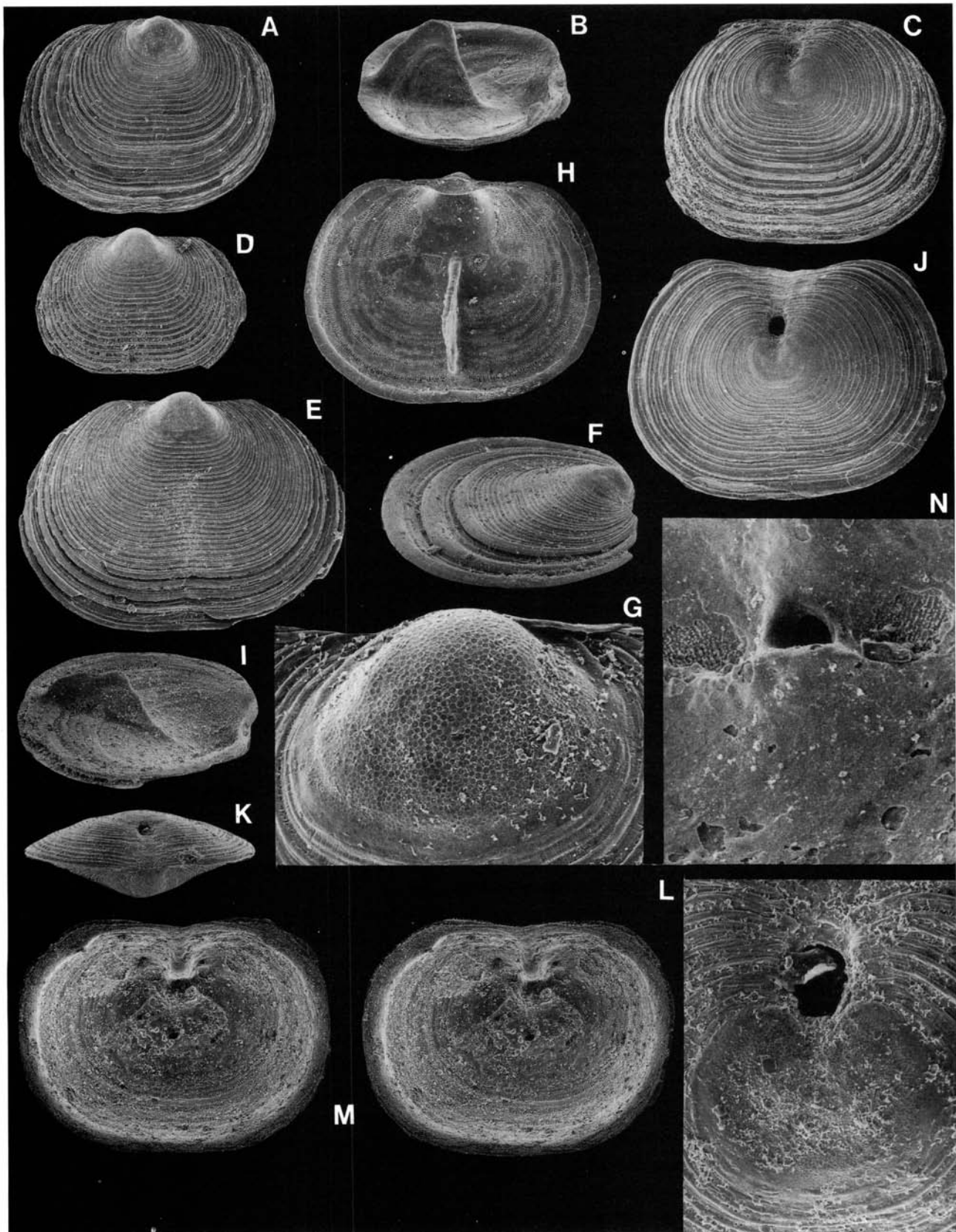


Fig. 99. □A–C. *Scaphelasma* sp. nov. a, Holen Limestone (sample GB81-0). □A. Dorsal exterior; Br128856, $\times 50$. □B. Side view of the interior of A; $\times 50$. □C. Exterior of a ventral valve; Br128857, $\times 50$. □D–N. *Scaphelasma mica* Popov, 1975. □D. Dorsal exterior; Kårgårde Limestone (sample DLK83-segk-1); Br128882, $\times 50$. □E. Exterior of a dorsal valve; Gullhøgen Formation (sample GB84-1-7); Br132619, $\times 50$. □F. Side view of a dorsal valve; Gullhøgen Formation (sample GB84-2-9); Br132689, $\times 50$. □G. Dorsal larval shell; Ryd Limestone (sample GB84-3-41); Br132853, $\times 200$. □H. Dorsal interior; Ryd Limestone (sample GB84-3-41); Br132854, $\times 50$. □I. Side view of the interior of a dorsal valve; Gullhøgen Formation (sample GB84-2-9); Br132690, $\times 50$. □J. Ventral exterior; Kårgårde Limestone (sample DLK83-segk-1); Br128880, $\times 50$. □K. Posterior view of a complete shell; Gullhøgen Formation (sample GB84-1-7); Br132618, $\times 50$. □L. The ventral larval shell of L; $\times 200$. □M. Stereo-pair; ventral interior; Gullhøgen Formation (sample GB84-2-9); Br132688, $\times 45$. □N. Detail of a ventral interior, showing the apical process and possible traces of antero-central muscle scars; Kårgårde Limestone (sample DLK83-segk-1); Br128883, $\times 200$.

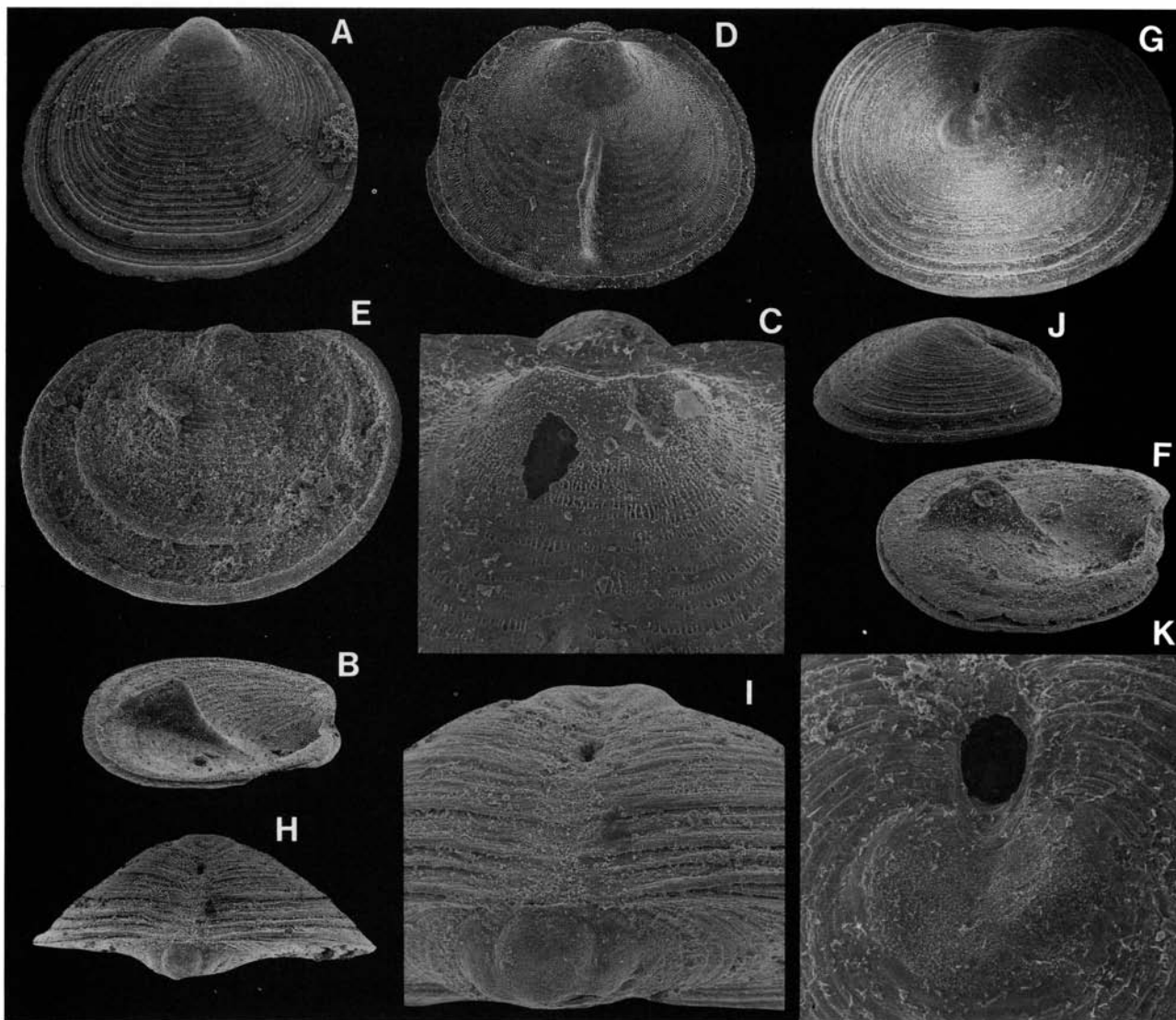


Fig. 100. *Scaphelasma mica* Popov, 1975; Karakan Formation (Middle Ordovician; coll. L.E. Popov), Karakan, Kazakhstan. □A. Dorsal exterior; Br133670, $\times 56$. □B. Side view of the interior of A; $\times 56$. □C. Detail of the pseudointerarea of A; $\times 150$. □D. Interior of a dorsal valve; Br133672, $\times 56$. □E. Dorsal exterior; Br133671, $\times 56$. □F. Side view of the interior of E; $\times 56$. □G. Ventral view of a complete shell; Br133673, $\times 56$. □H. Posterior view of G; $\times 56$. □I. Detail of H; $\times 120$. □J. Side view of a ventral valve; Br133674, $\times 56$. □K. Detail of the larval shell and pedicle foramen of J; $\times 186$.

tral outline slightly concave (Fig. 99I). The dorsal cardinal muscle scars are poorly defined, but there is a pair of anterocentral muscle scars at the posterior end of the median septum (Fig. 99H). The valves are ornamented with evenly spaced fila, about 60 per mm (Fig. 99D), and strongly developed lamellae, with up to a total of six lamellae per valve; the ornamentation starts on the anterior portion of the valve, about 0.6 mm from the posterior margin (Figs. 36A, D, 99E–F, J). The outline of the larval shell is poorly delineated; it varies in size and shape, from oval – about 0.23 mm wide and 0.17 mm long (Fig. 99G), to circular – about 0.19 mm in diameter (Figs. 99L, 101H). The larval shell has large pits, up to 4 μm across, surrounded by clusters of small pits, up to 1 μm across (Fig. 101I). The shell structure is outlined above (p. 47; Fig. 36).

Ontogeny. – In one dorsal larval shell (W 0.22, L 0.19; Fig. 103A) an incipient pseudointerarea (WI 0.11, LI 0.03) is

present; the umbo is submarginal (Fig. 103A). The ventral larval shell is flattened and has an open pedicle notch (Figs. 99L, 103E). Early in the brephic stage (W 0.22–0.34, L 0.19–0.29) the dorsal valve lacks all traces of a median septum. During the middle part of the brephic stage (W 0.34–0.45, L 0.29–0.34) an incipient median septum (LS 0.26–0.29) is developed (Fig. 103B). The brephic ventral valve occasionally has traces of a small apical process (Fig. 103C). Complete brephic shells (T ?–0.17) are about 30–40% as thick as wide (Fig. 103E). The late part of the brephic stage (W 0.45–0.51, L 0.34–0.42) is reached when the pedicle foramen is formed (that is, the posteromedian portion of the ventral mantle starts to secrete shell material posterior to the pedicle notch; Fig. 103D). The late brephic pseudointerarea is not noticeably widened; the median septum (LS 0.29–0.36) is low (HS/W ratio 17–27%). The short neanic stage (W 0.51–0.71, L 0.42–0.60) is reached when the dorsal pseudointerarea is slightly widened (WI

0.11–0.17, LI 0.03–0.04) and develops a pair of incipient propareas. The adult stage (W 0.71–1.08, L 0.60–0.82) is reached approximately when the cardinal muscle scars are developed; the pseudointerarea (WI 0.17–0.39, LI 0.04–0.08) is widened, but only slightly elongated. Some possible gerontic stages (W 1.08–1.21, L 0.82–0.90) were also found (see also Fig. 46).

Discussion. – The Swedish specimens agree closely with *Scaphelasma mica* Popov, (1975, p. 39, Pl. 5:21–30; in Nazarov & Popov 1980:108, Pl. 25:12–14) from the Middle Ordovician (Karakan and Tselinograd stages) of Kazakhstan.

Table 25. *Scaphelasma mica* Popov, average dimensions and ratios of ventral valves.

	W	L	L/W	WP	LP
DLK83-se-5					
<i>n</i>	17	17	17	15	15
mean	0.78	0.61	78%	0.04	0.07
<i>s</i>	0.120	0.099	2.410	0.010	0.013
min	0.53	0.40	73%	0.03	0.05
max	1.01	0.81	82%	0.06	0.09
DLK83-dal-4					
<i>n</i>	18	18	18	18	18
mean	0.64	0.50	81%	0.03	0.04
<i>s</i>	0.094	0.056	4.400	0.010	0.012
min	0.45	0.39	74%	0.02	0.02
max	0.71	0.62	88%	0.04	0.05

Table 26. *Scaphelasma mica* Popov, average dimensions and ratios of dorsal valves.

	W	L	L/W	WI	LI	LI/WI	LS	BS
DLK83-se-5								
<i>n</i>	16	16	16	16	16	16	15	15
mean	0.76	0.60	79%	0.17	0.05	27%	0.57	0.28
<i>s</i>	0.125	0.100	3.700	0.049	0.012	4.475	0.104	0.012
min	0.56	0.46	73%	0.09	0.03	18%	0.40	0.25
max	0.98	0.79	85%	0.25	0.06	33%	0.73	0.29
DLK83-fur-5								
<i>n</i>	13	13	13	13	13	13	13	13
mean	0.80	0.64	81%	0.19	0.05	24%	0.61	0.28
<i>s</i>	0.122	0.088	4.419	0.038	0.011	3.203	0.089	0.010
min	0.46	0.39	71%	0.09	0.02	18%	0.36	0.26
max	0.95	0.73	86%	0.28	0.06	26%	0.67	0.29
DLK83-dal-4								
<i>n</i>	18	18	18	18	18	18	18	18
mean	0.62	0.51	82%	0.18	0.04	20%	0.46	0.23
<i>s</i>	0.139	0.113	2.562	0.068	0.012	5.031	0.099	0.011
min	0.34	0.29	76%	0.11	0.02	11%	0.26	0.22
max	0.88	0.70	85%	0.39	0.06	27%	0.62	0.25

Table 27. *Scaphelasma mica* Popov, average dimensions and ratios of dorsal valves.

	W	L	L/W	WI	LI	LI/WI	LS	BS
Karakan, Kazakhstan								
<i>n</i>	7	7	7	7	7	7	7	7
mean	0.76	0.59	78%	0.19	0.03	19%	0.50	0.25
<i>s</i>	0.152	0.124	3.579	0.074	0.011	3.078	0.092	0.018
min	0.53	0.39	74%	0.09	0.02	15%	0.34	0.23
max	0.99	0.76	80%	0.33	0.05	23%	0.60	0.28

In order to facilitate comparison, some specimens from the Karakan Formation (supplied by L. E. Popov) are figured here (Fig. 100; Table 27). The two main differences between the Swedish and Kazakhstani specimens lie in the complete lack of an apical process, and a slightly larger pedicle foramen (Fig. 100K) in the type material. However, in the Swedish material these two characters are extremely variable. The differences between *S. mica* and previously described species were discussed by Popov (1975, p. 41). The three Whiterock species, *S. lamellosum*, *S. tumidatum*, and *S. anomalatum*, from Nevada (Krause & Rowell 1975), differ from *S. mica* in that all three have relatively wider pseudointerareas. Within the Swedish assemblages of *S. mica* there is variation in (1) the relative convexity of both valves, (2) the proportional size of the dorsal pseudointerarea, (3) the size and outline of pedicle foramen, and (4) the development of lamellose ornamentation. There is also some temporal variation (Tables 25, 26), but a detailed study of this is outside the scope of this paper.

Occurrence. – *Scaphelasma mica* is the second most abundant species in the Viru sequence considered in this monograph; it is also very long ranging, appearing in the Segerstad Limestone and ranging into the lower Dalby Limestone (Figs. 9, 10) of Dalarna. In Västergötland it extends from the Skövde beds to the Ryd Limestone, and there are questionable occurrences from the Våmb and the lowermost Dalby limestones (Fig. 8A–C). Holmer (1986) also recorded the species from the upper Viru of the same

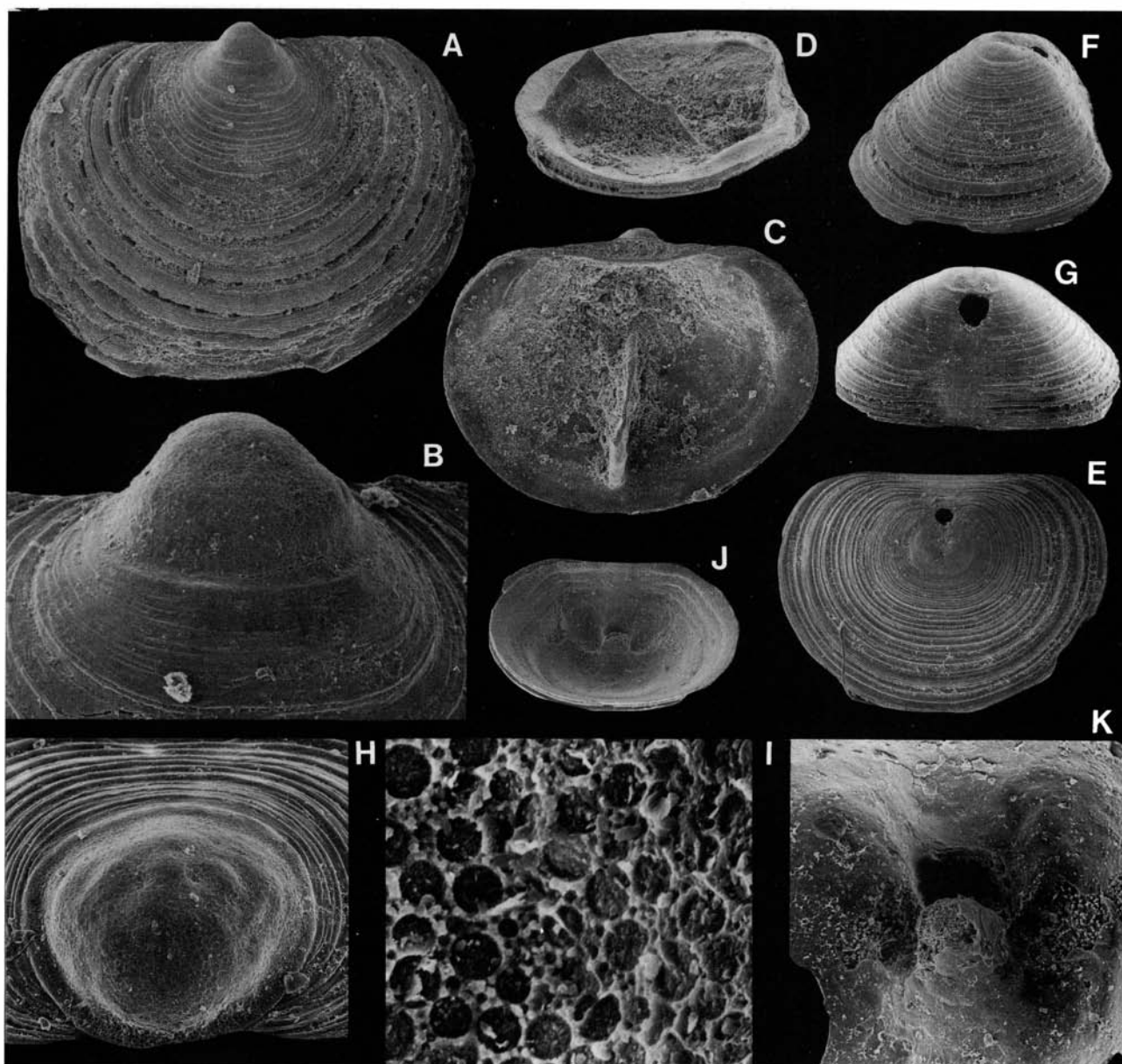


Fig. 101. □A–G. *Scaphelasma* cf. *pusillum* Popov, 1980. □A. Dorsal exterior; Dalby Limestone (sample DLK83-dal-8); Br132490, $\times 50$. □B. The larval shell of A; $\times 200$. □C. Interior of a dorsal valve; Dalby Limestone (sample DLK83-dal-8); Br132491, $\times 50$. □D. Side view of C; $\times 50$. □E. Ventral exterior; Dalby Limestone (sample DLK83-dal-8); Br132492, $\times 50$. □F. Side view of E; $\times 50$. □G. Posterior view of a ventral valve; Dalby Limestone (sample D60-205); Br128722, $\times 50$. □H–K. *Scaphelasma mica* Popov, 1975. □H. Posterior view of a dorsal larval shell; Dalby Limestone (sample D60-214); Br128717, $\times 200$. □I. Ornamentation of the larval shell of H; $\times 2000$. □J. Ventral interior; Dalby Limestone (sample DLK83-dal-4); Br132464, $\times 50$. □K. Detail of a pedicle foramen; note the apical process; Dalby Limestone (sample D60-206); Br128791, $\times 200$.

district. On Öland the species is known from the Källa Limestone. It was also found in an erratic boulder of the lower Dalby Limestone from Uppland.

Scaphelasma sp. nov. a

Figs. 99A–C, 104

Material. – Figured; Br128856 (W 0.88, L 0.68), Br128857 (W 0.93, L 0.73, H 0.50). Total of 37 dorsal and 10 ventral valves.

Description. – The valves average 81% as long as wide (Table 28). The ventral valve is highly conical, more than 50% as

high as wide (Fig. 99C). In lateral profile the dorsal valve is convex, with a slightly recurved umbo (Fig. 99A–B). The dorsal pseudointerarea is on average 18% as long as wide (Table 28), extending 37% of the total width (OR 32–40%; $N=9$). The median septum originates about 0.27 mm from the posterior margin (Table 28); it is relatively high (HS/W ratio about 40%), and extends 92% of the total length (OR 87–98%; $N=9$; Fig. 99B). The valves are ornamented with lamellae (Fig. 99A, C). The larval shell is similar to that of *S. mica*.

Discussion. – *Scaphelasma* sp. nov. a differs from *S. mica* in having proportionally (1) a higher ventral valve, (2) a

Table 28. *Scaphelasma* sp. nov. a, average dimensions and ratios of dorsal valves.

	W	L	L/W	WI	LI	LI/WI	LS	BS
GB81-0								
<i>n</i>	9	9	9	9	9	9	9	9
mean	0.73	0.60	81%	0.27	0.05	18%	0.55	0.27
<i>s</i>	0.142	0.128	3.060	0.052	0.011	4.003	0.109	0.022
min	0.56	0.45	76%	0.19	0.03	13%	0.40	0.23
max	0.98	0.84	82%	0.36	0.06	24%	0.73	0.31

higher median septum, and (3) a longer dorsal pseudo-interarea. The species has its main range in the Kundan Stage; the formal erection of a new species is postponed until it has been studied in detail.

Occurrence. – In Västergötland and Dalarna this species is restricted to the Holen Limestone (Figs. 8A, 9A).

Scaphelasma cf. *pusillum* Popov, 1980

Figs. 101A–G, 104

Synonymy. – □v cf. 1980, *Scaphelasma pusilla* [sic] Popov, sp. nov. – Nazarov & Popov, p. 109, Pl. 26:12–14.

Material. – Figured; Br132490 (W 1.30, L 1.04), Br132491 (W 1.07, L 0.82), Br132492 (W 0.93, L 0.71, H 0.36), Br128722 (W 0.84, L 0.65, H 0.34). Total of 260 dorsal valves, 21 ventral valves and 3 complete shells.

Diagnosis. – See Popov (in Nazarov & Popov 1980, p. 109).

Description. – The valves average 80% as long as wide (OR 74–92%; *N*=25; Tables 29, 30). The ventral valve is about 40% as high as wide with the highest point situated near the centre (Fig. 101F). The intertrough is wide and the ventral posterior margin is almost straight (Fig. 101E, G). The ventral larval shell has a median sulcus and a small, rounded pedicle foramen (WP/LP ratio about 80%; Table 29). The ventral interior is without recognizable structures. In lateral profile the dorsal valve is convex (Fig. 101D), with a slightly recurved umbo (Fig. 101B). The dorsal pseudo-interarea is on average 19% as long as wide (Table 30), and

Table 29. *Scaphelasma* cf. *pusillum* Popov, average dimensions and ratios of ventral valves.

	W	L	L/W	WP	LP
DLK83-dal-8, 14					
<i>n</i>	4	4	4	3	3
mean	0.67	0.53	76%	0.04	0.05
min	0.45	0.36	74%	0.03	0.04
max	0.93	0.70	80%	0.05	0.05

Table 30. *Scaphelasma* cf. *pusillum* Popov, average dimensions and ratios of dorsal valves.

	W	L	L/W	WI	LI	LI/WI	LS	BS
DLK83-dal-8, 14, 16								
<i>n</i>	21	21	21	21	21	21	21	21
mean	0.80	0.64	81%	0.34	0.05	19%	0.57	0.24
<i>s</i>	0.279	0.204	5.006	0.168	0.015	8.906	0.181	0.020
min	0.39	0.36	74%	0.11	0.02	11%	0.34	0.22
max	1.30	1.02	92%	0.62	0.09	42%	0.93	0.29

occupies 40% of the total width (OR 27–52%; *N*=21). The median groove is wide and the propareas are reduced (Fig. 101C). The median septum originates about 0.24 mm from the posterior margin (Table 30), and extends 90% of the length of the valve (OR 77–97%; *N*=21). A pair of dorsal cardinal muscle scars are sometimes present. The valves are ornamented with strongly developed, closely spaced lamellae. Adult shells have up to 9–10 lamellae, which start immediately anterior to the larval shell (Fig. 101A, E). The larval shell is similar to that of *S. mica*.

Discussion. – This material agrees closely with the Upper Ordovician *Scaphelasma pusillum* described by Popov (in Nazarov & Popov 1980) from the Dulankara Stage of Kazakhstan. Both have (1) an almost straight posterior margin, (2) a wide dorsal pseudointerarea, and (3) a comparatively high ventral valve that lacks recognizable interior structures. The Swedish species differs from true *S. pusillum* mainly in being more strongly lamellose, and in having a somewhat higher ventral valve.

Occurrence. – In Dalarna and Västergötland *Scaphelasma* cf. *pusillum* is restricted to the Dalby Limestone (Figs. 8C–D, 9B–C, 10).

Scaphelasma? *rugosum* Goryanskij, 1969

Figs. 102, 103F–H, 104

Synonymy. – □v*1969 *Scaphelasma septatum rugosum* Gorjansky subsp. nov. – Goryanskij, p. 70, Pl. 12:1–4.

Remark. – Herein elevated to species rank.

Holotype. – CNIGR Museum no. 166/9960 (VSEGEI, Leningrad), Dorsal valve, Goryanskij, 1969, Pl. 12:2 (W 0.9, L 0.6), from the Aserian Stage of the Pechory core (459.4 m), Pskov district, Russia, U.S.S.R.

Material. – Figured; Br128956 (W 1.27, L 1.01), Br128951 (W 1.27, L 0.98), Br128954 (W 0.95, L 0.71, H 0.34), Br128950 (W 0.57, L 0.45, T 0.26), Br128953 (W 0.60, L 0.46), Br128952 (0.48, L 0.39, T 0.19). Total of 225 dorsal valves, 33 ventral valves and 3 complete shells.

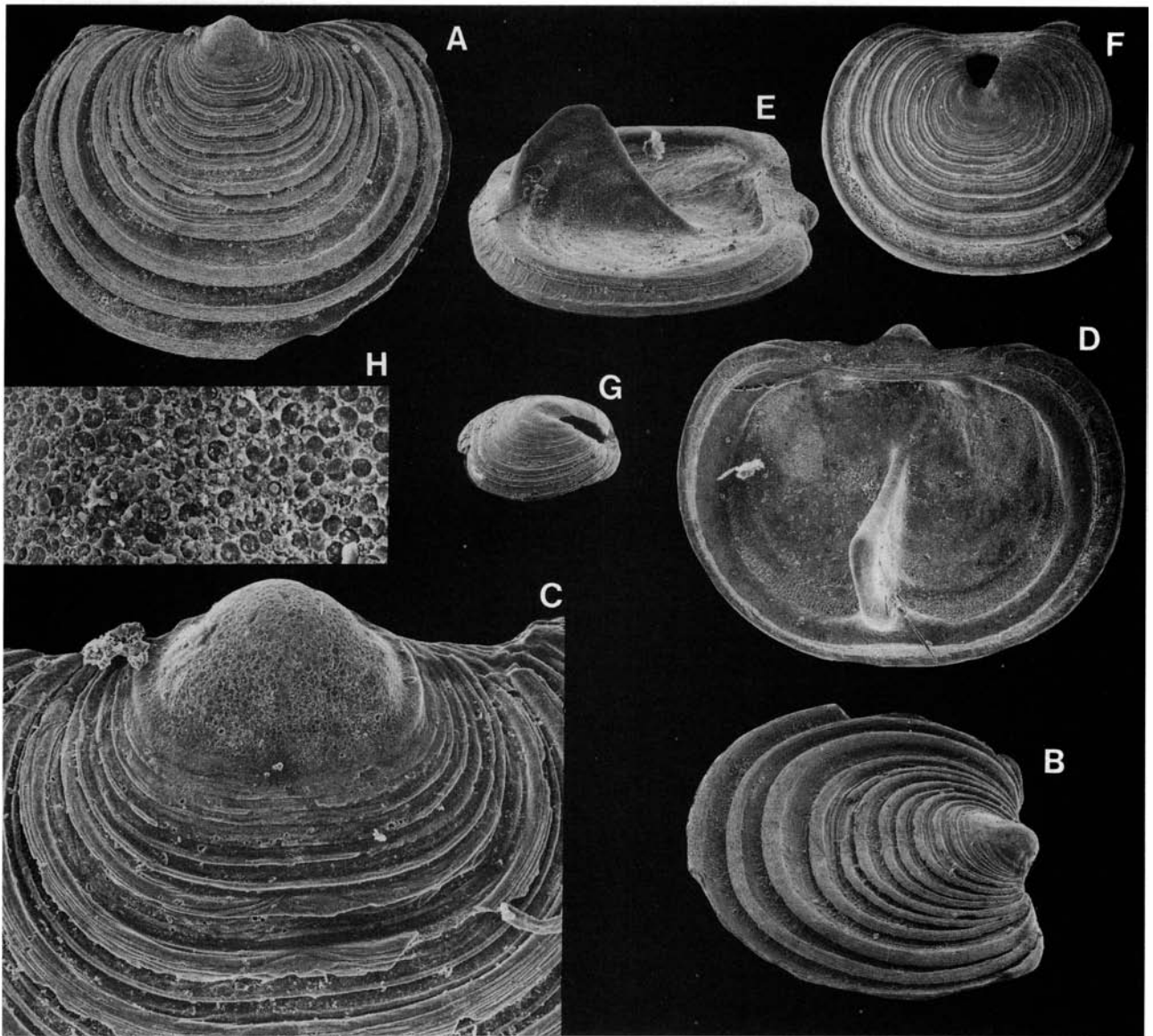


Fig. 102. *Scaphelasma rugosum* Goryanskij, 1969. □A. Dorsal exterior; Kårgårde Limestone (sample DLK83-segk-8); Br128956, $\times 50$. □B. Side view of A; $\times 50$. □C. The larval shell of A; $\times 200$. □D. Interior of a dorsal valve; Kårgårde Limestone (sample DLK83-segk-7); Br128951, $\times 50$. □E. Side view of D; $\times 50$. □F. Ventral exterior; Kårgårde Limestone (sample DLK83-segk-8); Br128954, $\times 50$. □G. Side view of a complete juvenile shell; Kårgårde Limestone (sample DLK83-segk-3); Br128950, $\times 50$. □H. Ornamentation of the ventral larval shell of G; $\times 700$.

Diagnosis. – Valves with straight posterior margin. Lamellose ornamentation with up to 11 lamellae per valve. Ventral valve with large pedicle opening, low apical process. Dorsal pseudointerarea wide and comparatively long.

Description of the Swedish material. – The valves average 78% as long as wide (OR 71–85%; $N=32$; Table 31). The ventral valve is about 30–40% as high as wide; the highest point is situated slightly subcentrally towards the posterior margin. The pedicle foramen is relatively large, up to 0.6 mm wide and long, triangular in outline, widening posteriorly (Fig. 102F–G). The interior of one ventral valve (Fig. 102F) has traces of a pair of cardinal muscle scars, as well as a low, wide and ridge-like apical process. In ventral view the ventral posterior margin is almost straight; in posterior profile the ventral pseudointerarea is triangular and lacks an intertrough (Fig. 102F). The dorsal valve is flattened in lateral

profile and has a convex, recurved umbo; the posterior margin is almost straight (Fig. 102B, E). The dorsal pseudointerarea is relatively long, undivided (maximum LI/L ratio about 15%), and on average 27% as long as wide (Table 31); in dorsal view it is triangular and occupies on average 40% of the total width (Fig. 102D). The median septum originates about 0.29 mm from the posterior margin (Table 31), extending on average 89% of the total length; it is high with a maximum HS/W ratio about 42%; the highest point is situated close to the anterior margin (Fig. 102D–E). The dorsal cardinal muscle scars are about 60–87% as long as wide; the anterocentral muscle scars are situated at the posterior end of the median septum (Fig. 102D). The valves are ornamented with evenly spaced fila superposed on strongly developed, evenly spaced lamellae, up to 0.05 mm across; the ornamentation originates immediately outside the larval shell; each valve has up to 11

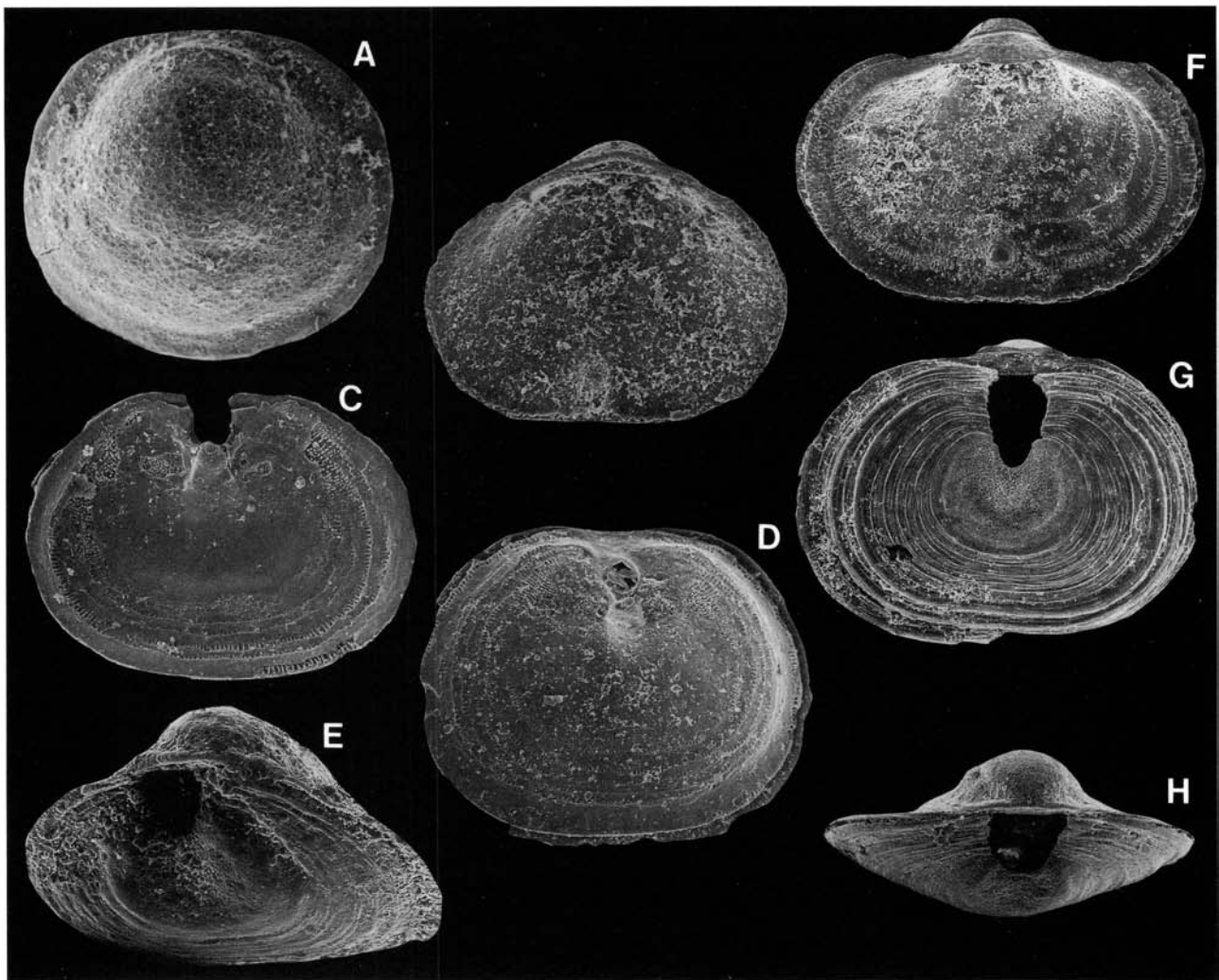


Fig. 103. □A–E. Ontogeny of *Scaphelasma mica* Popov, 1975. □A. Exterior of a dorsal larval shell; Ryd Limestone (sample GB84-3-59); Br132879, $\times 242$. □B. Interior of a juvenile dorsal valve; Ryd Limestone (sample GB84-3-61); Br132908, $\times 144$. □C. Interior of a juvenile ventral valve; Ryd Limestone (sample GB84-3-61); Br132909, $\times 135$. □D. Adult ventral interior; Ryd Limestone (sample GB84-3-61); Br132910, $\times 117$. □E. Oblique posterior view of a complete juvenile shell; Dalby Limestone (sample D60-214); Br128718, $\times 140$. □F–H. Ontogeny of *Scaphelasma? rugosum* Goryanskij, 1969. □F. Juvenile dorsal interior; Kårgårde Limestone (sample DLK83-segk-7); Br128953, $\times 90$. □G. Ventral view of a complete juvenile shell; Kårgårde Limestone (sample DLK83-segk-3); Br128950, $\times 106$. □H. Posterior view of a complete juvenile shell; Kårgårde Limestone (sample DLK83-segk-7); Br128952, $\times 106$.

lamellae (Fig. 102A, F) which are incurled downwards in lateral profile (Fig. 102B–C). The larval shell is circular to slightly oval, with an ornamentation like that of *Scaphelasma mica* (Figs. 102C, H, 103G).

Ontogeny. – The larval shell is about 0.17 mm across. The ventral larval shell has a median sulcus running towards the pedicle foramen. The posterior commissure has a pedicle notch (Figs. 102G, 103G–H). During the brephic stage (W

0.17–0.51, L 0.17–0.40) the dorsal valve lacks a median septum. The brephic pseudointerarea (WI \approx 0.16, LI \approx 0.06) occupies about 15% of the total length; the LI/L ratio varies between 8 and 15% throughout ontogeny. The brephic shells have up to three lamellae. The neanic stage (W 0.51–0.70, L 0.40–0.51) is reached when the dorsal pseudointerarea (WI 0.16–0.19, LI 0.06) is widened and develops a pair of propareas; the dorsal median septum (LS 0.37–0.48) is formed (Fig. 103F). At about the point when

Table 31. *Scaphelasma? rugosum* Goryanskij, average dimensions and ratios of dorsal valves.

	W	L	L/W	WI	LI	LI/WI	LS	BS
DLK83-segk-3, 4, 7, 8								
<i>n</i>	28	28	28	28	28	28	18	18
mean	0.66	0.51	78%	0.26	0.07	27%	0.54	0.29
<i>s</i>	0.290	0.225	3.848	0.140	0.028	8.150	0.180	0.022
min	0.29	0.25	71%	0.17	0.02	12%	0.33	0.26
max	1.30	1.04	85%	0.70	0.16	42%	0.90	0.33

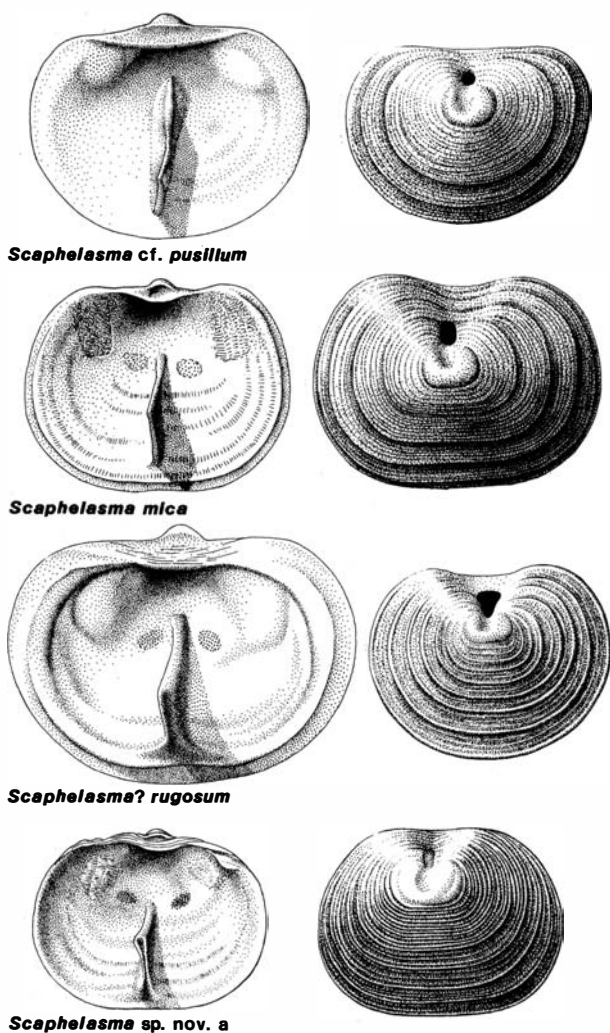


Fig. 104. Comparison between species of *Scaphelasma*. Figure prepared by Lennart Andersson (Stockholm).

the shell is 0.57–0.60 m wide the posteromedian sector of the ventral valve develops a pedicle foramen (Fig. 103G). The neanic shells have up to five lamellae. The adult stage (W 0.70–1.19, L 0.51–0.85) is reached when the dorsal cardinal muscle scars are formed and the shells have about seven lamellae. Some possible gerontic individuals (W 1.19–1.30, L 0.85–1.04) have clearly raised dorsal cardinal muscle scars, and up to 11 lamellae.

Discussion. – The Swedish material of *Scaphelasma? rugosum* is closely similar to the type specimens from the Aserian Stage of the Pskov district. *S.? rugosum* is assigned tentatively to the genus as it differs from most other members in having (1) a more lamellose ornamentation, with incurled lamella, (2) a proportionally longer dorsal pseudointerarea, and (3) a pair of well developed dorsal cardinal muscle scars; these characters are more suggestive of *Rhysotreta* Cooper. However, all described species of *Rhysotreta* have a highly conical ventral valve, generally more than 100% as high as wide. In contrast the H/W ratio of the ventral valve of *S.? rugosum* is only up to 40%.

Occurrence. – In Dalarna and on Öland *Scaphelasma? rugosum* is restricted to the Segerstad Limestone (Fig. 9A). The

species is also known from this formation in Jämtland (samples J70–165, J69–35, 37, 40–42).

Family Eoconulidae Rowell, 1965.

Genus *Eoconulus* Cooper, 1956

Type species. – Original designation; *Eoconulus rectangulatus* Cooper, 1956, p. 282, from the Middle Ordovician (*Pygodus anserinus* Biozone) Pratt Ferry beds, Pratt Ferry, Alabama, U.S.A.

Diagnosis. – See Krause & Rowell (1975, p. 64).

Species assigned. – *Eoconulus rectangulatus* Cooper, 1956; *E. transversus* Wright, 1963; *E. cryptomyus* Goryanskij, 1969; *E. antelopensis* Krause & Rowell, 1975; *E. clivosus* Popov, 1975; *E. dyminensis* Bednarczyk & Biernat 1978; *E. robustus* sp. nov.

Discussion. – The taxonomy of *Eoconulus* is very complex; meaningful definitions of new species as well as comparison with previously described taxa present problems, since the outline and convexity of both valves depend almost entirely on the configuration of the substrate. Moreover, most previously described species are known only from their dorsal valves. Rowell & Krause (1973) first identified the cementing ventral valve of a lower Whiterock species from Meiklejohn Peak, Nevada, which was later referred to *E. antelopensis* Krause & Rowell, 1975. The Middle Ordovician *E. clivosus* Popov, 1975, from Kazakhstan, was also represented by both valves, and the ventral valve of the Arenig *E. dyminensis* Bednarczyk & Biernat, 1978, from Poland is also known.

In my material all species of *Eoconulus* possess mineralized (or partly mineralized) ventral valves. In the Swedish material of *E. cf. cryptomyus* Goryanskij and *E. robustus*, the adults possessed a thin and poorly mineralized ventral valve, whilst the younger stages only had thickened cardinal muscle scars. As noted by Krause & Rowell (1975, p. 65) such a retardation of mineralisation of the cementing ventral valve is also found in Recent craniaceans; the strongly unequal proportions of ventral and dorsal valves of species of *Eoconulus* (Figs. 11, 12) are probably due to comparable factors. Moreover, the thin ventral valves of *E. cf. cryptomyus* and *E. robustus* are easily broken into indeterminable fragments.

At present eight named species are assigned to *Eoconulus*; the genus has a range from the Upper Cambrian (L. E. Popov, personal communication 1985) to the Upper Ordovician (Cautleyan; Wright 1963). Previous investigations of the taxon were summarized by Krause & Rowell (1975).

In addition to the occurrences mentioned above, an unnamed Lower Ordovician species from the Tourmakedy Limestone of Ireland was recorded by Williams & Curry (1985). Popov (*in* Nazarov & Popov 1980) described some possible Middle Ordovician occurrences of *E. clivosus* from the Karakan Stage of Kazakhstan. Juveniles referred tentatively to the same species were figured by Holmer (1986) from the upper Middle Ordovician of Västergötland. Unpublished work on the group by L. E. Popov (personal communication 1985) indicates that eoconulids

are closely related to, and probably derived from the scaphelasmatines. McClean (1988) illustrated an unnamed species of *Eoconulus* from the Upper Ordovician Kildare Limestone of Ireland.

In view of the above discussion, the following taxonomic assessment necessitates frequent use of open nomenclature. Consideration of the differences in ontogeny, shell structure, and morphology of the ventral valve of various species of *Eoconulus* suggests that the genus may be further subdivided in the future.

Eoconulus cf. *clivus* Popov, 1975

Figs. 38A–B, 39A–H, 105G–I, 110A–H, 111

Synonymy. – □ v cf. 1975 *Eoconulus clivus* Popov, sp. nov. – Popov, p. 41, Pl. 5:31–35. □ v? 1980 *Eoconulus* cf. *clivus* Popov, 1975 – Nazarov & Popov, p. 112, Pl. 29:1–3. □ v? 1986 *Eoconulus* cf. *clivus* Popov, 1975 – Holmer, p. 122, Fig. 11E–G.

Material. – Figured; Br133605d (section), Br128907 (W 0.91, L 0.84, H 0.29), Br133608c (section), Br132576 (section), Br128962 (W 0.84, L 0.84), Br128960 (W 1.08, L 0.91, H 0.65), Br133618b (W 0.78, L 0.74, H 0.34), Br133618a (W 0.56, L 0.50, H 0.25), Br128961 (W 0.90, L 0.79). Total of 245 dorsal and 144 ventral valves.

Diagnosis. – See Popov (1975, p. 41).

Description. – The valves have an irregular, circular or slightly subrectangular outline, and average 93% as long as wide (OR 84–108%; $N=25$; Tables 32, 33). The ventral valve has a flattened (Fig. 39E) or completely irregular attachment scar (Fig. 39A, G). The ‘pedicle foramen’ is closed in most specimens, and scattered over the exterior and interior there are ‘pores’ (up to about 50 per valve) that do not penetrate the entire thickness of the valve (Fig. 39A–D). In lateral profile the ventral valve has a broadly triangular outline (Fig. 105I); it averages 39% as high as wide (Table 32). The maximum height is situated most commonly at some distance (up to 0.30 mm) from the anterior margin (Figs. 39E, 105I). The ventral posterior margin is almost straight (Figs. 39C, 105H). The ventral cardinal muscle scars are well developed and thick, oval in outline, and on average 62% as long as wide (Table 32), occupying up to 82% of the total width (Fig. 105H). A well developed, knob-like apical process (up to 0.08 mm high) is situated at about the centre of the valve (Figs. 39D, 105H). Immediately posterior to the apical process there is a possible pedicle foramen which is closed with shell material in most adult specimens (Fig. 39E). The ventral visceral area generally has a mosaic of shallow polygonal pits, defined by low ridges (Fig. 39C–D). In lateral profile the dorsal valve is regularly to irregularly conical, low to high, and on average 42% as high as wide (Table 33); the maximum height occurs near the centre of the valve (Fig. 110D) or slightly subcentrally, towards the posterior margin (Fig. 110A). The dorsal larval shell is commonly broken in adults, and in some specimens the remaining hole is partly or completely plugged by shell material (Figs. 105G, 110H). The dorsal interior has a pair of well developed and raised

cardinal muscle scars on the posterior wall, occupying up to 82% of the total width; on the anterior wall there are raised markings of unknown function (Fig. 105G). The dorsal valve is ornamented with faint, closely spaced, slightly irregular fila (Fig. 110B, F). For shell structure, see above (p. 48, Fig. 39A–H).

Ontogeny. – The dorsal larval shell is nearly circular, about 0.20 mm across. It is ornamented with large, circular pits, 9 μ m in diameter, separated by clusters of small pits, 800 nm across (Fig. 110B–D). In some specimens the shape of the dorsal larval shell appears to reproduce the configuration of the substrate; some larval shells have circular and bulbous nodes, each up to 0.05 mm across (Fig. 110B, F). The ventral larval shell is poorly defined, about 0.20 mm in diameter (Fig. 39B). There are no larval pits, but the exterior has scattered shallow ‘pores’, of which the central one could possibly represent a sealed pedicle foramen (Fig. 39B). In some dorsal valves the boundary between the larval and bryophic stages is transitional; there is a gradual decrease in size of larval pits towards the edge of the shell (Fig. 110A–C). More rarely the boundary is sharply delineated (Fig. 110D–F). Juvenile dorsal valves (W 0.19–0.74) have traces of cardinal muscle scars. Juvenile ventral valves were poorly mineralized or not mineralized at all; they probably consisted of a periostracum pierced by numerous ‘pores’. The adult stage (W 0.74–1.02) was reached when the mineralization of the ventral valve was initiated. The ventral valve was thickened by the accretion of successively parallel apatite lamellae, secreted on the inside of the previous ones. However, the valve was not further widened (Fig. 39E–H). This ‘inside growth’ was most rapid along the anterior margin of the ventral valve (Figs. 39F, 105I). The adult dorsal valve did not increase apparently beyond a certain size, and through later growth it became thickened by the accretion of parallel lamellae. During a possible gerontic stage the dorsal larval shell was closed off by a partition (Figs. 105G, 110G). The dorsal larval shell is much thinner than the rest of the shell and is generally broken in large specimens; for this feature there are two possible main explanations: (1) the shell material was resorbed, or (2) the dorsal larval shell was poorly mineralized. The breakage could have taken place either during the life of the brachiopod or postmortally.

Discussion. – The Swedish material is close morphologically to *Eoconulus clivus* Popov from the Middle Ordovician Bestamak Formation of Kazakhstan (Popov 1975, Pl. 5:31–35) in having (1) a comparatively high (H/W ratio about 40%) irregular ventral valve with a nearly straight posterior margin, (2) a triangular lateral outline of the ventral valve with maximum height near the anterior margin, and (3) a pair of well developed, large cardinal muscle scars in both valves. *E. cf. clivus* also resembles the lower Whiterock species *E. antelopensis* Krause & Rowell (1975) from Nevada, which differs, however in having (1) proportionally smaller cardinal muscle scars, (2) a proportionally higher ventral valve (H/W ratio about 58%), and (3) a conical dorsal valve, with concave anterior and posterior surfaces. The Swedish material is also close to *E. cf. clivus* described

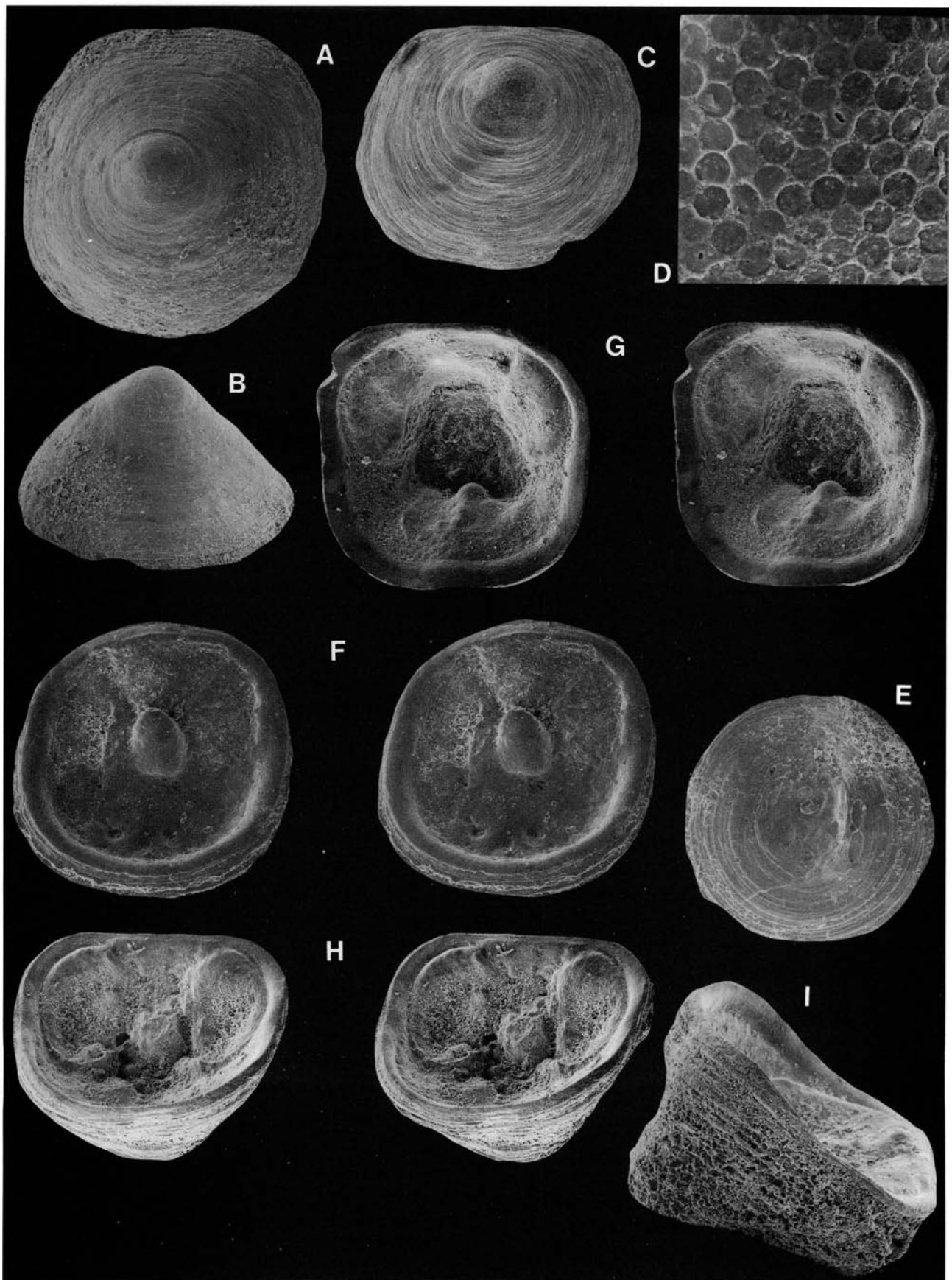


Fig. 105. □A–B. *Eoconulus* sp. nov. a?; Holen Limestone (sample GB81-0); Br132584. □A. Dorsal exterior; $\times 76$. □B. Side view of A; $\times 76$. □C–F. *Eoconulus* sp. nov. a. □C. Exterior of a dorsal valve; Kårgårde Limestone (sample DLK83-segk-4); Br128918, $\times 100$. □D. Ornamentation of the larval shell of C; $\times 757$. □E. Ventral exterior, showing a cylindrical attachment scar; note the central protogulum with bulla; Kårgårde Limestone (sample DLK83-segk-4); Br128922, $\times 100$. □F. Stereo-pair; interior of a ventral valve, showing the apical process and cardinal muscle scars; Kårgårde Limestone (sample DLK83-segk-4); Br128920, $\times 81$. □G–I. *Eoconulus* cf. *clivus* Popov, 1975; Skårlöv Limestone (sample DLK83-sä-2). □G. Stereo-pair; dorsal interior; Br128962, $\times 57$. □H. Stereo-pair; interior of a ventral valve; Br128960, $\times 45$. □I. Side view of H; $\times 60$.

Table 32. *Eoconulus* cf. *clivus* Popov, average dimensions and ratios of ventral valves.

	W	L	L/W	WM	LM	LM/WM	H	H/W
DLK83-sä-2								
<i>n</i>	11	11	11	5	5	5	10	10
mean	0.86	0.80	93%	0.68	0.41	62%	0.34	39%
<i>s</i>	0.073	0.051	6.000	0.039	0.049	7.797	0.097	9.920
min	0.74	0.71	85%	0.62	0.36	51%	0.22	26%
max	1.02	0.87	104%	0.71	0.46	71%	0.51	58%

Table 33. *Eoconulus* cf. *clivus* Popov, average dimensions and ratios of dorsal valves.

	W	L	L/W	H	H/W
DLK83-sä-1, 2					
<i>n</i>	14	14	14	9	9
mean	0.72	0.67	93%	0.29	42%
<i>s</i>	0.109	0.107	6.847	0.054	9.262
min	0.50	0.43	84%	0.20	29%
max	0.88	0.84	108%	0.36	54%

by Popov (*in* Nazarov & Popov 1980, Pl. 29:1–3) from the Middle Ordovician Karakan Formation of Kazakhstan.

McClellan (1988) described a polygonal mosaic from the visceral area of the dorsal valve of an unnamed *Eoconulus*. A similar pattern is also present in the Swedish material of *E. cf. clivus*; in all probability this polygonal pattern represents epithelial moulds (McClellan 1988).

Occurrence. – *Eoconulus* cf. *clivus* is known from the Skärlov, Seby Limestone, and Folkeslunda limestones of Dalarna (Fig. 9A).

Eoconulus cf. *semiregularis* Biernat, 1973

Figs. 39I, 106, 107, 111

Synonymy. – □v cf. 1973 *Eoconulus semiregularis* n.sp. – Biernat, p. 112, Pl. 36:1–8. □v cf. 1982 *Eoconulus semiregularis* Biernat, 1973 – Popov et al., p. 101, Fig. 2:6.

Material. – Figured; Br132719d (W 0.74, L 0.70, H 0.19), Br132682 (W 0.62, L 0.60, H 0.09), Br132719e (W 0.74, L 0.74, H 0.22), Br132719b (W 0.76, L 0.70, H 0.29), Br132791 (W 0.54, L 0.54, H 0.23), Br132701a (W 0.71, L 0.62, H 0.12). Total of 2248 dorsal and 707 ventral valves.

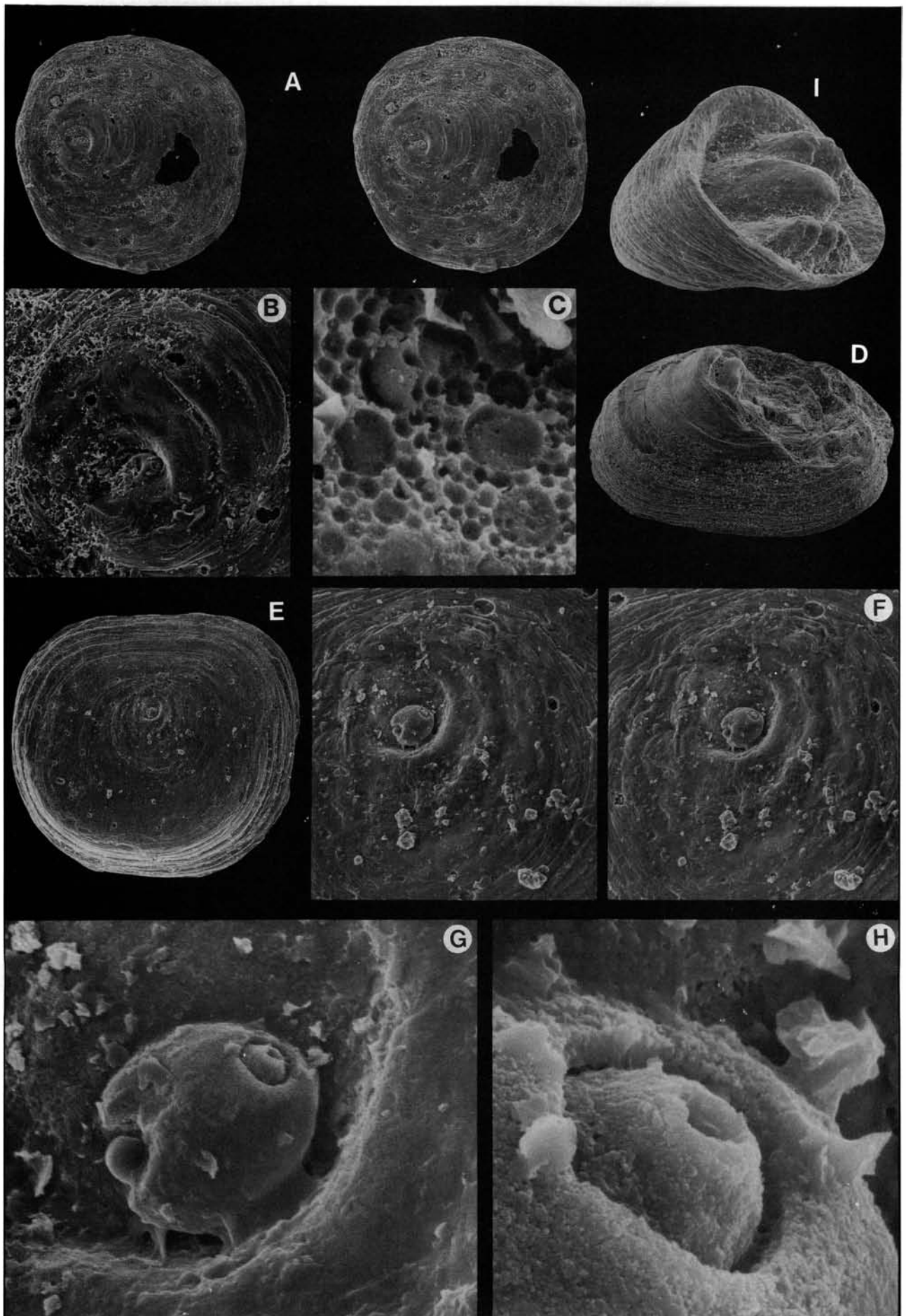
Diagnosis. – See Biernat (1973, p. 113).

Description. – The valves are almost circular, on average 97% as long as wide (OR 84–113%; *N*=36; Tables 34, 35). The cemented ventral valve has an attachment scar that is either flat (Fig. 106E), irregular (Figs. 106D, 107C), or most commonly cylindrical. In a few specimens the attachment scar reproduces a pattern with one or several parallel ridges (Fig. 107A) that sometimes bear regularly spaced nodes (Fig. 106A). The concentric growth lines are poorly defined (Fig. 106E) and there are a few scattered exterior ‘pores’ (Fig. 39I). The ventral valve averages 28% as high as wide (Table 34), with the maximum height some distance from the anterior margin (Fig. 106I); in lateral profile the posterior margin is most frequently low and rounded (Fig. 106D–E, 107C). The ventral cardinal muscle

scars are well developed and raised (Fig. 106I), averaging 77% as long as wide (Table 34), forming about 70–80% of the total width. Near the centre of the valve a distinct apical process is present; it is of varying shape, low to high, in places forked and elongated, and occupies up to about 50% of the total length (Fig. 106I). In some specimens a rounded or triangular pedicle foramen is situated directly posterior to the apical process. The dorsal valve (Fig. 111) is almost identical to that of *Eoconulus* sp. nov. a (Fig. 105A–D; see also Biernat 1973); it commonly lacks a pronounced beak and the interior is without recognizable structures. The dorsal valve is highly conical, generally above half as high as wide (Table 35); the maximum height is generally at about the centre of the valve, but some specimens have a pronounced beak towards the posterior margin.

Ontogeny. – The cemented ventral valve of *Eoconulus* cf. *semiregularis* has a possible protogulum (or early larval shell), about 0.07 mm wide, the morphology of which is described and discussed above (p. 63, Figs. 106, 107). The larval shell is circular, about 0.25 mm across. The dorsal larval shell is about 0.08 mm high and distinctly pitted with pits closely similar to those of *Eoconulus* sp. nov. a (Fig. 105C–D). In contrast, the ventral larval shell completely lacks pits. Growth lines are also absent, but it has numerous irregular wrinkles and some scattered ‘pores’ (Figs. 106B, F, 107B, D). The boundary between the larval and juvenile shell is sharply delineated on both valves; on the ventral valve there is a line of disturbance in growth (Fig. 107B, D). During the juvenile stage (W 0.25–0.51, L 0.25–0.46) the ventral valve was either poorly mineralized or not mineralized at all. The juvenile dorsal valve is up to 0.31 mm high. The adult stage (W 0.51–0.68, L 0.46–0.60) was reached at about the point when the ventral valve became thickened by interior accretion (as described above in *E. cf. clivus*). Occasionally, the ‘inside growth’ of the ventral valve was

Fig. 106. *Eoconulus* cf. *semiregularis* Biernat, 1973. □A. Stereo-pair; ventral exterior, showing the attachment scar; Gullhøgen Limestone (sample GB84-2-9); Br132682, ×72. □B. The larval shell of A; ×229. □C. Protogular ornamentation of a ventral valve; Gullhøgen Limestone (sample GB84-2-19); Br132719e, ×4134. □D. Side view of exterior of a ventral valve; Gullhøgen Limestone (sample GB84-2-19); Br132719b, ×85. □E. Ventral exterior; Gullhøgen Limestone (sample GB84-2-19); Br132719d, ×72. □F. Stereo-pair; the larval shell of E; ×286. □G. Detail of the protogulum of E, showing the bulla; ×1500. □H. Detail of G, showing the protogular apertures; ×6900. □I. Side view of interior of a ventral valve; Gullhøgen Limestone (sample GB84-2-27); Br132791, ×100.



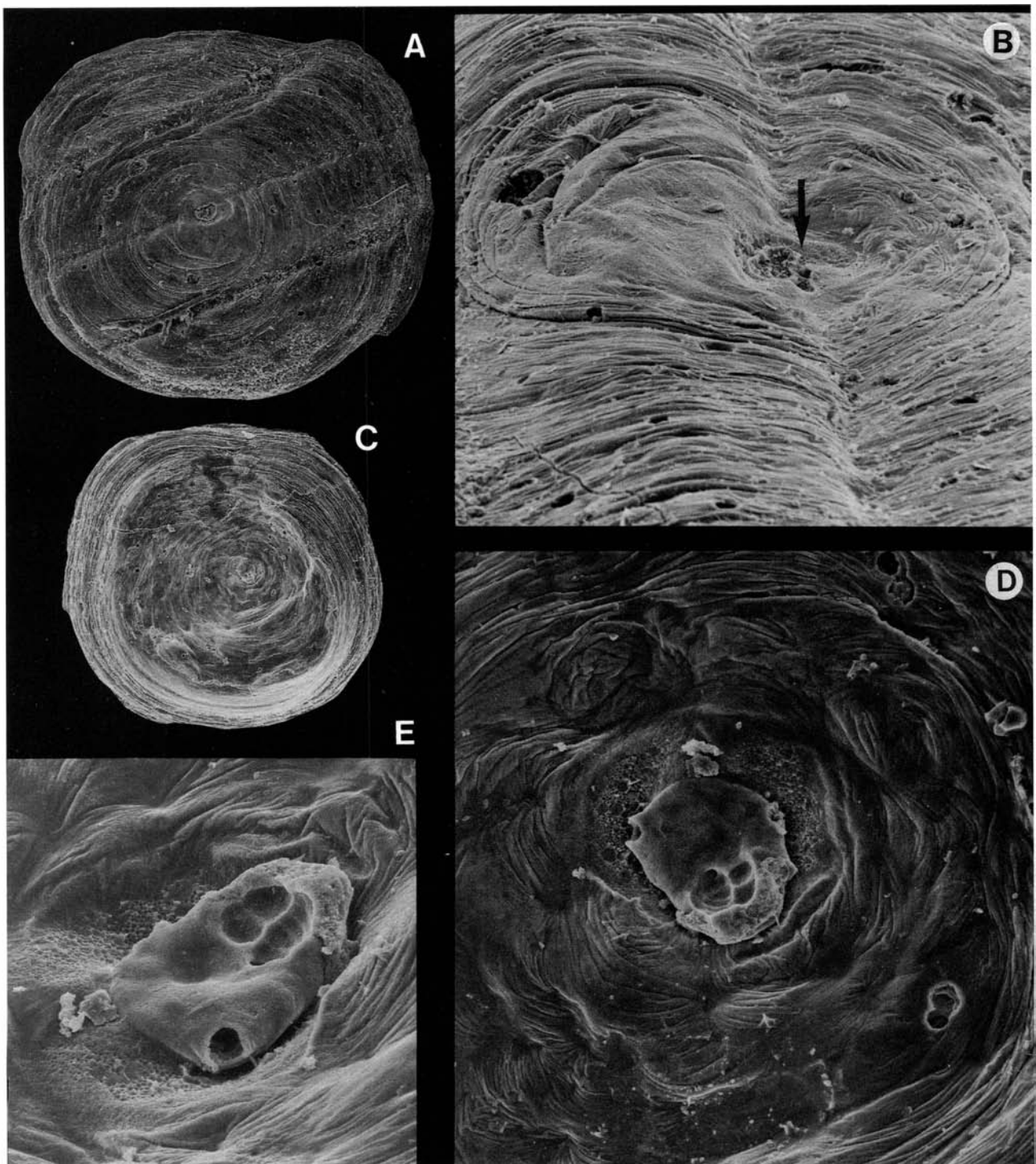


Fig. 107. *Eoconulus* cf. *semiregularis* Biernat, 1973. □A. Ventral exterior, showing attachment scar with three parallel ridges; Gullhøgen Formation (sample GB84-2-11); Br132701a, $\times 100$. □B. Oblique side view of the larval shell of A, the protegulum indicated by an arrow; $\times 450$. □C. Exterior of a ventral valve, showing an irregular attachment scar; Gullhøgen Formation (sample GB84-2-19); Br132719e, $\times 70$. □D. Detail of C, showing the larval shell, protegulum; $\times 600$. □E. Side view of the protegulum of C; note the bulla and the lateral aperture; $\times 950$.

most rapid along the anterior margin (Fig. 106I), but more commonly the ventral valve forms a truncated cone (Figs. 106D, 107C). During the adult stage the raised ventral cardinal muscle scars and the apical process were formed. The adult dorsal valve is up to 0.46 mm high. Some very thick ventral valves (more than 0.68 mm wide) possibly belong to the gerontic stage (e.g., Fig. 106E; see also Fig. 46).

Discussion. – The type material of *Eoconulus semiregularis* Biernat (1973, Pl. 36:1–8) is known from the dorsal valve only, derived from an Ordovician erratic boulder the exact age of which is unknown. The shape, size and convexity of the dorsal valve of Biernat's species is very suggestive of the dorsal valves in the Swedish specimens, but as the Polish species is still poorly known, open nomenclature is preferred here as means of expressing the comparison.

Table 34. *Eoconulus* cf. *semiregularis* Biernat, average dimensions and ratios of ventral valves.

	W	L	L/W	WM	LM	LM/WM	H	H/W
DLK83-fur-6								
<i>n</i>	18	18	18	17	17	17	18	18
mean	0.62	0.63	95%	0.47	0.36	77%	0.19	28%
<i>s</i>	0.086	0.066	7.448	0.077	0.041	9.192	0.082	11.730
min	0.51	0.46	84%	0.36	0.28	53%	0.09	15%
max	0.81	0.73	108%	0.62	0.42	95%	0.33	48%

Table 35. *Eoconulus* cf. *semiregularis* Biernat, average dimensions and ratios of dorsal valves.

	W	L	L/W	H	H/W
DLK83-fur-6					
<i>n</i>	18	18	18	17	17
mean	0.46	0.46	99%	0.29	59%
<i>s</i>	0.126	0.120	6.922	0.117	13.535
min	0.26	0.28	93%	0.12	43%
max	0.68	0.60	113%	0.46	90%

Occurrence. – *Eoconulus* cf. *semiregularis* is the fourth most common species in the Viru sequence investigated for this monograph. It ranges from the Gullhögen Formation to the Ryd Limestone in Västergötland (Fig. 8B–C), and in Dalarna it is restricted to the Furudal Limestone (Fig. 9A–B). On Öland the species is known from the Källa Limestone.

Eoconulus sp. nov. a

Figs. 37, 38D, ?105A–B, 105C–F, 110I, 111

Material. – Figured; Br133595c (section), Br128923 (W 0.45, L 0.47; section), ?Br132584 (W 0.71, L 0.76, H 0.45), Br128918 (W 0.57, L 0.57, H 0.29), Br128922 (W 0.43, L 0.46), Br128920 (W 0.60, L 0.62). Total of 184 dorsal and 53 ventral valves.

Description. – The valves are almost circular, on average 102% as long as wide (OR 92–115%; *N*=26). The ventral valve (\bar{W} 0.51, \bar{L} 0.52; *N*=11; DLK83-segk-4) is less than 0.10 mm high. In most specimens the attachment scar is cylindrical in cross-section (Figs. 37, 105E); there are some scattered ‘pores’ that occasionally penetrate the entire thickness of the valve. The ventral cardinal muscle scars are either poorly developed or most commonly not preserved (Fig. 105F). The apical process is small and low. Some specimens have a circular to triangular pedicle foramen immediately posterior to the apical process. The dorsal valve (\bar{W} 0.49, \bar{L} 0.49; *N*=15; DLK83-segk-4, 6) is generally more than half as high as wide; the apex is subcentral, but is sometimes recurved and submarginal (Fig. 105A–C). The dorsal interior lacks recognizable structures. The ontogeny was not examined in detail, but it appears to be close to that of *E. cf. semiregularis*. The ventral larval shell is circular, about 0.25 mm across (Fig. 110I). The dorsal larval shell is ornamented with large pits, up to 9 µm across, sometimes overlapping, separated by clusters of smaller pits up to 800 nm across (Fig. 105D). The shell structure is outlined above (p. 48, Figs. 37, 38D).

Discussion. – *Eoconulus* sp. nov. a is similar to *E. cf. semiregularis*. The dorsal valves are indistinguishable. However, the maximum size of *E. sp. nov. a* is smaller, and the ventral valve appears to be much thinner, with more poorly developed cardinal muscle scars and apical process. Specimens from the Holen Limestone of Västergötland (Fig. 105A–B) cannot be assigned unconditionally to this species, because the ventral valve has not been identified. The formal erection of a new species is postponed until more material has been isolated from other regions.

Occurrence. – In Dalarna *Eoconulus* sp. nov. a is restricted to the Kårgårde Limestone (Fig. 9A). In Västergötland there is a questionable occurrence in the Holen Limestone (Fig. 8A). In Jämtland (samples J70-161, J69-37–38, 43) and on Öland the species is known from the Segerstad Limestone.

Eoconulus cf. *cryptomys* Goryanskij, 1969

Figs. 38E, 108A, 109A, 111

Synonymy. – □ v cf. 1969 *Eoconulus cryptomys* Gorjansky sp. nov. – Goryanskij, p. 108, Pl. 20:5–8. □ v cf. 1973 *Eoconulus cryptomys* Gorjansky, 1969 – Biernat, p. 112, Pl. 34, 35, 36:9–10.

Material. – Figured; Br133595n (section), Br129035 (W 1.12, L 0.91), Br128926 (W 0.91, L 0.78). Total of 36 dorsal and 2 ventral valves.

Diagnosis. – See Goryanskij (1969, p. 108).

Description. – The valves are subrectangular, on average 82% as long as wide (OR 77–89%; *N*=9). The ventral valve is thin, most commonly fragmentary, flattened in lateral profile; the posterior margin is almost straight. The interior is surrounded by a narrow rim (Fig. 109A). The exterior is without growth lines. The apical process is poorly developed or lacking. The ventral cardinal muscle scars are small and widely spaced, up to 0.28 mm apart, and about 40% as long as wide (Fig. 109A). The dorsal valve (\bar{W} 1.13, \bar{L} 0.92; OR W 0.93–1.44, L 0.73–1.21; *N*=8) is regularly conical with a subcentral apex that is almost invariably broken (Fig. 108A). In some specimens the ornamentation of the dorsal valve reproduces the configuration of the substrate (Fig. 108A). The dorsal interior any lacks recognizable structures.

Remarks on ontogeny. – The ontogeny is not known in detail. Apparently the ventral valve became mineralized fairly late in its development, and during earlier stages possibly only the ventral cardinal muscle scars were mineralized. No brephic or juvenile dorsal valves were identified. Appar-

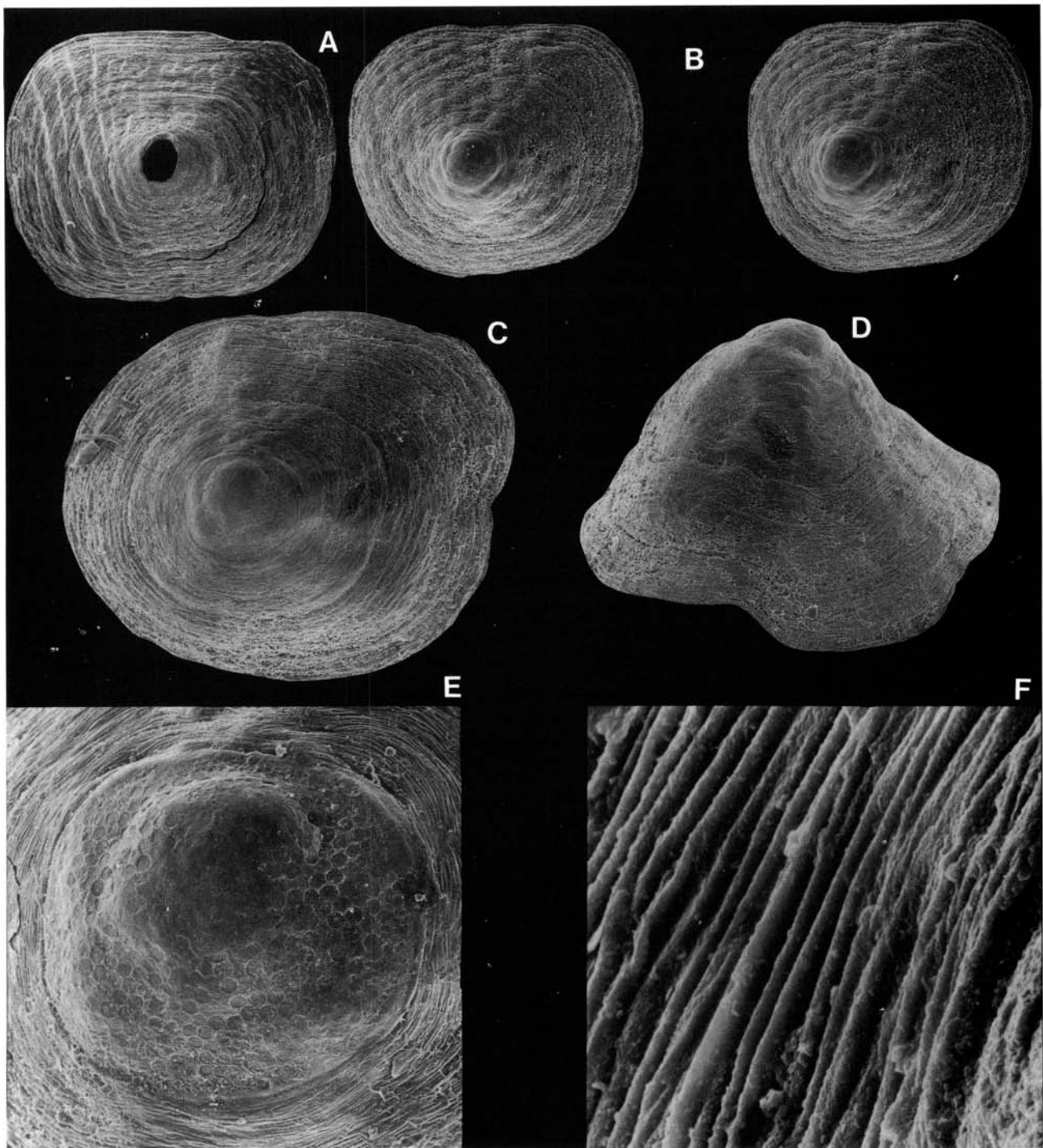


Fig. 108. □A. *Eoconulus* cf. *cryptomyus* Goryanskij, 1969; dorsal exterior; note the attachment scar with three parallel ridges; Folkeslunda Limestone (sample DLK83-Fo-1); Br129035, $\times 47$. □B–F. *Eoconulus robustus* sp. nov. □B. Stereo-pair; exterior of a dorsal valve; Ryd Limestone (sample GB84-3-59); Br132877, $\times 65$. □C. Holotype; dorsal exterior; Dalby Limestone (sample D60-214); Br128712, $\times 100$. □D. Side view of C; $\times 110$. □E. The larval shell of C; $\times 332$. □F. Detail of the ornamentation of C; $\times 3320$.

ently, the dorsal larval shell on older individuals is very easily broken; the broken apex appears to have been plugged by shell material.

Discussion. – *Eoconulus cryptomyus* was described from the Aserian Stage in the Pskov district by Goryanskij (1969, Pl. 20:5–7), who also illustrated material from the Kundan Stage at Paldiski, Estonia (Pl. 20:8). The dorsal valves illustrated by Goryanskij compare closely with those illus-

trated here. The ventral valve of *E. cryptomyus* is not known. Some dorsal valves from the Volkhovian Stage of Suhkrumägi quarry, Tallinn, Estonia, were referred to *E. cryptomyus* by Biernat (1973). The broken apex of one dorsal valve (Biernat, 1973, Pl. 34:4) in her material appears to be plugged by shell material.

Occurrence. – In Dalarna and on Öland *Eoconulus* cf. *cryptomyus* is restricted to the Segerstad Limestone (Fig.

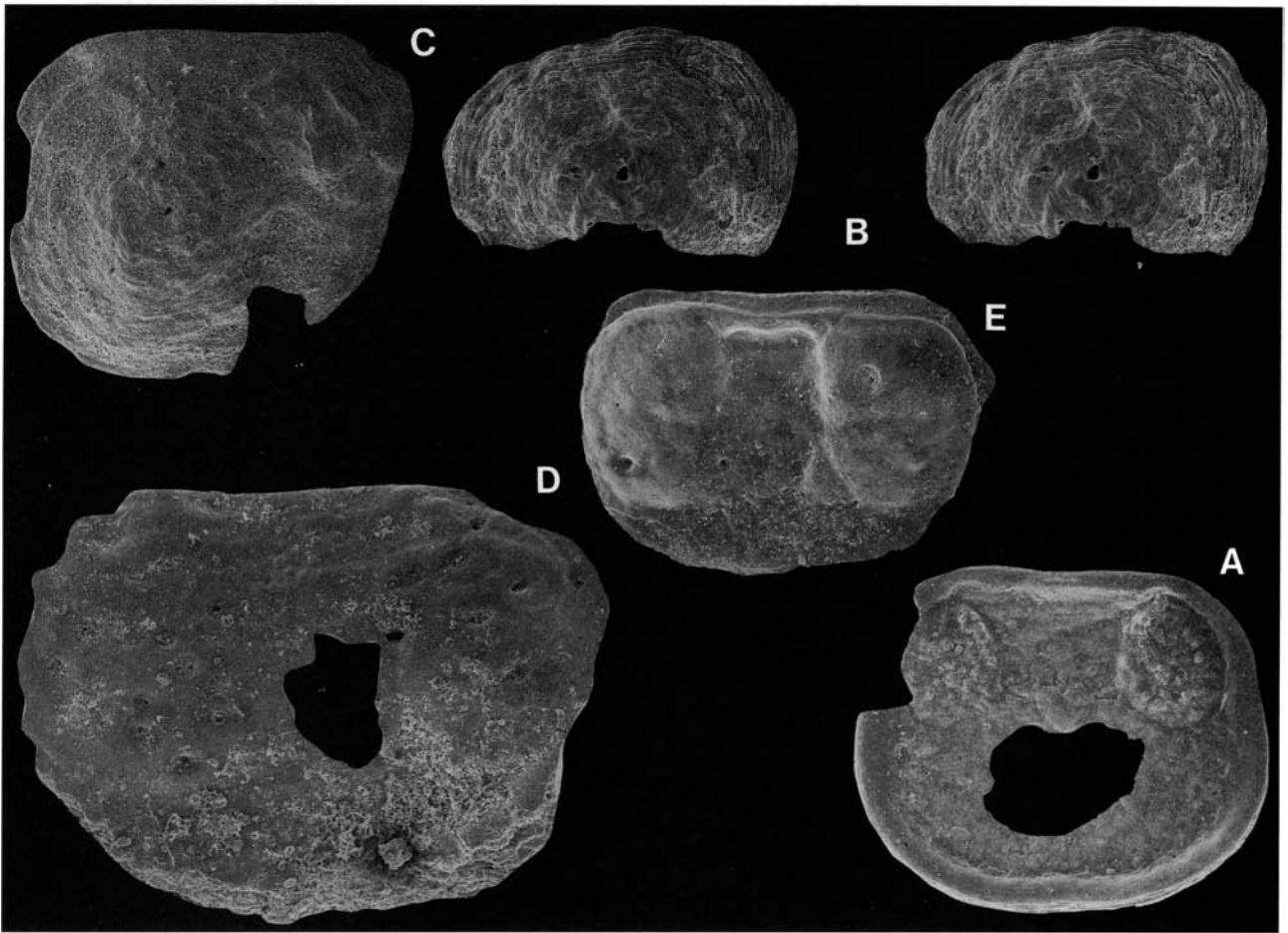


Fig. 109. □A. *Eoconulus* cf. *cryptomyus* Goryanskij, 1969; ventral interior; Kårgårde Limestone (sample DLK83-segk-2); Br128926, ×57. □B–E. *Eoconulus robustus* sp. nov. □B. Stereo-pair; exterior of a ventral valve; Dalby Limestone (sample GB84-3-49); Br132860b, ×43. □C. Ventral exterior; Dalby Limestone (sample DLK83-dal-12); Br132511, ×57. □D. Interior of a ventral valve; Dalby Limestone (sample DLK83-dal-9); Br132498, ×57. □E. Ventral interior; Dalby Limestone (sample GB84-3-49); Br132860a, ×50.

9A). It is also known from the Segerstad (samples J70-165–166, J69-35, 37–38, 41) and the Skårlöv limestones (sample J70-167) of Jämtland.

Eoconulus robustus sp. nov.

Figs. 108B–F, 109B–E, 111

Name. – Latin *robustus*, strong; alluding to the thick dorsal valves.

Holotype. – Br128712, complete dorsal valve, Fig. 108C–F (W 0.78, L 0.67, H 0.45), from the Dalby Limestone, Fjåcka section (sample D60-214), Dalarna.

Paratypes. – Figured; Br132877 (W 0.95, L 0.81, H 0.50), Br132860b (W 1.07, L ~0.78), Br132511 (W 0.88, L 0.78), Br132498, Br132860a (W 1.04, L ~0.78). Total of 2258 dorsal valves and 12 ventral valves.

Diagnosis. – Valves subrectangular, ventral valve thin, with regular to irregular attachment scar. Ventral interior dominated by large cardinal muscle scars. Apical process lacking. Ventral valve mineralized late in ontogeny. Dorsal valve with subcentral apex. Dorsal interior with well developed cardinal muscle scars.

Description. – The valves are subrectangular, on average 82% as long as wide ($N=20$; Table 36). The ventral valve is thin and has a smooth, regular (Fig. 109D–E) or irregular (Fig. 109B) attachment scar with growth lines and numerous exterior shallow ‘pores’ (Fig. 109B). The ventral interior is surrounded by a raised rim (Fig. 109E). The cardinal muscle scars are large (\overline{WM} 1.02, \overline{LM} 0.64; OR WM 0.81–1.24, LM 0.57–0.78; $N=4$), 63% as long as wide (OR 56–73%); they occupy well over 90% of the total width and slightly less than 80% of the total length (Fig. 109D–E). The ventral interior has some scattered shallow ‘pores’ (Fig. 109B). The dorsal valve is on average 48% as high as wide (Table 36). In lateral profile the outline is regularly to slightly irregularly conical, generally with a subcentral apex (Fig. 108B, D). In dorsal view the posterior margin is almost straight (Fig. 108B) or rounded (Fig. 108C). The ornamentation of the dorsal valve sometimes reproduces the configuration of the substrate (Fig. 108B). The dorsal valve is ornamented with closely spaced, irregular, minute fila (Fig. 108F). The dorsal cardinal muscle scars are large, on average 64% as long as wide (Table 36).

Remarks on ontogeny. – The ventral larval shell of *Eoconulus robustus* could not be identified. The dorsal larval shell is

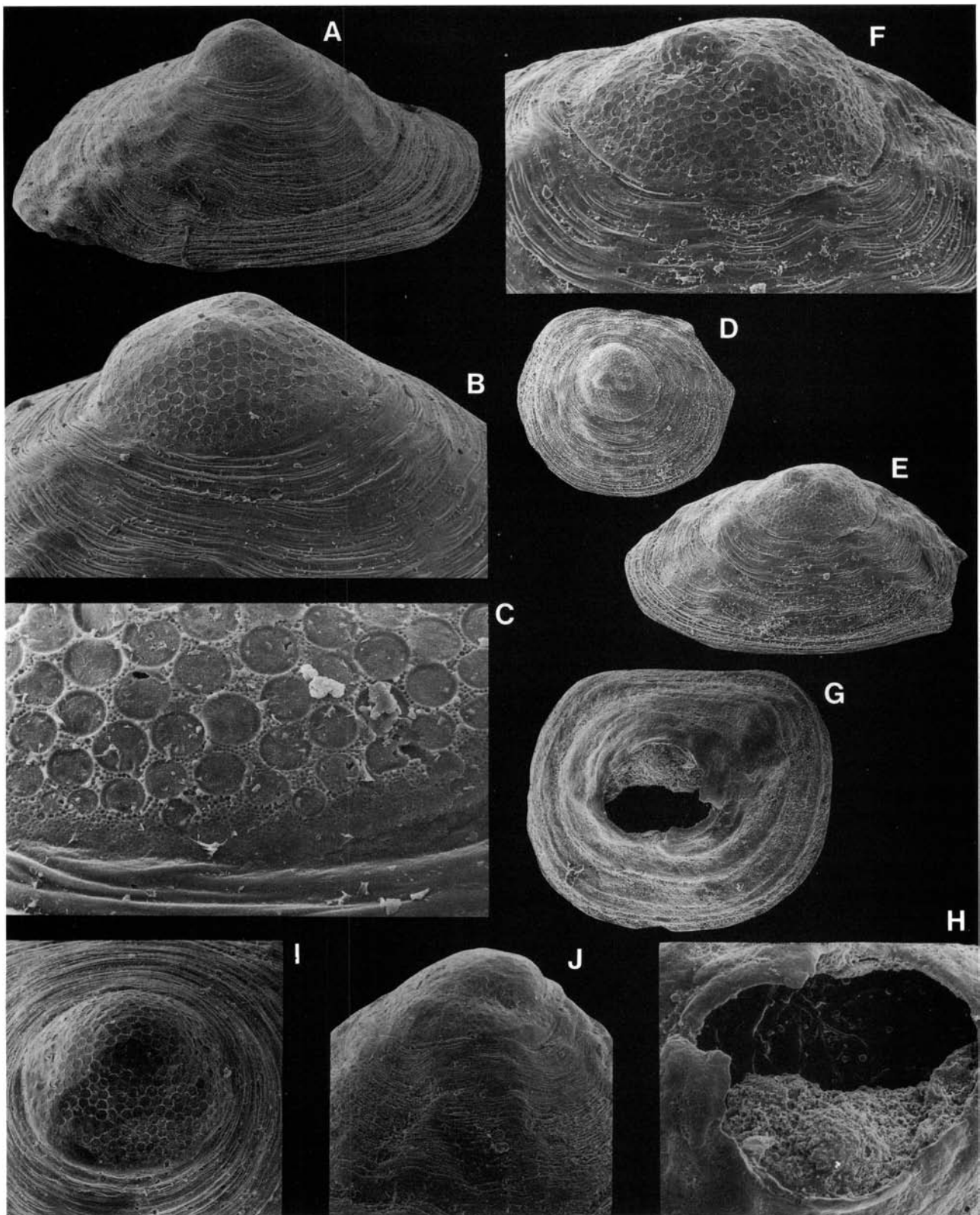
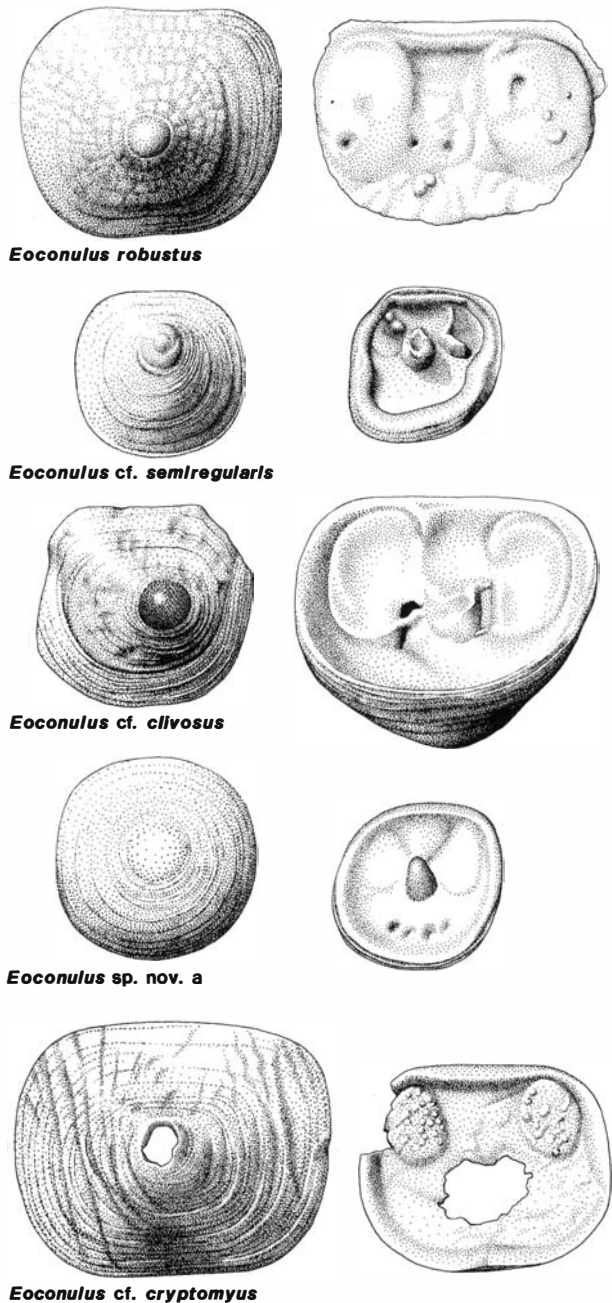


Fig. 110. □A–H. *Eoconulus* cf. *clivusos* Popov, 1975. □A. Side view of a dorsal exterior; Seby Limestone (sample DLK83-se-5); Br133618b, $\times 115$. □B. Detail of A, showing the larval shell; $\times 290$. □C. Detail of B, showing the edge of larval shell; $\times 1200$. □D. Dorsal exterior; Seby Limestone (sample DLK83-se-5); Br133618a, $\times 80$. □E. Side view of D; $\times 120$. □F. Detail of E, showing the larval shell; $\times 300$. □G. Exterior of a dorsal valve; Skårlöv Limestone (sample DLK83-sä-2); Br128961, $\times 41$. □H. Detail of the apex of G, showing the broken larval shell; $\times 106$. □I. *Eoconulus* sp. nov. a; detail of a dorsal larval shell (see also Fig. 105C); Kårgårde Limestone (sample DLK83-segk-4); Br128918, $\times 195$. □J. *E. robustus* sp. nov.; side view of a dorsal larval shell (see also Fig. 108C); Dalby Limestone (sample D60-214); Br128712, $\times 180$.

Table 36. *Eoconulus robustus* sp. nov., average dimensions and ratios of dorsal valves.

	W	L	L/W	WM	LM	LM/WM	H	H/W
DLK83-dal-4								
<i>n</i>	18	18	18	9	9	9	18	18
mean	0.70	0.57	82%	0.60	0.39	64%	0.33	48%
<i>s</i>	0.282	0.204	5.117	0.220	0.148	6.021	0.139	4.947
min	0.37	0.31	73%	0.36	0.23	56%	0.14	35%
max	1.43	1.05	91%	1.04	0.67	77%	0.62	56%

Fig. 111. Comparison between species of *Eoconulus*. Figure prepared by Lennart Andersson (Stockholm).

almost circular, about 0.20 mm across (Fig. 108E). In most specimens the boundary with the juvenile stage is not sharply delineated. In some specimens there is a line of growth disturbance at the edge of the dorsal larval shell,

the irregular outline of which reproduces the configuration of the substrate (Figs. 108B, E, 110J). Mineralization of the ventral valve did not take place until late in ontogeny. Some isolated cardinal muscle scars were found, probably indicating that they became mineralized before the rest of the valve.

Discussion. – The dorsal valve of *Eoconulus robustus* is similar to that of *E. rectangulatus* Cooper (1956, Pl. 10B:11–13), *E. transversus* Wright (1963, Pl. 3:4, 8, 12, 13), and *E. cryptomyus* Goryanskij. However, the ventral valve is unknown from any of these species. The dorsal valve of *E. rectangulatus* differs from the Swedish species in having a median septum (Cooper 1956, Pl. 10B:13). *E. transversus* differs from *E. robustus* in having a less conical dorsal valve. The dorsal valve of *E. cryptomyus* completely lacks all traces of cardinal muscle scars. The ventral valve of *E. robustus* is most similar to that of *E. cf. cryptomyus* from the Kårgårde Limestone. However, the ventral cardinal muscle scars of this species are proportionally much smaller than those of *E. robustus* (e.g. Fig. 111).

Occurrence. – In the Swedish Viru sequence *Eoconulus robustus* is the fifth most abundant species. It ranges from the Ryd to the lower Dalby limestones of Västergötland (Fig. 8C), and in Dalarna it is known from the Furudal to Dalby limestones, and questionably from the uppermost Folkeslunda Limestone (Figs. 9, 10). It has also been recorded from an erratic boulder of lower Dalby Limestone from Uppland.

Order Discinida Kuhn, 1949 (*sensu* Kuhn 1949, p. 99)

[*nomen correctum* herein (*pro* Order Discinacea Kuhn, 1949, p. 99, *nomen imperfectum*)]

Superfamily Discinacea Gray, 1840

Diagnosis. – See Rowell (1965, p. H282).

Discussion. – The first records of undisputed discinaceans are of early Ordovician age, when the stock is already split into two well separated families; the Trematidae, in which the central posterior sector of the ventral mantle edge never secreted shell, and the Discinidae, in which the ventral pedicle opening was enclosed by an entire posterior margin in the adult shell (Williams & Rowell 1965b). Williams & Rowell (1965a, p. H78) pointed to similarities in shell structure between discinaceans and acrotretaceans that are not confirmed here (see above, p. 35). As shown by Koneva & Popov (1983), the formation of an 'acrotretid-

like' pedicle foramen from a lingulid ventral valve is comparatively simple. This change could have taken place convergently several times in different stocks (see above, p. 69). The suggestion of Wright (1979) and Popov (*in* Nazarov & Popov 1980), to exclude the Discinacea from the Acrotretida and include it in the separate order Discinida, is accepted here.

Family Trematidae Schuchert, 1893.

Genus *Trematis* Sharpe, 1848

Type species. – Subsequent designation by Davidson 1853, p. 130; *Orbicula terminalis* Emmons, 1842, from the Middle Ordovician of New York State, U.S.A.

Diagnosis. – See Rowell (1965, p. H283).

Trematis? sp.

Material. – Total of 3 dorsal and 2 ventral valves (not illustrated).

Remarks. – The fragments of this unidentified species are referred tentatively to *Trematis*. The dorsal valve is somewhat similar to the Middle Ordovician *Trematis?* *spinosa* Cooper (1956, Pl. 111:22–24) from the Pratt Ferry beds of Alabama, in having a narrow shelf-like pseudointerarea and a slightly spinose posterior margin. The valves are ornamented with poorly developed, shallow pits.

Occurrence. – Fragments of *Trematis?* sp. are known only from the Furudal and Dalby limestones of Dalarna (Figs. 9B–C, 10).

Family Discinidae Gray, 1840.

Subfamily Orbiculoideinae Schuchert & LeVene, 1929

Diagnosis. – See Rowell (1965, p. H285).

Discussion. – Throughout the sequence an as yet undetermined number of taxa occur that are referable to this subfamily. Some of the better preserved orbiculoideines are considered briefly below, under open nomenclature. A special study of the group is outside the scope of the present paper; this requires additional selective collecting of macroscopic specimens in the field. Much of the material is highly fragmented and/or represents juveniles; the identification of dorsal and ventral valves belonging to the same species is commonly not obvious. The stratigraphic distribution of orbiculoideines is recorded in the faunal logs at the subfamily level only.

Genus *Orbiculoidea* D'Orbigny, 1847

Type species. – Subsequent designation by ICZN plenary powers, opinion 722, 1965; *Orbicula forbesi* Davidson, 1848, from the Wenlock (Homerian) of West Midlands, England.

Diagnosis. – See Rowell (1965, p. H285).

Discussion. – Most species referred to the genus have valves with a nearly circular outline and are regularly conical with a subcentral apex. In addition, there is a well developed listrium running from the apex to the anterior end of the pedicle foramen. However, none of the species described below can be assigned unconditionally to the genus.

Orbiculoidea? sp. a

Fig. 112A–B

Material. – Figured; Br129025 (W 3.41, L ~3.41). Total number of specimens not determined.

Remarks. – Only the dorsal valve of this strongly ornamented species could be identified (Fig. 112A). The valve is nearly circular, depressed in lateral profile with the apex situated about 1/10 the distance of the total length from the posterior margin. The valves are ornamented with high rugae, up to five per mm (Fig. 112B); the postlarval surface is covered with pits, similar to those in *Orbiculoidea?* sp. b. The larval valve is about 0.50 mm across.

Occurrence. – The species is restricted to the Folkeslunda Limestone of Dalarna.

Orbiculoidea? sp. b

Figs. 19D–J, 44A–C, 112C–D, ?E–F, 113D, ?E–F

Material. – Figured; Br132676f, g (sections), Br132613, Br132723 (damaged), ?Br128957 (damaged), Br132612 (damaged), ?Br129000 (damaged). Total number of specimens not determined.

Description. – The valves are almost circular in outline. In lateral profile the outline is flattened. The dorsal valve has a submarginal apex (Fig. 112D), whilst the ventral apex is subcentral (Fig. 113D–E). The ventral valve has a well developed, wide, long listrium that is up to about 40% as long as wide and occupies up to about 90% of the distance from the posterior margin to the larval shell (Fig. 113D). The valves are ornamented with rugae (Figs. 112F, 113F), up to seven per mm. For ontogeny and shell structure see above (pp. 35, 59, Figs. 19D–J, 45A–C).

Occurrence. – In Västergötland *Orbiculoidea?* sp. b is known from the Gullhögen Formation, and it also occurs questionably in the Kårgärde and Skårlöv limestones of Dalarna.

Orbiculoidea? sp. c

Fig. 113A–C

Material. – Figured; Br128997 (damaged), Br132804 (damaged). Total number of specimens not determined.

Remarks. – Only the ventral valve of this species is known (Fig. 113A–C). It appears to be almost circular in outline, with a subcentral apex. The larval shell appears to be very large, possibly up to 0.88 mm across. However, its outline is not sharply delineated. A very short listrium begins immediately outside the larval shell. The central portion of the

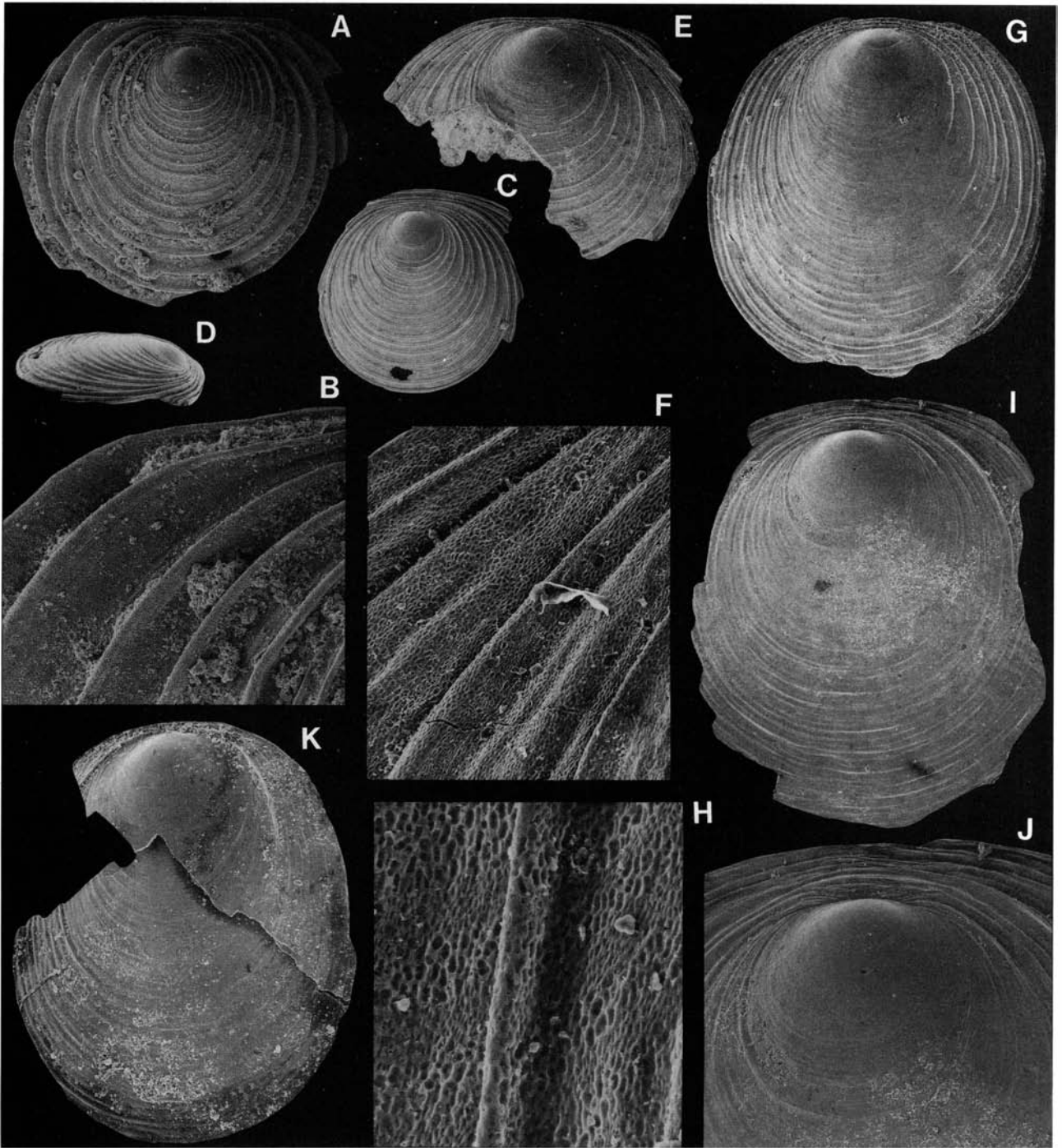


Fig. 112. □A–B. *Orbiculoidea?* sp. a; Folkeslunda Limestone (sample DLK83-fo-1); Br129025. □A. Exterior of the dorsal valve; $\times 14$. □B. Detail of the ornamentation of A; $\times 71$. □C–D. *Orbiculoidea?* sp. b. □C. Dorsal exterior; Gullhöggen Formation (sample GB84-2-19); Br132723, $\times 14$. □D. Side view of C; $\times 14$. □E–F. *Orbiculoidea?* sp. b?, □E. Exterior of a dorsal valve; Kårgårde Limestone (sample DLK83-segk-7); Br128957, $\times 25$. □F. Detail of the ornamentation of E; $\times 225$. □G–K. *Schizotreta* sp. a. □G. Dorsal exterior; Folkeslunda Limestone (sample DLK83-fo-1); Br129023, $\times 25$. □H. Detail of the ornamentation of G; $\times 679$. □I. Exterior of a dorsal valve; Holen Limestone (sample DLK84-hol-25); Br128861, $\times 25$. □J. Detail of the apex of J; $\times 44$. □K. Dorsal exterior; Gullhöggen Formation (sample GB84-2-37); Br132829, $\times 25$.

ventral posterior margin apparently started to secrete shell material at a relatively early stage in ontogeny.

Occurrence. – In Dalarna the species occurs in the Skärlov Limestone and in Västergötland in the Gullhöggen Formation.

Genus *Schizotreta* Kutorga, 1848

Type species. – Original designation; *Orbicula elliptica* Kutorga, 1846, p. 123, probably from the Lower Ordovician (Volkhovian or Kundan stages; L. E. Popov, personal communication, 1985), Pulkova, Leningrad district, U.S.S.R.

Diagnosis. – See Rowell (1965, p. H275).

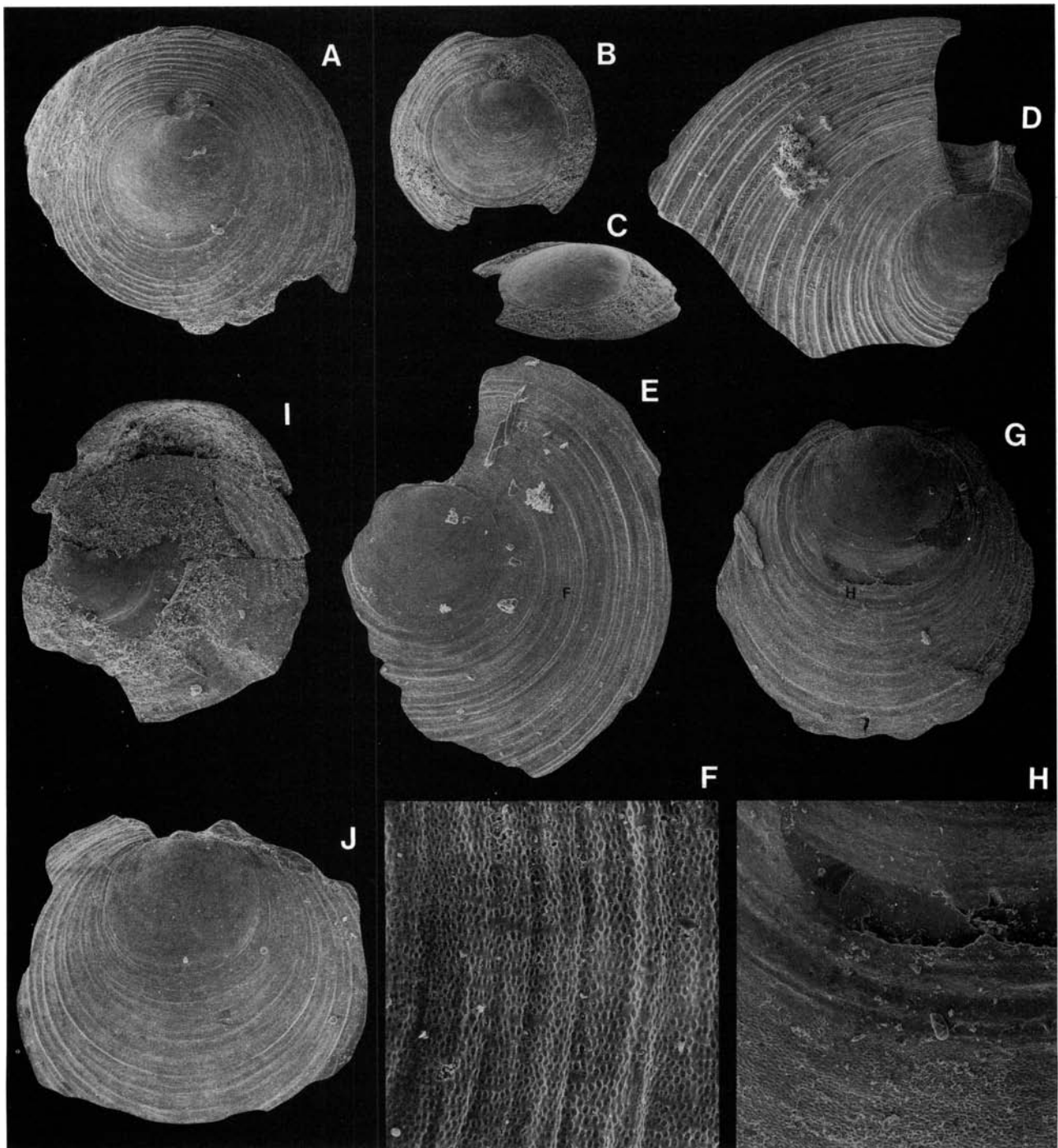


Fig. 113. □A–C. *Orbiculoidea?* sp. c. □A. Ventral exterior; Skärlov Limestone (sample DLK83-sä-6); Br128997, ×25. □B. Exterior of a ventral valve; Gullhögen Formation (sample GB84-2-35); Br132804, ×25. □C. Side view of B; ×25. □D. *Orbiculoidea?* sp. b; ventral exterior; Gullhögen Formation (sample GB84-1-3); Br132612, ×45. □E–F. *Orbiculoidea?* sp. b?. □E. Exterior of a ventral valve; the location of F is indicated; Skärlov Limestone (sample DLK83-sä-7); Br129000, ×45. □F. Detail of the pitted ornamentation of F; ×318. □G–J. *Schizotreta?* sp. a? □G. Ventral exterior; Dalby Limestone (sample DLK83-dal-12); Br132516, ×45. □H. Detail of the ornamentation of G, showing the larval and juvenile shells; ×171. □I. Ventral view of a complete juvenile shell; Furudal Limestone (sample DLK83-fur-17); Br132434, ×45. □J. Ventral exterior; Skärlov Limestone (sample DLK83-sä-6); Br128998, ×45.

Discussion. – Species of *Schizotreta* differ from most species of *Orbiculoidea* in having elongated and flattened valves with a submarginal apex; the ventral valve has a short, marginal listrium.

Schizotreta sp. a

Figs. 19A–C, 45D–F, 112G–K, ?113G–J

Material. – Figured; Br133608d (section), Br129053 (damaged), Br129023 (W 2.05, L 2.23), Br128861 (damaged),

Br132829 (W 2.32, L 2.72), Br132516 (damaged), Br132434 (damaged), Br128998 (damaged). Total number of specimens not determined.

Description. – The valves are elongate oval in outline, about 80–90% as wide as long. The ventral valve is poorly known; in lateral profile it is flattened, with a submarginal apex, and there is a short marginal pedicle notch that lies outside the larval shell. Apparently no listrium is developed (Fig. 113G, I–J). In lateral profile the dorsal valve is flattened and has a submarginal apex (Fig. 112G, I–K). The valves are ornamented with fila (Figs. 112G, I, 113G, J). The ontogeny and postlarval pitting are described above (p. 59, Figs. 45D–F, 112H, 113H). For shell structure see above (p. 35, Fig. 19A–C).

Occurrence. – *Schizotreta* sp. a ranges from the Holen Limestone up into the Folkeslunda Limestone, and questionably also into the Furudal Limestone of Dalarna. In Västergötland it occurs in the Gullhøgen Formation and questionably in the Dalby Limestone.

Order Siphonotretida Kuhn, 1949 (*sensu* Kuhn 1949, p. 101)

Superfamily Siphonotretacea Kutorga, 1848

Diagnosis. – See Rowell (1965, p. H287).

Discussion. – The siphonotretaceans have usually been placed within the Acrotretida. Rowell (1962, p. 151, and 1965, p. H287) suggested that the morphology of the dorsal pseudointerarea of the siphonotretaceans (e.g., *Dysoristus* Bell, 1944) indicates an acrotretacean affinity. However, the early history of the group is not well known. Goryanskij (1960, 1969), Goryanskij & Popov (1985), and Popov & Nölvak (1987) considered the siphonotretaceans as a separate order, the Siphonotretida. This suggestion is supported here. Members of the Siphonotretacea differ from the acrotretids (*sensu stricto*) mainly in shell structure (Biernat & Williams 1971, Popov & Nölvak 1987) and ontogeny. The siphonotretacean larval shell is completely smooth and the formation and development of the siphonotretacean pedicle foramen commonly differs from that of the acrotretaceans (see also above, p. 65).

Family Siphonotretidae Kutorga, 1848

Subfamily Schizamboninae Havlíček, 1982

Genus *Nushbiella* Popov, 1986

Type species. – Original designation; *Multispinula? dubia* Popov, 1977, p. 104, from the Middle Ordovician (Llandeilo–Caradoc) Bestamak Formation, Chingiz range, Kazakhstan, U.S.S.R.

Diagnosis. – See Popov (*in* Kolobova & Popov 1986, p. 252).

Species assigned. – *Multispinula? dubia* Popov, 1977; *?Multispinula parvula* Popov, 1980; *Nushbiella lillianae* sp. nov.

Discussion. The relation of *Nushbiella* to other siphonotretid genera was discussed by Popov (*in* Kolobova & Popov 1986); it differs from other schizambonines in having a well defined procline ventral pseudointerarea, whilst the dorsal pseudointerarea is reduced or lacking. Moreover, unlike most other siphonotretids, no resorption seems to have taken place during the formation of the pedicle foramen. The genus seems to be related somehow to the Lower Ordovician (Arenig) *Cyrbasiotreta* Williams & Curry, 1985, from Ireland; it was not included originally in the Schizamboninae by Williams & Curry (1985) as the type species differs from the schizambonines in lacking an interior pedicle tube. However, *Cyrbasiotreta* is clearly distinguished from the Siphonotretinae Kutorga, 1848, in possessing a sharply delineated procline ventral pseudointerarea.

Nushbiella lillianae sp. nov.

Fig. 114

Name. – After my wife Lillian.

Holotype. – Br132543, complete dorsal valve, Fig. 114A–E (W 2.20, L 1.98) from the Dalby Limestone, Kårgårde (sample DLK83-dal-15), Dalarna.

Paratypes. Figured; Br132493 (W 1.30, L 1.12, H 0.39), Br128730 (damaged). Total of 169 dorsal and 188 ventral valves.

Diagnosis. – Ventral valve conical, strongly procline, with apex about 33% of total length from posterior margin. Pedicle foramen small, continued as thickened interior pedicle tube. Valves with well developed spine-bearing lamellae.

Description. – The valves are about 90% as long as wide. The ventral valve is conical, about 30% as high as wide. In lateral profile it is strongly procline (Fig. 114G) with the maximum height situated at about 33% of the total length from the posterior margin. The ventral pseudointerarea is poorly defined and triangular (Fig. 114H). In ventral view the posterior margin is rounded (Fig. 114F). The outline of the pedicle foramen is keyhole-shaped and relatively short and narrow (\overline{WP} 0.11, \overline{LP} 0.21; OR WP 0.09–0.12, LP 0.20–0.23; $N=9$; sample GB84-3-59). The posterior part of the ‘keyhole’ is generally plugged, thus leaving an open pedicle foramen, rounded to oval in outline, about 90% as wide as long, tapering slightly towards the posterior margin (Fig. 114F); a bulbous projection is present immediately posterior to the pedicle foramen (Fig. 114F–H). The foramen is apparently formed without resorption (see also above, p. 65). The ventral interior has a well developed pedicle tube (Fig. 114I), and the cardinal muscle scars appear to be situated directly lateral to this tube. The dorsal valve is gently convex and sulcate (Fig. 114A, C); in lateral profile it has a strongly recurved beak that extends beyond the posterior margin (Fig. 114B). There is no dorsal pseudointerarea. The dorsal cardinal muscle scars are well developed; the interior is divided by a low median ridge (Fig. 114E). The valves are ornamented with radial costa

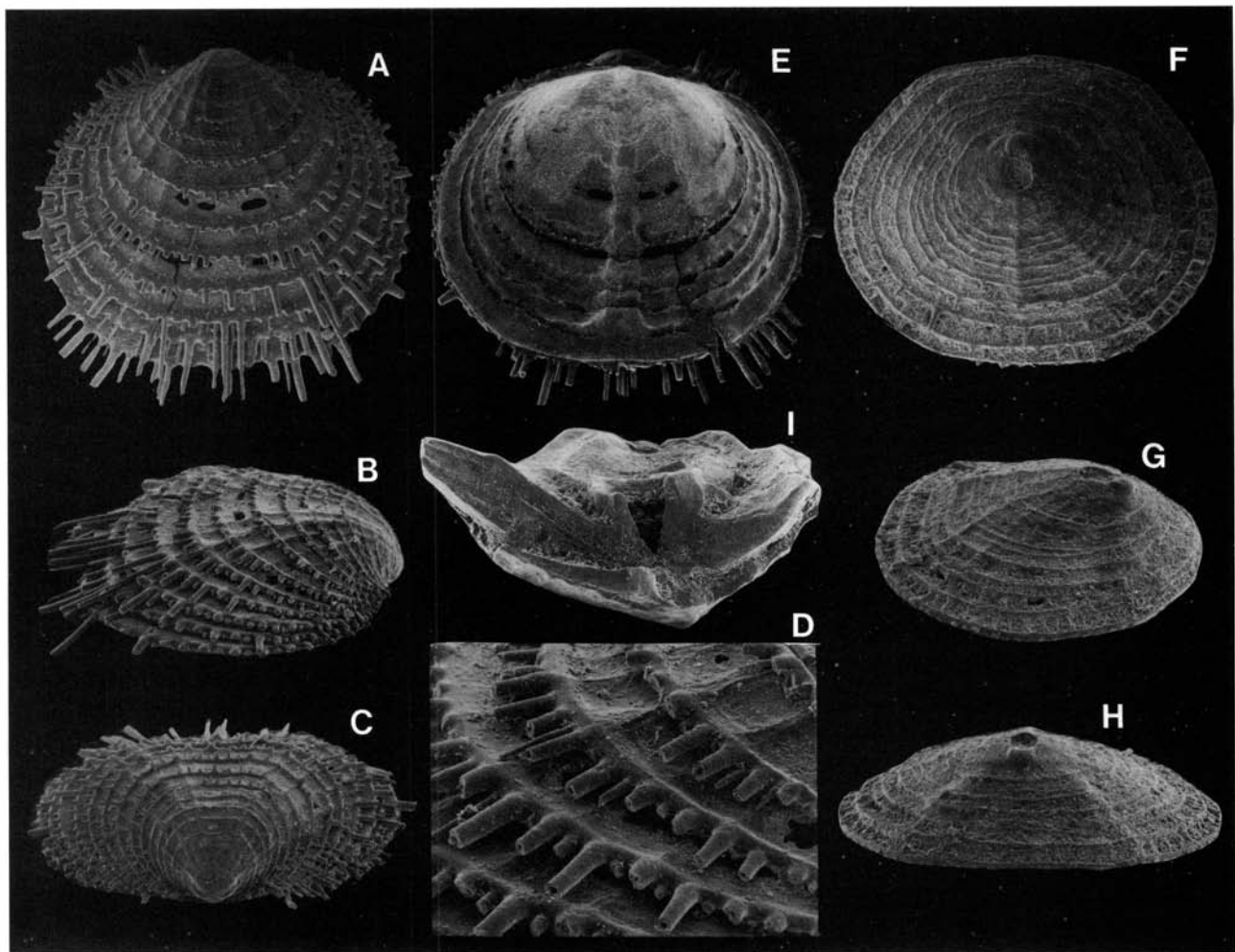


Fig. 114. *Nushbiella lillianae* sp. nov. □A. Holotype; dorsal exterior; Dalby Limestone (sample DLK83-dal-15); Br132543, $\times 22$. □B. Side view of A; $\times 22$. □C. Posterior view of A; $\times 22$. □D. Detail of the spinose ornamentation of A; $\times 68$. □E. Interior of A, showing the median ridge and cardinal muscle scars; $\times 22$. □F. Exterior of a ventral valve; Dalby Limestone (sample DLK83-dal-8); Br132493, $\times 39$. □G. Side view of F; $\times 39$. □H. Posterior view of F; $\times 39$. □I. Side view of the interior of a fragmentary ventral valve, showing the pedicle tube; Dalby Limestone (sample D60-203); Br128730, $\times 54$.

superposed on the lamellae (Fig. 114A, F), and successive lamellae are clearly separated, up to 0.18 mm apart (Fig. 114A, F); the edge of each lamella bears a single row of hollow, tapering spines. Large spines with a basal diameter of 0.04 mm alternate with small spines that have a basal diameter of 0.02 mm (Fig. 114D); thus a fine-meshed trellis is formed, together with the protruding spines of the previous lamellae (Fig. 114A). The ontogeny is described above (p. 65).

Discussion. – *Nushbiella lillianae* is closely related to the type species *N. dubia* (Popov, 1977, p. 104, Pl. 25:8–11) from the Middle Ordovician of Kazakhstan; like the Swedish species, it has a procline ventral valve with a keyhole-shaped pedicle foramen continued as an interior pedicle tube. However, the foramen is about twice as large in *N. dubia*. The foramen of the Lower Ordovician (Arenig) *N.?* *parvula* (Popov, 1980, p. 117, Pl. 29:8–11, 30:1–4) is also much larger than in *N. lillianae*, and it appears to have been formed through some resorption. *N. lillianae* differs from all previously described schizambonine genera (*Schizambon* Walcott, 1884; *Dysoristus* Bell, 1944; *Multispinula* Rowell, 1962;

Ferrobolus Havlíček, 1982; *Karnotreta* Williams & Curry, 1985) in having a short pedicle track and in lacking a dorsal pseudointerarea. The Irish *Cyrbasiotreta cirrata* is similar to *N. lillianae* in having (1) a conical and procline ventral valve, (2) a comparatively small and short pedicle track, and (3) an ornamentation with spinose lamellae. It differs from *N. lillianae* mainly in having (1) a proportionally higher ventral valve, (2) a dorsal pseudointerarea, and (3) more closely spaced spinose lamellae. Moreover, the Swedish species has an interior pedicle tube, which is lacking in *C. cirrata*.

Occurrence. – In Västergötland *N. lillianae* is restricted to the upper Ryd and lower Dalby limestones (Fig. 8C–D). In Dalarna it ranges from the Furudal to the Dalby limestones (Figs. 9B–C, 10).

Subfamily Acanthamboniinae Cooper, 1956

Diagnosis. – Siphonotretids with exclusively hemiperipheral growth; of linguloid outline. Shell gently biconvex. Minute

marginal pedicle foramen, continued as interior pedicle tube. Both valves spinose, with pseudointerareas.

Genera assigned. – *Helmersen*a Pander, 1861; *Acanthambonia* Cooper, 1956; ?*Quasithambonia* Bednarczyk & Biernat, 1978.

Discussion. – Previous studies of acanthamboniines were summarized recently by Popov & Nölvak (1987). The subfamily was assigned originally to the obolids by Cooper (1956, p. 211), and this placement was followed by Wright (1963, p. 231), Rowell (1965, p. H269), and Williams & Curry (1985, p. 196). Goryanskij (1969, p. 99) suggested that *Acanthambonia* was closely related to the siphonotretid *Helmersen*a, but noted that no pedicle foramen had been found in the former. Havlíček (1982, p. 73) followed the notion of Goryanskij and referred the Acanthamboniinae to the Siphonotretidae, and this placement was supported by Popov (personal communication 1985, in Holmer 1986; see also Popov & Nölvak 1987). The lingulid-shaped, flattened valves of acanthamboniines, in combination with their minute pedicle foramen and lingulid-like pseudo-interareas, clearly distinguish them from all other siphonotretids. The genus *Quasithambonia* Bednarczyk & Biernat, 1978 is most probably referable to the subfamily, but its exact relation to *Acanthambonia* cannot be determined at present. According to Popov & Nölvak (1987), *Helmersen*a Pander, 1861 also should be assigned to the subfamily.

Genus *Acanthambonia* Cooper, 1956

Type species. – Original designation; *Acanthambonia minutissima* Cooper, 1956, p. 212, from the Middle Ordovician (*Pygodus anserinus* Biozone) Pratt Ferry beds, Pratt Ferry, Alabama, U.S.A.

Diagnosis. – See Popov & Nölvak (1987, p. 17).

Species assigned. – *Acanthambonia minutissima* Cooper, 1956; *A. virginensis* Cooper, 1956; *A. portranensis* Wright, 1963; *A. klabavensis* Havlíček, 1982; *A. delicata* sp. nov.

Discussion. – As noted by Popov & Nölvak, many previous descriptions of *Acanthambonia* have identified the ventral valve as the dorsal, and vice versa. For example, the ventral valve of the type species, *Acanthambonia minutissima* illustrated by Cooper (1956, Pl. 18D:23, 25; note the interior pedicle tube), is referred to as ‘the dorsal valve’ and the dorsal valve (Pl. 18D:24, 26) is called ‘the ventral valve’. At present five species have been referred to the genus, which has a range from the Arenig to the Upper Ordovician. In addition to the type species, Cooper (1956, p. 213) described *A. virginensis* from the Middle Ordovician Botetourt Formation of Virginia. The youngest member of the genus, *A. portranensis*, was described by Wright (1963, p. 231) from the Upper Ordovician (Cautleyan) Portrane Limestone of Ireland. This species was later recorded also by Goryanskij (1969, p. 49) and by Popov & Nölvak (1987) from the Upper Ordovician Vormsian to Pirguan stages of Estonia. Havlíček (1982, p. 73) described the oldest known member of the genus from the Arenig Klabava Formation

in the Prague Basin, Bohemia. Some unnamed species of *Acanthambonia* have been recorded from the Arenig Tourmakeady Limestone of Ireland by Williams & Curry (1985, p. 196) and from the uppermost Middle Ordovician and lower Upper Ordovician in Västergötland, by Holmer (1986, p. 123). Some undescribed species of the genus are also present in the Tremadoc and Arenig of Sweden (Holmer, unpublished).

Acanthambonia delicata sp. nov.

Fig. 115A–K

Name. – Latin *delicatus*, delightful.

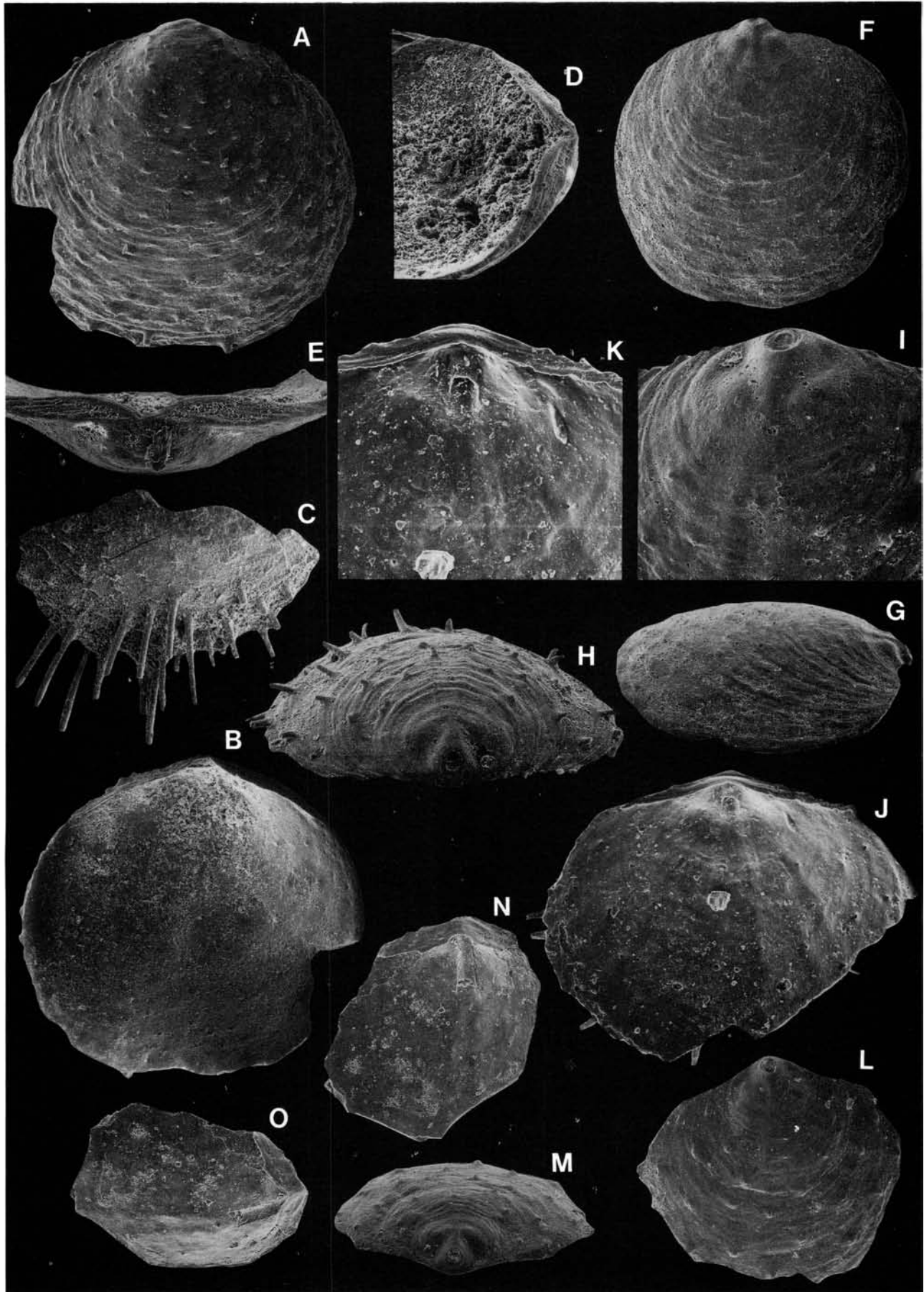
Holotype. – Br128934, complete ventral valve, Figs 115F–G (W 0.95, L 0.93), from the Kårgårde Limestone, Kårgårde section (sample DLK83-segk-3), Dalarna.

Paratypes. – Figured; Br129048a (W 1.01, L 0.99), Br129048b (fragmentary), Br129933 (damaged), Br128935 (damaged). Total of 77 dorsal valves and 37 ventral valves.

Diagnosis. – Valves almost circular with crescent-shaped pseudointerareas, short but wide. Ventral pseudointerarea undivided; dorsal pseudointerarea divided by median groove. Sealed pedicle foramen with short exterior and interior tubes. Moderately spinose valves.

Description. – The valves are almost circular, on average 99% (OR 91–109%; $N=19$) as long as wide. The ventral valve (\bar{W} 0.90, \bar{L} 0.89; OR W 0.57–1.10, L 0.54–1.20; $N=11$; samples DLK83-fo-4, 5, fur-1) is gently convex, about 20% as high (maximum H 0.23) as wide (Fig. 115G–H). The pedicle foramen is minute, circular, and marginal, about 0.05 mm in diameter. The short exterior pedicle tube (Fig. 115H–I) continues as a short interior tube; it is sealed in adults (Fig. 115J–K). The ventral pseudointerarea is undivided, anacline, and wide, occupying 72% (OR 60–79%; $N=9$) of the total width; it is slightly crescent-shaped and short, with a midsagittal length of about 0.06 mm, occupying about 4% of total length (Fig. 115J–K). The dorsal valve (\bar{W} 0.96, \bar{L} 0.95; OR W 0.71–1.10, L 0.67–1.13; $N=9$; samples DLK83-fo-4, 5, fur-1) is very gently sulcate (Fig. 115A–B), and slightly more convex than the ventral valve; it is about 30% as high (maximum H 0.31) as wide. In some specimens the umbo is recurved beyond the posterior margin (Fig. 115D–E). The dorsal pseudointerarea occupies 72% (OR 65–79%; $N=7$) of the total width; it is divided by a triangular median groove (referred to as the pedicle groove by many previous workers), and has strongly anacline propareas (Fig. 115B, D–E). The dorsal interior occasionally has a pair of weakly impressed, closely spaced muscle scars, in about the centre of the valve. The valves are ornamented with regularly spaced, hollow spines, 0.03 mm in diameter (Fig. 115A, C, H, F). The smooth marginal larval shell is sharply delineated, circular, up to about 0.25 mm across (Fig. 115H–I).

Discussion. – The pedicle foramen of *Acanthambonia* has previously been illustrated only in *A. portranensis* Wright, 1963 (Popov & Nölvak 1987), and the morphology of the pseudointerareas of most other acanthamboniines is un-



known. The type species, *A. minutissima* Cooper, differs from *A. delicata* in being more oblong (L/W ratio about 111% in the holotype and paratype; Pl. 18D:23–24) and in having a proportionally longer ventral pseudointerarea (LI/L ratio about 8% in the holotype). *A. virginensis* Cooper (1956, Pl. 9A:1–6) is more spinose than the Swedish species. *A. delicata* appears to be related closely to the Irish *A. portranensis* Wright (1963, Pl. 1:29–31; Popov & Nölvak 1987, Pl. 1–2), the holotype of which is a dorsal valve with a divided pseudointerarea and two central cardinal muscle scars. The wide and long ventral pseudointerarea of this species was well illustrated by Popov & Nölvak (1987, Pl. 2:1A). The dorsal pseudointerarea of the Irish species is comparatively narrower than in *A. delicata*, whereas the ventral pseudointerarea is longer. The large (maximum W 3.1 mm) Bohemian species, *A. klabavensis* Havlíček, 1982 differs from all other species in having interior tubercles.

Occurrence. – *Acanthambonia delicata* ranges from the Segerstad to Furudal limestones of Dalarna (Fig. 9A). There is also a questionable record from the Skärlov Limestone of Jämtland (sample J70-167).

Acanthambonia sp. nov. a

Fig. 115L–O

Material. – Figured; Br133003 (damaged), Br133002 (damaged). Total of 7 ventral valves.

Remarks. – *Acanthambonia* sp. nov. a is closely related to *A. delicata*. However, the ventral valve is flatter and has a more protruding larval shell (Fig. 115L–M). The ventral pseudointerarea and pedicle tube are proportionally longer than in *A. delicata* (Fig. 115N–O), and the ornamentation is sparsely spinose. No dorsal valves were isolated.

Occurrence. – A few fragmentary valves of *Acanthambonia* sp. nov. a are known from the upper Dalby Limestone of Dalarna (Fig. 9C).

Order Paterinida Rowell, 1965

Superfamily Paterinacea Schuchert, 1893

Family Paterinidae Schuchert, 1893.

Genus *Dictyonites* Cooper, 1956

Type species. – Original designation; *Dictyonites perforata* Cooper, 1956, p. 187, from the Middle Ordovician (*Pygodus anserinus* Biozone) Pratt Ferry beds, Pratt Ferry, Alabama, U.S.A.

Diagnosis. – See Rowell (1965, p. H295).

Species assigned. – *Dictyonites perforata* Cooper, 1956; *D. fredriki* sp. nov.

Discussion. – One unnamed species of *Dictyonites* from the lower Whiterock of Nevada was illustrated by Krause & Rowell (1975, p. 70, Pl. 9:18–22). Popov (*in* Nazarov & Popov 1980, p. 119, Pl. 32:5–9) questionably recorded the type species from the Lower and Middle Ordovician Kogashi and Kopalin stages of Kazakhstan.

Dictyonites fredriki sp. nov.

Fig. 116A–H

Name. – After my son Fredrik.

Holotype. – Br128495, slightly damaged dorsal valve, Fig. 116A–C (W c2.64, L 1.49), from the Furudal Limestone (sample DLK83-fur-11), Kårgårde section, Dalarna.

Material. – Figured; Br128494 (damaged), Br128493 (W 1.70, L 0.96, H 0.68). Total of 2 dorsal and 3 ventral valves.

Diagnosis. – Ventral valve relatively low. Poorly developed divaricate ornamentation of open pores; diameter of pores relatively small.

Description. – The valves average 56% as long as wide ($N=2$), with an almost straight posterior margin (Fig. 116A, G). One ventral valve is about 40% as high as wide; in lateral profile it is regularly conical with the maximum height near the centre of the valve (Fig. 116D–E, G–H). The ventral pseudointerarea is procline, wide, and occupies about 80–90% of the total width; in posterior view it is triangular and has a pair of well defined, flattened propareas. The delthyrium is partly closed by a raised, convex homeodeltidium, which has strongly developed growth lines (Fig. 116D–G). The ventral interior has a knob-like apical process on the anterior apical surface. In lateral profile the dorsal valve is flattened, approximately less than 10% as high as wide. The dorsal pseudointerarea is poorly defined, broadly triangular and wide, occupying about 80–90% of the total width; the notothyrium appears to be unrestricted (Fig. 116A–C). The dorsal valve is ornamented with pores in a divaricate pattern; the pores, which generally are open, vary considerably in size, but are always less than 0.10 mm across. The divaricate pattern is more poorly developed on the ventral valve (Fig. 116A, G–H); on both valves it is commonly disturbed (Fig. 116A, D). The larval shell is about 0.70 mm wide and 0.45 mm long; it is sharply delineated and has a raised rim. In ventral view the ventral larval shell is slightly

Fig. 115. □A–K. *Acanthambonia delicata* sp. nov. □A. Dorsal exterior; Folkeslunda Limestone (sample DLK83-fo-4); Br129048a, ×60. □B. Interior of A; ×60. □C. Fragmentary valve, showing the spinose ornamentation; Folkeslunda Limestone (sample DLK83-fo-4); Br129048b, ×60. □D. Side view of a dorsal pseudointerarea; Kårgårde Limestone (sample DLK83-segk-3); Br128933, ×82. □E. Posterior view of the pseudointerarea of D; ×82. □F. Holotype; ventral exterior; Kårgårde Limestone (sample DLK83-segk-3); Br128934, ×60. □G. Side view of F; ×60. □H. Posterior view of a ventral valve; Kårgårde Limestone (sample DLK83-segk-3); Br128935, ×60. □I. The larval shell of H; ×151. □J. Interior of H; ×100. □K. Detail of the pseudointerarea and pedicle tube of H; ×170. □L–O. *Acanthambonia* sp. nov. a; Dalby Limestone (sample DLK83-dal-36). □L. Ventral exterior; Br133003, ×82. □M. Posterior view of L; ×82. □N. Interior of a ventral valve; Br133002, ×82. □O. Side view of N; ×82.

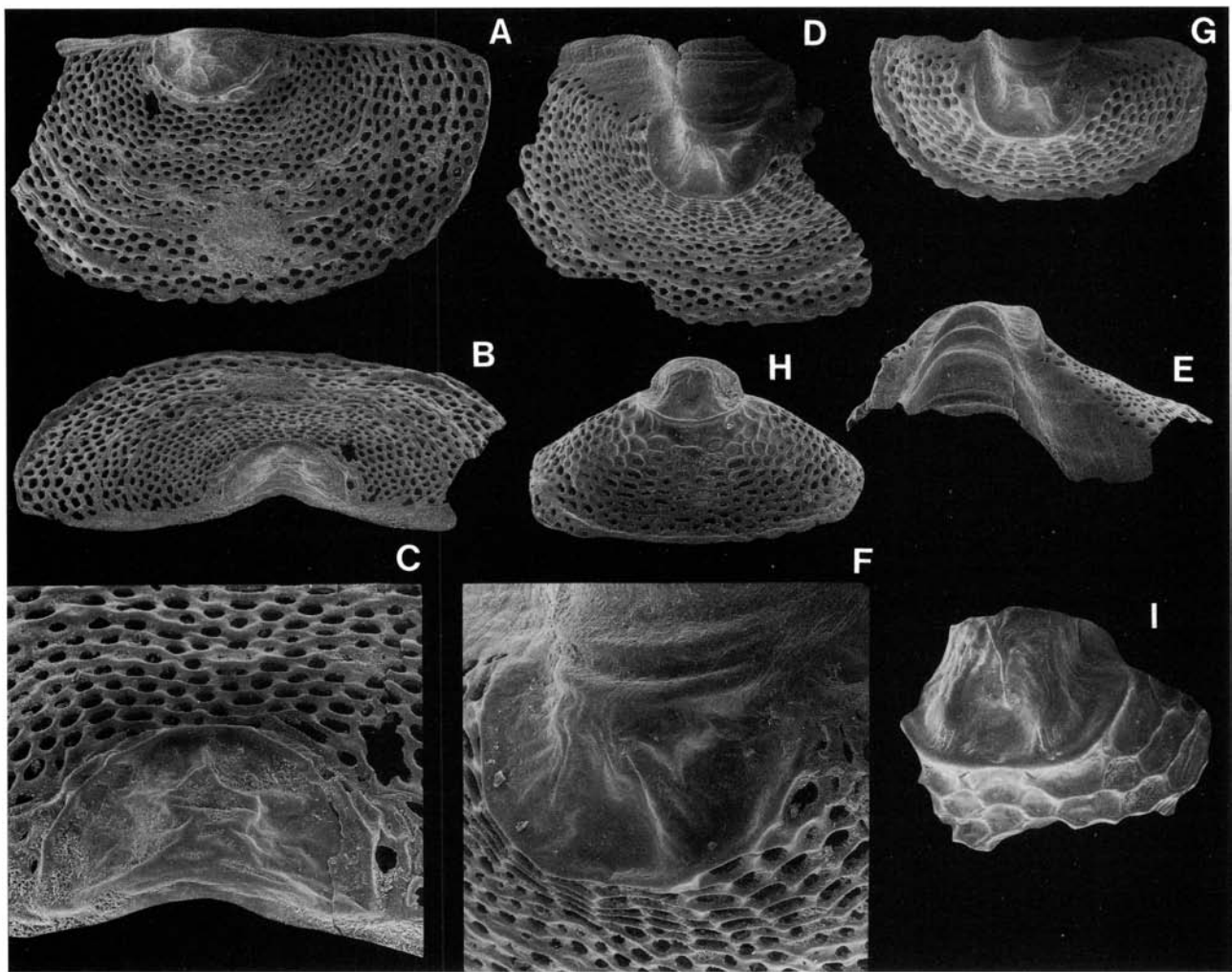


Fig. 116. □A–H. *Dictyonites fredriki* sp. nov.; Furudal Limestone (sample DLK83-fur-11). □A. Holotype; dorsal exterior; Br128495, $\times 25$. □B. Posterior view of A; $\times 25$. □C. Posterior view of the larval shell of A; $\times 67$. □D. Exterior of a ventral valve; Br128494, $\times 25$. □E. Posterior view of D; $\times 25$. □F. The larval shell of D; $\times 67$. □G. Exterior of a ventral valve; Br128493, $\times 25$. □H. Anterior view of G; $\times 25$. □I. *Dictyonites* sp.; Exterior of a fragmentary ventral valve; Kårgårde Limestone (sample DLK83-segk-5); Br128932, $\times 25$.

crescent-shaped with rounded anterior margin (Fig. 116F). The marginal dorsal larval shell has an almost straight posterior and a convex anterior margin (Fig. 116C). The surface of both larval shells lacks micro-ornamentation. The shell appears to consist entirely of CCP, which shows no birefringence.

Discussion. – *Dictyonites fredriki* compares closely with the roughly contemporaneous type species *Dictyonites perforata* Cooper (1956, Pl. 9D:11–13, 10A:1–10) from the southern Appalachians, but the latter, however, differs mainly in having (1) larger pores (diameter generally above 0.10 mm), (2) a somewhat higher ventral valve (H/W ratio around 42–48% in two paratypes), and (3) a better developed divaricate ornamentation of pores. The presence of a homoeochilidium was reported by Cooper from the dorsal valve of *D. perforata*. However, the notothyrium is unrestricted in the Swedish specimens. An apical process (referred to as a septum by Cooper 1956, p. 188) is present on the ventral interior in both Cooper's specimens (Pl. 10B:9–10) and in the material under consideration.

Occurrence. – In Dalarna *Dictyonites fredriki* is known from the Furudal Limestone, and there is a questionable record from the Dalby Limestone (Fig. 9B–C).

Dictyonites sp.

Fig. 116I

Material. Figured; Br128932 (damaged). Total of one ventral valve.

Remarks. – The apical portion of the ventral valve is damaged in the only known specimen. It appears to be close to *Dictyonites fredriki*, but the larval shell is proportionally somewhat higher and more wrinkled, and the post-larval shell is ornamented with closed pores (Fig. 116I).

Occurrence. – The sole specimen is from the Kårgårde Limestone of Dalarna, but there are also some questionable fragments in the Vikarby and Seby limestones (Fig. 9A).

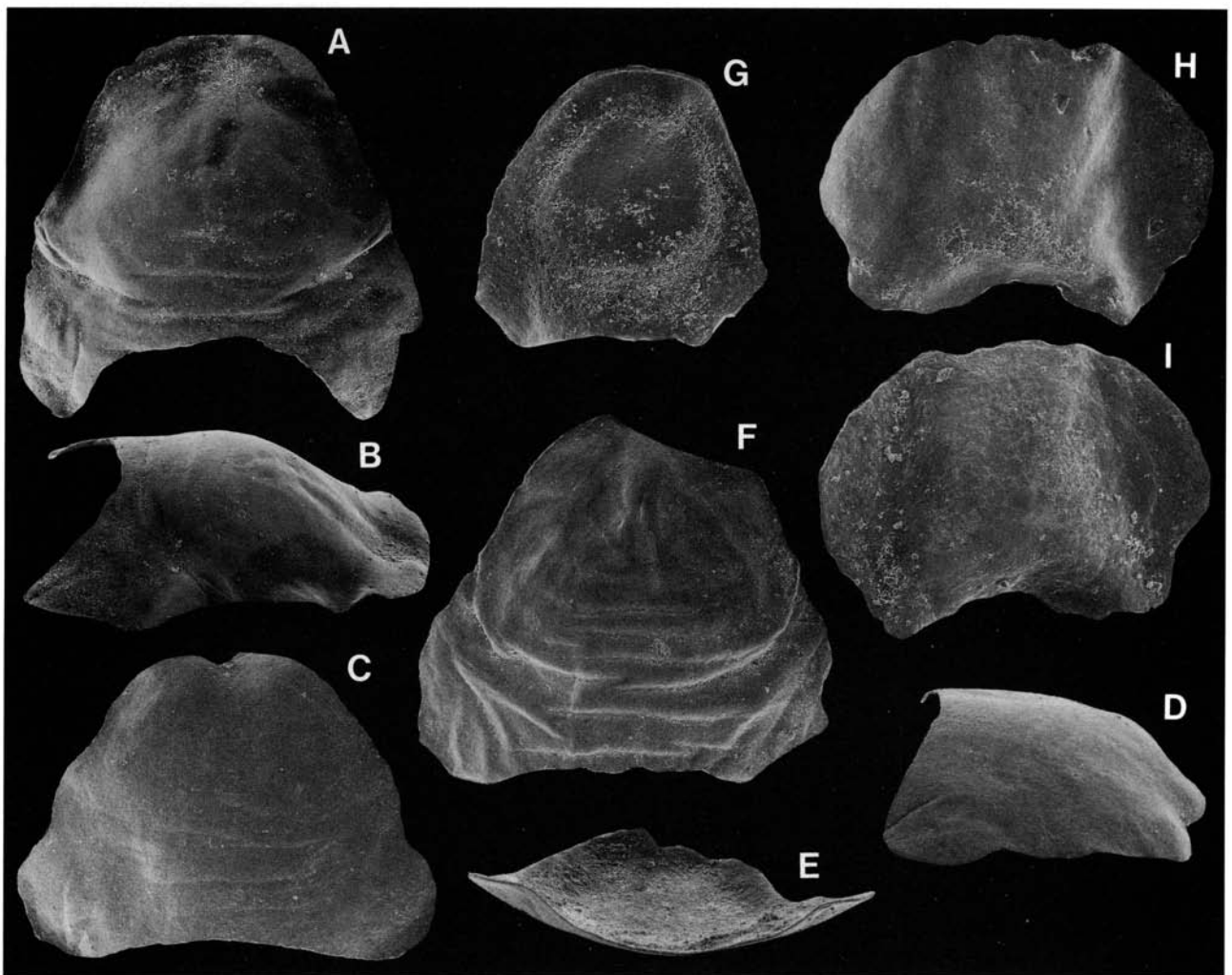


Fig. 117. *Tegulella minuta* gen. et sp. nov. □A. Holotype; dorsal exterior; Furudal Limestone (sample DLK83-fur-11); Br128492, ×47. □B. Side view of A; ×47. □C. Exterior of a dorsal valve; Holen Limestone (sample DLK84-hol-25); Br128846, ×47. □D. Side view of C; ×47. □E. Posterior view of the interior of C; ×47. □F. Dorsal exterior; Furudal Limestone (sample DLK83-fur-6); Br129061, ×47. □G. Interior of a dorsal valve; Furudal Limestone (sample DLK83-fur-6); Br129060, ×47. □H. Ventral exterior; Furudal Limestone (sample DLK83-fur-6); Br129063, ×86. □J. Interior of H; ×86.

Problematica

Genus *Tegulella* gen. nov.

Name. – Latin *tegulum*, small roof; alluding to the slightly arched roof-like shape of the ventral valve.

Type species. – *Tegulella minuta* gen. et sp. nov., from the Furudal Limestone, Kårgärde quarry, Dalarna.

Species assigned. – Type species only.

Diagnosis. – Bivalved, chitinophosphatic shells; bilaterally symmetrical. Exterior of concave ventral valve with central depression and two lateral 'wings'. Crescent-shaped dorsal valve larger than ventral valve, with wrinkled exterior but without growth lines; rounded, convex anterior margin and convex posterior margin; gently convex in lateral profile.

Tegulella minuta sp. nov.

Figs. 117, 118

Name. – Latin *minutus*, small.

Holotype. – Br128492, complete dorsal valve, Fig. 117A–B (W 1.12, L 1.10), from the Furudal Limestone, Kårgärde section (sample DLK83-fur-11), Dalarna.

Paratypes. – Figured; Br133595k (section), Br128846 (W 1.15, L 0.96), Br129061 (W ~1.16, L 1.12), Br129060 (W ~0.93, L 0.87), Br129063 (W 0.59, L 0.46). Total of 103 dorsal and 6 ventral valves.

Diagnosis. – As for genus.

Description. – The concave ventral valve is about 78% as long as wide in one specimen. The anterior margin is convex, with the posterior margin slightly concave. The ventral exterior is smooth, with a median depression and two lateral 'wings' (Fig. 117H). The ventral interior lacks recognizable structures (Fig. 117I). In lateral profile the dorsal valve is 'roof-like' and convex, with the maximum height

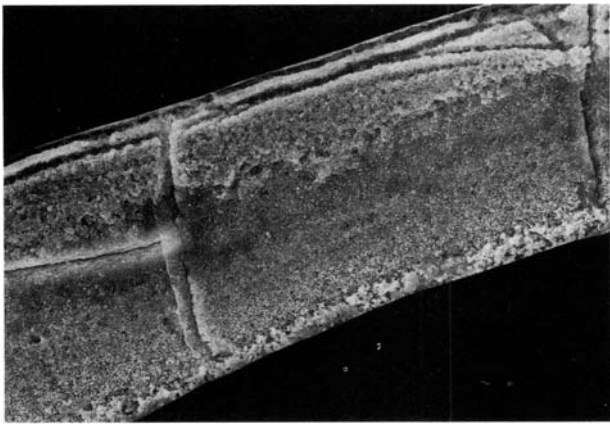


Fig. 118. Midsagittal section through the dorsal valve of *Tegulella minuta* gen. et sp. nov.; note that the shell consists entirely of CCP; Kårgårde Limestone (sample DLK83-segk-6); Br133595k, $\times 1100$.

near the centre of the valve (Fig. 117B, D–E). In dorsal view it is more varying in outline, on average 93% as long as wide ($N=4$); it is commonly crescent-shaped with a convex anterior and concave posterior margin (Fig. 117A, C). In some specimens it is more triangular in outline (Fig. 117F–G). The dorsal exterior is smooth (Fig. 117A, C), but commonly also wrinkled (Fig. 117F). There are no recognizable structures on the dorsal interior, but the valve is generally slightly thicker near its centre (Fig. 117G). The exterior of both valves lacks all traces of growth lines. In sections examined under the SEM and in polarized light, the shell is seen to have a thin outer layer, about $4\ \mu\text{m}$ thick, and a thicker inner layer, about $27\ \mu\text{m}$ thick (Fig. 118). Both layers consist of CCP and do not show birefringence.

Discussion. – Only the type species can be referred to this problematical genus, whose affinities remain obscure. It is comparable with brachiopods because it is bivalved and bilaterally symmetrical. It is comparable with the phosphatic inarticulates in shell composition. However, *Tegulella* cannot be compared with any previously described taxa. The correct orientation of the valves of *T. minuta* is not known and consequently the dorsal–ventral and anterior–posterior directions cannot be identified with certainty. An articulated (although somewhat crushed) shell of *T. minuta* was found in the Kålla Limestone on Öland, providing evidence that the two described valves belong to the same species. It does not appear to be a broken part of some larger animal, but there is no evidence of accretionary growth. The size range of *T. minuta* is very restricted. The width of the dorsal valves varies from 0.93 to 1.16 mm. The shell structure and the lack of evidence of accretionary growth could indicate that the valves were secreted as entire plates over an epithelial surface.

Occurrence. – *Tegulella minuta* is a common, widely distributed and long ranging species. It appears in the Hølen Limestone and ranges up into the Dalby Limestone of Dalarna (Figs. 9, 10). In Västergötland it is restricted to the Gullhögen Formation and the lowermost Ryd Limestone (Fig. 8B–C). *T. minuta* has also been recorded from the Kålla Limestone on Öland, and from the Pratt Ferry beds of Alabama, U.S.A.

References

- Ager, D.V. 1967: Brachiopod palaeoecology. *Earth-Science Reviews* 3, 157–179.
- Angelin, N.P. & Lindström, G. 1880: *Fragmenta Silurica e dono Caroli Henrici Wegelin*. 60 pp. Holmiae [Stockholm].
- Bassett, M.G. 1984: Life strategies of Silurian brachiopods. *Special Papers in Paleontology* 32, 237–263.
- Bednarczyk, W. 1964: Stratygrafia i fauna tremadoku i arenigu (Oelandianu) regionu kieleckiego Gór Swietokrzyskich. [The stratigraphy and fauna of the Tremadocian and Arenigian (Oelandian) in the Kielce region of the Holy Cross Mountains.] *Biuletyn Geologiczny Uniwersytetu Warszawskiego* 4, 1–216.
- Bednarczyk, W. 1971: Stratigraphy and palaeogeography of the Ordovician in the Holy Cross Mts. *Acta Geologica Polonica* 21, 573–616.
- Bednarczyk, W. 1986: Inarticulate brachiopods from the Lower Ordovician in northern Poland. *Annales Societatis Geologorum Poloniae* 56, 409–418.
- Bednarczyk, W. & Biernat, G. 1978: Inarticulate brachiopods from the Lower Ordovician of the Holy Cross Mountains. *Acta Paleontologica Polonica* 23, 293–316.
- Beecher, C.E. 1891: Development of the Brachiopoda. Part 1: Introduction. *American Journal of Science* 41, 343–357.
- Beecher, C.E. 1892: Development of the Brachiopoda. Part 2: Classification of the stages of growth and decline. *American Journal of Science* 44, 133–155.
- Bell, W.C. 1946: Etching 'corneous' brachiopods (Abstract). *Geological Society of America Bulletin* 57, 117.
- Bell, W.C. 1948: Acetic acid etching technique applied to Cambrian brachiopods. *Journal of Paleontology* 22, 101–102.
- Bergström, J. 1968a: Some Ordovician and Silurian brachiopod assemblages. *Lethaia* 1, 230–237.
- Bergström, J. 1968b: Upper Ordovician brachiopods from Västergötland, Sweden. *Geologica et Palaeontologica* 2, 1–35.
- Bergström, S.M. 1971: Conodont biostratigraphy of the Middle and Upper Ordovician of Europe and eastern North America. *Geological Society of America Memoir* 127, 83–157.
- Biernat, G. 1973: Ordovician inarticulate brachiopods from Poland and Estonia. *Paleontologica Polonica* 28, 1–116.
- Biernat, G. & Williams, A. 1970: Ultrastructure of the protogulum of some acrotretide brachiopods. *Palaentology* 13, 491–502.
- Biernat & Williams, A. 1971: Shell structure of the siphonotretacean Brachiopoda. *Palaentology* 14, 423–430.
- Bitter, P.H. von & Ludvigsen, R. 1979: Formation and function of protogular pitting in some North American acrotretid brachiopods. *Palaentology* 22, 705–720.
- Blochmann, F. 1900: *Untersuchungen über den Bau der Brachiopoden I. Die anatomie von Discinisca lamellosa (Broderip) und Lingula anatina Bruguiere*. 66–124. Gustav Fischer, Jena.
- Boucot, A.J. 1975: *Evolution and extinction rate controls*. 427 pp. Developments in Palaeontology and Stratigraphy, 1. Elsevier, Amsterdam.
- Bulman, O.M.B. 1964: Lower Palaeozoic plankton. *Quarterly Journal of the Geological Society of London* 120, 455–476.
- Chatterton, B.D.E. & Whitehead, H.L. 1987: Predatory borings in the inarticulate brachiopod *Artiotreta* from the Silurian of Oklahoma. *Lethaia* 20, 67–74.
- Cherns, L. 1979: The environmental significance of *Lingula* in the Ludlow Series of the Welsh Borderland and Wales. *Lethaia* 12, 35–46.
- Chuang, S.H. 1961: Growth of the postlarval shell in *Lingula unguis* (L.) (Brachiopoda). *Proceedings of the Zoological Society of London* 137, 299–310.
- Chuang, S.H. 1962: Statistical study of variations in the shell of *Lingula unguis* (Linnaeus). *Videnskaphige Meddelelser fra Dansk Naturhistorisk Forening* 124, 199–215.
- Chuang, S.H. 1971a: New interpretation of the morphology of *Schizambon australis* Ulrich and Cooper (Ordovician siphonotretid inarticulate brachiopod). *Journal of Paleontology* 45, 824–832.

- Chuang, S.H. 1971b: The morphology and paleobiology of *Trematis elliptopora* Cooper (Inarticulata, Brachiopoda). In Dutro, J. T., Jr. (ed.): *Paleozoic perspectives: A paleontological tribute to G. Arthur Cooper*. *Smithsonian Contributions to Paleobiology* 3, 93–100.
- Chuang, S.H. 1977: Larval development in *Discinisca* (inarticulate brachiopod). *American Zoologist* 17, 39–53.
- Cisne, J.L. 1973: Beecher's Trilobite Bed revisited: ecology of an Ordovician deepwater fauna. *Postilla* 160, Peabody Museum Yale University, 1–25.
- Conklin, E.G. 1902: The embryology of a brachiopod, *Terebratulina septentrionalis* Couthony. *Proceedings of the American Philosophical Society* 40, 41–76.
- Conway Morris, S., Whittington, H.B., Briggs, D.E.G., Hughes, C.P. & Bruton, D.L. 1982: *Atlas of the Burgess Shale*. 31 pp. Palaeontological Association, London.
- Cooper, G.A. 1956: Chazyan and related brachiopods. *Smithsonian Miscellaneous Collection* 127, 1–1245.
- Curry, G.B., & Williams, A. 1983: Epithelial moulds on the shells of the early Palaeozoic brachiopod *Lingulella Lethaia* 16, 111–118.
- Fåhræus, L.E. 1966: Lower Viruan (Middle Ordovician) conodonts from the Gullhögen quarry, southern central Sweden. *Sveriges Geologiska Undersökning C* 610, 1–40.
- Fortey, R.A. & Owens, R.M. 1987: The Arenig Series in South Wales: Stratigraphy and Palaeontology. *Bulletin of the British Museum of Natural History (Geology)* 41, 69–307.
- Franzén, Å. 1969: On larval development and metamorphosis in *Terebratulina*, Brachiopoda. *Zoologiska Bidrag, Uppsala universitet* 38, 155–178.
- Funkquist, H.P.A. 1919: Asaphusregionens omfattning i sydöstra Skåne och på Bornholm. *Lunds Universitets Årsskrift N.F.* 2, 16, 1–55.
- Fürsich, F.T. & Hurst, J.M. 1974: Environmental factors determining the distribution of brachiopods. *Palaeontology* 17, 879–900.
- Gilmour, T.H.J. 1978: Ciliation and function of the food-collecting and waste-rejecting organs of lophophorates. *Canadian Journal of Zoology* 56, 2142–2155.
- Gilmour, T.H.J. 1981: Food-collecting and waste-rejecting mechanisms in *Glottidia pyramidata* and the persistence of lingulacean inarticulate brachiopods in the fossil record. *Canadian Journal of Zoology* 59, 1539–1547.
- Goryanskij, V.Yu. 1960: Klass Inarticulata. In Sarycheva, T.G. (ed.): *Mshanki Brakhiopody*. In Orlov, U.A. (ed.): *Osnovy Paleontologii*. 172–182. Akademii Nauk SSSR, Moskva.
- Goryanskij, V.Yu. 1969: Bezzamkovye brakhiopody kembrijskikh i ordovikskikh otlozhenij severo-zapada Russkoj platformy. [Inarticulate brachiopods of the Cambrian and Ordovician of the northwest Russian Platform.] *Ministerstvo Geologii RSFSR, Severo-Zapadnoe Territorialnoe Geologicheskoe Upravlenie* 6, 1–173.
- Goryanskij, V.Yu. & Popov, L.E. 1985: Morfologiya, sistemicheskoe polozenie i proiskhozhdenie bezzamkovykh brakhiopod s karbonatnoj rakovinoj. [Morphology, systematic position and origin of the inarticulate brachiopods with carbonate shells.] *Paleontologicheskij Zhurnal* 1985:3, 3–14.
- Goryanskij, V.Yu. & Popov, L.E. 1986: On the origin and systematic position of the calcareous-shelled inarticulate brachiopods. *Lethaia* 19, 233–240.
- Grahn, Y. 1981: Ordovician Chitinozoa from the Stora Åsbotorp boring in Västergötland south-central Sweden. *Sveriges Geologiska Undersökning C* 787, 1–40.
- Grant, R.E. 1980: Koskinoid perforations in brachiopod shells: function and mode of formation. *Lethaia* 13, 313–319.
- Hadding, A. 1913: Undre dicellograptusskiffern i Skåne jämte några därmed ekvivalenta bildningar. *Lunds Universitets Årsskrift N.F.* 2, 9, 1–93.
- Hammond, L.S. 1980: The larvae of a discinid (Brachiopoda: Inarticulata) from inshore waters near Townsville, Australia, with revised identifications of previous records. *Journal of Natural History* 4, 647–661.
- Hammond, L.S. 1982: Breeding season, larval development and dispersal of *Lingula anatina* (Brachiopoda, Inarticulata) from Townsville, Australia. *Journal of the Zoological Society of London* 198, 183–196.
- Harper, D.A.T., Owen, A.W. & Williams, S.H. 1984: The Middle Ordovician of the Oslo Region, Norway, 34. the type Nakholmen Formation (Upper Caradoc), Oslo, and its faunal significance. *Norsk Geologisk Tidsskrift* 64, 293–311.
- Havlíček, V. 1967: Brachiopoda of the Suborder Strophomenidina in Czechoslovakia. *Rozpravy Ústředního ústavu geologického* 33, 1–235.
- Havlíček, V. 1972: Life habit of some Ordovician inarticulate brachiopods. *Vestník Ústředního ústavu geologického* 47, 229–233.
- Havlíček, V. 1982: Lingulacea, Paterinacea and Siphonotretacea (Brachiopoda) in the Lower Ordovician sequence of Bohemia. *Sborník geologických věd, Paleontologie* 25, 9–82.
- Hede, J.E. 1951: Boring through Middle Ordovician – Upper Cambrian strata in the Fågelsång district, Scania (Sweden). *Lunds Universitets Årsskrift N.F.* 2, 7, 1–84.
- Helmcke, J. 1939: Brachiopoda. In Kükenthal, W. & Krumbach, T. (eds.): *Handbuch der Zoologie* 3:2, 139–262.
- Henningsmoen, G. 1948: The Tretaspis Series of the Kullatorp core. In Waern, B., Thorslund, P., & Henningsmoen, G.: Deep boring through Ordovician and Silurian strata at Kinnekulle, Västergötland. *Bulletin of the Geological Institutions of the University of Uppsala* 32, 374–432.
- Hewitt, R.A. 1980: Microstructural contrasts between some sedimentary francolites. *Journal of the Geological Society of London* 137, 661–667.
- Hisinger, W. 1837: *Lethaea Svecica seu Petrificata Sveciae, iconibus et characteribus illustrata*. 124 pp. Holmiae [Stockholm].
- Holmer, L.E. 1983: Lower Viruan discontinuity surfaces in central Sweden. *Geologiska Föreningens i Stockholms Förhandlingar* 105, 29–42.
- Holmer, L.E. 1986: Inarticulate brachiopods around the Middle-Upper Ordovician boundary in Västergötland. *Geologiska Föreningens i Stockholms Förhandlingar* 108, 97–126.
- Holmer, L.E. 1987a: Ordovician mazuelloids and other microfossils from Västergötland. *Geologiska Föreningens i Stockholm Förhandlingar* 109, 67–71.
- Holmer, L.E. 1987b: Discinacean brachiopods from the Ordovician Kullsberg and Boda limestones of Dalarna, Sweden. *Geologiska Föreningens i Stockholm Förhandlingar* 109, 317–326.
- Hurst, J.M. 1979: Evolution, succession and replacement in the type upper Caradoc (Ordovician) benthic faunas of England. *Paleogeography, Paleoclimatology, Paleoecology* 27, 189–246.
- Hyman, L.H. 1959: *The invertebrates 5. Smaller coelomate groups*. 516–609. McGraw Hill, New York.
- Iwata, K. 1981a: Ultrastructure and mineralization of the shell of *Lingula unguis* Linne, (Inarticulate brachiopod). *Journal of the Faculty of Science, Hokkaido University, Serie 4:20*, 35–65. [In Japanese.]
- Iwata, K. 1981b: Ultrastructure and calcification of the shells in inarticulate brachiopods. Part 1. Ultrastructure of the shells of *Lingula unguis* (Linnaeus). *Journal of the Geological Society of Japan* 87, 405–415.
- Iwata, K. 1982: Ultrastructure and calcification of the shells in inarticulate brachiopods. Part 2. Ultrastructure of the shells of *Glottidia* and *Discinisca*. *Journal of the Geological Society of Japan* 88, 957–966. [In Japanese with English abstract.]
- Jaanusson, V. 1957: Middle Ordovician ostracodes of central and southern Sweden. *Bulletin of the Geological Institutions of the University of Uppsala* 37, 1–442.
- Jaanusson, V. 1960: The Viruan (Middle Ordovician) of Öland. *Bulletin of the Geological Institutions of the University of Uppsala* 38, 207–288.
- Jaanusson, V. 1963: Lower and Middle Viruan (Middle Ordovician) of the Siljan district. *Bulletin of the Geological Institutions of the University of Uppsala* 42, 1–40.
- Jaanusson, V. 1964: The Viruan (Middle Ordovician) of Kinnekulle and Northern Billingen, Västergötland. *Bulletin of the Geological Institutions of the University of Uppsala* 43, 1–73.
- Jaanusson, V. 1966: Fossil brachiopods with probable aragonitic shell. *Geologiska Föreningens i Stockholm Förhandlingar* 88, 279–281.
- Jaanusson, V. 1972: Constituent analysis of an Ordovician limestone from Sweden. *Lethaia* 5, 1–73.

- Jaanusson, V. 1973: Aspects of carbonate sedimentation in the Ordovician of Baltoscandia. *Lethaia* 6, 11–34.
- Jaanusson, V. 1976: Faunal dynamics in the Middle Ordovician (Viruan) of Balto-scandia. In Bassett, M.G. (ed.): *The Ordovician System. Proceedings of a Palaeontological Association symposium*. 301–326. University of Wales Press and National Museum of Wales, Cardiff.
- Jaanusson, V. 1982a: Introduction to the Ordovician of Sweden. In Bruton, D.L. (ed.): Field excursion guide. IV International Symposium on the Ordovician System. *Paleontological Contributions from the University of Oslo the University of Oslo* 279, 1–9.
- Jaanusson, V. 1982b: Ordovician in Dalarna. In Bruton, D.L. (ed.): Field excursion guide. IV International Symposium on the Ordovician System. *Paleontological Contributions from the University of Oslo the University of Oslo* 279, 15–42.
- Jaanusson, V. 1982c: Ordovician in Västergötland. In Bruton, D.L. (ed.): Field excursion guide. IV International Symposium on the Ordovician System. *Paleontological Contributions from the University of Oslo the University of Oslo* 279, 164–183.
- Jaanusson, V. 1984: Ordovician benthic macrofaunal associations. In Bruton, D.L. (ed.) 1984: Aspects of the Ordovician System. *Paleontological Contributions from the University of Oslo*, 295, 127–139. Universitetsförlaget.
- Jaanusson, V. & Bergström, S.M. 1980: Middle Ordovician faunal spatial differentiation in Baltoscandia and the Appalachians. *Alcheringa* 4, 89–110.
- Jaanusson, V. & Martna, J. 1948: A section from the Upper Chasmops Series to the Lower Tretaspis Series at Fjäckå rivulet in the Siljan area, Dalarna. *Bulletin of the Geological Institution of the University of Upsala* 32, 183–193.
- Jaanusson, V. & Mutvei, H. 1953: Stratigraphie und Lithologie der unterordovizischen Platyrurus-Stufe im Siljan-Gebiet, Dalarna. *Bulletin of the Geological Institutions of the University of Upsala* 35, 7–34.
- Jaanusson, V. & Mutvei, H. 1982: *Ordovician of Öland. Guide to Excursion 3*. IV International Symposium on the Ordovician System, Oslo. 23 pp. Swedish Museum of Natural History, Stockholm.
- Jaanusson, V. & Skoglund, R. 1963: Graptoloids from the Viruan (Ordovician) Dalby and Skagen limestones of Västergötland. *Geologiska Föreningens i Stockholm Förhandlingar* 85, 341–357.
- Jeppsson, L., Fredholm, D. & Mattiasson, B. 1985: Acetic acid and phosphatic fossils – A warning. *Journal of Paleontology* 59, 952–956.
- Kaljo, D., Röömusoks, A. & Männil, R. 1958: O seriyakh pribaltijskogo ordovika i ikh znachenii. [On the Series of the Baltic Ordovician and their significance.] *Eesti NSV Teaduste Akadeemia Toimetised. Tehniliste ja füüsilis-matemaatiliste teaduste seeria* 7, 71–74.
- Kaljo, D., Borovko, N., Heinsalu, H., Khazanovich, K., Mens, K., Popov, L., Sergejeva, S., Sobolevskaya, R. & Viira, V. 1986: The Cambrian–Ordovician boundary in the Baltic–Ladoga clint area (north Estonia and Leningrad region, USSR). *Eesti NSV Teaduste Akadeemia Toimetised. Geologia* 35, 97–108.
- Kolobova, I.M. & Popov, L.E. 1986: K paleontologicheskoy kharakteristike anderkenskogo gorizonta srednego ordovika v Chuilijksikh gorakh (yuzhnyj Kazakhstan). [On the palaeontological characteristics of the Middle Ordovician Anderken Formation in the Chu-ilijski mountains (southern Kazakhstan).] *Ezhegodnik vsesoyuznogo paleontologicheskogo obshchestva* 29, 246–261.
- Koneva, C.P. & Popov, L.E. 1983: Nektorye novy lingulidy iz verchnego kembriya i nizhnego ordovika Malogo Karatau. [Some new lingulids from the Upper Cambrian and Lower Ordovician of Malij Karatau.] In Satpaeva, K.I. (ed.): *Stratigrafiya i paleontologiya nizhnego paleozoya Kazakhstana*. 110–124. Alma-Ata 1983.
- Krause, F.F. 1972: Distributional patterns of some inarticulate brachiopods on a Middle Ordovician bioherm [abstract]. *Geological Society of America, Abstract with Programs* 4, 282–283.
- Krause, F.F. & Rowell, A.J. 1975: Distribution and systematics of the inarticulate brachiopods of the Ordovician carbonate mud mound Meiklejohn Peak, Nevada. *The University of Kansas Paleontological Contributions* 61. 74 pp.
- Kuhn, O. 1949: *Lehrbuch der Paläozoologie*. 326 pp. E. Schweizerbart'sche Verlagsbuchhandlung, Stuttgart.
- Larsson, K. 1973: The lower Viruan in the autochthonous Ordovician sequence of Jämtland. *Sveriges Geologiska Undersökning C683*, 1–82.
- Laufeld, S. 1967: Caradocian Chitinozoa from Dalarna, Sweden. *Geologiska Föreningens i Stockholm Förhandlingar* 89, 275–349.
- Lindström, G. 1888: *List of the fossil faunas of Sweden 1. Cambrian and Lower Silurian*, 1–24.
- Lindström, M. 1963: Sedimentary folds and the development of limestones in an Early Ordovician sea. *Sedimentology* 2, 243–292.
- Lindström, M. 1972: Vom Anfang, Hochstand und Ende eines Epikontinentalmeeres. *Geologische Rundschau* 60, 419–438.
- Lindström, M. 1979: Diagenesis of Lower Ordovician hardgrounds in Sweden. *Geologica et Palaeontologica* 13, 9–30.
- Lindström, M. 1984: The Ordovician climate based on the study of carbonate rocks. In Bruton, D.L. (ed.): Aspects of the Ordovician System. *Paleontological Contributions from the University of Oslo* 295, 81–88. Universitetsförlaget.
- Lindström, M., Simon, S., Paul, B. & Kessler, K. 1983: The Ordovician and its mass movements in the Lockne Area near the Caledonian margin, Central Sweden. *Geologica et Palaeontologica* 17, 17–27.
- Lindström, M. & Vortisch, W. 1983: Indications of upwelling in the Lower Ordovician of Scandinavia. In Thiede, J. & Suess, E. (eds.): *Coastal Upwelling*. 535–551. Plenum Publishing co.
- Lockley, M.G. & Antia, D.D.J. 1980: Anomalous occurrences of the Lower Palaeozoic brachiopod *Schizocrania*. *Palaentology* 23, 707–713.
- Lockley, M.G. & Williams, A. 1981: Lower Ordovician Brachiopoda from mid and southwest Wales. *Bulletin of the British Museum of Natural History (Geology)* 35, 1–78.
- Logan, B.W., Rezak, R. & Ginsburg, R.N. 1964: Classification and environmental significance of algal stromatolites. *Journal of Geology* 72, 68–83.
- Ludvigsen, R. 1974: A new Devonian acrotretid (Brachiopoda, Inarticulata) with unique protegular ultrastructure. *Neues Jahrbuch für Geologie und Paläontologie, Monatshefte*, 3 133–148.
- Löfgren, A. 1978: Arenigian and Llanvirnian conodonts from Jämtland, northern Sweden. *Fossils & Strata* 13, 1–129.
- Martna, J. 1955: Studies on the Macrourus and Slandrom Formations I. Shell fragment frequencies of the Macrourus Formation and adjacent strata at Fjäckå, Gräsgård, and File Haidar. *Geologiska Föreningens i Stockholm Förhandlingar* 77, 229–256.
- McClellan, A.E. 1988: Epithelial moulds from some Upper Ordovician acrotretide brachiopods of Ireland. *Lethaia* 21, 43–50.
- McConnell, D. 1963: Inorganic constituents in the shell of the living brachiopod *Lingula*. *Bulletin of the Geological Society of America* 74, 363–364.
- Männil, R. 1966: *Istoriya razvitiya Baltijskogo basseyna v ordovike*. (Evolution of the Baltic Basin during the Ordovician). 201 pp. Eesti NSV Teaduste Akadeemia Geoloogia Instituudi, Tallin.
- Mickwitz, A. 1896: Über die Brachiopodengattung *Obolus* Eichwald. *Memoires de l'academie imperiale des sciences de St.-Petersbourg* 4, 1–215.
- Moberg, J.C. & Segerberg, C.O. 1906: Bidrag till kännedomen om ceratopygeregionen med särskild hänsyn till dess utveckling i Fogelsångstrakten. *Lunds Universitets Årsskrift N.F.* 2, 2, 1–116
- Muir-Wood, H.M. 1955: *A history of the classification of the phylum Brachiopoda*. 124 pp. British Museum (Natural History), London.
- Müller, F. 1860: Beschreibung einer Brachiopodenlarve. *Archiv für Anatomie, Physiologie und Wissenschaftliche Medicin*, 72–81.
- Nazarov, B.B. & Popov, L.E. 1976: Radiolyarii, bezzamkovyye brachiopody i organizmy neyasnogo sistematicheskogo položeniya iz srednego ordovika vostochnogo Kazakhstana. [Radiolarians, inarticulate brachiopods and organisms of uncertain systematic position from the Middle Ordovician of eastern Kazakhstan.] *Paleontologicheskij Zhurnal* 1976:4, 33–42.
- Nazarov, B.B. & Popov, L.E. 1980: Stratigrafiya i fauna kremnistokarbonatnykh tolshch ordovika Kazakhstana. [Stratigraphy and fauna of Ordovician siliceous-carbonate deposits of Kazakh-

- stan.] *Trudy Geologicheskogo Instituta Akademiyi Nauk SSSR* 331, 1–190.
- Nilsson, R. 1977: A boring through Middle and Upper Ordovician Strata at Koängen in western Scania. *Sveriges geologiska Undersökning C 733*, 1–58.
- Owen, A.W. 1987: The trilobite *Tretaspis* at the Middle–Upper Ordovician boundary in Västergötland. *Geologiska Föreningens i Stockholm Förhandlingar* 109, 259–266.
- Owens, R.M., Fortey, R.A., Cope, J.C.W., Rushton, A.W.A. & Bassett, M.G. 1982: Tremadoc faunas from the Carmarthen district, South Wales. *Geological Magazine* 119, 1–38.
- Paine, R.T. 1963: Ecology of the brachiopod *Glottidia pyramidata*. *Ecological Monographs* 33, 187–213.
- Paine, R.T. 1970: The sediment occupied by Recent lingulid brachiopods and some paleoecological implications. *Paleogeography, Paleoclimatology, Paleocology* 7, 21–31.
- Percival, E. 1944: A contribution to the life-history of the brachiopod *Terebratalia inconspicua* Sowerby. *Transactions of the Royal Society of New Zealand* 74, 1–23.
- Percival, E. 1953: Orientation of Telotrematous Brachiopoda. *Nature* 171, 436.
- Percival, I.G. 1978: Inarticulate brachiopods from the Late Ordovician of New South Wales, and their palaeoecological significance. *Alcheringa* 2, 117–141.
- Pickerill, R.K., Harland, T.L. & Fillion, D. 1984: *In situ* lingulids from deep-water carbonates of the Middle Ordovician Table Head Group of Newfoundland and the Trenton Group of Quebec. *Canadian Journal of Earth Science* 21, 194–199.
- Popov, L.E. 1975: Bezzamkovyye brachiopody iz srednego ordovika khrebtu Chingiza. [Middle Ordovician inarticulate brachiopods from the Chingiz ridge.] *Paleontologicheskij Zhurnal* 1975:4, 32–41.
- Popov, L.E. 1977: Novye vidy sredneordovikskikh bezzamkovykh brachiopod Chingiza. [New species of Middle Ordovician inarticulate brachiopods from the Chingiz ridge.] *Novye vidy drevnykh rasteniy i bespozvonochnykh SSSR* 4, 102–105.
- Popov, L.E. & Nölvak, J. 1987: Revision of the morphology and systematic position of the genus *Acanthambonia* (Brachiopoda, Inarticulata). *Eesti NSV Teaduste Akadeemia Toimetised, Geoloogia* 36, 14–18.
- Popov, L.E. & Ushatinskaya, G.T. 1986: O vtorichnykh izmeneniyakh mikrostruktury fosfatno-kal'tsievnykh rakovin bezzamkovykh brachiopod. (On secondary changes in the microstructure of calcium-phosphatic shells of inarticulate brachiopods.) *Izvestiya Akademii Nauk SSSR, Seriya Geologicheskaya* 10, 135–137.
- Popov, L.E., Zezina, O. N. & Nölvak, J. 1982: Mikrostruktura apikal'noj chasti rakoviny bezzamkovykh brachiopod i ee ekologicheskoe znachenie. [Microstructure of the apical parts of inarticulates and its ecological importance.] *Byulleten' Moskovskogo obshchestva ispytatelej prirody, otdel biologicheskij* 87, 94–104.
- Poulsen, V. 1971: Notes on an Ordovician acrotretacean brachiopod from the Oslo region. *Geological Society of Denmark, Bulletin* 20, 265–278.
- Rhodes, F.H.T. & Bloxham, T.W. 1971: Phosphatic organisms in the Paleozoic and their evolutionary significance. *Proceedings of the North American Paleontological Convention, Part K: Phosphate in Fossils*, 1485–1513.
- Ross, R.J. Jr., Jaanusson, V. & Friedman, J. 1975: Lithology and origin of Middle Ordovician calcareous mudmound at Meiklejohn Peak, southern Nevada. *U.S. Geological Survey Professional Paper* 871, 1–48.
- Rowell, A.J. 1960: Some early stages in the development of the brachiopod *Crania anomala* (Muller). *Annales and Magazine of Natural History* 13:3, 35–52.
- Rowell, A.J. 1962: The genera of the brachiopod superfamilies Obolllacea and Siphonotretacea. *Journal of Paleontology* 36, 136–152.
- Rowell, A.J. 1965: Inarticulata. In Moore, R.C. (ed.). *Treatise on Invertebrate Palaeontology, Part H*. H260–H296. Geological Society of America, Lawrence.
- Rowell, A.J. 1966: Revision of some Cambrian and Ordovician inarticulate brachiopods. *The University of Kansas Paleontological Contributions* 7, 1–36.
- Rowell, A.J. 1981a: The Cambrian brachiopod radiation: monophyletic or polyphyletic origins? In Taylor, M.E. (ed.): Short papers for the Second International Symposium on the Cambrian System. *U.S. Geological Survey Open File Report* 81-743, 184–187.
- Rowell, A.J. 1981b: The origin of the Brachiopoda. In Broadhead, T.W. (ed.): *Lophophorates – Notes for a short course*, 97–109. University of Tennessee, Department of Geological Sciences, Studies in Geology 5.
- Rowell, A.J. 1982: The monophyletic origin of the Brachiopoda. *Lethaia* 15, 299–307.
- Rowell, A.J. 1986: The distribution and inferred larval dispersion of *Rhondellina dorei*: A new Cambrian brachiopod (Acrotretida). *Journal of Paleontology* 60, 1056–1065.
- Rowell, A.J. & Brady, M.J. 1976: Brachiopods and biomerer. *Brigham Young University Geology Studies* 23, 165–180.
- Rowell, A.J. & Krause, F.F. 1973: Habitat diversity in the Acrotretacea (Brachiopoda, Inarticulata). *Journal of Paleontology* 47, 791–800.
- Rowell, A.J. & Henderson, R.A. 1978: New genera of acrotretids from the Cambrian of Australia and the United States. *The University of Kansas Paleontological Contributions* 93, 1–12.
- Ruedemann, R. 1934: Paleozoic plankton of North America. *Geological Society of America, Memoir* 2, 1–144.
- Savazzi, E. 1986: Burrowing sculptures and life habits in Paleozoic lingulacean brachiopods. *Paleobiology* 12, 46–63.
- Schallreuter, R.E.L. 1984: Middle Ordovician ostracodes from Sweden. *Geologiska Föreningens i Stockholm Förhandlingar* 106, 93–99.
- Schuchert, C. 1911: Paleogeographic and geologic significance of Recent Brachiopoda. *Geological Society of America, Bulletin* 22, 258–275.
- Seilacher, A. 1972: Divaricate patterns in pelecypod shells. *Lethaia* 5, 325–343.
- Sheehan, P.M. 1977: Ordovician and Silurian brachiopods from graptolite shales and related deep-water argillaceous rocks. *Lethaia* 10, 201–203.
- Sheehan, P.M. 1979: Swedish Late Ordovician marine benthic assemblages and their bearing on brachiopod zoogeography. In Gray, J. & Boucot, A.J. (eds.): *Historical Biogeography, Plate Tectonics, and the Changing Environment*. 61–73. The Oregon State University Press.
- Skoglund, R. 1963: Uppermost Viruan and lower Harjuan (Ordovician) stratigraphy of Västergötland and lower Harjuan graptolite faunas of central Sweden. *Bulletin of the Geological Institutions of the University of Uppsala* 42, 1–55.
- Spjeldnaes, N. 1978: Epiplanktoniske brachiopoder og bryozoaer fra en sort skifer [abstract]. *XIII Nordiska Geologiska Vintermötet* 1978, 11.
- Starobogatov, Ya.I. 1979: Evolyutsiya pelagicheskikh lichinok pervichnorotykh zhivotnykh i problema osnovnykh komponentov tela. [Evolution of the pelagic larvae of Protostomia and problem of the main body components.] *Zoologicheskij Zhurnal* 78, 149–160.
- Stricker, S.A. & Reed, C.G. 1985a: The ontogeny of shell secretion in *Terebratalia transversa* (Brachiopoda, Articulata) 1. Development of the mantle. *Journal of Morphology* 183, 233–250.
- Stricker, S.A. & Reed, C.G. 1985b: The ontogeny of shell secretion in *Terebratalia transversa* (Brachiopoda, Articulata) 2. Formation of the Protegulum and juvenile shell. *Journal of Morphology* 183, 251–271.
- Stricker, S.A. & Reed, C.G. 1985c: The protegulum and juvenile shell of a Recent articulate brachiopod: patterns of growth and chemical composition. *Lethaia* 18, 295–303.
- Stricker, S.A. & Reed, C.G. 1985d: Development of the pedicle in the articulate brachiopod *Terebratalia transversa* (Brachiopoda, Terebratulida). *Zoomorphology* 105, 253–264.
- Sturesson, U. 1988a: Lower Ordovician ferriiferous ooids from the Siljan district, Sweden. *Bulletin of the Geological Institutions of the University of Uppsala, N.S.* 12, 109–212.

- Stuesson, U. 1989: Coated grains in the Lower Viruan limestone in Västergötland, central Sweden. *Geologiska Föreningens i Stockholm Förhandlingar* 111, 273–284.
- Sweet, W.C. & Bergström, S.M. 1962: Conodonts from the Pratt Ferry Formation (Middle Ordovician) of Alabama. *Journal of Paleontology* 36, 1214–1252.
- Szymanski, B. 1985: Stromatolity lanwirnu górnego z północno-wschodniej części obniżenia podlaskiego. [Upper Llanvirnian Stromatolites from the north-eastern part of the Podlasie depression.] *Kwartalnik Geologiczny* 29, 597–624.
- Temple, J.T. 1965: Upper Ordovician brachiopods from Poland and Britain. *Acta Palaeontologica Polonica* 10, 379–422.
- Thayer, C.W. 1975: Morphologic adaptations of benthic invertebrates to soft substrata. *Journal of Marine Research* 33, 177–189.
- Thorslund, P. & Jaanusson, V. 1960: The Cambrian, Ordovician, and Silurian in Västergötland, Närke, Dalarna, and Jämtland, Central Sweden. Guide to excursions A 23 and C 18. *International Geological Congress, 21 Session, Copenhagen 1960*, 3–51.
- Törnquist, S.L. 1867: Om lagerföljden i Dalarnes Undersiluriska bildningar. *Lunds Universitets Årsskrift* 3, 1–20.
- Törnquist, S.L. 1883: Öfversigt öfver bergbyggnaden inom Siljansområdet i Dalarna, med hänsyn företrädesvis fäst vid dess paleozoiska lag. *Sveriges Geologiska Undersökning C* 57, 1–59.
- Troedsson, G.T. 1918: Om skånes brachiopods-kiffer. *Lunds Universitets Årsskrift N. F. 2, 15(3)*, 1–104.
- Valentine, J.W. 1973: Coelomate superphyla. *Systematic Zoology* 22, 97–102.
- Valentine, J.W. 1975: Adaptive strategy and the origin of grades and ground plans. *American Zoologist* 15, 391–404.
- Valentine, J.W. 1977: General patterns of Metazoan Evolution. In Hallam, A. (ed.): *Patterns of Evolution as illustrated by the Fossil Record*. 27–57. Elsevier, Amsterdam.
- Valentine, J.W. 1981: The lophophorate condition. In Broadhead, T.W. (ed.): *Lophophorates – Notes for a short course*. 190–204. University of Tennessee, Department of Geological Sciences, Studies in Geology 5.
- Valentine, J.W. & Erwin, D.H. 1987: Interpreting great developmental experiments: the fossil record. In Raff, R.A. & Raff, E.C. (eds): *Development as an Evolutionary Process. Marine Biological Laboratory Lectures in Biology* 8, 71–107. Alan R. Liss, New York, N.Y.
- Waern, B. 1952: Palaeontology and Stratigraphy of the Cambrian and Lowermost Ordovician of the Bödahamn Core. *Bulletin of the Geological Institutions of the University of Uppsala* 34, 224–250.
- Wahlenberg, G. 1818: Petrificata Telluris Svecanae. *Nova Acta Societatis Scientiarum Upsaliensis* 8, 1–116.
- Walcott, C.D. 1889: Description of a new genus and species of inarticulate brachiopod from the Trenton Limestone. *Proceedings of the United States National Museum* 12, 365–366.
- Walcott, C.D. 1908: Cambrian geology and Palaeontology 1:4. Classification and terminology of the Cambrian Brachiopoda. *Smithsonian Miscellaneous Collections* 53, 139–165.
- Walcott, C.D. 1912: Cambrian Brachiopoda. *Monograph of the U.S. Geological Survey* 51, 1–872.
- Wang, Y. 1949: Maquoketa Brachiopoda of Iowa. *Memoir of the Geological Society of America* 42, 1–55.
- Watabe, N. & Pan, C.-M. 1984: Phosphatic shell formation in atremate brachiopods. *American Zoologist* 24, 977–985.
- Westergård, A.H. 1909: Studier öfver dictyograpthuskiffern och dess gränslager med särskild hänsyn till i Skåne förekommande bildningar. *Lunds Universitets Årsskrift N.F. 2, 5*, 1–79.
- Wetzel, A. 1982: Cyclic and dyscyclic black shale formation. In Einsele, G. & Seilacher, A. (eds.): *Cyclic and Event Stratification*. 431–455. Springer-Verlag, Berlin.
- Williams, A. 1965: Stratigraphic distribution. In Moore, R.C. (ed.): *Treatise on Invertebrate Paleontology, Part H*. H237–H250. Geological Society of America, Lawrence.
- Williams, A. 1968: A history of skeletal secretion among articulate brachiopods. *Lethaia* 1, 268–287.
- Williams, A. 1974: Ordovician brachiopoda from the Shelve district, Shropshire. *Bulletin of the British Museum of Natural History (Geology), Supplement* 11, 1–163.
- Williams, A. 1977: Differentiation and growth of the brachiopod mantle. *American Zoologist* 17, 107–120.
- Williams, A. 1984: Lophophorates. In Bereiter-Hahn, J., Maltoltsy, A.G. & Rickards, K.S. (eds.): *Biology of the Integument 1. Invertebrates*. 728–745. Springer-Verlag, Berlin.
- Williams, A. & Curry, G.B. 1985: Lower Ordovician Brachiopoda from the Tourmakeady Limestone, Co. Mayo, Ireland. *Bulletin of the British Museum of Natural History (Geology)* 38, 183–269.
- Williams, A. & Hurst, J.M. 1977: Brachiopod evolution. In Hallam, A. (ed.): *Patterns of Evolution as Illustrated by the Fossil Record*. 79–121. Elsevier, Amsterdam.
- Williams, A. & MacKay, S. 1979: Differentiation of the brachiopod periostracum. *Palaeontology* 22, 721–736.
- Williams, A. & Rowell, A.J. 1965a: Morphology. In Moore, R.C. (ed.): *Treatise on Invertebrate Paleontology, Part H*, H57–H138. Geological Society of America, Lawrence.
- Williams, A. & Rowell, A.J. 1965b: Evolution and phylogeny. In Moore, R.C. (ed.): *Treatise on Invertebrate Palaeontology, Part H*. H164–H197. Geological Society of America, Lawrence.
- Williams, A. & Rowell, A.J. 1965c: Classification. In Moore, R.C. (ed.): *Treatise on Invertebrate Palaeontology, Part H*. H214–H237. Geological Society of America, Lawrence.
- Williams, A. & Wright, A.D. 1970: Shell structure of the Craniacea and other calcareous inarticulate brachiopods. *Special Papers in Palaeontology* 7, 1–51.
- Williams, S.H. & Lockley, G.M. 1983: Ordovician inarticulate brachiopods from graptolitic shales at Dob's Linn, Scotland; Their morphology and significance. *Journal of Paleontology* 57, 391–400.
- Williams, S.H. & Rickards, R.B. 1984: Palaeoecology of graptolitic black shales. In Bruton, D.L. (ed.): *Aspects of the Ordovician System. Palaeontological Contributions from the University of Oslo* 295, 159–166. Universitetsförlaget, Oslo.
- Wiman, C. 1905: Studien über das Nordbaltische Silurgebiet 1. *Bulletin of the Geological Institution of the University of Uppsala* 6, 12–76.
- Wiman, C. 1908: Studien über das Nordbaltische Silurgebiet 2. *Bulletin of the Geological Institution of the University of Uppsala* 8, 73–168.
- Wright, A.D. 1963: The fauna of the Portrane Limestone 1. The inarticulate brachiopods. *Bulletin of the British Museum of Natural History (Geology)* 8, 223–254.
- Wright, A.D. 1979: Brachiopod radiation. In House, M.R. (ed.): *The Origin of Major Invertebrate Groups*. 235–252. Academic Press.
- Wright, A.D. 1981: The external surface of *Dictyonella* and of other pitted brachiopods. *Palaeontology* 24, 443–481.
- Yatsu, N. 1902: On the development of *Lingula anatina*. *Journal of the College of Science, Imperial University of Tokyo, Japan* 17, 1–112.

Instructions to authors

Manuscripts are to be sent to the editor, and the author is requested to retain a complete copy. The text should initially be submitted as a paper copy for refereeing and eventually as word-processor text files; contact the editor for technical details. Figure and plate originals should not be submitted until the manuscript has been accepted for publication. The author is expected to read galley and page proofs carefully, making only necessary corrections, and to return them promptly to the editor. The author will receive 50 copies of the publication free of charge.

Language and style. – The principal language of *Fossils and Strata* is English. Authors are encouraged to write in a personal style, as long as it is (1) linguistically correct, (2) clear and unambiguous, and (3) concise.

Title. – The title should be short and concentrated, its purpose being to draw attention to the main subject of the paper. It should be 'clean', i.e. containing no 'noise words' ('Contributions to the knowledge of ...', 'Some preliminary notes on ...', 'On ...', etc.) or such extraneous characters as are likely not to survive treatment in information retrieval systems (question marks, parentheses, Greek letters, mathematical symbols, etc.).

Abstract. – The abstract, not exceeding 2000 characters and spaces, should be informative, stating the results presented in the paper rather than describing its contents. Avoid literature citations; if they must be provided they should be accompanied by abbreviated bibliographic references within parentheses. New systematic or stratigraphic names introduced in the paper should be mentioned in the abstract. Keywords (index entries) should be provided immediately after the main abstract text.

Manuscript. – The paper version of the manuscript submitted for refereeing should be submitted on white, standard-sized (A4 or Letter Size), consecutively numbered sheets of paper. Use double-spacing *throughout*, i.e. also for references, figure caption, tables, etc. Do not break words at the end of lines. Consult a recent issue of *Fossils and Strata* and arrange the text to conform with the typographic practices used therein. But consistency is more important than adherence to a template.

The manuscript should be arranged as follows: (1) Title of paper. (2) Name(s) of author(s), one or more forenames in full. (3) Bibliographic identification (biblid) as in the following example: Smith, John K. & Jones, Karen L. 19## ## #: Title of paper. *Fossils and Strata*, No. ##, pp. ###-###. Oslo. ISSN 0300-9491. ISBN ##-##-####-#. (4) Abstract. (5) Keywords. (6) Name and address(es) of author(s), followed by the date of completion of the paper. (7) Main text. (8) List of references. (9) Figure captions. (10) Plate captions. (11) Tables with captions.

Use four of fewer grades of heading in the main text: Large size roman (mark this heading with an initial '\$2'), smaller size roman ('\$3'), smaller size italics ('\$4'), and lower case italics flush with the text (followed by a full stop, space, double hyphen, space, and the subsequent text *en suite*). Do not number the headings.

Do not provide a separate table of contents. All detached headings (\$2-\$4) will be extracted by the editor for a table of contents.

Any character not available from the keyboard should be coded as a unique combination of keyboard characters (e.g., \$a, @1...).

Construct synonymy lists as run-on paragraphs with each new entry marked by a square symbol (may be coded as '\$F' in the word-processor), thus: □[year] [taxonomic name and authorship exactly as given in the cited publication] – [author(s) of paper], [page and figure references].

Avoid footnotes. Digressive material, not possible to place within parentheses, to delete, or to incorporate in the main text, may be set as discrete paragraphs in smaller type (mark this section with '[begin petit]' and '[end petit]' in the text).

SI (*Système International d'Unités*) units should be used wherever possible.

Literature citations in the text should be given as the author's surname followed by the year of publication with no intervening comma; placement of the parentheses depends on the structure of the sentence. Do not vex the reader with 'op. cit.', 'ibid.', etc. Note that an ampersand (&) is used for joint authorship in citations and

references. Entries in the reference list are to be listed alphabetically in order of authors' names in accordance with the following examples.

Henderson, R.A. 1974: Shell adaptation in acrothelid brachiopods to settlement on soft substrata. *Lethaia* 7, 57–61.

Lindström, M. 1971: Lower Ordovician conodonts of Europe. In Sweet, W.C. & Bergström, S.M. (eds.): Symposium on conodont biostratigraphy. *Geological Society of America, Memoir* 127, 21–61.

Popov, L.E. 1975: Bezzamkovye brachiopody iz srednego ordovika khrebta Chingiz. [Inarticulate brachiopods from the Middle Ordovician of the Chingiz Range.] *Paleontologicheskij zhurnal* 1975:4, 32–41.

Rudwick, M.J.S. 1970: *Living and Fossil Brachiopods*. 199 pp. Hutchinson, London.

If there are several references to any one author, the name should be repeated in each entry. Titles of *articles* should be decapitalized, except in cases where this would violate a language convention. Cyrillic letters should be transliterated according to the ISO Standard 833 (1974). Serial titles should not be abbreviated.

Figures, plates and table captions should be self-explanatory but as short as possible. If a figure contains lettered items, list them *en suite* in the caption and insert a square symbol (may be coded as '\$F') immediately in front of each entry (□A, etc.). All figured specimens should have a reference to their provenance and present location (museum or similar registration number).

Illustrations. – All illustrations must be clearly marked with the author's name and figure number. Plan the figures so that they take up the entire width of the type area (170 mm) or the width of one column (81 mm). If an intermediate width has to be used, do not exceed 127 mm. In the event of a full-page illustration, try to allow space for the caption to come within the page depth, 254 mm. Plates should be constructed for an area of 170×254 mm, but it is usually preferable to arrange all illustrations as figures to be placed in their proper positions in the text.

The cost of reproducing a figure is based on the smallest rectangular frame in which the figure can be inserted. Use that frame! Do not leave open corners or unnecessary space between items, Do not let text of lettering protrude outside the frame of the figure.

Photographs should be printed on white paper with glossy finish. They must be clear and sharply contrasted, but without pronounced light areas and heavy shadows. If incident light is used for illumination, the light should fall consistently from the upper left. Stereo-pairs should be mounted at a maximum distance of 70 mm. In a composite figure, all items should be of similar tone and contrast. Composite figures should consist of regular units as far as possible. Mount the photographs on cardboard. If a clean background is desired, provide originals that have an even *black* background tone or submit overlays for blocking out to an either black or white background (see Bengtson, S. 1986: Preparing clean backgrounds in published photographic illustrations. *Lethaia* 19:4, 361–362; available on request from the editor). If a photographic figure consists of several rectangular items, make sure that the intervening narrow strips are directly reproducible; i.e. cut the prints accurately and mount them on white cardboard, alternatively edge to edge with white adhesive strips over the joints.

Line drawings should have lines of even thickness and blackening. Do not use gray or too densely screened (more than 40 lines/cm) surfaces. If the figures include text, Do Not Monumentalize the Text by Capitalizing Words. For metric units, use the standard symbols – μm, mm, m, km – there should be no capitals (at least not for length units), not plural, no genitive, no hyphens, and no periods. Separate the symbols from the number by a space. Do not leave out zero before decimal points.

Line drawings and halftones should not be combined in the same figure without good reason. Place text and lettering *on* the figure, normally on its background portions.

Lettering of items in composite figures (A, B, C, etc.; *nota*, b, c...) and plates (1, 2, 3, etc.) should be distinct but not dominant, and placed as consistently as possible in the different items. Use transfer lettering (simple, sans-serif, semibold typefaces such as Helvetica) or stencils.

FOSSILS AND STRATA

ISSN 0300-9491

- No. 1 Jessen, H.L. 1972: Schultergürtel und Pectoralflosse bei Actinopterygiern. 101 pp. + 25 pls. ISBN 82-00-09288-7. NOK 249,00 (USD 35,00).
- No. 2 Bergström, J. 1973: Organization, life, and systematics of trilobites. 69 pp. + 5 pls. ISBN 82-00-09330-1. *Out of print.*
- No. 3 Bassett, M.G. & Cocks, L.R.M. 1974: A review of Silurian brachiopods from Gotland. 56 pp. + 11 pls. ISBN 82-00-09349-2. NOK 109,00 (USD 15,00).
- No. 4 1975: Evolution and morphology of the Trilobita, Trilobitoida and Merostomata. Proceedings of a symposium in Oslo, 1st-8th July, 1973. 468 pp. ISBN 82-00-04963-9. *Out of print.*
- No. 5 Laufeld, S. 1974: Silurian Chitinozoa from Gotland. 130 pp. ISBN 82-00-09358-1. NOK 249,00 (USD 35,00).
- No. 6 Jeppsson, L. 1974: Aspects of Late Silurian conodonts. 54 pp. + 12 pls. ISBN 82-00-09373-5. NOK 140,00 (USD 20,00).
- No. 7 Christensen, W.K. 1975: Upper Cretaceous belemnites from the Kristianstad area in Scania. 69 pp. + 12 pls. ISBN 82-00-09374-3. NOK 161,00 (USD 23,00).
- No. 8 Bjerreskov, M. 1975: Llandoveryan and Wenlockian graptolites from Bornholm. 93 pp. + 13 pls. ISBN 82-00-09392-1. NOK 249,00 (USD 35,00).
- No. 9 Vidal, G. 1976: Late Precambrian microfossils from the Visingsö Beds in southern Sweden. 57 pp. ISBN 82-00-09418-9. NOK 161,00 (USD 23,00).
- No. 10 Hansen, H.J. & Lykke-Andersen, A.-L. 1976: Wall structure and classification of fossil elphidiid and non-ionid Foraminifera. 37 pp. + 22 pls. ISBN 82-00-09427-9. NOK 175,00 (USD 25,00).
- No. 11 Larsson, K. 1979: Silurian tentaculitids from Gotland and Scania. 180 pp. ISBN 82-00-09483-9. *Out of print.*
- No. 12 Bengtson, P. 1983: The Cenomanian-Coniacian of the Sergipe Basin, Brazil. 78 pp. ISBN 82-00-09484-7. NOK 199,00 (USD 28,00).
- No. 13 Löfgren, A. 1978: Arenigian and Llanvirnian conodonts from Jämtland, northern Sweden. 129 pp. + 16 pls. ISBN 82-00-09476-6. *Out of print.*
- No. 14 Björck, S. 1981: A stratigraphic study of Late Weichselian deglaciation, shore displacement and vegetation history in south-eastern Sweden. 93 pp. ISBN 82-00-09520-6. NOK 199,00 (USD 28,00).
- No. 15 1983: Taxonomy, ecology and identity of conodonts. Proceedings of the Third European Conodont Symposium (ECOS III) in Lund, 30th August to 1st September, 1982. 192 pp. ISBN 82-00-06737-8. NOK 339,00 (USD 48,00).
- No. 16 Stouge, S.S. 1984: Conodonts of the Middle Ordovician Table Head Formation, western Newfoundland. 145 pp. ISBN 82-00-09548-7. NOK 259,00 (USD 37,00).
- No. 17 Müller, K.J. & Walossek, D. 1985: Skaracarida, a new order of Crustacea from the Upper Cambrian of Västergötland, Sweden. 65 pp. ISBN 82-00-07498-6. NOK 147,00 (USD 21,00).
- No. 18 Stridsberg, S. 1985: Silurian oncocerid cephalopods from Gotland. 65 pp. ISBN 82-00-07575-3. NOK 147,00 (USD 21,00).
- No. 19 Müller, K.J. & Walossek, D. 1987: Morphology, ontogeny, and life habit of *Agnostus pisiformis* from the Upper Cambrian of Sweden. 124 pp. ISBN 82-00-07511-7. NOK 245,00 (USD 35,00).
- No. 20 Johansen, M.B. 1987: Brachiopods from the Maastrichtian-Danian boundary sequence at Nye Kløv, Jylland, Denmark. 99 pp. ISBN 82-00-02558-6. NOK 189,00 (USD 26,00).
- No. 21 Berthou, P.-Y. & Bengtson, P. 1988: Stratigraphic correlation by microfacies of the Cenomanian-Coniacian of the Sergipe Basin, Brazil. 88 pp. ISBN 82-00-37413-0. NOK 189,00 (USD 27,00).
- No. 22 Hessel, M.H.R. 1988: Lower Turonian inoceramids from Sergipe, Brazil: systematics, stratigraphy and palaeoecology. 49 pp. ISBN 82-00-37414-9. NOK 126,00 (USD 18,00).
- No. 23 Müller, K.J. & Walossek, D. 1988: External morphology and larval development of the Upper Cambrian maxillopod *Bredocaris admirabilis*. 70 pp. ISBN 82-00-37412-2. NOK 161,00 (USD 23,00).
- No. 24 Qian Yi & Bengtson, S. 1989: Palaeontology and biostratigraphy of the Early Cambrian Meishucunian Stage in Yunnan Province, South China. 156 pp. ISBN 82-00-37415-7. NOK 315,00 (USD 45,00).
- No. 25 Bergman, C.F. 1989: Silurian paulinitid polychaetes from Gotland. 128 pp. ISBN 82-00-37424-6. NOK 259,00 (USD 37,00).
- No. 26 Holmer, I.E. 1989: Middle Ordovician phosphatic inarticulate brachiopods from Västergötland and Dalarna, Sweden. 172 pp. ISBN 82-00-37425-4. NOK 336,00 (USD 48,00).
- No. 27 Majoran, S. 1989: Mid-Cretaceous Ostracoda of north-eastern Algeria. 68 pp. ISBN 82-00-37426-2. NOK 154,00 (USD 22,00).

